

3. SUMMARY OF WESTERN NORTH PACIFIC AND NORTH INDIAN OCEAN TROPICAL CYCLONES

3.1 WESTERN NORTH PACIFIC OCEAN TROPICAL CYCLONES

The year of 1994 included ~~five~~^{six} super typhoons, 16 lesser typhoons, 15 tropical storms and five tropical depressions (Table 3-1). The calendar year total of 41 significant tropical cyclones (TCs) in the western North Pacific was the highest since 1967 when there were also 41 (Table 3-2). The year's total of six super

typhoons was two above the 35-year (1960-1994) average (Figure 3-1), and the year's total of 36 named TCs was eight above the 35-year average (1960-1994) (Figure 3-2). Thirty-five of the 41 significant TCs in the western North Pacific during 1994 originated in the low-level monsoon trough or near-equatorial trough. Two — Tropical Depression 31W and Yuri (36W) — formed in direct association with cold-core

Table 3-1 WESTERN NORTH PACIFIC SIGNIFICANT TROPICAL CYCLONES FOR 1994

TROPICAL CYCLONE		PERIOD OF WARNING	NUMBER OF WARNINGS ISSUED	ESTIMATED MAXIMUM SURFACE WINDS KT (M/SEC)	ESTIMATED MSLP (MB)
01W	TD	04 JAN - 06 JAN	5	25 (13)	1002
02W	TY OWEN	01 MAR - 08 MAR	32	75 (39)	968
03W	TY PAGE	11 MAY - 17 MAY	25	90 (46)	954
04W	TD	24 MAY - 26 MAY	11	30 (15)	1000
05W	TS RUSS	04 JUN - 09 JUN	20	55 (28)	984
06W	TS SHARON	21-22 JUN/22-25 JUN	14	45 (23)	991
07W	TD	03 JUL - 04 JUL	7	30 (15)	1000
08W	TY TIM	07 JUL - 11 JUL	18	125 (64)	916
09W	TS VANESSA	09 JUL - 11 JUL	10	45 (23)	991
10W	STY WALT	14 JUL - 26 JUL	50	130 (67)	910
11W	TS YUNYA	18 JUL - 21 JUL	14	45 (23)	991
12W	TY ZEKE	18 JUL - 24 JUL	26	65 (33)	976
13W	TD	25 JUL - 26 JUL	4	25 (13)	1002
14W	TS BRENDAN	29 JUL - 01 AUG	15	50 (26)	987
15W	TS AMY	29 JUL - 31 JUL	8	40 (21)	994
16W	TS CAITLIN	02 AUG - 04 AUG	9	60 (31)	980
17W	STY DOUG	02 AUG - 13 AUG	42	140 (72)	898
18W	TY ELLIE	08 AUG - 16 AUG	33	80 (41)	963
08E	TS LI	13 AUG - 18 AUG	21	55 (28)	984
19W	STY FRED	14 AUG - 22 AUG	33	130 (67)	910
20W	TY GLADYS	22 AUG - 02 SEP	45	105 (54)	938
21W	TS HARRY	25 AUG - 29 AUG	15	60 (31)	980
22W	TY IVY	28 AUG - 03 SEP	26	75 (39)	968
10E	TY JOHN	28 AUG - 08 SEP	45	105 (54)	938
23W	TS JOEL	04 SEP - 07 SEP	15	45 (23)	991
24W	TY KINNA	05 SEP - 11 SEP	27	85 (44)	958
25W	TS LUKE	09 SEP - 14 SEP	22	50 (26)	987
26W	STY MELISSA	11 SEP - 18 SEP	29	135 (69)	904
27W	TS NAT	15 SEP - 22 SEP	29	45 (23)	991
28W	STY ORCHID	18 SEP - 30 SEP	48	135 (69)	904
29W	TY PAT	21 SEP - 26 SEP	18	95 (49)	949
30W	TS RUTH	24 SEP - 28 SEP	18	45 (23)	991
31W	TD	29 SEP - 03 OCT	11	30 (15)	1000
32W	TY SETH	02 OCT - 11 OCT	37	120 (62)	922
33W	TY VERNE	15 OCT - 31 OCT	66	115 (59)	927
34W	TY TERESA	17 OCT - 26 OCT	37	80 (41)	963
35W	TY WILDA	20 OCT - 01 NOV	49	125 (64)	916
36W	TS YURI	23 OCT - 25 OCT	9	35 (18)	997
37W	STY ZELDA	28 OCT - 08 NOV	44	135 (69)	904
38W	TY AXEL	13-14 DEC/15-25 DEC	42	115 (59)	927
39W	TS BOBBIE	17 DEC - 25 DEC	29	50 (26)	987

TOTAL: 1058

Table 3-2 **DISTRIBUTION OF WESTERN NORTH PACIFIC TROPICAL CYCLONES**
FOR 1959 - 1994

<u>YEAR</u>	<u>JAN</u>	<u>FEB</u>	<u>MAR</u>	<u>APR</u>	<u>MAY</u>	<u>JUN</u>	<u>JUL</u>	<u>AUG</u>	<u>SEP</u>	<u>OCT</u>	<u>NOV</u>	<u>DEC</u>	<u>TOTALS</u>
1959	0	1	1	1	0	1	3	8	9	3	2	2	31
	000	010	010	100	000	001	111	512	423	210	200	200	17 7 7
1960	1	0	1	1	1	3	3	9	5	4	1	1	30
	001	000	001	100	010	210	210	810	041	400	100	100	19 8 3
1961	1	1	1	1	4	6	5	7	6	7	2	1	42
	010	010	100	010	211	114	320	313	510	322	101	100	20 11 11
1962	0	1	0	1	3	0	8	8	7	5	4	2	39
	000	010	000	100	201	000	512	701	313	311	301	020	24 6 9
1963	0	0	1	1	0	4	5	4	4	6	0	3	28
	000	000	001	100	000	310	311	301	220	510	000	210	19 6 3
1964	0	0	0	0	3	2	8	8	8	7	6	2	44
	000	000	000	000	201	200	611	350	521	331	420	101	26 13 5
1965	2	2	1	1	2	4	6	7	9	3	2	1	40
	110	020	010	100	101	310	411	322	531	201	110	010	21 13 6
1966	0	0	0	1	2	1	4	9	10	4	5	2	38
	000	000	000	100	200	100	310	531	532	112	122	101	20 10 8
1967	1	0	2	1	1	1	8	10	8	4	4	1	41
	010	000	110	100	010	100	332	343	530	211	400	010	20 15 6
1968	0	1	0	1	0	4	3	8	4	6	4	0	31
	000	001	000	100	000	202	120	341	400	510	400	000	20 7 4
1969	1	0	1	1	0	0	3	3	6	5	2	1	23
	100	000	010	100	000	000	210	210	204	410	110	010	13 6 4
1970	0	1	0	0	0	2	3	7	4	6	4	0	27
	000	100	000	000	000	110	021	421	220	321	130	000	12 12 3
1971	1	0	1	2	5	2	8	5	7	4	2	0	37
	010	000	010	200	230	200	620	311	511	310	110	000	24 11 2
1972	1	0	1	0	0	4	5	5	6	5	2	3	32
	100	000	001	000	000	220	410	320	411	410	200	210	22 8 2
1973	0	0	0	0	0	0	7	6	3	4	3	0	23
	000	000	000	000	000	000	430	231	201	400	030	000	12 9 2
1974	1	0	1	1	1	4	5	7	5	4	4	2	35
	010	000	010	010	100	121	230	232	320	400	220	020	15 17 3
1975	1	0	0	1	0	0	1	6	5	6	3	2	25
	100	000	000	001	000	000	010	411	410	321	210	002	14 6 5
1976	1	1	0	2	2	2	4	4	5	0	2	2	25
	100	010	000	110	200	200	220	130	410	000	110	020	14 11 0
1977	0	0	1	0	1	1	4	2	5	4	2	1	21
	000	000	010	000	001	010	301	020	230	310	200	100	11 8 2
1978	1	0	0	1	0	3	4	8	4	7	4	0	32
	010	000	000	100	000	030	310	341	310	412	121	000	15 13 4
1979	1	0	1	1	2	0	5	4	6	3	2	3	28
	100	000	100	100	011	000	221	202	330	210	110	111	14 9 5
1980	0	0	1	1	4	1	5	3	7	4	1	1	28
	000	000	001	010	220	010	311	201	511	220	100	010	15 9 4
1981	0	0	1	1	1	2	5	8	4	2	3	2	29
	000	000	100	010	010	200	230	251	400	110	210	200	16 12 1
1982	0	0	3	0	1	3	4	5	6	4	1	1	28
	000	000	210	000	100	120	220	500	321	301	100	100	19 7 2
1983	0	0	0	0	0	1	3	6	3	5	5	2	25
	000	000	000	000	000	010	300	231	111	320	320	020	12 11 2
1984	0	0	0	0	0	2	5	7	4	8	3	1	30
	000	000	000	000	000	020	410	232	130	521	300	100	16 11 3
1985	2	0	0	0	1	3	1	7	5	5	1	2	27
	020	000	000	000	100	201	100	520	320	410	010	110	17 9 1
1986	0	1	0	1	2	2	2	5	2	5	4	3	27
	000	100	000	100	110	110	200	410	200	320	220	210	19 8 0
1987	1	0	0	1	0	2	4	4	7	2	3	1	25
	100	000	000	010	000	110	400	310	511	200	120	100	18 6 1

TABLE CONTINUED ON TOP OF NEXT PAGE

CONTINUED FROM PREVIOUS PAGE													
YEAR	JAN	FEB	MAR	APR	MAY	JUN	JUL	AUG	SEP	OCT	NOV	DEC	TOTALS
1988	1	0	0	0	1	3	2	5	8	4	2	1	27
	100	000	000	000	100	111	110	230	260	400	200	010	14 12 1
1989	1	0	0	1	2	2	6	8	4	6	3	2	35
	010	000	000	100	200	110	231	332	220	600	300	101	21 10 4
1990	1	0	0	1	2	4	4	5	5	5	4	1	31
	100	000	000	010	110	211	220	500	410	230	310	100	21 9 1
1991	0	0	2	1	1	1	4	8	6	3	6	0	32
	000	000	110	010	100	100	400	332	420	300	330	000	20 10 2
1992	1	1	0	0	0	3	4	8	5	6	5	0	33
	100	010	000	000	000	210	220	440	410	510	311	000	21 11 1
1993	0	0	2	2	1	2	5	8	5	6	4	3	38
	000	000	011	002	010	101	320	611	410	321	112	300	21 9 8
1994	1	0	1	0	2	2	9	9	8	7	0	2	41
	001	000	100	000	101	020	342	630	440	511	000	110	21 15 5
(1959-1994)													
MEAN	0.6	0.3	0.6	0.8	1.3	2.1	4.6	6.4	5.7	4.7	2.9	1.4	31.4
CASES	21	10	23	27	45	77	165	231	205	169	105	51	1129

The criteria used in Table 3-2 are as follows:

- 1) If a tropical cyclone was first warned on during the last two days of a particular month and continued into the next month for longer than two days, then that system was attributed to the second month.
- 2) If a tropical cyclone was warned on prior to the last two days of a month, it was attributed to the first month, regardless of how long the system lasted.
- 3) If a tropical cyclone began on the last day of the month and ended on the first day of the next month, that system was attributed to the first month. However, if a tropical cyclone began on the last day of the month and continued into the next month for only two days, then it was attributed to the second month.

TABLE 3-2 LEGEND

Total for the month/year → 41

Typhoons → 21 15 5

Tropical Storms →

Tropical Depressions →

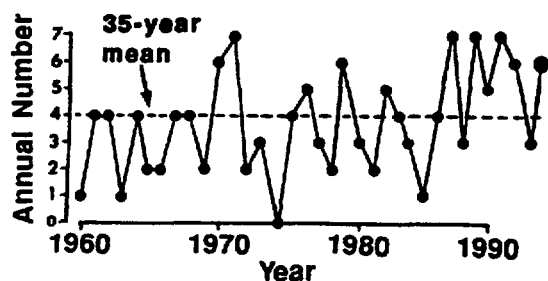


Figure 3-1 Number of western North Pacific super typhoons (1960-1994).

cyclonic vortices in the tropical upper tropospheric trough (TUTT). Ivy (22W) and Ellie (25W) formed in the subtropics from disturbances at the southern end of midlatitude troughs. Two of the year's named TCs — Li (06E) and John (08E) — formed in the monsoon trough of the eastern North Pacific and survived the long westward passage across the central Pacific to the western North Pacific.

Some of the large-scale atmospheric and

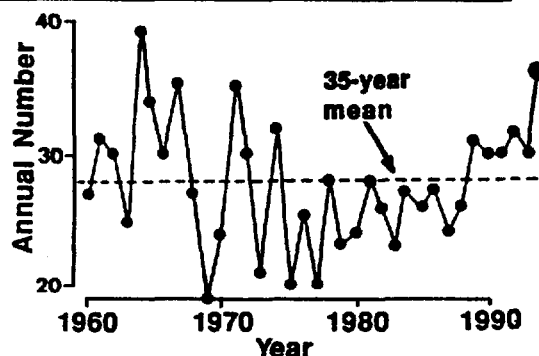


Figure 3-2 Tropical cyclones of tropical storm or greater intensity in the western North Pacific (1960-1994).

oceanic climatic parameters continued to be indicative of El Niño conditions during most of 1994: the sea surface temperature (SST) over much of the eastern equatorial Pacific — especially near the international date line — was consistently warmer than normal, and the Southern Oscillation Index (SOI) (Climate Analysis Center, 1994) was strongly negative for most of the year (Figure 3-3). From September through the remainder of the year,

low-level westerly winds penetrated far to the east of normal (Figure 3-4). By the end of December, monsoonal low-level westerly wind flow was straddling the equator and had penetrated well-beyond the international date line to near 160°W. Based on the Pacific basin SST patterns and the distribution of wind and surface pressure in the tropics of the Pacific basin, the U.S. Climate Analysis Center (along with other international meteorological centers) officially declared that an El Niño event was under way, and predicted that it would reach its mature phase in early 1995. With the anomalous eastward push of monsoonal westerlies, several of the year's tropical cyclones formed east of 160°E and south of 20°N (Figure 3-5a). The number of tropical cyclones that form in this region is highly dependent upon El Niño, with more during El Niño years and less in other years. Unlike most El Niño years, however, there were several tropical cyclones that formed east of 160°E and north of 20°N. These tropical cyclones formed in association with TUTT cells, mid-latitude troughs, or were at the eastern end of a reverse-oriented monsoon trough. Despite a high number of tropical cyclones which formed well to the east of normal, there were a significant number of tropical cyclones that formed in the western part of the basin (including four that formed in the South China Sea); hence the 1994 annual mean genesis location was close to normal (Figure 3-5b).

The monsoon circulation of the western North Pacific (WNP) was very active during 1994 and was highlighted by three major episodes — one each during July, September and October— of reverse orientation of the trough axis. A reverse-oriented monsoon trough in the WNP is an episodic event that occurs on average about once each typhoon season sometime between mid-July and mid-October. During some years it is not seen; but during other years (such as 1989 and 1994) the monsoon trough repeatedly organizes in a reverse orientation. The distinguishing charac-

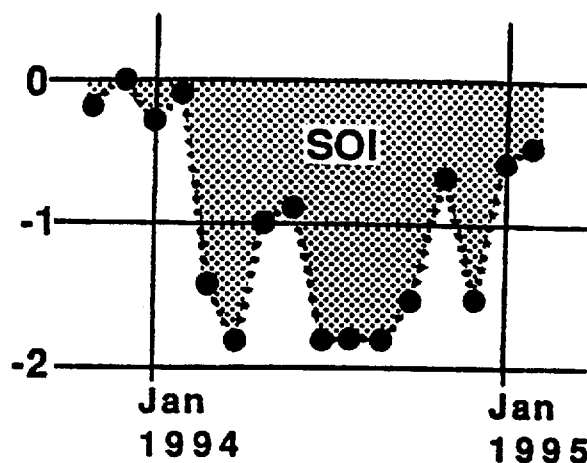


Figure 3-3 The Southern Oscillation Index (SOI) (shaded) for 1994 (adapted from Climate Analysis Center, 1994).

teristics of a reverse-oriented monsoon trough are a SW-NE (i.e., reverse) orientation of the trough axis with respect to the normal NW-SE orientation of the trough axis, and the penetration of the trough axis into subtropical areas normally the province of easterly flow (Figure 3-6a,b). When the monsoon trough axis acquires a reverse orientation, tropical cyclones along it tend to move on north-oriented tracks (JMA 1976) and may undergo binary interactions with other tropical cyclones or monsoon depressions located along the trough axis (Lander 1995).

The first occurrence during 1994 of reverse orientation of the monsoon trough in the WNP was during July. By mid-July, an active reverse-oriented monsoon trough stretched across the tropics of the WNP from the South China Sea northeastward into sub-tropical latitudes near the international date line. Three tropical cyclones formed in this trough — Walt (10W), Yunya (11W), and Zeke (12W). Each of these tropical cyclones moved on north-oriented tracks, and each exhibited unusual eastward motion at low latitude.

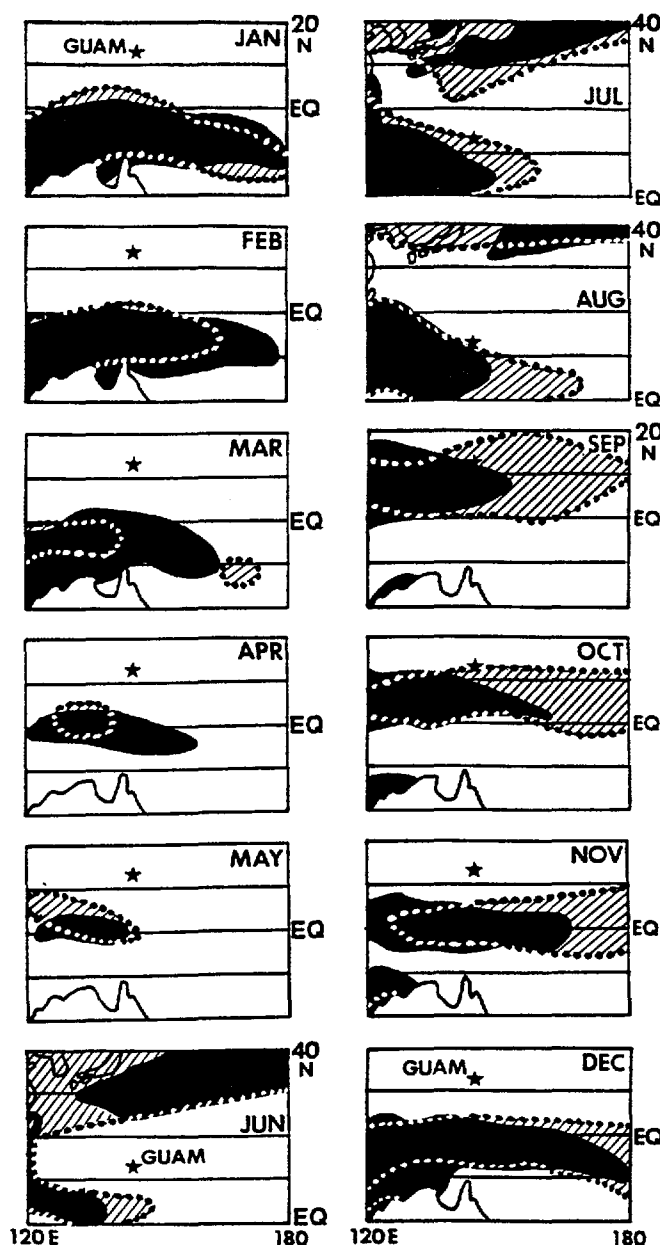


Figure 3-4 Comparison between climatological (black) and analyzed (hatched) mean monthly winds with a westerly component for the western North Pacific in 1994. For June, July, and August the area of coverage is shifted northward to include the subtropics of the North Pacific. For reference, the star indicates the location of Guam. The outline of Australia appears in the lower left of each panel except for June, July, and August where the Korean Peninsula and Japan appear in the upper left. The climatology is adapted from Sadler *et al.*, 1987. The 1994 monthly mean winds were adapted from the Climate Analysis Center, 1994.

The second occurrence during 1994 of reverse orientation of the monsoon trough in the WNP was during September. For a full two weeks in the middle of September, an active reverse-oriented monsoon trough dominated the large-scale circulation of the WNP. Five tropical cyclones formed in this trough — Melissa (26W), Nat (27W), Orchid (28W), Pat (29W), and Ruth (30W). All of them moved on north-oriented tracks. Nat, Orchid, and Ruth exhibited unusual eastward motion at low-latitude. Pat and Ruth underwent a binary interaction that resulted in the merger of the two systems into one.

The third occurrence during 1994 of reverse orientation of the monsoon trough in the WNP occurred in October. By mid-October, the monsoon trough was oriented zonally at low latitude and in the eastern portion of the basin. Three tropical cyclones — Teresa (34W), Verne (33W), and Wilda (35W) — formed in succession in this monsoon trough and initially moved westward. By the end of October, Teresa, Verne and Wilda had moved relative to each other so as to bring the axis of the monsoon trough into a reverse orientation. As soon as this occurred, the westward motion of Verne ceased, and Wilda began to move on a north-oriented “S-shaped” track.

The tracks of the TCs which formed in the WNP during 1994 indicates a high number of north-oriented tracks. Of the 39 TCs which formed in the WNP during 1994: fifteen (38%) were straight moving, only six (15%) were recurvers, thirteen (33%) moved on north-oriented tracks, and five were designated as “other” (Table 3-3). Of the 13 tropical cyclones which moved on north-oriented tracks during 1994, five underwent “S” motion. Four of the five “other” storms remained in or near the South China Sea. Ten of the thirteen tropical cyclones during 1994 which moved on north-oriented tracks occurred in association with the three episodes of reverse orientation of the monsoon trough.

(a)

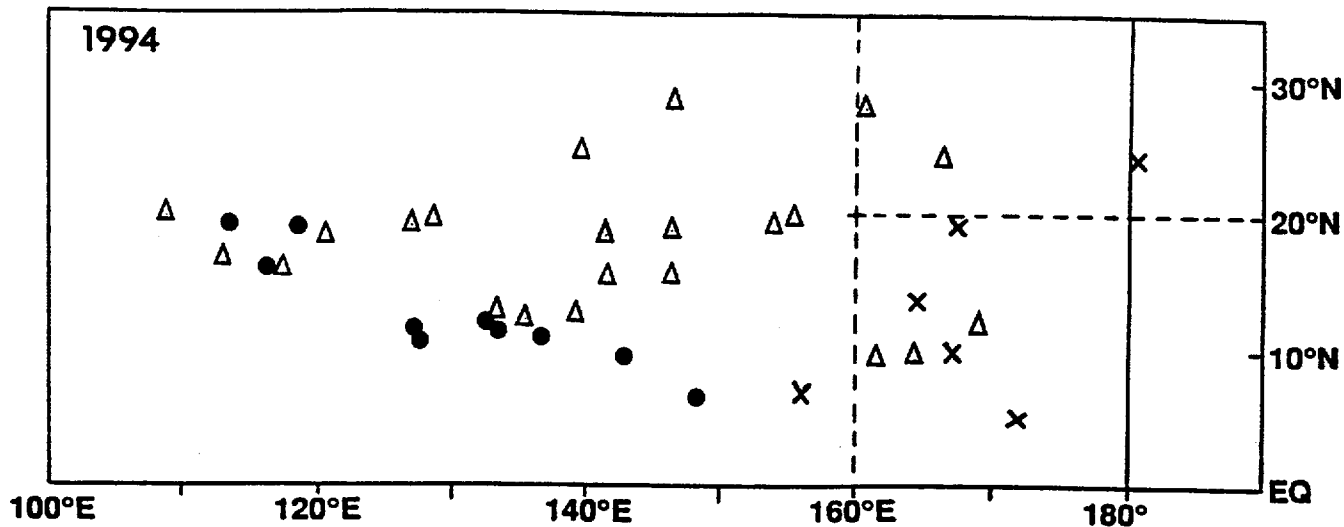


Figure 3-5a Point of formation of significant tropical cyclones in 1994 as indicated by the initial intensity of 25 kt (13 m/sec) on the best track. The symbols indicate: solid dots = 01 January to 15 July; open triangles = 16 July to 15 October; and, X = 16 October to 31 December.

(b)

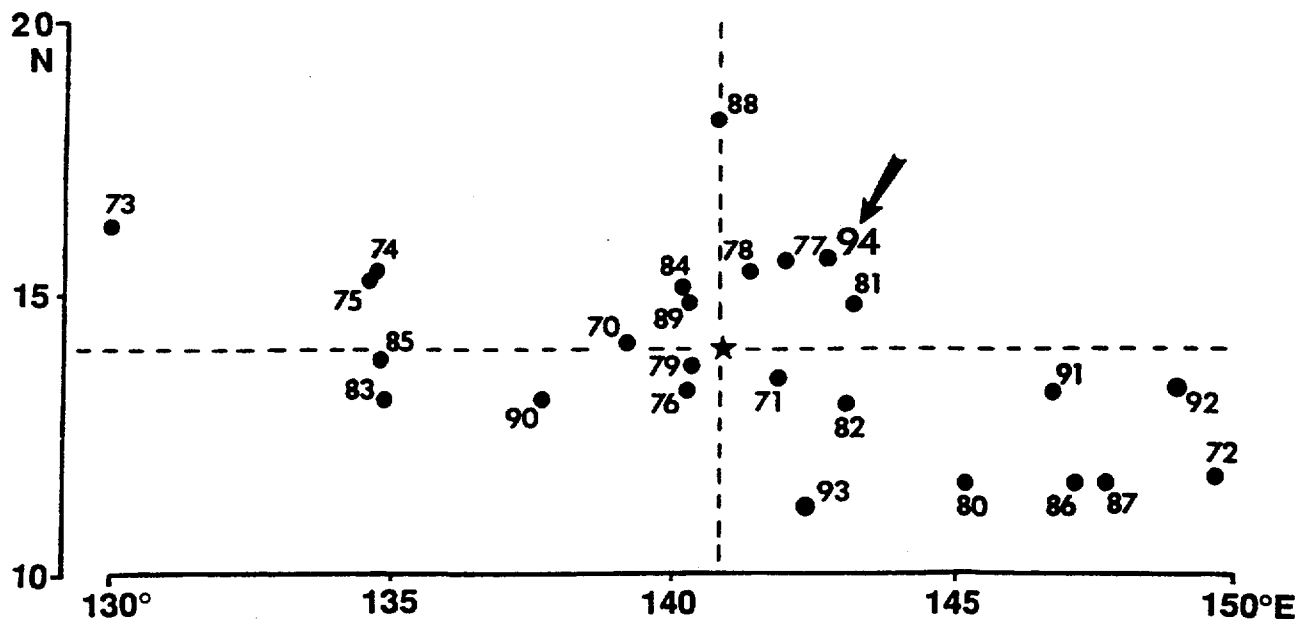


Figure 3-5b Mean annual genesis locations for the period 1970-1994. 1994's location is indicated by the arrow. The star lies at the intersection of the 25-year average latitude and longitude of genesis. For statistical purposes, genesis is defined as the first 25 kt (13 m/sec) intensity on the best track.

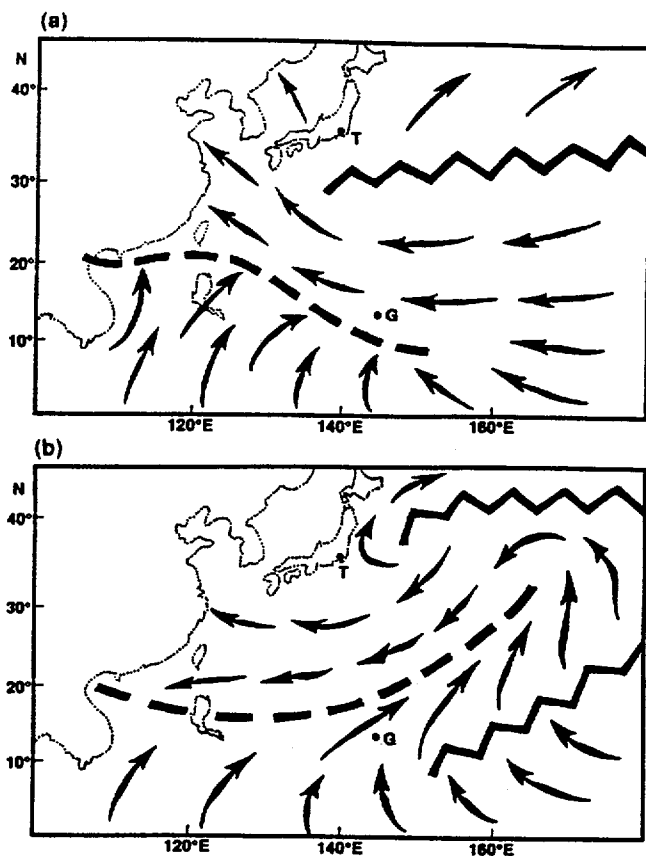


Figure 3-6 The low-level circulation during the summer in the tropics of the western North Pacific: (a) The long-term average; and (b) a schematic example of the low-level circulation associated with a reverse-oriented monsoon trough. Bold zig-zag lines indicate ridge axes, and bold dashed line indicated the axis of the monsoon trough. Arrows indicated wind direction. The locations of Guam (G) and Tokyo (T) are indicated.

In summary, an illustration of all the tropical cyclone activity in the WNP and North Indian Oceans is provided in Figure 3-7. Table 3-4 includes: a climatology of typhoons, and tropical storms and typhoons for the WNP for the period 1945-1959 and 1960-1994; and a summary of warning days. Table 3-5 is a summary of the TCFA's for the WNP for 1976-1994. Composite best tracks for the WNP Ocean tropical cyclones are provided for the periods: 01 January to 28 July (Figure 3-8), 16 July to 02 September (Figure 3-9), 20 August to 29 September (Figure 3-10), and 28 September to 26 December (Figure 3-11).

3.1.1 MONTHLY ACTIVITY SUMMARY

JANUARY

Tropical cyclone activity got off to an early start during 1994. **Tropical Depression 01W** occurred in January in the near-equatorial trough. January TCs are most properly considered to be late-season storms, born in atmospheric conditions that evolved during November and December of the previous calendar year.

FEBRUARY

The month with the lowest average number of tropical cyclones in the western North Pacific is February. In keeping with climatology, there were no significant tropical cyclones in the western North Pacific basin during February 1994.

MARCH

There were no significant tropical cyclones in the western North Pacific basin during March 1994, however, the tropical disturbance which became **Typhoon Owen (02W)** was first detected in late March in a near-equatorial trough in the Caroline islands.

APRIL

One tropical cyclone — **Owen (02W)** — was active during April. The tropical disturbance from which it developed formed in the Caroline islands at the end of March. Tracking westward, Owen reached peak intensity of 75 kt (39 m/sec) one day before it crossed several islands of the Philippine archipelago where three people were killed and four were reported missing. Emerging into the South China Sea, it turned northward, steadily weakened, and dissipated over water northwest of Luzon. The rest of April was quiet.

MAY

During early May, the Mei-yu front became established from Hong Kong to Japan. In the

deeper tropics, a near-equatorial trough became established across the western North Pacific between 5°N and 10°N. On 08 May, a cloud cluster in the near-equatorial trough began to organize and drift toward the northwest. Four days later, this disturbance became **Page (03W)** at a location about 300 nm (550 km) west of Guam. It continued to move northwestward and became a typhoon on 15 May. Shortly thereafter, it recurved. Page reached its peak intensity of 90 kt (46 m/sec) 30 hours after the point of recurvature. On 18 May, Page accelerated into the midlatitudes and became extratropical. The tropics then became quiet until 23 May when **Tropical Depression 04W** developed east of the Philippines. This tropical depression never became a tropical storm. It crossed the South China Sea and dissipated over Vietnam. The remainder of May was inactive as the amount of deep convection in the tropics was suppressed.

JUNE

During early June, tropical cyclone activity was focused in the South China Sea. On 04 June, **Russ (05W)** developed and moved northward toward Hong Kong. When about 100 nm (185 km) south of Hong Kong, Russ turned toward the west and went ashore in southern China just east of the Luichow peninsula on 09 June. Russ was the first of a series of tropical cyclones that hit southern China and contributed to destructive flooding. During the middle of June, deep convection increased across the western North Pacific south of 10°N to the international date line. Despite the increase of deep convection, no tropical cyclones formed until 22 June when a tropical depression formed east of the Philippines. After crossing the Philippines, this tropical depression became **Sharon (06W)** on 23 June. Sharon made landfall in central Vietnam on 28 June.

JULY

One of the busiest Julys on record, a total of nine tropical cyclones occurred during the month. Tropical cyclone activity for the month began in the South China Sea with the development of **Tropical Depression 07W** south of Hong Kong on 03 July. This short-lived system moved westward and made landfall in southern China, just northeast of the Luichow Peninsula on 04 July. During the first week of July, a very intense TUTT established from the east coast of China to the international date line. South of this TUTT, large-scale deep convection increased. On 07 July, the tropical disturbance that became **Tim (08W)** appeared in the Philippine Sea. While on a northwestward track, this system rapidly reached a peak intensity of 125 kt (64 m/sec), and on 10 July, it made landfall on the east coast of Taiwan. As Tim neared the Taiwan coast, **Vanessa (09W)** formed in the South China Sea. Vanessa was short-lived, moved northeastward, and was absorbed by the circulation of the larger Tim.

On 14 July, a reverse oriented monsoon trough developed east of the Philippines. The first super typhoon of the season, **Walt (10W)** formed along the axis of this trough. Walt underwent unusual northeastward motion along the trough axis, and reached its 130 kt (67 m/sec) peak intensity on 19 July before turning back to the northwest. As Walt weakened, it slowly tracked to the west and dissipated during the early morning hours of 27 July near western Japan after a total of 50 warnings.

Along with Walt (10W), two other tropical cyclones formed along the axis of the reverse oriented monsoon trough — **Yunya (11W)**, west of Walt; and **Zeke (12W)**, northeast of Walt. Yunya developed in the South China Sea west of Luzon. It underwent unusual eastward motion and crossed Luzon from west to east on 19 July with a landfall intensity of 45 kt (23 m/sec). Heading east, Yunya dissipated over water in the Philippine Sea on 21 July. Meanwhile, Zeke (12W) developed northeast of

Walt and moved on an unusual "S-shaped" track. Zeke reached its maximum intensity of 65 kt (33 m/sec) on 22 July as it made a sharp turn toward the north. It later turned northeastward and became extratropical poleward of 40°N on 24 July.

On 24 July, the large-scale low-level circulation of the western North Pacific became organized as a monsoon gyre. **Tropical Depression 13W** developed on 25 July in a monsoon surge along the southeastern periphery of the gyre. Tropical depression 13W dissipated on 26 July. Its remnants accelerated to the north within a band of large-scale deep convection that formed a fish-hook pattern on the eastern side of the gyre.

On 28 July, the gyre that had dominated the flow gave way to a more typical monsoon cloud band stretching from the South China Sea eastward into Micronesia. On 29 July, a tropical disturbance that formed in this monsoon trough became **Brendan (14W)**. It moved rapidly to the north and was located over Korea by the end of the month. Two other tropical cyclones also formed in the monsoon trough during the last week of July — **Amy (15W)** and **Caitlin (16W)**. Amy formed in the South China Sea near Hainan Island on 28 July, and made land-fall near Haiphong in northern Vietnam on 31 July. The tropical disturbance that became Caitlin formed near Guam on 29 July, and moved west-northwestward. It did not become a tropical storm until early August.

AUGUST

August 1994 was a very active month. There were a total of nine significant tropical cyclones: eight that formed during the month and one that was still active from July. On the first day of the month, Brendan, which developed in July, became extratropical in the Sea of Japan. On 02 August, Caitlin developed northeast of the Philippines and moved northwestward over Taiwan and into southeastern China. A few days later, the disturbance that became

Doug (17W) developed east of the Philippines. It moved northwestward passing just off the northeastern tip of Taiwan. Doug then moved northward toward Korea. Close to the resort island of Cheju on 10 August, it created poor weather and gusty winds which contributed to the crash of a Korean Air Lines A-300 jet trying to land at Cheju International Airport.

On 08 August, the tropical disturbance that became **Ellie (18W)** developed in the subtropics (i.e., north of 25°N) at the base of a midlatitude trough. Ellie passed southwest of Kyushu on 13 August where wind gusts up to 87 kt (45 m/sec) were recorded. It later recurved in the Yellow Sea and dissipated over land in northeastern China. On 13 August Hurricane **Li (06E)** approached 180°E from the central Pacific, weakened as it crossed into JTWC's area of responsibility, and dissipated near Wake Island on 16 August. On 14 August, the tropical disturbance that became **Fred (19W)** became a tropical depression near 19°N ; 139°E. Fred tracked just north of Taiwan and went ashore south of Shanghai on 22 August as one of the most destructive typhoons to hit that region in decades.

On 20 August, a midlatitude trough in combination with the tropical upper tropospheric trough (TUTT) produced several areas of deep convection in the subtropics (i.e., approximately 25°N) from 160°E to the international date line. Two typhoons — **Gladys (20W)** and **Ivy (22W)** — formed in this area. Gladys was a very small tropical cyclone that had its first warning on 22 August as it moved westward. The first warning on Ivy was issued on 28 August as it moved toward the northwest.

On 25 August, a tropical disturbance in the monsoon trough became a tropical depression east of the Philippines on 25 August. This tropical depression moved across Luzon and became **Harry (21W)** on 26 August. Harry passed south of Hong Kong, crossed Hainan Island, and went ashore near Haiphong, Vietnam. It dissipated over land on 29 August.

On 28 August, **John (10E)** moved from the central Pacific across 180°E, forming an east-west chain of tropical cyclones with Gladys and Ivy. By the end of August, Gladys was approaching northern Taiwan as a typhoon, Ivy was heading northwestward near 30°N ; 159°E, and John was weakening near 29°N ; 172°E.

SEPTEMBER

September was even more active than August, with a total of 12 tropical cyclones: nine that formed during the month and three that were still active from August. On the first day of the month, Gladys, which developed in August, crossed Taiwan, and dissipated over China on 02 September. Ivy, which also developed during August, recurved far to the east of Japan and became extratropical on 03 September. John (10E), the last of the August tropical cyclones overlapping into September, weakened during the first few days of September, but on 06 September, it began to reintensify. John recurved, and on 08 September, it moved back across 180°E into the central North Pacific as a Hurricane.

During the first week of September, after Gladys (20W) moved into China, monsoon southwesterlies began to strengthen over the South China Sea and across low latitudes of the western North Pacific. Joel (23W), formed in the South China Sea along the axis of the monsoon trough, moved northwestward across Hainan Island and then went ashore in Vietnam near Haiphong on 07 September. On 05 September, a large monsoon depression formed west of the Mariana island chain. A separate tropical disturbance which formed on the northeastern side of this monsoon depression broke free of it, and moved northward. This tropical disturbance became **Kinna (24W)**. Kinna recurved south of Tokyo, accelerated to the northeast, and became extratropical on 11 September. On 09 September, a tropical disturbance developed in the Philippine Sea, moved northwestward, and passed across northern

Luzon. Once it entered the South China Sea, it intensified and became **Luke (25W)**. Luke moved westward and passed over Hainan Island, and then moved ashore in northern Vietnam close to where Harry (21W) and Joel (23W) had made landfall earlier.

On 10 September a monsoon depression (which later became **Melissa (26W)**) formed in the Marshall Islands. The large circulation of Melissa at one point covered a substantial portion of the western North Pacific basin from 180°E to the Philippines. Melissa moved on a north-oriented "S-shaped" track. It recurved southeast of Hokkaido, Japan, on 19 September and became extratropical.

By mid-September, a reverse-oriented monsoon trough stretched from the South China Sea, east-northeastwards into the cloud bands south of Melissa's large circulation. **Nat (27W)** formed in the Philippine Sea along the axis of this monsoon trough and moved eastward. Nat followed an "S-shaped" track: initially moving eastward, it turned northward along 150°E, and recurved near 30°N. Nat dissipated over water on 22 September. On 18 September, another tropical disturbance formed in the Philippine Sea along the monsoon trough axis in approximately the same location where Nat (27W) originated. This tropical disturbance became **Orchid (28W)**. Like Nat, Orchid initially moved eastward followed by a turn to the north. On 25 September, Orchid became the fourth super typhoon of 1994. It accelerated toward the north-northeast on 28 September and made landfall on the Japanese main island of Shikoku on 29 September.

As Orchid intensified, two more tropical disturbances formed to its east along the monsoon trough axis — **Pat (29W)** and **Ruth (30W)**. Pat (29W) and Ruth (30W) underwent a binary interaction. During the night of 26 September, Pat and Ruth merged to become one tropical cyclone. The merged Pat and Ruth recurved and dissipated over open water on 28 September. On 29 September, **Tropical**

Depression 31W developed near 22°N ; 150°E in association with a TUTT cell. It dissipated over water on 03 October.

OCTOBER

The fourth consecutive month of above normal tropical cyclone activity in the western North Pacific basin had five typhoons, one of them a super typhoon, and two tropical storms. The tropical cyclones of October were notable for their longevity: three of the seven longest-lived tropical cyclones of 1994 occurred. Verne (33W), for example, persisted for more than half the month, and required 66 warnings.

On the first day of the month, the tropical disturbance that became **Seth (32W)** formed in the Marshall Islands. This disturbance moved toward the west-northwest, intensified, and passed south of Guam as a tropical storm on 05 October. Seth reached a peak intensity of 120 kt (62 m/sec) while southeast of Taiwan on 07 October. It later skirted the northeastern tip of Taiwan, recurved along the China coast south of Shanghai, and went ashore in Korea where wind gusts to near 70 kt (36 m/sec) and rainfall in excess of 300 mm (11.8 inches) were experienced. Seth became extratropical in the Sea of Japan on 11 October.

The three days 12 through 14 October were the only days during the month without a tropical cyclone active in the western North Pacific basin. During the period 15 to 20 October, three tropical cyclones — **Teresa (34W)**, **Verne (33W)**, and **Wilda (35W)** — formed in a monsoon trough which stretched east-west across Micronesia. On 21 October, the westernmost of the three, Teresa, crossed the Philippine Islands very close to Manila. Loss of life was reported. On 19 October, the middle tropical cyclone, Verne (33W), passed very close to the island of Rota in the Mariana Island chain. Verne later stalled in the Philippine Sea west of Guam before recurving and moving northeastward, well east of Japan. The easternmost tropical cyclone of these three, Wilda (35W), formed

north of the Marshall Island group on 19 October. It moved westward, and then stalled for 24-hours northeast of Saipan where high winds downed trees and power lines, and pulled tin roofs from houses. Eleven people were injured in typhoon-related accidents. Wilda then moved turned north-northeastward and moved on an unusual “S-shaped” track. It was accelerating into the midlatitudes on the last day of the month.

Toward the end of the month, a tropical disturbance developed east of the international date line at relatively high latitude (25°N), in direct association with a TUTT cell. This disturbance moved rapidly westward, crossed the international date line, and became **Yuri (36W)** on 24 October. Yuri slowed, turned north, and dissipated over water on 27 October.

And finally, **Zelda (37W)** formed and spent the majority of its life in November. As Verne (33W) and Wilda (35W) were undergoing extratropical transition on the last day of October, Zelda (37W) was intensifying near 10°N ; 150°E.

NOVEMBER

Zelda (37W) was located southeast of Guam and intensifying as the month of November began. It became a typhoon on 02 November, moved west-northwestward and passed directly over Anatahan (a small island of the Northern Marianas located about 70 nm (130 km) north of Saipan). The large eye of Zelda passed over Anatahan where the homes and crops of the 39 residents were devastated. On 05 November, Zelda reached peak intensity of 135 kt (69 m/sec), making it the sixth and final super typhoon of 1994. Zelda recurved and dissipated over water south of Japan on 08 November.

Despite the presence of a near-equatorial trough, and westerly low-level winds extending to the international date line, deep convection was largely absent over most of the area, and no significant tropical cyclones formed in the western North Pacific basin during November.

DECEMBER

The first half of December was very quiet, continuing the break in tropical cyclone activity that began in early November. Amounts of deep convection began to increase in the Marshall Islands during mid-December in association with a twin-trough monsoon flow pattern. Two tropical cyclones — **Axel (38W)** and **Bobbie (39W)** — began as tropical disturbances that formed in the Marshall Islands in the near-equatorial trough of the northern hemisphere. On 16 December, Axel reached minimal tropical storm intensity while passing well south of Guam. Moving steadily westward along about 10°N, Axel crossed through the Philippine Archipelago on 21 December where at least 12 people died.

While Axel was intensifying in the Philippine Sea on 17 December, the final tropical cyclone of 1994, Bobbie (39W) was forming in the southern Marshall Islands. Bobbie moved toward the west-northwest, and reached peak intensity of 50 kt (26 m/sec) on 22 December. On 23 December, it passed north of Saipan with winds of 45 kt (23 m/sec). Bobbie had no significant impact on Saipan or on other islands of the Northern Marianas. On Christmas Day, Bobbie dissipated as a significant tropical cyclone, closing out the 1994 tropical cyclone season. The remainder of December was quiet, as deep convection and tropical cyclone activity shifted to the southern hemisphere.

3.1.2 IMPACTS OF THE TROPICAL CYCLONES OF 1994

Twenty-three of the 41 significant tropical cyclones in the western North Pacific basin during 1994 made landfall in Asia. The Philippine islands were especially hard hit with eight significant landfalling tropical cyclones. Other countries experiencing significant impacts from landfalling tropical cyclones were Taiwan (three major landfalling typhoons and two close passes), Korea (one major landfalling typhoon —

Seth (32W) — one tropical storm, and a damaging close pass by Doug (17W)), China (eleven significant tropical cyclones made landfall somewhere along its extensive coastline), Japan (only one major typhoon — Orchid (28W) — and one tropical storm), the Ryukyu Islands (three major typhoons passed through the southern end of this island chain), Vietnam (four significant landfalling tropical cyclones), and the islands of Micronesia (Saipan and Anatahan of the Northern Mariana island group were severely impacted by Zelda (37W)). The greatest loss of life occurred in southern China where the landfall of three tropical cyclones — Russ (05W), Sharon (06W), and Tropical Depression 07W contributed to widespread flooding that left more than 1,400 people dead. The damage, which included the destruction of nearly one million houses in southern China, was estimated in excess of US\$6 billion. Loss of life also occurred in the Philippines and Taiwan. Reports of the loss of life due to the impact of tropical cyclones in any of the other countries were not received. The greatest loss of life at sea occurred when a Maltese oil tanker, the *Thanassis A*, sank in the South China Sea in heavy seas associated with Teresa (34W) and the northeast monsoon. Seventeen people were reported to be dead or missing and nineteen other crew members were rescued. The JTWC received no additional reports indicating loss of life at sea.

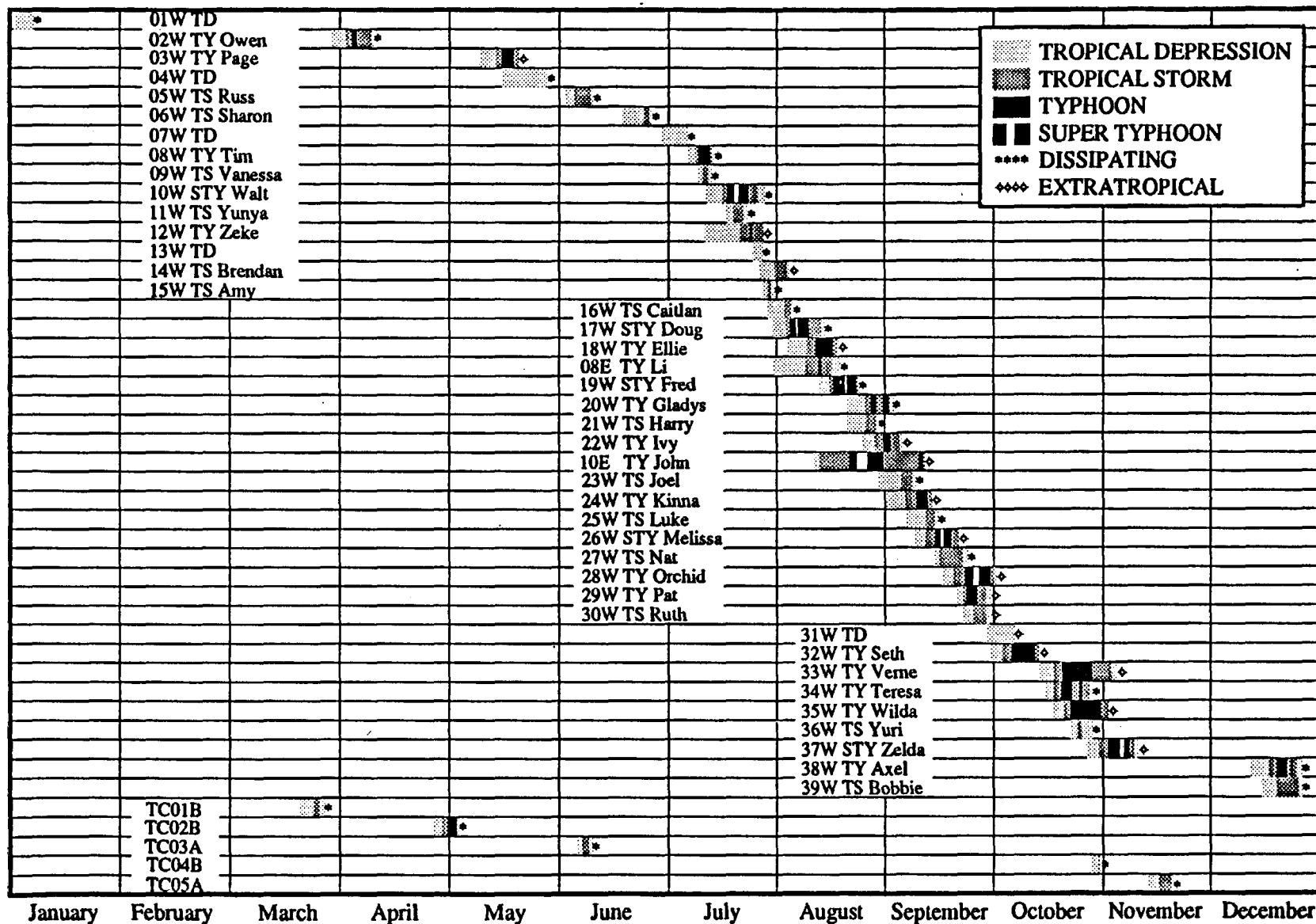


Figure 3-7 Chronology of western North Pacific and North Indian Ocean tropical cyclones for 1994.

Table 3-3 Individual 1978-1994 tropical cyclone (TC) track types. The observed track classes are defined as straight moving (SM), recurving (R), north-oriented (NO), "S"-track (S), and "other". Further subdivisions of the "other" category are indicated by icons: ■ = TC remained in or near South China Sea for its whole life; W = TC made many loops and meanders but made little overall forward progress; O = TC formed in Mei-yu cloud band and tracked rapidly to the northeast; < = TC formed over open Pacific and died over water after a short track; c = TC formed in the lee of Taiwan during conditions of monsoonal southwesterly flow and tracked northward then westward around the top of Taiwan to make landfall on the China coast.

YEAR	SM	R	NO+S	OTHER	■	<	W	O	c
1978	5	10	10	7	4	3	-	-	-
1979	9	12	2	5	2	2	1	1	-
1980	10	7	6	5	4	1	1	-	-
1981	11	7	5	6	2	2	1	-	1
1982	9	5	7	6	2	1	1	2	-
1983	11	5	4	5	4	1	1	-	-
1984	6	5	11	8	5	3	1	-	-
1985	7	3	9	8	5	2	1	-	-
1986	9	12	2	3	1	1	1	1	-
1987	7	2	10	5	2	3	-	-	-
1988	9	4	8	5	2	-	1	2	1
1989	15	5	9	6	3	3	-	-	-
1990	8	11	5	7	5	1	-	-	1
1991	11	14	2	4	3	1	1	-	-
1992	8	11	9	4	3	1	-	-	-
1993	15	10	4	8	2	6	-	-	-
1994	15	6	13	5	4	1	-	-	-
	165	129	116	97	53	32	10	6	3

Table 3-4

WESTERN NORTH PACIFIC TROPICAL CYCLONES

TYPHOONS													
(1945 - 1959)													
	JAN	FEB	MAR	APR	MAY	JUN	JUL	AUG	SEP	OCT	NOV	DEC	TOTALS
MEAN	0.3	0.1	0.3	0.4	0.7	1.0	2.9	3.1	3.3	2.4	2.0	0.9	16.4
CASES	5	1	4	6	10	15	29	46	49	36	30	14	245
(1960 - 1994)													
	JAN	FEB	MAR	APR	MAY	JUN	JUL	AUG	SEP	OCT	NOV	DEC	TOTALS
MEAN	0.3	0.1	0.2	0.4	0.7	1.1	2.7	3.4	3.3	3.2	1.7	0.7	17.9
CASES	10	2	8	15	25	38	96	118	116	113	61	24	626
TROPICAL STORMS AND TYPHOONS													
(1945 - 1959)													
	JAN	FEB	MAR	APR	MAY	JUN	JUL	AUG	SEP	OCT	NOV	DEC	TOTALS
MEAN	0.4	0.1	0.5	0.5	0.8	1.6	2.9	4.0	4.2	3.3	2.7	1.2	22.2
CASES	6	2	7	8	11	22	44	60	64	49	41	18	332
(1960 - 1994)													
	JAN	FEB	MAR	APR	MAY	JUN	JUL	AUG	SEP	OCT	NOV	DEC	TOTALS
MEAN	0.5	0.3	0.5	0.6	1.1	1.9	4.3	5.6	5.1	4.3	2.7	1.2	27.9
CASES	19	9	17	22	38	65	149	195	177	150	94	43	978

Table 3-5

TROPICAL CYCLONE FORMATION ALERTS FOR THE WESTERN NORTH PACIFIC OCEAN 1976-1994

YEAR	INITIAL TCFAS	TROPICAL CYCLONES WITH TCFAS	TOTAL TROPICAL CYCLONES	FALSE ALARM RATE*	PROBABILITY OF DETECTION
1976	34	25	25	26%	100%
1977	26	20	21	23%	95%
1978	32	27	32	16%	84%
1979	27	23	28	15%	82%
1980	37	28	28	24%	100%
1981	29	28	29	3%	96%
1982	36	26	28	28%	93%
1983	31	25	25	19%	100%
1984	37	30	30	19%	100%
1985	39	26	27	33%	96%
1986	38	27	27	29%	100%
1987	31	24	25	23%	96%
1988	33	26	27	21%	96%
1989	51	32	35	37%	91%
1990	33	30	31	9%	97%
1991	37	29	31	22%	94%
1992	36	32	32	20%	100%
1993	50	35	38	30%	92%
1994	50	40	40 **	20%	100%
(1976-1994)					
MEAN:	35.4	27.4	28.8	23%	95%
TOTALS:	637	493	519		

* The false alarm rate is the difference between the number of initial TCFA's and the number of tropical cyclones with TCFA's divided by the number of initial TCFA's and is expressed as a percentage.

** Note: The total of 40 tropical cyclones (TCs) results from 41 TCs minus two (TC08E and 10E), plus one for the regeneration of TC38W.

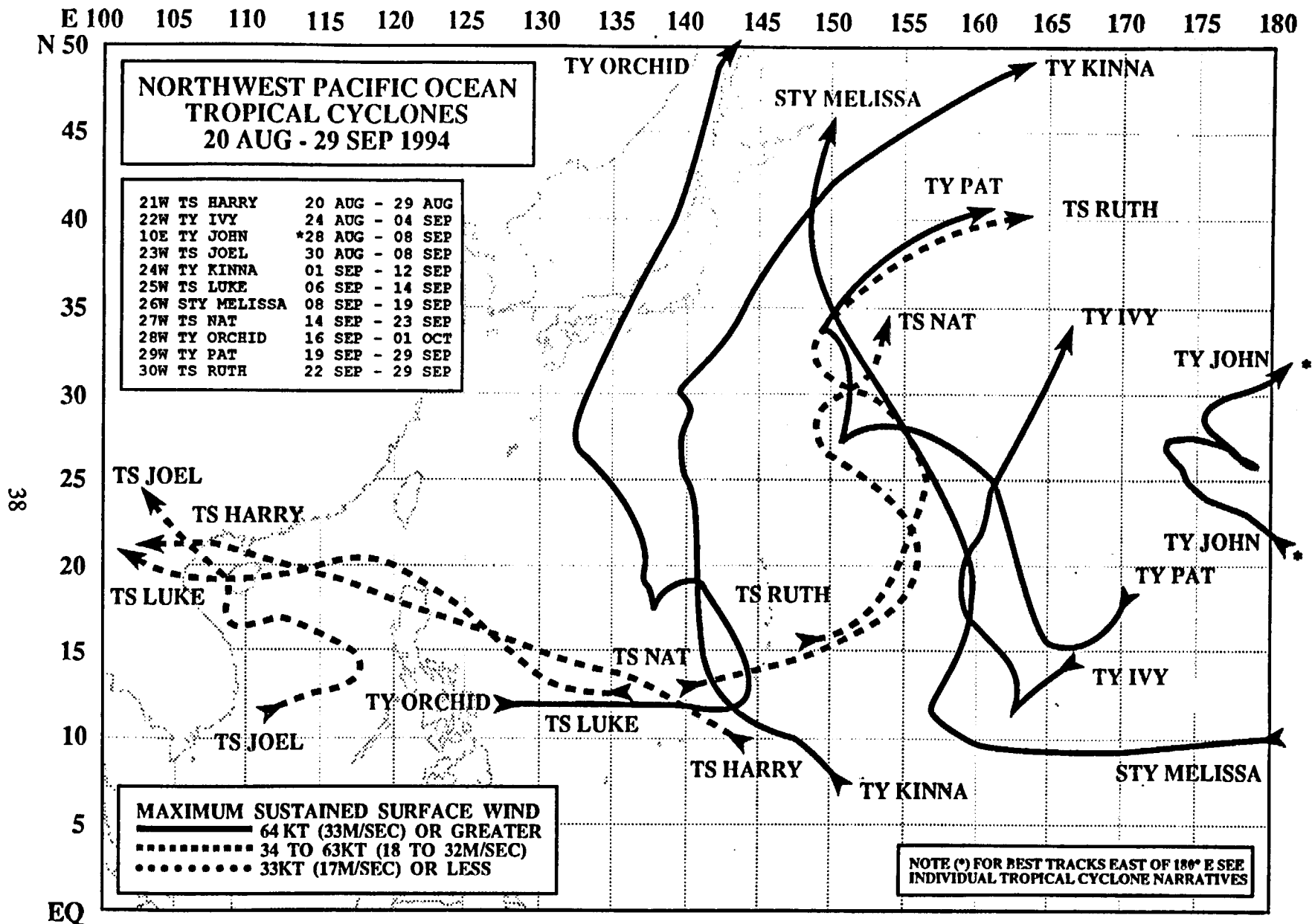


Figure 3-10 Composite best tracks for the North West Pacific Ocean tropical cyclones for the period 20 August to 29 September 1994.

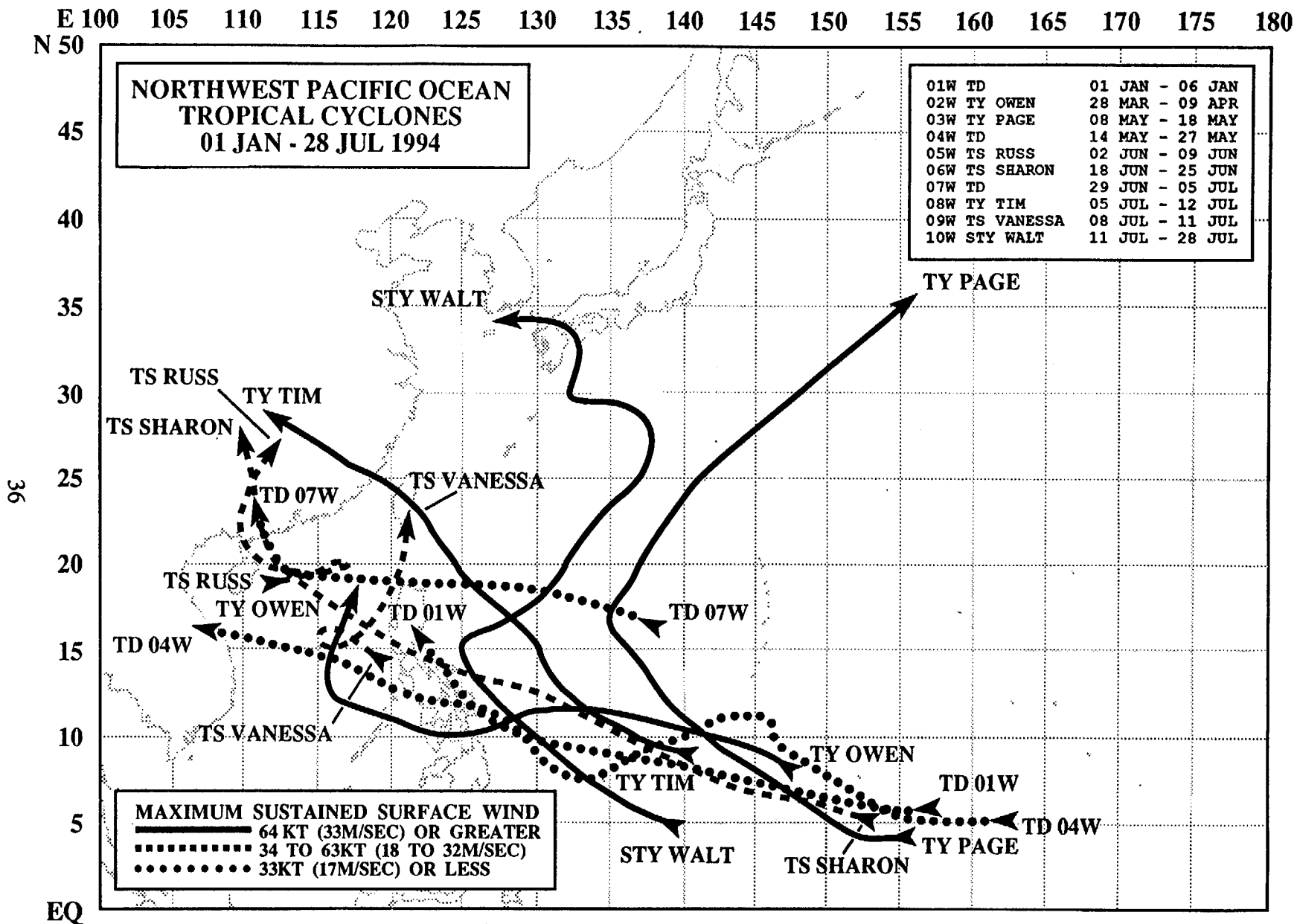


Figure 3-8 Composite best tracks for the North West Pacific Ocean tropical cyclones for the period 1 January to 28 July 1994.

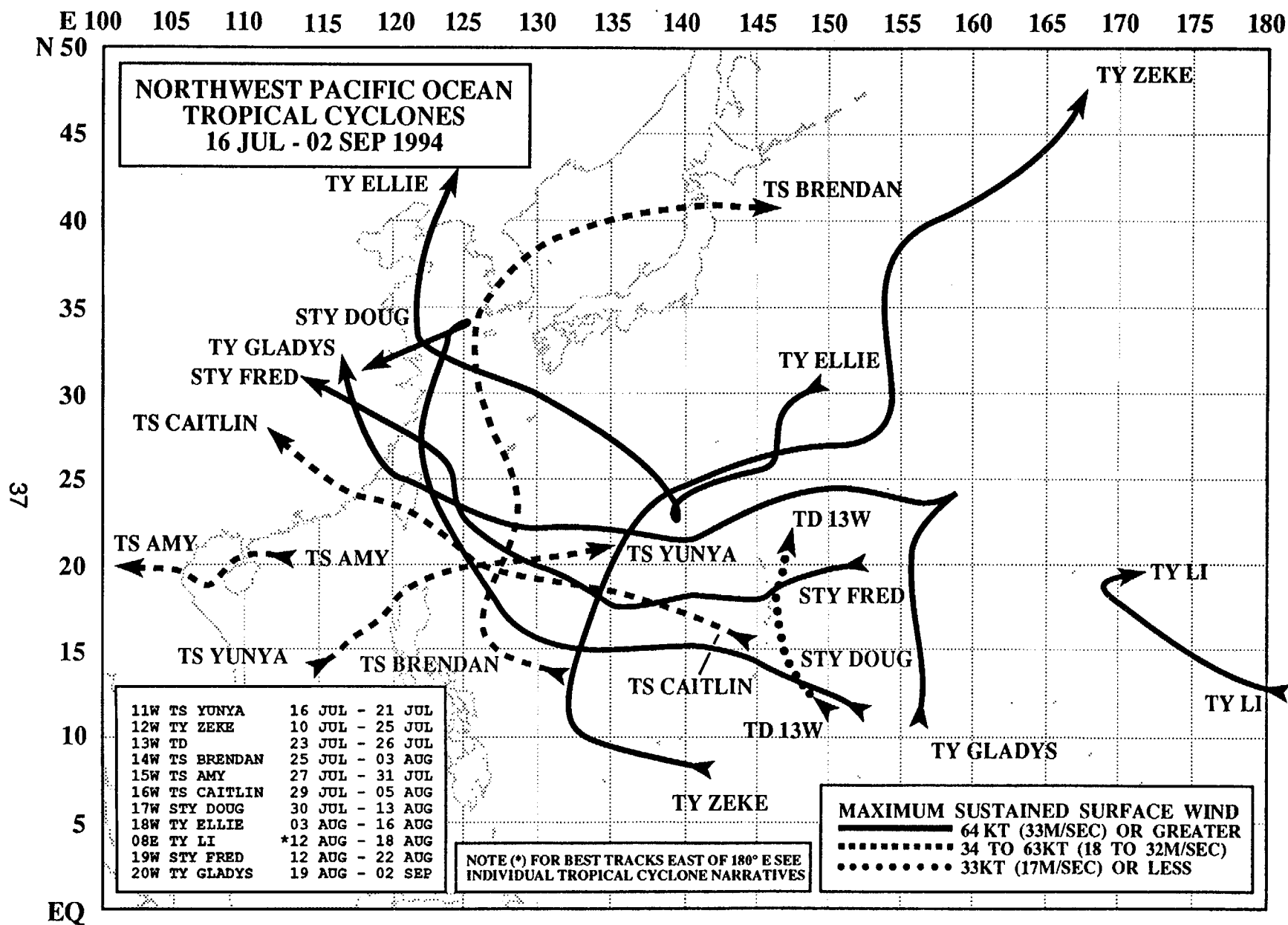


Figure 3-9 Composite best tracks for the North West Pacific Ocean tropical cyclones for the period 16 July to 02 September 1994.

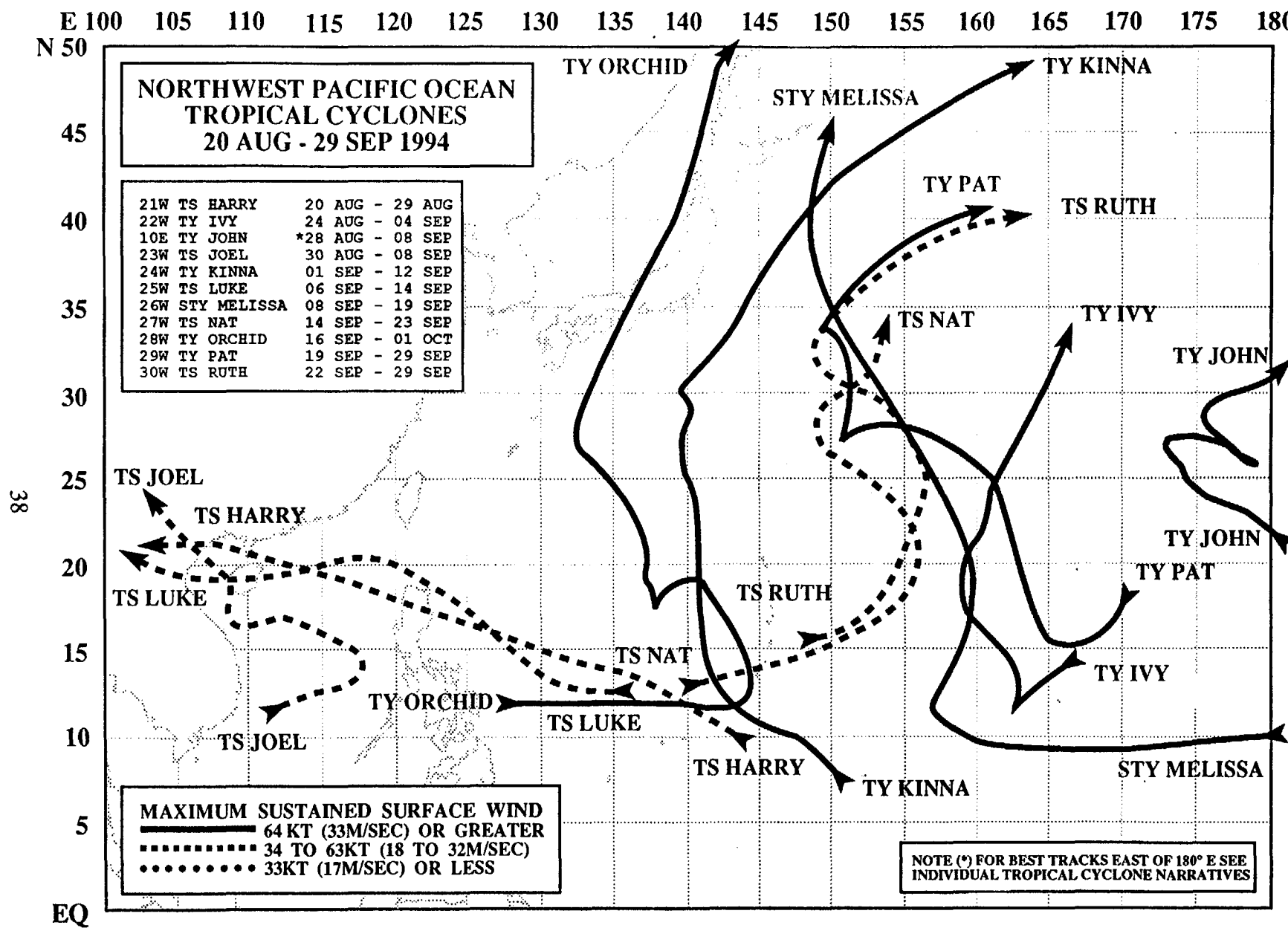


Figure 3-10 Composite best tracks for the North West Pacific Ocean tropical cyclones for the period 20 August to 29 September 1994.

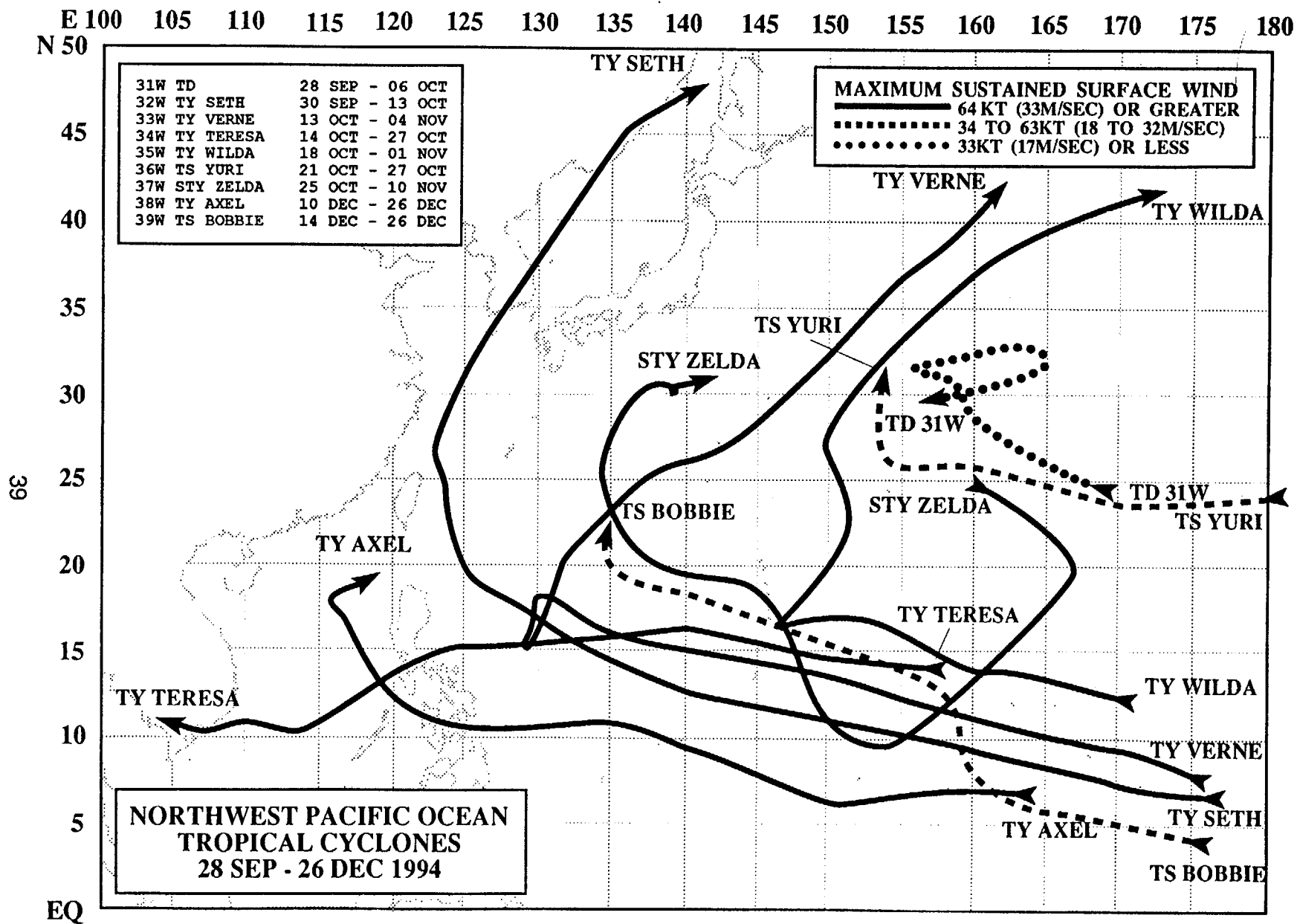
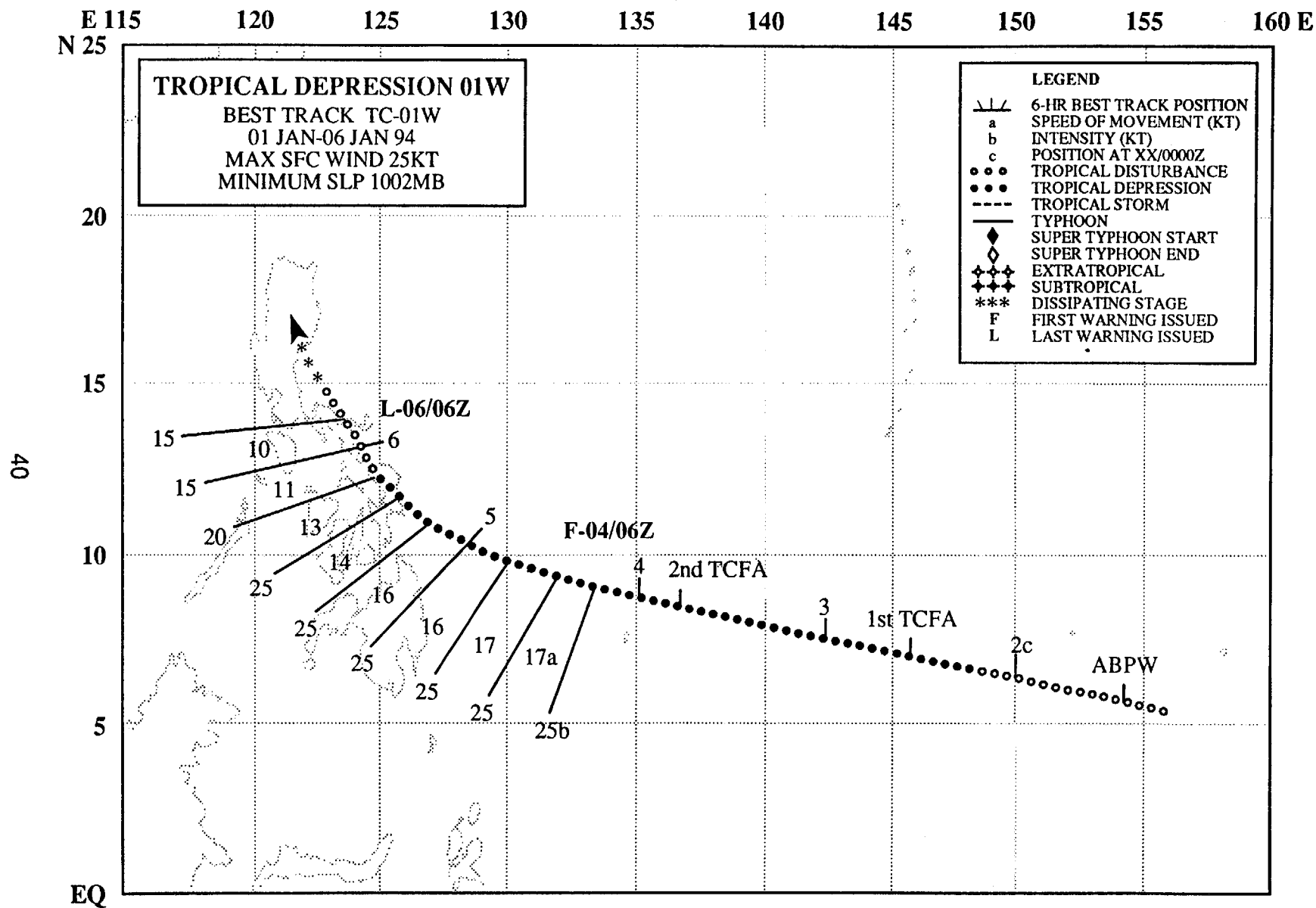


Figure 3-11 Composite best tracks for the North West Pacific Ocean tropical cyclones for the period 28 September to 26 December 1994.



TROPICAL DEPRESSION 01W

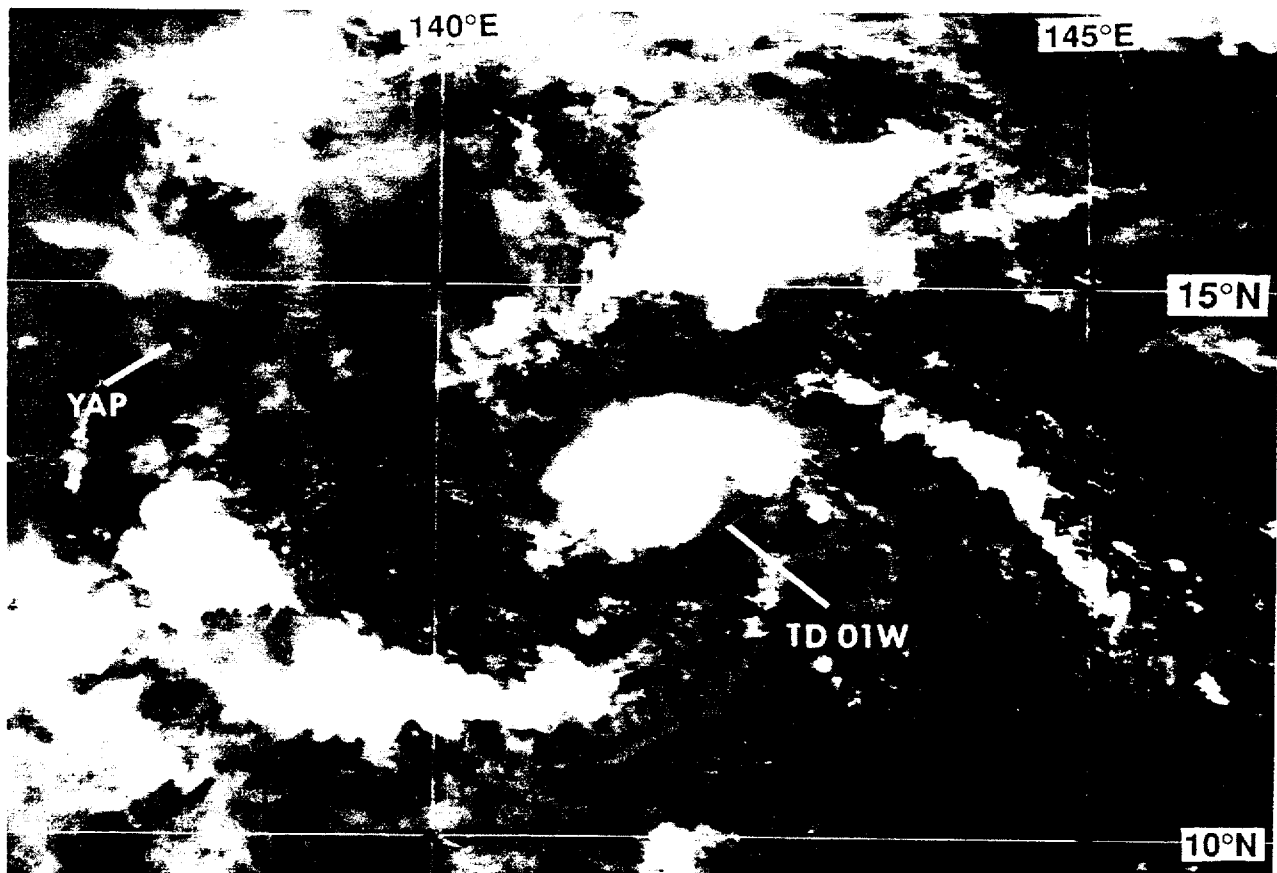


Figure 3-01-1 The disturbance which would later become TD 01W shows cyclonically curved lines of cumulonimbus clouds surrounding a small central cluster of deep convection (030231Z January visible GMS imagery).

I. HIGHLIGHTS

The first significant tropical cyclone of 1994 in the western North Pacific, Tropical Depression 01W reached a maximum intensity of only 25 kt (13 m/sec). Tropical Depression 01W formed in the near-equatorial trough of the Northern Hemisphere at a time when the monsoon trough of the Southern Hemisphere was also active.

II. TRACK AND INTENSITY

Tropical Depression 01W was first detected as a poorly organized area of cloudiness in the near-equatorial trough in the eastern Caroline islands. The disturbance was first mentioned on the 010600Z January Significant Tropical Weather Advisory. An increase in convective organization and a gradient-level wind of 30 kt (15 m/sec) at Chuuk (WMO 91334) prompted a Tropical Cyclone Formation Alert at 021400Z. During the daylight hours of 03 January (022100Z to 030800Z) the disturbance lost much of its deep convection; and, although it retained organized curved cloud lines (Figure 3-01-1), it had yet to intensify into a significant tropical cyclone. A dramatic flare-up of deep convection between 031800Z and 040000Z, that produced a large cold cirrus cloud shield with anticyclonic outflow, prompted a second Tropical Cyclone Formation Alert which was issued at 031900Z followed by the first warning at 040600Z. This first cold cloud shield collapsed by evening (040600Z), and the intensity was held at 25

kt (13 m/sec). A second flare-up of deep convection between 041800Z and 050000Z resulted in another large cold cirrus cloud shield. The system appeared to be somewhat sheared with the low-level circulation center located at the southeastern edge of this cloud shield. Synoptic wind and pressure reports and satellite intensity estimates indicated that the system had still failed to mature and the intensity was kept at 25 kt (13 m/sec). At 051200Z, Tropical depression 01W made landfall on the island of Samar in the central Philippines. Convection became disorganized and synoptic reports from land and ships indicated that the disturbance was weakening. The last warning on Tropical Depression 01W was issued at 060600Z as the system tracked along the east coast of Luzon, and lost its deep convection.

III. DISCUSSION

Tropical Depression 01W was forming in the Northern Hemisphere near-equatorial trough at the same time as the Australian Northwest Monsoon was reaching a peak of activity. When the first Tropical Cyclone Formation Alert was issued for Tropical Depression 01W, two named tropical cyclones, Rewa (05P) and Oscar (06S), and a tropical disturbance were active in the Australian region of the monsoon trough of the Southern Hemisphere (Figure 3-01-2). Tropical Depression 01W formed in a wind pattern with some similarity to the twin-trough pattern that is commonly observed during the simultaneous occurrence of tropical cyclones on both sides of the equator. In this case, however, the southern monsoon trough was clearly dominant and further from the equator than the northern near-equatorial trough.

Another interesting feature of the evolution of Tropical Depression 01W was the strong diurnal periodicity of the flare-up of large cold cirrus shields near the circulation center. On two occasions, once on the early morning of 04 January, and again during the early morning of 05 January, a large mesoscale convective system developed on the northwestern side of the circulation center and produced an extensive area of very cold dense cirrus cloud cover. During the afternoon, after both of these early morning flare-ups, the convection collapsed and the cirrus canopy thinned. Despite the increase of convection near the low-level circulation center, Tropical Depression 01W failed to intensify. A possible reason may be the presence of persistent southeasterly shear across the system. A large-scale collapse of the Australian Northwest Monsoon occurred concurrently with the dissipation of Tropical Depression 01W.

IV. IMPACT

Although Tropical Depression 01W brought heavy rains to some areas of the Philippine Islands, no reports of significant damage or fatalities were received.

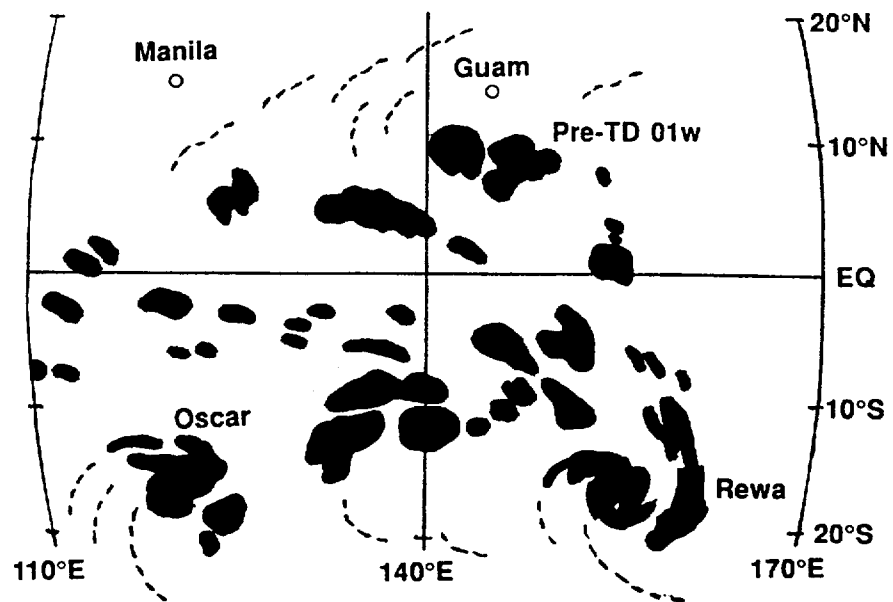


Figure 3-01-2 Cloud silhouettes adapted from the 021234Z infrared GMS imagery show two named tropical cyclones — Rewa (05P) and Oscar (06S) — along the axis of low pressure of an active Australian monsoon. The disturbance which would later intensify to become Tropical Depression 01W is seen south of Guam. Thin dashed lines show streamers of high-thin cirrus.

E 110 115 120 125 130 135 140 145 150 155 E

N 25

20

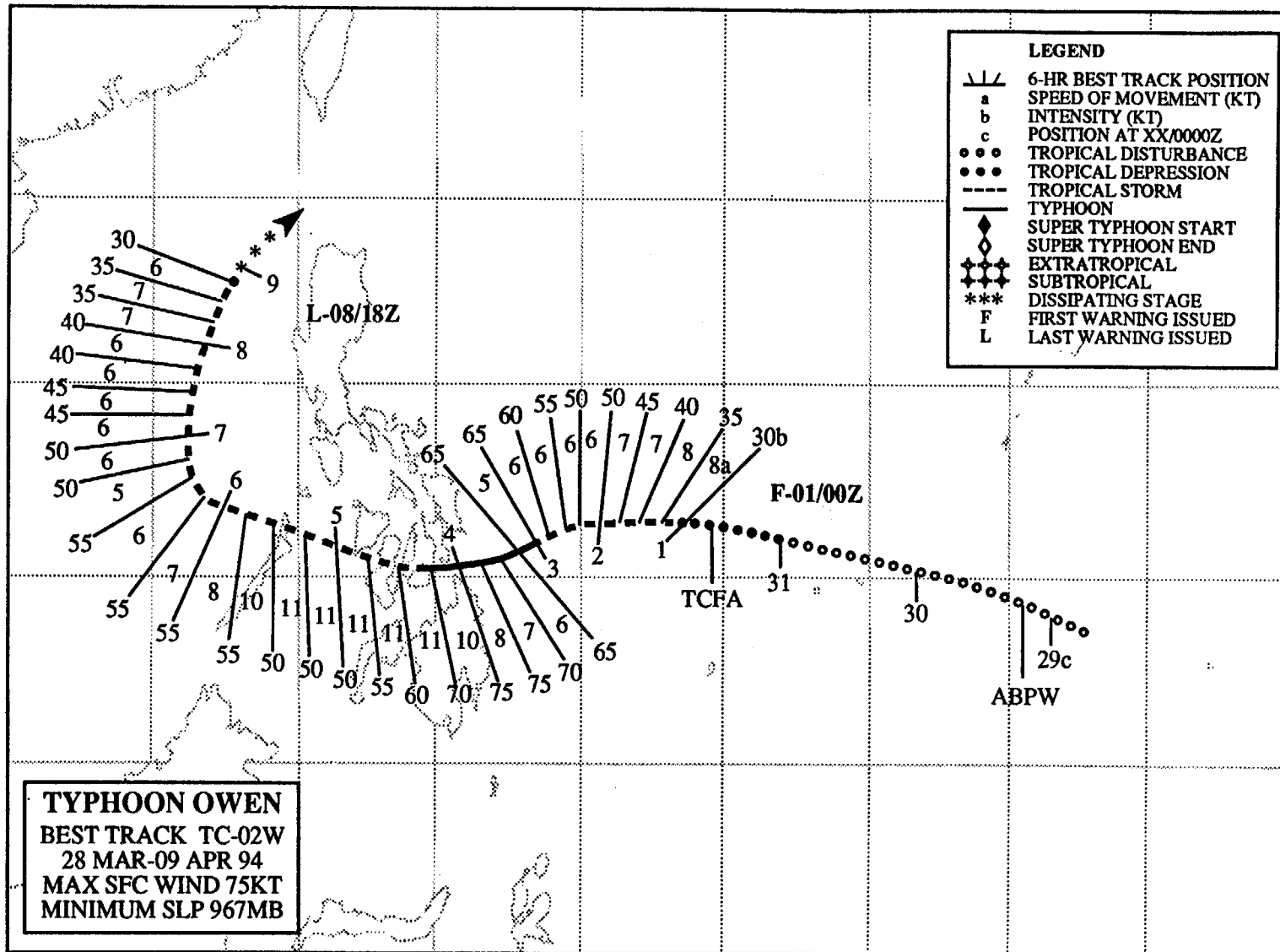
15

10

5

EQ

44



TYPHOON OWEN (02W)

I. HIGHLIGHTS

Unusual southwestward motion brought Owen from the Philippine Sea across the southern islands of the Philippine Archipelago. Like many typhoons which track across the Philippine islands on a southwestward trajectory, Owen was small-sized. Until typhoon intensity was diagnosed, Owen was not forecast to reach typhoon intensity.

II. TRACK AND INTENSITY

During the last week of March, there was extensive deep convection in Micronesia associated with a near-equatorial trough in the region. The first mention of a tropical disturbance embedded within this large-scale cloudiness over Micronesia appeared on the 290600Z March Significant Tropical Weather Advisory. On 30 March, deep convection flared along the equator in association with low-level westerly winds. The disturbance (pre-Owen) in the near-equatorial trough appeared to be shearing and losing its separate identity in the extensive cloudiness. By 31 March, the equatorial cloudiness had collapsed, and a distinct cloud cluster appeared in the near-equatorial trough that exhibited cyclonic curvature. A Tropical Cyclone Formation Alert was issued at 311800Z, followed by a warning at 010000Z.

Owen's development was contrary to expectations. It was not forecasted to become a typhoon until satellite imagery at 030000Z April indicated typhoon intensity. The presence of upper-level shear from the southeast, large diurnal fluctuations in the amount and organization of Owen's deep convection, and interaction with the Philippine Islands were considered to be factors unfavorable for intensification.

Also unanticipated was Owen's southwestward motion during the two days prior to landfall in the Philippine islands. At 020600Z, Owen began to move toward the west-southwest. By the time it passed between the islands of Leyte and Mindanao, Owen had lost nearly 1.5° of latitude. The peak intensity of 75 kt (39 m/sec) was reached shortly before passage between these two islands (Figure 3-02-1). Owen weakened to tropical storm intensity as it crossed several islands of the Philippine archipelago. Emerging into the South China Sea, it turned northward, steadily weakened, and dissipated over water northwest of Luzon. The final warning was issued at 090000Z.

III. DISCUSSION

Typhoons have occurred in the month of April for fifteen of the past 36 years. Of these, six (including Owen) have made landfall in the Philippine Islands. Four (including Owen) of these six moved into the Philippine Archipelago near the island of Samar, one struck northern Luzon, and another moved westward at very low latitude (6°N) and crossed over the southern end of Mindanao.

Owen's west-southwestward motion prior to landfall in the Philippines was somewhat unusual. Climatology for the region indicates northwestward motion. Of the six typhoons impacting the Philippines in April during the past 36 years, only two — Owen and Wanda (1971) — were moving west-southwestward at landfall. Owen's later recurvature in the South China Sea at low latitude (13°N) is about 3° south of the average latitude of recurvature for all tropical cyclones in that region during April.

IV. IMPACT

As Owen swept across the central Philippines, three people were killed and four were reported missing. On the island of Cebu, more than 7000 villagers living in the coastal areas were affected by flash

floods. Emerging into the South China Sea west of the Philippine islands, Owen passed to the south of the drilling rig, SEDCO 709 (11.6°N ; 118.9°E). Maximum sustained winds measured on the rig were 50 kt (26 m/sec) with a peak gust of 67 kt (35 m/sec). No damage or fatalities were reported on the rig.

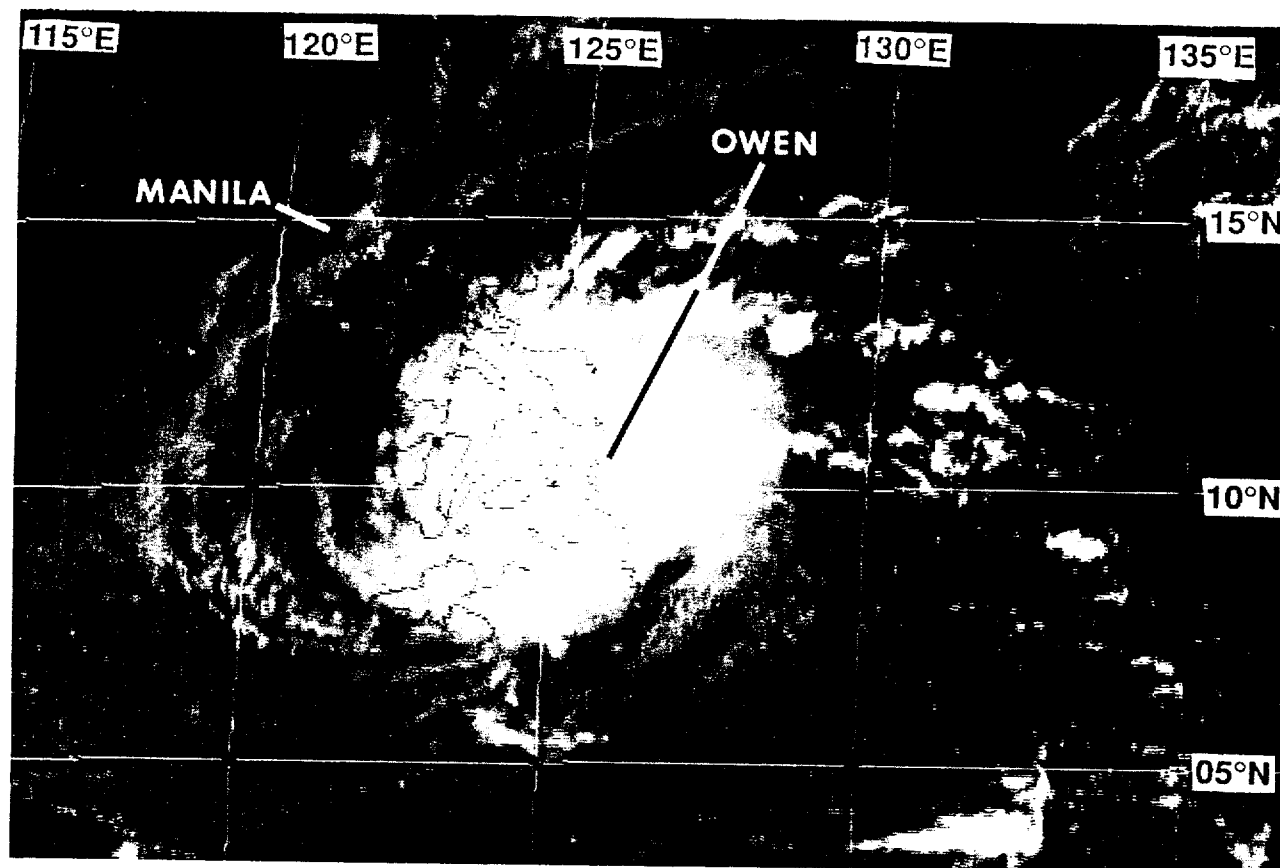

















Figure 3-02-1 Owen passes between the islands of Leyte and Mindanao at its peak intensity of 75 kt (39 m/sec)
(0322331Z April visible GMS imagery)

E 120 125 130 135 140 145 150 155 160 165 170 E
N 45

TYPHOON PAGE

BEST TRACK TC-03W
08 MAY-18 MAY 94
MAX SFC WIND 90KT
MINIMUM SLP 954MB

LEGEND

-  6-HR BEST TRACK POSITION
-  a SPEED OF MOVEMENT (KT)
-  b INTENSITY (KT)
-  c POSITION AT XX/0000Z
-  TROPICAL DISTURBANCE
-  TROPICAL DEPRESSION
-  TROPICAL STORM
-  TYPHOON
-  SUPER TYPHOON START
-  SUPER TYPHOON END
-  EXTRATROPICAL
-  SUBTROPICAL
-  DISSIPATING STAGE
-  F FIRST WARNING ISSUED
-  L LAST WARNING ISSUED

40

35

30

25

20

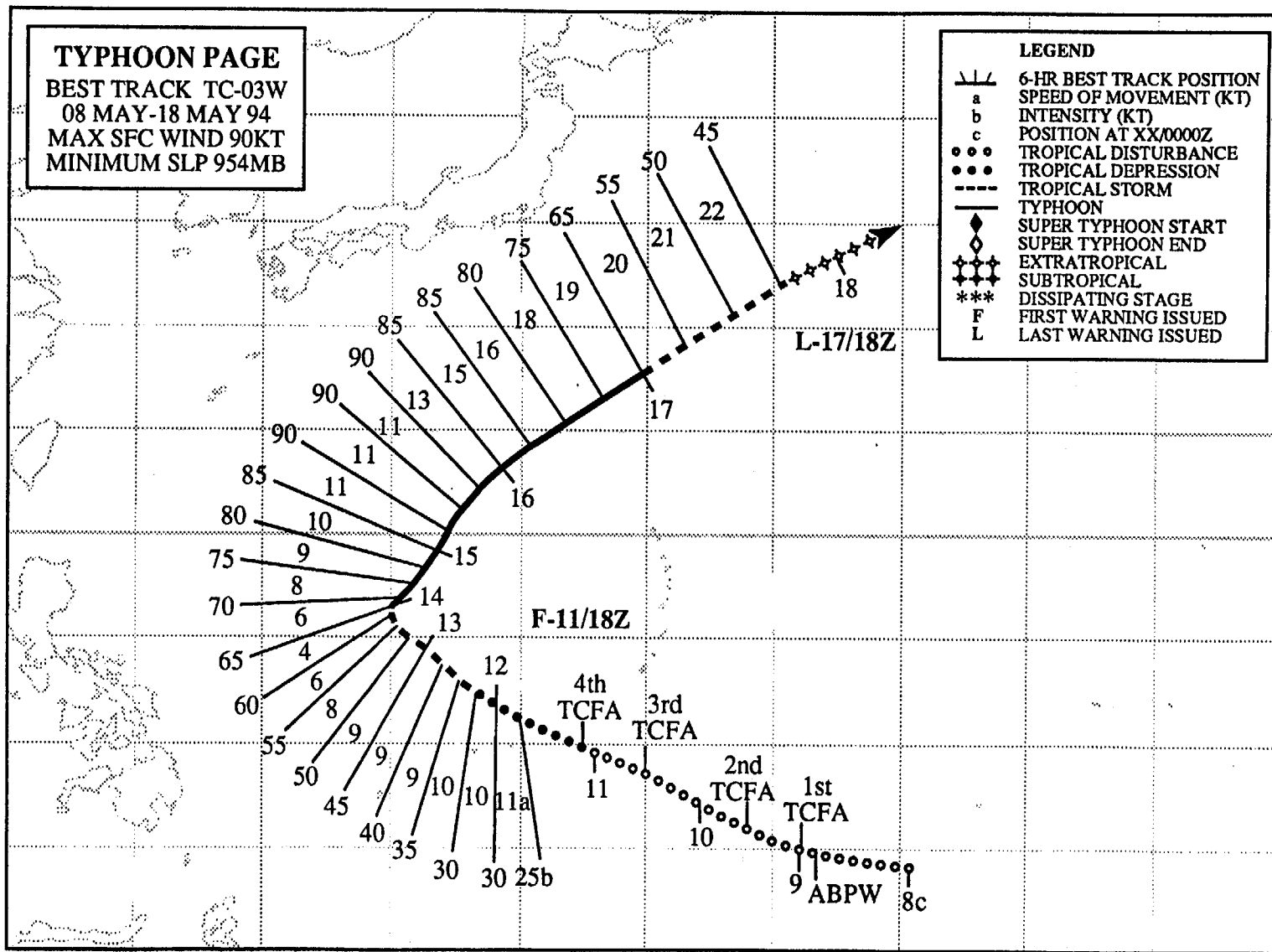
15

10

5

EQ

47



TYPHOON PAGE (03W)

I. HIGHLIGHTS

Forming at very low latitude in the northern of twin near-equatorial troughs (i.e., one trough north of the equator, and the other south of the equator); Page was very slow to develop, with four Tropical Cyclone Formation Alerts issued prior to the first warning. Page was one of relatively few tropical cyclones that reach peak intensity well past the point of recurvature. The recurvature of Page was not well-anticipated, and the average 72-hour forecast error of 475 nm (880 km) was the largest for any western North Pacific typhoon during 1994.

II. TRACK AND INTENSITY

During the first week of May, there was extensive deep convection in Micronesia associated with a near-equatorial trough in the region. On 08 May, a flare-up of deep convection in the eastern Caroline Islands was included as a suspect area on the 081800Z May Significant Tropical Weather Advisory. By the morning of 09 May, visible satellite imagery indicated an increase in the organization of the deep convection in this tropical disturbance, and synoptic reports confirmed the presence of a low-level circulation center located near 5°N 153°E. The first of four Tropical Cyclone Formation Alerts was issued at 082355Z. A second Tropical Cyclone Formation Alert was issued at 091330Z because the estimated location of the low-level circulation center was nearing the edge of the previous alert box. The disturbance failed to intensify, but since conditions were deemed favorable for intensification, a third Tropical Cyclone Formation Alert was issued at 101330Z. By the evening of 11 May, a large convective band formed to the north of the estimated low-level circulation center, but the overall organization of deep convection within the system still did not indicate an increased intensity, so the fourth Tropical Cyclone Formation Alert was issued at 110530Z. During the early morning hours of 12 May, the organization of the deep convection improved rapidly, and the first warning was issued at 111800Z.

Page moved steadily on a northwestward track and slowly intensified during the 42 hours following the first warning. At 131200Z, the system abruptly slowed and began its turn toward the northeast, reaching its point of recurvature at 131800Z. Page became a typhoon at 140000Z. At 150000Z, thirty hours after the point of recurvature, Page's intensity peaked at 90 kt (46 m/sec) (Figure 3-03-1). After recurvature, Page gradually accelerated to a maximum forward speed of 22 kt (41 km/hr). The final warning was issued at 171800Z as Page began its transition to an extratropical low about 600 miles east-southeast of Tokyo.

III. DISCUSSION

a. Forecast performance

The average track forecast errors for Page were the worst for any typhoon during 1994. The main factor contributing to these large average errors was a failure to anticipate the recurvature of Page (Figure 3-03-2a). The NOGAPS model and its derived track guidance (Figure 3-03-2b) gave early indications of recurvature, but the repetition of numerical forecasts of northward motion during a period of ongoing westward motion eroded the forecasters confidence in the numerical guidance. As a result, JTWC forecasters relied more on a consensus of various climatological, statistical and dynamic aids, which correctly indicated a decrease in the forward speed of motion, but were late to forecast recurvature.

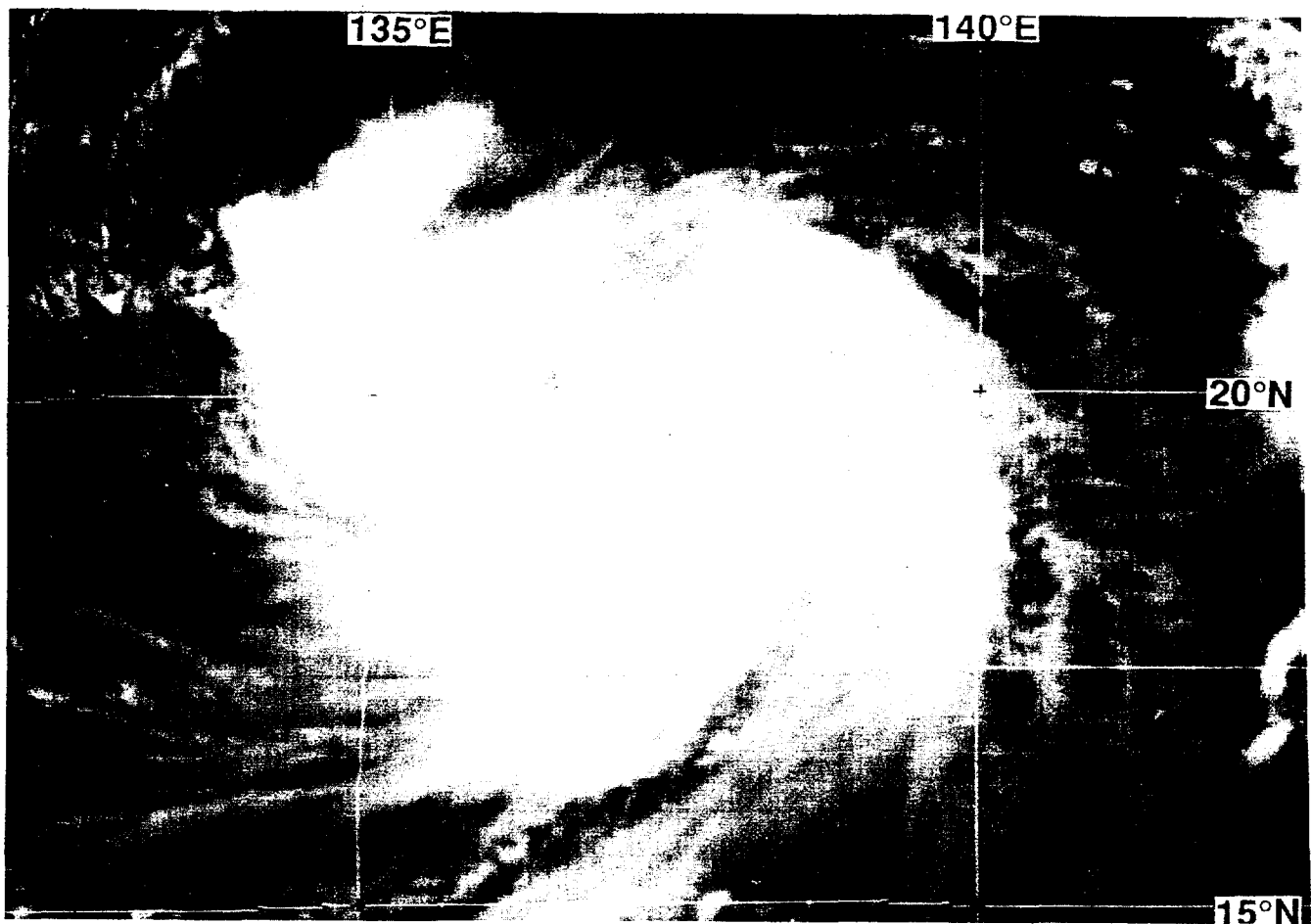
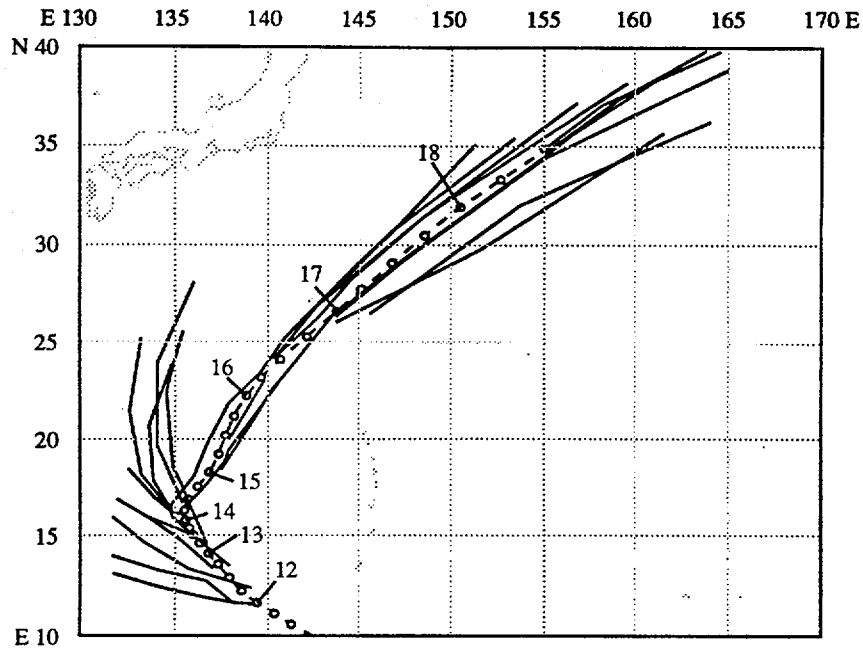


Figure 3-03-1 Page at peak intensity (150231Z May visible GMS imagery).

b. Peak intensity after recurvature

Of 77 cases of typhoons that exhibited classical recurvature (i.e., a roughly "<"-shaped track that features initial steady west-northwestward motion, then a northward turn while slowing, followed by an acceleration toward the northeast) during the period 1978 to 1993, about three-fourths (57) reached peak intensity at, or before, the point of recurvature (Figure 3-03-3); where the point of recurvature is identified as that point where the typhoon reaches its western-most longitude as it moves poleward. A much smaller group (seven) reached peak intensity 24 hours or more after the point of recurvature. Page reached its peak intensity of 90 kt (46 m/sec) 30 hours after the point of recurvature placing it in the very small group of typhoons that have waited that long. Another interesting feature of Figure 3-03-3, is an apparent relationship (represented by the best-fit curve) between typhoon peak intensity and its timing with respect to the point of recurvature. The higher the peak intensity of a recurving typhoon, the greater the delay of recurvature with respect to the timing of the peak intensity. Of the 30 recurving typhoons reaching peak intensities of 120 kt (62 m/sec) or greater during the period 1978 to 1993, only three reached peak intensity after recurvature. On average, recurving typhoons attaining peak intensities less than 120 kt (62 m/sec) reached peak intensity about 12 hours prior to the point of recurvature; recurving typhoons attaining peak intensities of 120 kt (62 m/sec) or greater reached peak intensity about 48 hours prior to the point of recurvature.

(a)



(b)

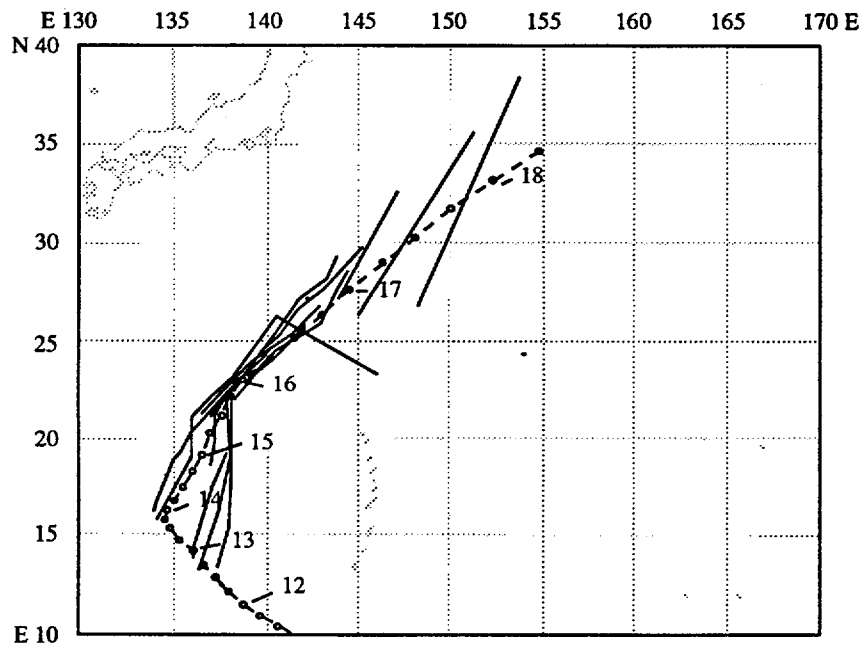


Figure 3-03-2 (a) JTWC forecast tracks prior to the point of recurvature of Page. (b) NOGAPS forecast tracks prior to the point of recurvature of Page.

IV. IMPACT

Typhoon Page remained over open ocean its entire life, and no reports of fatalities or significant damage were received. Large westerly swell generated by Page while it was in the Philippine Sea impacted the western shores of the Mariana Islands. Several tourists required rescue from high surf and strong currents along Guam's western reefs.

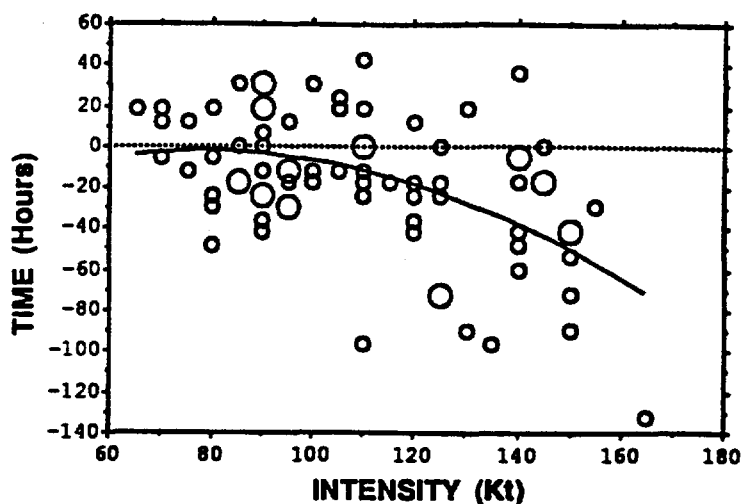
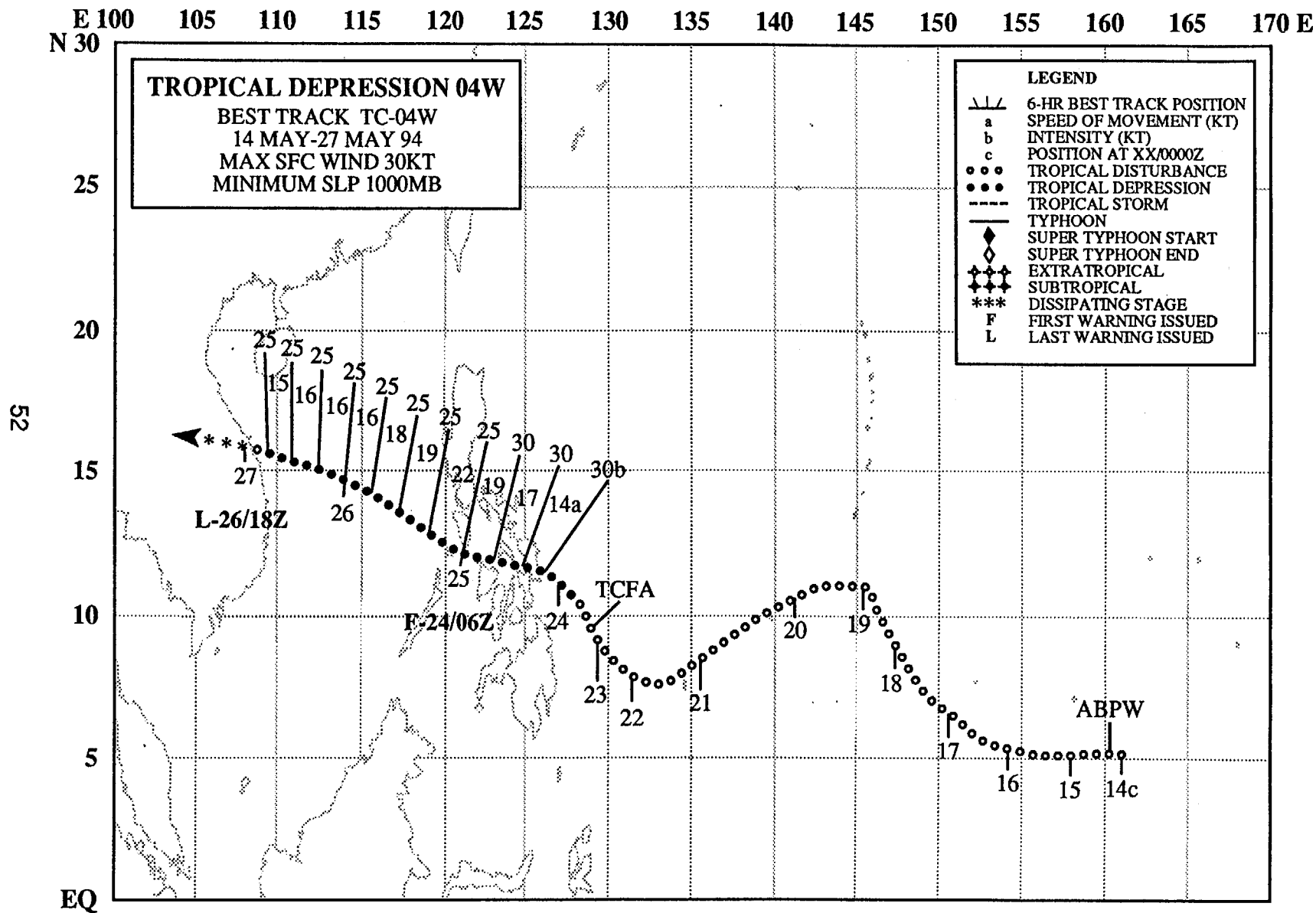


Figure 3-03-3 Timing of peak intensity (kt) with respect to the time of recurvature (+/- hours) versus peak intensity for 77 recurving typhoons during the period 1978 to 1993. Open circles indicate individual typhoons, larger open circles indicate more than one typhoon occupies that point on the graph. A circle on the dashed zero line is indicative of a typhoon that reached peak intensity at the same time that it reached its point of recurvature; typhoons reaching peak intensity after recurvature are plotted above this line, those reaching peak intensity prior to recurvature are plotted below. The best-fit second-order polynomial is indicated by the curve defined by: $Y = -58.315 + 1.453 X - .009 X^2$. If the peak intensity, X , is known, this equation estimates the number of hours, Y , between the time of peak intensity and the time when the typhoon reaches its point of recurvature.



TROPICAL DEPRESSION 04W

As Typhoon Page (03W) was undergoing its recurvature, westerly monsoonal winds extended eastward at low latitude into the eastern Caroline Islands. An area of deep convection straddled the equator which was associated with a weak cyclonic circulation near Kosrae. This weak circulation was first mentioned on the 140600Z May significant tropical weather advisory. For about five days, the weak low-level circulation moved west-northwestward toward Guam, however, convection failed to consolidate in the center. As the disturbance neared Guam it turned to the west-southwest and passed very close to Palau at 210600Z. After passing Palau, the system turned northwestward into the Philippine Sea. SSM/I imagery at 230101Z indicated a well-defined low-level circulation center. Visible and infrared satellite imagery also indicated an increase in organization of the system and a consolidation of deep convection near the low-level circulation center. These data prompted the issuance of a Tropical Cyclone Formation Alert at 230600Z. As the system neared the Philippines, the amount of deep convection near the low-level center increased, and the first warning was issued at 240600Z. Tropical Depression 04W entered the South China Sea by 250600Z. Twice, once while over the Philippine islands, and again 24 hours later over water west of Luzon, a large mesoscale convective system (MCS) formed near the center of Tropical Depression 04W and produced an extensive cold cirrus cloud shield (Figure 3-04-1a,b). On both occasions, the MCS began to grow explosively at sunset, with the maximum extent of cold cirrus observed during the pre-dawn hours. After the decay of the second large MCS during the daylight hours of 26 May, the low-level circulation center of Tropical Depression 04W moved westward and made landfall along the coast of central Vietnam. The final warning was issued at 261800Z. No reports of damage or injuries were received.

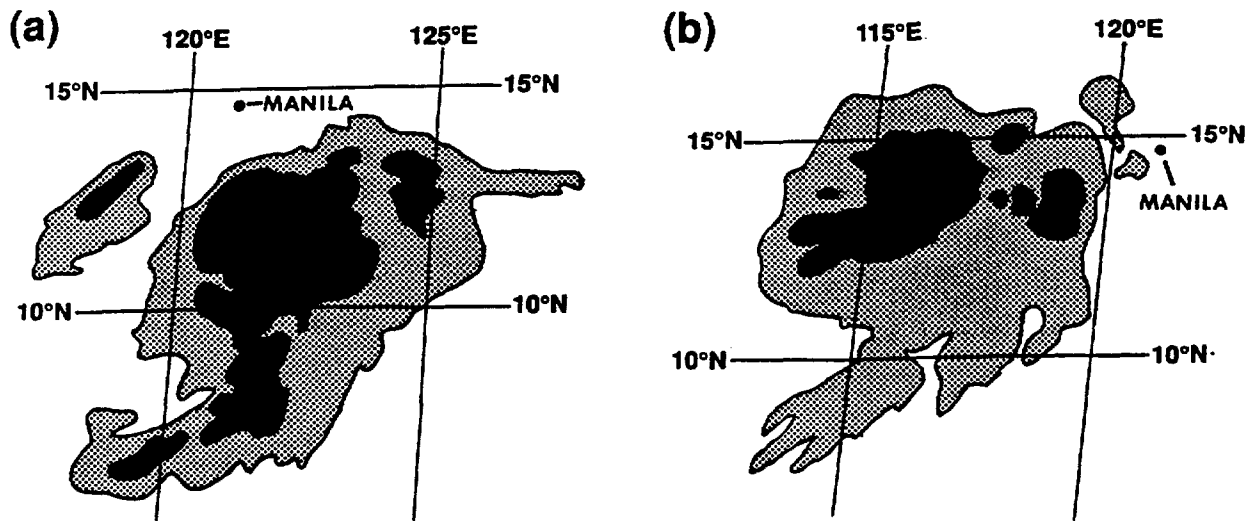


Figure 3-04-1 Schematic illustration of two episodes of early morning flare-up of the deep convection associated with Tropical Depression 04W based on: (a) 241931Z May enhanced infrared GMS imagery; and, (b) 251931Z May enhanced infrared GMS imagery. Shaded regions indicate cloud-top temperatures less than -60°C ; black regions indicate cloud-top temperatures less than -75°C .

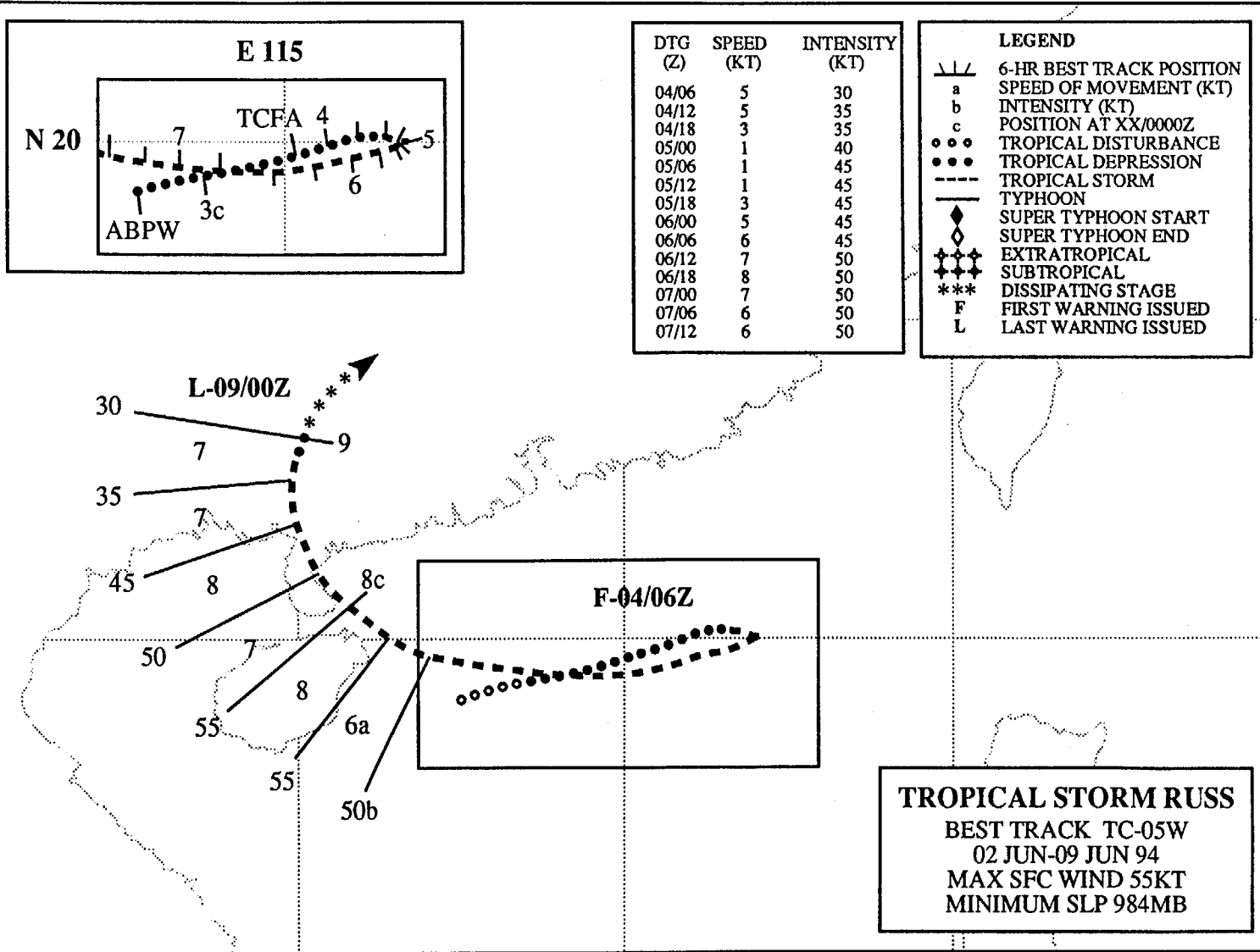
E 105
N 30

110

115

120

125 E



25

54

20

N 15

TROPICAL STORM RUSS (05W)

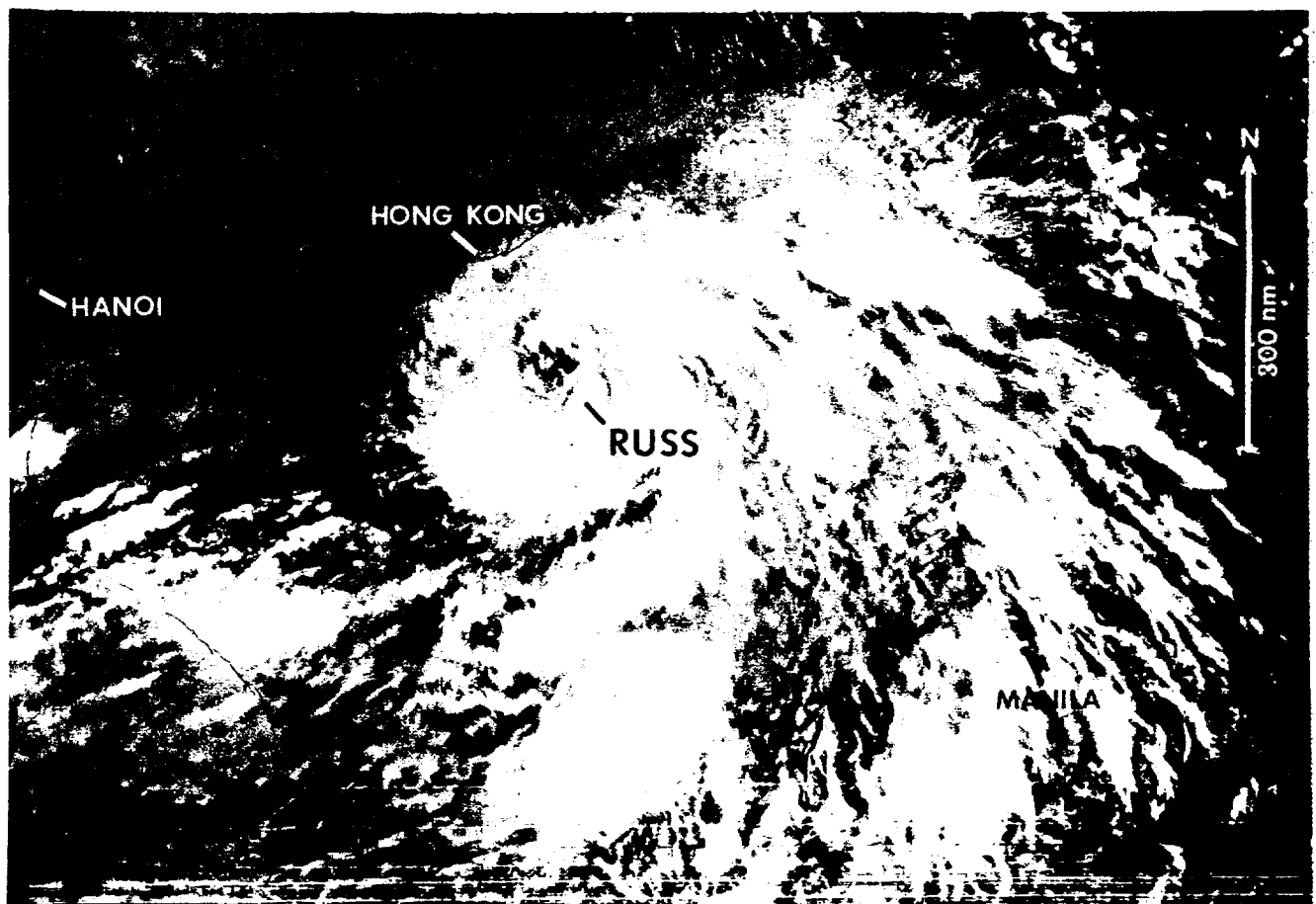
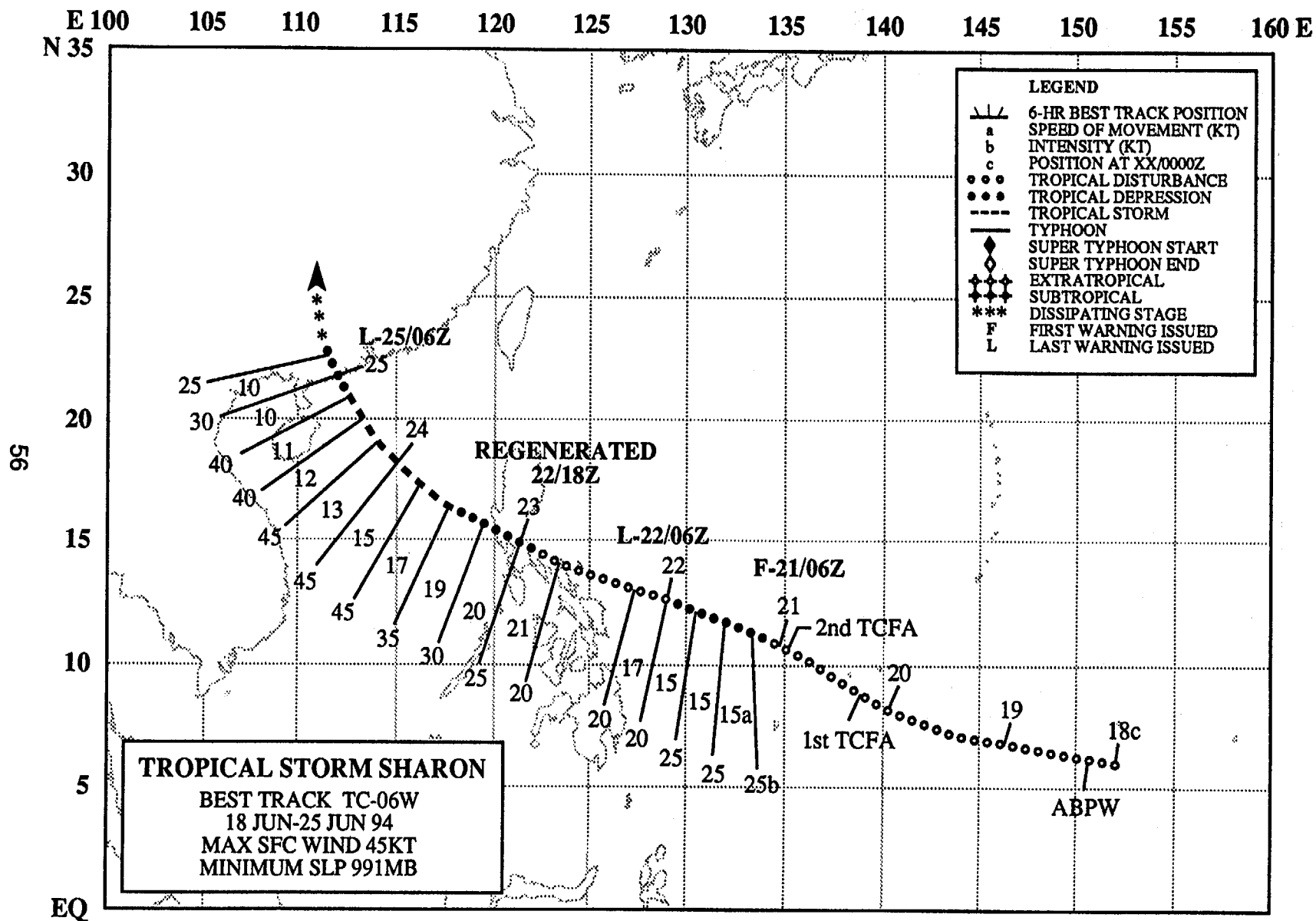


Figure 3-05-1 Russ with a ragged eye nears its peak intensity to the south of Hong Kong (060214Z June infrared DMSP imagery).

On 02 June, as the low-level southwest monsoonal flow over the South China Sea interacted with the well-anchored Mei-yu front (see Appendix A) that extended from south of Japan to near Hong Kong, surface pressures began to fall at the extreme southern end of the front. A tropical disturbance, about 75 nm (140 km) east of Hainan Island, was first mentioned on the Significant Tropical Weather Advisory at 020600Z May. By the evening of 03 June, with deep convection consolidated over the circulation center of this tropical disturbance, a Tropical Cyclone Formation Alert was issued at 031900Z. During the following day, the convection remained over the circulation center, and the JTWC issued the first warning on Tropical Depression 05W at 040600Z. The tropical depression slowly tracked in a northeastward direction for two days in association with deep southwesterly monsoonal steering flow. As the southwest monsoon weakened, Russ executed a clockwise loop back toward the west and slowly began to intensify. Russ reached its maximum intensity of 55 kt (28 m/sec) on 06 June as it developed a ragged banding-type eye (Figure 3-05-1). Russ went ashore at 080700Z on the northeastern Luichow Peninsula, and dissipated over southern China. Torrential rains caused severe flooding that killed hundreds of people and destroyed thousands of houses. The combined impacts of Russ and Sharon (06W) are discussed in the Tropical Storm Sharon narrative.



TROPICAL STORM SHARON (06W)

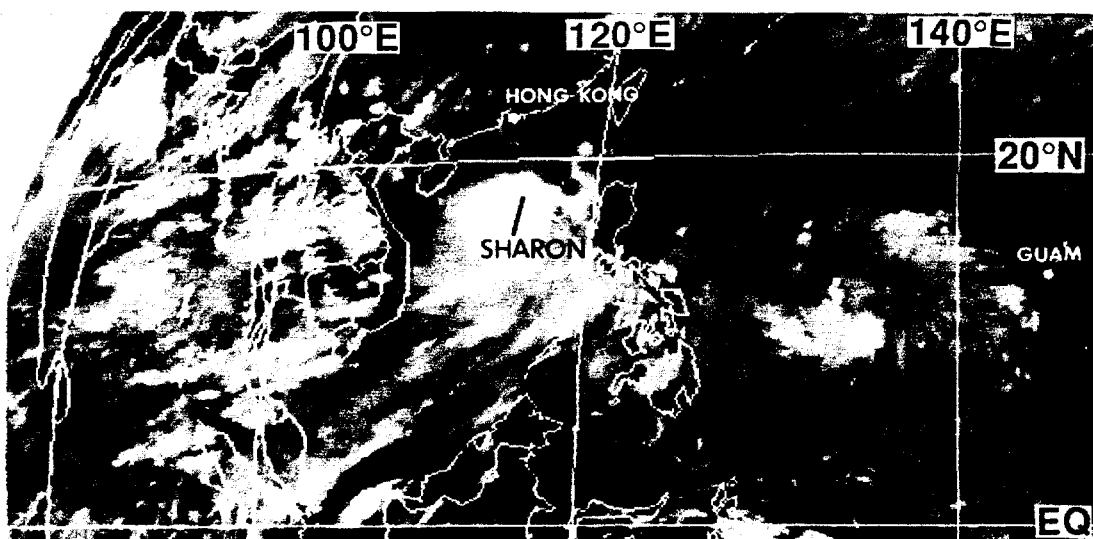
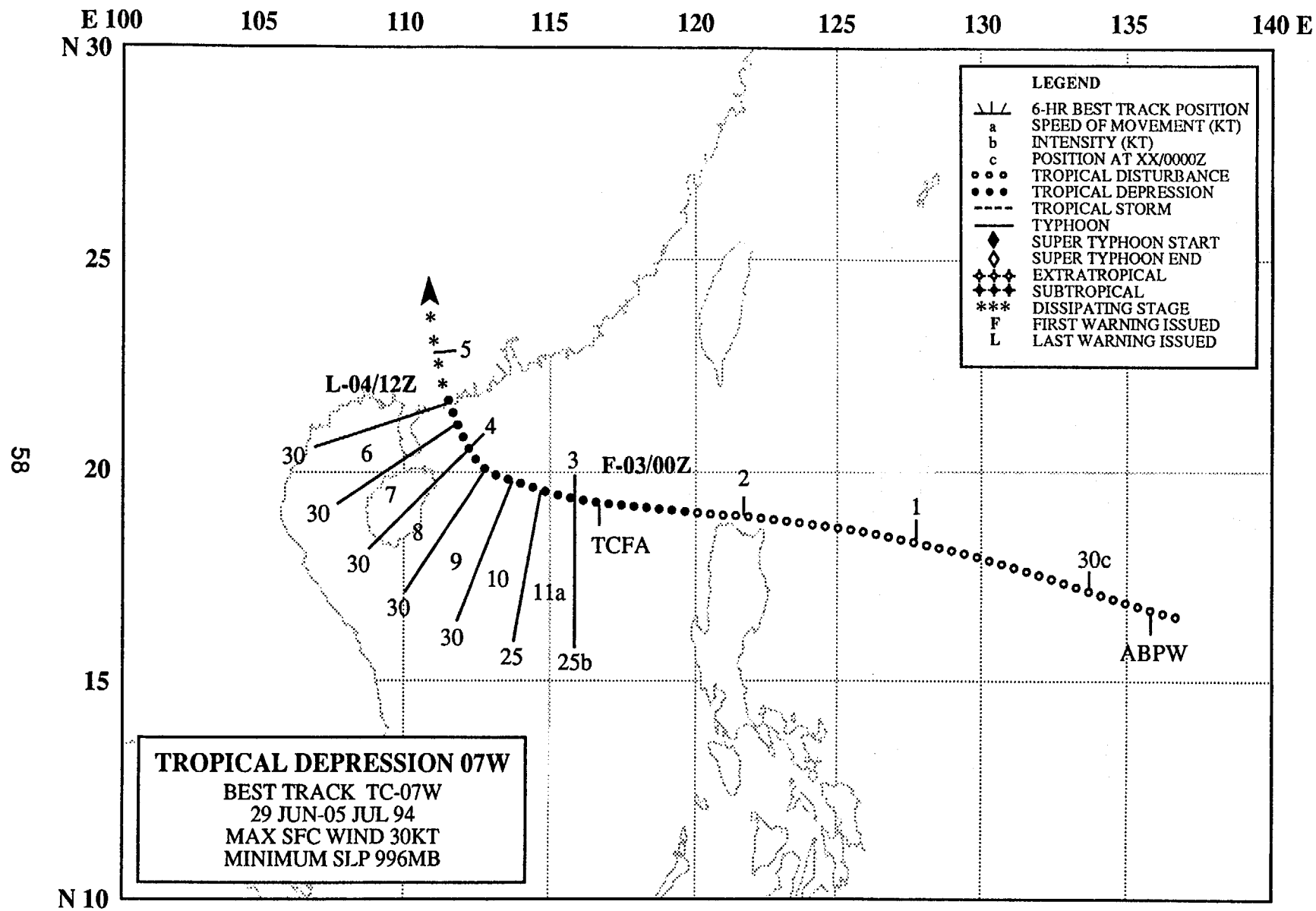


Figure 3-06-1 Just prior to its upgrade to Tropical Storm Sharon, TD 06W is located in the South China Sea to the south of Hong Kong. The lack of cirrus outflow northeast of the system center suggests that Sharon is being sheared by strong upper-level northeasterly winds (231230Z June infrared GMS imagery).

After Tropical Storm Russ (05W) went ashore in southern China on 08 June, the tropical western North Pacific quieted until mid-June when the convection in the near equatorial trough began to increase. An area of convection just south of Chuuk in the eastern Caroline Islands began to consolidate, and was first mentioned on the 180600Z June Significant Tropical Weather Advisory. The tropical disturbance moved west-northwestward at 15 kt (28 km/hr) and became more organized, prompting issuance of a Tropical Cyclone Formation Alert (TCFA) at 200730Z. When the tropical disturbance moved out of the predicted development area, a second TCFA (valid at 202300Z) was issued, followed by a 210600Z warning. Shortly thereafter, intensification arrested; most likely due to an increase in vertical wind shear. Twenty-four hours after the first warning, a final warning was issued. However, as the disturbance approached southeastern Luzon, it linked to the southwest monsoonal flow in the South China Sea that extended eastward. The convection flared again, which led to a regenerated warning valid at 221800Z. After crossing Luzon and entering the South China Sea, Sharon reached its peak intensity of 45 kt (23 m/sec) on the morning of 24 June. Vertical shearing due to strong upper-level northeasterly winds stymied further intensification (Figure 3-06-1). At 250600Z, the final warning was issued after the tropical storm went ashore in southern China, about 60 nm (110 km) east of the location where Tropical Storm Russ (05W) had gone ashore a week earlier. The combined flooding associated with Russ and Sharon left more than 1,400 people dead. The damage, which included the destruction of nearly one million houses in southern China, was estimated in excess of US\$6 billion.



TROPICAL DEPRESSION 07W

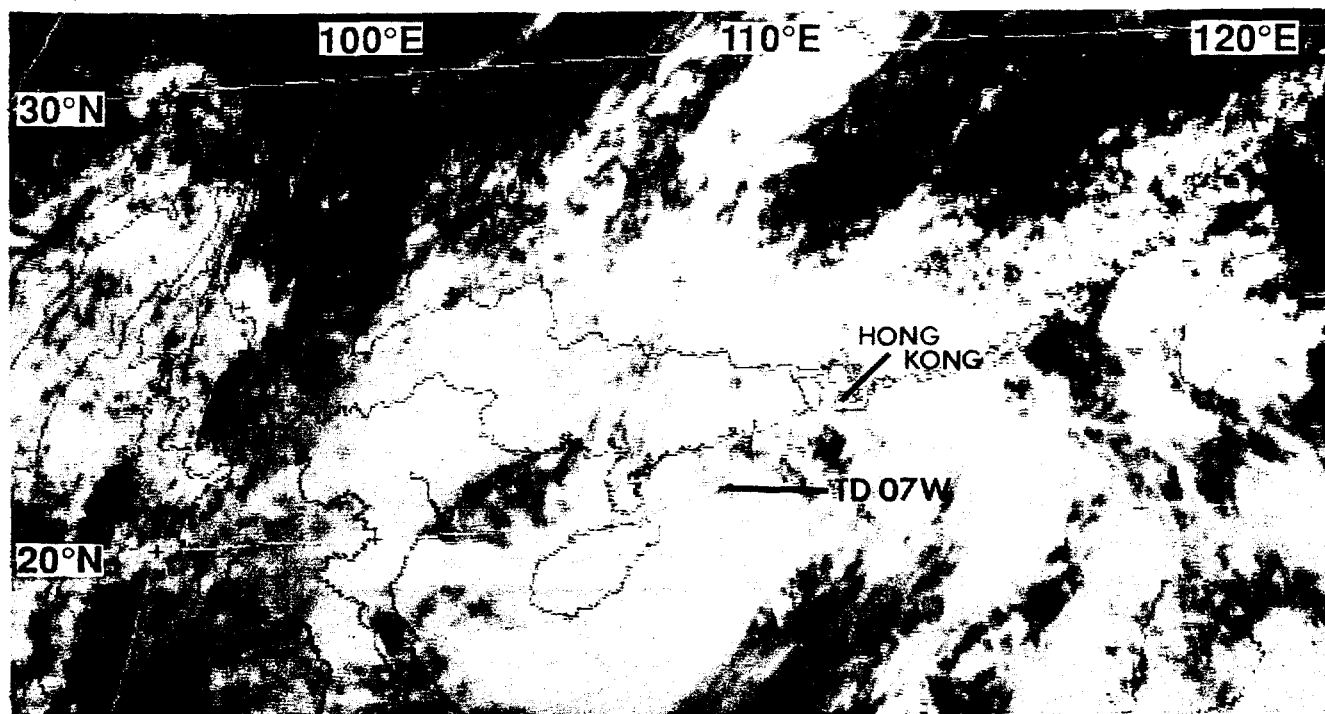
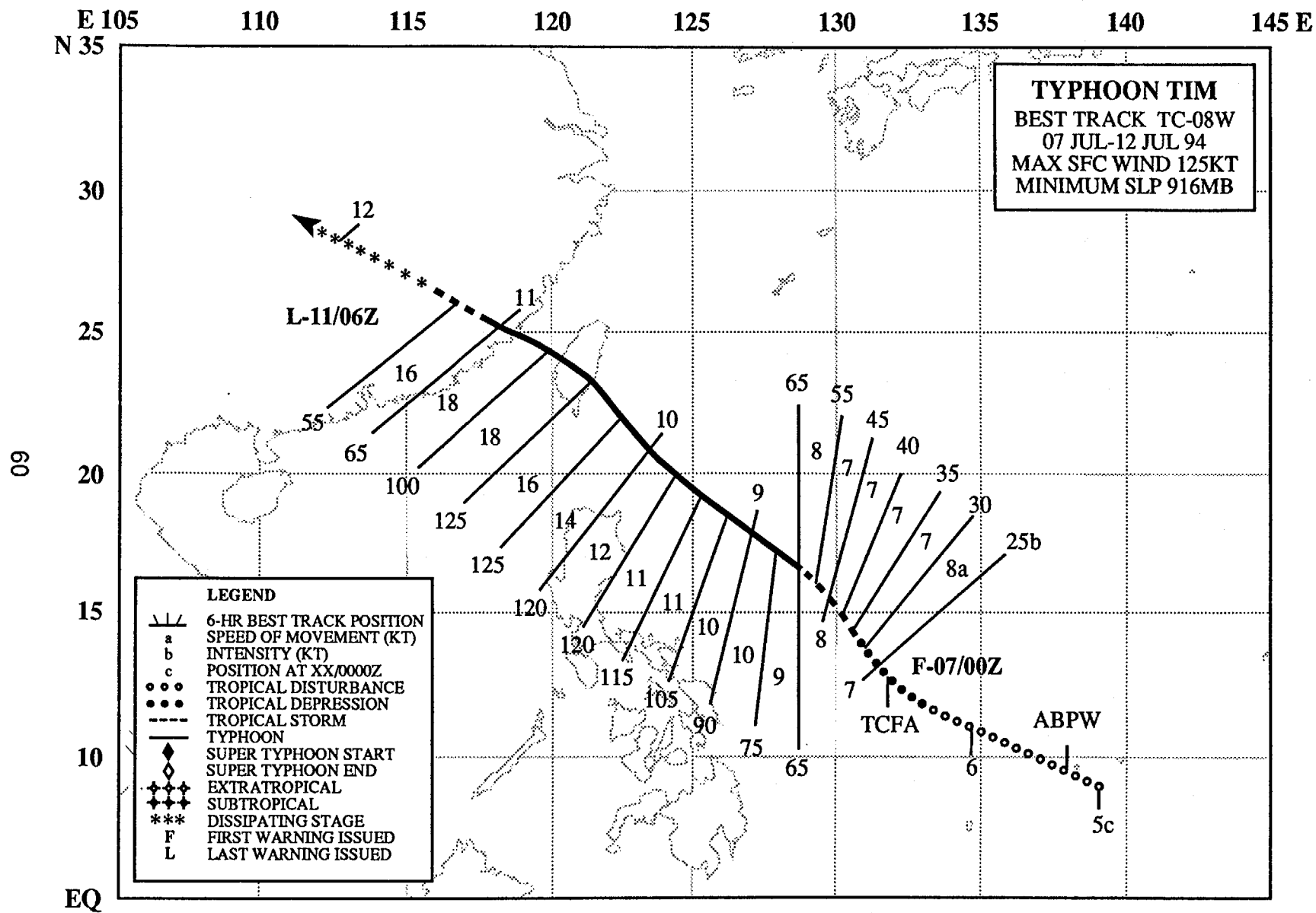


Figure 3-07-1 The result of strong northeasterly upper-level shear, Tropical Depression 07W exhibits a partially exposed low-level circulation center (LLCC) (040031Z July visible GMS imagery).

Tropical Depression (TD) 07W, the third tropical cyclone of June, developed in the monsoon trough around 17°N 135°E, late on 29 June. Under the influence of strong vertical shear, it never intensified above tropical depression intensity. The system moved across the Philippine Sea at 14-15 kt (26-28 km/hr). On 02 June, it passed north of Luzon into the South China Sea. Influenced by deep steering associated with the southwest monsoon, TD 07W slowed in forward speed, and turned toward the northwest. It reached its 30 kt (15 m/sec) maximum intensity just prior to making landfall in southern China (Figure 3-07-1), virtually in the same spot that Tropical Storm Sharon (06W) had gone ashore two weeks earlier. TD 07W dissipated over southern China. Heavy rains and flooding associated with TD 07W led to four people killed, two people missing, 6,700 houses destroyed, another 50,000 damaged, and 365 mines and factories forced to close. Total losses were estimated at \$US 114 million.



TYPHOON TIM (08W)

I. HIGHLIGHTS

After a week of relative calm in the western North Pacific, a tropical disturbance developed in the Caroline Islands on 05 July. The disturbance moved northwestward and was upgraded to Tropical Storm Tim. On 08 July, it underwent an episode of rapid intensification. A peak intensity of 125 kt (64 m/sec) was reached at 100600Z. Tim and Vanessa (09W) underwent a binary interaction that resulted in the decay and absorption of the smaller Vanessa into Tim's outer circulation. Tim made landfall in central Taiwan at 101200Z. Gusts to 98 kt (51 m/sec) were reported at Chengkung (WMO 46761).

II. TRACK AND INTENSITY

In early July, the Tropical Upper Tropospheric Trough (TUTT) intensified across the western North Pacific. Trade winds beneath the TUTT dominated the low-level flow over most of the region, except south of 10°N where the axis of a weak monsoon trough extended across Micronesia to about 160°E. By 05 July, convection over the Philippine Sea had increased south of the TUTT, and the disturbance that would become Typhoon Tim was first mentioned on the Significant Tropical Weather Advisory at 050600Z July as an area of enhanced convection south of Chuuk. On the early morning of 06 July, a Tropical Cyclone Formation Alert was issued, followed two hours later by the first warning on Tropical Depression 08W. As this system approached 130°E, it was upgraded to Tropical Storm Tim. After Tim crossed 130°E, the southwest monsoon surged across the Philippines and into the storm.

Tim reached an intensity of 55 kt (28 m/sec) at about 080600Z, then started to rapidly intensify. It reached typhoon intensity at 081200Z enroute to its peak intensity of 125 kt (64 m/sec) on the morning of 10 July. From 09 to 11 July, Tim underwent a binary interaction with Tropical Storm Vanessa (09W) (See Vanessa's Summary). Tim, much larger than Vanessa, showed little track deviation as a result of the interaction.

Tim weakened rapidly after it made landfall at Hualien County in central Taiwan at 101200Z where maximum winds of 79 kt (41 m/sec) with gusts to 98 kt (51 m/sec) were reported at Chengkung (WMO 46761) and 64 kt with gusts to 81 kt (33 m/sec with gusts to 42 m/sec) at Hualien City (WMO 46763). Ten hours later, Tim moved into mainland China as a minimal typhoon where it dissipated a day-and-a-half later over the inland mountains. The final warning on Tim was issued at 110600Z.

III. DISCUSSION

There are two primary areas of interest concerning Typhoon Tim. The first is its rapid intensification, and the second is Tim's binary interaction with Tropical Storm Vanessa. The latter is covered in the Tropical Storm Vanessa (09W) summary.

Tim intensified normally from 070000Z to 080000Z July. During this interval the developing eye wall was suppressed on the west side, most probably by upper-level westerly wind flow south of the TUTT axis (Figure 3-8-1a,b). Twelve hours later (081200Z), the shear had relaxed. A complete eye wall formed, and peripheral bands of deep convection developed in all quadrants and an episode of rapid intensification began. From 081200Z until 091200Z, Tim intensified at a rate of 49 mb/day or 2.04 mb/hr. This meets the requirement for rapid intensification — 42 mb/day or 1.75 mb/hr — as designated by Holliday and Thompson (1979). After 091200Z, Tim's rate of intensification slowed, and it reached its peak intensity of 125 kt (64 m/sec) at 100600Z (Figure 3-08-2).

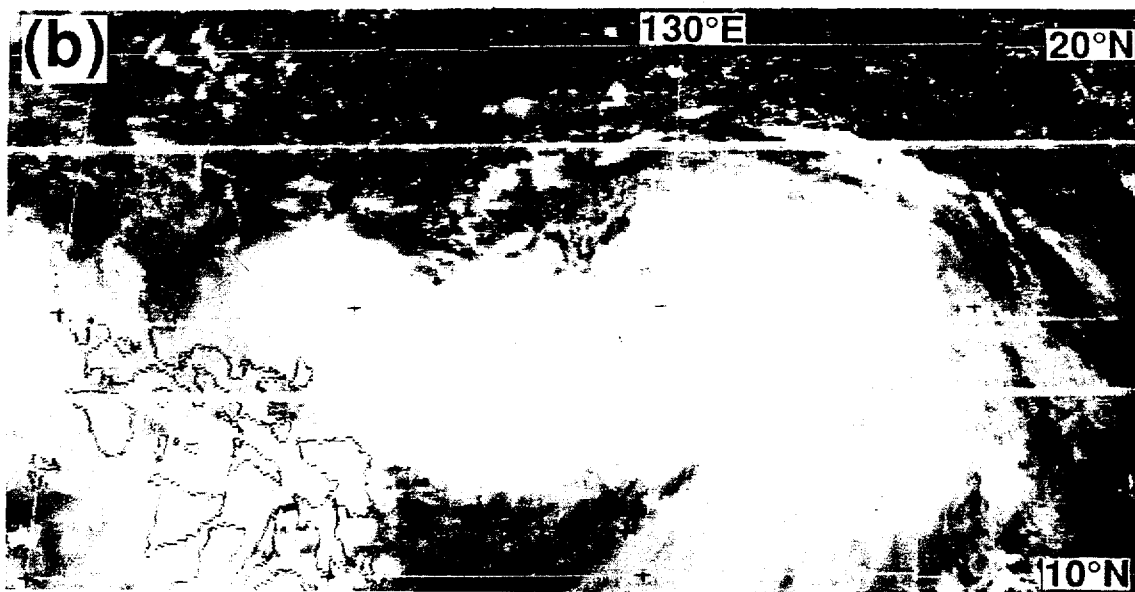
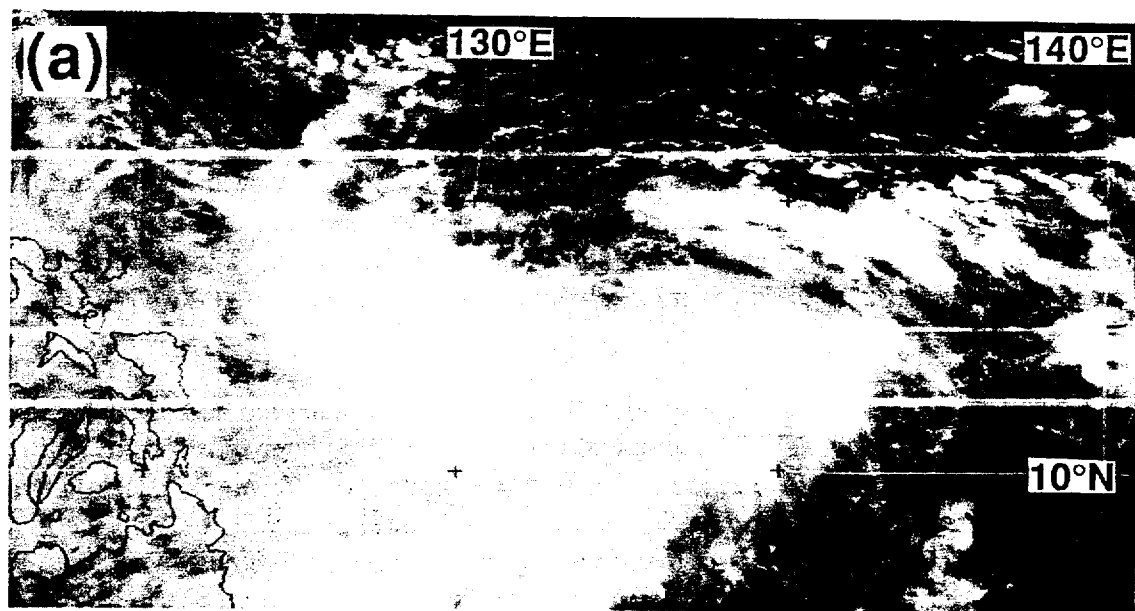


Figure 3-08-1 Tim intensifies despite apparent shearing from the west: (a) 070031Z July visible GMS imagery; (b) 080031Z July visible GMS imagery.

IV. IMPACT

In Taiwan, 39 fishermen were missing as a result of Tim when their fishing trawler ran aground near the eastern coastal city of Ilan. Elsewhere in Taiwan, four people were killed, and several highways were closed as a result of landslides from torrential rains.

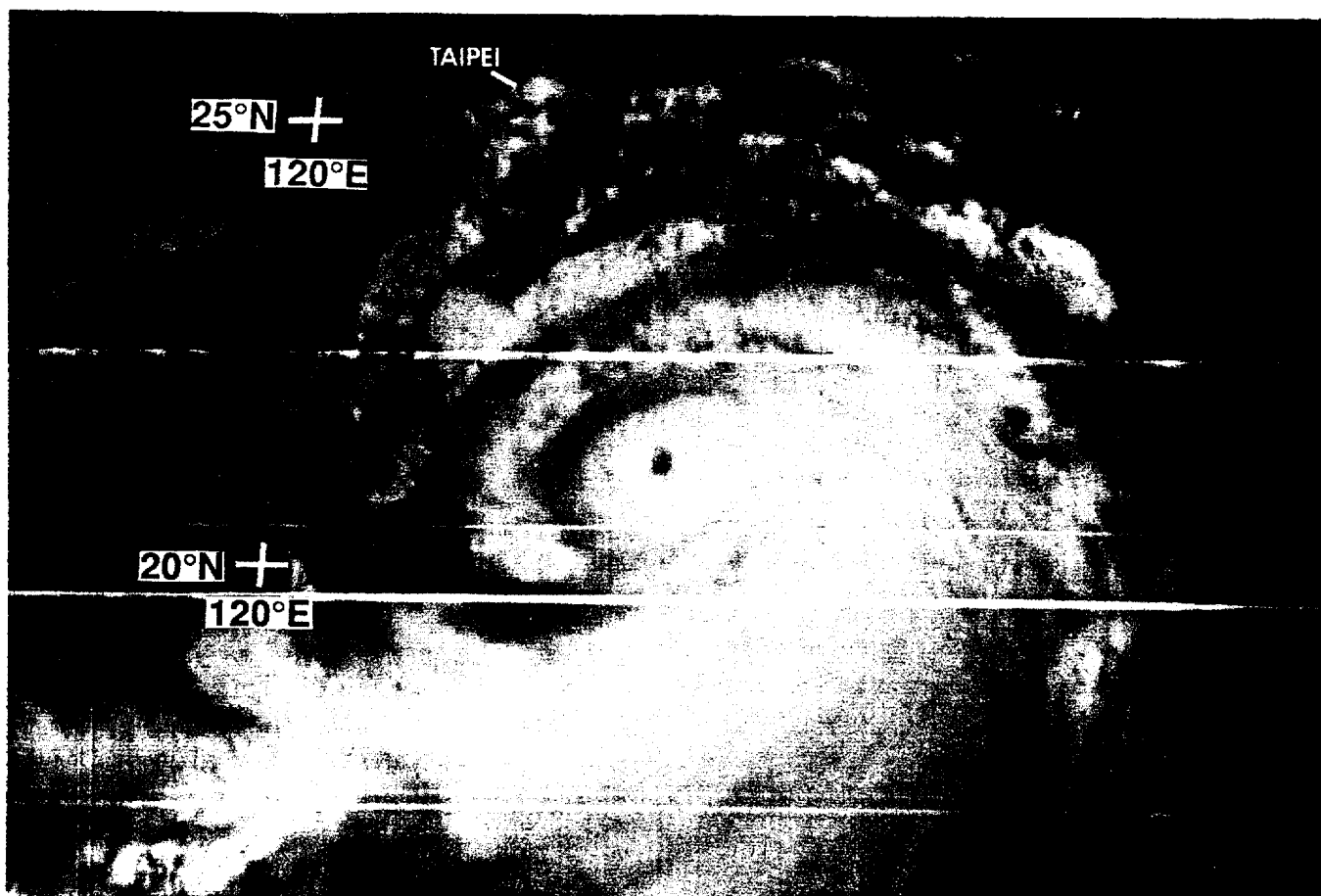


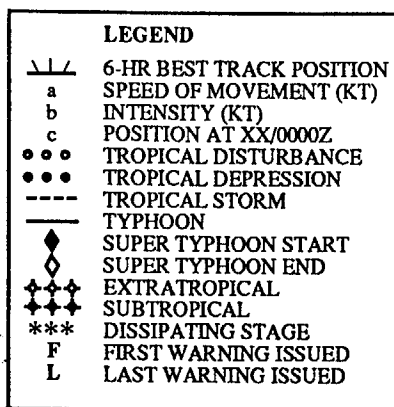
Figure 3-08-2 Tim at 120 kt (62 m/sec) six hours prior to reaching its peak intensity of 125 kt (64 m/sec) (100031Z July visible GMS imagery).

E 110
N 25

115

120

125 E

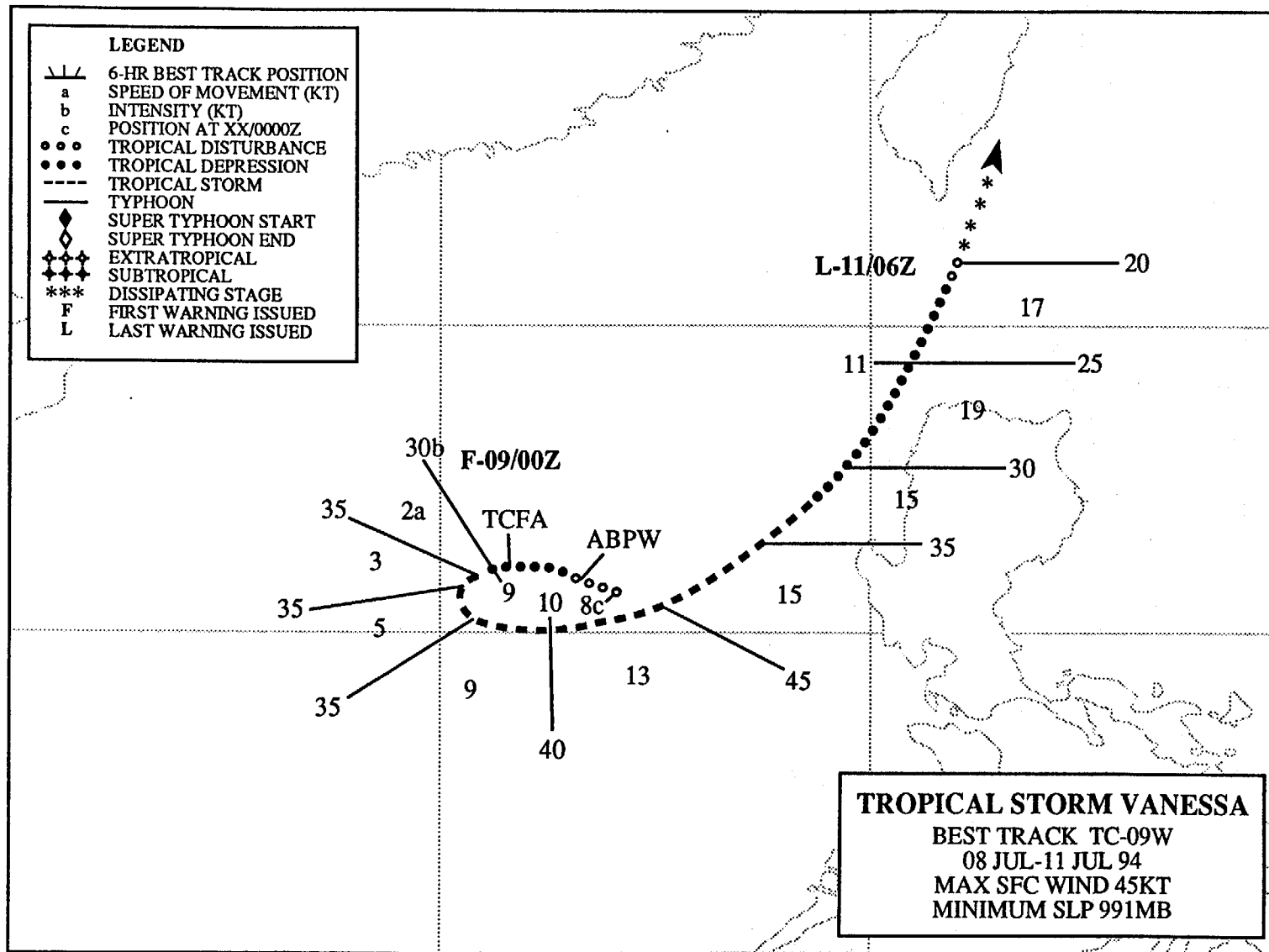


64

20

15

N 10



TROPICAL STORM VANESSA (09W)

I. HIGHLIGHTS

The second of five tropical cyclones to form in the South China Sea during 1994, Vanessa was small. Interacting with the larger Typhoon Tim (08W), Vanessa moved northeastward, closing to within about 400 nm (740 km) of Tim. Vanessa's convection then was sheared away and its low-level circulation center was absorbed by Tim's outer circulation.

II. TRACK AND INTENSITY

During the first week of July, the monsoon trough extended across the South China Sea at about 15°N, and from there, east-southeastward into Micronesia. A few days prior to the formation of Vanessa in the South China Sea, larger-sized Typhoon Tim (08W) formed in the Philippine Sea and moved west-northwestward towards Taiwan. As Tim matured in the Philippine Sea, a tropical disturbance in the South China Sea, located just west of Luzon, began to show signs of development. Synoptic data and satellite imagery showed that a low-level circulation center had persisted for 24 hours, and this tropical disturbance was mentioned on the 080600Z July Significant Tropical Weather Advisory. Satellite imagery on the morning of 09 July showed that this system had become well organized (Figure 3-09-1). A Tropical Cyclone Formation Alert was issued at 082200Z followed by the first warning at 090000Z. After an initial period of slow westward motion, Vanessa executed a counter-clockwise loop, and then tracked northeastward under the steering influence of Tim's larger circulation and deep southwesterly monsoon flow.

Vanessa reached a peak intensity of only 45 kt (23 m/sec), possibly due to vertical and horizontal shearing imposed on it by the larger Typhoon Tim (08W) (Figure 3-09-2), before it was destroyed in a merger with Tim. The final warning was issued at 110600Z when satellite imagery and synoptic data indicated that Vanessa's circulation had disappeared into Tim's southeastern quadrant.

III. DISCUSSION

Asymmetrical tropical cyclone merger — wherein one tropical cyclone loses its deep convection and its remnant low-level circulation is swept into the remaining intact tropical cyclone — is the norm for a binary interaction that ends in merger (Lander and Holland 1993). Vanessa's binary interaction with Typhoon Tim (Figure 3-09-3) was a typical case of the merger of two tropical cyclones. In contrast, the first-ever observed case of symmetrical dissolution of deep convection and merger of two tropical cyclones occurred later in the year when Pat (29W) and Ruth (30W) merged (see their summaries later in this chapter).

IV. IMPACT

Tropical Storm Vanessa battered the northern Philippines with strong winds and heavy rains. Torrential rains triggered landslides along major highways and explosions of superheated material on the slopes of Mount Pinatubo. One person was killed and three injured by flying debris from the Pinatubo explosions. In northern Luzon, a man was killed when the roof of his house collapsed.

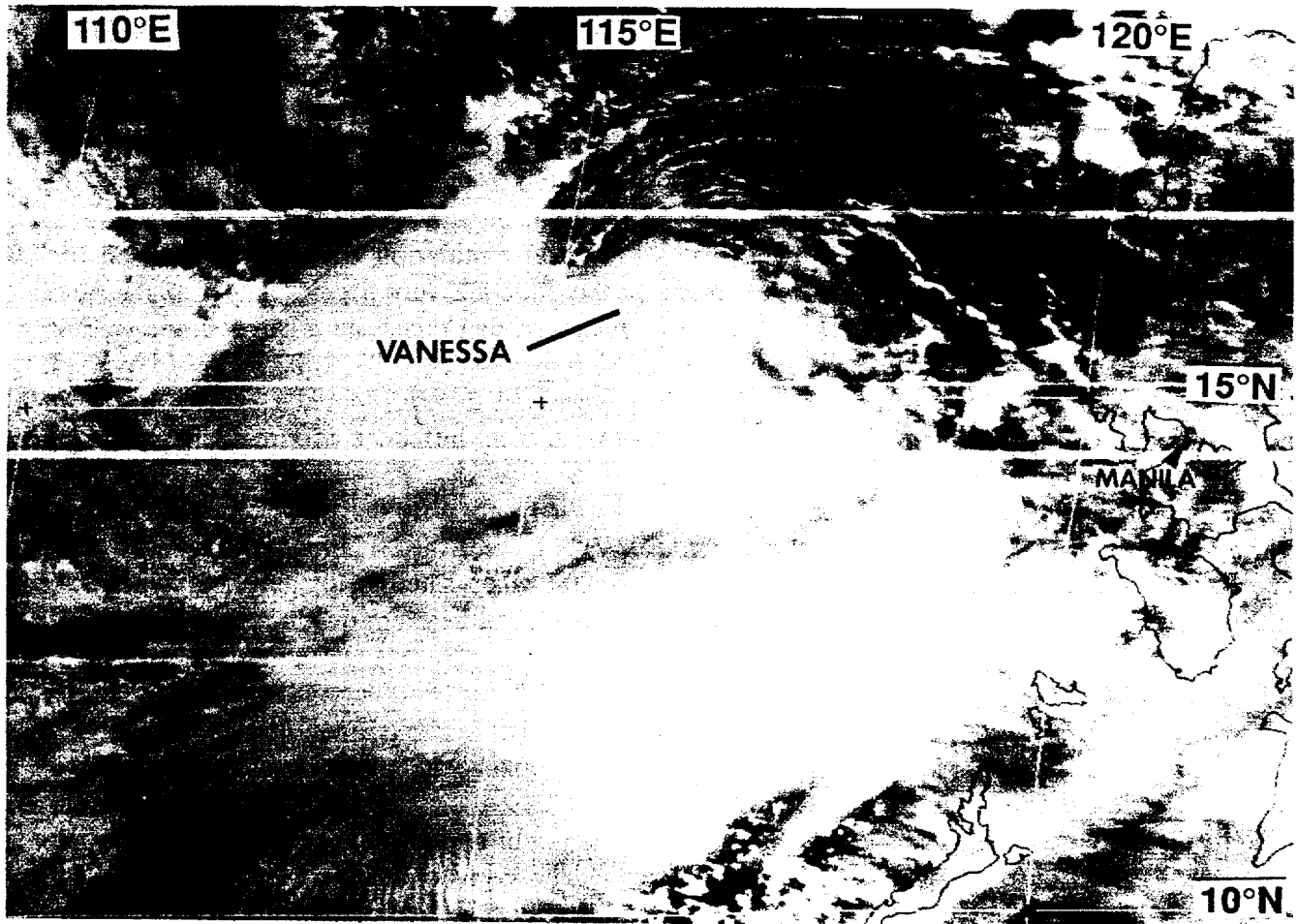


Figure 3-09-1 Well-organized low-level cloud lines and a central dense overcast prompted the first warning on Tropical Storm Vanessa (082331Z July visible GMS imagery).

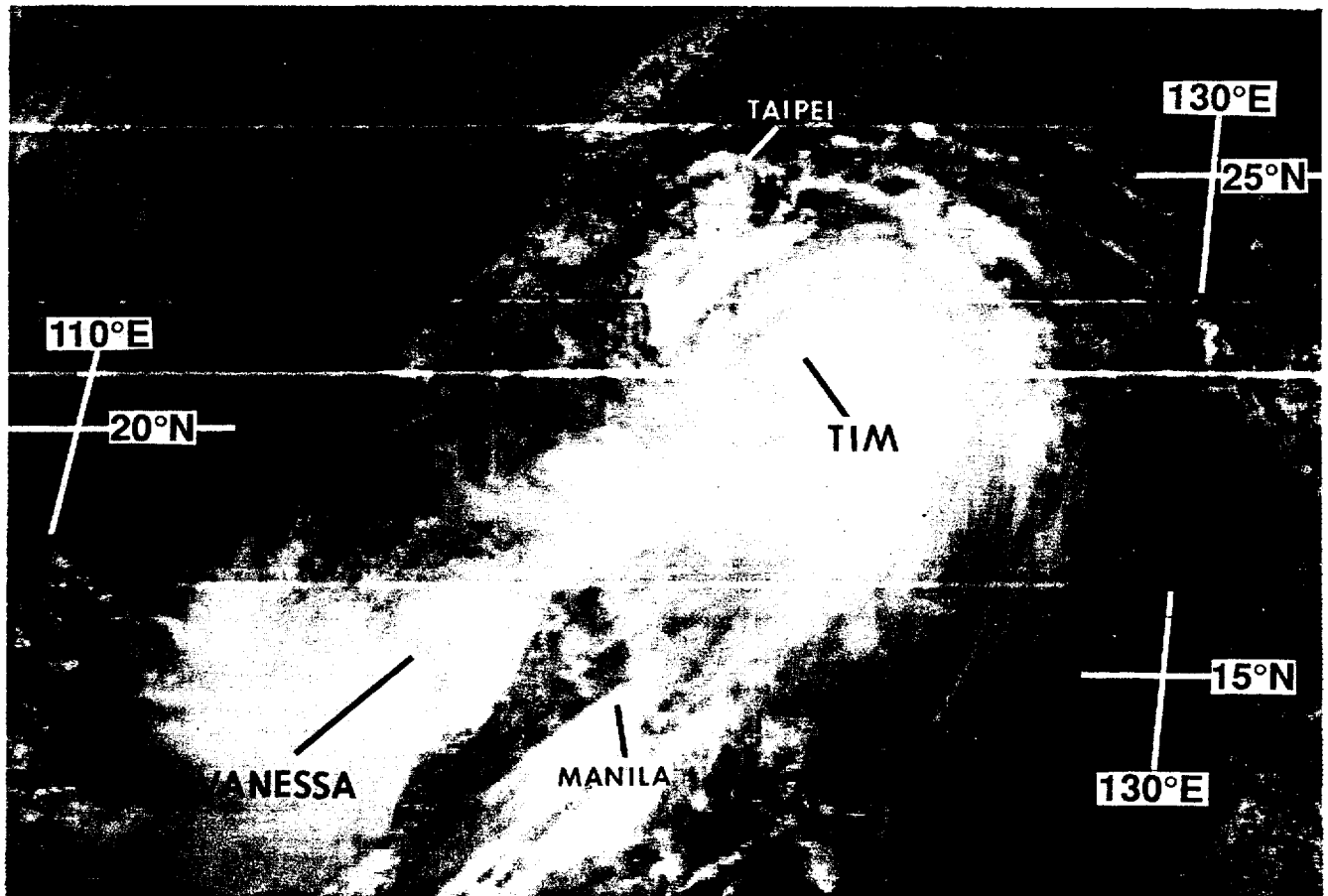


Figure 3-09-2 Vanessa is moving northeastward under the influence of the outer circulation of Typhoon Tim (08W) and strong southwesterly monsoonal flow (100131Z July visible GMS imagery).

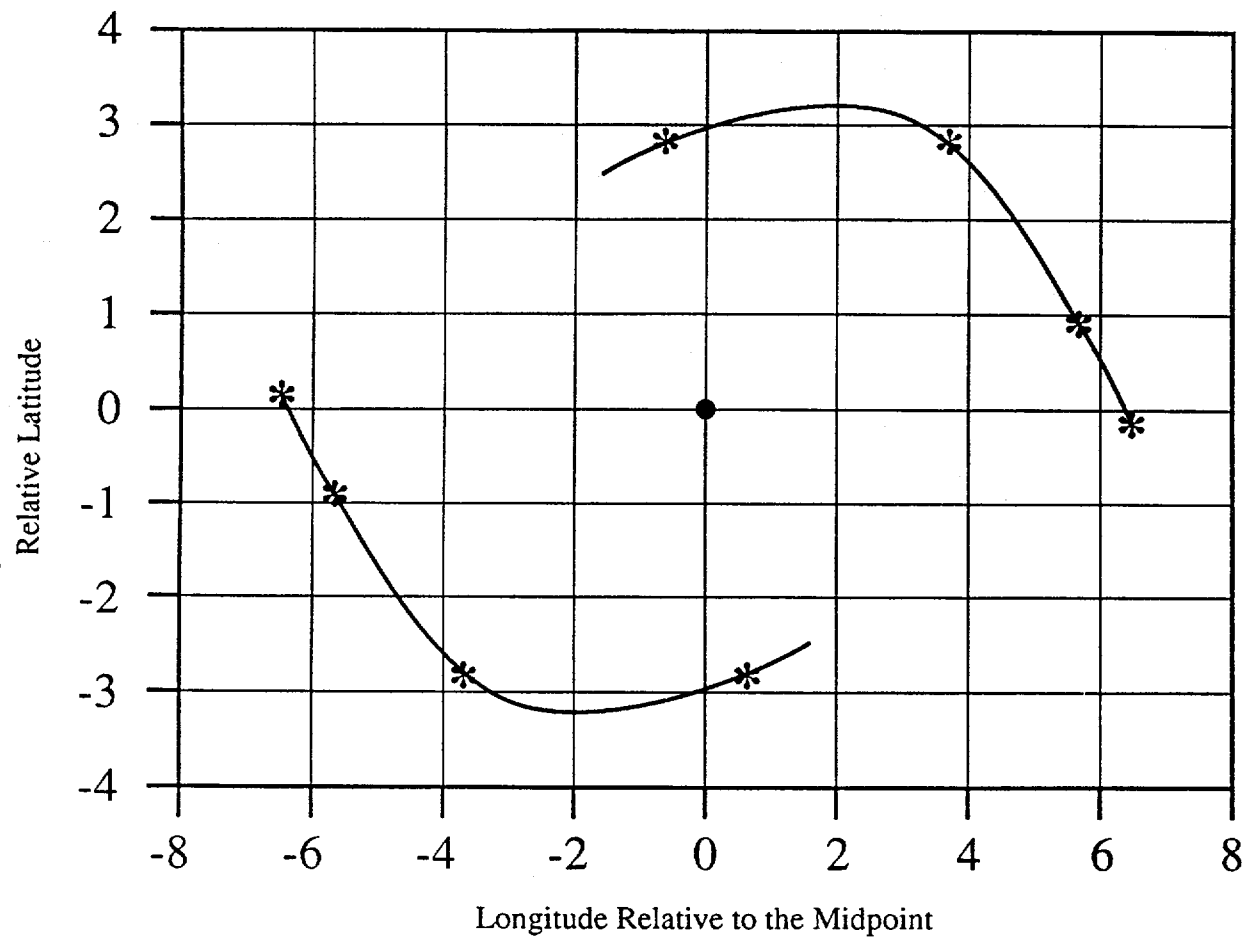
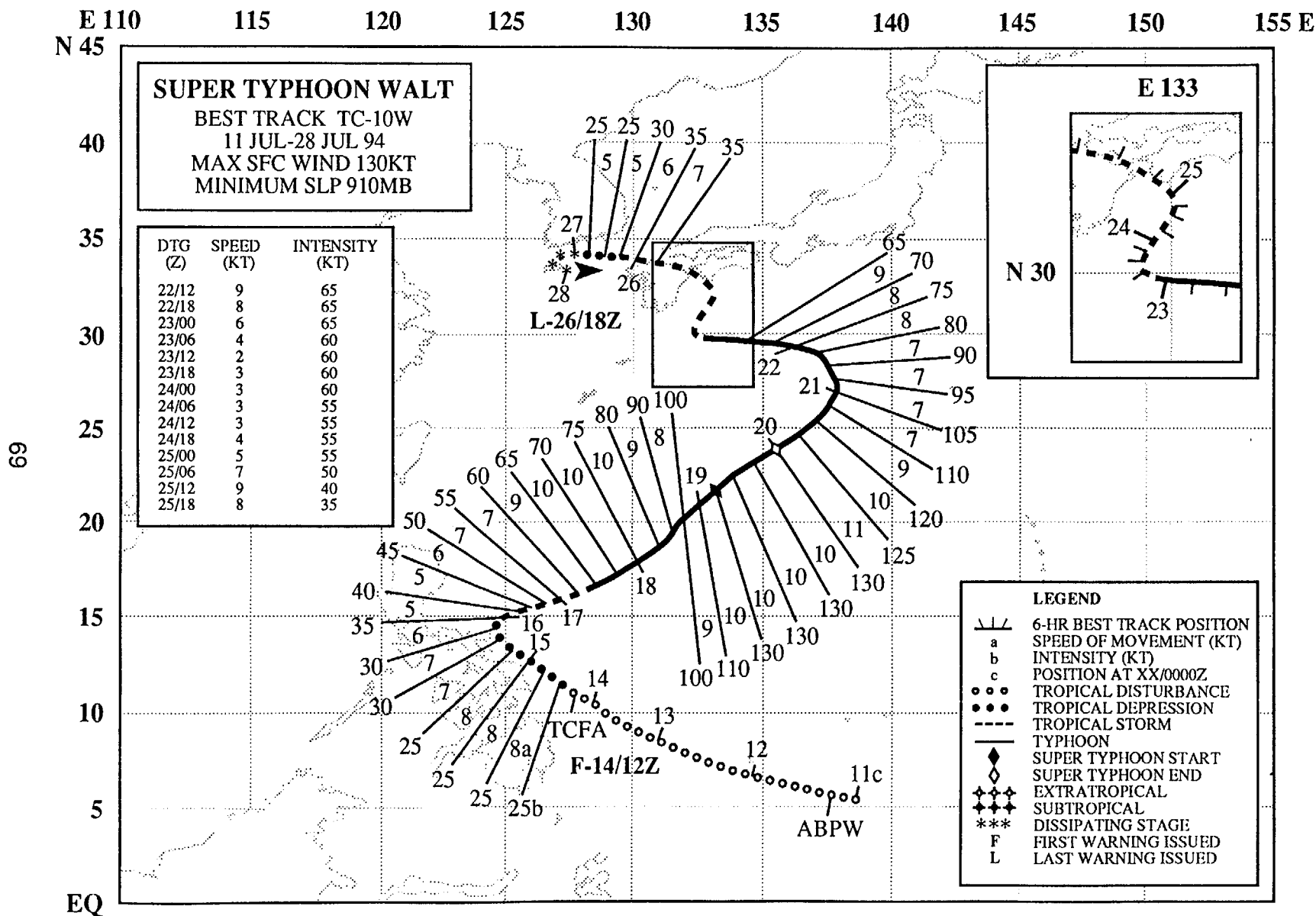


Figure 3-09-3 The binary interaction of Vanessa with Tim (08W) in a centroid-relative frame of reference.



SUPER TYPHOON WALT (10W)

I. HIGHLIGHTS

The first tropical cyclone of 1994 in the western North Pacific to become a super typhoon, Walt was the larger and more intense of three named tropical cyclones which, for several days, were located along the axis of a reverse-oriented monsoon trough (Figure 3-10-1 and Figure 3-10-2). Typical of tropical cyclones embedded in a reverse-oriented monsoon trough, Walt exhibited unusual motion: eastward motion at low latitudes followed by a turn to the north. After reaching its peak intensity of 130 kt (67 m/sec), Walt slowly decayed as it made a gradual turn from a northward to a westward track. Before dissipating in the Korea Strait, its remnant cloud system brought much needed rain to some drought-stricken portions of South Korea.

II. TRACK AND INTENSITY

During early July, the axis of the monsoon trough extended across much of Micronesia at rather low latitudes (5° - 7° N). Most of the deep convection associated with this monsoon trough was located south of 10° N. By 11 July, a persistent cloud cluster had consolidated near Palau. The first mention of this

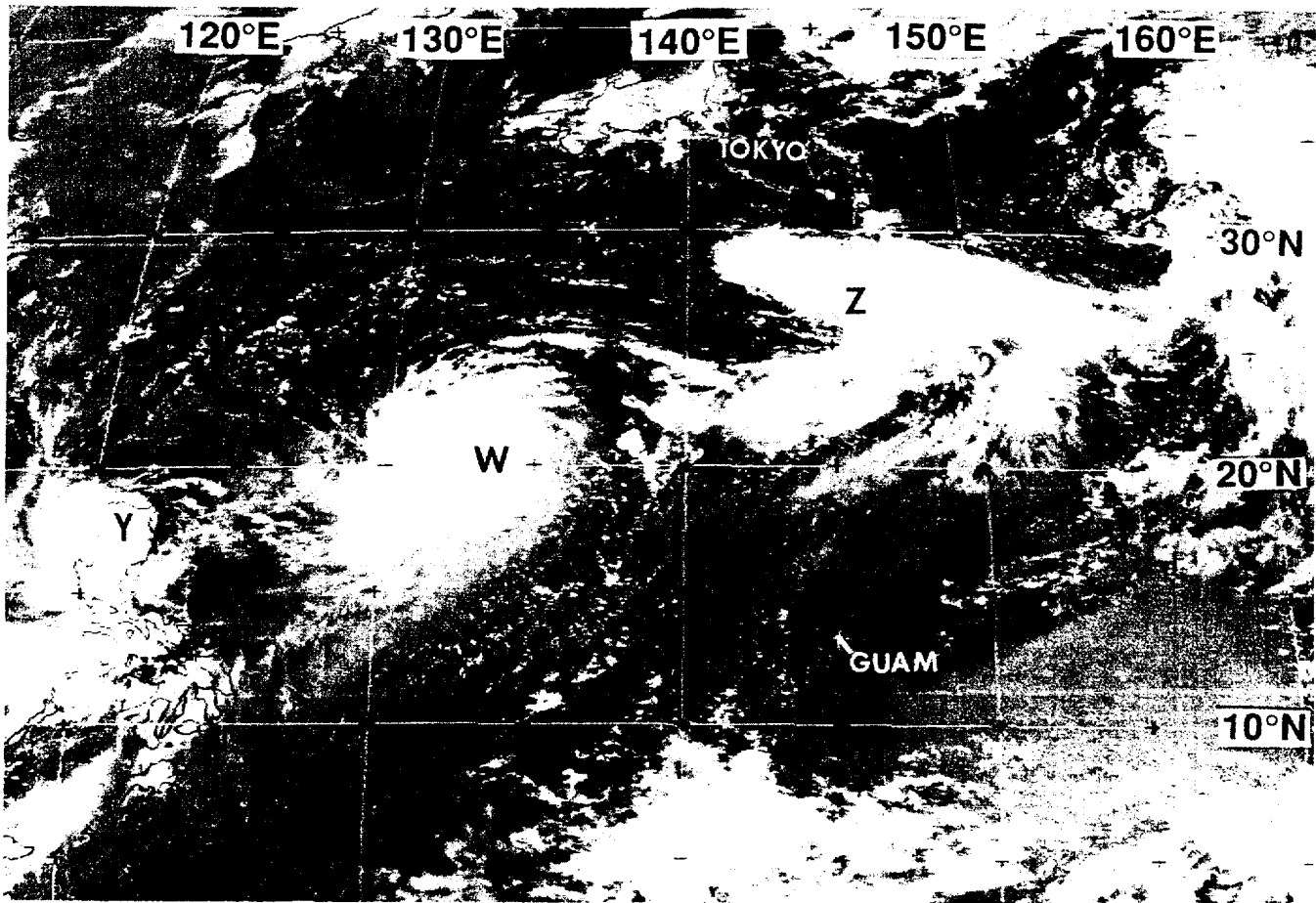


Figure 3-10-1 Yunya (11W), Walt, Zeke (12W), and a subtropical disturbance are aligned SW-NE along the axis of a reverse-oriented monsoon trough (190031Z July visible GMS imagery).

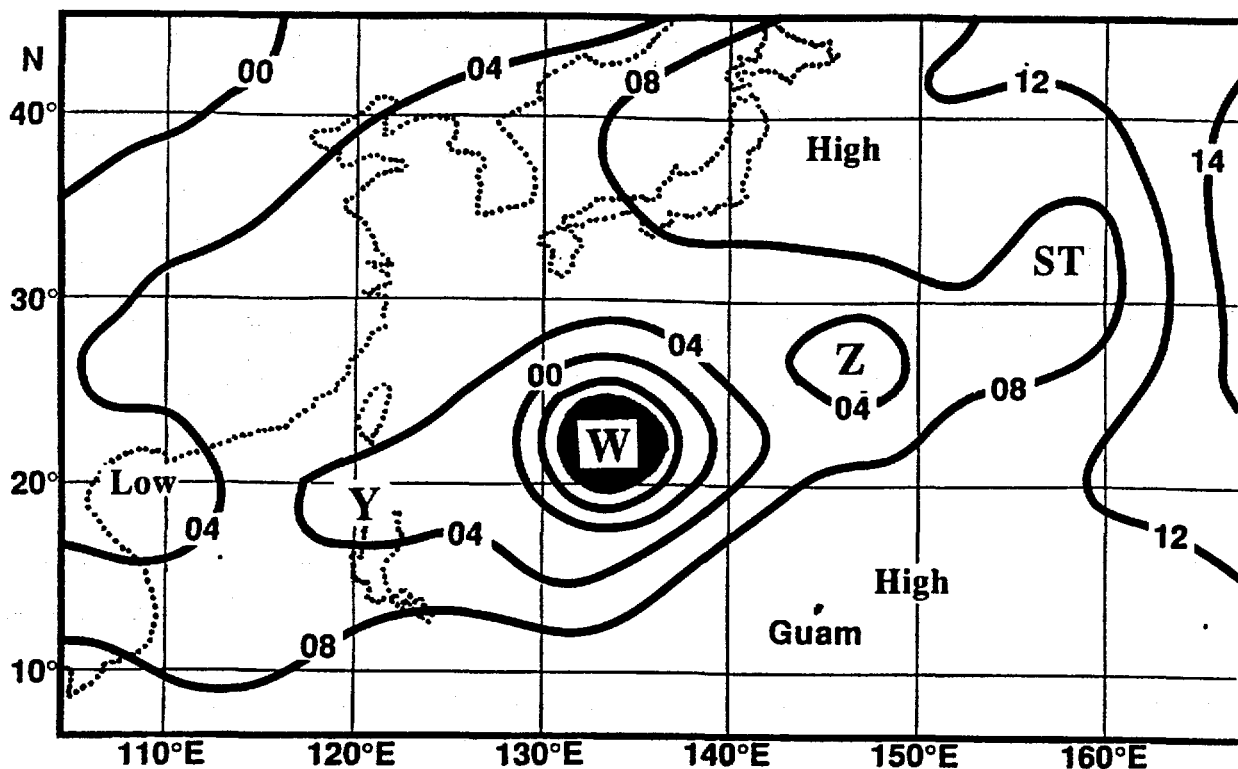


Figure 3-10-2 As in Figure 3-10-1, except sea-level pressure analysis at 190000Z July.

cloud cluster as a suspect tropical disturbance appeared on the 110600Z July Significant Tropical Weather Advisory. During the next few days, this tropical disturbance moved slowly northwestward. At 140800Z, the organization of the deep convection had further improved, and a Tropical Cyclone Formation Alert was issued. The first warning was issued soon thereafter at 141200Z.

Initially, Walt (as a tropical depression) moved northwestward towards Luzon. Then it slowed and turned towards the northeast at a relatively low latitude (15°N), and intensified. Concurrent with Walt's low-latitude turn toward the northeast, a long band of deep convective cloud clusters (which included Walt's cloud system) acquired a SW-NE (i.e., reverse) orientation, and extended from 15°N in the South China Sea to 30°N near the international date line. This cloud band signaled the onset of the year's first of three episodes of reverse orientation of the monsoon trough.

As Walt moved northeastward, it continued to intensify. By 190600Z its intensity peaked at the 130 kt (67 m/sec) super typhoon threshold (Figure 3-10-3). This peak intensity remained until 200000Z, when it began to slowly weaken. At 210000Z, Walt turned towards the west. Dropping below typhoon intensity shortly after 230000Z, Walt then tracked northward for two days. A westward turn at 250000Z led Walt to landfall at 250600Z on the southwestern end of the Japanese island of Shikoku. The estimated intensity at landfall was 50 kt (26 m/sec). Walt dissipated over water south of Korea after crossing southern Japan. The final warning was issued at 261800Z.

III. DISCUSSION

a. Unusual motion

The track of Super Typhoon Walt was north-oriented (JMA 1976). Tropical cyclones which move

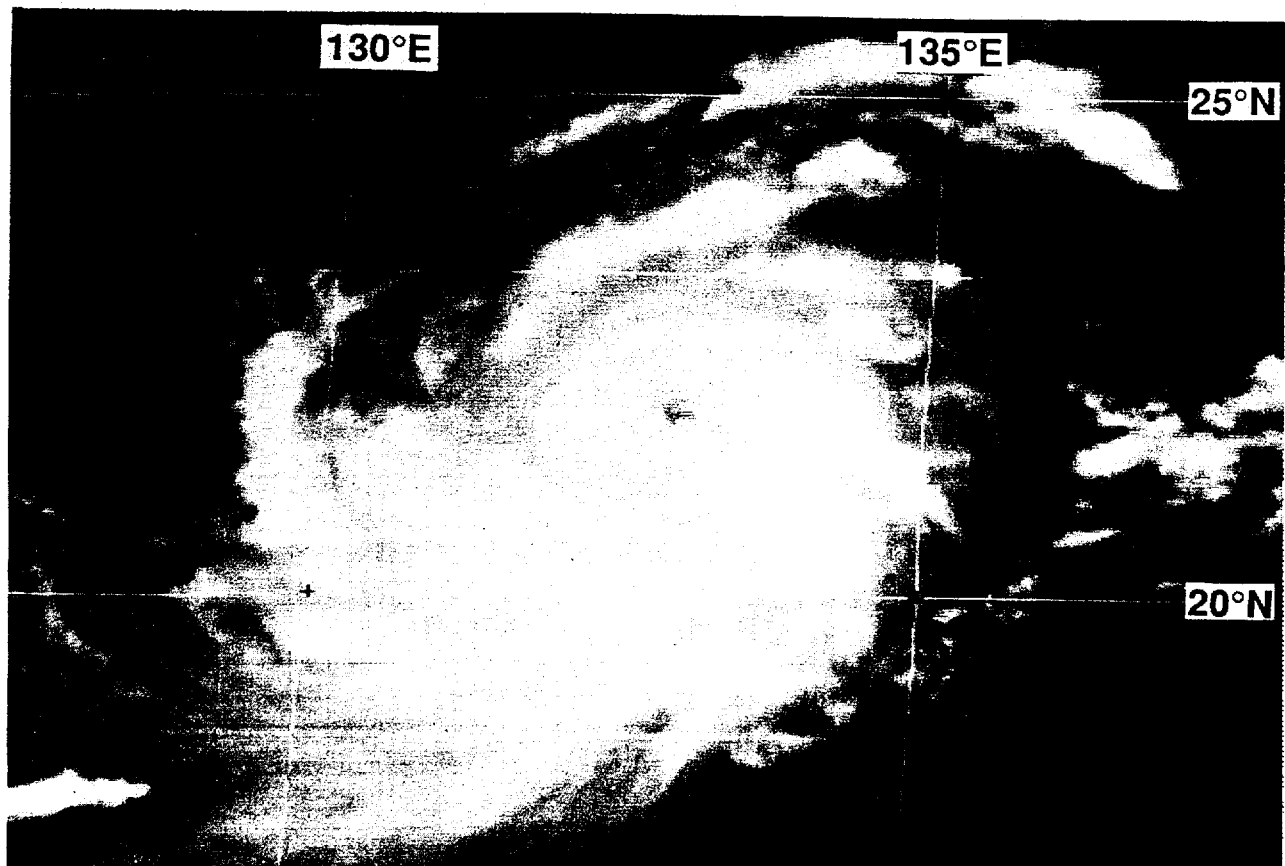


Figure 3-10-3 Walt at peak intensity (190600Z July visible GMS imagery).

on such tracks follow long generally northward paths from their genesis location into the mid-latitudes. A north-oriented track may feature large meanders and abrupt turns to the left or right. The speed of forward motion is often slower than average. Many north-oriented tracks feature eastward motion at low latitudes, and some even have an eastward component of motion for their entire track. Most north-oriented motion occurs during July through September (Lander 1995a).

The pattern of the large-scale low-level monsoon circulation of the western North Pacific has been shown to be a discriminator of tropical cyclone track type (Harr and Elsberry 1991; Lander 1995a). One pattern in particular, the reverse-oriented monsoon trough, has been shown by Lander (1995a) to be almost exclusively associated with north-oriented motion.

In its simplest description, the large-scale low-level circulation of summer over the western North Pacific can be described in terms of low-latitude southwesterlies, a monsoon trough and a subtropical ridge (Figure 3-10-4a). The axis of the summer monsoon trough of the western North Pacific usually emerges from East Asia at about 20° N to 25°N, and extends southeastward to a terminus southeast of Guam (13°N ; 145°E) (Sadler et al. 1987). Most of the tropical cyclones which develop in the western North Pacific form in the monsoon trough. When the axis of the monsoon trough is in its normal orientation (NW-SE), tropical cyclones tend to move northwestward on tracks close to those expected from climatology. As an episodic event, the axis of the monsoon trough becomes displaced to the north of its usual location and takes on a SW-NE (i.e., reverse) orientation (see Figure 3-10-4b). When the monsoon trough acquires a reverse orientation, tropical cyclones along it tend to move on north-oriented tracks, as was the case with Walt.

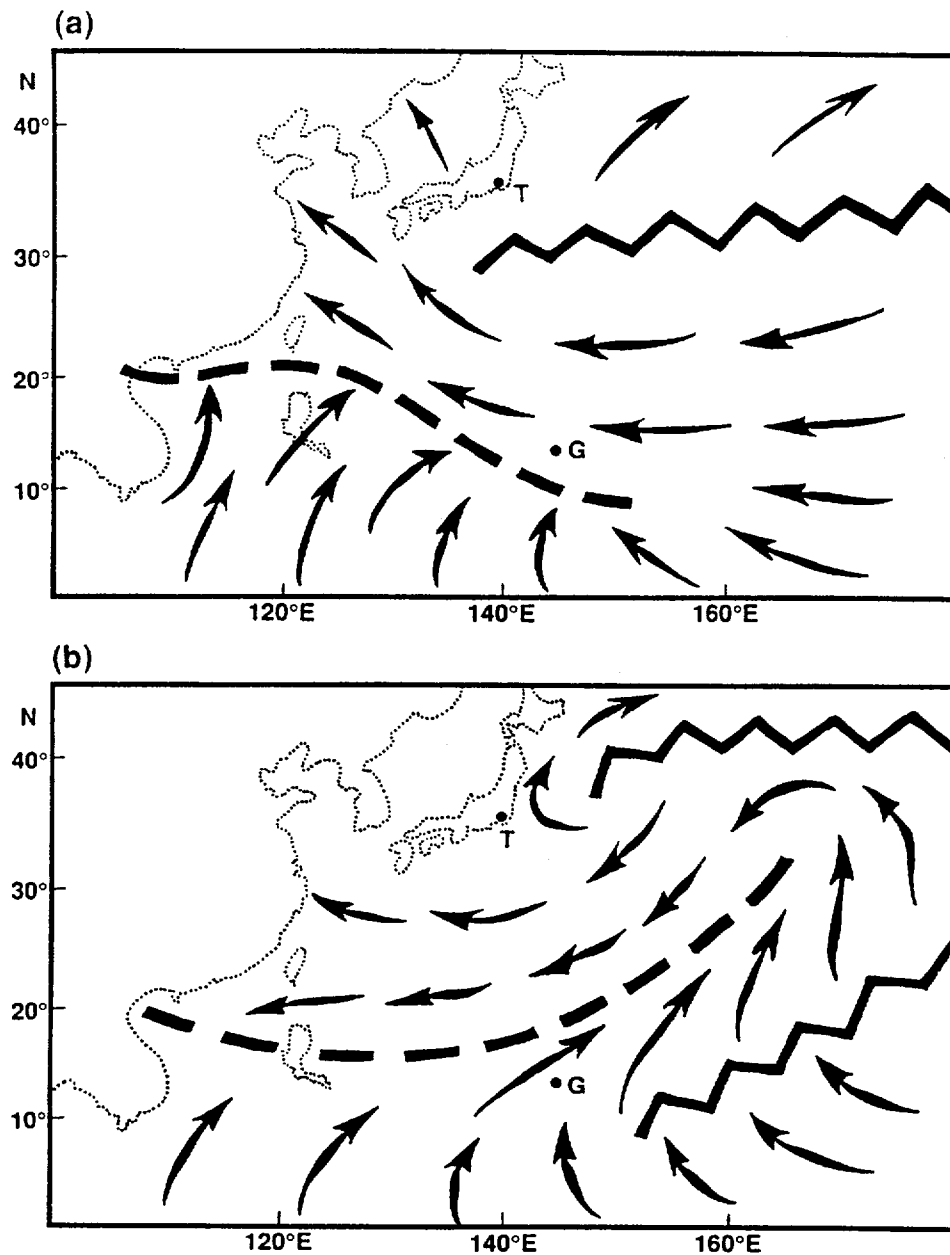


Figure 3-10-4 The low-level circulation of summer in the tropics of the western North Pacific: (a) the long-term average; and (b) a schematic illustration of the low-level circulation associated with a reverse-oriented monsoon trough. Bold zig-zag lines indicate ridge axes, and bold dashed line indicates the axis of the monsoon trough. Arrows indicate wind direction. The location of Guam (G) and Tokyo (T) are indicated.

b. Decay over warm water

After reaching super typhoon intensity over the warm waters of the Philippine Sea, Walt gradually weakened while moving slowly northward towards southern Japan. Although it was over warm sea surface temperatures, Walt weakened from 130 kt (67 m/sec) at 200000Z to 50 kt (26 m/sec) by 250600Z (the time of landfall in southern Japan) without any signs of appreciable vertical shear. By 280600Z Walt had completely dissipated.

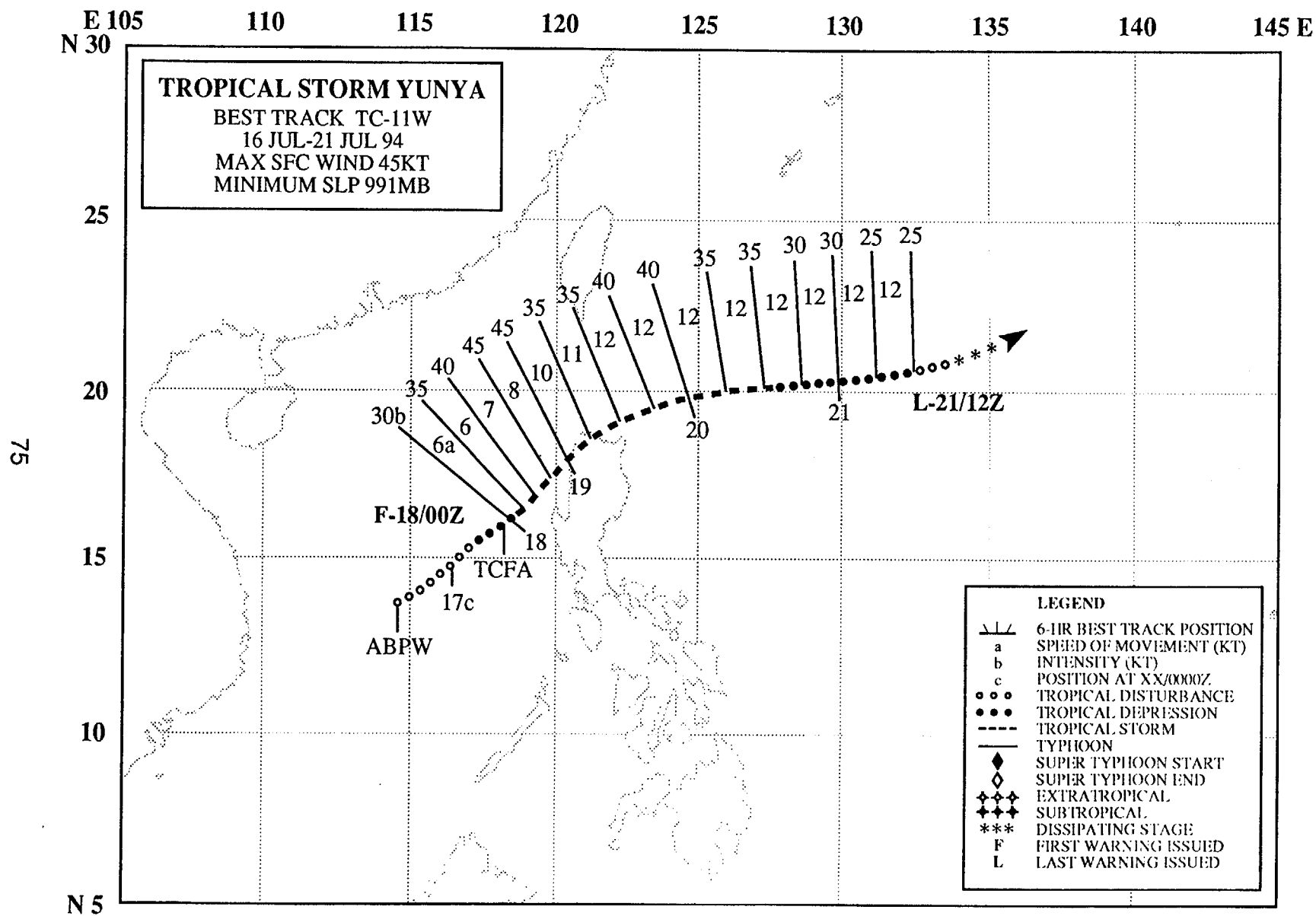
c. Forecast performance

Overall, the official forecasts for Walt were good. The track forecast extracted from the NOGAPS model (the objective aid, "NGPS", received at the JTWC) and the forecast low-level wind fields made by the NOGAPS model had two periods of difficulty during the lifetime of Walt. The biggest problem with the numerical guidance provided by the Navy's NOGAPS model (e.g., wind and height fields, and the track aid "NGPS") was in the prediction of the size of Walt in relation to the prediction of the sizes of two other tropical cyclones, Yunya (11W) and Zeke (12W), that accompanied Walt along the axis of the monsoon trough. Early in Walt's life, the NOGAPS model was greatly over-forecasting the size and intensity of the pre-Zeke tropical disturbance that was located to the east of Walt. At the same time, the size and intensity of Walt were under-forecast by NOGAPS. As a result, the model output showed Walt dissipating and being swept eastward into the exaggerated circulation of Zeke (12W).

A few days later, the NOGAPS forecasts radically changed. They began to over-forecast the size of Walt, causing the model-predicted track of the smaller Zeke (12W) to be affected (i.e., to undergo a binary interaction with Walt that moved it too far to the north and west). Walt did eventually become a large and very intense typhoon, so the NOGAPS forecasts which called for Walt to grow extremely large verified reasonably well; however, this relatively minor error had significant consequences on the track forecasts of Zeke (12W) (see Zeke's summary).

IV. IMPACT

No reports of fatalities or significant damage were received. As a weak tropical storm passing over southern Japan, peak recorded wind gusts were near 35 kt (17 m/sec). Rainfall in southern portions of the Korean Peninsula caused by Walt helped to alleviate ongoing severe drought conditions.



TROPICAL STORM YUNYA(11W)

I. HIGHLIGHTS

Yunya was a very small tropical cyclone that formed along the axis of a reverse-oriented monsoon trough. It was the westernmost of three tropical cyclones along this trough. The other two were Walt (10W) and Zeke (12W). Yunya exhibited unusual eastward motion for its entire track which resulted in a rare west-to-east crossing of Luzon. Weakened by its passage over Luzon, it briefly re-intensified over water in the Philippine Sea before dissipating.

II. TRACK AND INTENSITY

During mid-July, an active reverse-oriented monsoon trough dominated the low-level circulation of the western North Pacific. The cloudiness associated with the southwesterly monsoon flow stretched eastward from Southeast Asia, across the South China Sea and the Philippine islands; then east-northeastward across the Philippine Sea toward sub-tropical latitudes near the international date line. On or about 16 July, the monsoon cloud band evolved into a sequence of several distinct cloud clusters, three of which became named tropical cyclones: Walt (10W), Yunya, and Zeke (12W). By 160000Z, animated satellite imagery and synoptic data indicated that a weak low-level circulation center was associated with a cloud cluster over the South China Sea. This tropical disturbance was first mentioned in the 160600Z July Significant Tropical Weather Advisory. As the low-level circulation center moved toward the east-northeast, the organization of the associated deep convection improved (Figure 3-11-1), and at 172300Z a Tropical Cyclone Formation Alert was issued. The first warning was issued an hour later at 180000Z. The system was upgraded to Tropical Storm Yunya at 181800Z. Post analysis indicated that tropical storm intensity had most probably occurred 12 hours earlier at 180600Z. As Yunya neared landfall on the northwest corner of Luzon, its satellite cloud signature improved (Figure 3-11-2). At the landfall, shortly after 190000Z, its intensity was estimated to be 45 kt (23 m/sec). During the six-hour passage over land, its cloud structure became disorganized, and the best-track intensity was lowered to 35 kt (17 m/sec) at 190600Z. Moving eastward, Yunya was soon over water in the Philippine Sea. A brief period of re-intensification to 40 kt (21 m/sec) took place and persisted for six hours (191800Z to 200000Z). Deep convection then decreased, and the final warning was issued at 211200Z as Yunya moved eastward over water and dissipated.

III. DISCUSSION

a. Unusual motion

Yunya's motion had an eastward component for its entire track. This type of unusual motion is commonly associated with tropical cyclones which are located within a reverse-oriented monsoon trough. For a more thorough discussion of the characteristics of a reverse-oriented monsoon, and of its impacts upon the motion of tropical cyclones, see Walt's (10W) summary.

b. Small Size

Developing from a cloud cluster in the South China Sea, Yunya consolidated into a small core of deep convection to the north of an area of extensive deep convection in the southwesterly monsoon flow. Yunya's small cloud system appeared to be undergoing rapid improvement in organization as it made landfall on northern Luzon (Figure 3-11-2). Brand (1972) noted a preference for very small tropical cyclones to be located in the extreme western Pacific Ocean within a corridor extending from Luzon to Tokyo.

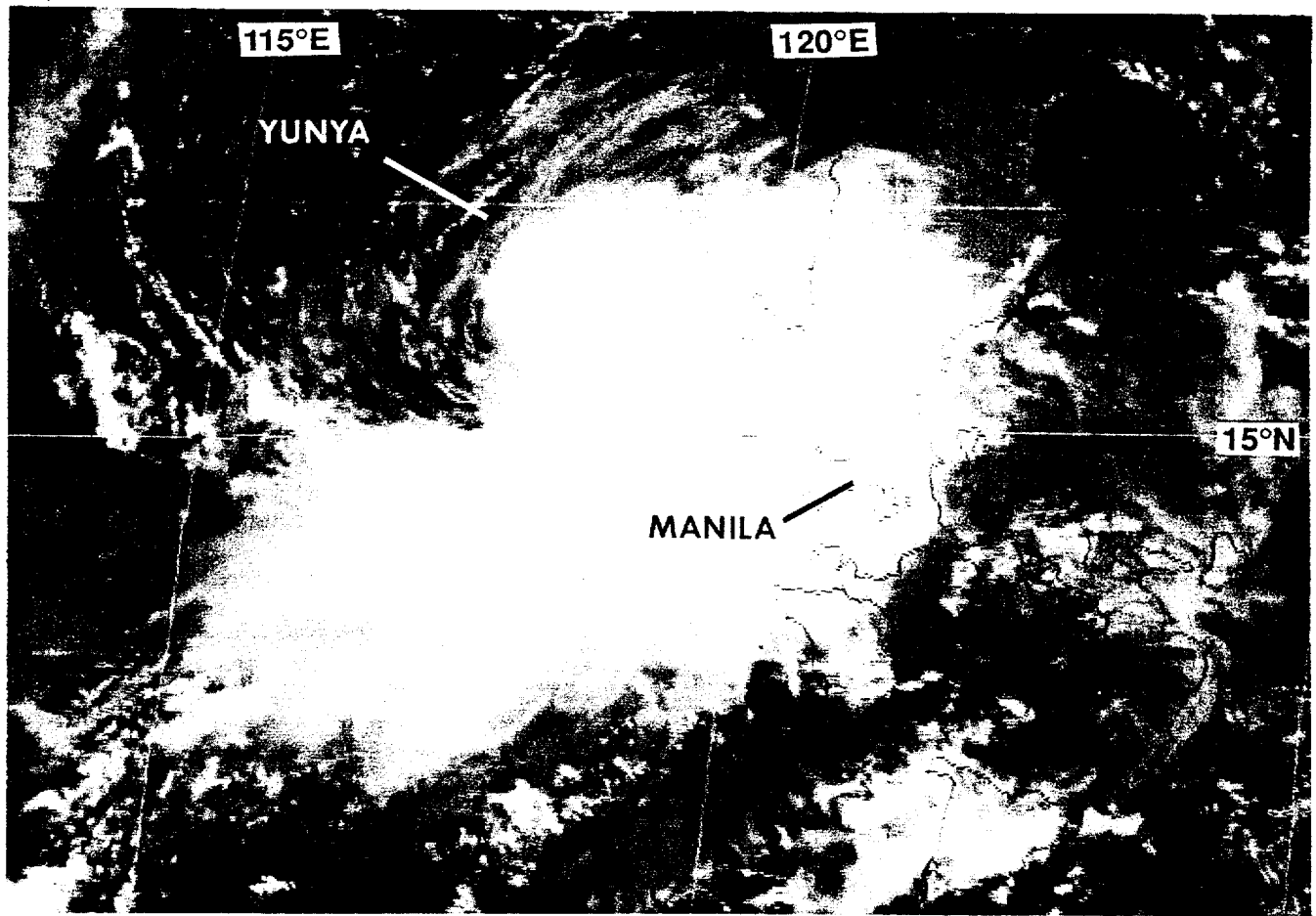


Figure 3-11-1 Curving low-level cloud lines, and organization of the deep convection into a curved band prompted the the first warning on Yunya. (180131Z July visible GMS imagery).

IV. IMPACT

Heavy rains from Yunya triggered landslides of volcanic debris from Mount Pinatubo. Monsoon flow to the south of Yunya had gusts in excess of 60 kt (31 m/sec) across the central plains of Luzon. No reports of serious damage were received. One man reportedly died of a heart attack in central Luzon after seeing his house swept away by floodwaters.

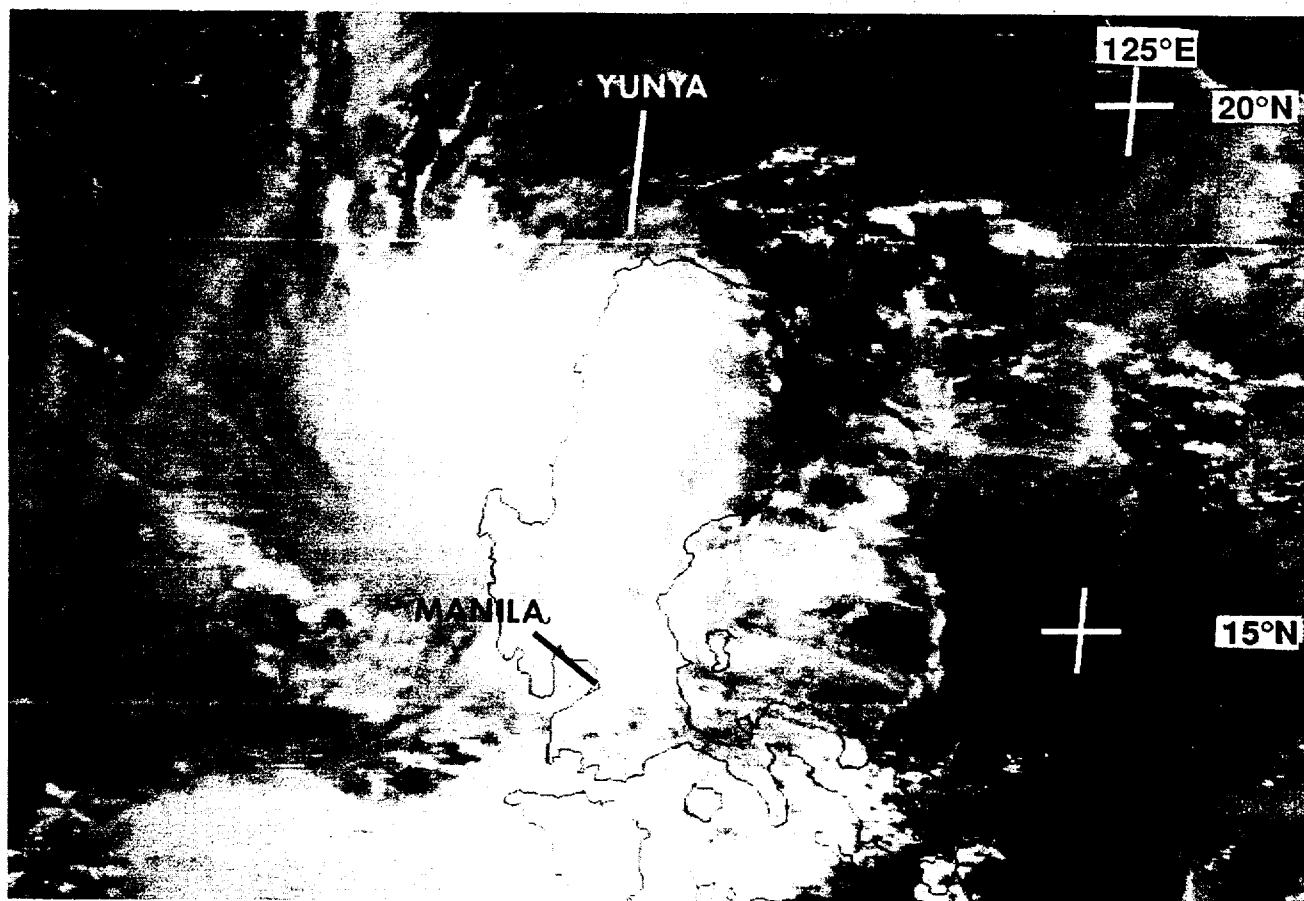
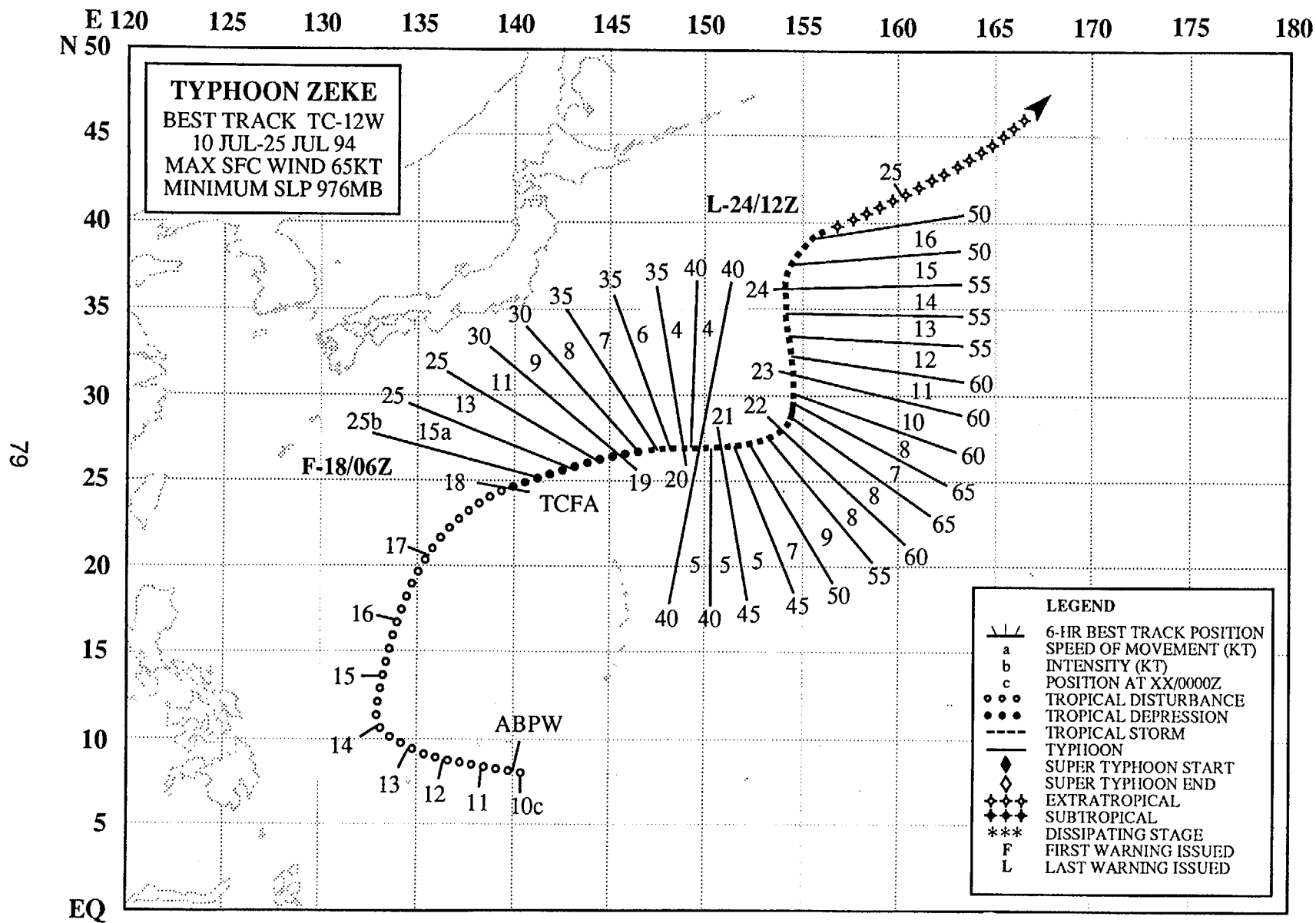


Figure 3-11-2 Yunya reaches its peak intensity of 45 kt (23 m/sec) as it makes landfall on the northwestern corner of Luzon. (182331Z July visible GMS imagery).



TYPHOON ZEKE (12W)

I. HIGHLIGHTS

Zeke was a small tropical cyclone that formed along the axis of a reverse-oriented monsoon trough. It was the easternmost of three tropical cyclones along this trough (see Figure 3-10-1 in Walt's (10W) summary). Zeke exhibited unusual "S" track motion which is almost exclusively associated with tropical cyclones embedded in a reverse-oriented monsoon trough (Lander 1995a). Zeke's brief attainment of typhoon intensity was verified by ship observation. Satellite imagery at the time of typhoon intensity winds was atypical: ragged, but tightly coiled spirals of relatively warm-topped convection, and alone did not support typhoon intensity.

II. TRACK AND INTENSITY

During early July, the axis of the monsoon trough extended across much of Micronesia at rather low latitudes (5° - 7° N). Most of the deep convection associated with this monsoon trough resided south of 10° N. On 14 July, two persistent cloud clusters had consolidated in the Philippine Sea to the east of Luzon. The westernmost cloud cluster became Walt (10W), while the easternmost later became Zeke. The first mention of the incipient tropical disturbance that would become Zeke appeared on the 140600Z July Significant Tropical Weather Advisory. This tropical disturbance was followed for several days as it moved first northward, then northeastward. During this time, Walt (10W) formed to the east of Luzon, southwest of the pre-Zeke tropical disturbance. Concurrent with Walt's (10W) low-latitude turn toward the northeast and the gradual turn to the northeast of the pre-Zeke disturbance, a long band of deep convective cloud clusters, that included the cloud systems of Walt (10W), Yunya (11W) and the pre-Zeke disturbance, had acquired a SW-NE (i.e., reverse) orientation. This reverse-oriented monsoon trough was the first of three reverse-oriented monsoon troughs during 1994, and stretched from 15° N in the South China Sea to 30° N near the international date line.

As the pre-Zeke tropical disturbance moved northeastward, it slowly intensified. At 180000Z, a Tropical Cyclone Formation Alert was issued. This alert stated, in part:

"... satellite and synoptic data indicate an active area of convection northeast of Tropical Storm Walt (10W) is showing signs of development. The disturbance is located beneath an area of light upper level winds with a TUTT cell located to the northwest of the system. ..."

Based upon improved banding of the deep convection and the appearance of well-defined cyclonically curved low-level cloud lines, the first warning on Tropical Depression 12W was issued at 180600Z. Upper-level shear from the west seemed to be preventing intensification, and the system remained at tropical depression intensity until 191200Z. During the early morning of 20 July, tropical depression warning number 7 (191200Z) was amended to tropical cyclone warning number 7A. The amended warning stated, in part:

"... visual satellite imagery indicates Tropical Storm Zeke (12W) has a well defined low level circulation beneath an area of active convection ... For this reason, TD 12W has been upgraded to tropical storm intensity and named 'Zeke'. ..."

Moving eastward until 220000Z, Zeke then slowed and turned to the north. Shortly after turning northward, about 220600Z, synoptic data indicated that Zeke possessed winds of 65 kt (33m/sec), and at 220600Z, Zeke was upgraded to a typhoon. Zeke's life as a typhoon was short-lived, however, and at 221800Z it was downgraded to a 60 kt (31 m/sec) tropical storm. Moving on a track slightly west of north until 240000Z, Zeke gradually weakened. Turning gradually to the northeast after 240000Z, and

accelerating, Zeke began to acquire extratropical characteristics, and the final warning was issued at 241200Z.

III. DISCUSSION

a. Unusual motion

Zeke's track is a good example of the "S" motion, which is defined by Lander (1995a). This north-oriented motion features eastward movement at low latitude, a later bend to the north or northwest, and then eventually north-eastward motion as the system enters the mid-latitude westerlies. Of the 103 north-oriented tracks during the period 1978 to 1993, thirty five (34%) could be categorized as "S" motion. Of the 35 cases of "S" motion during the period 1978 to 1993, twenty eight cases (80%) occurred in association with a reverse-oriented monsoon trough, five cases occurred in association with a monsoon gyre, and two cases were associated with other environmental flow patterns. For a more thorough discussion of the characteristics of a reverse-oriented monsoon trough see Walt's (10W) summary.

b. Unusual satellite signature for a typhoon

During the morning of 22 July, the cloud signature of Zeke rapidly improved as a spiral band of cold-

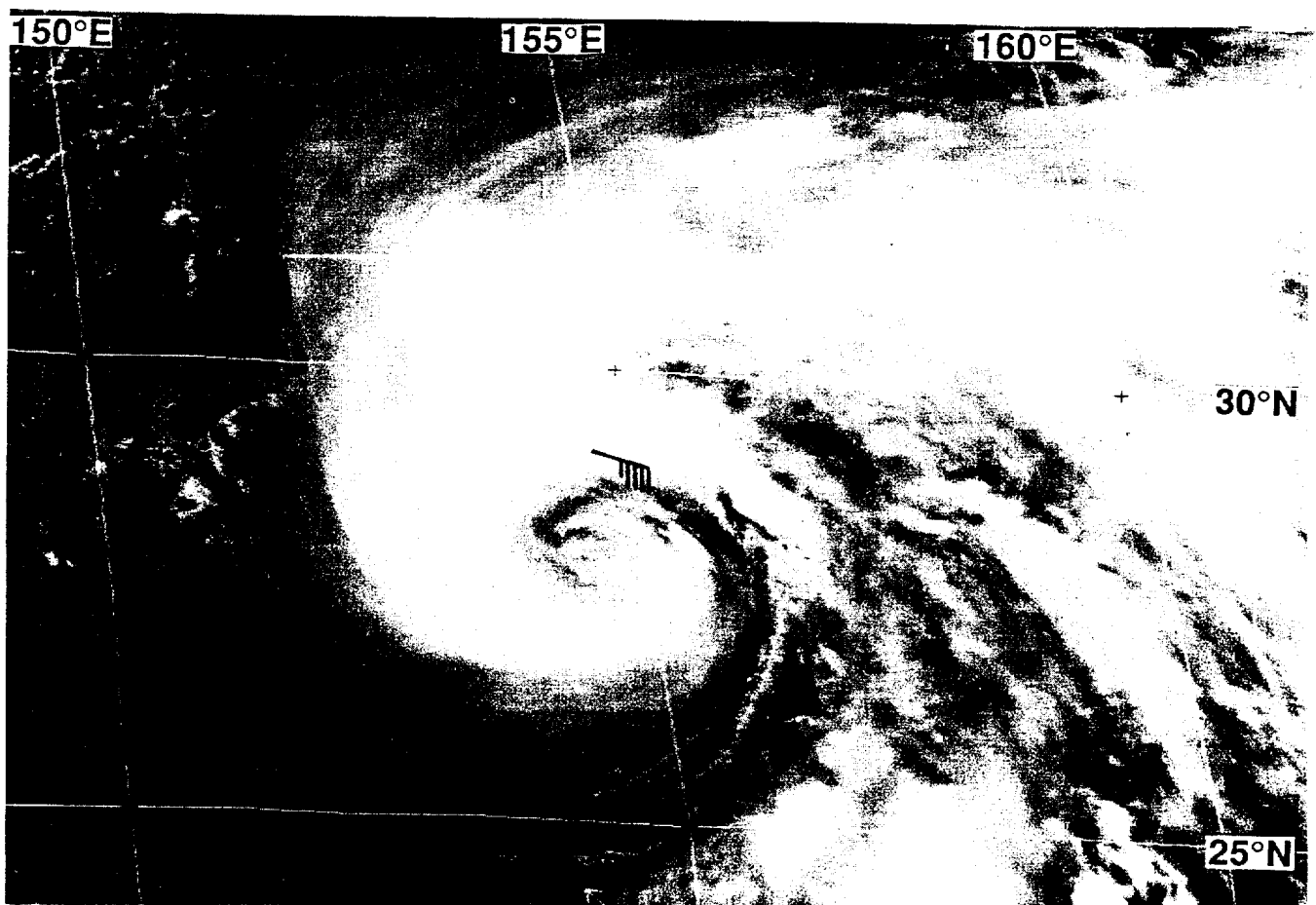


Figure 3-12-1 The deep convection begins to coil tightly around Zeke's low-level center (220031 July visible GMS imagery).

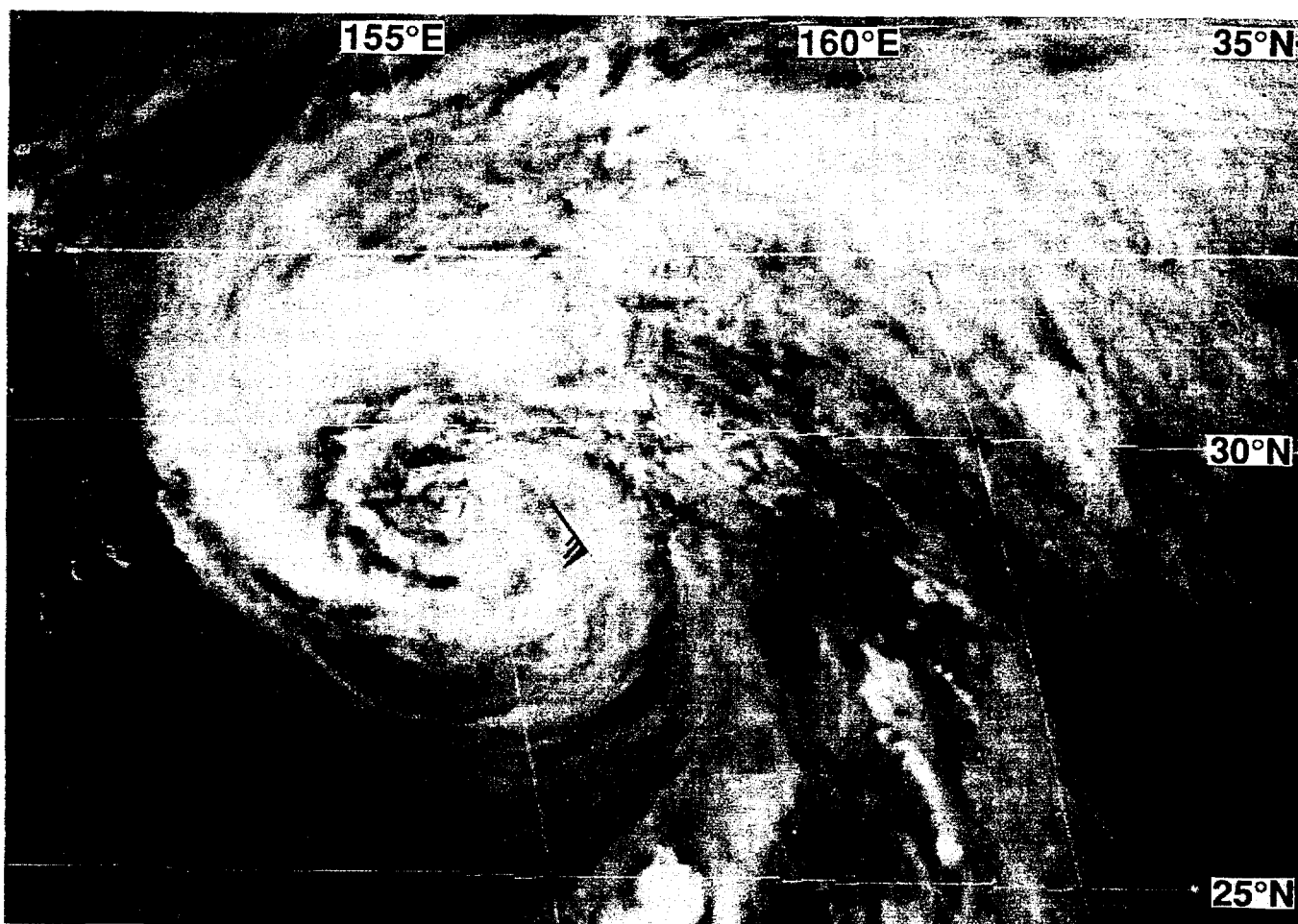


Figure 3-12-2 Bands of towering cumulus and relatively shallow convection are tightly wound and multi-coiled when a ship near Zeke's center reported typhoon intensity wind (220531Z July visible GMS imagery).

topped deep convection began to coil tightly around the exposed low-level center (Figure 3-12-1). At this time, a ship located north of the center of Zeke reported 45 kt (23 m/sec) sustained winds. Towards the evening of July 22, the single, cold-topped spiral of deep convection had evolved into a multi-coiled spiral of ragged warmer-topped convection (Figure 3-12-02). At the time of the imagery in Figure 3-12-2, the aforementioned ship had progressed into the eastern semi-circle of Zeke's circulation and reported typhoon-force winds. A satellite intensity estimate made at 220424Z July (an hour before the satellite imagery shown in Figure 3-12-2) indicated an intensity of T2.5 (minimal tropical storm intensity), and remarks on this fix stated:

... "Zeke is becoming extratropical. Only a little deep convection remains near the center . . ."

If not for the 65 kt (33 m/sec) ship report, it is doubtful that the JTWC would have upgraded Zeke to a typhoon.

c. Forecast performance

Overall, the official forecasts for Typhoon Zeke were quite good. Similar to problems with the objective guidance described in the summary of Walt (10W), the track forecast extracted from the NOGAPS model (the objective aid, "NGPS", received at the JTWC) and the forecast low-level wind fields made

by the NOGAPS model had two periods of difficulty during the lifetime of Zeke. First, early in Zeke's life, the NOGAPS model over-developed its circulation into a very large tropical cyclone. Zeke, however, remained small for its entire life. Rather, it was Walt (10W) which became the largest and most intense of the three named tropical cyclones (Walt (10W), Yunya(11W), and Zeke) which were aligned SW-NE along the axis of a reverse-oriented monsoon trough. The erroneous initial over-development of Zeke caused the model to subsume Walt (10W) into Zeke's artificially large circulation by the 48-hour point of the forecast. The second problem occurred later in Zeke's life when the NOGAPS model over-developed the size of Walt's circulation. This, along with the model's loss of the eastern reaches of the reverse-oriented monsoon trough, contributed to NOGAPS forecasts of Zeke's motion too far to the north and west during the period 200000Z through 230000Z.

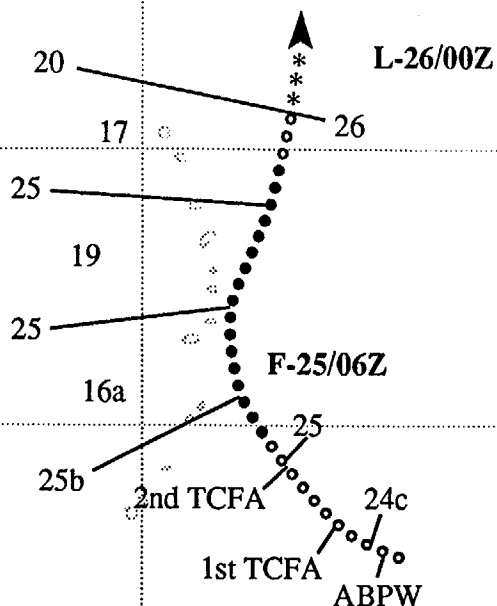
IV. IMPACT

Typhoon Zeke remained over open ocean its entire life, and no reports of fatalities or significant damage were received.

E 135 140 145 150 155 E
N 25
84
15
10
N 5

TROPICAL DEPRESSION 13W
BEST TRACK TC-13W
23 JUL-26 JUL 94
MAX SFC WIND 25KT
MINIMUM SLP 1000MB

LEGEND	
△/△/△	6-HR BEST TRACK POSITION
a	SPEED OF MOVEMENT (KT)
b	INTENSITY (KT)
c	POSITION AT XX/0000Z
○ ○ ○	TROPICAL DISTURBANCE
● ● ●	TROPICAL DEPRESSION
---	TROPICAL STORM
—	TYPHOON
◆	SUPER TYPHOON START
◇	SUPER TYPHOON END
+	EXTRATROPICAL
+	SUBTROPICAL
***	DISSIPATING STAGE
F	FIRST WARNING ISSUED
L	LAST WARNING ISSUED



TROPICAL DEPRESSION 13W

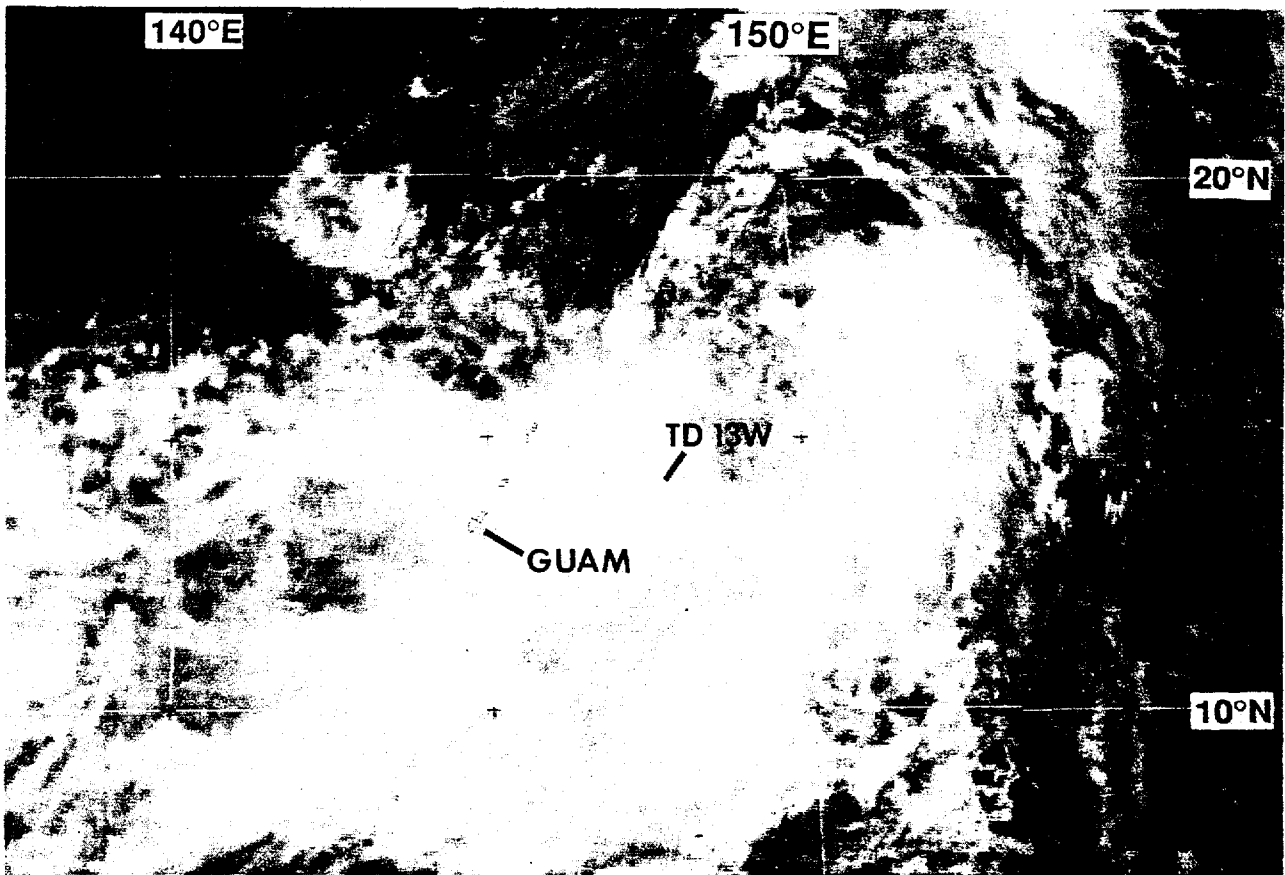
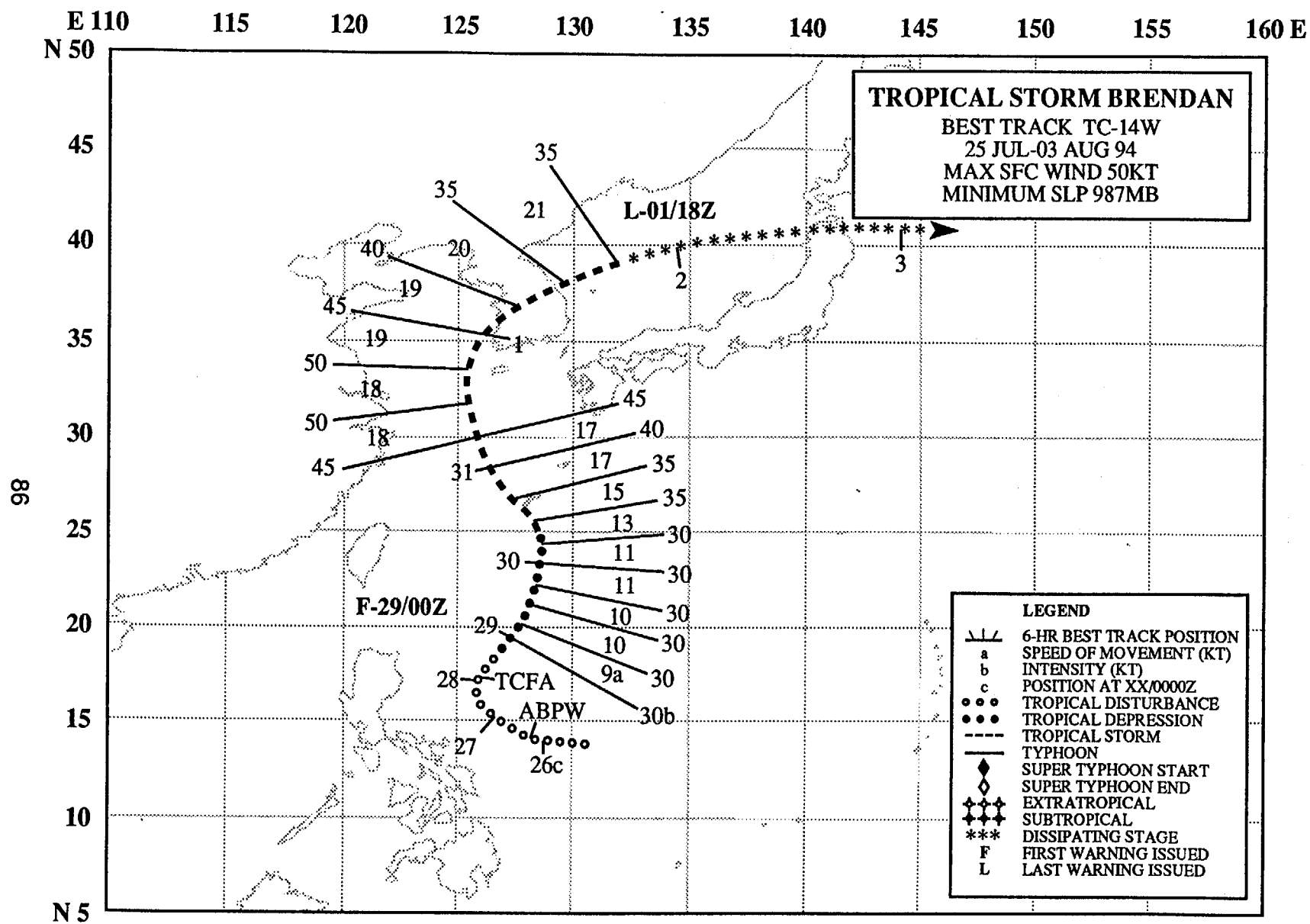


Figure 3-13-1 Tropical Depression 13W forms in the monsoon cloud band east of Guam (250424Z July visible GMS imagery).

Tropical Depression 13W, formed on 24 July, in association with a surge of the southwest monsoon across the Philippine Sea. Two Tropical Cyclone Formation Alerts were issued on the system: the first at 241051Z July, the second was at 242251Z after the disturbance center was relocated to the south. The first warning on Tropical Depression 13W was issued at 250600Z as the system passed about 40 nm (74 km) east of Saipan (WMO 91222) (Figure 3-13-1) while moving northward at 10-12 kt (19-22 km/hr) along the east side of a monsoon gyre. The depression was short-lived, however, as it dissipated less than a day later east of the northernmost of the Mariana Islands.



TROPICAL STORM BRENDAN (14W)

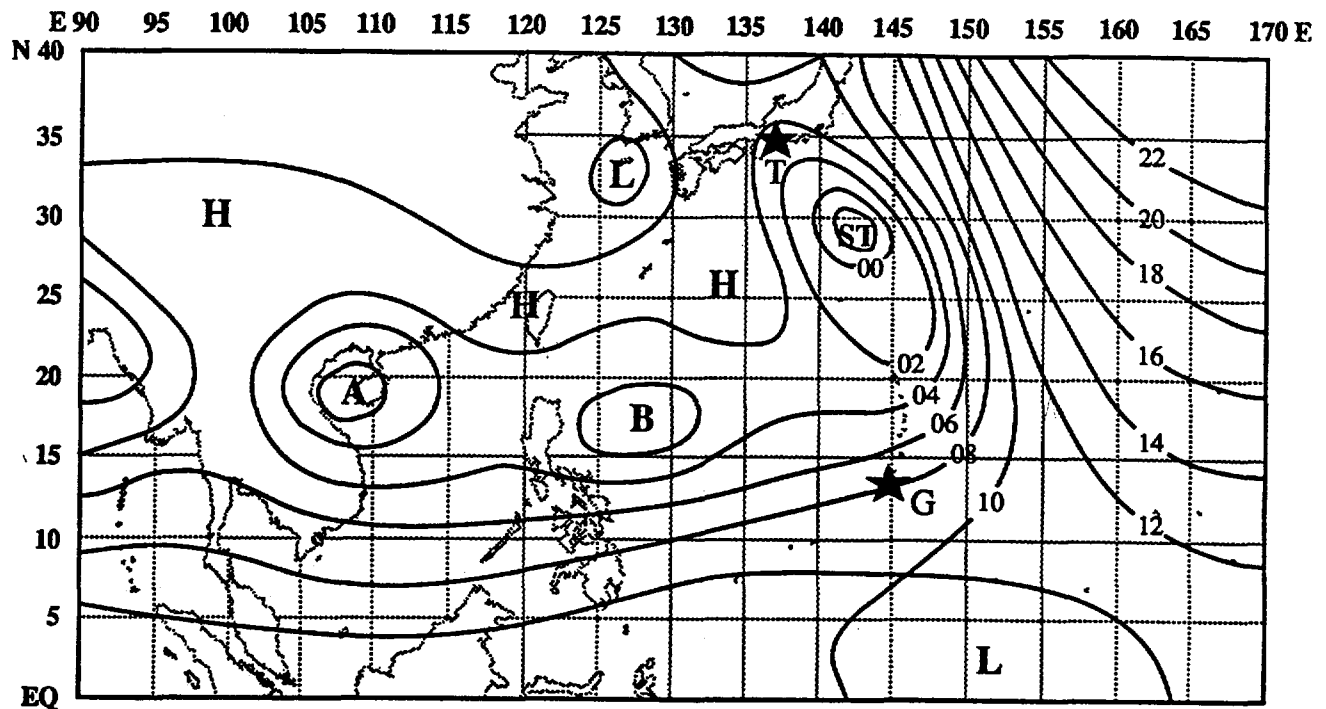


Figure 3-14-1 Sea-level pressure analysis at 280000Z July showing the location of the pre-Brendan (B) tropical disturbance in an active monsoon trough. A sub-tropical cyclone (ST) — possibly the continuation of Tropical Depression 13W — is seen southeast of Tokyo. A low pressure area in the Tonkin Gulf would later become Amy (15W) (A). Dotted lines outline major land masses, bold lines are isobars at 2 mb intervals, stars are labeled G for Guam and T for Tokyo.

I. HIGHLIGHTS

For six days, Brendan meandered northward in a sinusoidal pattern, passing over Okinawa, and eventually striking Korea on 01 August. Up to 8 inches (203 mm) of rain helped to alleviate drought conditions in some areas of the Korean peninsula.

II. TRACK AND INTENSITY

On 26 July, convection began to consolidate into a discrete tropical disturbance in the monsoonal cloud band over the Philippine Sea. This disturbance — the precursor to Brendan — was first mentioned on the 260600Z July Significant Tropical Weather Advisory. During the next two days, the disturbance moved at an average speed of 6 kt (11 km/hr), initially to the northwest, and then, in association with a surge in the southwest monsoon, it turned northward. Based upon improved organization of the deep convection, a Tropical Cyclone Formation Alert was issued at 280200Z. At this time the monsoon circulation was very active (Figure 3-14-1). The first warning on Tropical Depression 14W was issued at 290000Z based upon ship reports of 25 kt (13 m/sec) wind and sea-level pressure below 1000

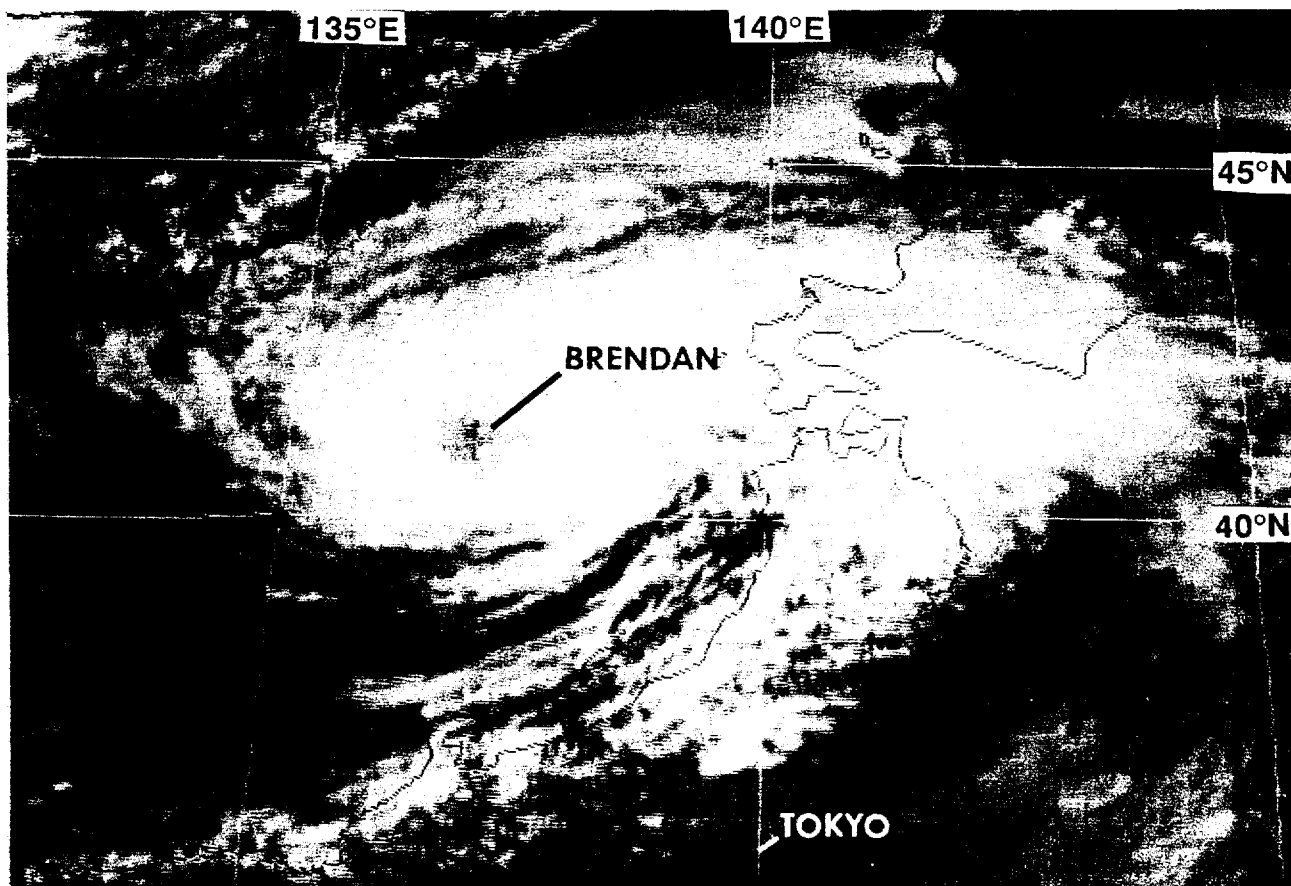


Figure 3-14-2 Brendan exhibits a well-defined exposed low-level circulation center as it approaches Okinawa (300631Z July visible GMS imagery).

mb. As Tropical Depression 14W accelerated northward, it reached tropical storm intensity on the evening of 30 July (Figure 3-14-2) just prior to crossing Okinawa.

Brendan was moving at 18 kt (33 km/hr) when it reached its maximum intensity of 50 kt (26 m/sec) about 120 nm (220 km) south of Cheju Island, Korea. The system reached its point of recurvature at 311800Z in the Yellow Sea, and then accelerated northeastward passing over the Korean peninsula. After weakening over Korea, Brendan continued to accelerate while crossing the Sea of Japan, became extra-tropical, and reintensified to 45 kt (23 m/sec). The system passed near Misawa, Japan at 021500Z August, and later merged with a frontal cloud band after crossing Japan.

III. DISCUSSION

As Brendan passed over Korea, it acquired characteristics of a hybrid tropical cyclone (i.e., possessing characteristics of both a tropical and extratropical cyclone) (Gray 1968, Hebert and Poteat 1975). As the system moved into the Sea of Japan, it elongated in an east-west direction, characteristic of an occlusion, but maintained organized convection near the central eye-like feature (Figure 3-14-3).

IV. IMPACT

Brendan's path over Korea left two dead and 28 missing as high waves overturned fishing boats. No other reports of significant damage were received.

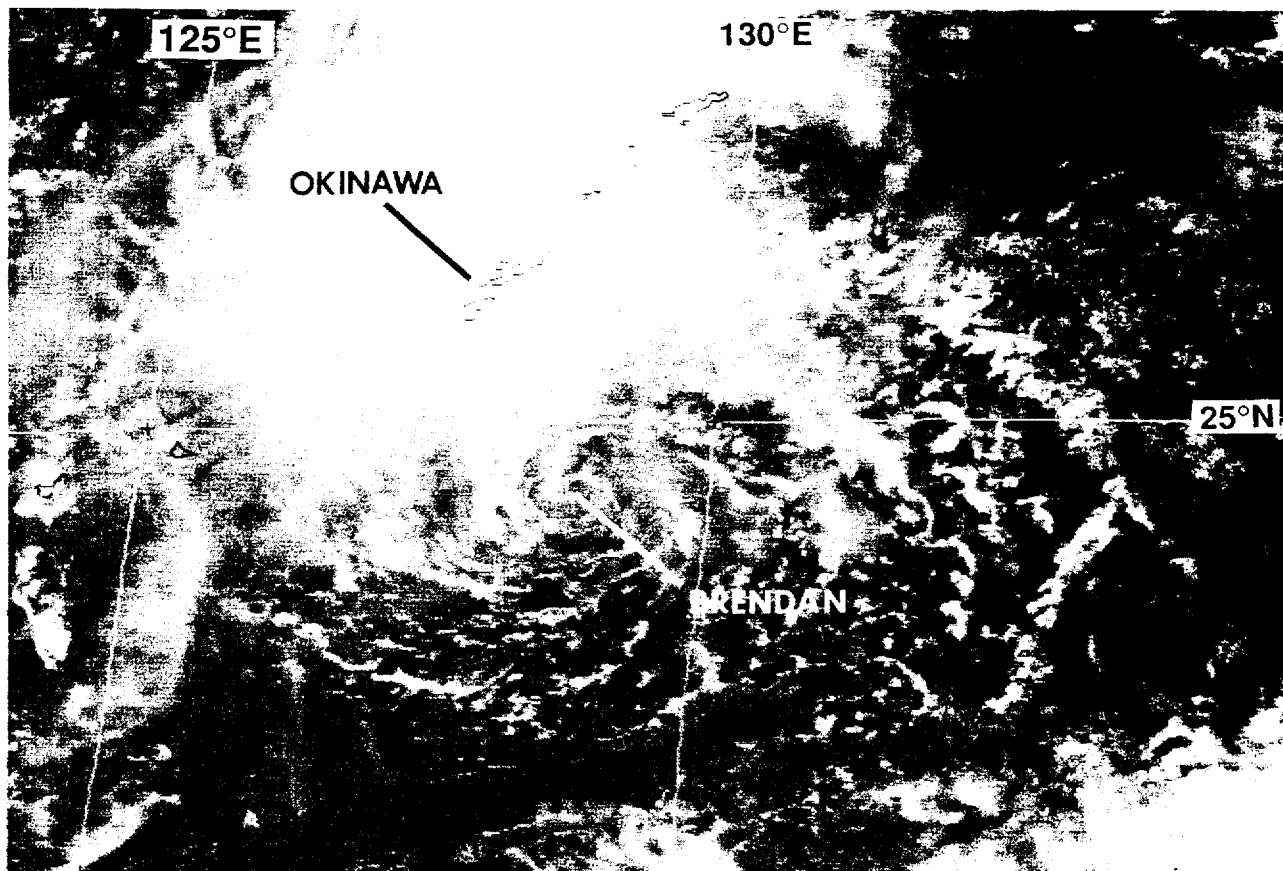


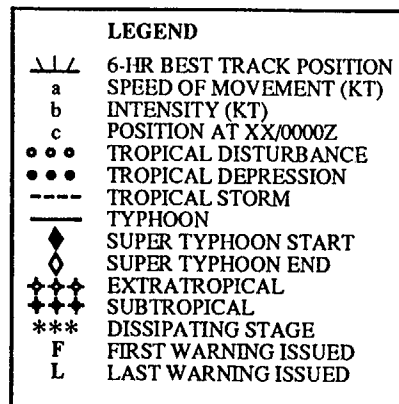
Figure 3-14-3 As a hybrid system, Brendan exhibits both tropical (e.g., organized central convection and an eye-like feature) and extratropical (e.g., the beginnings of a frontal cloud band in its eastern periphery) characteristics (020531Z August visible GMS imagery).

E 100
N 25

105

110

115 E

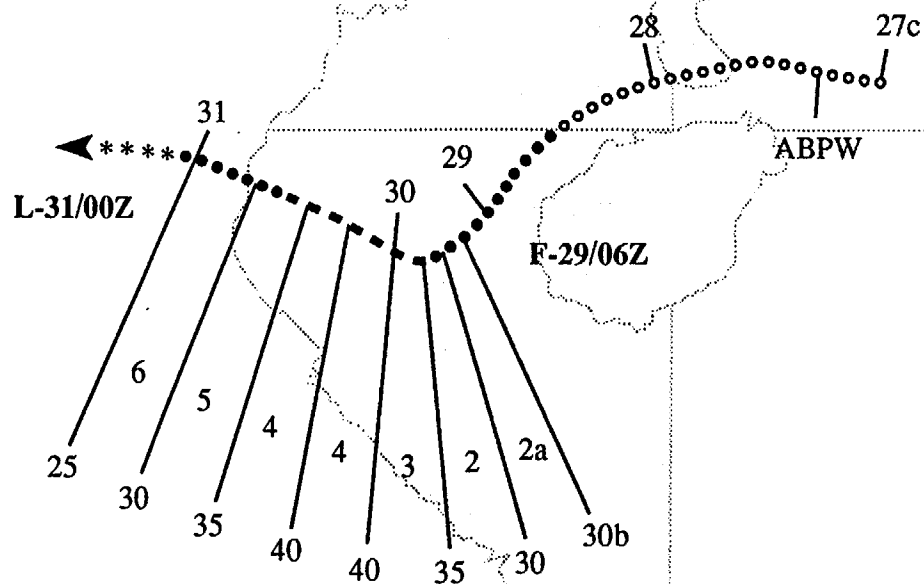


TROPICAL STORM AMY
BEST TRACK TC-15W
27 JUL-31 JUL 94
MAX SFC WIND 40KT
MINIMUM SLP 994MB

06

20

N 15



TROPICAL STORM AMY (15W)

Throughout most of July, an area of low sea-level pressure persisted in the region of the Gulf of Tonkin. This low-pressure area was a regional feature at the western end of the over-water portion of the monsoon trough [see Figure 3-14-1 in Brendan's (14W) summary]. For many days, thick layered cloudiness with embedded deep convection covered southern China, portions of Southeast Asia, and much of the South China Sea. On 29 July, an area of persistent convection associated with a low-level cyclonic circulation that had previously been located over Hainan Dao, moved over water. Based upon synoptic data and satellite imagery (Figure 3-15-1), the first warning on Tropical Storm Amy was issued at 290600Z. Amy reached an estimated peak intensity of 40 kt (20 m/sec) at 300000Z while over the Gulf of Tonkin. Moving slowly westward, it began to weaken while still over water, and later dissipated over land south of Hanoi.

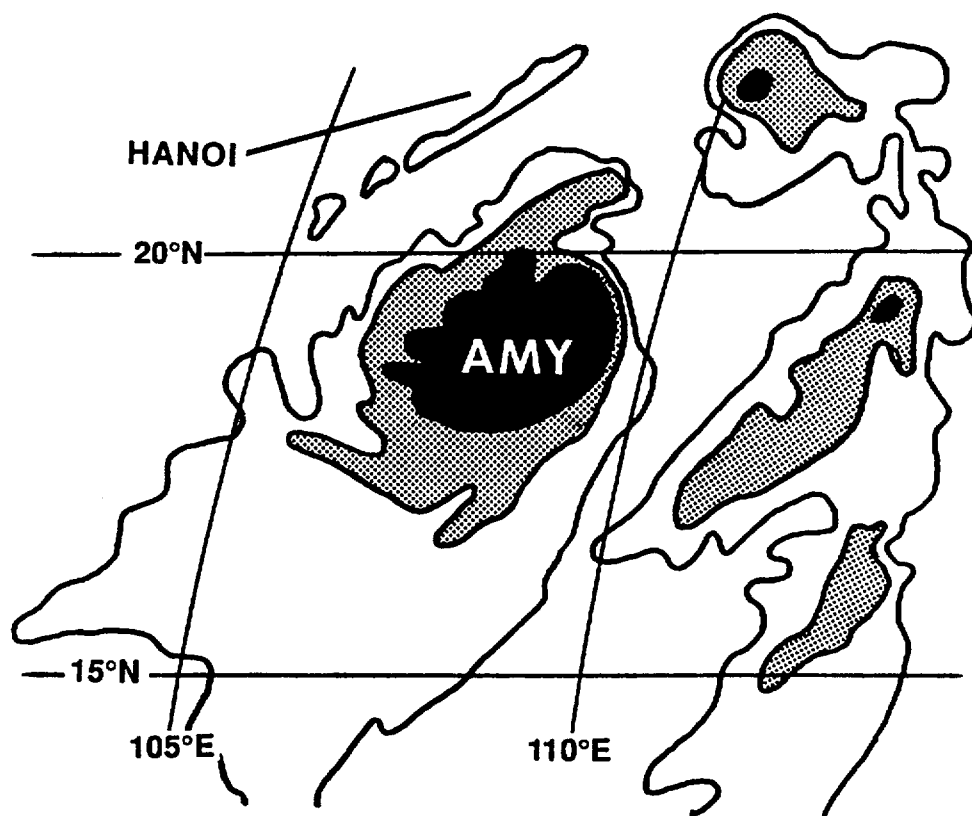
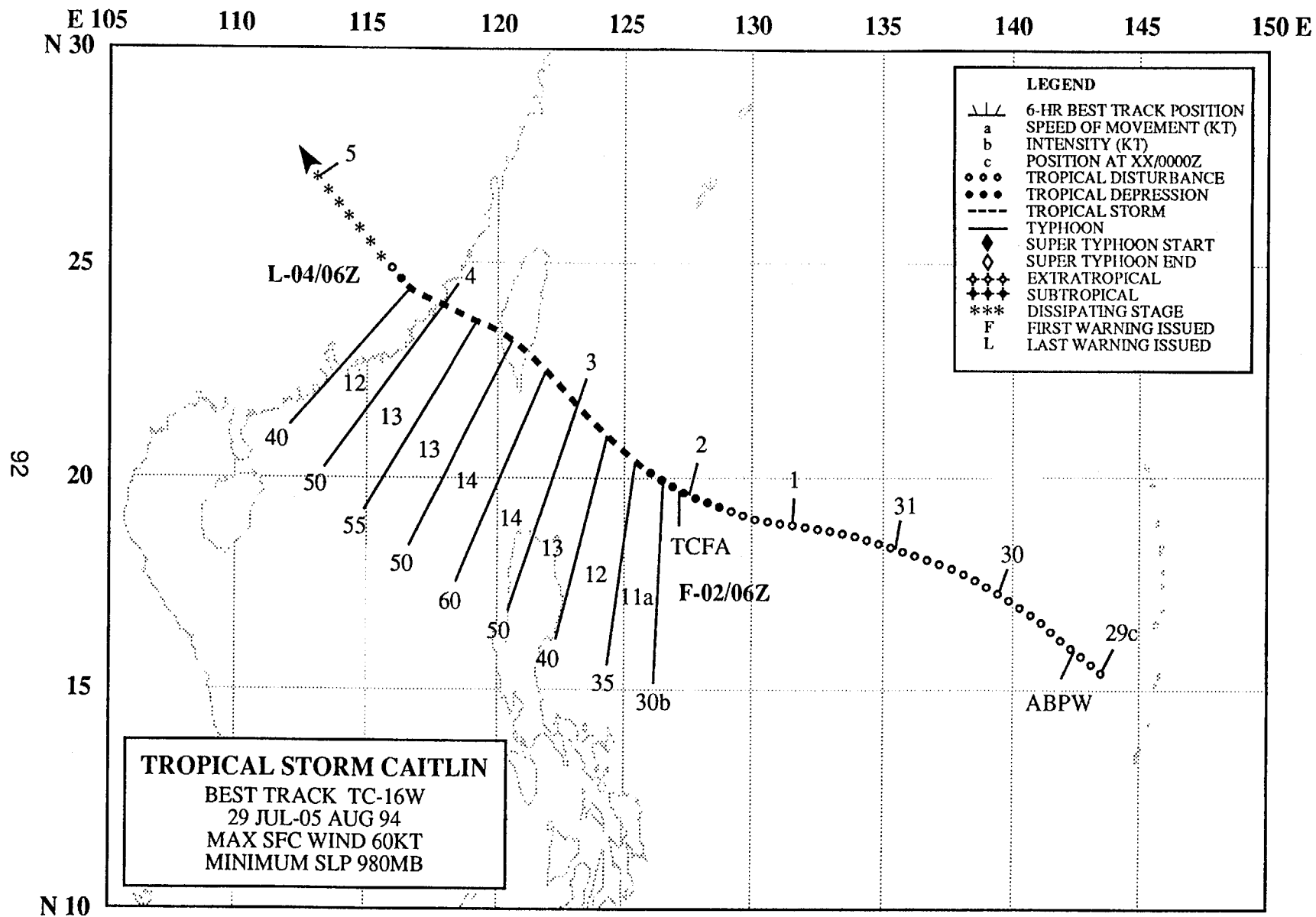


Figure 3-15-1 Schematic illustration of Amy's deep convection as it intensifies over water to the west of Hainan Dao. Cloud-top temperatures are indicated: outer contour = -31°C , shaded region $\leq -54^{\circ}\text{C}$, black region $\leq -70^{\circ}\text{C}$. (Adapted from 290424Z July enhanced infrared imagery.)



TROPICAL STORM CAITLAN (16W)

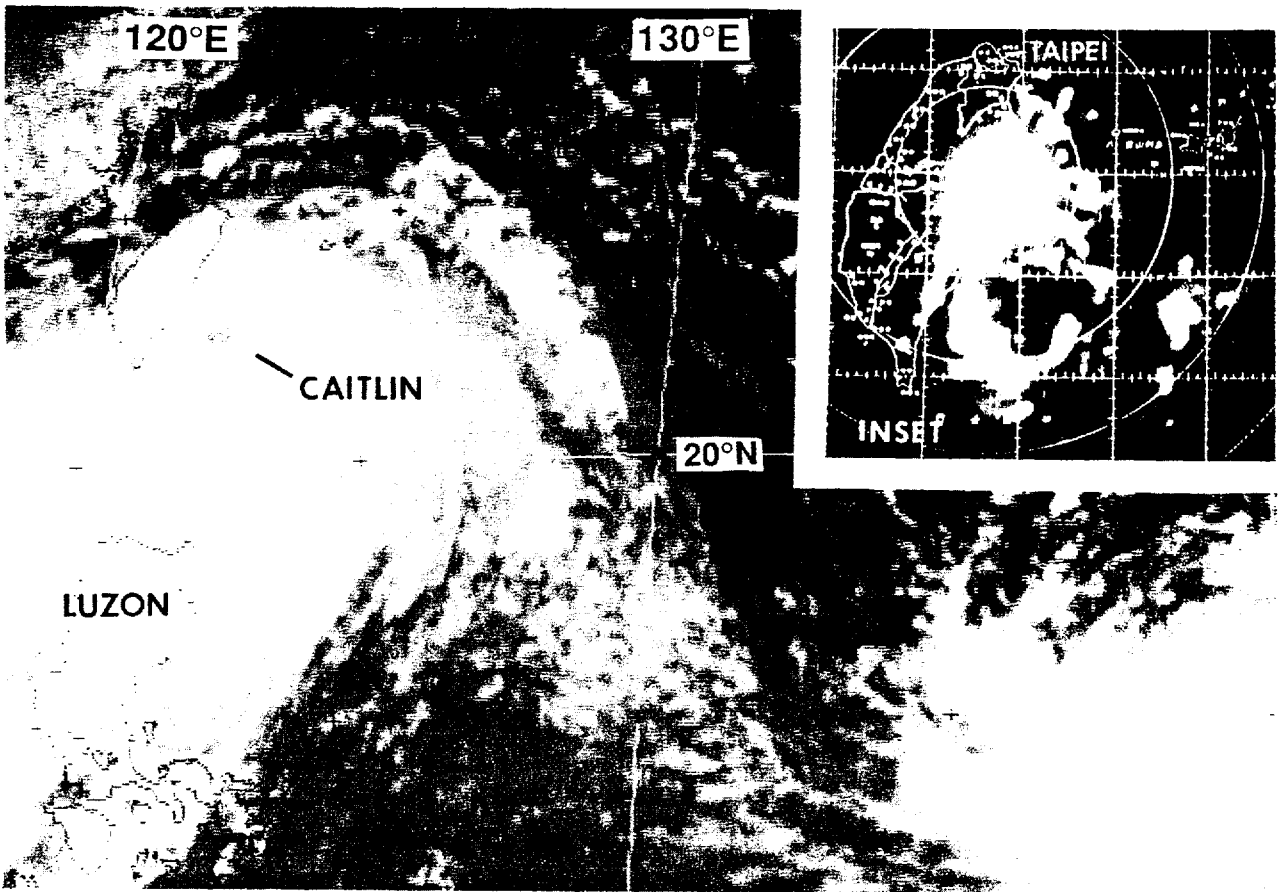


Figure 3-16-1 Tropical Storm Caitlin with a ragged banding type eye, some 60 nm (111 km) east of Taiwan (030424Z August visible GMS imagery). Inset shows Caitlin's radar reflectivity at 030700Z August. (Radar imagery courtesy of Taiwan Central Weather Bureau.)

On the morning of 29 July, a tropical disturbance developed in the monsoon trough northwest of Guam and west of Saipan. It was mentioned on the Significant Tropical Weather Advisory that afternoon (290600Z July). Development was very slow, but after four days, satellite imagery and synoptic data indicated that the disturbance was beginning to intensify, so a Tropical Cyclone Formation Alert was issued at 020000Z August. The first warning on Tropical Depression 16W was issued four hours later as the system continued to show signs of improving organization (e.g., convective curvature of the deep convection). In another six hours (at 021200Z), the system was upgraded to Tropical Storm Caitlin. It appeared to interact with a surge in the southwest monsoon, which resulted in a turn to the northwest, and an acceleration to 15 kt (28 km/hr) toward south central Taiwan. Caitlin reached its maximum intensity of 60 kt (31 m/s) at 030600Z (Figure 3-16-1a,b), three hours before going ashore in Hualien County, Taiwan, at 031015Z. Wind gusts in excess of typhoon force were experienced for a 21-hour period (030900Z to 040600Z) at Green Island, Taiwan (WMO 46760) as Caitlin passed a short distance to the north of the island. The system crossed Taiwan in six hours, and entered the Taiwan Straits at about 031500Z. Approximately ten hours later (040100Z), Caitlin went ashore on mainland China where it dissipated on 05 August. Caitlin caused heavy rains, as much as 3.3 inches (84 mm) in one hour, in China's Ningxia Hui Autonomous Region. The resulting mountain flooding killed eight people and left nine missing.

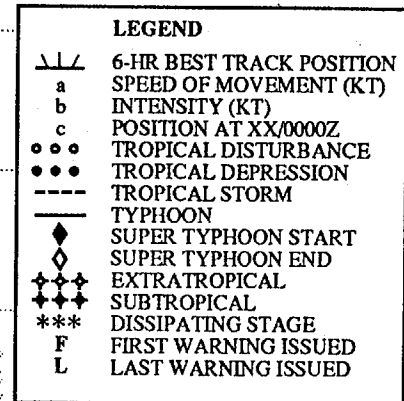
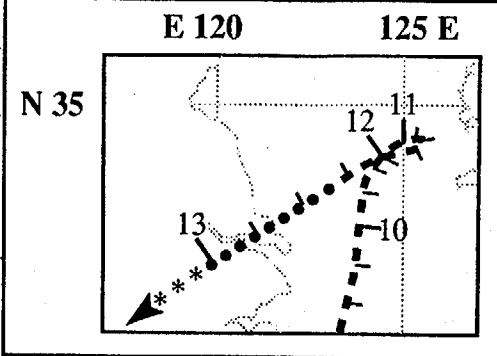
E 110 115 120 125 130 135 140 145 150 155 160 E

N 45

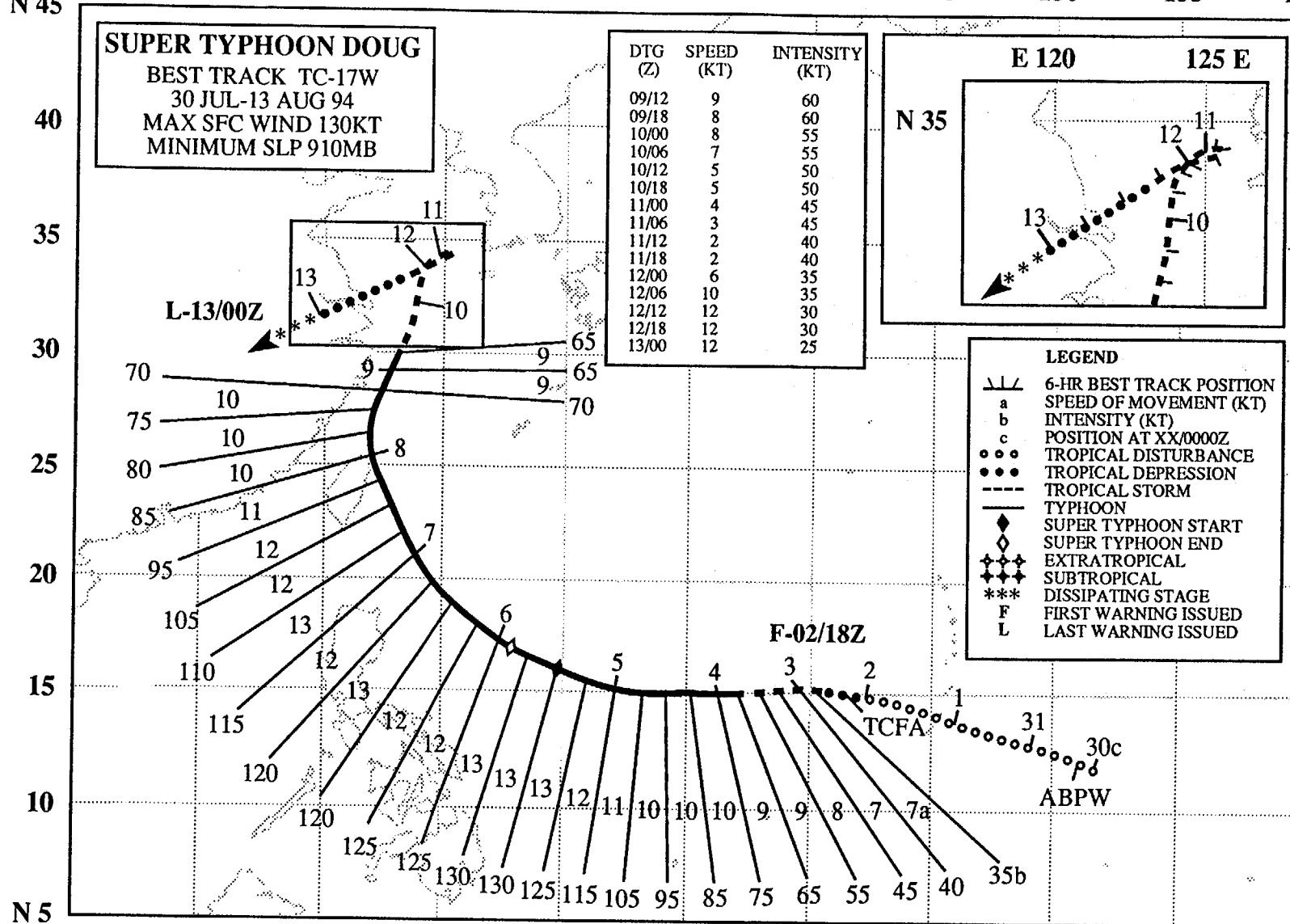
SUPER TYPHOON DOUG

BEST TRACK TC-17W
30 JUL-13 AUG 94
MAX SFC WIND 130KT
MINIMUM SLP 910MB

DTG (Z)	SPEED (KT)	INTENSITY (KT)
09/12	9	60
09/18	8	60
10/00	8	55
10/06	7	55
10/12	5	50
10/18	5	50
11/00	4	45
11/06	3	45
11/12	2	40
11/18	2	40
12/00	6	35
12/06	10	35
12/12	12	30
12/18	12	30
13/00	12	25



94



N 5

SUPER TYPHOON DOUG (17W)

I. HIGHLIGHTS

Doug was the second of six tropical cyclones to attain super typhoon intensity in the western North Pacific basin during 1994. Doug exhibited some unusual structural characteristics: it had an abnormally large eye for a system of its intensity, which grew larger as the system intensified. Doug also went through an unusually long period of rapid intensification. Doug caused extensive damage and loss of life in Taiwan. After affecting Taiwan, Doug moved northward to Korea, creating the conditions which led to a Korean Air Lines A-300 crash landing at Cheju International Airport.

II. TRACK AND INTENSITY

The tropical disturbance that eventually became Super Typhoon Doug was first mentioned on the 300600Z July Significant Tropical Weather Advisory as an area of enhanced convection on the eastern end of a relatively weak monsoon trough that extended eastward across the southern Mariana Islands. After several episodes of normal diurnal fluctuations in deep convection (i.e., night maximum, day minimum), the disturbance began to maintain daytime convection. A Tropical Cyclone Formation Alert was issued at 020700Z August. The amount and organization of the convection increased during that night, and the first warning on Tropical Depression 17W was issued at 021800Z. At this time, the system was moving slowly westward at a speed of 7-8 kt (13-14 km/hr).

Doug began to increase its rate of intensification during the evening of 03 August, and reached typhoon intensity at 031800Z. For the following 48 hours, the system intensified at a steady rate of 10 kt (5 m/sec) / 6 hr or 40 kt (21 m/sec) per day. After reaching a peak intensity of 140 kt (72 m/sec) at 051800Z, Doug began to slowly weaken (Figure 3-17-1). Doug maintained an eye diameter of over 50 nm (95 km) from 051200Z to 060000Z. The Taiwanese radar at Hualien (46699) confirmed Doug's very large eye (Figure 3-17-2) when its intensity was estimated to be 125 kt (64 m/sec). A few hours later, Doug passed between the Taiwanese station of Suao (WMO 46706) and the Japanese station of Yonaguni-Shima (WMO 47912) (the southern-most of the Ryukyu islands). Table 3-17-1 shows the maximum wind speeds observed at these stations (based on the peak observed gust) as Doug passed between them over a 4-hour period. When the translation speed of 11 kt (20 km/hr) is factored into the winds at these stations to account for the asymmetry, the winds at the stations agree very well with each other and with the estimated sustained wind of 110 kt (57 m/sec) for Doug.

After passing very near the extreme northeastern tip of Taiwan (the western half of Doug's eye wall moved over land there), Doug turned to the north and then to the north-northeast. Doug weakened to tropical storm intensity after 090600Z when approximately 100 nm (185 km) southeast of Shanghai. At 091800Z, Doug produced sustained winds of 60 kt (31 m/sec) with a gust to 72 kt (37 m/sec) at Mosulpo, Cheju-Do (WMO 47187) when the storm was 180 nm (335 km) south-southwest of the island (Figure 3-17-3). The weakening system meandered toward the small islands at the southwestern tip of the Korean peninsula, and its convective organization and circulation weakened drastically. The remaining low-level circulation was redirected by low- to mid-level northeasterly flow on the southern periphery of a blocking high-pressure system over northern China. Doug, now downgraded to Tropical Depression 17W, then moved to the southwest across the Yellow Sea, and into mainland China. The final warning was issued at 120000Z as it dissipated northwest of Shanghai.

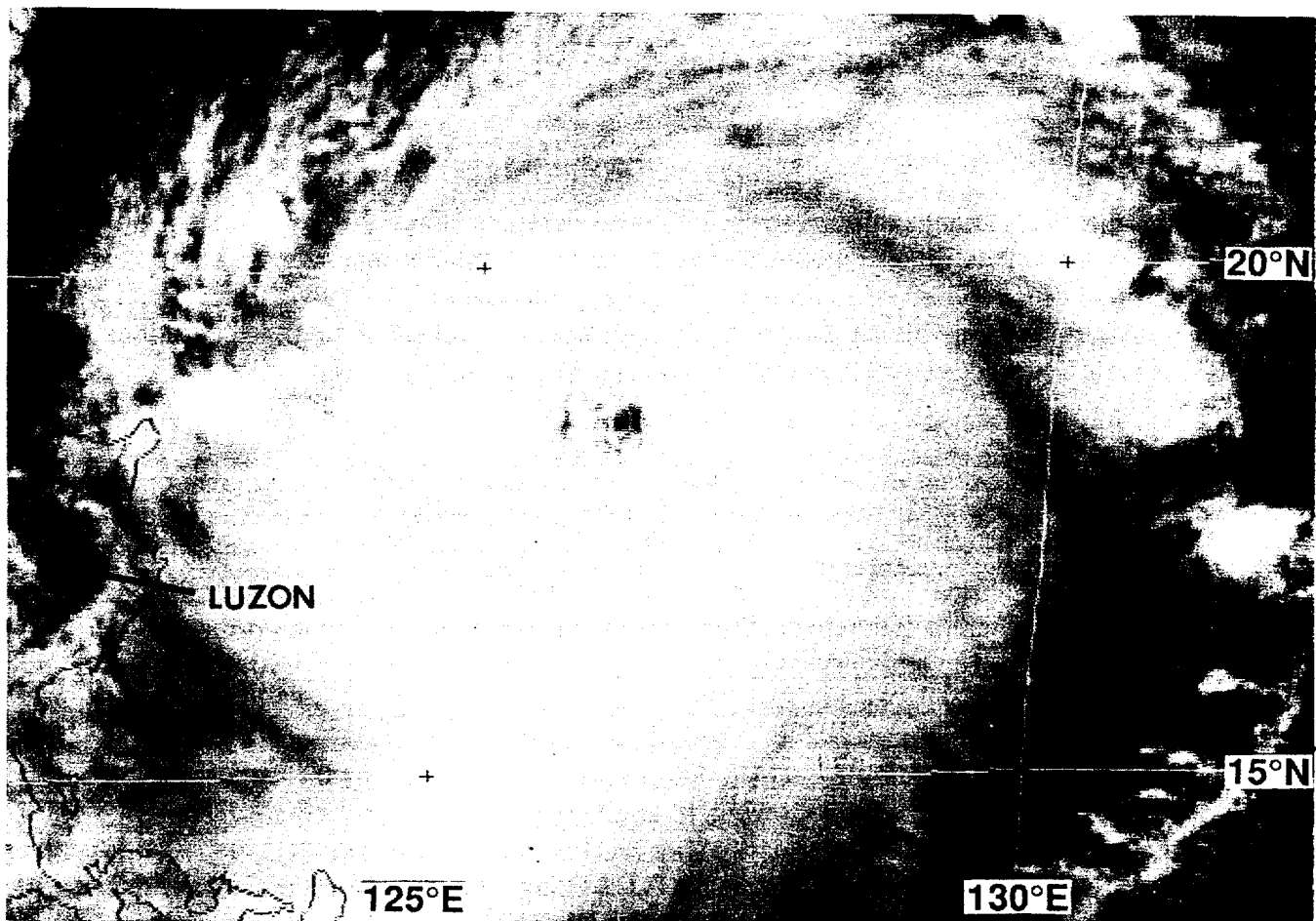


Figure 3-17-1 Super Typhoon Doug is located 240 nm (445 km) east of the northeast tip of Luzon just after reaching its 140 kt (72 m/sec) peak intensity (060530Z August visible GMS imagery).

III. DISCUSSION

There are two aspects of Doug's structure and evolution that were of special interest. The first was its long period of a high rate of intensification, and the second was the diameter of its eye that enlarged during intensification and shrunk during much of its weakening.

a. Unusual intensification rate of Doug.

Mundell (1990) indicates that most of the western North Pacific typhoons that reach super typhoon intensity undergo an episode of rapid intensification (central pressure falls > 42 mb/day (Holliday and Thompson 1979)), that usually lasts about 24 hours. From 030600Z to 051200Z, Doug increased in intensity at a rate of 10 kt (5 m/sec)/6 hr and peaked at 140 kt (72 m/sec) at 051800Z. The 24-hour falls of central pressure during much of Doug's intensifying phase gradually increased from the low 30s (mb per day) to values in the low 40s (mb per day) (Table 3-17-2). The periods 040600Z-050600Z and 041200Z-051200Z exhibited pressure falls of 42 mb and 43 mb respectively. The evolution of the intensities of Doug and Super Typhoon Yuri (1991), are representative of the minority of western North Pacific typhoons that intensify at rapid or near-rapid rates for unusually long periods (at least 48 hours). Characteristics common to both Doug and Super Typhoon Yuri (1991) include: very large size, an extended period of intensification rates near the lower threshold of the established criteria for rapid

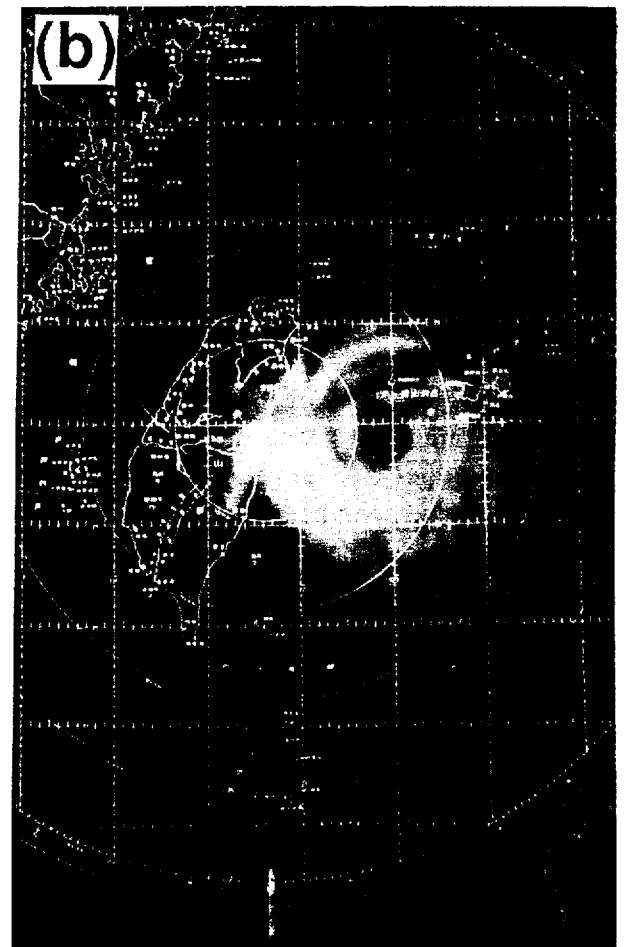


Figure 3-17-2 Two radar images of Typhoon Doug from the Hualien, Taiwan (WMO 46669) radar at: (a) 071000Z August , and (b) 071300Z August. In (a) the center of Doug's large eye was approximately 120 nm (220 km) southeast of the radar. In (b) the eye wall is nearing Yonaguni-Shima which recorded its peak gust of 136 kt (70.2 m/sec) at 131337Z. (Radar photos courtesy of the Central Weather Bureau, Taipei, Taiwan.)

intensification (> 42 mb per day), peak intensity in the 140-150 kt (75-77 m/sec) range, and relatively large eye diameters that bordered on the 45 nm (85 km) large-eye threshold set by Dvorak (1984) for purposes of capping intensity at 115 kt (59 m/sec).

b. Unusual eye behavior

Doug's eye diameter showed an unusual evolution. It increased in size from 11 to 47 nm (20 to 87 km) during Doug's intensification phase; expanded further to 57 nm (106 km) just after peaking; but then decreased in size as it weakened. Except for the six hours of expansion after reaching peak intensity, the trends were opposite to those normally observed, and lend further support to the premise that Doug did not undergo the typical process of rapid intensification, since the process normally involves shrinking of the eye.

The diameter of Doug's eye was abnormally large for a very intense typhoon, similar to the case of Super Typhoon Yuri (1991). The potential problem that occurs is with the rule in the technique that restricts the intensity of tropical cyclones for eye diameters of 45 nm (85 km) or greater: for large ragged eyes the intensity is capped at 90 kt (46 m/sec); for large well-defined eyes the intensity is capped at 115 kt (59 m/sec). It is likely that both Doug and Yuri had large eyes with accompanying

intensities in excess of the Dvorak caps. During Doug's intensification phase, the large eye was embedded in the deep (eye wall area) convection by average distances over 120 nm (220 km). These are extraordinarily large embedded distances. Also, the percentage of cloud within three degrees latitude (180 nm) of the center that was colder than -70°C remained relatively high, even during the weakening phase. Super typhoons like Doug and Yuri may represent a special case of very large tropical cyclones with large eyes and very wide eye walls that can exceed the intensity bounds which Dvorak placed on tropical cyclones with large eyes.

IV. IMPACT

Doug spent much of its life over open ocean. However, during its passage near Taiwan, it produced torrential rains and strong winds, blowing vehicles off of highways. At least 19 people lost their lives, 45 were injured, and damage in Taiwan was estimated to be in excess of US \$110 million. Destruction must also have been heavy in the southwestern Ryukyu islands, although no reports were received. The anemometer at Yonaguni-Shima (WMO 47912) failed when wind gusts reached 136 kt (70.2 m/sec). Doug also caused considerable flooding in China, but reports of damage were not received. As the system approached Korea, it created poor weather and gusty winds on Cheju-Do. A Korean Air Lines A-300 jet trying to land at Cheju International Airport (WMO 47182), buffeted by 40 kt (20 m/sec) winds, skidded on the wet runway into a barrier. Fortunately, all 160 passengers and crew got off the aircraft before it was engulfed in flames.

Table 3-17-1 Observed maximum winds at Suao, Taiwan (WMO 46706) and Yonaguni-Shima, Japan (WMO 47912), as Typhoon Doug passed between the two stations. Peak gusts are observed, but sustained winds are one-minute average based on 0.88 of peak gust (Atkinson 1974). "Distance" refers to the distance from the station to the typhoon center at the time of peak wind. "COR Vmax" shows what the expected peak gust would be when corrected for the 11 kt (20 km/hr) translation speed of Doug. "BT" is the best-track intensity at the time of the peak wind at each site.

Location	Date / Time (Z)	Peak Wind (kt)	Distance (nm)	COR Vmax (kt)	BT (kt)
Suao	071657	95G115	25	126	110
Yonaguni	071337	110G136	30	125	115

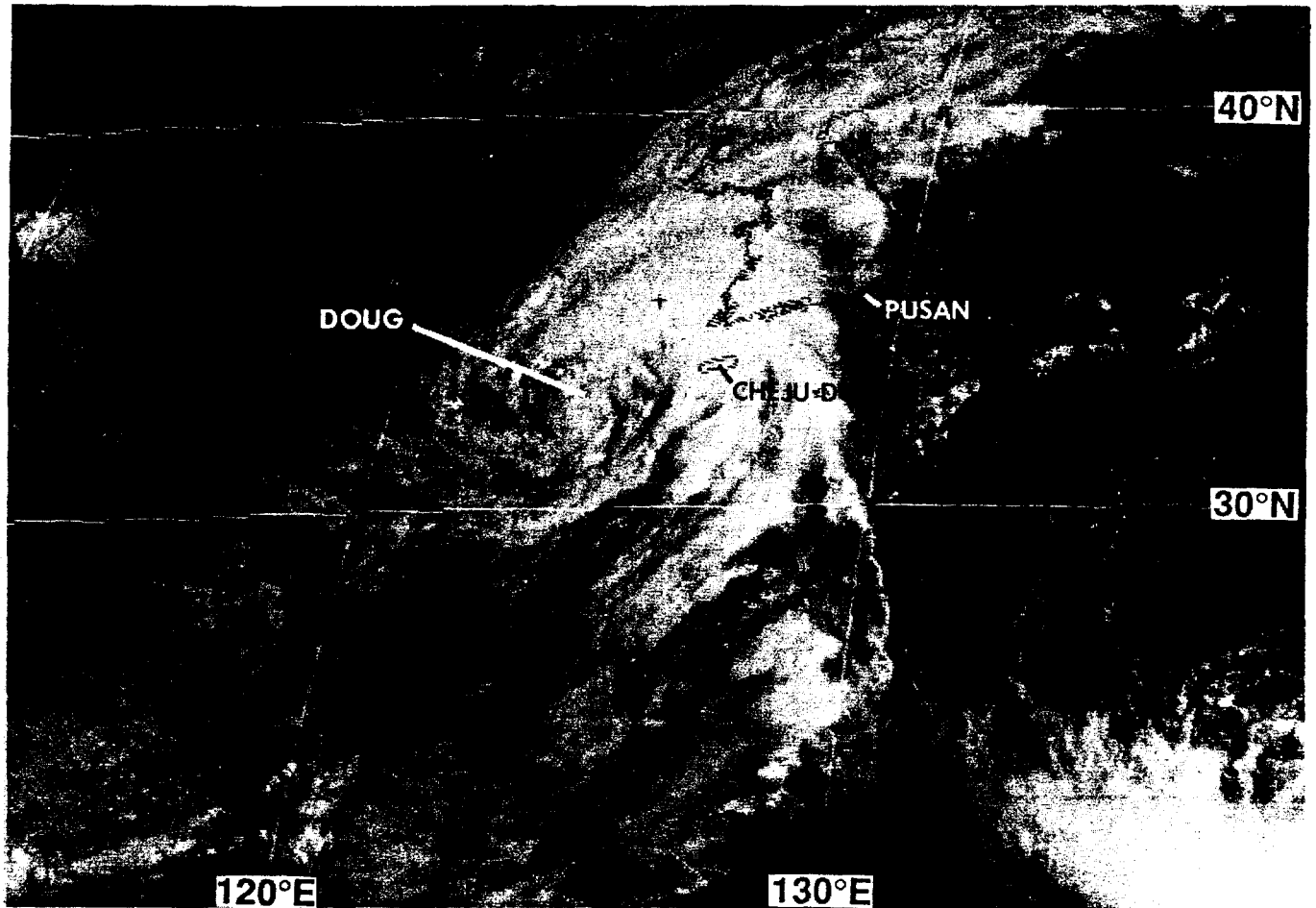


Figure 3-17-3 Tropical Storm Doug at 55 kt (28 m/sec) intensity as it moves toward Korea. Approximately six hours prior to picture time (091800Z), Cheju-Do (WMO 47187) received its peak wind gust of 72 kt (37 m/sec) (092331Z August visible GMS imagery).

Table 3-17-2 Twenty-four hour pressure changes for each six-hour warning period prior to Doug's maximum intensity, beginning at 030600Z and ending at 050600Z.

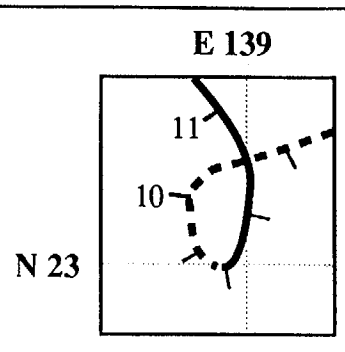
Date/Time Period	Wind Change (kt)	Pressure change (mb)
030600 - 040600	+40 (45 - 85)	-33 (991 - 958)
031200 - 041200	+40 (55 - 95)	-35 (984 - 949)
031800 - 041800	+40 (65 - 105)	-38 (976 - 938)
040000 - 050000	+40 (75 - 115)	-41 (968 - 927)
040600 - 050600	+40 (85 - 125)	-42 (958 - 916)
041200 - 051200	+40 (95 - 135)	-43 (949 - 906)
041800 - 051800	+35 (105 - 140)	-40 (938 - 898)
050000 - 060000	+25 (115 - 140)	-29 (927 - 898)
050600 - 060600	+15 (125 - 140)	-18 (916 - 898)

E 115 120 125 130 135 140 145 150 155 E

N 50

TYPHOON ELLIE
 BEST TRACK TC-18W
 03 AUG-16 AUG 94
 MAX SFC WIND 80KT
 MINIMUM SLP 963MB

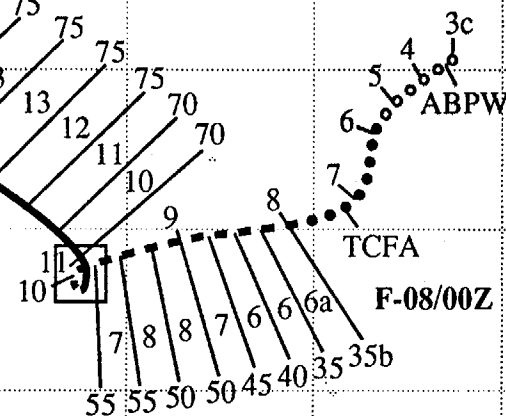
L-16/06Z



LEGEND

- 6-HR BEST TRACK POSITION
- a SPEED OF MOVEMENT (KT)
- b INTENSITY (KT)
- c POSITION AT XX/0000Z
- TROPICAL DISTURBANCE
- TROPICAL DEPRESSION
- TROPICAL STORM
- TYPHOON
- ◆ SUPER TYPHOON START
- ◆ SUPER TYPHOON END
- ◆◆◆ EXTRATROPICAL
- ◆◆◆ SUBTROPICAL
- *** DISSIPATING STAGE
- F FIRST WARNING ISSUED
- L LAST WARNING ISSUED

DTG (Z)	SPEED (KT)	INTENSITY (KT)
09/18	7	55
10/00	6	60
10/06	4	60
10/12	2	65
10/18	4	65
11/00	7	70



100

N 15

TYPHOON ELLIE (18W)

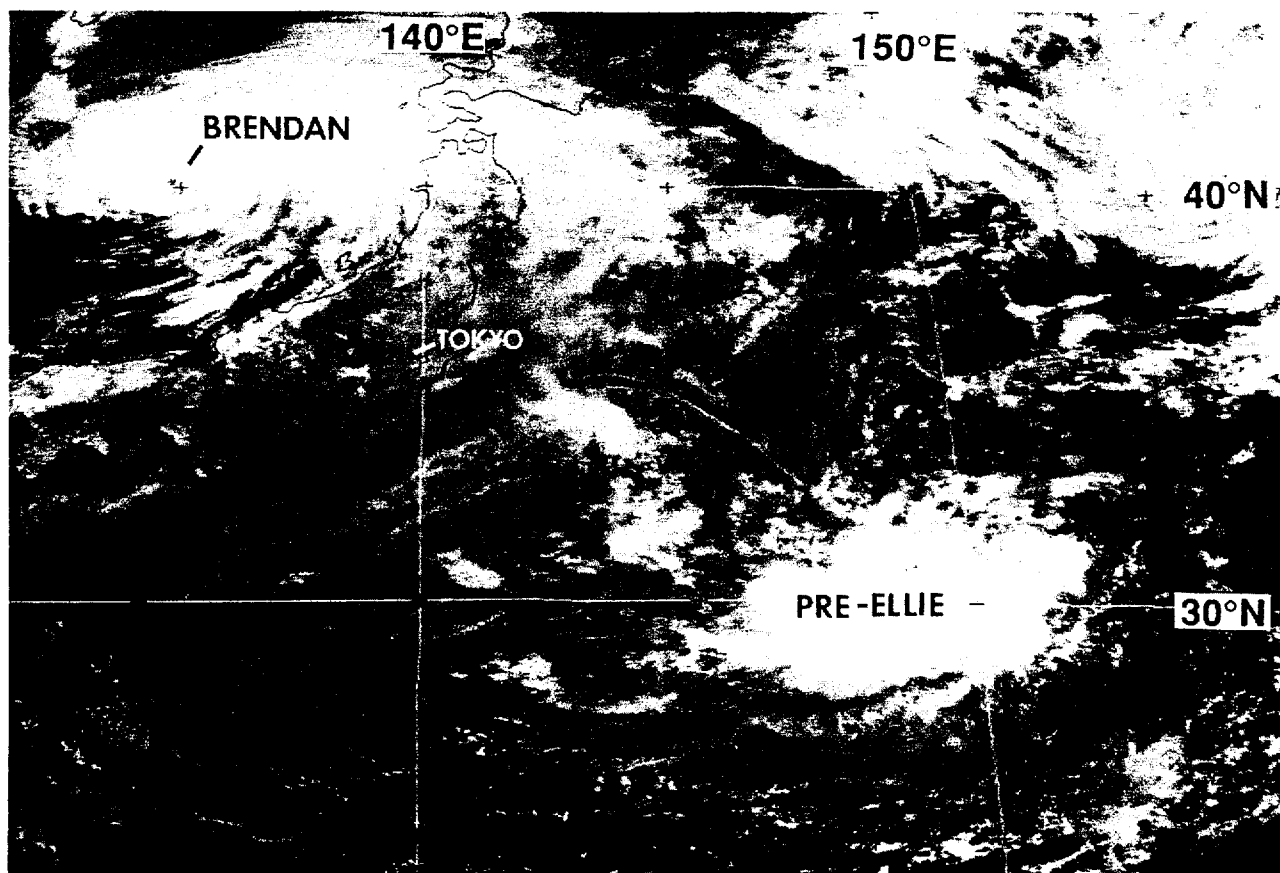


Figure 3-18-1 The small area of deep convection at the base of a weak mid-latitude trough drifted southward and became Ellie. The recurving Brendan is seen in the Sea of Japan (020031Z August visible GMS imagery).

I. HIGHLIGHTS

The tropical disturbance that became Ellie had an atypical origin in the sub-tropics about 500 nm (900 km) east-southeast of Tokyo. Ellie became a large typhoon with a large ragged eye. Prior to recurvature in the Yellow Sea, it moved on a westward track at high latitude (25°N). A peak wind gust of 87 kt (45 m/sec) was recorded by a station on the south coast of Kyushu, Japan, as Ellie passed 60 nm (110 km) to the south.

II. TRACK AND INTENSITY

On 02 August, an area of deep convection was observed at the base of a weak trough of low pressure which was moving eastward away from Japan (Figure 3-18-1). Drifting slowly southward, this area of deep convection persisted, prompting its first mention on the 030600Z August Significant Tropical Weather Advisory. For the next several days, this tropical disturbance continued to move slowly southward, and the areal extent of deep convection increased. An exposed low-level circulation center on the northern side of the deep convection became increasingly well defined. At 070630Z, a Tropical Cyclone Formation Alert was issued based upon increasing curvature of the main band of deep convection. At 080000Z, the first warning was issued on Tropical Depression 18W. By 081200Z, the

system was upgraded to Tropical Storm Ellie based upon synoptic data from the Volcano Islands [Chi Chi Jima (WMO 47971) recorded a peak gust of 48 kt (25 m/sec) and a minimum sea-level pressure of 1002.1 mb as the system passed nearby]. The system gradually turned to the west-southwest. On the morning of 09 August, a large ragged eye formed (Figure 3-18-2). On 10 August, the system stalled for approximately 24 hours, intensified, and grew in size. As it came out of its stall, Ellie moved on a west-northwestward track at a steady 13 kt (24 km/hr) for the next 72 hours (110600Z to 140600Z). At 110600Z, the system was upgraded to Typhoon Ellie, however post-analysis indicated that typhoon intensity was most probably reached at 101200Z. After becoming a typhoon, Ellie's intensity increased very slowly, reaching a peak of 80 kt (41 m/sec) at 121200Z. Throughout the entire period during which Ellie was at typhoon intensity (101200Z to 150000Z), the eye remained large (i.e., diameter in excess of 45 nm) and ragged, and the areal extent of the outer circulation was very large (Figure 3-18-3). At 130000Z, Ellie passed within 90 nm (170 km) of the southern coast of Kyushu. A comprehensive data set of peak wind and minimum sea-level pressure was obtained from stations in Japan (Figure 3-18-4). After 140600Z, Ellie turned northward and slowly weakened. It briefly touched land at Wendeng, China, then made final landfall midway between Dairen and the China-North Korea border with an intensity of 45 kt (23 m/sec). The final warning was issued at 160600Z as the remnants of Ellie moved northward over rugged terrain in northeastern China.

III. DISCUSSION

a. Unusual genesis

Most tropical cyclones of the western North Pacific form in the monsoon trough. Ellie was one of few that did not. Some of the few, like Tropical Depression 31W and Yunya (36W), form in the low-level tradewind easterly flow in association with cyclonic disturbances in the tropical upper tropospheric trough (TUTT). Others, like Ellie, form in the subtropics at the base of mid-latitude low-pressure troughs.

The disturbance that became Ellie evolved from an area of deep convection that first appeared at relatively high latitude (30°N) at the base of a weak mid-latitude trough. This area of convection drifted slowly southward and was associated with an intensifying low-level cyclonic circulation. After several days of slow improvement in the organization of deep convection, and a gradual increase in the intensity and size of the low-level circulation, this subtropical disturbance became a tropical cyclone.

b. Large eye and large size.

In its intensifying tropical storm stage, the deep convection near the center of Ellie gradually wrapped around a large (60 nm) relatively cloud-free center (Figure 3-18-2). Satellite analysts were reluctant to call this feature an eye, as significant breaks in the deep convection were evident. However, as the deep convection formed a more complete ring, it was diagnosed as a ragged eye wall at 120530Z, roughly six hours after the image in Figure 3-18-3. For most of its life, Ellie had a large ragged eye with a diameter of approximately 60 nm (110 km). The maximum intensity of Ellie as derived from application of Dvorak satellite imagery analysis was 80 kt (41 m/sec). The Dvorak technique caps intensity at 90 kt (46 m/sec) for typhoons with large ragged eyes; where large is defined as an eye diameter of 45 nm (85 km) or more.

Another of Ellie's structural characteristics was its large size. The size of a tropical cyclone is a fairly difficult parameter to objectively specify. The average radius to the outer-most closed isobar has been suggested as an objective measure of size (Merrill 1984). Another parameter suggested as a measure of size is the average radial distance to the point where the streamlines of the low-level flow become unidi-

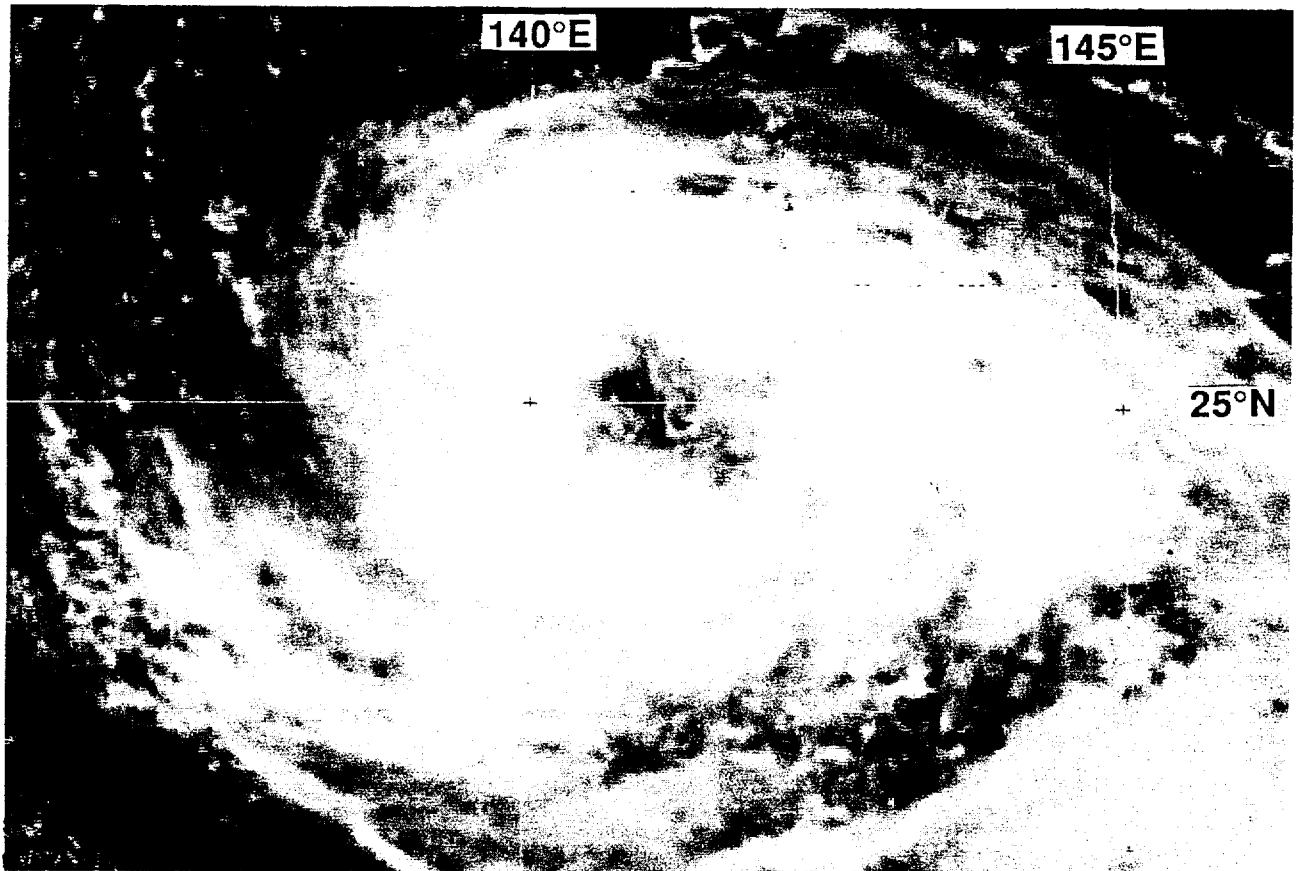


Figure 3-18-2 Ellie's deep convection begins to consolidate around a 60 nm (110 km) cloud-free center that would not be diagnosed as an eye for over another 72 hours (090231Z August visible GMS imagery).

rectional or anticyclonic. In the North Atlantic, where tropical cyclones are usually embedded in low-level easterly flow, the aforementioned size parameters may yield consistent results. However, in the western North Pacific, where tropical cyclones are usually embedded in the monsoon trough, the aforementioned parameters lead to an ambiguity: where does the tropical cyclone circulation end and the monsoon circulation begin? Disregarding the problems of objective determination of tropical cyclone size, it is certainly apparent on satellite imagery (Figure 3-18-3), that Ellie was large.

IV. IMPACT

No reports of injuries or of serious damage were received.

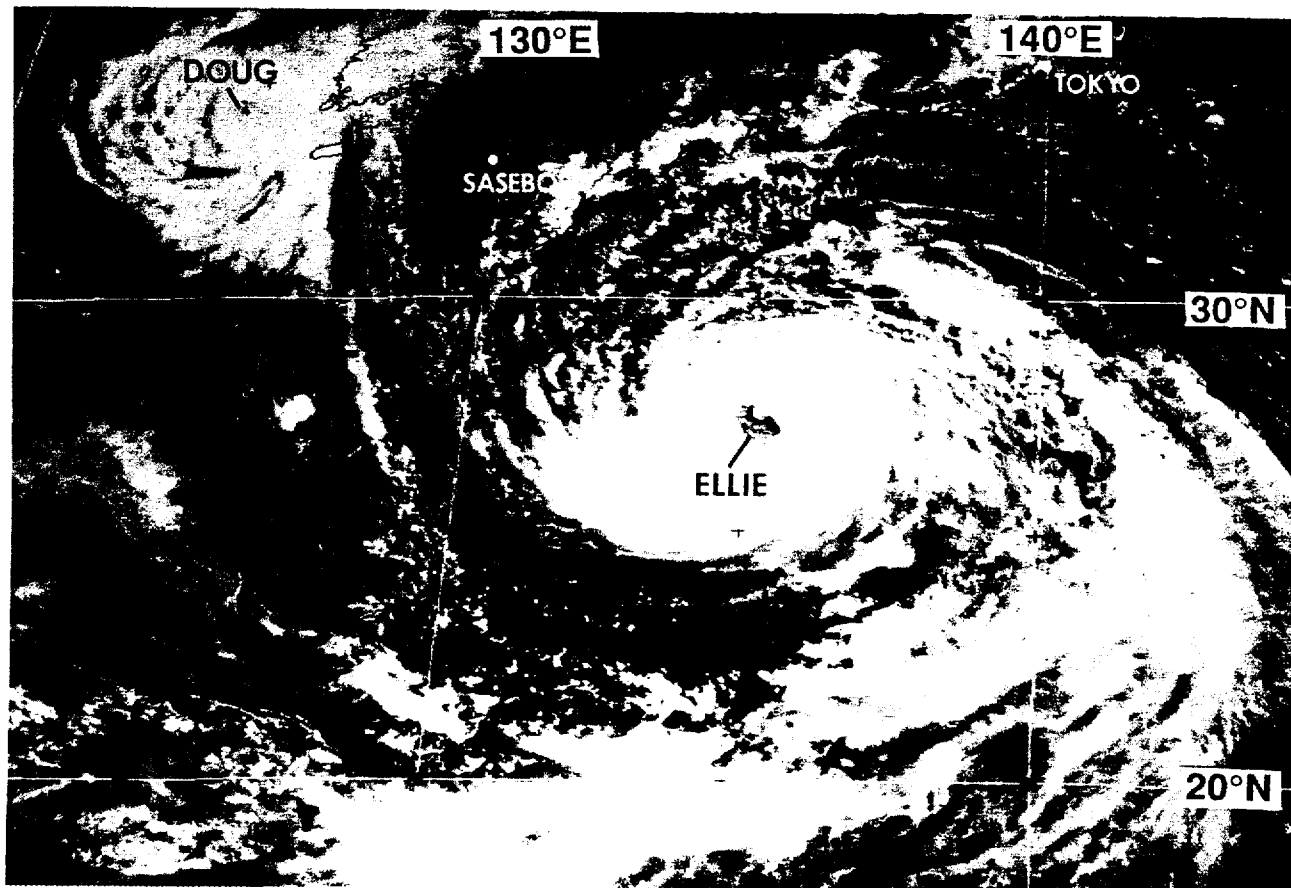


Figure 3-18-3 Ellie possesses a large ragged eye and a large outer circulation (112331Z August visible GMS imagery).

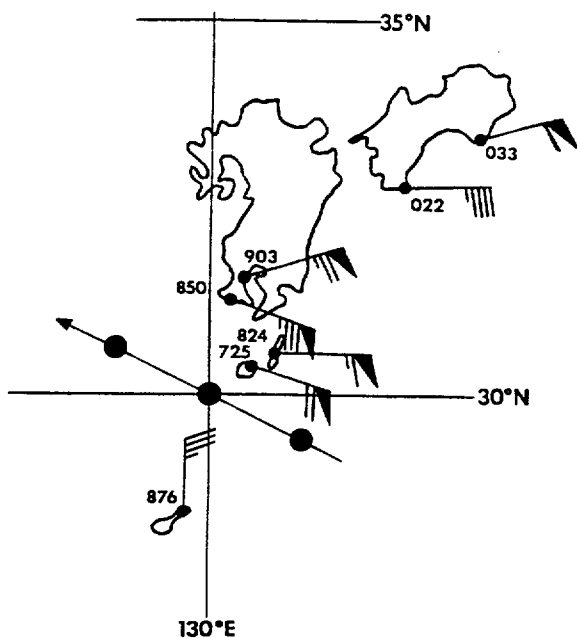


Figure 3-18-4 Maximum wind gusts and minimum sea-level pressure reported at several stations in southwestern Japan as Ellie passed through the region. Ellie's best-track is indicated by large dots. Wind is coded as follows: full barb = 10 kt, flag = 50 kt. Pressure is coded as follows: divide indicated value by 10 and add 900 (or add 1000 to values less than 100) to get pressure in units of millibars.

E 160 165 170 175 180 175 170 165 160 155 150 145 140 135 130 125 120 115 W

N 35

TROPICAL STORM LI

BEST TRACK TC-08E
30 JUL-18 AUG 94
MAX SFC WIND 55KT
MINIMUM SLP 984MB

30

25

20

15

10

5

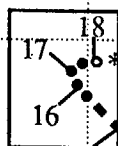
EQ

5

S 10

LEGEND

- △/△ 6-HR BEST TRACK POSITION
- a SPEED OF MOVEMENT (KT)
- b INTENSITY (KT)
- c POSITION AT XX/0000Z
- TROPICAL DISTURBANCE
- TROPICAL DEPRESSION
- TROPICAL STORM
- TYPHOON
- ◆ SUPER TYPHOON START
- ◇ SUPER TYPHOON END
- ◆◆◆ EXTRATROPICAL
- ◆◆◆ SUBTROPICAL
- *** DISSIPATING STAGE
- F FIRST WARNING ISSUED
- L LAST WARNING ISSUED

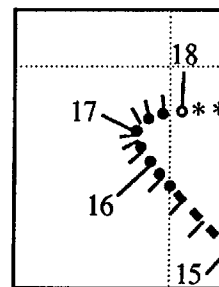


L-18/00Z

F-13/00Z

E 170

N 20



DTG (Z)	SPEED (KT)	INTENSITY (KT)
15/00	9	35
15/06	9	35
15/12	8	35
15/18	6	30
16/00	3	30
16/06	3	30
16/12	3	25
16/18	2	25
17/00	1	25
17/06	2	25
17/12	3	25
17/18	5	25
18/00	5	20

TYPHOON LI (08E)

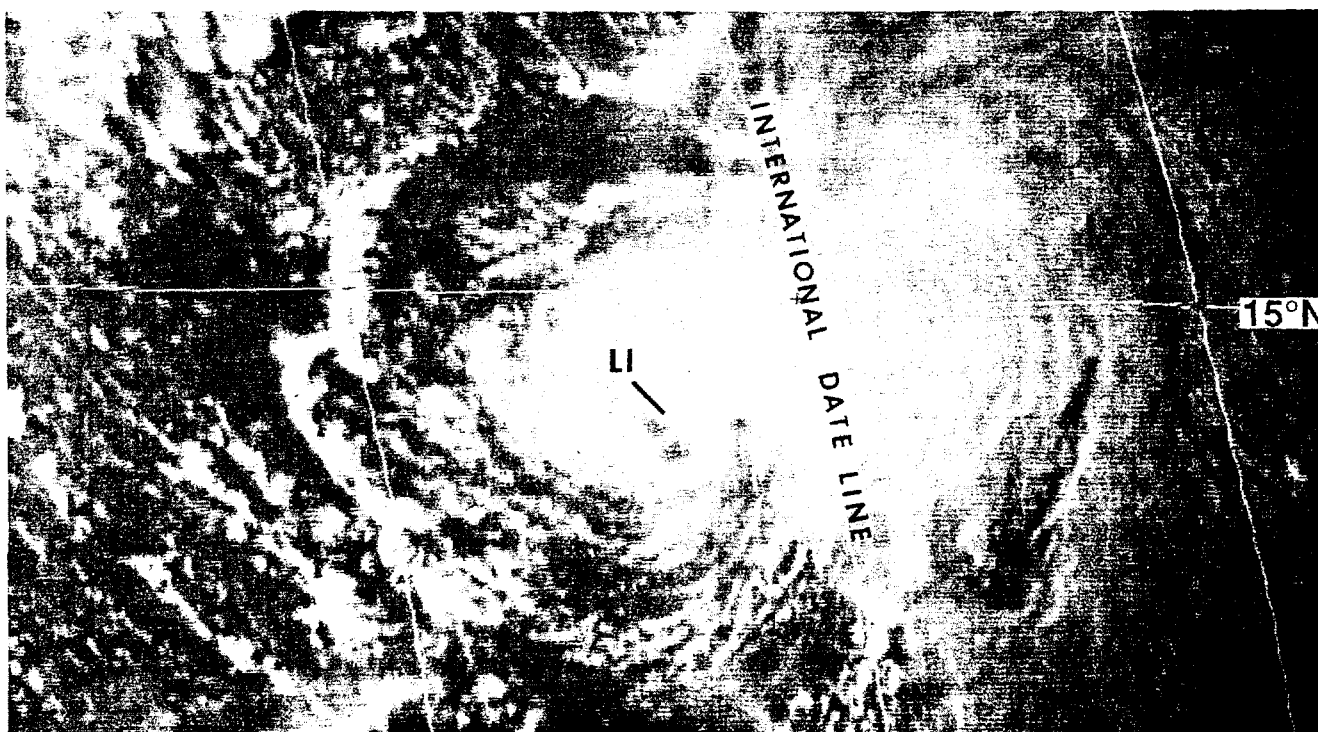
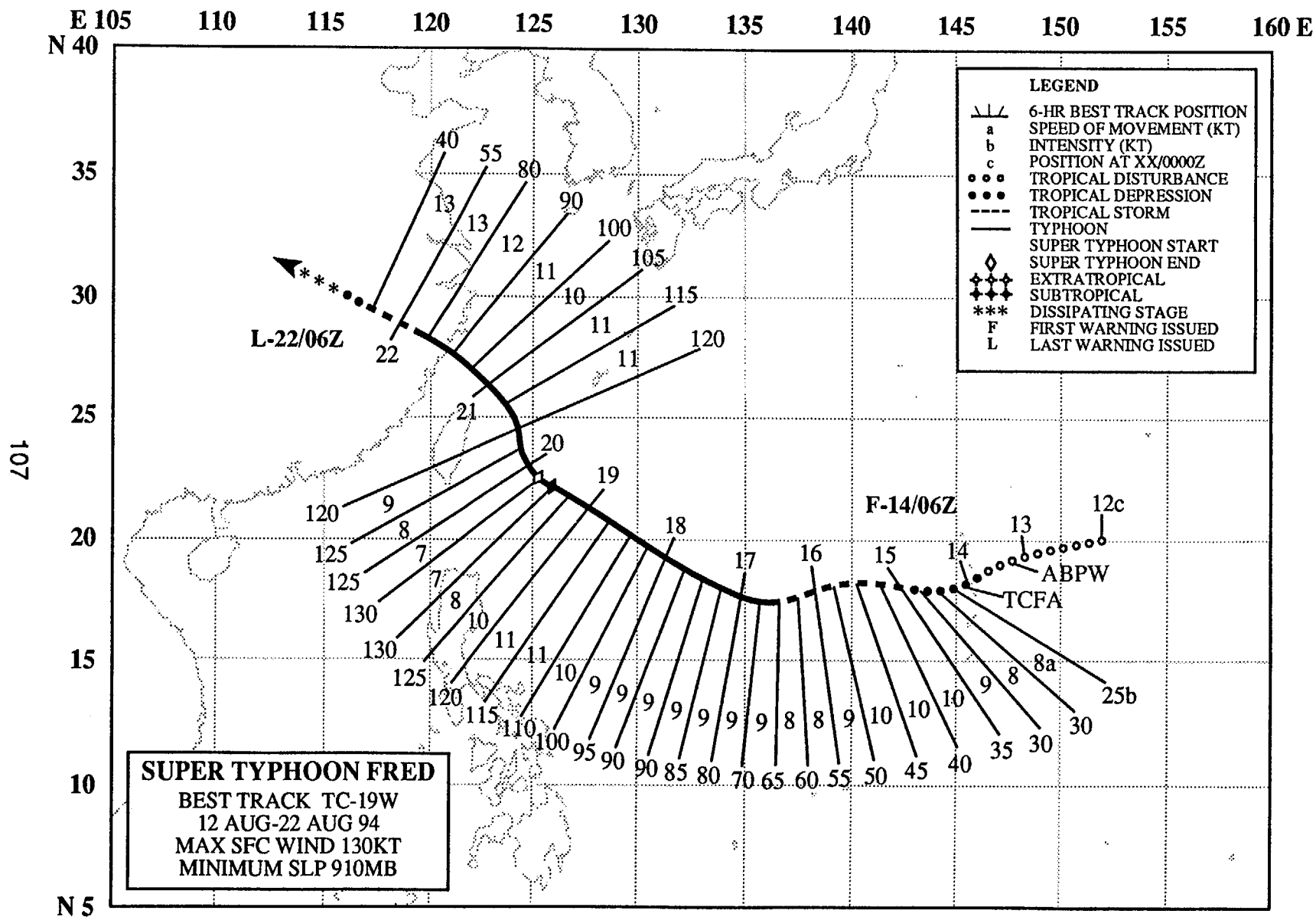


Figure 3-08E-1 Tropical Storm Li just after crossing the international date line with 50 kt (26 m/sec) (130531Z August visible GMS imagery). Li is about 250 nm (465 km) east of Wake Island.

Li, like John (08E), was unusual in that it traversed the areas of responsibility of all three US tropical cyclone warning centers — the National Hurricane Center (NHC), the Central Pacific Hurricane Center (CPHC), and the Joint Typhoon Warning Center (JTWC). During its 18-day life, it traveled over 3600 nm (6670 km), and 59 warnings were issued on the system.

Li was first observed as a disturbance in the monsoon trough of the eastern North Pacific, near 11°N; 120°W on 30 July. As it moved westward, it slowly intensified, and on 03 August, the disturbance crossed 140°W. At 030600Z, CPHC issued the first warning on Tropical Depression 08E. For the next two days, the depression tracked west-southwestward at 12-18 kt (22-33 km/hr) with 25 kt (13 m/sec) winds. On 05 August, the system turned toward the northwest; lost nearly all of its deep convection, and warnings were discontinued. A day later, warnings were reissued after convection again flared. On 06 and 07 August, the tropical depression passed about 600 nm (1111 km) south of the Hawaiian Island chain. Late on 07 August, TD 08E took a westward track, and at 081200Z, it was upgraded to Tropical Storm Li. A day later, it passed 180 nm (333 km) south of Johnston Island with 45 kt (23 m/sec) sustained winds. For the next 48 hours, Li slowly intensified, and at 121200Z, it was upgraded by the CPHC to Hurricane Li. Peak intensity was 65 kt (33 m/s). The CPHC issued its final warning on Hurricane Li at 121800Z as it crossed the international date line into the JTWC's area of responsibility. At 130000Z, JTWC issued its first warning on the system, downgrading Li to a 55-kt (28-m/sec) tropical storm, as strong upper level westerly winds south of a TUTT cell sheared the convection on Li's west side (Figure 3-08E-1). Li steadily weakened, and at 160600Z it was downgraded to a tropical depression. The depression continued to drift to the northwest, and the 59th and final warning was issued at 180000Z as TD 08E dissipated over water.



SUPER TYPHOON FRED (19W)

I. HIGHLIGHTS

As Typhoon Ellie (18W) approached southwestern Japan, the embryo of Super Typhoon Fred was developing about 1200 nm (2200 km) to the southeast. The developing system moved west-southwestward for four days, reaching typhoon intensity on 16 August. Like Doug (17W), which occurred earlier in the month, Fred reached super typhoon intensity without going through an episode of rapid intensification. Near the southern Ryukyu Islands, Fred began to weaken from its 130 kt (67 m/sec) peak intensity and veered to the northwest. It passed about 120 nm (220 km) north of Taipei before the system resumed a west-northwestward track and continued to weaken. Fred's landfall on mainland China on 21 August near the city of Wenzhou coincided with an unusually high astronomical tide, generating some of the highest tides of the last two decades in that region. Resultant flooding and strong winds took an estimated 1,000 lives in Wenzhou alone.

II. TRACK AND INTENSITY

The tropical disturbance that would become Fred was first mentioned on the 130600Z August Significant Tropical Weather Advisory. It initially tracked toward the west-southwest, equatorward of the mid-level subtropical ridge. The disturbance continued to develop, a Tropical Cyclone Formation Alert was issued at 140400Z followed by the first warning at 140600Z. On the morning of 15 August, Tropical Depression 19W was upgraded to Tropical Storm Fred. For the next five days the storm intensified at a rate of 20 kt (10 m/sec) per day, reaching typhoon intensity on the night of 16 August (Figure 3-19-1) and super typhoon intensity on the night of 19 August (Figure 3-19-2).

When Fred became a super typhoon, it was heading to the west-northwest on a course toward Taiwan. About 250 nm (460 km) southwest of Okinawa, Fred began to rapidly weaken, and veered north-northwestward passing to the north of Taiwan. The period of north-northwestward motion was short-lived, leading to passage between Ishigaki-jima (WMO 47918) and Miyako-jima (WMO 47927) (Figure 3-19-3). After passing through the southern Ryukyu islands, Fred resumed its previous west-northwestward heading, and continued to weaken (but at a much slower rate) as it approached mainland China. At 211200Z, Nanji Shan (WMO 58765) (a small island about 120 nm southeast of Wenzhou) recorded ten-minute sustained winds of 80 kt (41 m/sec) (92 kt one-minute average sustained wind) and a sea-level pressure of 956.7 mb (Figure 3-19-5). The final warning was issued at 220600Z as Fred dissipated over the Yangtze River valley near Wuhan.

III. DISCUSSION

a. Rate of intensification

Most super typhoons undergo a period of rapid intensification (Mundell 1990); where rapid intensification is defined as a 24-hour period during which the central pressure falls by at least 42 mb. However, Fred did not go through a period of rapid intensification (Table 3-19-1). In addition, the eye did not shrink significantly as usually occurs with rapid intensification, nor did it expand and develop a very thick eye wall as did Doug (17W). In fact, the size of the eye vacillated considerably (Table 3-19-2). Beginning on 15 August at 1200Z, Fred moved westward in tandem with a TUTT cell to its northeast. The effects (if any) of TUTT cells upon tropical cyclone motion and intensity are not well-understood.

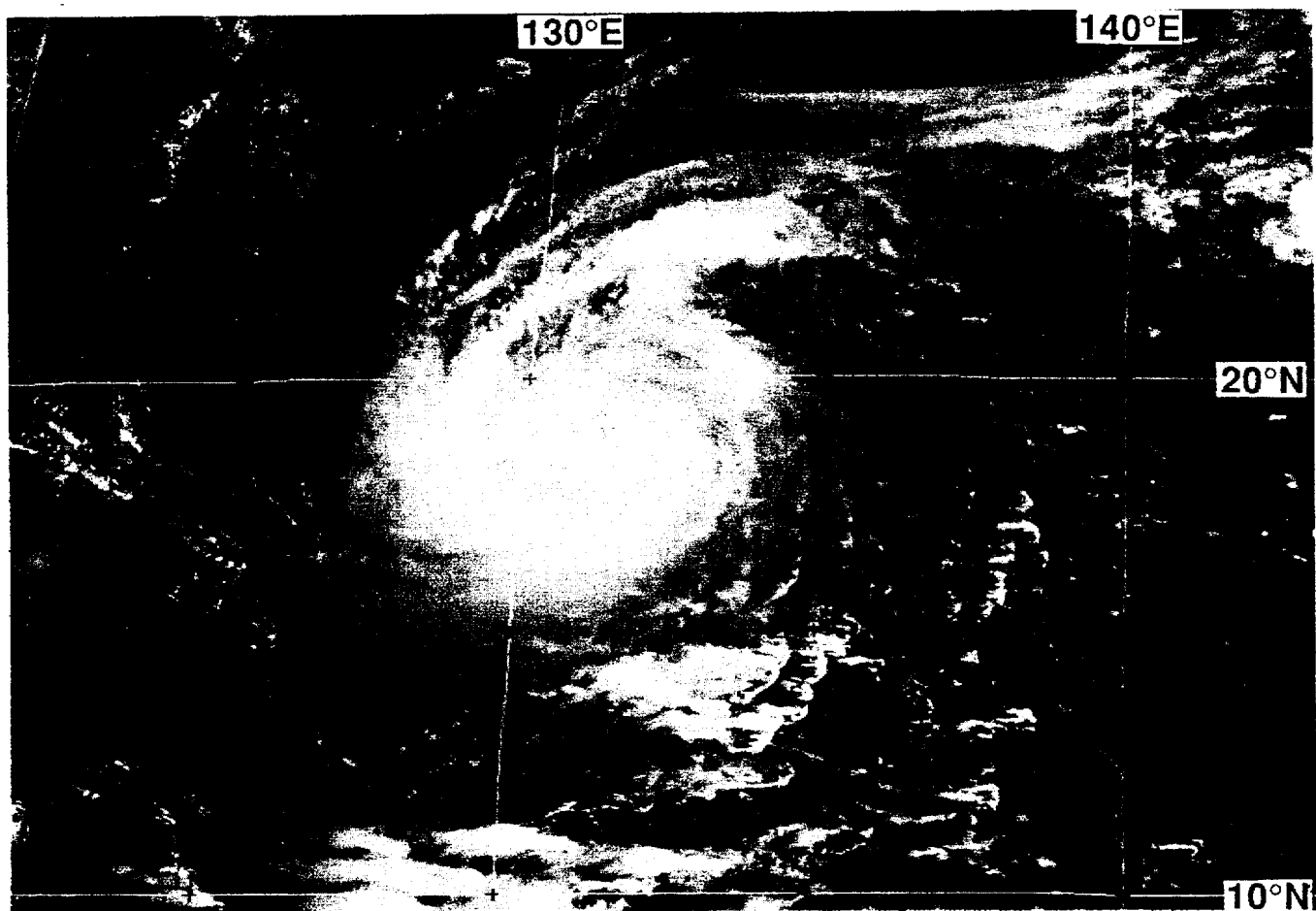


Figure 3-19-1 Fred attains typhoon intensity (172331Z August visible GMS satellite imagery).

b. Rate of weakening

Fred weakened rapidly following its peak of 130 kt (67 m/sec). This rapid weakening is substantiated by the observed minimum pressure and maximum wind during eye passage over Ishigaki-jima (WMO 47918), and by the maximum winds seen at Miyako-jima (see Figure 3-19-4). After leaving these stations, however, it appears that the rate of weakening slowed to less than 5 kt (2.6 m/sec) per 6-hour interval, since 92 kt (converted 1-min average) maximum sustained winds were observed at Nanji Shan (WMO 58765), China, as Fred struck the coast. Since this report was obtained at the synoptic hour of 211200Z it is likely that it represents neither the maximum wind nor the lowest pressure in Fred's core at landfall.

As with Doug (17W), Fred's eye did not expand after reaching peak intensity (Table 3-19-2). After 201800Z, the eye diameter began to shrink from 32 nm (59 km) to 11 nm (20 km) before it disappeared from the satellite imagery.

IV. IMPACT

No information was received concerning damage from Fred in the southern Ryukyu Islands. Damage in China was summarized in the August 31, 1994 Weekly Climate Bulletin of the U.S. National Climate Analysis Center of NOAA:

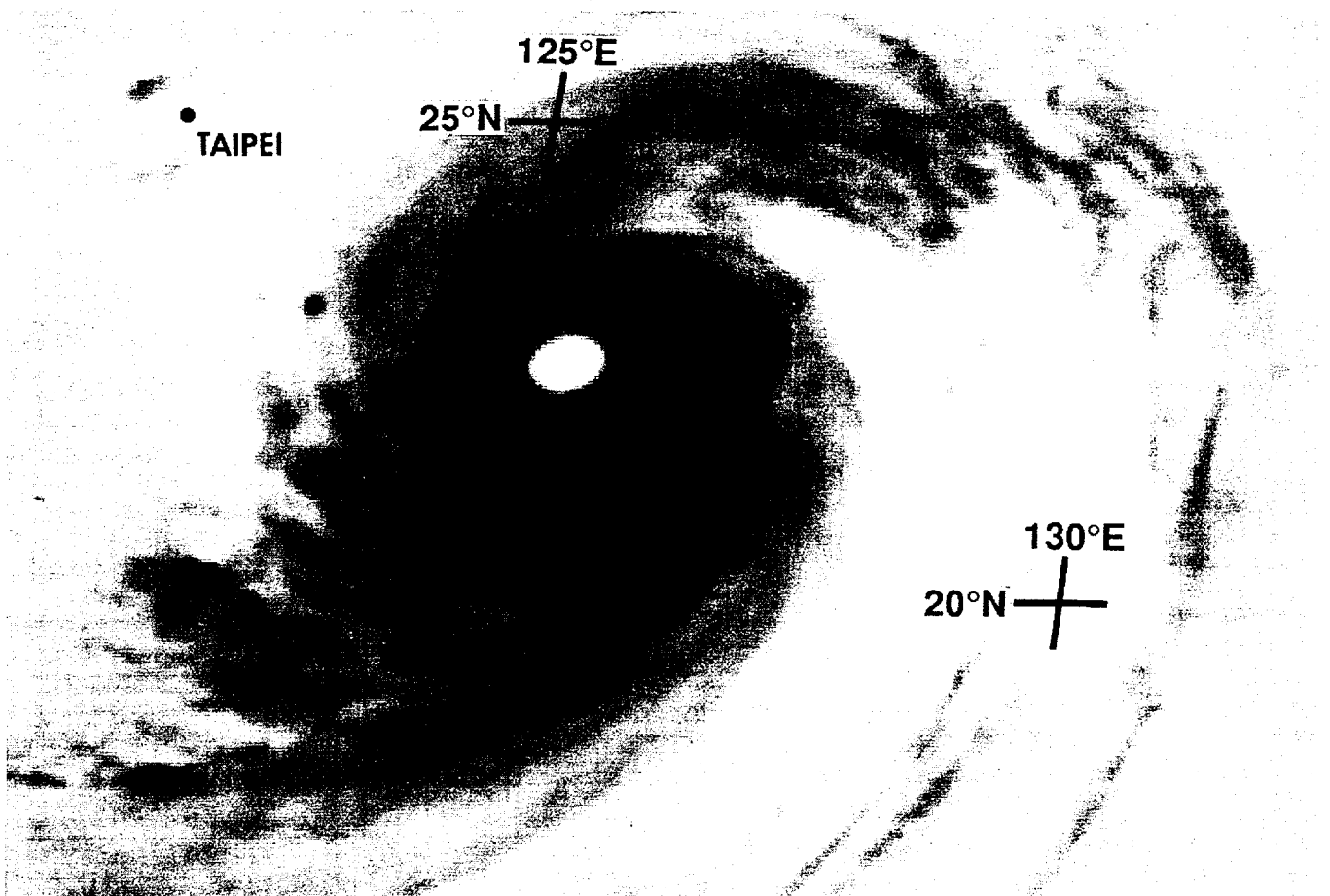


Figure 3-19-2 Fred at its peak intensity of 130 kt (67 m/sec) (191831Z August inverse infrared GMS imagery). Note: in an inverse infrared image, the cold clouds are dark and the warm sea surface is white.

“Typhoon Fred, packing wind gusts over 295 kph [160 kt] at one time, slowly weakened as it tracked north of Taiwan and into southern Zhejiang province in China. Generally, 100-225 mm (3.9-8.9 in) of rain fell along and near the path of the storm, flooding large sections of northern Taiwan and southern Zhejiang province. According to press reports, Fred’s landfall near the city of Wenzhou coincided with an unusually high astronomical tide, thereby generating some of the highest tides of the last two decades in and near Wenzhou. Resultant flooding combined with strong winds to take an estimated 1,000 lives in Wenzhou alone, according to city officials. In addition, local officials indicated that Fred, the region’s worst storm in over a century, demolished 100,000 homes, damaged another 700,000 dwellings, isolated more than two million individuals, forced the closure of Wenzhou airport for at least two weeks, damaged over 3000 km² (875 mi²) of farmland, caused flooding in more than 180 towns, and forced 90,000 enterprises to suspend production. Total economic losses may top \$1.2 billion (U.S.).”

Table 3-19-1 Twenty-four hour pressure fall for each 6-hour interval during the intensification of Typhoon Fred. Winds are in knots and represent best-track winds; pressures are in millibars and are derived from winds using the Atkinson-Holliday wind-pressure relationship (Atkinson and Holliday 1977).

Time (Z)	24-hr Wind Range	24-hr Pressure Range	24-hr Pressure Fall
1600-1700	55-75 kt	984-968 mb	16 mb
1606-1706	60-80	980-963	17
1612-1712	65-85	976-959	17
1618-1718	70-90	971-954	17
1700-1800	75-95	968-949	19
1706-1806	80-100	963-943	20
1712-1812	85-110	961-932	29
1718-1818	90-115	954-927	27
1800-1900	95-120	949-922	27
1806-1906	100-125	939-916	23
1812-1912	110-130	932-910	22
1818-1918	115-125	927-916	11

Table 3-19-2 Comparison of Dvorak T-number, best track intensity and infrared eye diameter for Typhoon Fred from initial 55 kt (28 m/s) intensity to after landfall in China.

Date/Time (Z)	T-number	Intensity (kt)	Eye Diam (nm)
160000	3.5	55	NA
160600	3.5	60	NA
161200	4.0	65	27
161800	4.5	70	24
170000	5.0	75	25
170600	5.0	80	17
171200	5.0	85	29
171800	5.0	90	24
180000	5.0	95	22
180600	5.0	100	21
181200	6.0	110	16
181500	6.0	115	16
181800	6.0	115	25
182100	6.0	120	35
190000	6.0	120	24
190300	6.0	120	29
190600	6.5	125	30
190900	6.5	125	30
191200	7.0	130	33
191800	6.0	125	38
200000	6.0	120	32
200600	5.5	110	26
201200	6.0	105	34
201800	5.0	100	26
210000	4.5	95	18
210600	4.5	95	11
211200	4.0	90	NA
211800	4.0	80	NA

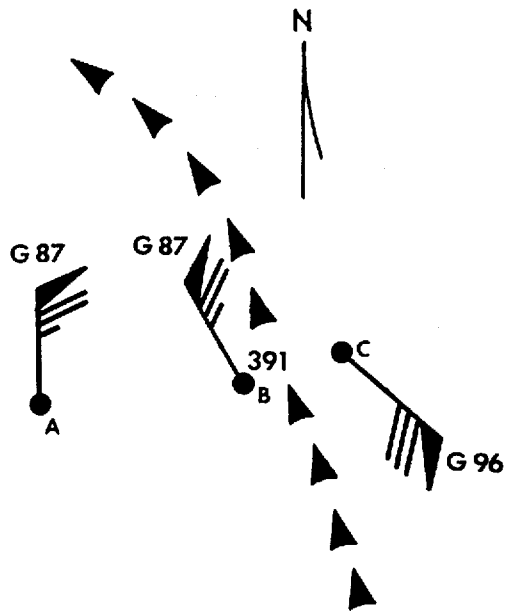


Figure 3-19-3 Wind and pressure data at Yonaguni-jima (WMO 47912) (labeled A), Ishigaki-jima (WMO 47918) (labeled B), and Miyako-jima (WMO 47927) (labeled C) at 201200Z. Peak 10-minute sustained winds are plotted and peak gusts are indicated. The pressure of 939.1 mb recorded at Ishigaki-jima is plotted as 391. The track of Fred is indicated by the trail of arrows.

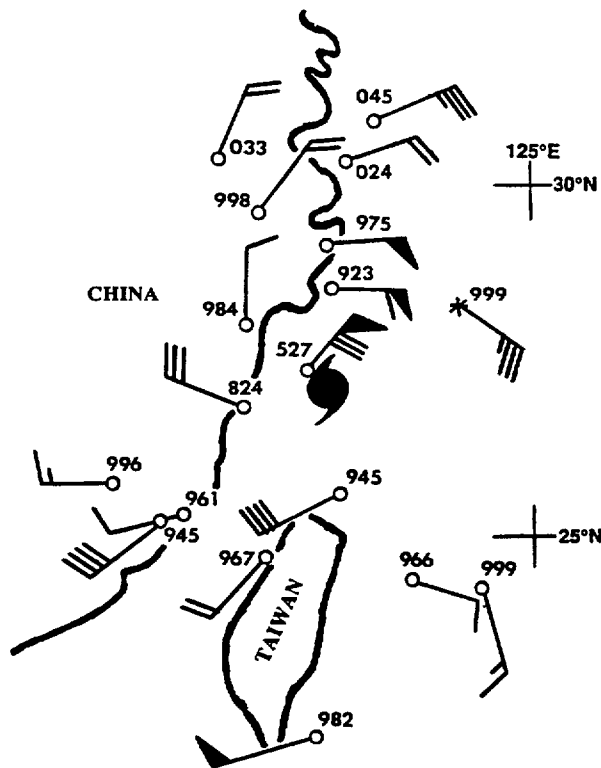


Figure 3-19-4 Synoptic reports at 211200Z August as Fred makes landfall on the east coast of China. Winds are 10-minute sustained averages.

E 105 110 115 120 125 130 135 140 145 150 155 160 165 170 E

N 40

35

30

25

20

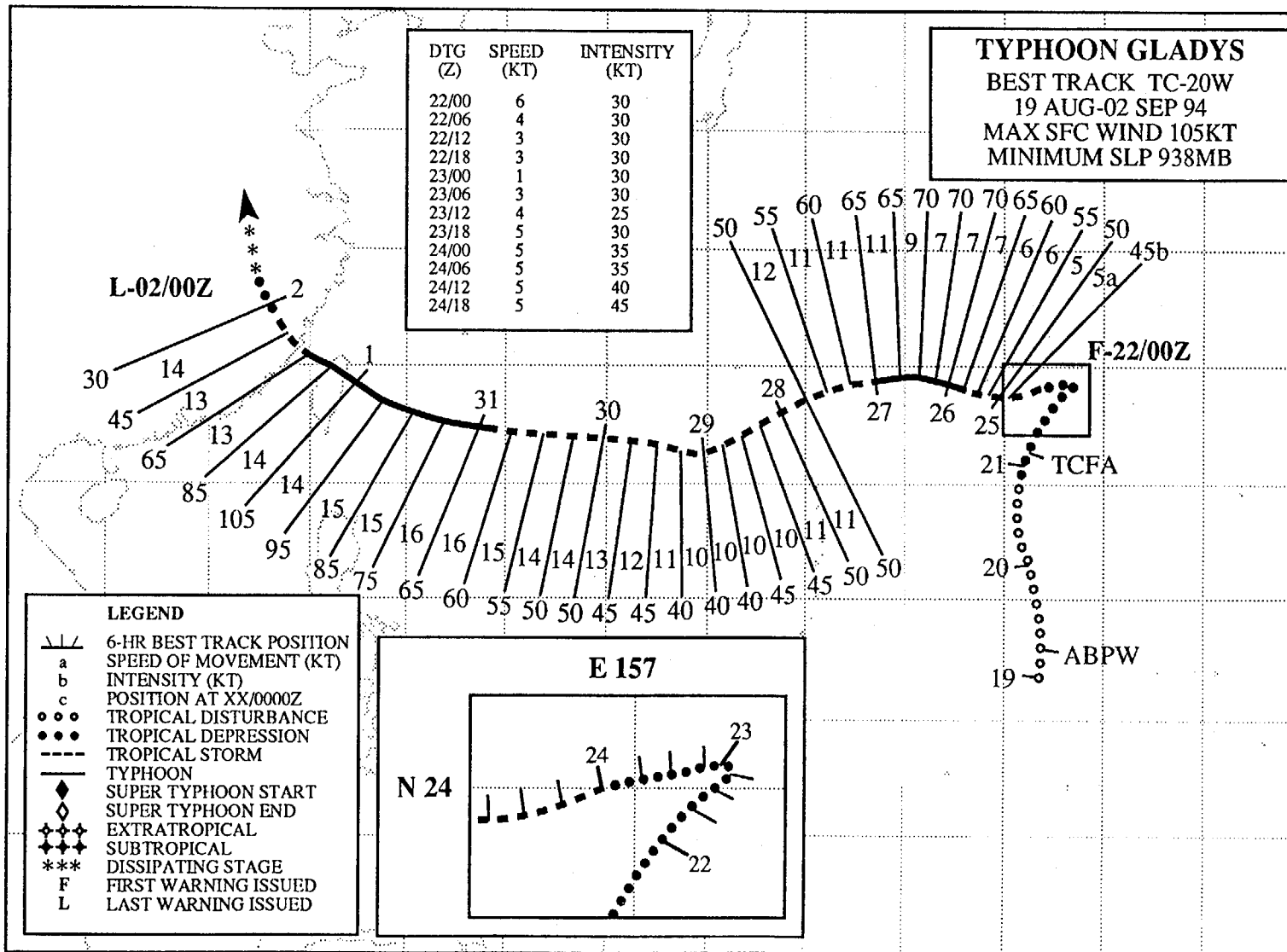
15

10

5

EQ

113



TYPHOON GLADYS (20W)

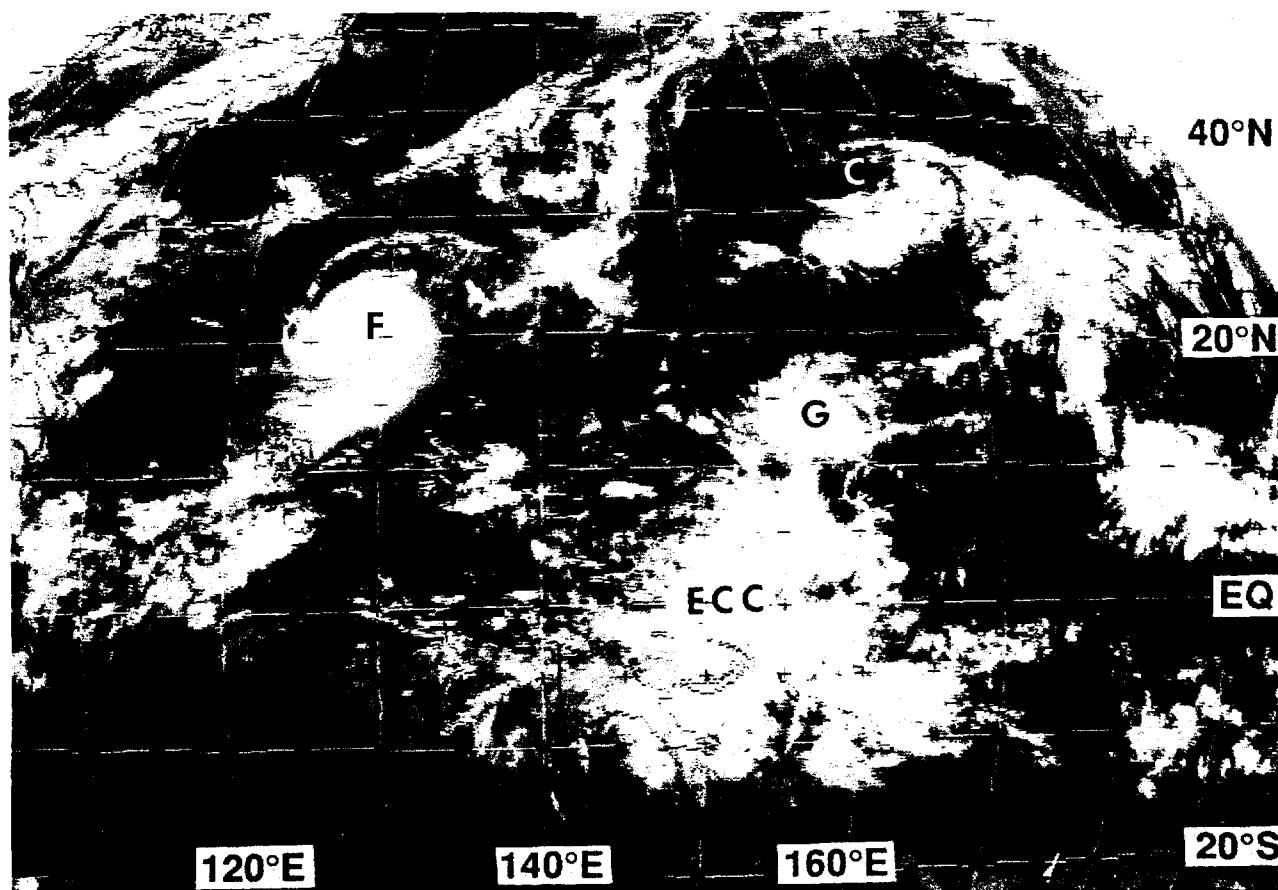


Figure 3-20-1 A complex cloud pattern over the western North Pacific basin preceded the formation of Gladys. An equatorial cloud cluster (ECC), an upper tropospheric cut-off low (C), and Typhoon Fred (F) figure prominently in the large-scale environment of the pre-Gladys tropical disturbance (G) (190031Z August infrared GMS imagery).

I. HIGHLIGHTS

For the first half of its life, Gladys was a very small tropical cyclone that exhibited large fluctuations of intensity. Ground-truth wind measurements from Minami-Torishima (WMO 47991) and from a station at its landfall site in Taiwan indicated that real-time estimates of Gladys' intensity (when near these sites) were too low. Images from Taiwan-based radar showed that as Gladys approached Taiwan it had well-developed concentric eye walls.

II. TRACK AND INTENSITY

As Gladys was forming, the large-scale distribution of cloudiness (Figure 3-20-1) and the large-scale structure of the troposphere over the western North Pacific had become quite complex. An upper-tropospheric cold-core low dominated the distribution of cloudiness in the subtropics of the western North Pacific, near the international date line, and had induced an inverted trough of low pressure in the sea-level pressure field there. A weak monsoon trough extended east-southeastward from near Taiwan to about 13°N 160°E. A large cluster of deep convection and associated cirrus debris accompanied monsoonal westerly winds along the equator from 150°E to 160°E.

During the daylight hours of 19 August, a small area of persistent deep convection embedded in anti-

cyclonically curved cirrus debris (Figure 3-20-2) was observed at the eastern end of the monsoon trough where synoptic data indicated the presence of a weak surface circulation. This tropical disturbance was first mentioned on the 190600Z August Significant Tropical Weather Advisory. After drifting northward for almost two days, satellite imagery showed low-level cloud lines wrapping underneath a convective cloud mass. A Tropical Cyclone Formation Alert was issued at 210430Z. The first warning was issued at 220000Z; it stated, in part:

“... [Tropical Depression] 20W has an organized low level circulation which is partially exposed on the northwest side of the convective cloud mass. The deep convection is displaced less than 30 nm southeast of the cyclone center. This is a small tropical cyclone ... SSM/I data does not indicate that gale-force winds exist near the center. ... The NOGAPS model does not analyze Tropical Depression 20W as a distinct feature, nor does it develop the system in the prog series. ... Climatology favors a peak intensity of less than 55 kt ... we anticipate that Tropical Depression 20W will reach minimal tropical storm intensity in about 24 hours, and peak at about 50 knots in 60 hours. ...”

After 221800Z, Tropical Depression 20W made an abrupt turn toward the west. This may have been in response to the sub-tropical ridge building to its north as two upper-tropospheric cold-core lows, one near the international date line, and another near Japan, weakened. After the system turned toward the west, it began to intensify. It was upgraded to Tropical Storm Gladys at 240000Z. By the morning of 25 August, it developed an eye (Figure 3-20-3). About nine hours after the imagery in Figure 3-20-3, Gladys passed about 30 nm (50 km) south of Minami-Torishima (WMO 47991), where a peak gust of 74 kt (38 m/sec) was recorded at 250956Z. Continuing on a westward track, Gladys appeared to come under the influence of westerly shear and weakened considerably (Figure 3-20-4). At 281800Z, its intensity dropped to 40 kt (21 m/sec). As Gladys moved westward toward Taiwan, it underwent a second period of intensification. At 010000Z September, shortly before Gladys' landfall on Taiwan, the intensity reached 105 kt (54 m/sec) (Figure 3-20-5). Gladys increased in size from very small to average during this second intensification phase. While crossing the northern half of Taiwan, Gladys weakened considerably. It then tracked inland over mainland China. The final warning was issued at 020000Z September as Gladys dissipated over land.

III. DISCUSSION

a. Ground-truth intensity verification

Ground-truth verification of Gladys' intensity was obtained at two points along its track: (1) Minami-Torishima (WMO 47991), and (2) northern Taiwan. At 250900Z, Gladys passed about 30 nm (50 km) south-southwest of Minami-Torishima (WMO 47991), (Figure 3-20-6). This island experienced a seven-hour period of sustained gale-force wind. The peak gust of 74 kt (38 m/sec) was recorded at 250956Z, and the minimum sea level pressure of 1001.4 mb was recorded at 250951Z. This peak wind and minimum pressure indicate that Gladys was a typhoon when it passed south of Minami-Torishima. Based on these measurements, the final best-track intensity of Gladys was increased to 65 kt (33 m/sec) from the real-time 55 kt (28 m/sec) satellite-derived estimate.

The second ground-truth verification was obtained when Gladys came ashore in northern Taiwan. Suao (WMO 46706), recorded a peak gust of 133 kt (68.6 m/sec) at 010232Z and a minimum sea level pressure reading of 960.3 mb at 010247Z. The over-water one-minute sustained wind speed associated with a 133 kt gust is 105 kt (54 m/sec). Thus, the peak gust measured at Suao was used to increase the final best-track intensity to 105 kt from the real-time satellite-derived intensity estimate of 85 kt (44 m/sec).

b. Concentric eye walls

As Gladys approached Taiwan's northeastern coast, weather radar located at Hualien (WMO 46699) was able to gather some detailed images of the structure of its core. From the time when the eye first appeared at the outer range of the radar, until approximately one hour before landfall, the core was comprised of concentric eye walls (Figure 3-20-7). At 311600Z, the inner eye wall was a complete ring about 10 nm (20 km) in thickness that surrounded a small central clearing about 6 nm (10 km) across (Figure 3-20-7c). A 10 nm (20 km) moat surrounded the inner eye wall and separated it from a 10 nm (20 km)-thick outer eye wall. For nearly ten hours, this structure prevailed. There was no evidence of contraction of the outer eye wall. Few tropical cyclones are observed to have well-defined concentric eye walls, although it has been suggested that most very intense tropical cyclones (i.e., those tropical cyclones with intensities in excess of 100 kt) have concentric eye walls at some point in their evolution (Willoughby 1982, 1990). Another observation made by Willoughby is that when concentric eye walls are present, the outer eye wall tends to contract and eventually replace the inner eye wall. In the case of Gladys, it appears that a steady-state structure of well-defined concentric eye walls was maintained for 10 hours. Landfall ultimately disrupted that structure.

c. Forecast performance

The westward-moving Gladys presents an ideal case for illustrating the poleward bias reported by Carr (personal communication) to exist in the NOGAPS model for very small westward-moving tropical cyclones (Figure 3-20-8). According to Carr, NOGAPS effective grid spacing is too large to properly analyze a very small to small tropical cyclone. The bogus vortex inserted into the analysis starts out too large and usually expands if the model intensifies the system. Since the poleward propagation of a vortex is size-dependent (i.e., the larger the vortex, the greater the poleward prop-

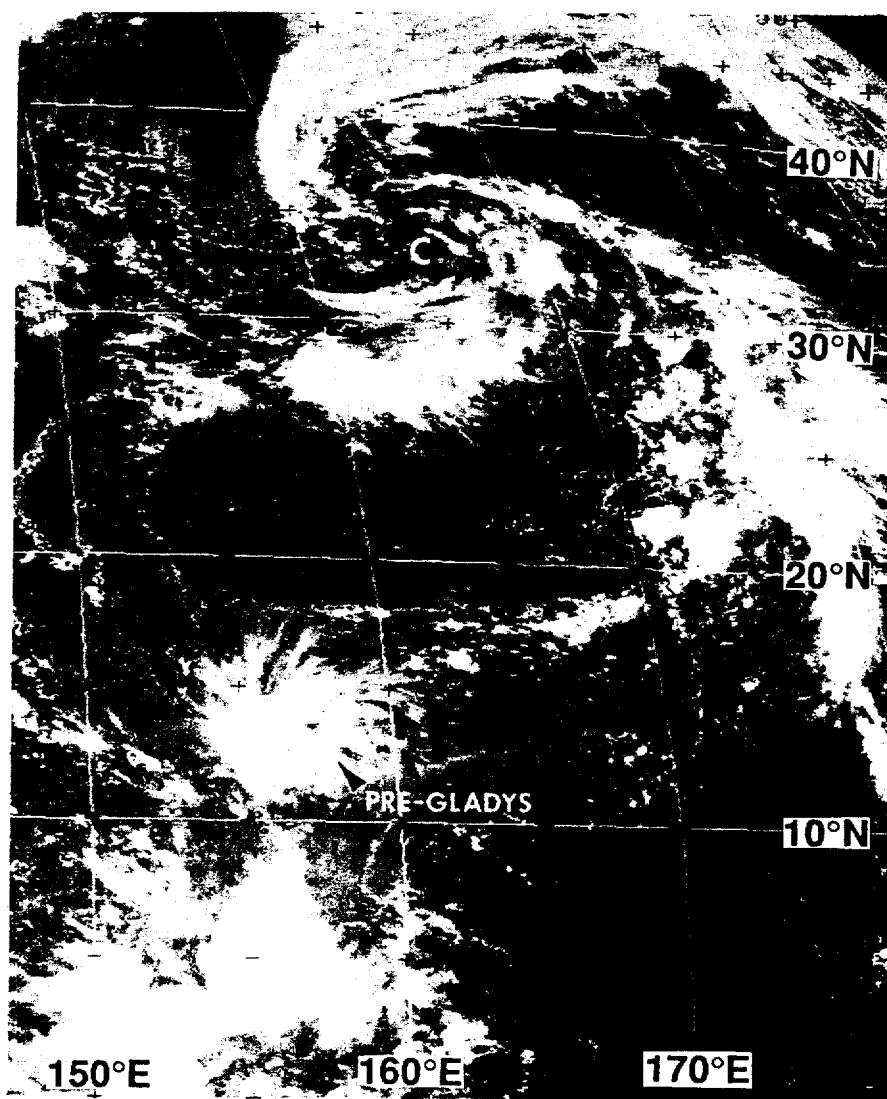


Figure 3-20-2 An area of persistent deep convection associated with anticyclonically curved cirrus outflow, defines the tropical disturbance that would later become Gladys (190031Z August visible GMS imagery). The "C" shows the location of a large upper-tropospheric cut-off low.

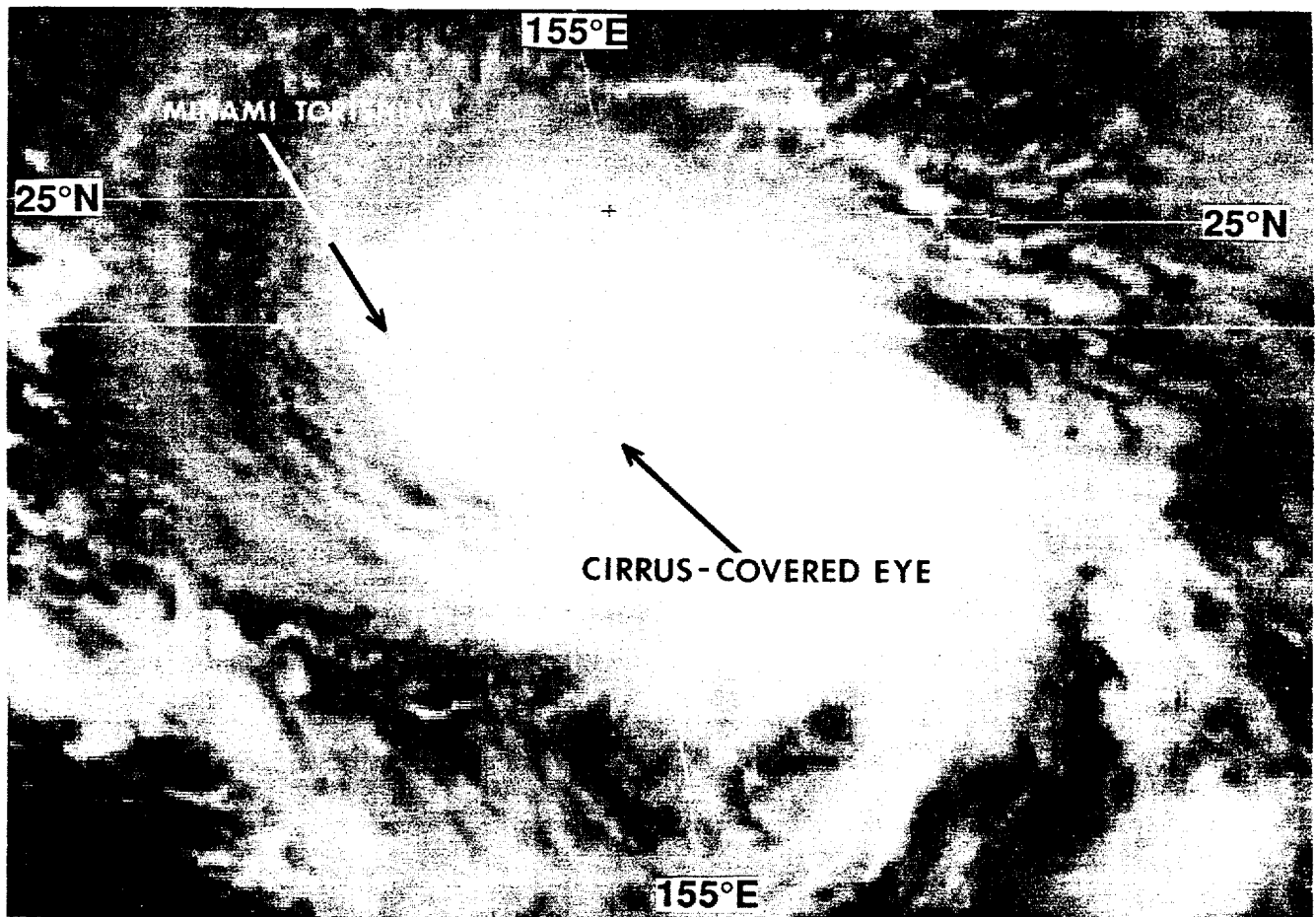


Figure 3-20-3 An eye appears in Gladys' central dense overcast (250131Z August visible GMS imagery).

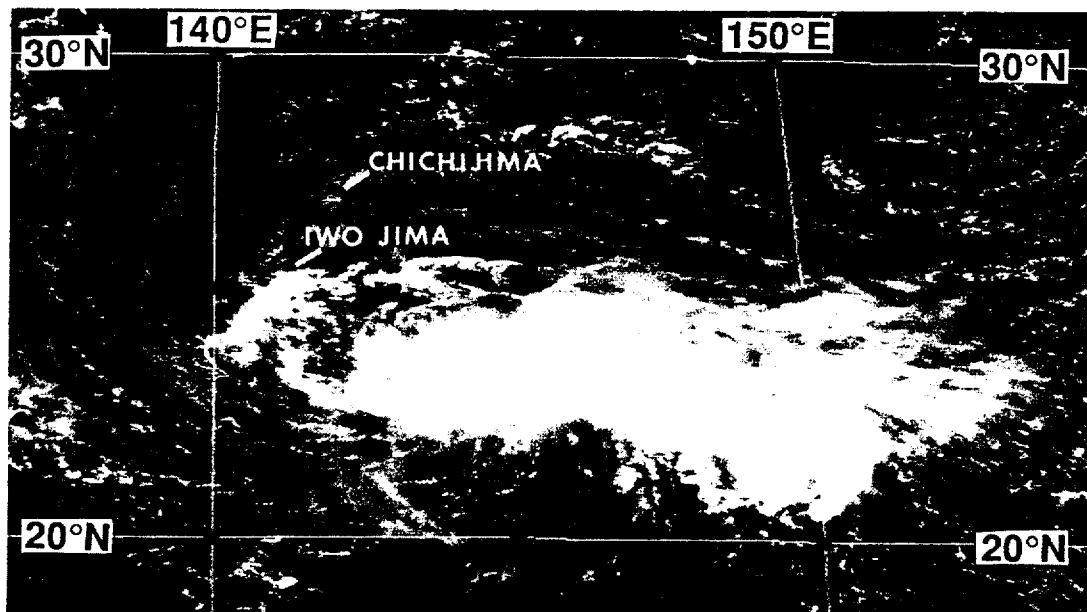


Figure 3-20-4 Gladys' low-level circulation center becomes partially exposed as the system experiences westerly shear (280031Z August visible GMS imagery).

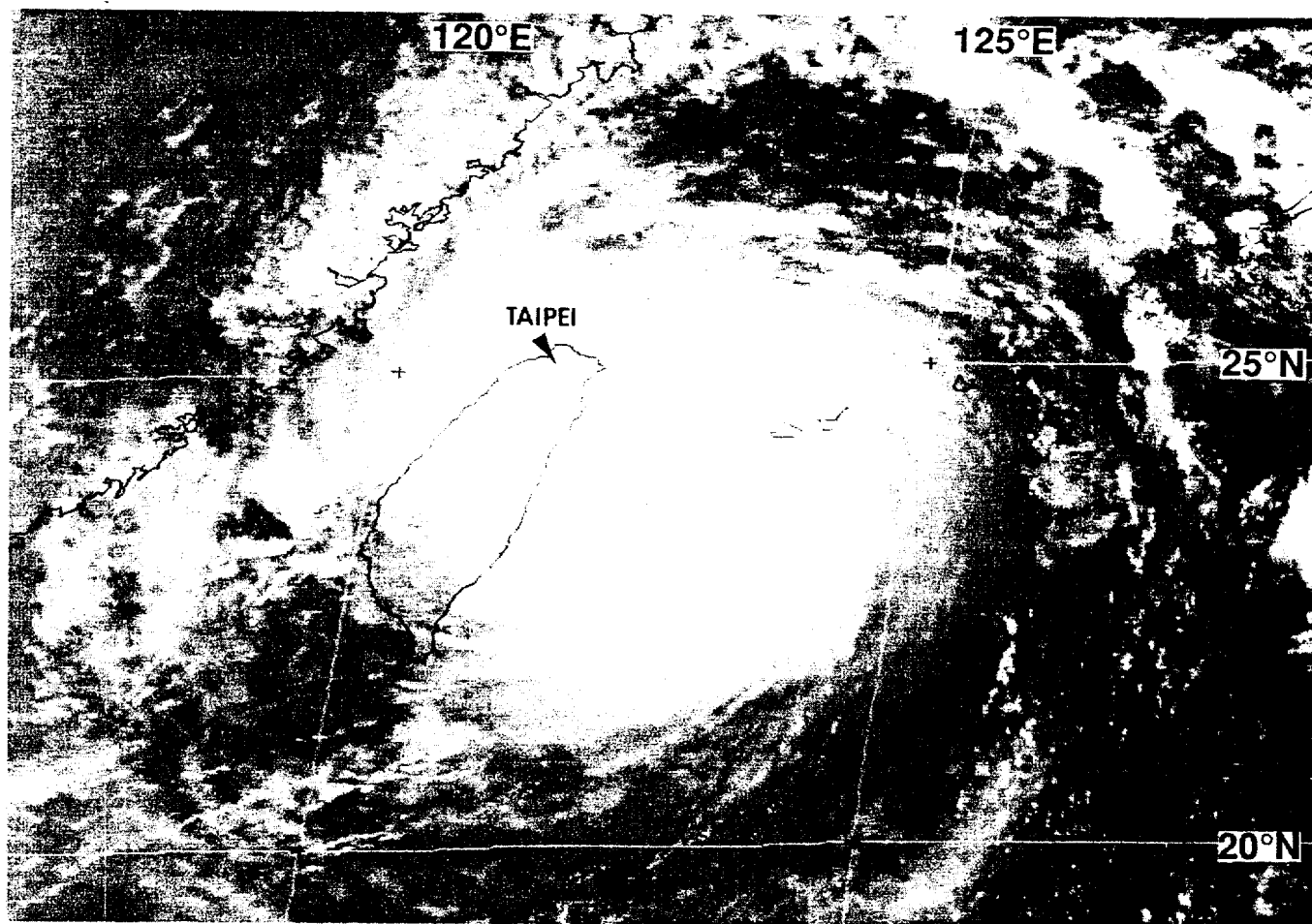


Figure 3-20-5 Gladys at peak intensity (312331Z August visible GMS imagery).

agation), it is almost a guarantee that the NOGAPS forecast will be to the right of track for a very small westward-moving tropical cyclone.

IV. IMPACT

Typhoon Gladys battered Taiwan with high wind and heavy rain. A peak wind gust of 133 kt (68.6 m/sec) was recorded at Suao (WMO 46706). Six deaths were recorded. A woman was killed when a utility pole fell on her car, a man drowned in a flooded river, and three other people were killed by falling objects. Another woman was killed when strong winds caused her house to collapse.

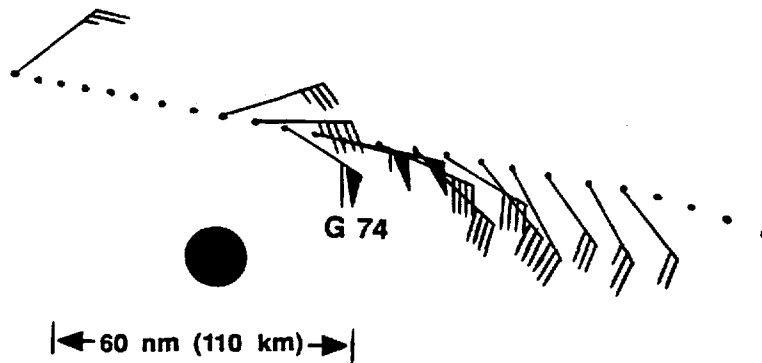


Figure 3-20-6 The wind recorded at Minami-Torishima (WMO 47991) as Gladys passed to the south (each small dot is a one-hour time step). The reference frame has been adjusted to the center of Gladys (large black dot).

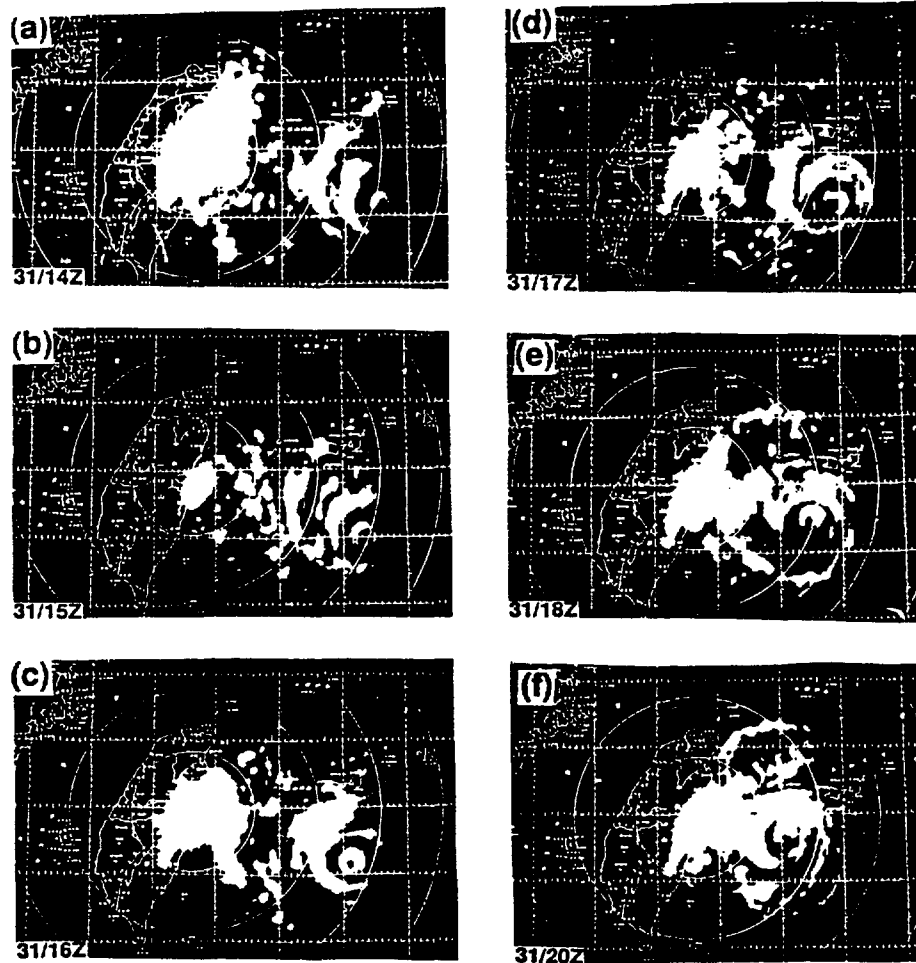


Figure 3-20-7 (a-f) Ground-based radar depictions of the concentric eye walls of Typhoon Gladys as it neared the coast of Taiwan. Time of radar image is indicated on each panel. (Radar images courtesy of the Taiwan Central Weather Bureau.)

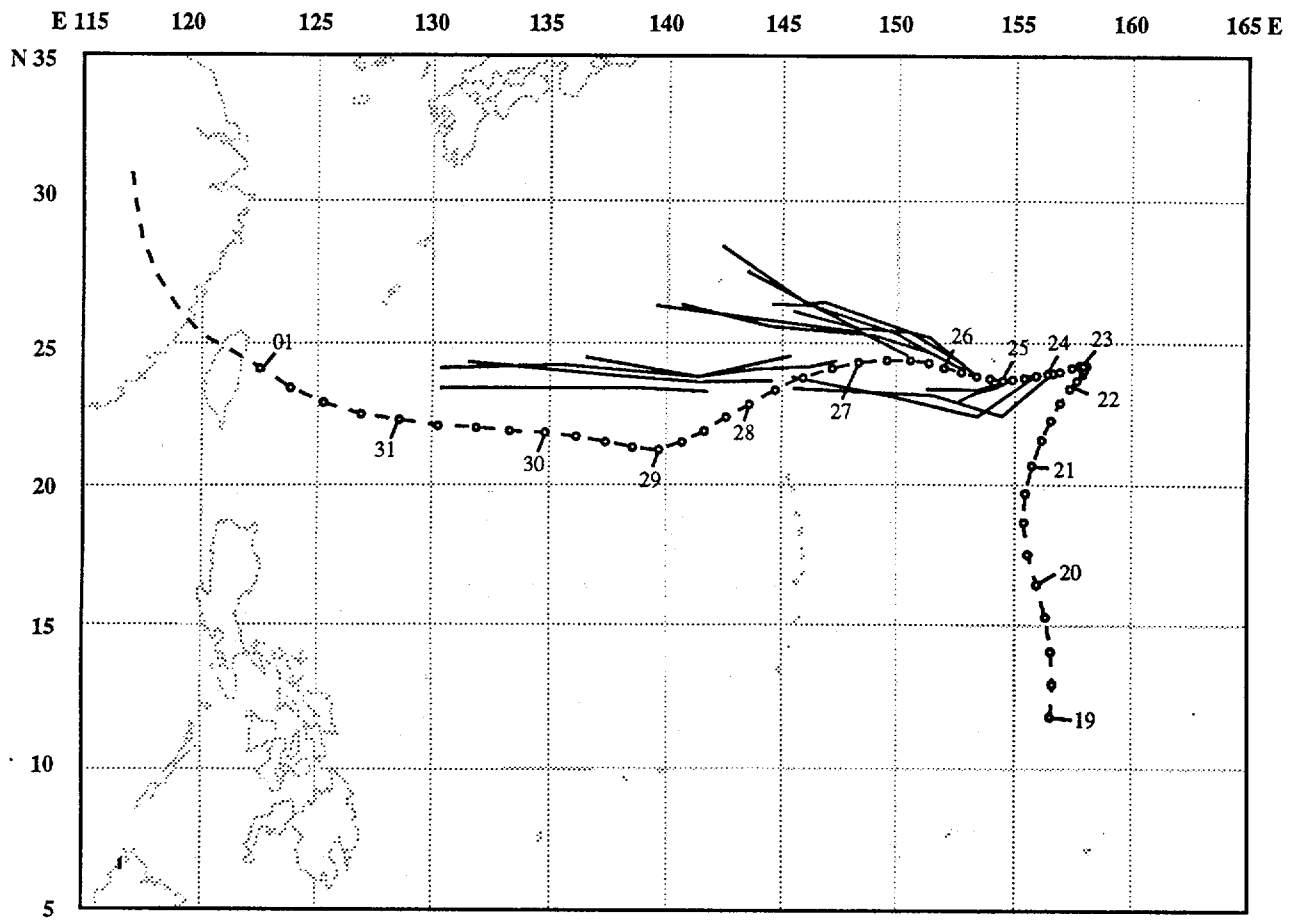
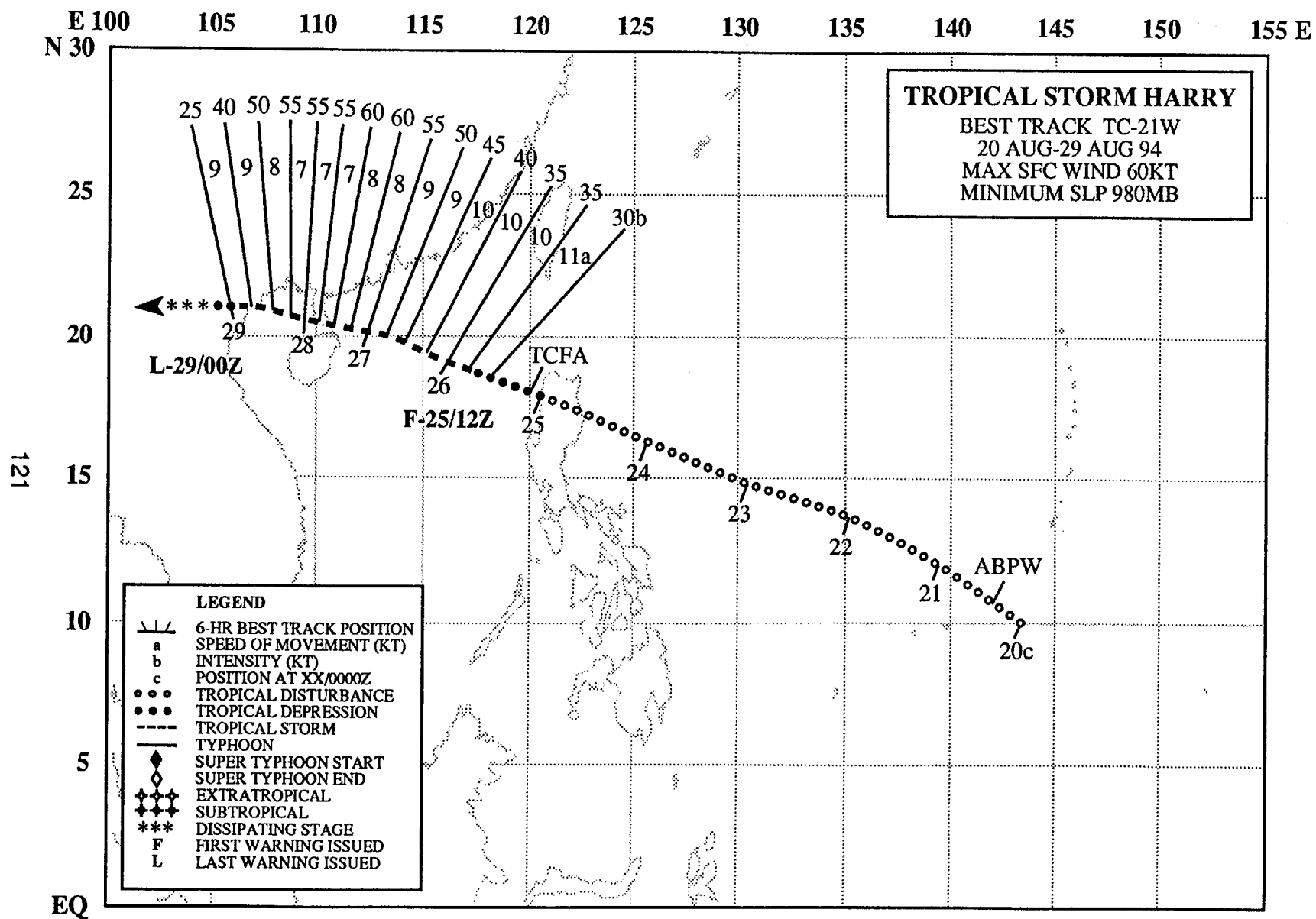


Figure 3-20-8 NOGAPS track forecasts show poleward bias.



TROPICAL STORM HARRY (21W)

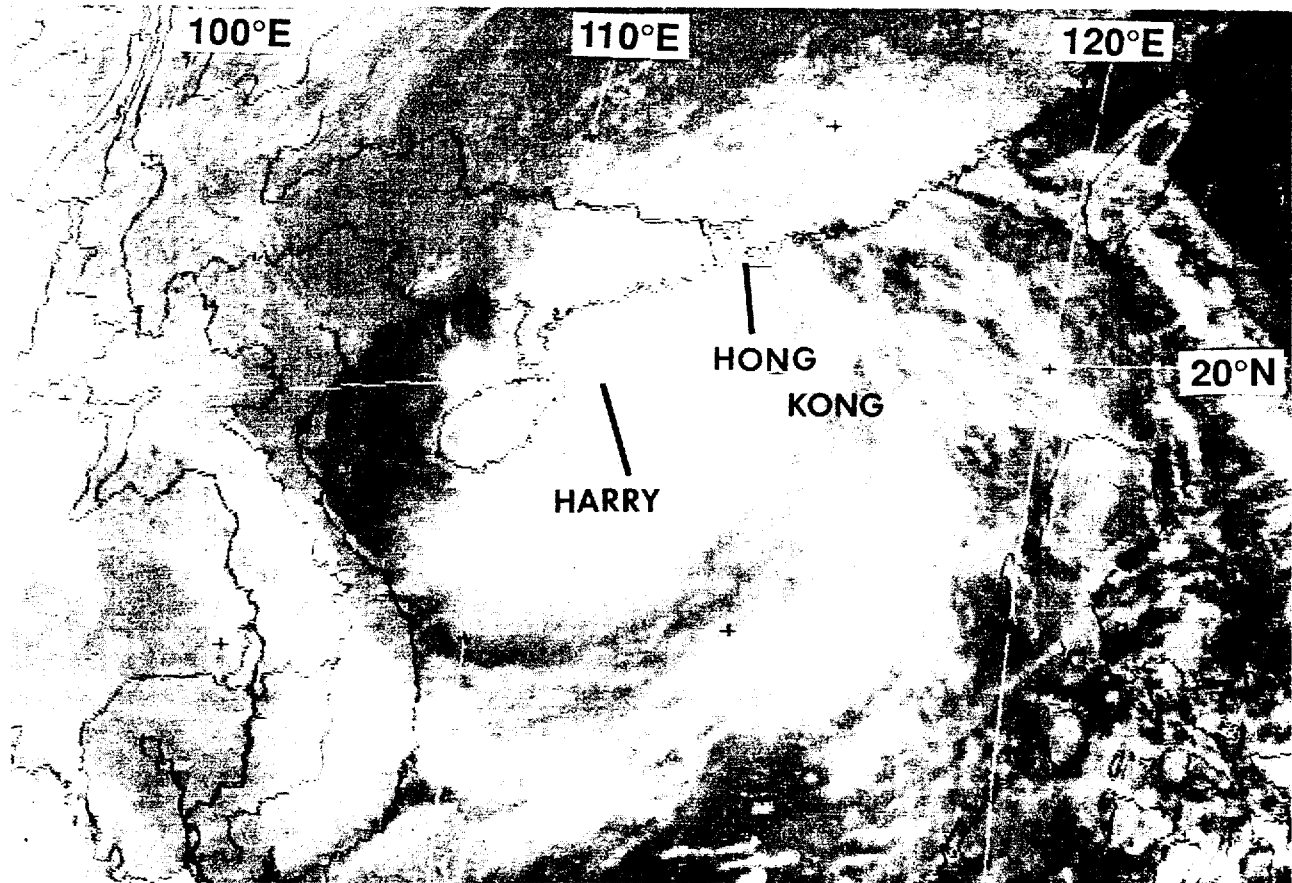
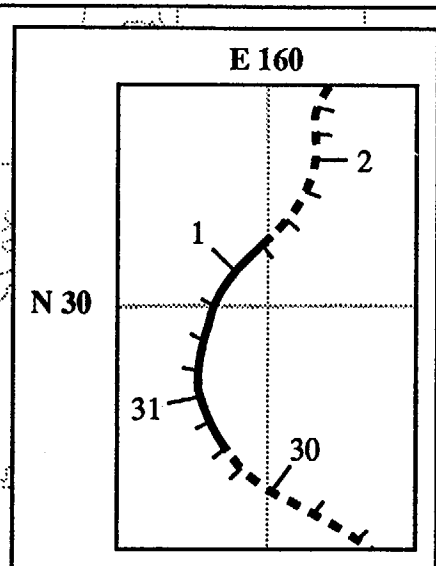


Figure 3-21-1 Harry near its peak intensity of 60 kt (31 m/sec) when located about 210 nm (390 km) southwest of Hong Kong (270231Z August visible GMS imagery).

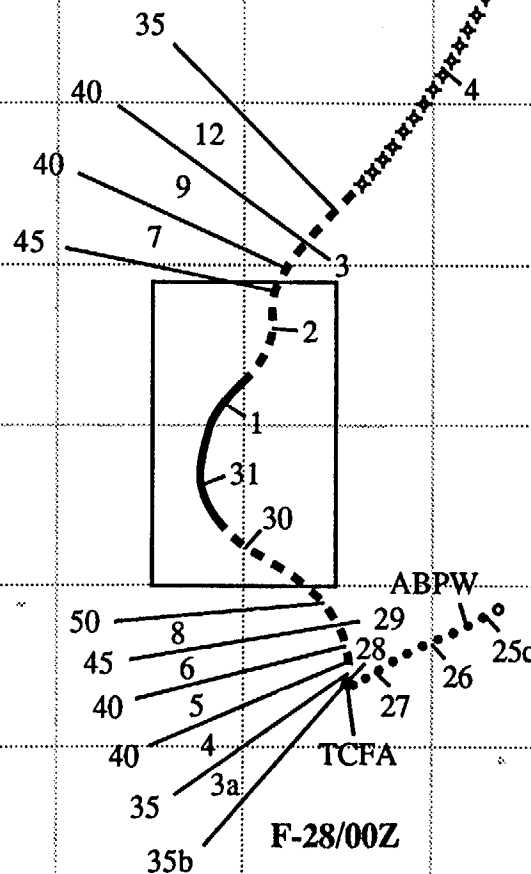
As Typhoon Fred approached the southwestern Ryukyu Islands of Japan on 20 August, convection began to reappear in the monsoon trough about 250 nm (463 km) southwest of Guam. A disturbance was mentioned that afternoon on the 200600Z August Significant Tropical Weather Advisory. For five days, the disturbance moved to the west-northwest with very little intensification. After it crossed the northern part of Luzon, a Tropical Cyclone Formation Alert was issued at 250000Z followed by the first warning on Tropical Depression 21W at 251200Z. By 251800Z, the system had reached tropical storm intensity. During the next 36 hours, Harry intensified at a rate of 5 kt (2.6 m/sec) per 6 hours while moving west-northwestward at 8-10 kt (15-19 km/hr). On the morning of 27 August, Harry passed 150 nm (278 km) south of Hong Kong where 79 km/hr (43 kt) 10-minute averaged sustained winds were recorded at Waglan Island at 270145Z. A peak gust of 104 km/hr (56 kt) was recorded at 270310Z at the same site. Less than three hours later, Harry reached its peak intensity of 60 kt (31 m/sec) (Figure 3-21-1), six hours before crossing the southern portion of the Luichou Peninsula of China. Harry slowly weakened as it crossed the Gulf of Tonkin, and went ashore at 281500Z just east of Haiphong, Vietnam, with 50 kt (26 m/sec) winds. The final warning was issued at 290000Z after Harry's weakened circulation had moved inland near Hanoi.

E 140 145 150 155 160 165 170 175 180
N 50



DTG (Z)	SPEED (KT)	INTENSITY (KT)
29/12	9	50
29/18	8	55
30/00	8	55
30/06	7	60
30/12	5	65
30/18	5	70
31/00	5	75
31/06	6	75
31/12	6	75
31/18	7	70
01/00	7	65
01/06	7	65
01/12	7	60
01/18	7	60
02/00	6	55
02/06	6	50
02/12	6	45

L-03/06Z



TYPHOON IVY
BEST TRACK TC-22W
24 AUG-04 SEP 94
MAX SFC WIND 75KT
MINIMUM SLP 968MB

LEGEND

—/—/—	6-HR BEST TRACK POSITION
a	SPEED OF MOVEMENT (KT)
b	INTENSITY (KT)
c	POSITION AT XX/0000Z
•••••	TROPICAL DISTURBANCE
•••••	TROPICAL DEPRESSION
-----	TROPICAL STORM
————	TYPHOON
◆	SUPER TYPHOON START
◆	SUPER TYPHOON END
◆◆◆◆	EXTRATROPICAL
◆◆◆◆	SUBTROPICAL
***	DISSIPATING STAGE
F	FIRST WARNING ISSUED
L	LAST WARNING ISSUED

N 15

123

TYPHOON IVY (22W)

I. HIGHLIGHTS

Ivy developed within an area of disturbed weather located in the subtropics (i.e., north of 20°N) at a time when the low-level and upper-level wind patterns throughout the western North Pacific were unusual. Ivy was a small tropical cyclone that moved on a north-oriented track.

II. TRACK AND INTENSITY

The tropical disturbance that would eventually become Ivy formed in the same complex environment within which Gladys (20W) formed. As Ivy was forming, the large-scale distribution of cloudiness (Figure 3-22-1 and Figure 3-22-2) and the large-scale structure of the troposphere over the western North Pacific was quite complex. [For a more complete description of the structure of the atmosphere during this time see the Track and Intensity section of Gladys' (20W) summary.]

During the daylight hours of 25 August, satellite imagery and synoptic data indicated that a low-level circulation center was exposed to the north of an area of deep convection near 24°N 166°E. This disturbance was first mentioned on the 250600Z August Significant Tropical Weather Advisory. For the next 36 hours, this disturbance drifted southwestward and showed signs of gradual intensification. A Tropical Cyclone Formation Alert was issued at 271700Z when satellite imagery depicted an increase in the amount of deep convection near the still-exposed low-level circulation center. The sea-level pressure at Wake Island (WMO 91245), located 200 nm (370 km) east-southeast of the low-level center, fell 3.5 mb over 24 hours. At 280000Z, a tropical depression warning was issued on Tropical Depression 22W. The system intensified more rapidly than anticipated, and on warning number 02, issued at 280600Z, Tropical Depression 22W was upgraded to Tropical Storm Ivy. Ivy then began to track slowly northward while embedded in a complex environment that also featured Gladys (20W) and John (10E). Ivy gradually intensified, and at 310000Z was upgraded to a typhoon. Peak intensity of 75 kt (39 m/sec) was reached at 310000Z (Figure 3-22-3). During the next three days (310000Z August to 030000Z September), Ivy drifted slowly north-northeastward and slowly weakened. After 030000Z, the system accelerated toward the northeast and was absorbed into the frontal cloud band of a midlatitude low. The final warning was issued at 030600Z, as the accelerating Ivy acquired extratropical characteristics.

III. DISCUSSION

a. Formation north of 20°

Ivy was one of five tropical cyclones during 1994 that first attained 25 kt (13 m/sec) (best-track) intensity north of 20°N. Two of these tropical cyclones, Tropical Depression 31W and Yuri (36W), formed in direct association with TUTT cells. The other three, Ellie (18W), Gladys (20W), and Ivy, formed in complex environments that featured TUTT cells and midlatitude troughs which penetrated into subtropical latitudes. Ivy did not form in direct association with the TUTT or a TUTT cell, but rather began as an area of enhanced convection beneath diffluent upper-level northwesterly winds at the base of a midlatitude trough (Figure 3-22-4). As a result, the system was sheared, with the low-level center located northwest of the primary deep convection. As Ivy intensified, a cut-off low formed at the base of the aforementioned midlatitude trough and moved to the west of Ivy. This cut-off low weakened the vertical shear, and contributed to weak, deep, southerly flow over Ivy. Drifting in a general

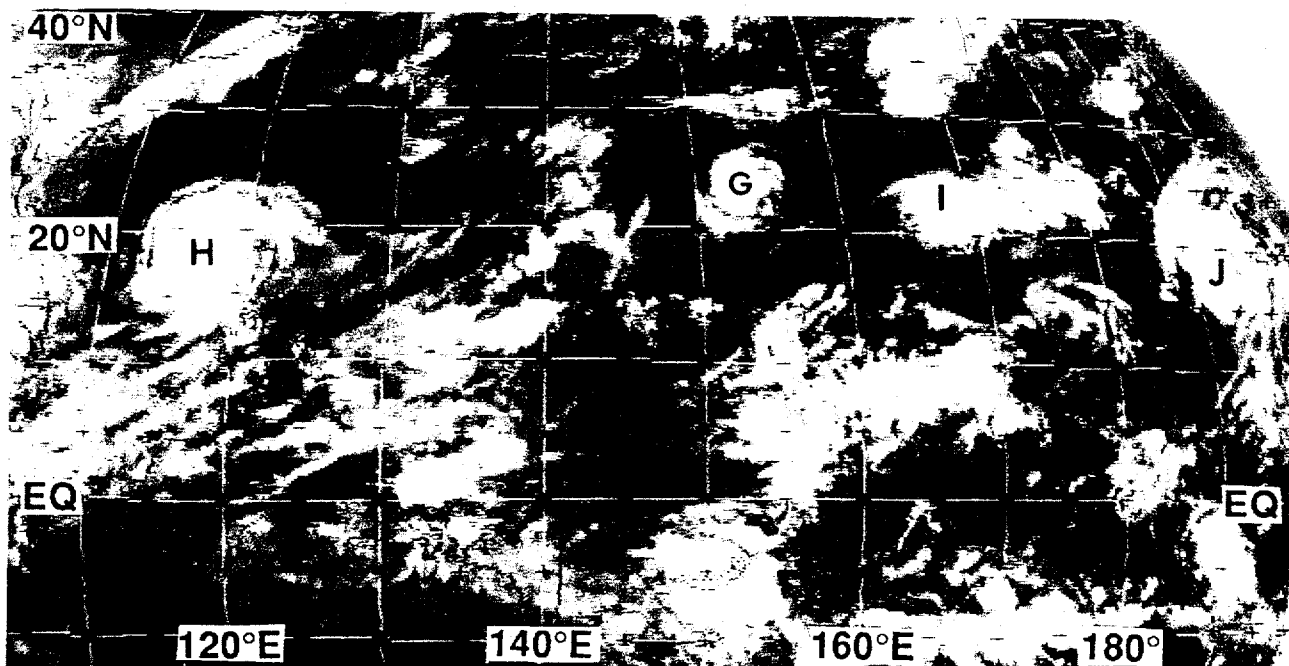


Figure 3-22-1 Ivy formed in a complex environment containing numerous clusters of deep convection and other tropical cyclones. G= Gladys (20W), H = Harry (21W), I = Ivy, and J = John (10E). (260031Z August infrared GMS imagery.)

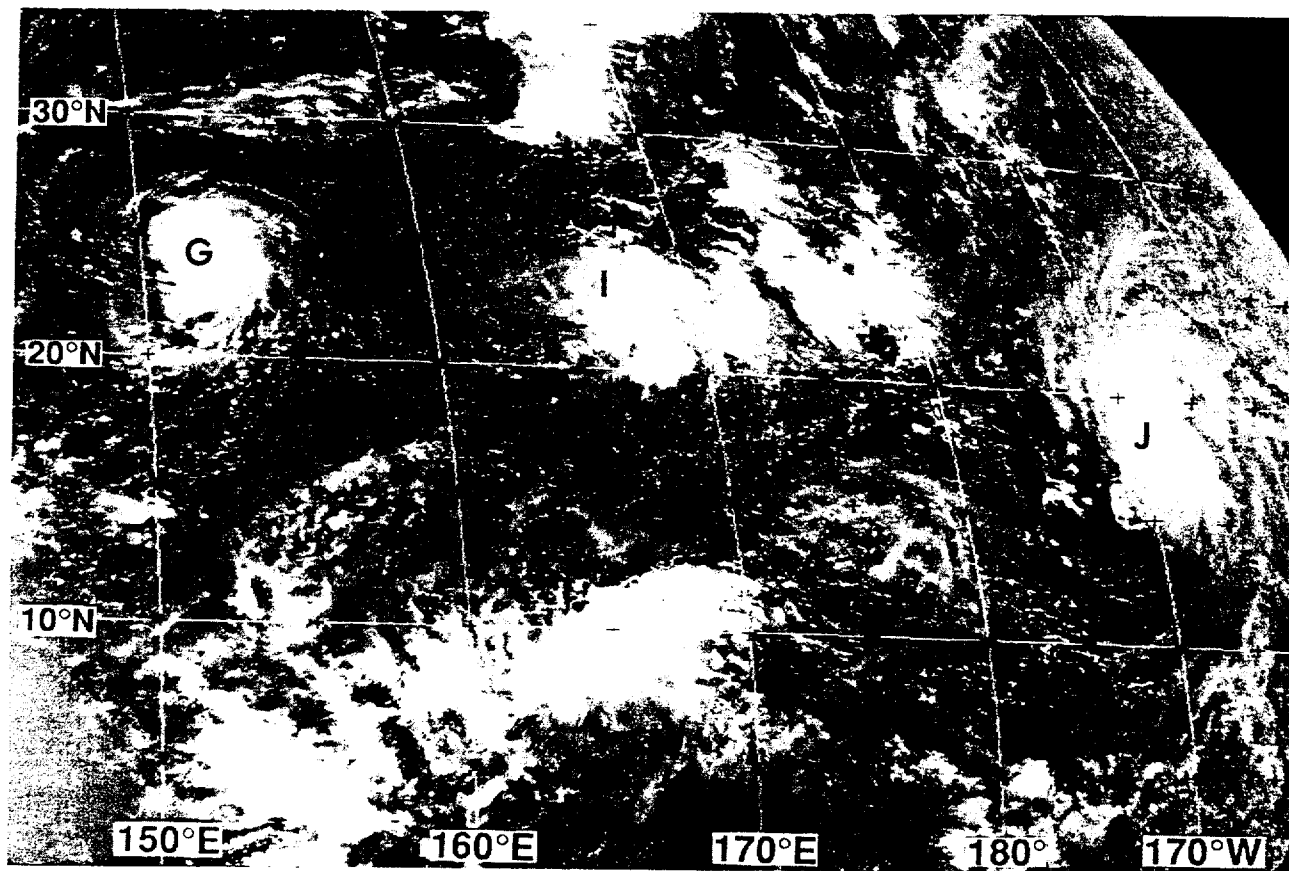


Figure 3-22-2 Ivy developed from a cluster of deep convection located about half way between Gladys (20W) and John (10E) (260231Z August visible GMS imagery). G = Gladys (20W), I = Ivy and J = John (10E)

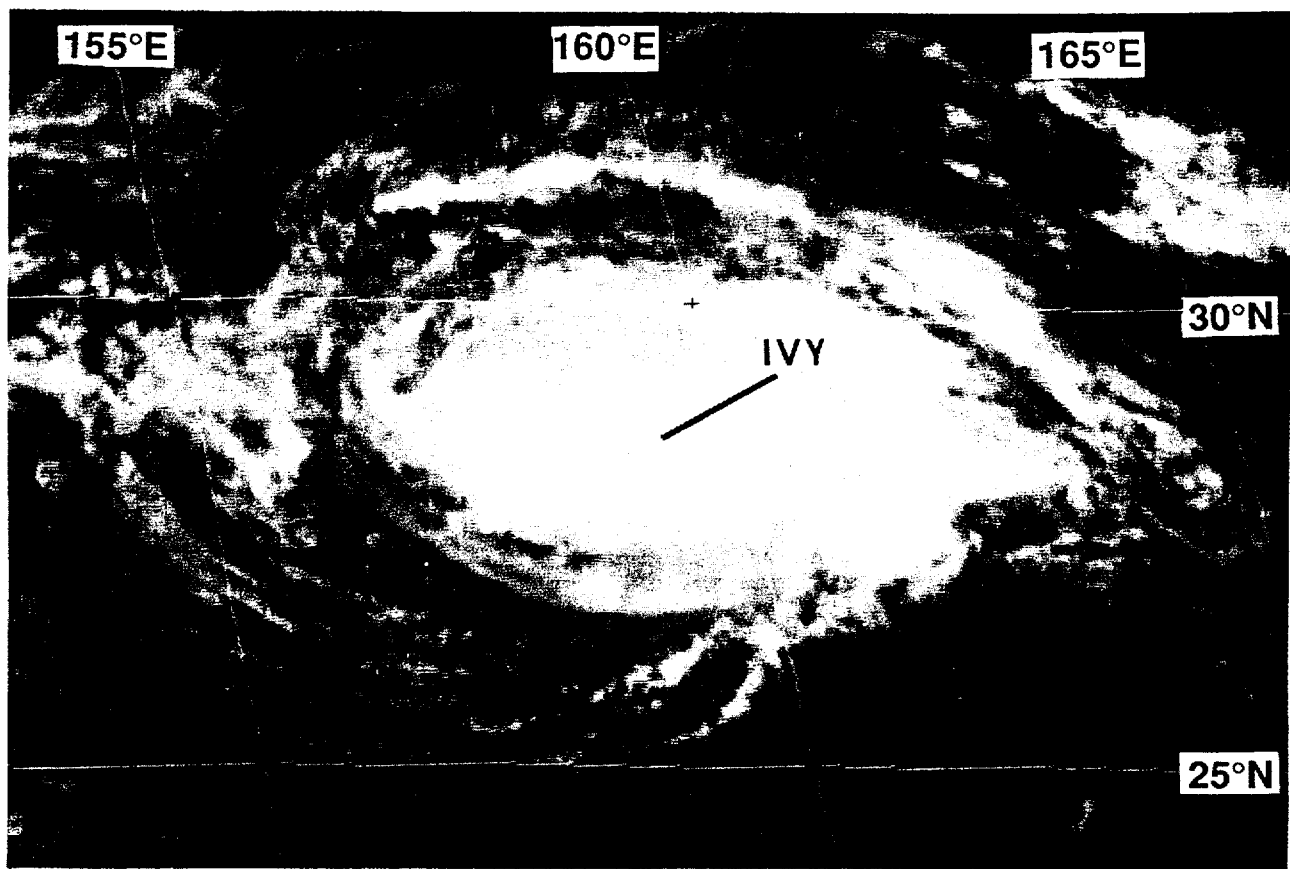


Figure 3-22-3 Ivy reaches its peak intensity of 75 kt (39 m/sec) (302331Z August visible GMS imagery)

northward direction, Ivy became a typhoon at 301200Z August. After moving poleward of 35°N shortly after 021800Z September, Ivy began to accelerate toward the north-northeast ahead of an advancing frontal system.

b. Unusual structure of the low-level wind field

As discussed above, Ivy formed within an area of deep convection associated with the extension into the subtropics of a mid-latitude trough (most tropical cyclones which develop in the western North Pacific form in the monsoon trough). This led to an unusual low-level wind field structure, in which an east-west chain of three tropical cyclones (with Ivy in the center) was positioned well north of a weak monsoon trough (Figure 3-22-5). A zone of light easterly winds separated the monsoon trough from the chain of cyclones.

IV. IMPACT

Ivy spent its entire life over open water. Its only impact was the diverting of shipping around its path.

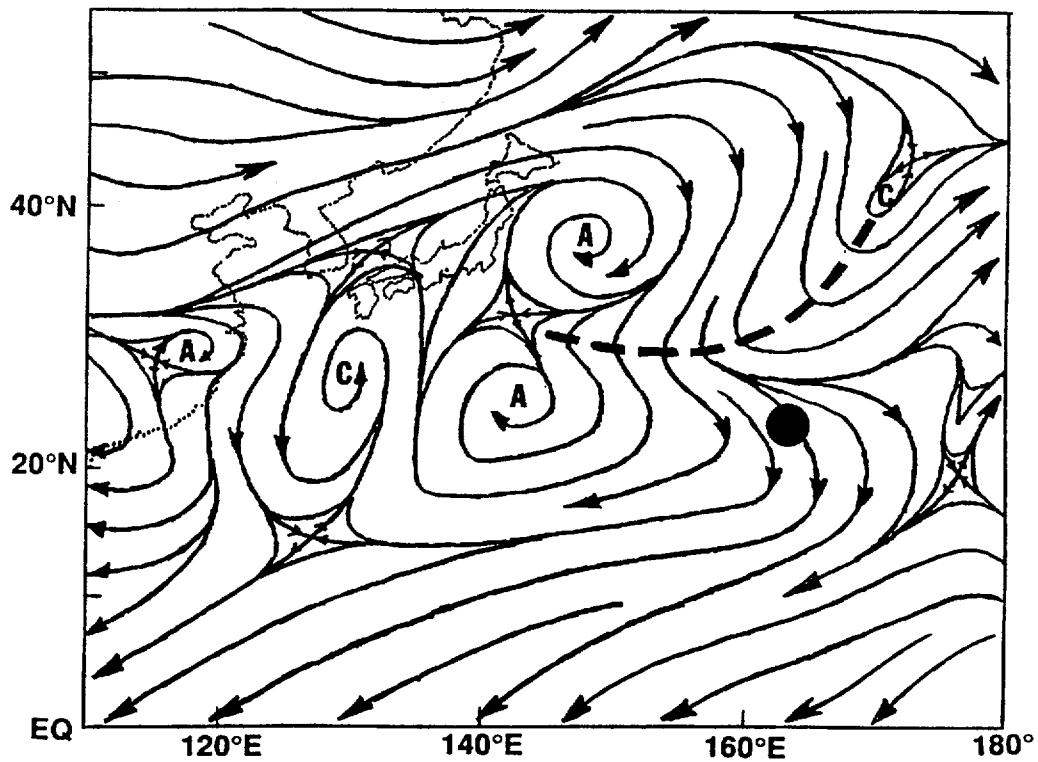


Figure 3-22-4 Streamlines of 200 mb wind (adapted from the 271200Z NOGAPS analysis. Dashed line indicates trough axis, c = cyclonic circulation centers, a = anticyclones, large dot indicates location of the developing Ivy.

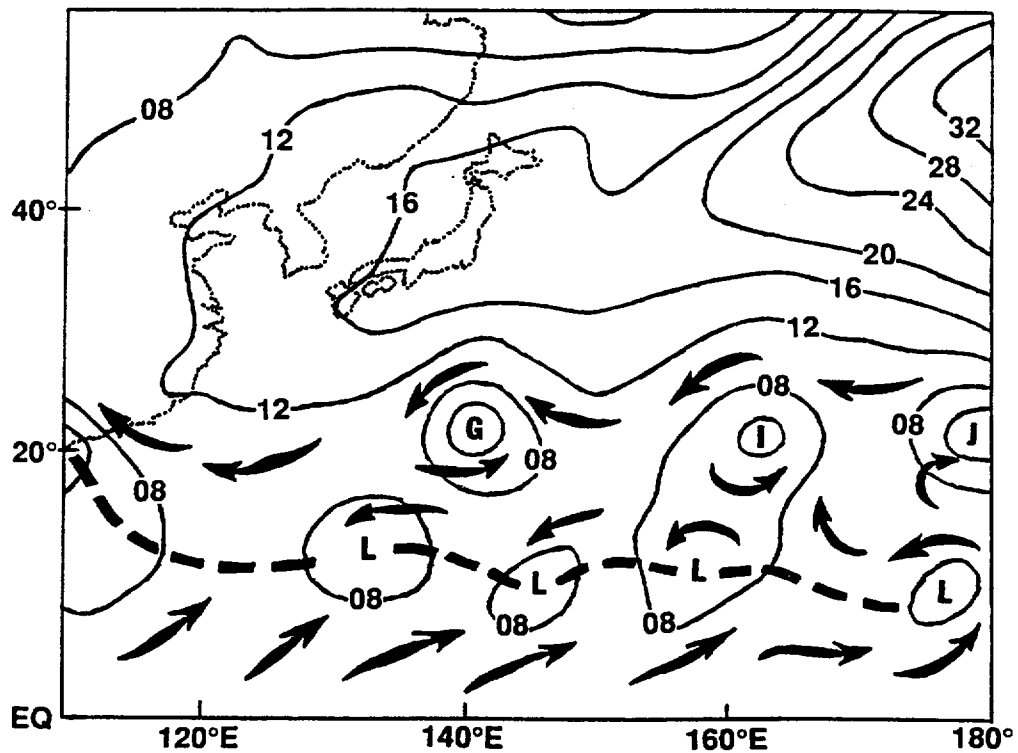
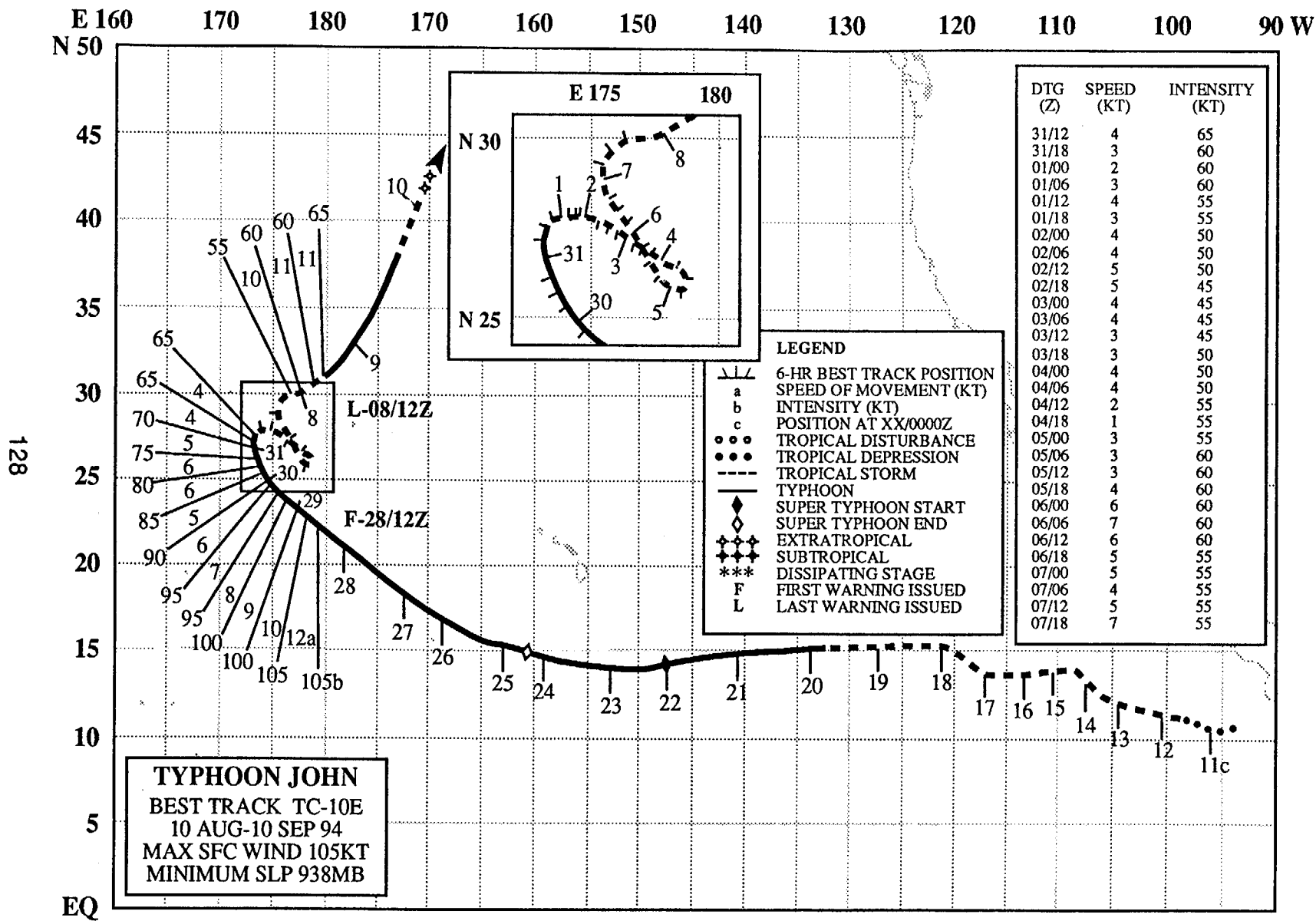


Figure 3-22-5 Contour analysis of the sea-level pressure (adapted from the 281200Z August NOGAPS surface pressure analysis). Dashed line = monsoon trough, C = cyclonic circulation center, G = Gladys (20W), I = Ivy, J = John (10E). Contours are at 4 mb intervals.



TYPHOON JOHN (10E)

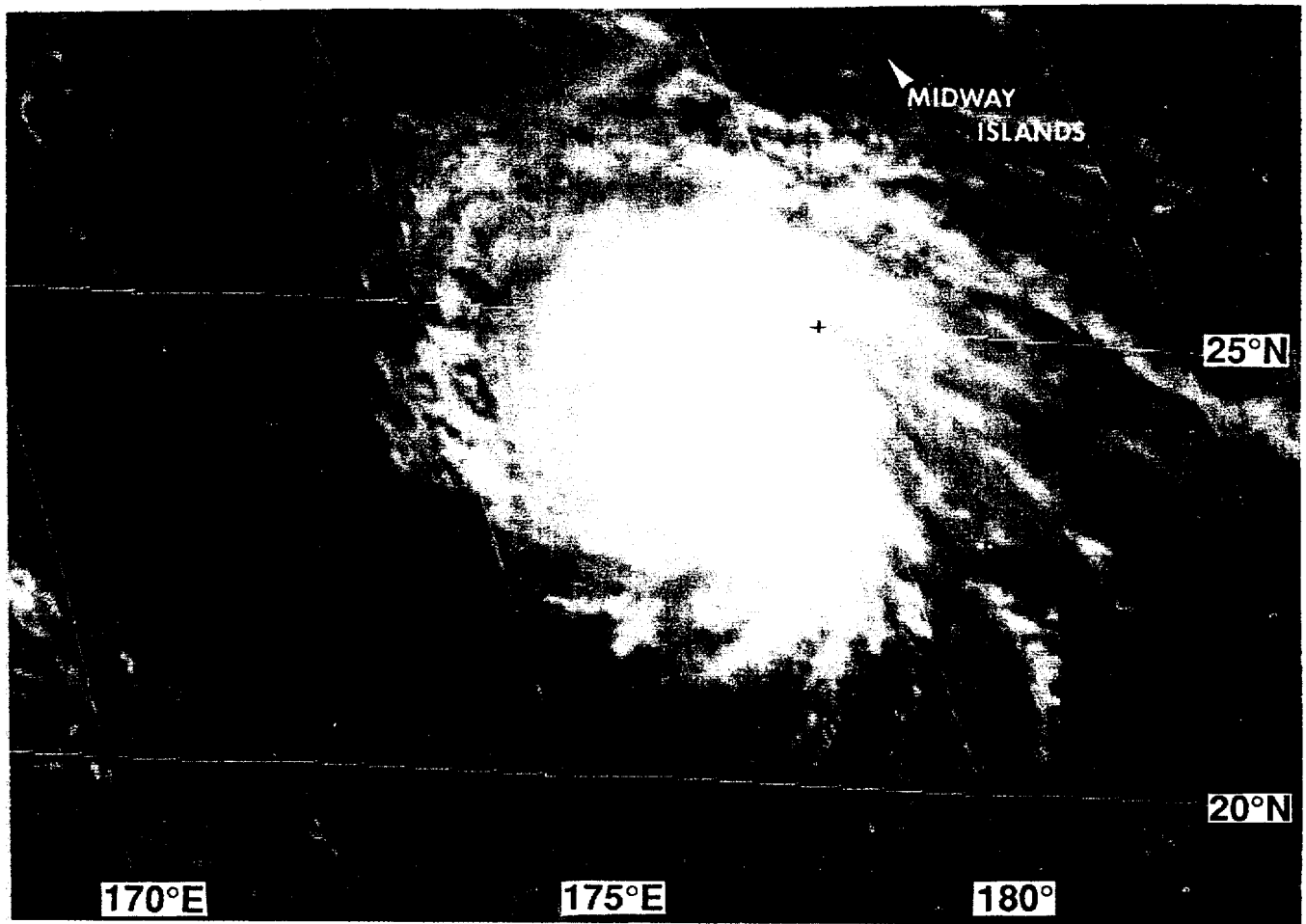


Figure 3-10E-1 A view of John shortly after it crossed the international date line (282331Z August visible GMS imagery).

I. HIGHLIGHTS

John was the longest-lived tropical cyclone on record. Between the National Hurricane Center (Miami), the Central Pacific Hurricane Center (Honolulu) and the JTWC (Guam), a cumulative total of 120 warnings were issued on this system over the course of 31 days. While in the western North Pacific (JTWC's area of responsibility), John weakened from typhoon intensity to tropical storm intensity. Just before it re-crossed the international date line, it reintensified to a typhoon. As John began to reintensify, diagnosed intensities from satellite imagery were much lower than indicated by ship reports near the system center.

II. TRACK AND INTENSITY

Beginning as a tropical depression off the southwest coast of Guatemala at 100600Z August, John traveled across the entire eastern North Pacific. It crossed the international date line and into the western North Pacific at 280900Z. When John was located 300 nm (555 km) south of the island of Hawaii at 230000Z, its intensity peaked at 150 kt (77 m/sec) — an unusually intense hurricane for that region. Moving steadily westward, it then weakened considerably (to 80 kt) and passed only 20 nm north of Johnston Atoll where some damage was reported (see Impact section). As it neared the international

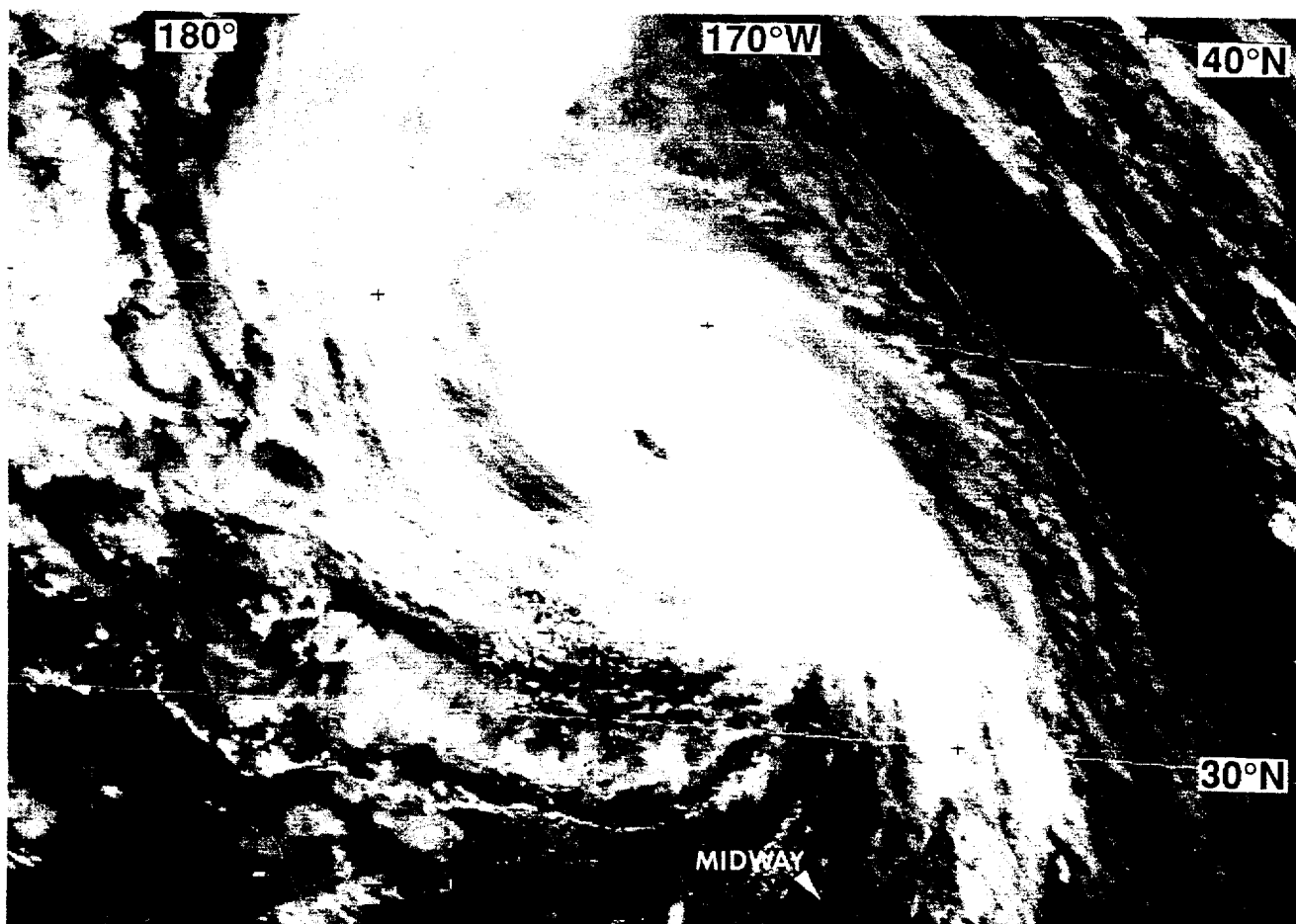


Figure 3-10E-2 Having moved back into the eastern North Pacific, John is once again at typhoon intensity (090031Z September visible GMS imagery).

date line from the east, John began to reintensify. It reached a secondary peak intensity of 105 kt (54 m/sec) at 281200Z as it entered the JTWC's area of responsibility (Figure 3-10E-1). The system weakened while meandering west of the international date line approximately 500 nm (925 km) west-southwest of Midway island. At 021800Z, real-time intensity estimates fell to 30 kt (15 m/sec) (these were later adjusted to 45 kt on the final best track), just prior to another period of intensification. A third and final peak intensity of 70 kt (36 m/sec) was attained at 081800Z after the system had recurved and moved back across the date line into the eastern North Pacific (Figure 3-10E-2 and Figure 3-10E-3). Rapid northeastward motion then ensued. The system became extratropical and gradually weakened, and the Central Pacific Hurricane Center, Honolulu, issued the final warning (warning number 120 — the most ever for a TC) at 100000Z September.

III. DISCUSSION

a. Long life

The average life span of a tropical cyclone in the western North Pacific is approximately 6.5 days. Of the 420 tropical cyclones during the period 1980-1993, 156 (37%) lasted seven days or more and only 11 (2.6%) persisted for 14 days or longer. Of the tropical cyclones that have spent their entire lives in the western North Pacific, the two longest-lived tropical were Wayne (1986) (with an 18-day life span) and Nat (1991) (with a 17-day life span). Some tropical cyclones which formed in the eastern or cen-

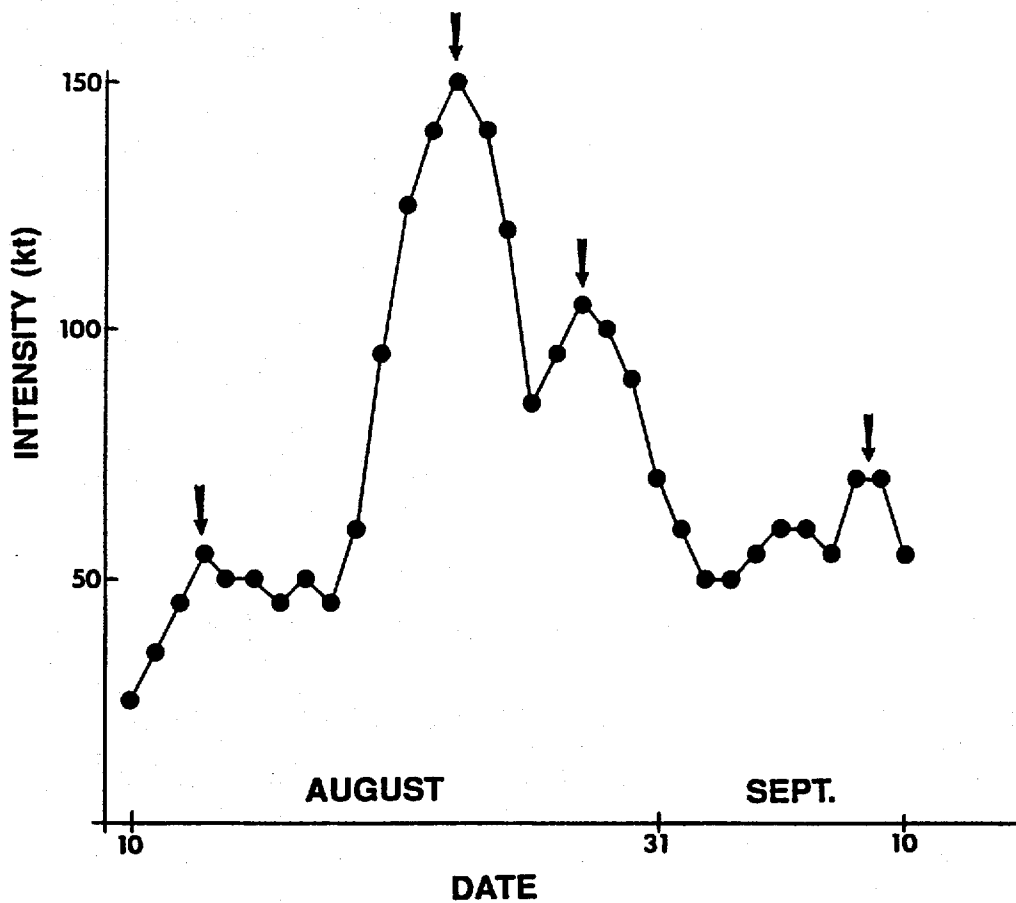


Figure 3-10E-3 A plot of John's intensity versus time. Each dot marks the highest intensity of each calendar day from August 10 to September 10.

tral Pacific and moved westward across the international date line into the western North Pacific have had longer life spans. For example, Enrique (1991), a tropical cyclone originating in the eastern North Pacific, lasted 20 days (including one day west of the date line). Keoni (1993), a tropical cyclone which originated in the central North Pacific, persisted for 24 days (including 9 days in the western North Pacific). John's total life span of 31 days (including 11 days in the western North Pacific) sets the record.

b. A problem with the intensity

After reaching a low-point of intensity at 021800Z September, John began to slowly reintensify. In real time, on or about 021800Z September, intensity estimates of John (based upon satellite imagery) fell below tropical storm intensity. Thus, John became a tropical depression on warning numbers 91 through 94 (the four warnings issued at six-hour intervals from 021800Z to 031200Z). On these warnings, the extended outlook beyond 48 hours called for dissipation as a significant tropical cyclone. However, on warning number 95 (031800Z September), John was upgraded to minimal tropical storm intensity with later weakening still indicated in the forecast. Twenty-four hours later, at 041800Z, the warning indicated that John was still at minimal tropical storm intensity, and the extended outlook continued to call for it to weaken. Two reports from a ship near John at this time, which were not received in real time at the JTWC, indicated that the intensity of John was under-estimated:

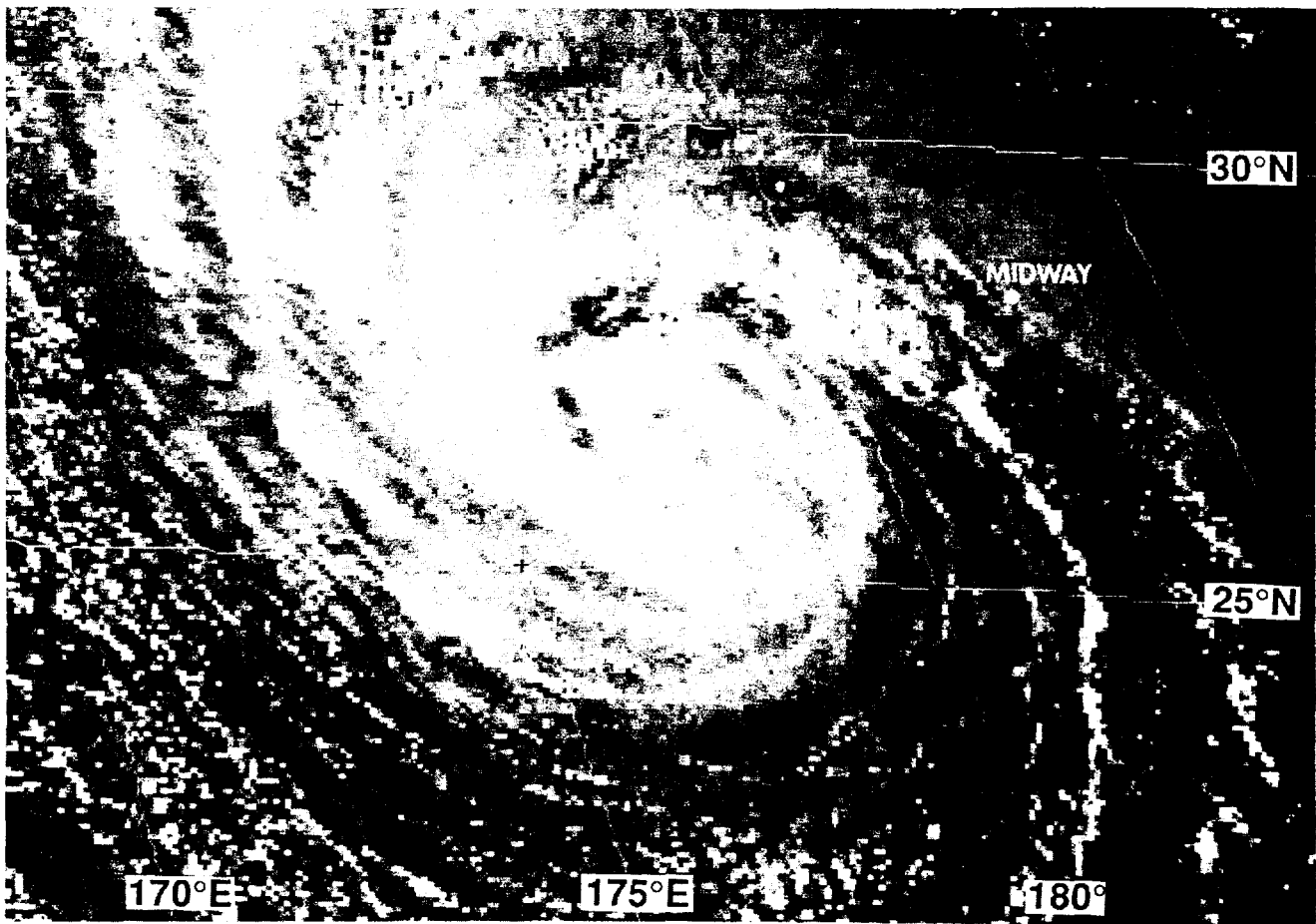


Figure 3-10E-4 John as seen in the low sun angle of evening. In real time, at the time of this picture, the warning intensity was 35 kt (18 m/sec). The final best-track intensity was upped to 60 kt (31 m/sec) based upon synoptic reports (050530Z September visible GMS imagery).

041500Z, 27.3°N 178.9°E, wind = 090 deg at 55 kt, SLP = 991.2 mb

041800Z, 27.6°N 177.7°E, wind = 050 deg at 55 kt, SLP = 993.5 mb.

Twelve hours after the valid time of these ship reports, the real-time intensity estimates were still probably too low. The 050530Z satellite imagery shown in Figure 3-10E-4 was diagnosed in real time to be of minimal tropical storm intensity. In post analysis, it was determined (based upon the aforementioned ship reports), that John was likely much more intense at this time — 60 kt vice 35 kt. With respect to the best-track intensity, each warning issued by the JTWC during the period 011200Z through JTWC's final warning at 081200Z, was anywhere from 5 to 25 kt too low.

IV. IMPACT

John spent all of its life over open water, and its greatest impact was felt when it skirted just north of Johnston Atoll. The Army's chemical weapons incinerator on Johnston Atoll had to be shut down, and all 1100 military and civilian personnel evacuated to Honolulu. The incinerator and ammunition storage areas weathered the storm well, but high winds caused minor to extensive damage to numerous support buildings and personnel billets. Electrical power and telephone communications were interrupted.

E 100 105 110 115 120 125 E
N 30

25

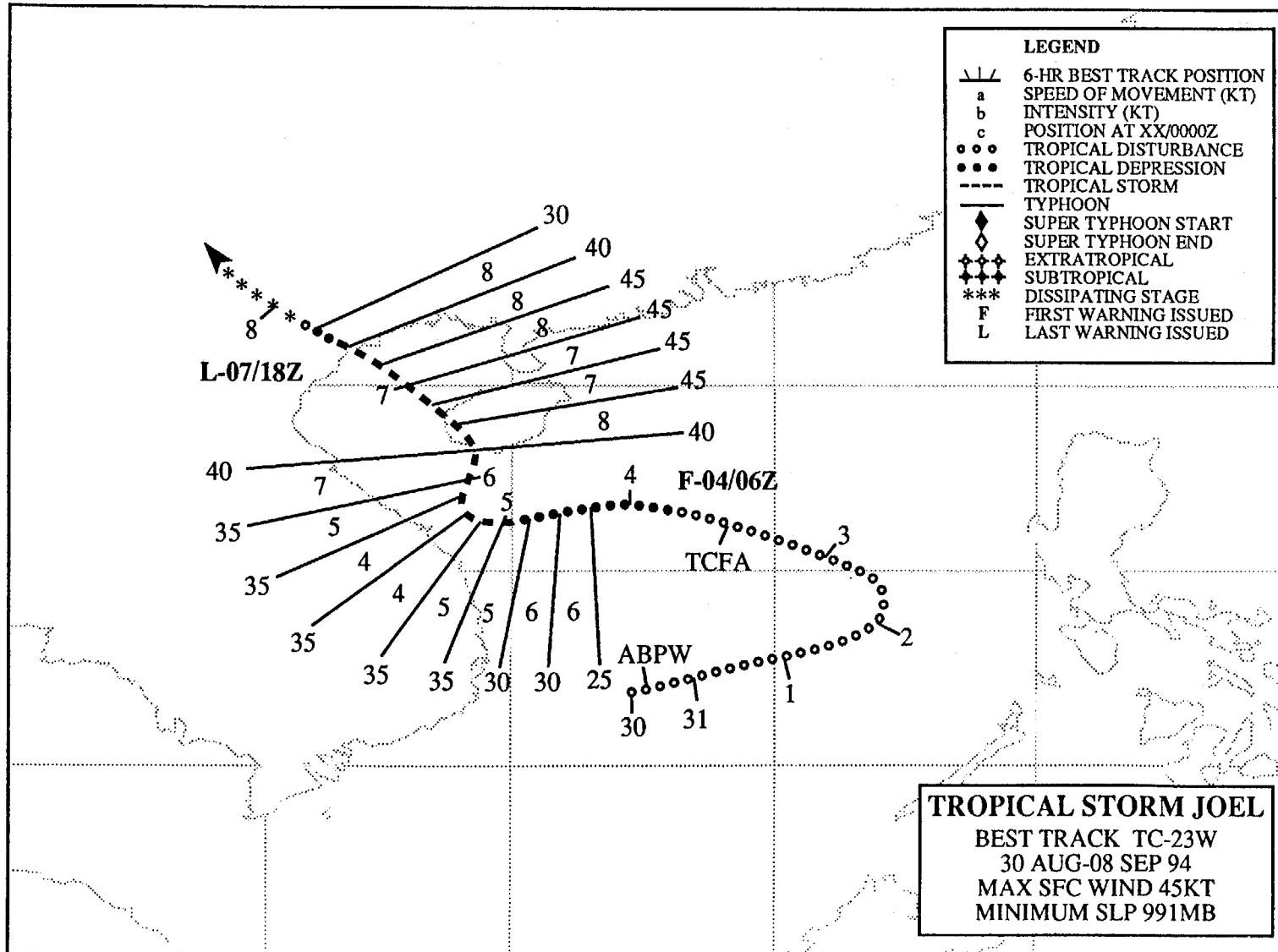
20

15

10

N 5

133



TROPICAL STORM JOEL (23W)

As Typhoon Gladys (20W) approached Taiwan, the monsoon trough in the South China Sea became active near 12°N. An area of persistent convection within this trough was first mentioned on the 300600Z August Significant Tropical Weather Advisory. For three days, the disturbance moved east-northeastward, and upon reaching 117°E at 020000Z September, it turned toward the west-northwest. At 031130Z, the JTWC issued a Tropical Cyclone Formation Alert, which was followed 19 hours later by the first warning on Tropical Depression 23W. During most of its westward track, strong upper level winds from the north-northeast kept the deep convection south of the small low level circulation center. By the morning of 05 September, the upper level winds began to weaken. This allowed the convection to wrap around the north side of the system, and the depression was upgraded to Tropical Storm Joel. About 50 nm (93 km) east-northeast of Da Nang and 70 nm (130 km) east of Hue, Vietnam, Joel turned sharply toward the north. At 060600Z, the tropical storm passed over the extreme southwestern edge of Hainan Island where it reached its estimated maximum intensity of 45 kt (23 m/sec). Joel then turned to the northwest. After entering the Gulf of Tonkin, a ragged, cloud-filled banding-type eye appeared (Figure 3-23-1). At about 071000Z, Joel went ashore near Haiphong, and moved inland toward Hanoi. News reports (09 September USA Today) indicated that Joel knocked down large trees in Hanoi. The final warning was issued on Tropical Depression 23W at 071800Z as it dissipated over land west of Hanoi.

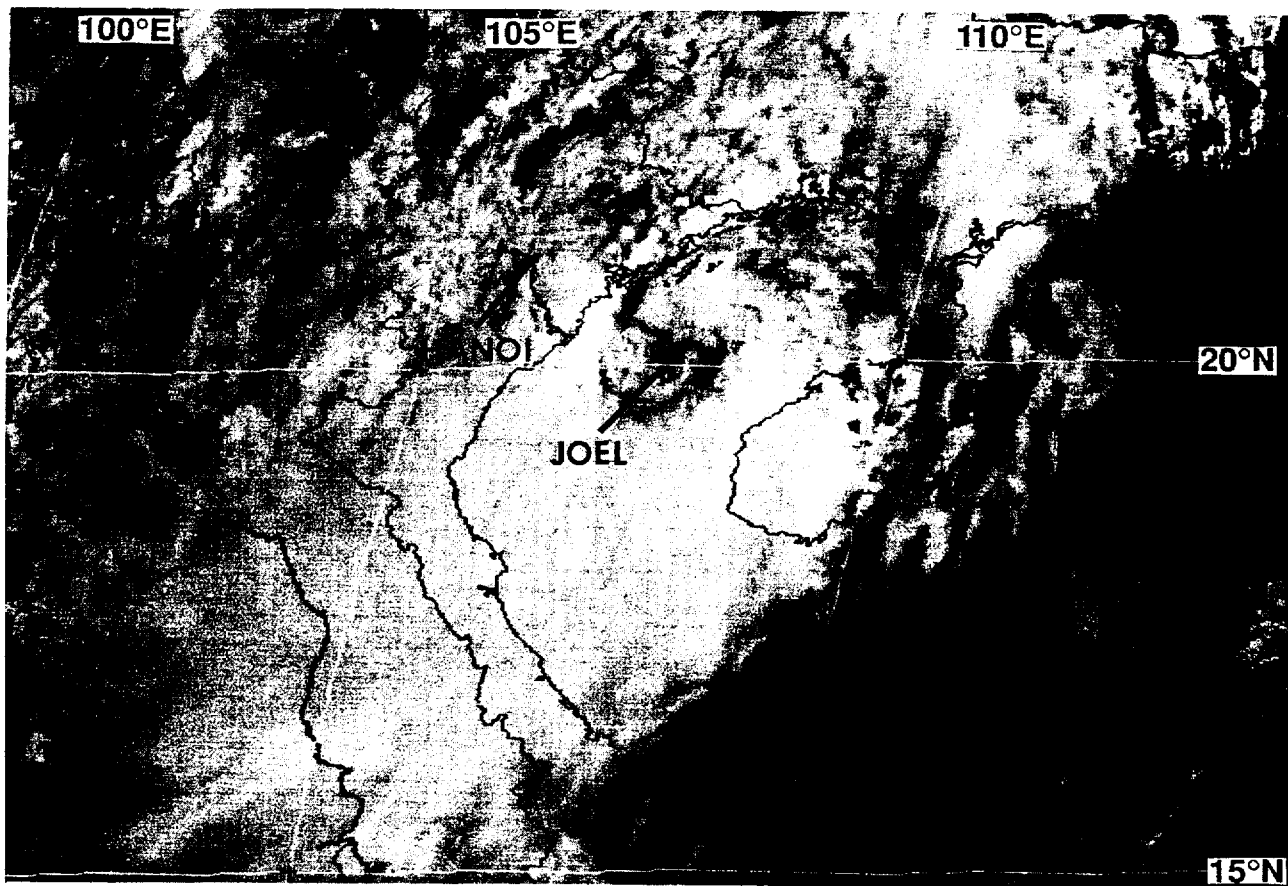
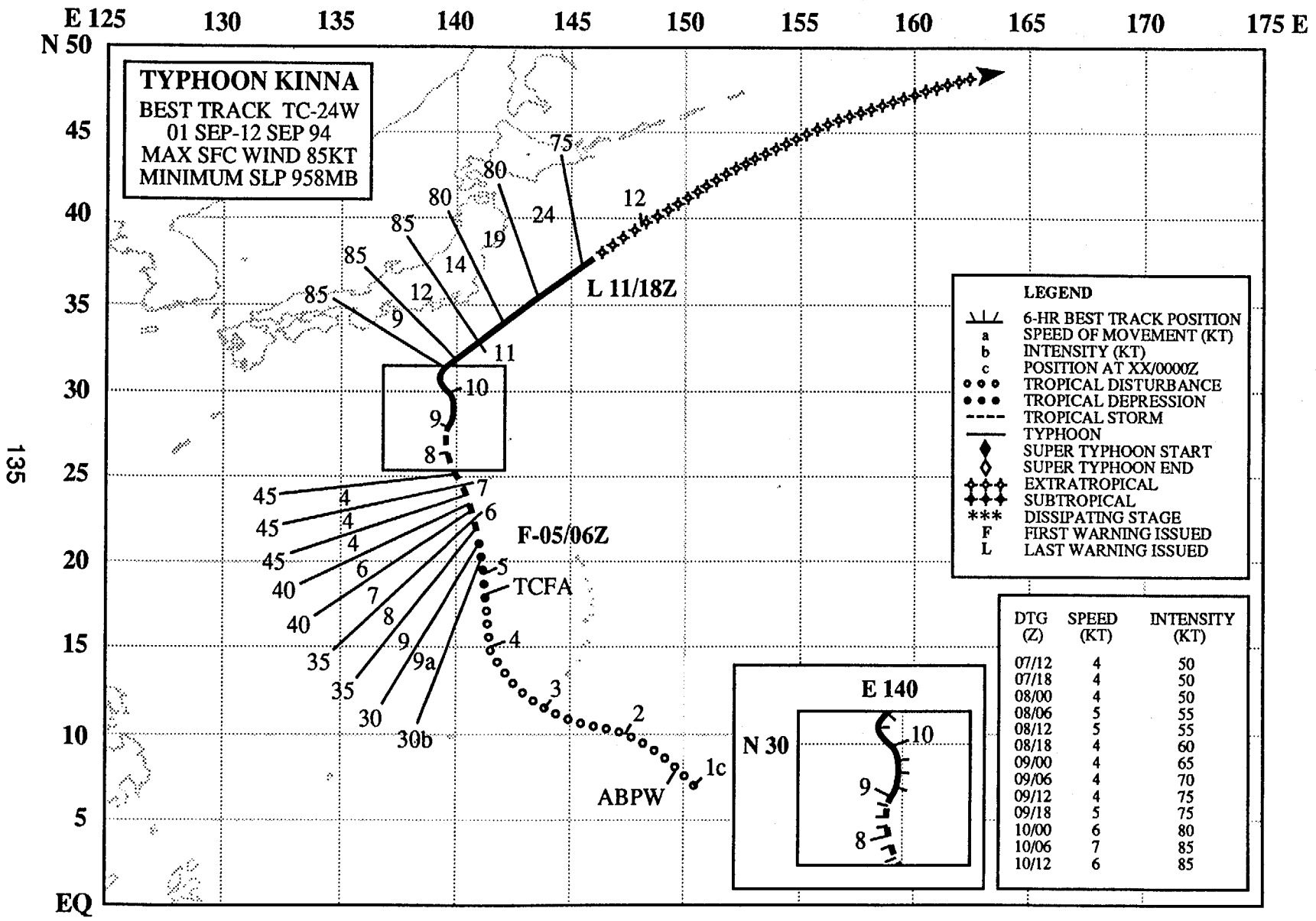


Figure 3-23-1 Tropical Storm Joel about 60 nm (111 km) southeast of the Vietnam coast, near Haiphong (070031Z September GMS visible imagery).



TYPHOON KINNA (24W)

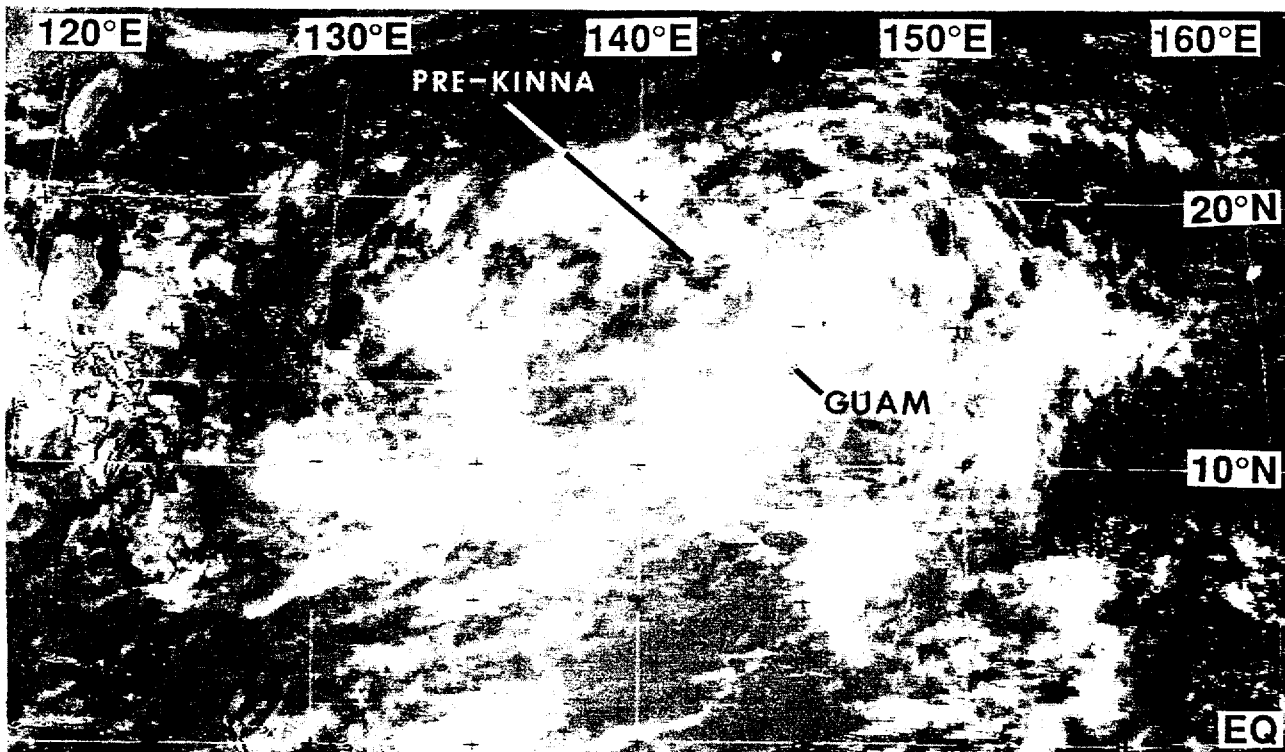


Figure 3-24-1 The pre-Kinna tropical disturbance is embedded within the cloudiness associated with a large monsoon depression (040231Z September visible GMS imagery).

I. HIGHLIGHTS

The tropical disturbance that became Kinna emerged from the northeastern quadrant of a monsoon depression. It moved on a north-oriented track. After peaking at 85 kt (44 m/sec), Kinna recurved and accelerated to more than 40 kt (74 km/hr). Kinna was a small tropical cyclone.

II. TRACK AND INTENSITY

At 010600Z September, the disturbance, that would eventually develop into Typhoon Kinna, was first mentioned on the Significant Tropical Weather Advisory when a small area of new convection appeared in the eastern Caroline Islands within the monsoon trough. For the next three-and-one-half days, the disturbance persisted as the monsoon trough moved northward, and a large monsoon depression formed near the Mariana Islands. The pre-Kinna disturbance became part of this monsoon depression on 04 September (Figure 3-24-1), and later moved north and detached from the monsoon depression (Figure 3-24-2). A Tropical Cyclone Formation alert was issued at 042000Z as an area of organized convection appeared to be emerging from the northeastern quadrant of the monsoon depression. When this convection became better organized, the JTWC issued the first warning on Tropical Depression 24W at 050600Z. Twelve hours later, the depression was upgraded to Tropical Storm Kinna. In addition to its intensification on 05 September, Kinna began to slow in forward speed as it entered a region of light southerly steering flow. Kinna remained under the influence of this weak northward steering until it moved poleward of the mid-level sub-tropical ridge on 10 September. At 070000Z, Tropical Storm Kinna passed 30 nm (56 km) west of Iwo Jima (WMO 47981) where a gust of 45 kt (23 m/sec) was

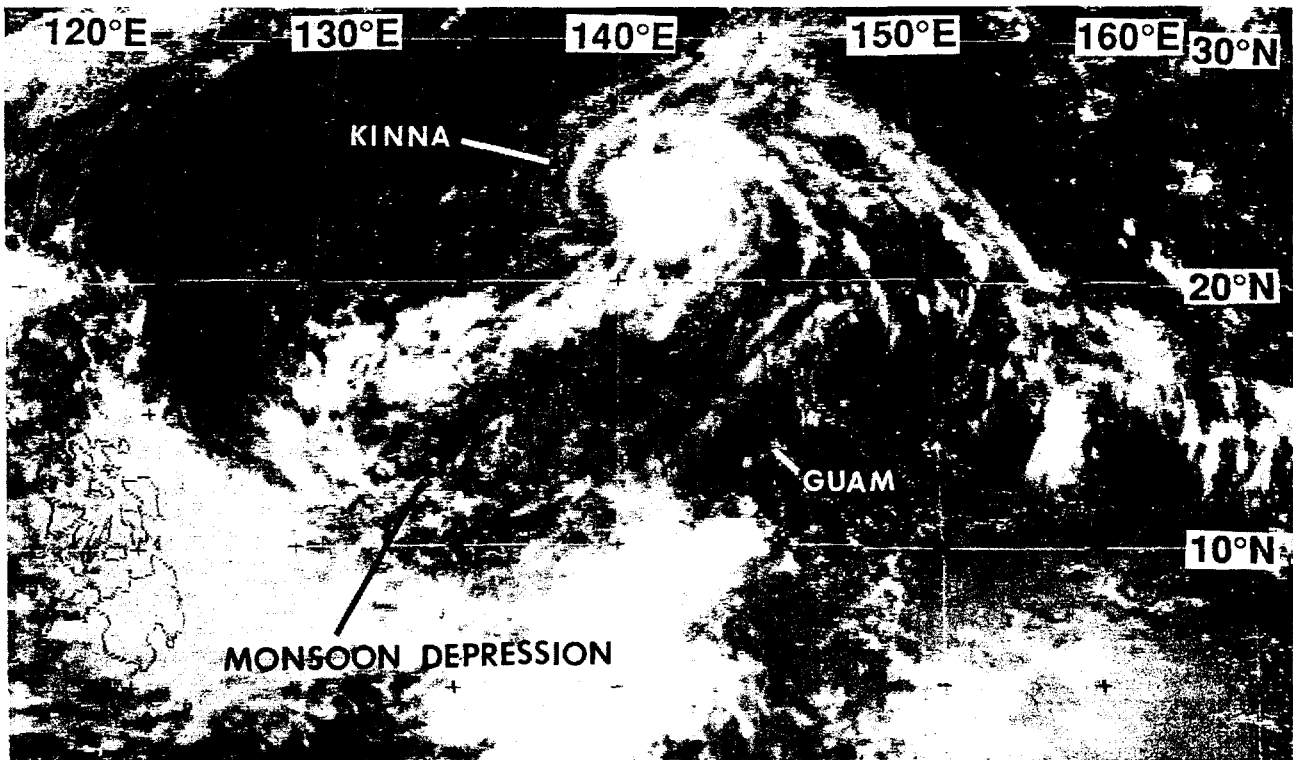


Figure 3-24-2 Kinna has moved north and become detached from the monsoon depression within which it had earlier been embedded (060031Z September visible GMS imagery).

recorded. Kinna was upgraded to typhoon intensity at 090000Z, and at 100600Z, just prior to recurvature, Typhoon Kinna reached its peak intensity of 85 kt (44 m/sec) (Fig. 3-24-3). Recurvature took the typhoon on a track that passed about 200 nm (370 km) east of Yokosuka, Japan. At 101700Z, Hachijojima (WMO 47678) recorded a peak gust of 30.8 m/sec (60 kt) as Typhoon Kinna was about 90 nm (167 km) to the south. Following recurvature, Kinna began to accelerate rapidly, eventually reaching speeds in excess of 40 kt (75 km/hr). The rapid acceleration kept Kinna's intensity high, despite its loss of symmetrical central deep convection. By the evening of 12 September, Kinna was absorbed into the cloud band of a rapidly moving front and acquired the appearance of a wave on the front.

III. DISCUSSION

The track forecasts for Kinna were challenging, as there were two plausible scenarios: one which favored northward motion, and another which favored west-northwestward motion. Both the statistical and the dynamic guidance oscillated between these scenarios during the period 06 to 10 September. Except for small, relatively short-lived meanders, the small-sized Kinna kept moving to the north, eventually passing through the mid-tropospheric sub-tropical ridge. Through-the-ridge motion (Sandgathe 1987) is typically expected of much larger tropical cyclones whose storm-induced changes to their environment allow them to modify and pass through a preexisting sub-tropical ridge (Elsberry and Abbey 1991). Overall, the track forecast errors for Typhoon Kinna were about 15 percent better than the long-term average at 24 and 48 hours, and close to average at 72 hours. Intensity forecast errors were less than 10 kt (5 m/s) at all forecast periods.

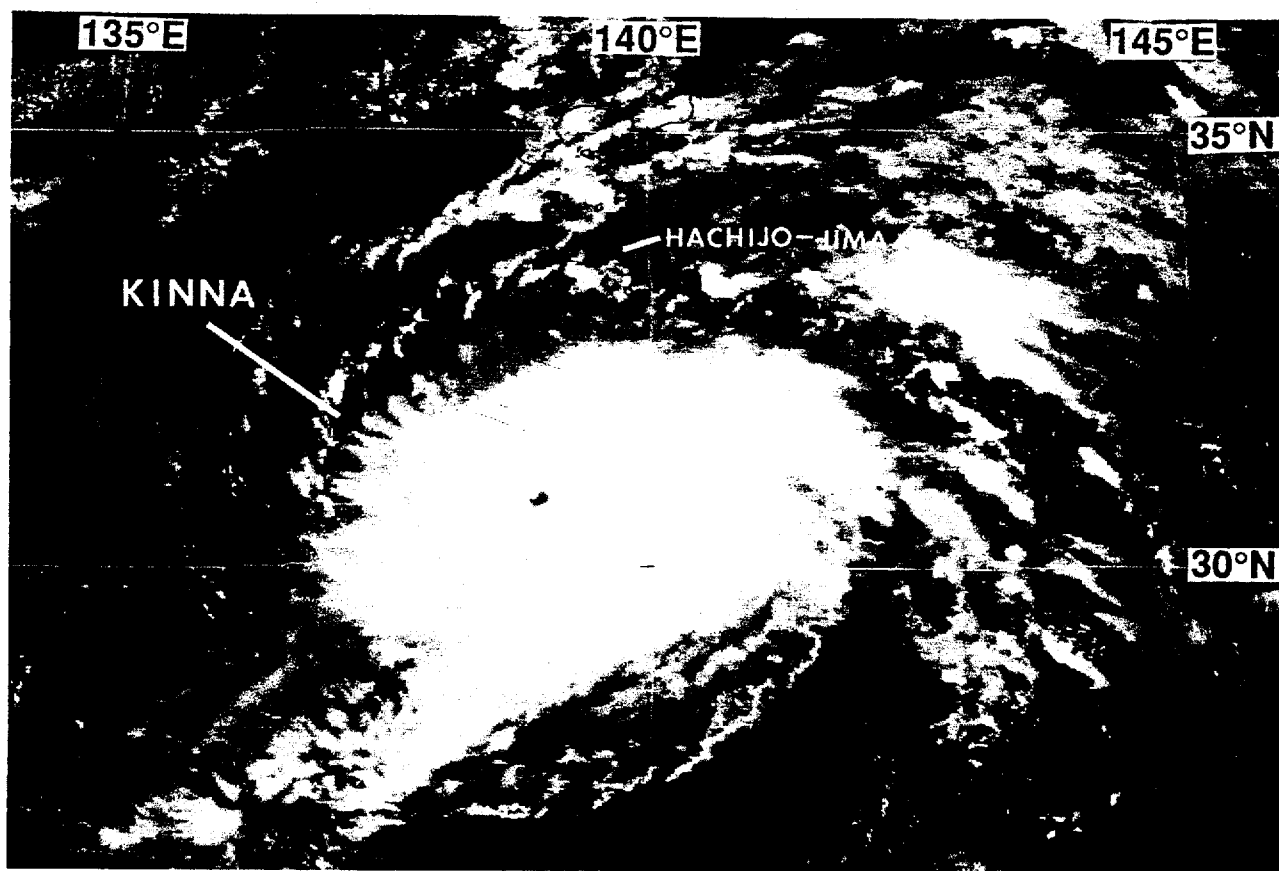
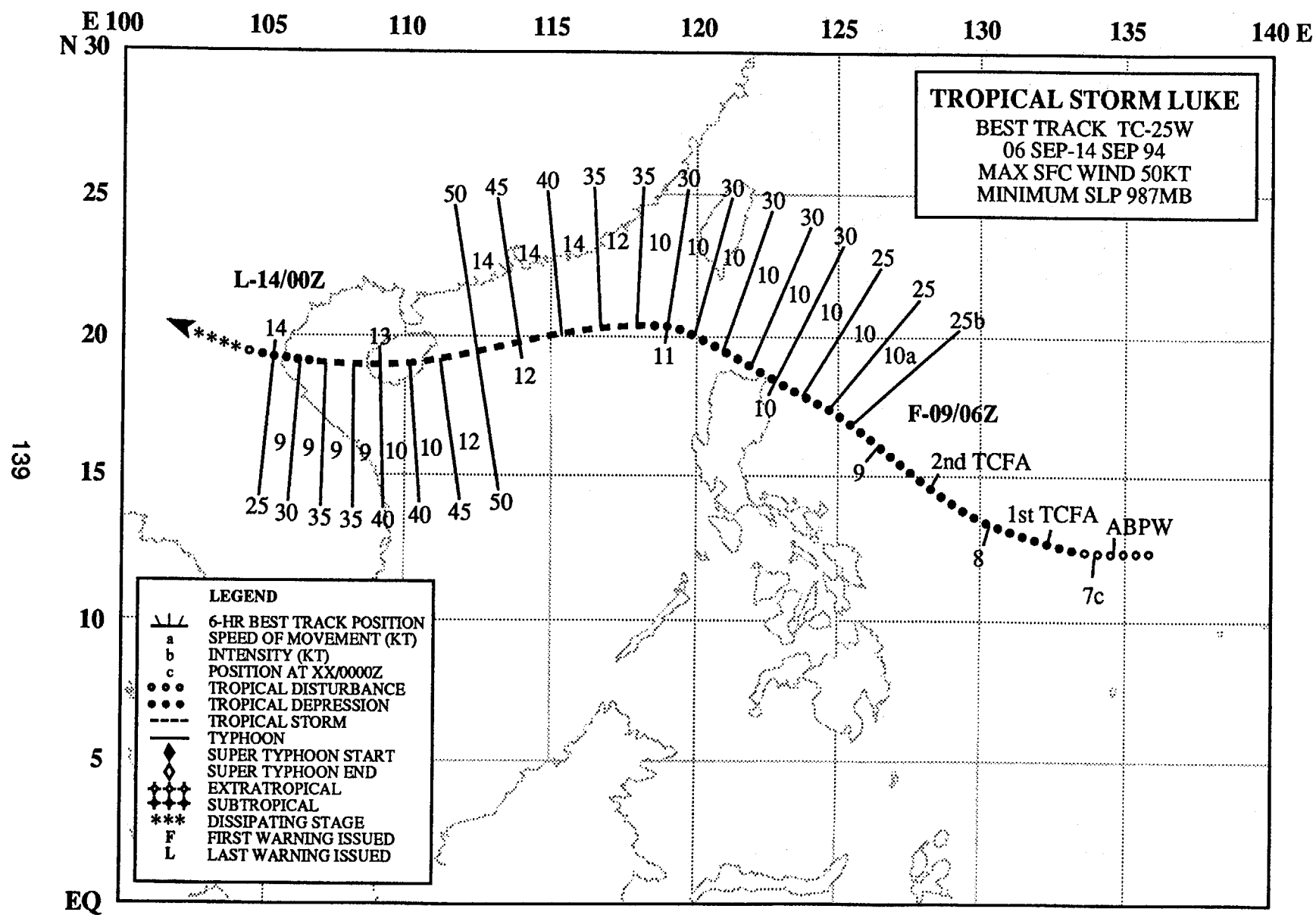


Figure 3-24-3 Kinna at its peak intensity of 85 kt (44 m/sec) (100531Z September visible GMS imagery).

IV. IMPACT

Kinna spent its entire life over open water. It turned away from the densely populated Kanto Plain area on the Japanese main island of Honshu, and produced potentially destructive winds only at Hachijo-jima, a small island about 150 nm (280 km) south of Tokyo.



TROPICAL STORM LUKE (25W)

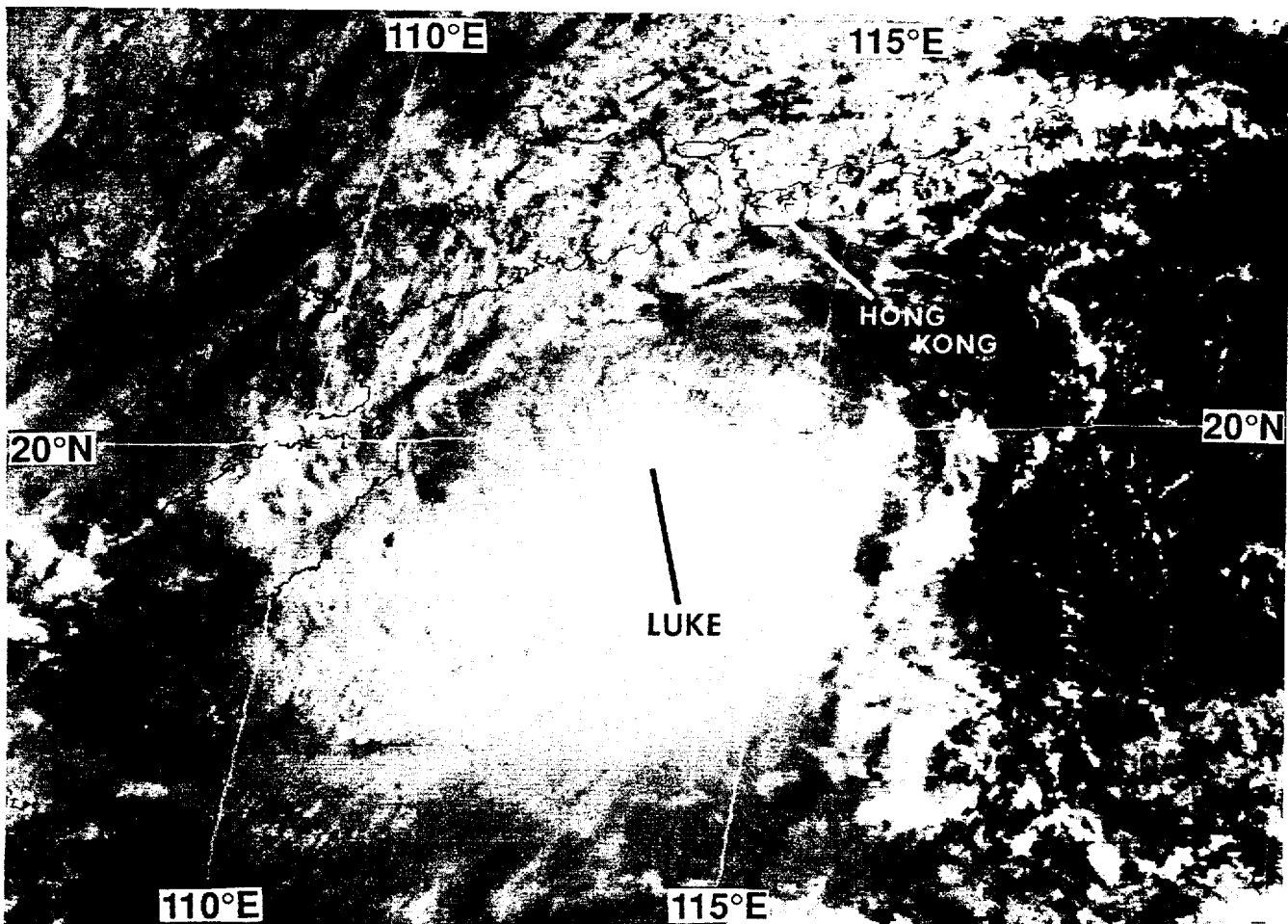
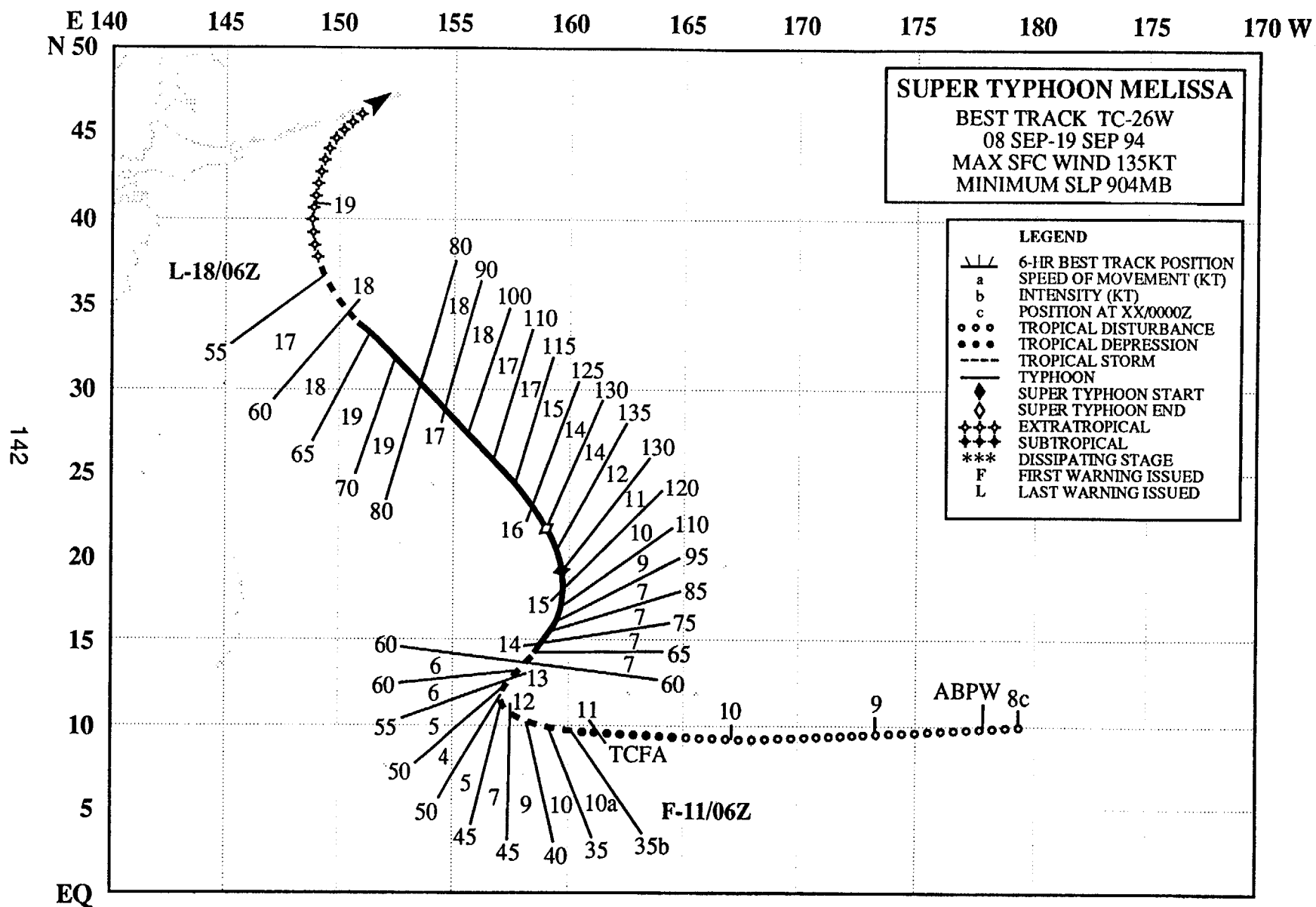


Figure 3-25-1 Tropical Storm Luke at 45 kt (23 m/sec) intensity and still intensifying while southwest of Hong Kong and east of Hainan Island (112331Z September visible GMS imagery).

While Tropical Storm Kinna (24W) was moving north along 140°E longitude, a monsoon depression covered an area from the Philippines to Yap [see Figure 3-24-2 in Kinna's (24W) summary]. This monsoon depression became Luke. When a large area of persistent deep convection to the west of the exposed low-level circulation center of this monsoon depression began to acquire cyclonic curvature, it was first mentioned on the 061800Z September Significant Tropical Weather Advisory. The disturbance moved slowly westward, and a Tropical Cyclone Formation Alert (TCFA) was issued at 071130Z. Intensification was slow. A second TCFA was issued 24 hours after the first. When the convection began to consolidate around a compact center, the first warning was issued on Tropical Depression 25W at 090600Z. For the next two days, the depression moved to the northwest at 10 kt (19 km/hr), passing just offshore of the northeastern tip of Luzon. On the afternoon of 11 September, the system was upgraded to Tropical Storm Luke, and turned to the west. On the morning of 12 September, Luke passed about 140 nm (260 km) south of Hong Kong. A peak gust of 94 km/hr (51 kt ; 26 m/sec) was recorded at Waglan Island (WMO 45009), Hong Kong, at 111422Z. Ten hours later, Luke reached

its 50 kt (26 m/sec) peak intensity 75 nm (140 km) east of Hainan Island (Figure 3-25-1). Hainan Island's rugged terrain, with mountains to 6,000 ft (1830 m), weakened the storm. Continuing westward, Luke went ashore in Vietnam as a tropical depression. The final warning was issued at 140000Z.



SUPER TYPHOON MELISSA (26W)

I. HIGHLIGHTS

Melissa was one of the largest and most intense September typhoons to develop east of Guam in recent history. The system first appeared on 08 September near the international date line in an El Niño / Southern Oscillation (ENSO)-induced region of abnormally warm sea surface temperatures. Melissa turned abruptly to the north as it became associated with a strong surge in the monsoonal southwesterly winds, and its subsequent track was north-oriented. It rapidly intensified, peaking at 135 kt (69 m/sec). On 15 September, a cross section of the cloud-top topography (which included the eye) was obtained by a Lidar (Light imaging and detection radar) as part of a Space Shuttle experiment. As a point of interest, meteorologists at Bracknell, England, indicated that Melissa was the "most severe tropical [cyclone]" ever developed by their operational global spectral model.

II. TRACK AND INTENSITY

Since 1991, warm sea surface temperatures associated with a prolonged ENSO event have persisted near the international date line, creating favorable conditions for eastward displacement of large-scale deep convection. On 08 September, the weakened remnants of Hurricane Kristy (11E), which developed in the eastern Pacific on 27 August, tracked westward at about 15 kt (28 km/hr) across the date line along the 10°N latitude line. This disturbance was first listed as a suspect area in the Western North Pacific on the Significant Tropical Weather Advisory at 080600Z September. On the night of 10 September, the remnants of Kristy (11E) disappeared in the eastern end of the monsoon cloud band which extended into the Marshall Islands. A low-level cyclonic circulation (most probably not the remnants of Kristy) with characteristics of a monsoon depression then grew dramatically, prompting forecasters at the JTWC to issue a Tropical Cyclone Formation Alert at 110000Z. Organization increased during the daylight hours of 11 September, and the first warning on Tropical Depression 26W was issued at 110600Z. Post analysis indicated that the winds at that time were most probably already at tropical storm intensity. Shortly afterward, cross-equatorial flow from the Southern Hemisphere began to strengthen between 150°E and 160°E. As Melissa crossed 160°E, it began to interact with a surge of deep southwesterly monsoon flow, and perhaps in response to this, it slowed and turned toward the north.

By 13 September, Melissa was moving to the northeast. It rapidly developed a deep central dense overcast (CDO) (Figure 3-26-1) and a small eye (Figure 3-26-3) as it was beginning to rapidly intensify (Holliday and Thompson, 1979). It attained typhoon intensity at 131800Z, and in 42 hours, Melissa had reached its peak intensity of 135 kt (69 m/sec). Pressures over the same period are estimated to have fallen 72 mb to a low of 904 mb. Near its peak intensity (Figure 3-26-2), astronauts in the Space Shuttle Discovery probed Melissa's eye with Lidar as part of the Lidar In-Space Technology Experiment (LITE) (Figures 3-26-4 and 3-26-5). Melissa's rapid intensification and Lidar imaging are discussed in greater detail in Section III.

As the large typhoon moved farther northward, it became less influenced by the monsoon flow to the south and more influenced by the strong ridge to the northeast. Melissa began to move to the northwest around the western periphery of the ridge, and accelerated from 10 kt (19 km/hr) on 14 September to 18 kt (33 km/hr) on 18 September (when it weakened to tropical storm intensity). Late on the morning of 19 September, Melissa passed through the axis of the sub-tropical ridge and recurved. By 20

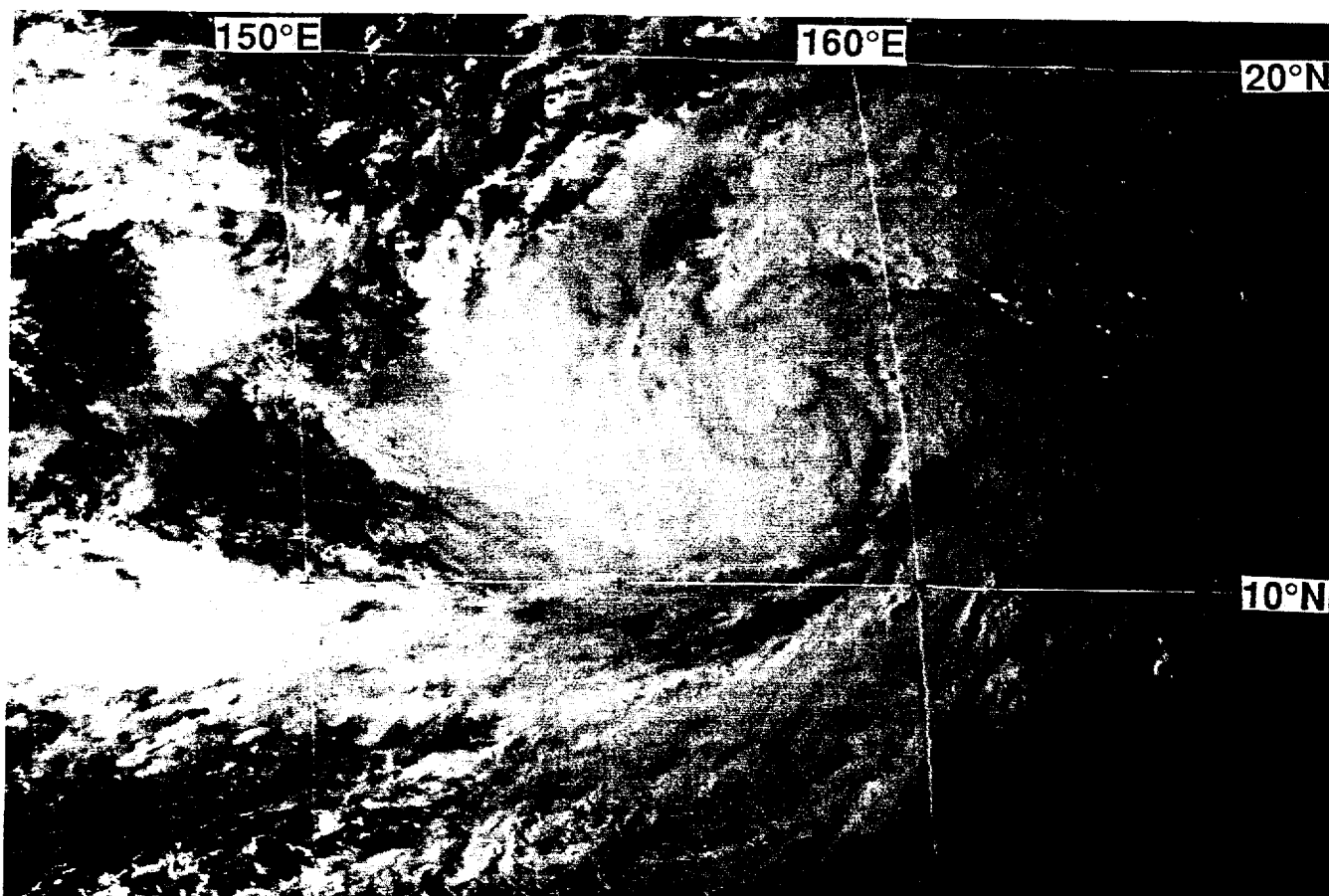


Figure 3-26-1 A very cold circular cirrus shield begins to grow near Melissa's center (130631Z September visible GMS imagery).

September, Melissa had undergone a compound transformation (Brand and Guard, 1977) into a large extratropical low.

Both track and intensity forecast errors for Melissa were larger than normal. Climatological- and statistical-based aids did not anticipate the northward turn near 160°E. Although forecast fields and derived track aids from dynamic models indicated a northward turn, they lacked consistency in their forecasts. Track errors were 113 nm (209 km), 252 nm (467 km), and 421 nm (780 km) at 24-, 48-, and 72-hours respectively. The intensity errors were 15 kt (7.7 m/sec) at 24 hours, and 27 kt (14 m/sec) at 48 and 72 hours.

III. DISCUSSION

a. Rapid intensification of Melissa

From 140600Z until 150600Z, Typhoon Melissa underwent a period of rapid intensification during which its intensity increased from 85 kt (44 m/sec) to 130 kt (67 m/sec) while pressures fell an estimated 49 mb. The rapid intensification process is defined by Holliday and Thompson (1979) as an episode of intensification where pressure falls are > 1.75 mb/hr or > 42 mb/day. Table 3-26-1 shows the best-track winds, the estimated 6-hourly change in pressures, and the 6-hourly and 24-hourly rates of change of these parameters during the rapid intensification of Melissa. Unlike the increase of the eye diameters of Doug (17W) and Fred (19W) as they rapidly intensified, Melissa's eye diameter decreased during its rapid intensification.

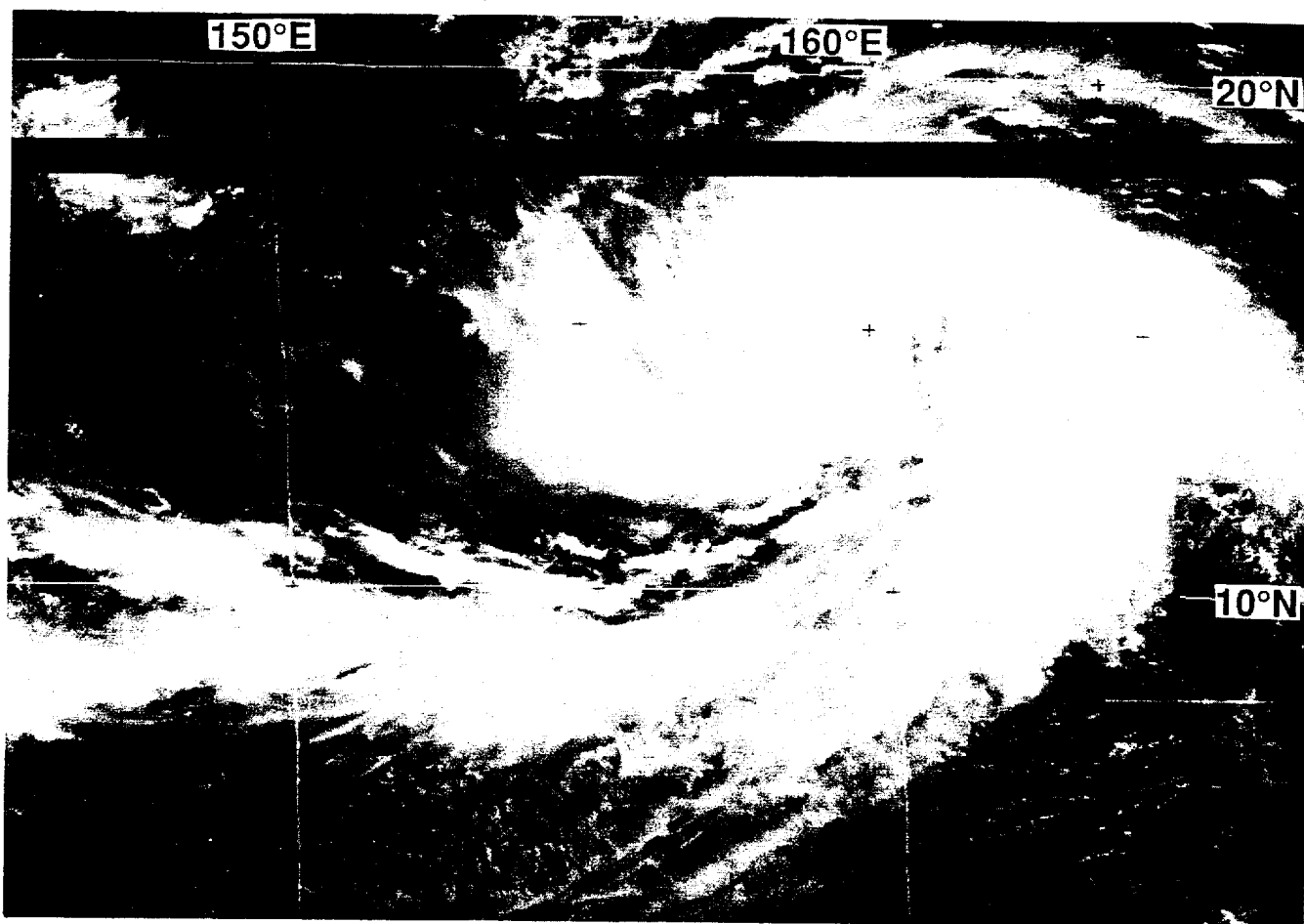


Figure 3-26-2 A small eye has formed (132331Z September visible GMS imagery).

b. Melissa imaged by Lidar

As Melissa was near maximum intensity, LITE on the Space Shuttle Discovery observed the typhoon with Lidar (Figures 3-26-4 and 3-26-5). Melissa's intensity at the time was 130 kt (67 m/sec) (Figure 3-26-3). The Lidar image shows the eye of the super typhoon, surrounded by a deck of cirrus near 15-17 km (8-9 nm) altitude. The inner edge of the wall cloud is visible, sloping inward from the top where the eye diameter is 45 km (25 nm) to the bottom where the eye diameter is 30 km (16 nm). Some scatterers (most probably thin cirrus) also appear over the eye itself. The data and its interpretation was provided by Mr. Charles Trepte, Aerosol Research Branch, NASA Langley Research Center.

IV. IMPACT

As large and intense as Super Typhoon Melissa was, it spent its life over open ocean, missing the many Mariana Islands and the Japanese island of Minami-Tori-Shima. The typhoon's large circulation covered nearly 1 million square miles of the Pacific.

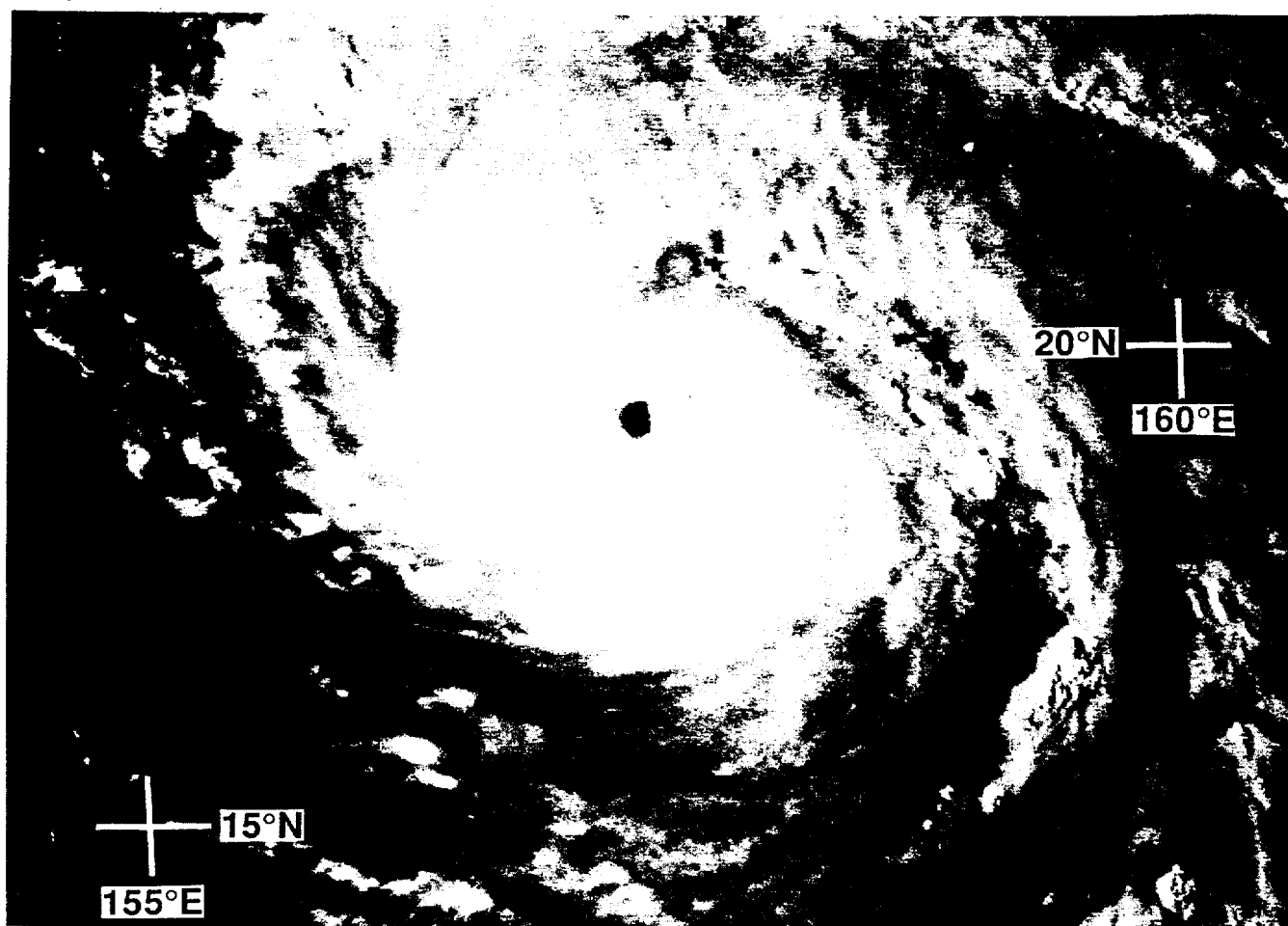


Figure 3-26-3 Melissa near peak intensity (150537Z September visible GMS imagery). Melissa was probed by a Lidar aboard the Space Shuttle Discovery at this time.

Date/Time (Z)	Wind Range (kt)	Pressure Rng (mb)	RateDP (mb)	
			1-hr	24-hr
13/12-13/18	60-65	980-976	-0.67	
13/18-14/00	65-75	976-968	-0.75	
14/00-14/06	75-85	968-959	-1.50	
14/06-14/12	85-95	959-949	-1.67	-31
14/12-14/18	95-110	949-933	-2.67	-43
14/18-15/00	110-120	933-922	-1.83	-46
15/00-15/06	120-130	922-910	-2.00	-49
15/06-15/12	130-135	910-904	-1.00	-45
15/12-15/18	135-130	904-910	1.00	23

Table 3-26-1 Pressure changes and rates of change for each six-hour warning period during the intensification of Super Typhoon Melissa, beginning at 131200Z and ending at 151800Z.

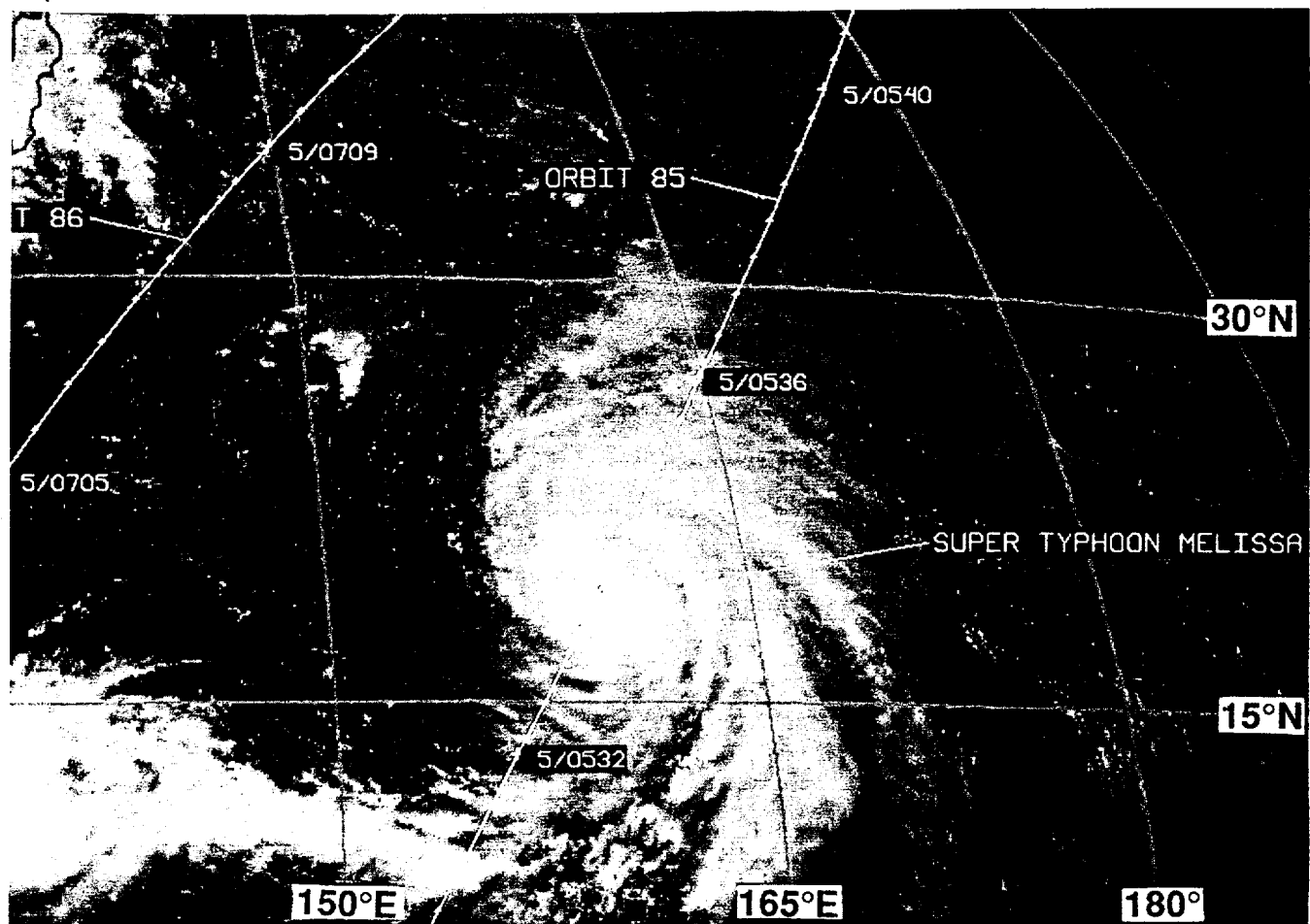


Figure 3-26-4 During orbit number 85, the Space Shuttle Discovery passes directly over Melissa.

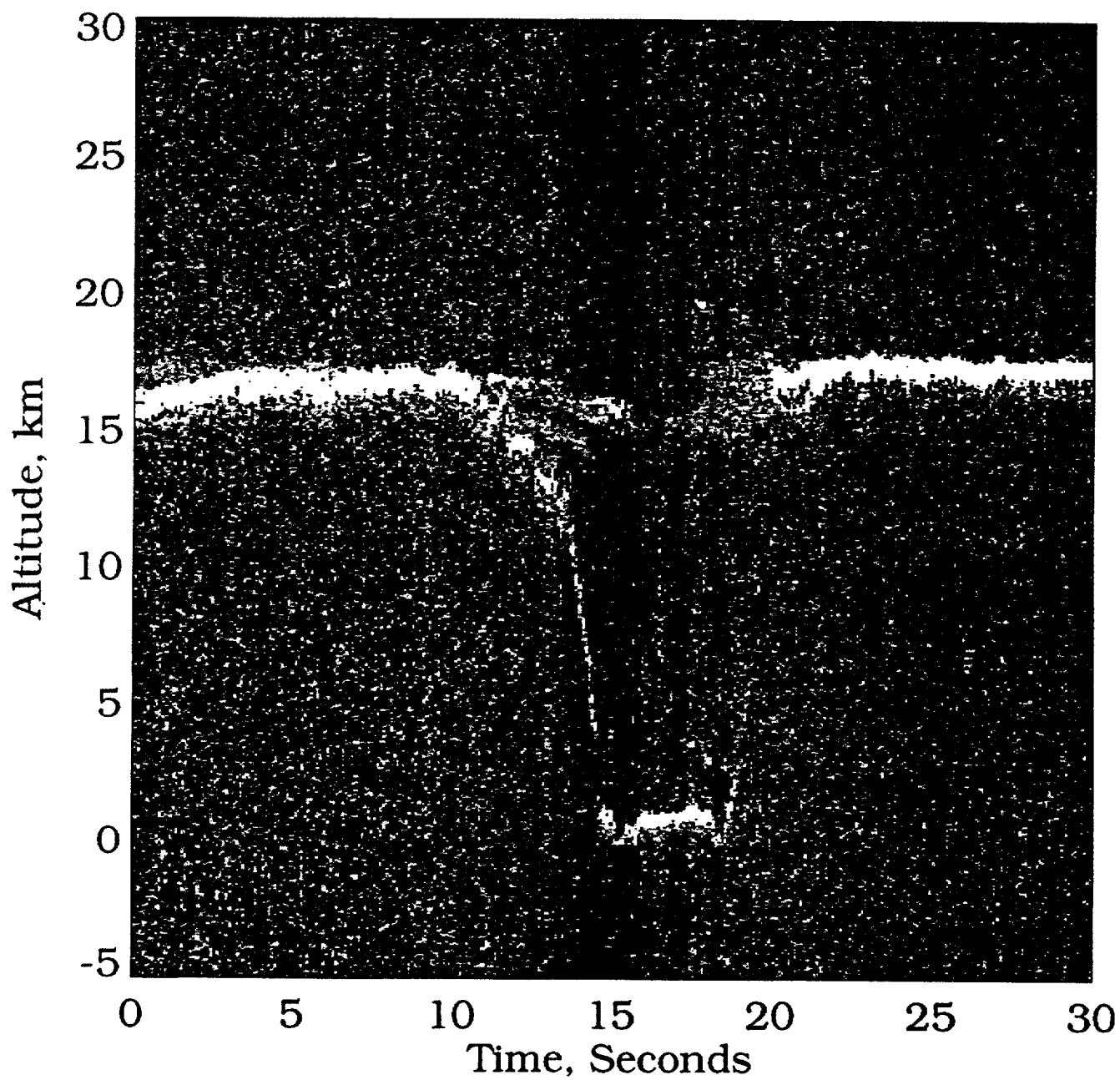
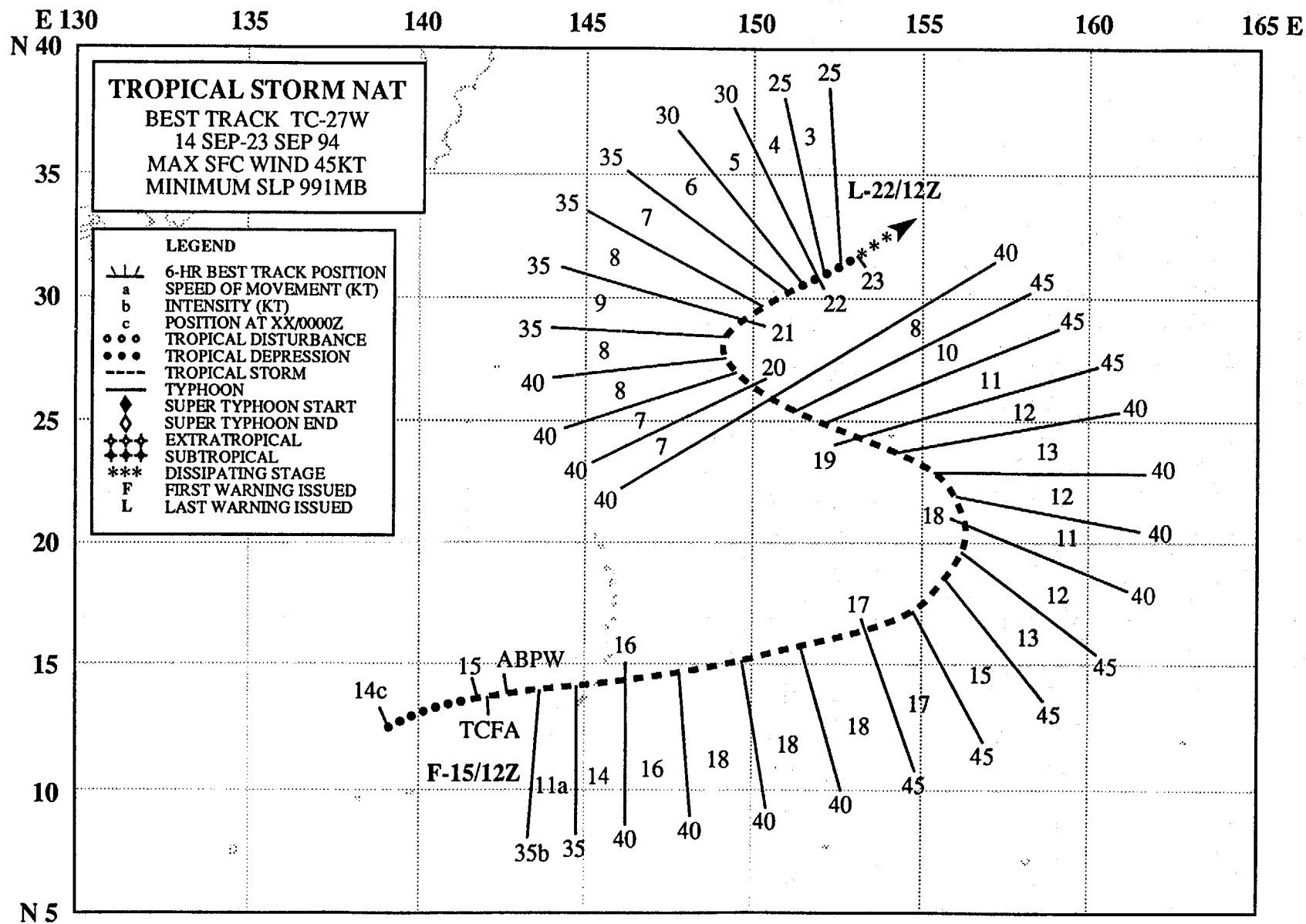


Figure 3-26-5 An altitude-time plot of the 532 nanometer LITE data raw signal distribution showing a cross-section of Melissa's eye at 150357Z September.



TROPICAL STORM NAT (27W)

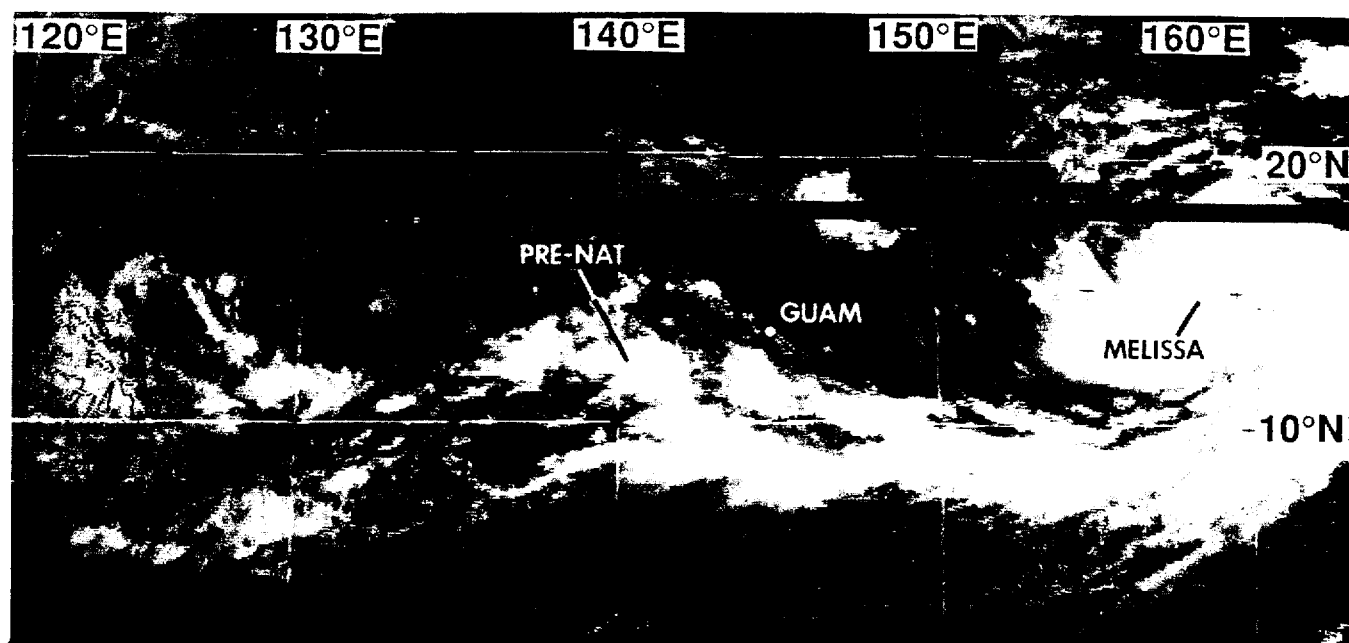


Figure 3-27-1 A monsoon cloud band stretches from the Philippines eastward toward Typhoon Melissa (26W). The first sign of organization of the tropical disturbance which became Nat is seen in the bulge of deep convection west of Guam (132331Z September visible GMS imagery).

I. HIGHLIGHTS

Nat was a small and relatively short-lived tropical cyclone that exhibited unusual “S” motion (Lander 1995a). Moving eastward at low latitude on the first leg of its “S” track, Nat passed to the north of Guam, and within range of Guam’s NEXRAD.

II. TRACK AND INTENSITY

By 14 September, a monsoon cloud band stretched from the Philippines eastward to the large cloud system associated with Super Typhoon Melissa (26W) (Figure 3-27-1). In response to the formation of a tropical disturbance to the west of Guam (Figure 3-27-2), a Tropical Cyclone Formation Alert was issued at 150230Z September that stated, in part:

“... surface pressures in the Marianas have fallen significantly over the past 24 hours, and winds on the south side of this ‘monsoon depression’ type of disturbance are approaching gale-force intensity. . . . This disturbance should continue to move east-northeastward with the prevailing southwest monsoon flow . . .”

The first warning on Tropical Depression 27W was issued at 151200Z when the system was located about 60 nm (110 km) west-northwest of Guam. It was upgraded to Tropical Storm Nat at 161200Z. In post-analysis, it was determined that Nat had most probably reached tropical storm intensity at 150000Z, and thus it was at minimal tropical storm intensity when it passed 40 nm (75 km) north of Guam at 151800Z. Wind and pressure measurements from conventional recording instruments located on Guam, and wind measurements obtained from Guam’s NEXRAD, were the basis of the final best-track intensity estimates.

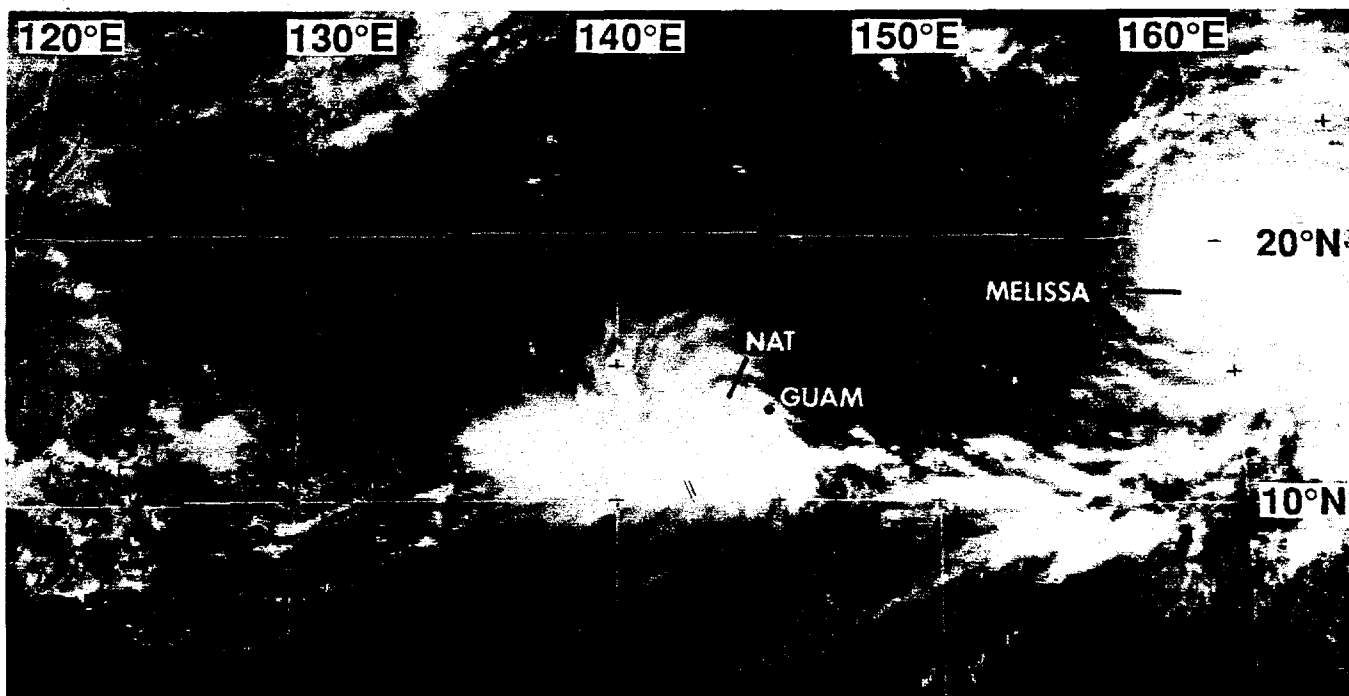


Figure 3-27-2 An area of deep convection has become organized west of Guam. Post analysis indicated that this system had already reached tropical storm intensity (150031Z September visible GMS imagery).

In the prognostic reasoning message (WDPN31 PGTW 151500) written to support the first warning, it was stated that:

“[the] track forecast philosophy is for this system to be a part of the overall monsoon surge that continues to move into Melissa (26W) . . . dynamic forecast aids indicate that the steering will be north-eastwards where the system will be absorbed into [Melissa]. . . . We expect this system [Nat] to be weak throughout its existence.”

As Nat continued on its northeastward track, it slowly intensified to a peak of 45 kt (23 m/sec). Considerable easterly shear appeared to be the major factor limiting Nat’s intensification (Figure 3-27-3). Nat was not absorbed into Melissa’s larger circulation as suggested earlier, but did remain weak throughout its life.

Between 170000Z and 190000Z, Nat’s heading backed from northeastward to northwestward. Then, between 190000Z and 220000Z, Nat’s heading veered from northwestward to northeastward to complete a nearly perfect “S” - shaped track. As Nat moved along the upper half of its “S” track, it separated from the major monsoon cloud band to the south, and decayed over open water near 30°N ; 150°E. The final warning was issued at 221200Z.

III. DISCUSSION

Nat was one of a very small percentage of tropical cyclones that move eastward at low latitude in the western North Pacific during the active months of July through September. Such cases of eastward motion most often occur when a tropical cyclone is embedded in the deep southwesterly flow of a very active monsoon. While on the lower east-bound leg of its “S”-shaped track, Nat passed 40 nm (74 km) to the north of Guam. Guam’s NEXRAD provided a unique look at the structure of this unusual tropical cyclone.

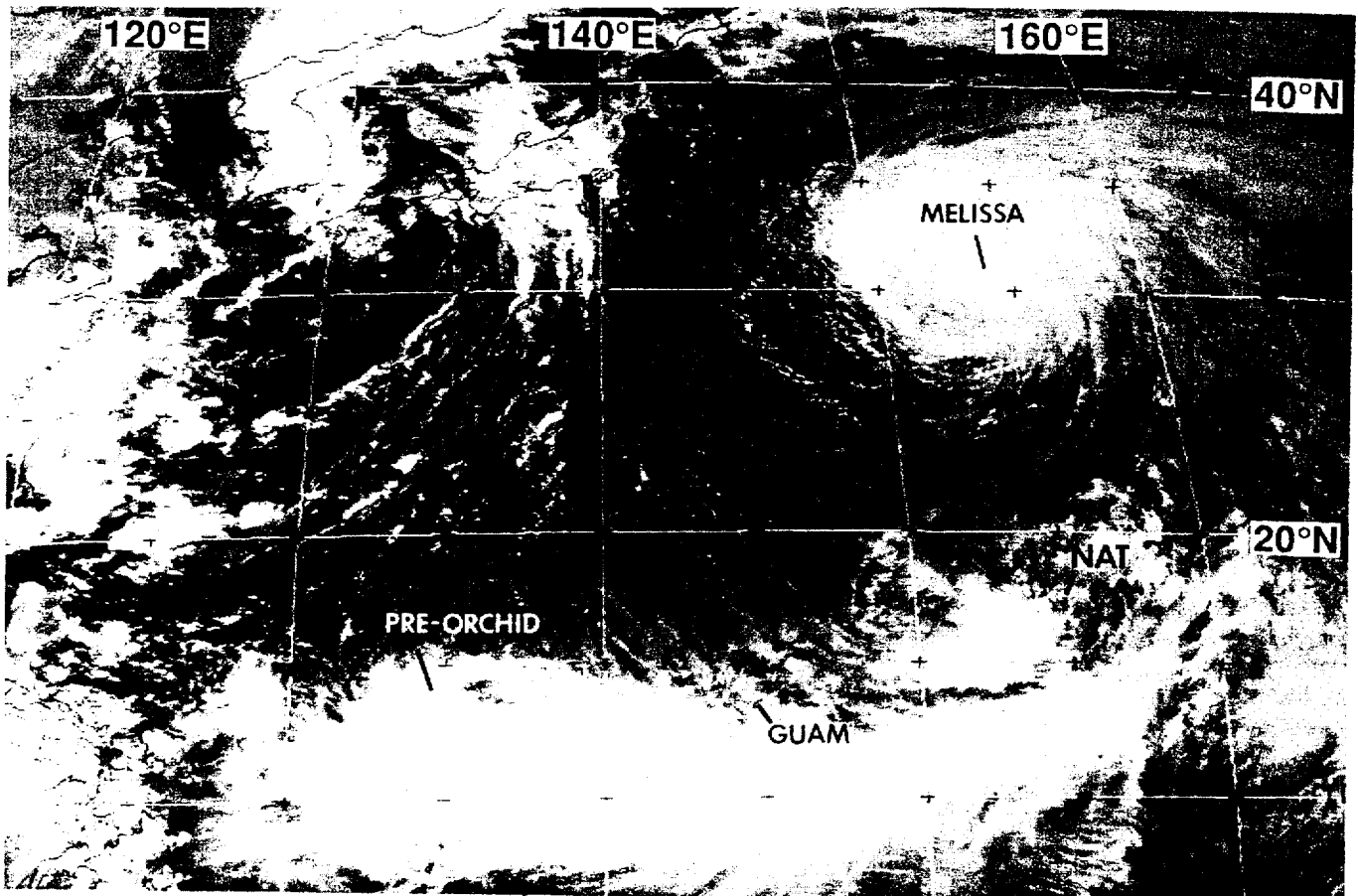


Figure 3-27-3 Nat's low-level circulation center is located to the east of its deep convection under the influence of easterly shear (170531Z September visible GMS imagery).

a. NEXRAD's view of a monsoon squall

On the morning of 15 September (at approximately 150000Z), a cloud band on the outer fringes of Nat's circulation (see Figure 3-27-2) passed over Guam from the southwest and was accompanied by a sudden wind squall. Peak gusts reached 48 Kt (24 m/sec) at the JTWC atop Nimitz Hill (see Figure 3-27-4). Using the "base velocity" product on the NEXRAD, the inbound squall was detected when it was about 40 nm (75 km) south of the island, or about one-half hour before its passage over Guam. A vertical cross section of the radial velocity, looking southwestward straight through the oncoming squall line, showed that the peak inbound winds with a velocity near 50 kt (25 m/sec) were confined within the lowest 10,000 feet of the troposphere. Shortly after the passage of the squall, the "velocity azimuth display" (VAD) product obtained from the NEXRAD showed another commonly observed property of high-wind events associated with the monsoon or with tropical cyclones affecting Guam: very deep unidirectional flow extending to at least 40,000 ft (200 mb).

b. Locating the center of Nat's poorly defined circulation

Nat's closest point of approach to Guam was 40 nm (75 km) to the north at 151800Z. This was well within the 124 nm (230 km) range of the NEXRAD's capability to observe radial velocity. Nat was poorly organized while passing to the north of Guam, and locating the center with the radar was difficult. Several radar products were examined in order to increase the confidence of the fix; these includ-

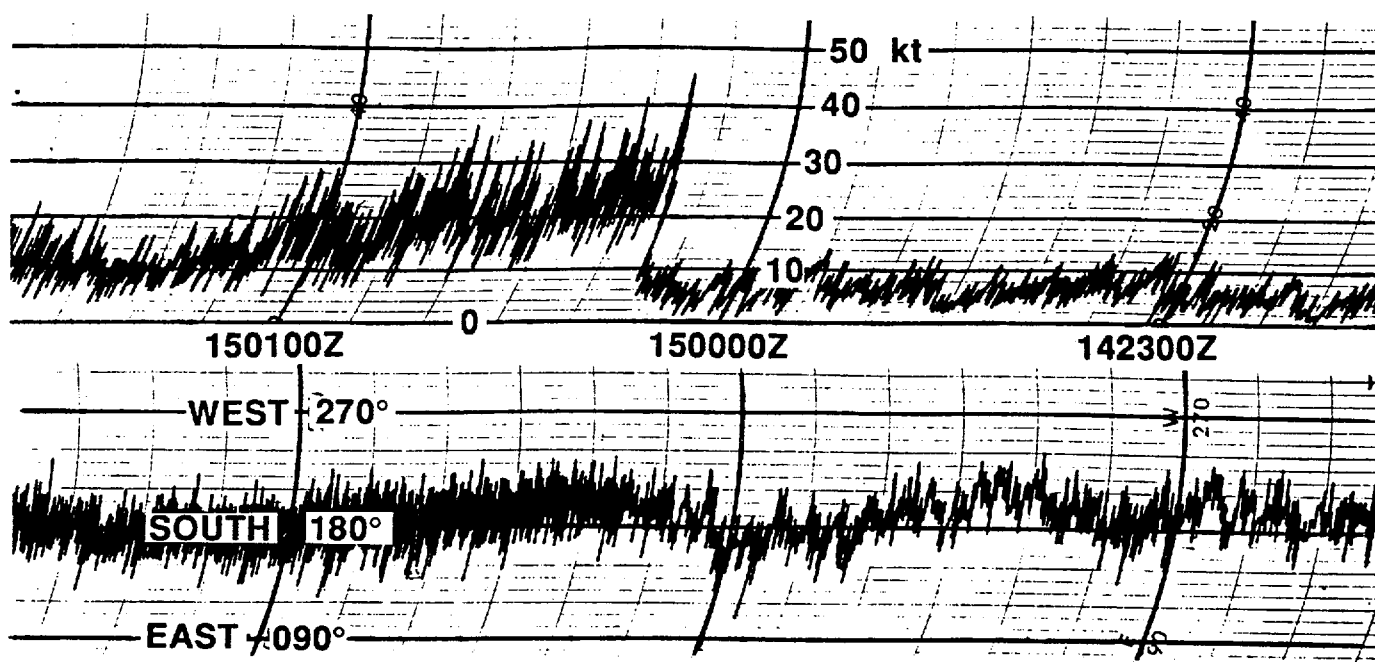


Figure 3-27-4 Recording anemometer trace at the JTWC showing the sudden onset of wind in the first squall associated with Nat.

ed: the base reflectivity, the base velocity, animation of the base reflectivity, convective cell tracking, and the one- and three-hour integrated rainfall products. In Nat's case, the distribution of deep convection as depicted by satellite (Figure 3-27-5a), and by the base reflectivity from the NEXRAD (Figure 3-27-5b), was poorly organized. The isodop (line of zero radial velocity) was useful for estimating the bearing of the center to the site (Figure 3-27-5c). The most striking depiction of the wind pattern in Nat was obtained from the three-hour precipitation product (Figure 3-27-5d). Despite the disorganized appearance of the cloud elements in satellite imagery and on the NEXRAD'S base reflectivity product, the short-term (i.e., one-hour and three-hour) integrated rainfall products showed a high degree of organization and helped increase the confidence of the estimated low-level center position.

IV. IMPACT

Throughout its entire life, Nat remained at sea and reached a peak intensity of only 45 kt (23 m/sec). However, for such a weak system, it had a disproportionate impact on the island of Guam, mostly in the form of freak accidents. As Nat approached the island of Guam on September 15, a squall line in the outer circulation of Nat passed across the island. Winds gusted to 48 kt (25 m/sec) at the JTWC as this squall passed. Two tourists who were parasailing were seriously injured when winds in this squall snapped the tow rope which attached their parasail to the boat. A second squall later in the evening damaged power lines, causing a half-hour loss of power to several villages. Strong winds on the morning of 16 September, when Nat was located about 100 nm (185 km) to the northeast of Guam, knocked a security guard off a gangplank and into the water at the commercial port. The man, who could not

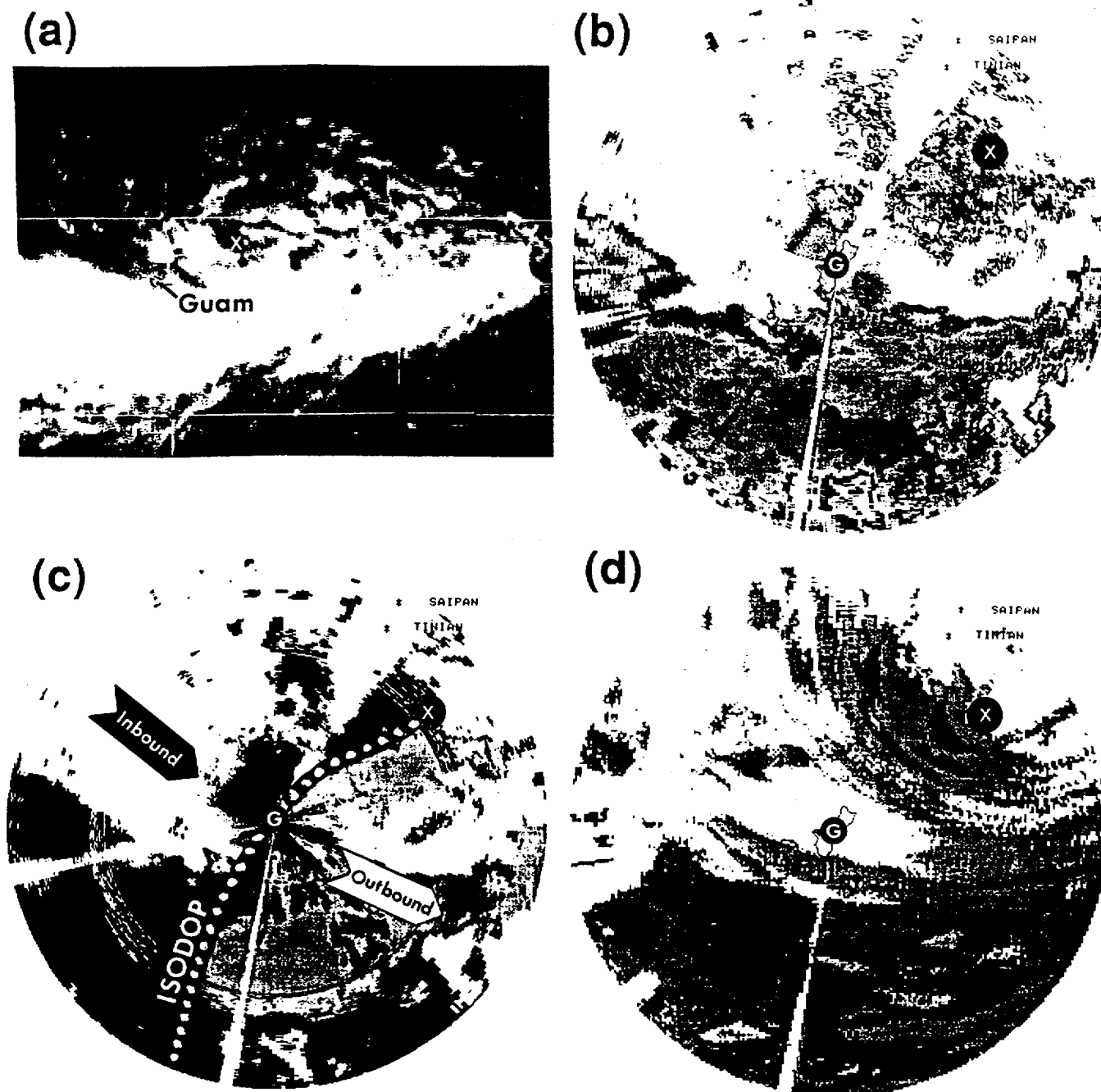


Figure 3-27-5 A combination of products from satellite and weather radar were used to locate the center of the poorly organized Nat as it passed north of Guam. (a) Nat's poorly organized central convection as seen by satellite (160031Z September visible GMS imagery), and (b) by Guam's NEXRAD (160058Z September NEXRAD base reflectivity). (c) The isodop (line of zero radial velocity) extends towards Nat's estimated center location (160058Z September NEXRAD base velocity). (d) Note the higher degree of organization apparent on the three-hour precipitation product (160058Z September NEXRAD three-hour precipitation). Nat's estimated center location is indicated by the small white "x" within the black dot.

swim, drowned. Two of his co-workers also were knocked into the water and nearly drowned. Later, on the morning of 17 September, when Nat was located about 500 nm (925 km) northeast of Guam, a thunderstorm developed over Guam in weak northwesterly wind flow. Lightning in this thunderstorm struck at a track meet and injured about 20 people. Most were treated for light electric shock and dizziness. Another lightning bolt from this same thunderstorm struck the commercial power line feeding Guam's NEXRAD, knocking the system out for over one month and causing \$90,000 worth of damage.

E 115 120 125 130 135 140 145 150 155 160 E

N 50

SUPER TYPHOON ORCHID

BEST TRACK TC-28W
16 SEP-01 OCT 94
MAX SFC WIND 135KT
MINIMUM SLP 904MB

45

40

35

30

25

20

15

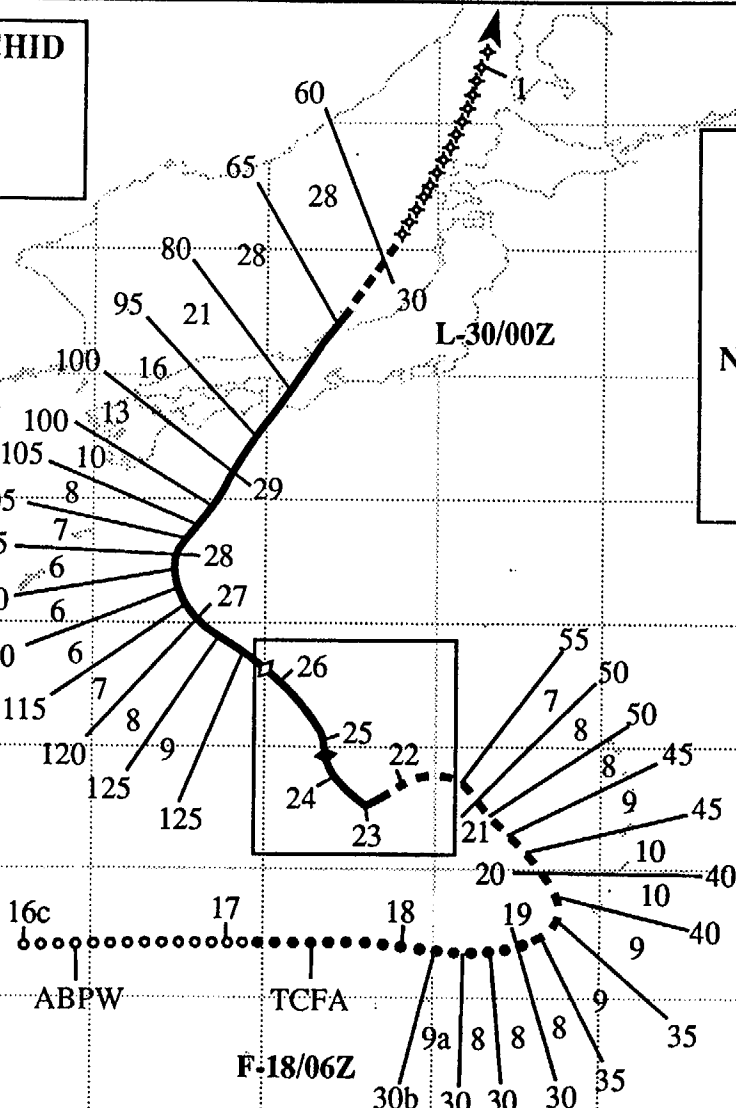
10

N 5

156

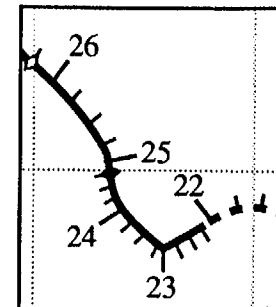
LEGEND

- 6-HR BEST TRACK POSITION
- a SPEED OF MOVEMENT (KT)
- b INTENSITY (KT)
- c POSITION AT XX/0000Z
- TROPICAL DISTURBANCE
- TROPICAL DEPRESSION
- TROPICAL STORM
- TYPHOON
- ◆ SUPER TYPHOON START
- ◇ SUPER TYPHOON END
- + + + EXTRATROPICAL
- * * * SUBTROPICAL
- *** DISSIPATING STAGE
- F FIRST WARNING ISSUED
- L LAST WARNING ISSUED



E 135 140 E

N 20



DTG (Z)	SPEED (KT)	INTENSITY (KT)
21/06	7	55
21/12	6	55
21/18	6	60
22/00	6	60
22/06	5	65
22/12	4	70
22/18	2	75
23/00	1	80
23/06	3	85
23/12	5	95
23/18	6	105
24/00	5	115
24/06	4	125
24/12	4	125
24/18	5	130
25/00	5	135
25/06	6	135
25/12	8	135
25/18	8	130
26/00	8	130
26/06	9	130

TYPHOON ORCHID (28W)

I. HIGHLIGHTS

The fifth super typhoon of 1994, Orchid was one of eight tropical cyclones to form during the very active month of September. Orchid underwent unusual motion (e.g., eastward motion at low latitude) that can be attributed to the influence of the large-scale monsoon circulation. Unlike most very intense tropical cyclones, Orchid did not appear to go through a period of rapid intensification. Orchid affected the island of Guam and later, after recurvature, it crossed the Japanese island of Honshu.

II. TRACK AND INTENSITY

The tropical disturbance that became Orchid was first detected about 100 nm (185 km) east of the Philippine island of Samar, and was mentioned on the 160600Z September Significant Tropical Weather Advisory. The disturbance moved slowly eastward under the influence of deep-layer westerly flow associated with an active monsoon. At 171130Z September, when the disturbance was located about 250 nm (460 km) north-northwest of Yap, a Tropical Cyclone Formation Alert was issued based upon improved organization of deep convection. The first warning was issued on Tropical Depression 28W at 180600Z as the organization of the satellite-observed deep convection continued to improve. The system continued eastward along about 12°N, towards the island of Guam. At 190000Z, Tropical Depression 28W began a turn toward the north. It was upgraded to Tropical Storm Orchid at 191200Z as the system (moving northward) passed 60 nm (110 km) to the west of Guam. During the next 48 hours (191200Z to 211200Z), Orchid moved northwestward at about 6 kt (11 km/hr) and slowly intensified. On the morning of 22 September, the system turned toward the southwest, then 24 hours later it turned back toward the northwest forming a V-shaped notch in its track. Typhoon intensity was first attained at 211800Z based upon its cloud structure as observed by satellite (Figure 3-28-1). During the next three days, Orchid's intensity increased at a normal rate of one "T" number per day, and by 250000Z it reached peak intensity of 135 kt (69 m/sec). After reaching peak intensity, the system accelerated toward the northwest, and slowly weakened (Figure 3-28-2). On 27 September, Orchid slowed its speed of forward motion as it approached its recurvature point. After 271800Z, Orchid turned toward the north-northeast and began to accelerate. At approximately 291000Z, Orchid made landfall on the Pii peninsula of the Japanese main island of Honshu. The eye passed just to the west of the coastal city of Tanabe (WMO 47778), where a minimum pressure of 960.9 mb and a peak gust of 92 kt (47 m/sec) were recorded. A central pressure of 961 mb supports an intensity of 85 kt (44 m/sec) sustained one-minute average wind with gusts to 105 kt (54 m/sec) using the Atkinson and Holliday (1977) wind-pressure relationship. Orchid crossed the mountainous island of Honshu at a forward speed of nearly 25 kt (46 km/hr) and entered the Sea of Japan as a minimal typhoon. On the afternoon of 30 September, Orchid passed over western Hokkaido with sustained winds of 55-60 kt (28-31 m/sec). On the evening of 01 October, the system dissipated over Sakhalin Island, at a latitude poleward of 50°N.

III. DISCUSSION

a. Monsoonal influences on Orchid's motion

From 160000Z (when Orchid was first detected) until 190600Z (when Orchid reached minimal tropical storm intensity), the system moved eastward more than 800 nm (1480 km). This unusual motion was the result of relatively deep westerly monsoon flow along the band of deep convection associated with a reverse-oriented monsoon trough that was connected to the major rain band on the south side of

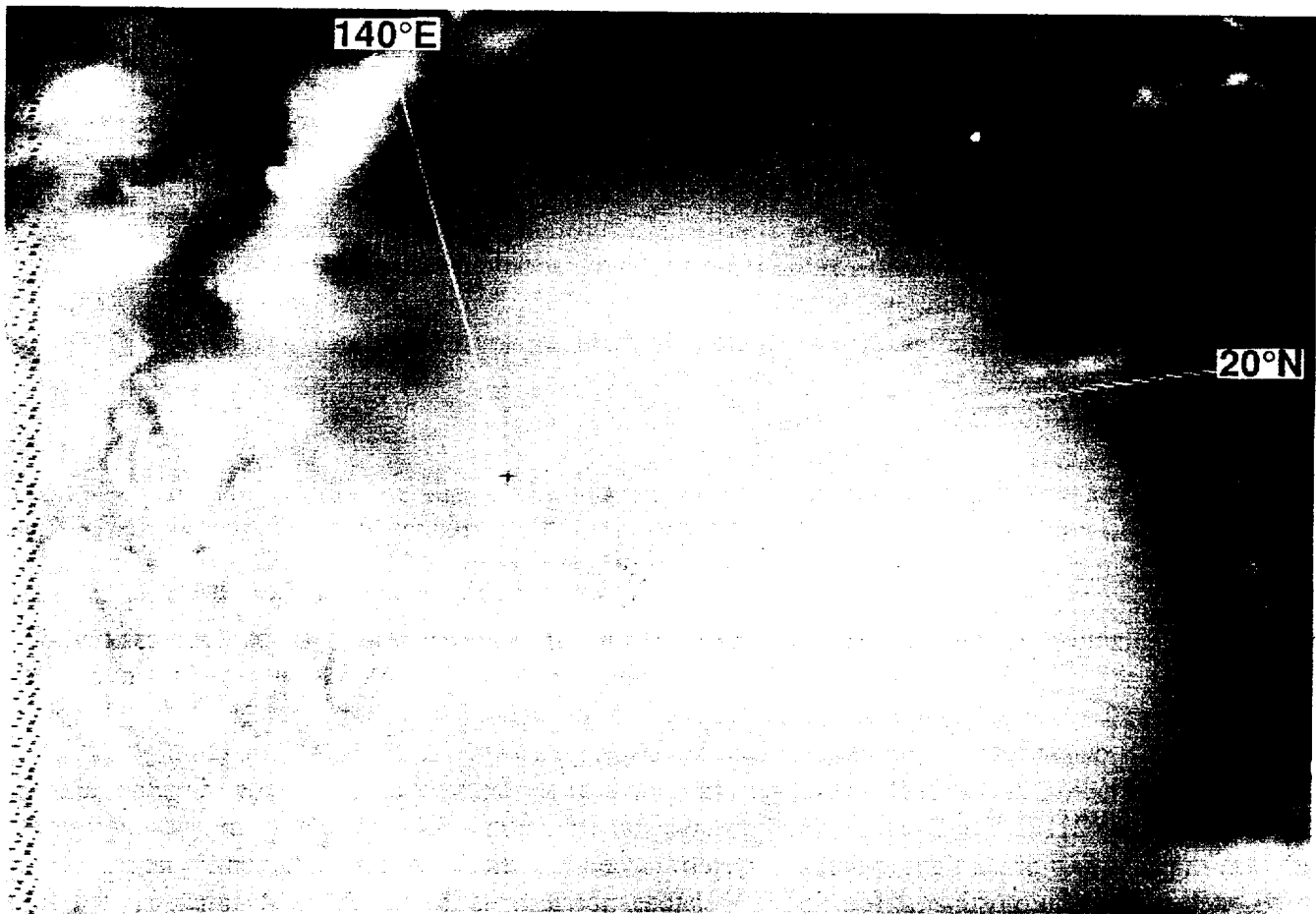


Figure 3-28-1 Orchid at 60 kt (31 m/sec) intensity at a location about 400 nm (750 km) northwest of Guam (212331Z September visible GMS imagery).

Melissa (26W). When Orchid reached about 142°E, it turned sharply to the north, passing 60 nm (110 km) west of Guam. After passing Guam, Orchid turned to the northwest. On 22 September, it turned abruptly to the southwest for 18 hours, then stalled and headed to the northwest, tracing a “V” shape.

The character and evolution of the mid-tropospheric subtropical ridge and the midlatitude disturbances passing poleward of this ridge have long been cited as the causative agents of the behavior of storms in most post analyses (e.g., Matsumoto 1984; Sandgathe 1987; and past ATCRs issued by the JTWC). Other factors deemed to be of importance to TC motion in the WNP include: binary interaction (Brand 1970, Dong and Neumann 1983, and Lander and Holland 1993), and the effects of the large-scale monsoon circulation (Harr and Elsberry 1991, Lander 1994a, and Carr and Elsberry 1994). The effects of the monsoon circulation on tropical cyclone motion have recently been receiving more attention.

A plausible explanation for the erratic “V” motion of Orchid is a monsoonal effect described by Carr and Elsberry (1995). They studied the properties of the motion of a tropical cyclone that resulted from the interaction between the tropical cyclone and a larger-sized “monsoon gyre” located to its north or west. The tropical cyclone undergoes about 180° of a counter-clockwise orbit around the gyre, and the two systems approach. Eventually the tropical cyclone merges with the gyre. Upon merger, the track abruptly changes to a steady northwestward drift (Figure 3-28-3). This theoretical motion and the actual

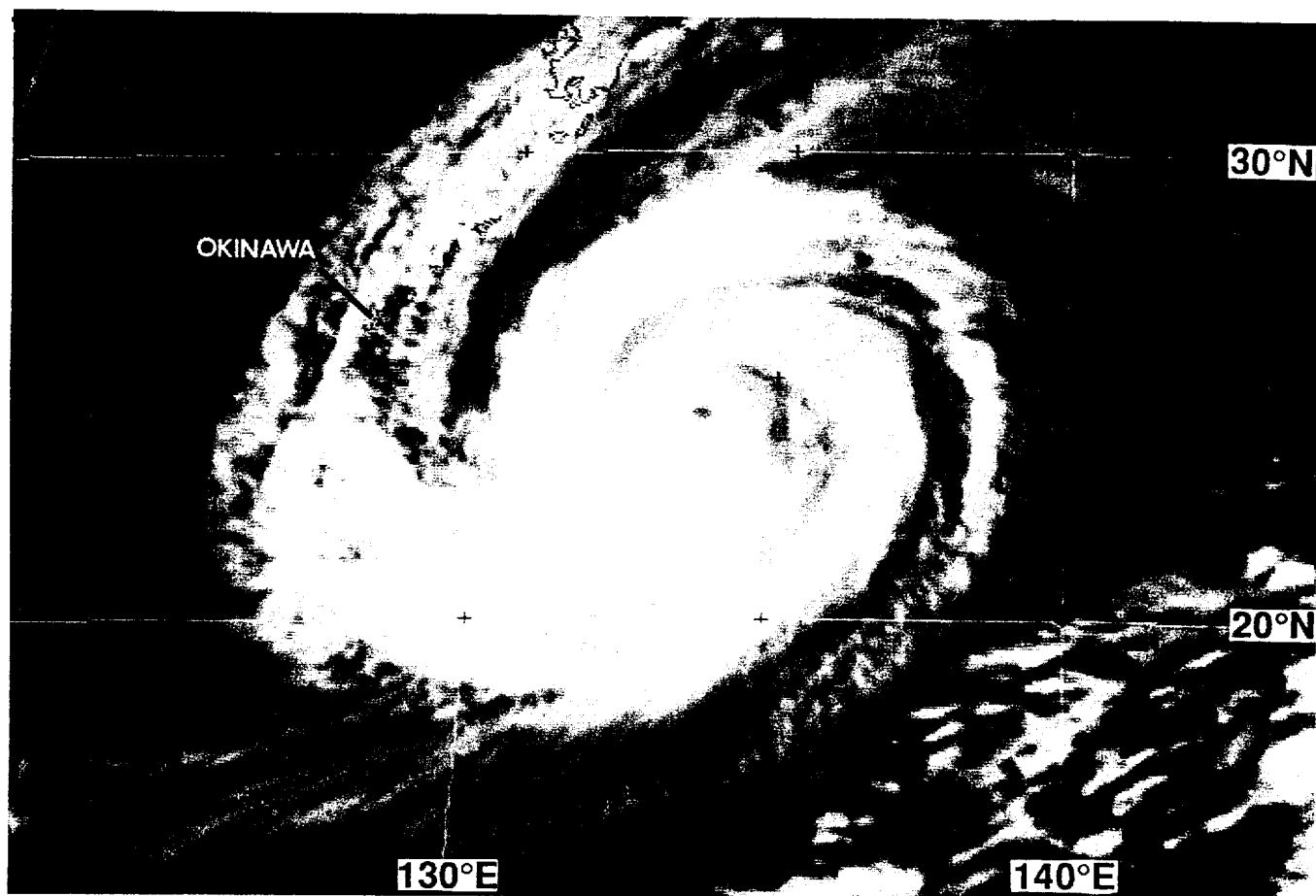


Figure 3-28-2 Orchid's intensity is 115 kt (59 m/sec) as it nears its point of recurvature (261538Z September infrared GMS imagery).

motion of Orchid are similar. Although Orchid was embedded in a reverse-oriented monsoon trough, there was, at the time of its "V" motion, a separate low-pressure area to its west (Figure 3-28-4a) with which Orchid could conceivably have orbited and merged (Figure 3-28-4b).

b. Changes in eye size during intensification

Orchid was the third super typhoon — the two others were Fred (17W) and Doug (19W) — that exhibited changes in the size of the eye that were contrary to those normally expected during the intensifying and weakening phases of a typhoon's life cycle. Orchid's eye expanded during the intensification period and it shrank during the weakening phase (see Figure 3-28-1). The changes in the size of Orchid's eye were not as dramatic as those that occurred with Doug (17W) or Fred (19W), but in each case, the changes were contrary to those expected.

IV. IMPACT

Orchid spent most of its life at sea. During its brush past Guam as a tropical storm, Orchid caused some local flooding. A peak gust of 46 kt (24 m/sec) was recorded at the JTWC. Orchid's passage over central Japan helped to alleviate a two-month drought which in some areas had left reservoirs dry. No reports of casualties or damage were received, however Orchid forced the cancellation of 400 international and domestic flights across Japan, and stopped the operation of over 100 ferry routes.

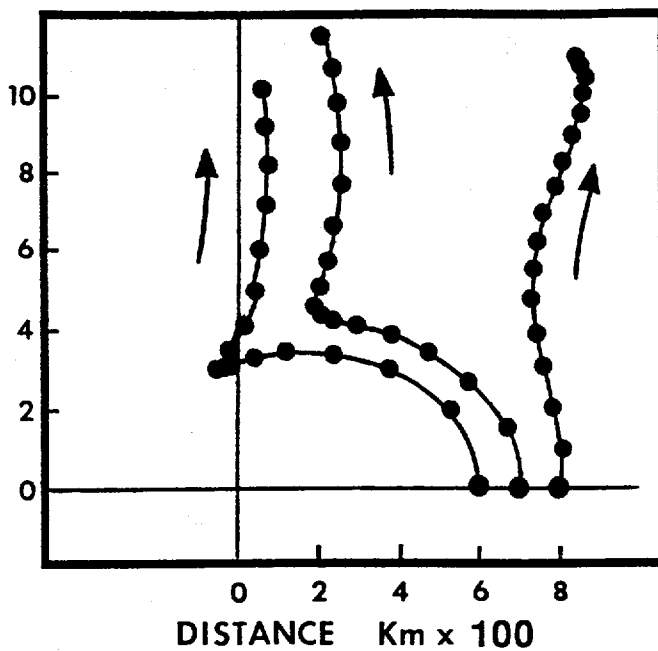


Figure 3-28-3 Typical track changes associated with the interaction of a tropical cyclone with a monsoon gyre. Dots show positions at six-hour intervals for 96 hours of the simulated tracks of three tropical cyclones placed at 600, 700, and 800 km respectively east of the center of a monsoon gyre. (Figure adapted from Carr and Elsberry, 1995.)

Table 3-28-1 Changes in the size of Orchid's eye diameter during the period when a well-defined eye was visible.

DATE/TIME (Z)	BEST-TRACK INTENSITY (kt)	EYE DIAMETER (nm)
23/00	80	26
23/06	85	17
23/12	95	18
23/18	105	17
24/00	115	16
24/06	125	14
24/12	125	18
24/18	130	14
25/00	135	21
25/06	135	18
25/12	135	11
25/18	130	19
26/00	130	23
26/06	130	30
26/12	125	26
26/18	125	22
27/00	120	22
27/06	115	13
27/12	110	11
27/18	110	14
28/00	105	12
28/06	105	17
28/12	105	14
28/18	100	14
29/00	100	9

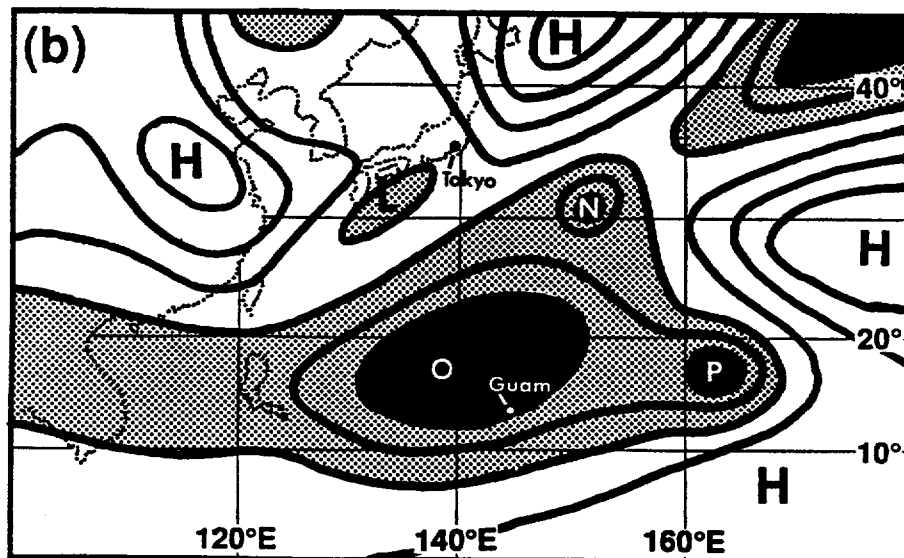
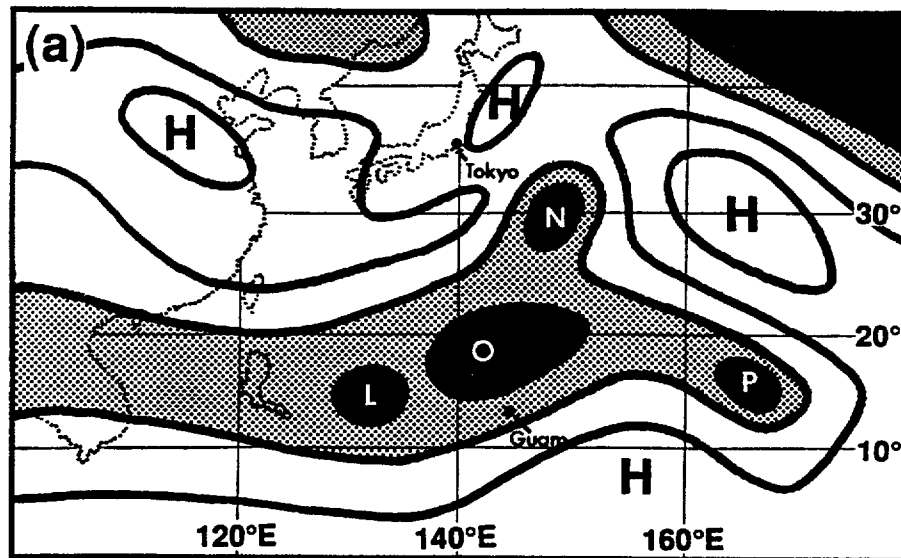
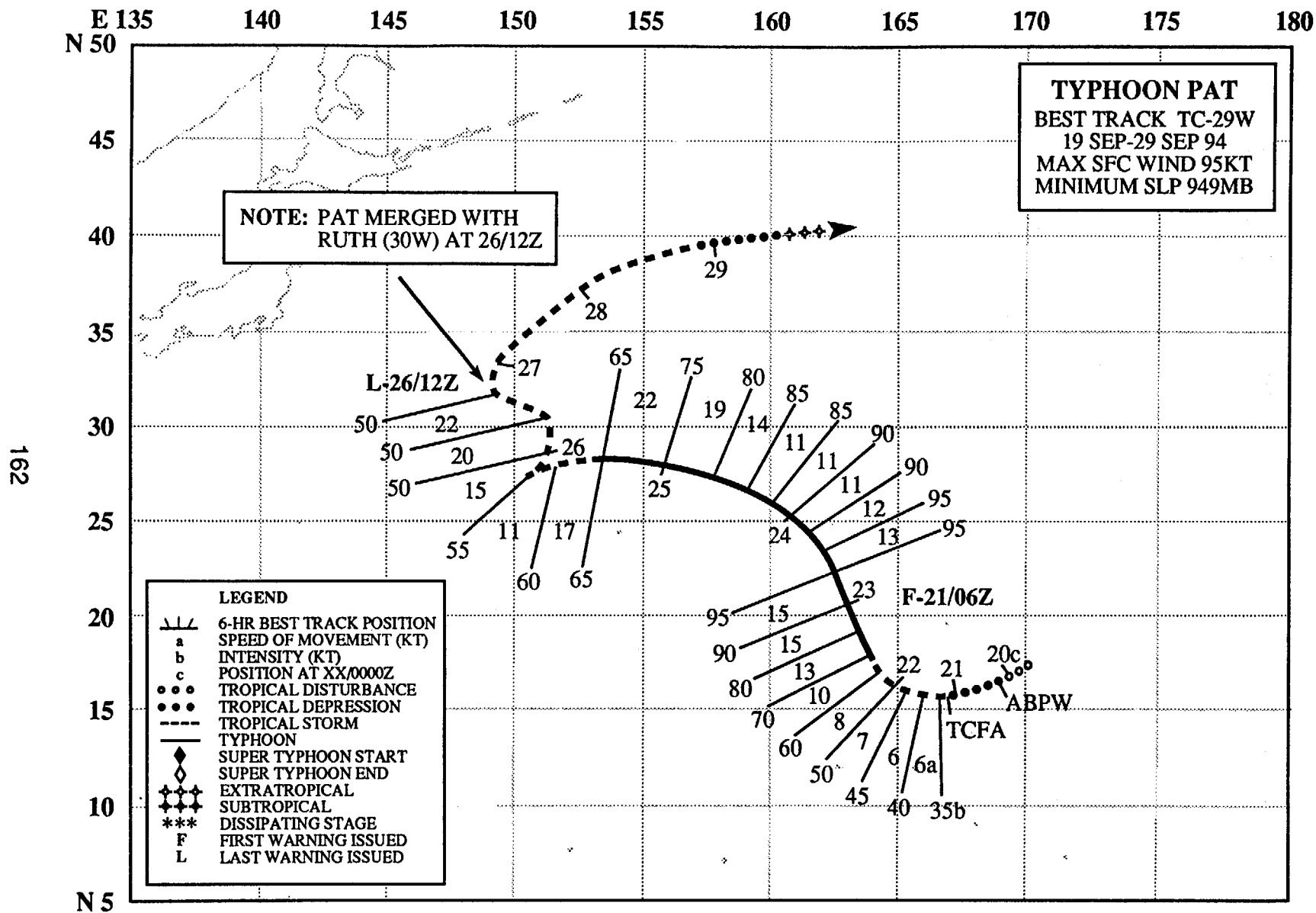


Figure 3-28-4 (a) Sea-level pressure (SLP) analysis at 210000Z October showing the location of Orchid in the monsoon trough. A low-pressure area to the west of orchid, labeled, L, may possibly have interacted with Orchid to cause Orchid's unusual southwestward motion which began at about this time. Key: Shaded regions are lower than 1010 mb, black regions are lower than 1008 mb. O = Orchid, N = Nat (27W), P = Pat (29), L = low-pressure area, and H = high pressure area. Contours are at 2 mb intervals. (b) SLP analysis at 231200Z October showing that Orchid has merged with the low-pressure area previously to its west. At this time, Orchid turned towards the northwest. Key: same as in (a) except that the black regions are lower than 1006 mb.



TYPHOON PAT (29W)

I. HIGHLIGHTS

The symmetrical collapse of deep convection during the merger of Pat with Tropical Storm Ruth (30W) is the first documented case of such an event. Pat developed at the extreme eastern terminus of a reverse-oriented monsoon trough. Pat's overall track pattern was an unusual north-oriented "S" shape that included a period of rapid counter-clockwise mutual orbit with Ruth (30W). Pat was a small typhoon.

II. TRACK AND INTENSITY

During the latter half of September, the circulation of the western North Pacific was dominated by an active monsoon trough. The low-level southwesterly winds associated with this trough had extended far to the north and east of normal, and the axis of this monsoon trough had a SW-NE (i.e., reverse) orientation. All of the tropical cyclones which formed in association with it — Melissa (26W), Nat (27W), Orchid (28W), Pat and Ruth (30W) — moved on north-oriented, "S"-shaped, tracks.

The tropical disturbance which became Typhoon Pat, was first observed at the far eastern reaches of the monsoon trough. It was listed as a suspect area on the 200600Z September Significant Tropical Weather Advisory when synoptic data and satellite imagery indicated that a low-level circulation center (with deep convection sheared to its southeast) had formed near Wake Island. An increase in the amount and organization of deep convection associated with this system prompted the JTWC to issue a Tropical Cyclone Formation Alert at 210400Z. The first warning followed at 210600Z.

Initially moving slowly west-southwestward, Pat turned toward the north-northwest and intensified. At 230000Z, when located about 270 nm (500 km) northwest of Wake Island, Pat reached 90 kt (46 m/sec) (Figure 3-29-1). It reached its peak intensity of 95 kt (48 m/sec) at 230600Z and began to weaken after 231200Z. At 240000Z, the system began to take a more westward course as it entered a easterly steering regime between a strong ridge to its north and another tropical cyclone — Tropical Storm Ruth (30W) — to its southwest. At 241200Z, Pat and Ruth (30W) abruptly increased their rate of centroid-relative cyclonic orbit. At 261200Z, the two tropical cyclones merged into a single vortex. The merged Pat and Ruth then recurved, and the final warning was issued at 281200Z. Post-analysis of synoptic data and satellite imagery indicated that the system most probably was a minimal tropical storm until 281800Z and a tropical depression until 291200Z.

III. DISCUSSION

The interaction of two adjacent tropical cyclones is often referred to as the Fujiwhara effect after the pioneering laboratory and observational studies of Fujiwhara (1921, 1923, and 1931). Fujiwhara demonstrated that the relative motion of two adjacent cyclonic vortices was composed of cyclonic orbit around their centroid, coupled with a mutual attraction. The rate of orbit steadily increases as the vortices spiral inward toward one another and eventually the two vortices coalesce into one vortex located at the centroid.

Usually the behavior of two adjacent tropical cyclones differs from the classical Fujiwhara effect in several aspects; prominent among these is the usual failure of tropical cyclones to merge. Because of these differences, the interaction between two tropical cyclones is usually called binary interaction. Dong and Neumann (1983) studied the behavior of interacting tropical cyclones and defined binary interaction as the occurrence of two named tropical cyclones which co-exist for at least 48 hours during

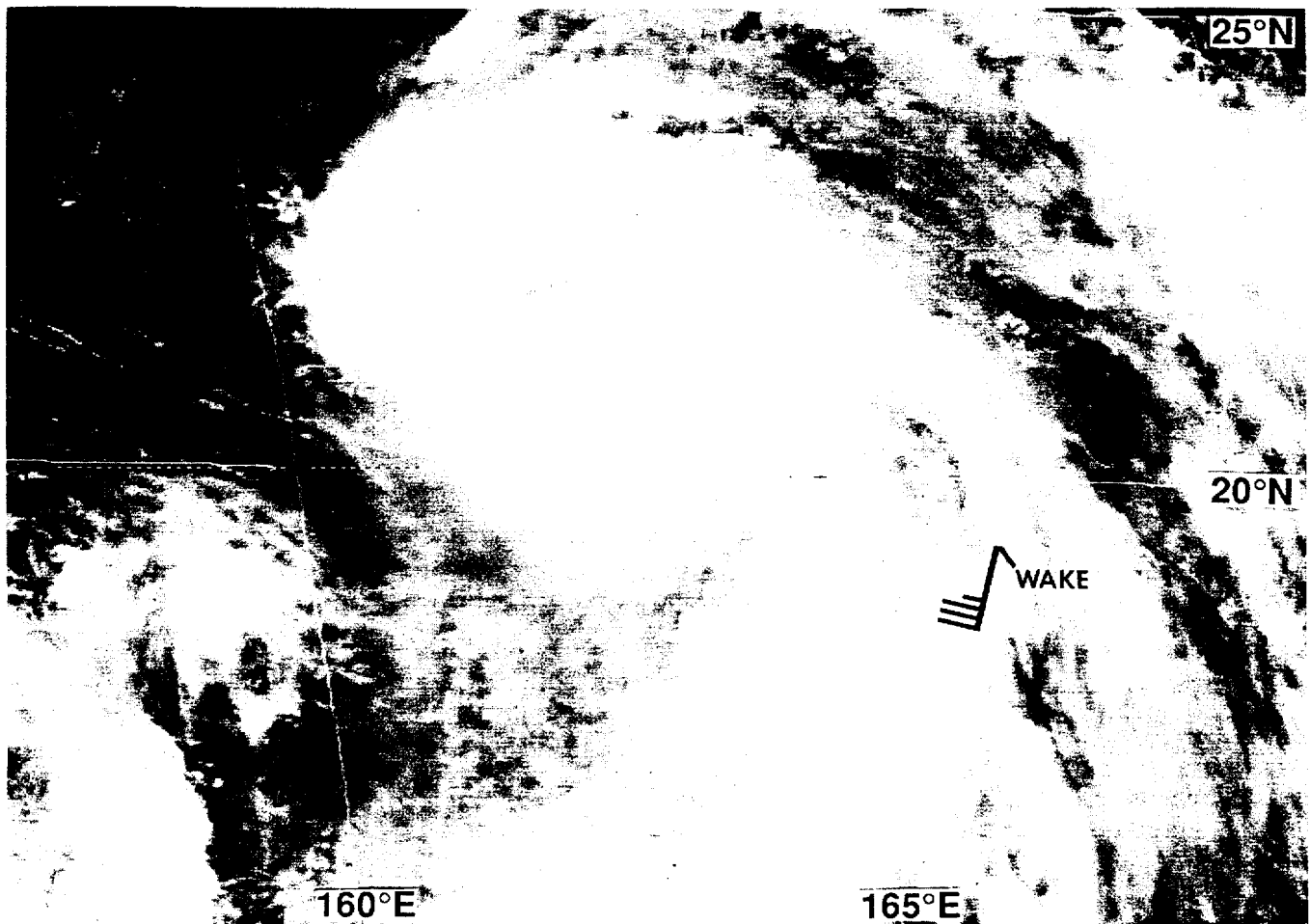


Figure 3-29-1 Pat at 90 kt (46 m/sec) six hours before its peak intensity of 95 kt (48 m/sec). The 230000Z gradient-level wind at Wake Island (WMO 91245) is plotted (230031Z September GMS visible imagery).

which time they approach within at least 780 nm (1450 km) and reach at least tropical storm intensity. The separation criterion was based on other studies by Brand (1970), which showed that mutual cyclonic orbit tends to dominate when storms approach within this distance. Brand further noted that mutual orbit tends to commence suddenly. Lander and Holland (1993) developed a generalized model of binary interaction (Figure 3-29-2), and showed that the classical Fujiwhara model of converging cyclonic rotation about a centroid followed by merger is rarely observed.

In all previously known cases of tropical cyclone merger, only one of the tropical cyclones experiences a loss of deep convection, followed by strong horizontal shearing and incorporation into the circulation of the surviving tropical cyclone. Prior to the interaction between Pat and Ruth, the symmetrical collapse of the deep convection of both tropical cyclones as they merge into a single vortex had not been documented (Lander 1995b).

During the last week of September, the tropical atmosphere over the western North Pacific Ocean was dominated by a very active monsoon trough. At the time of the satellite imagery in figure 3-29-3, two named tropical cyclones had formed in the monsoon cloud band — Orchid (28W) and Pat. A tropical depression (30W) (that later became Tropical Storm Ruth) was located between these two named storms. Over the next two days, Pat moved rapidly northwestward, and the tropical depression (30W) between Pat and Orchid (28W) was upgraded to Tropical Storm Ruth. Ruth (30W) initially moved northeastward and rapidly approached Pat. Over a 22-hour period, 250230Z to 260030Z, Pat and Ruth

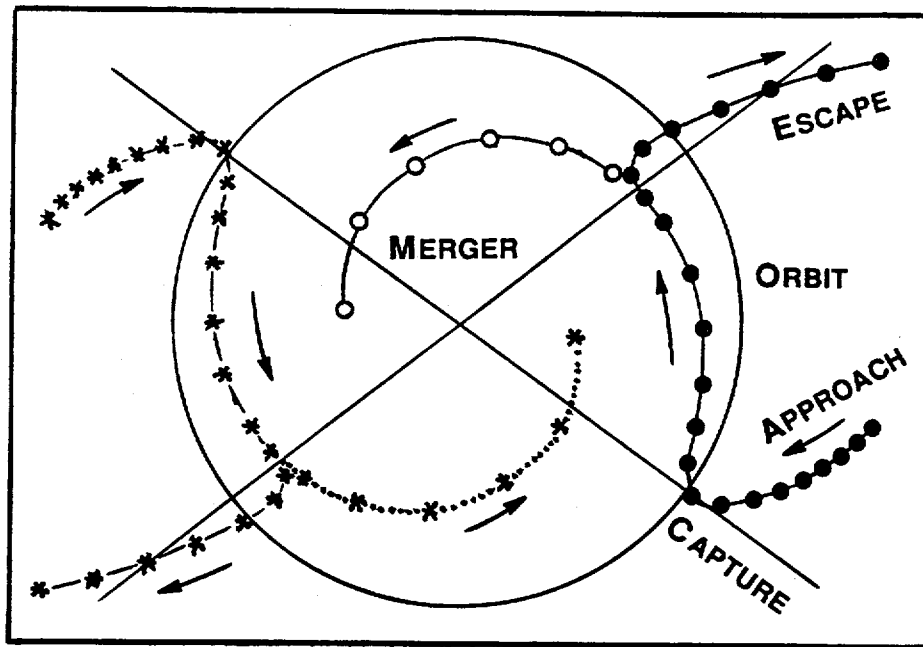


Figure 3-29-2 Model of binary interaction of two tropical cyclones containing the major elements of approach and capture, followed by mutual orbit, then escape or merger (from Lander and Holland 1993).

(30W) approached to within 200 nm (370 km) (Figure 3-29-4) and underwent about 180° of cyclonic orbit relative to their centroid (Figure 3-29-5a,b). The orbit continued during the night (260600Z to 261800Z), and during this period both systems lost their central convection and merged to become one vortex by the next morning (262330Z) (Figure 3-29-6).

At first, the merged vortex lacked significant central convection, but it still possessed tropical-storm intensity wind. The merged vortex (designated by the JTWC as Ruth) regained central convection within 24 hours following the merger (Figure 3-29-7). Later, Ruth (i.e., the merged Pat and Ruth) recurved into midlatitudes and decayed.

IV. IMPACT

No reports of significant damage or fatalities were received.

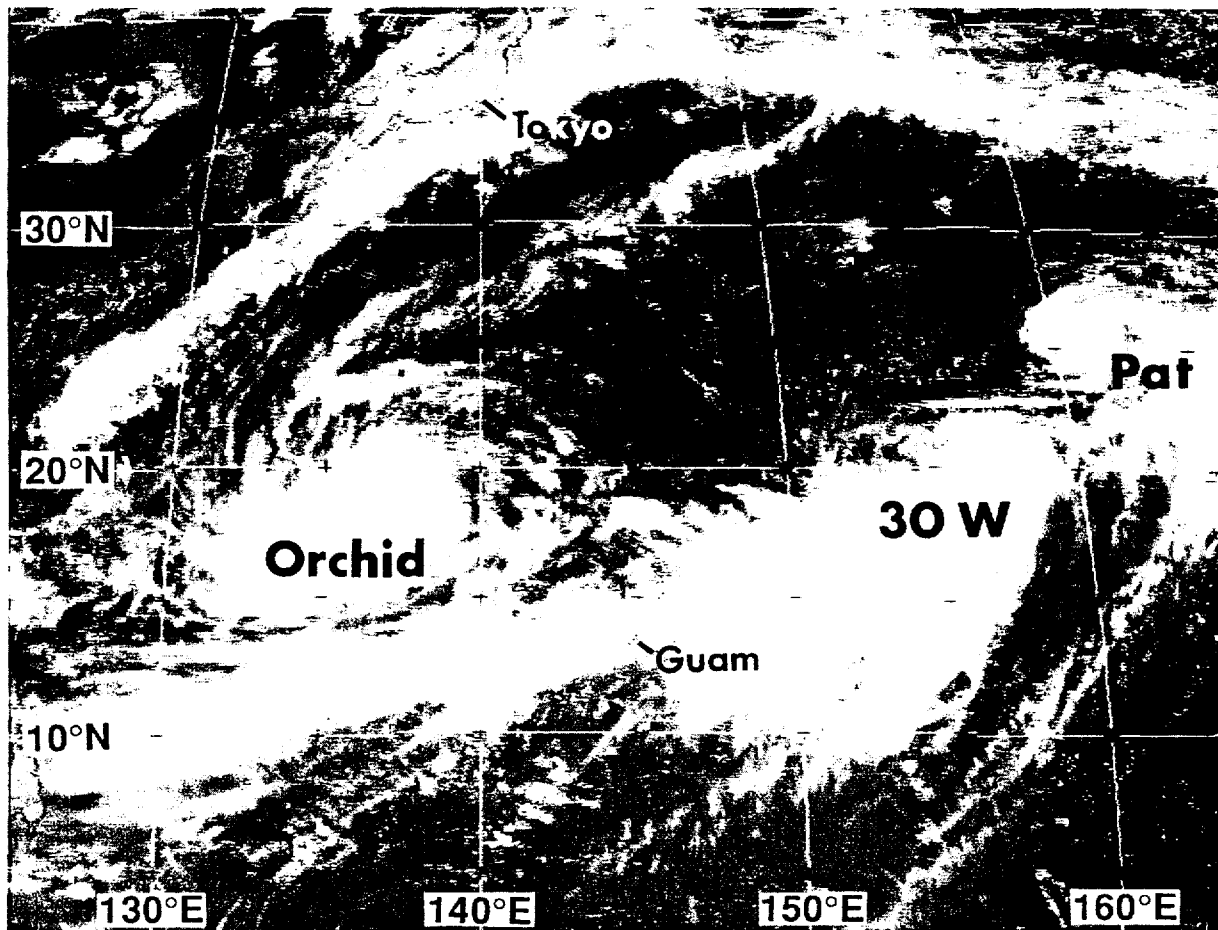


Figure 3-29-3 An active reverse-oriented monsoon trough. Typhoon Orchid, Tropical Depression 30W (later becoming Ruth), and Typhoon Pat are indicated (240031Z September GMS visible imagery).

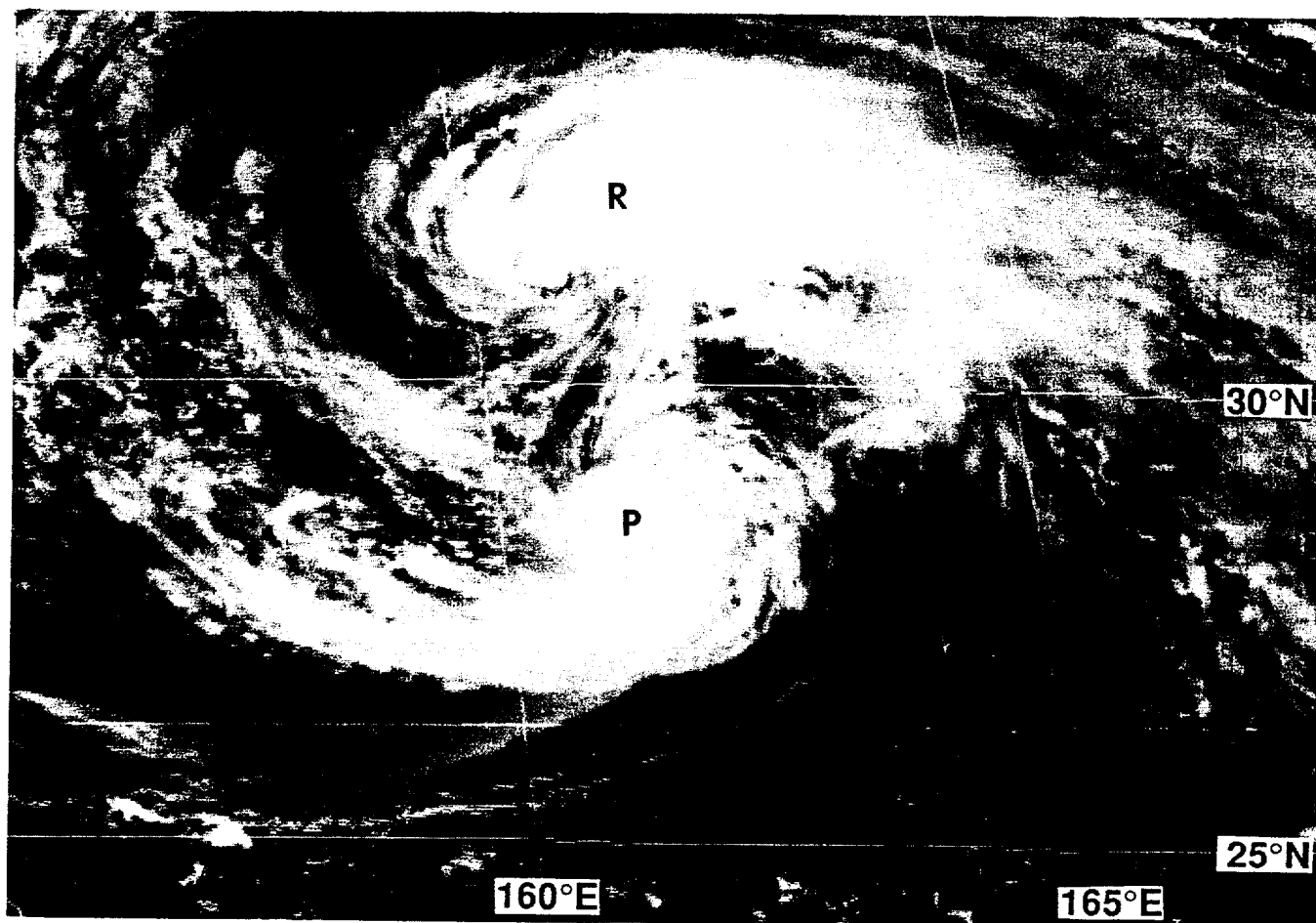


Figure 3-29-4 Pat and Ruth (30W) have moved to within 200 nm (370 km) of one another (260131Z September GMS visible imagery).

(a)

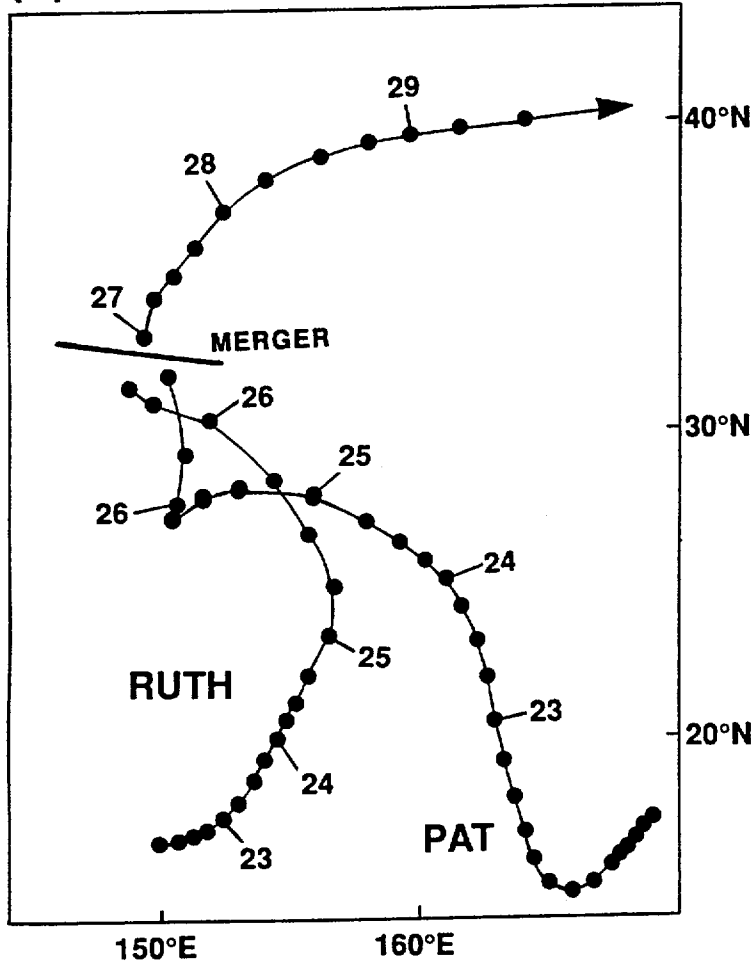
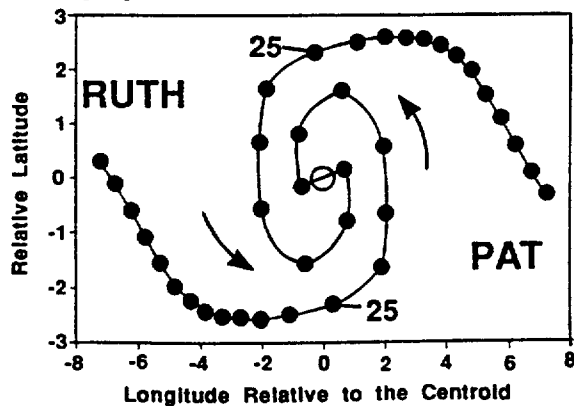


Figure 3-29-5 The tracks of Pat and Ruth (30W) in two reference frames: (a) Earth-relative [Black dots are at six-hour intervals. The positions at 0000Z are indicated. The merger location is shown as a solid bar, after which the two tracks become one], and (b) Centroid-relative [Black dots are at six-hour intervals. Positions at 250000Z September are indicated. The open circle is the centroid, where merger takes place shortly after 261200Z September]. (Adapted from Lander, 1995b).

(b)



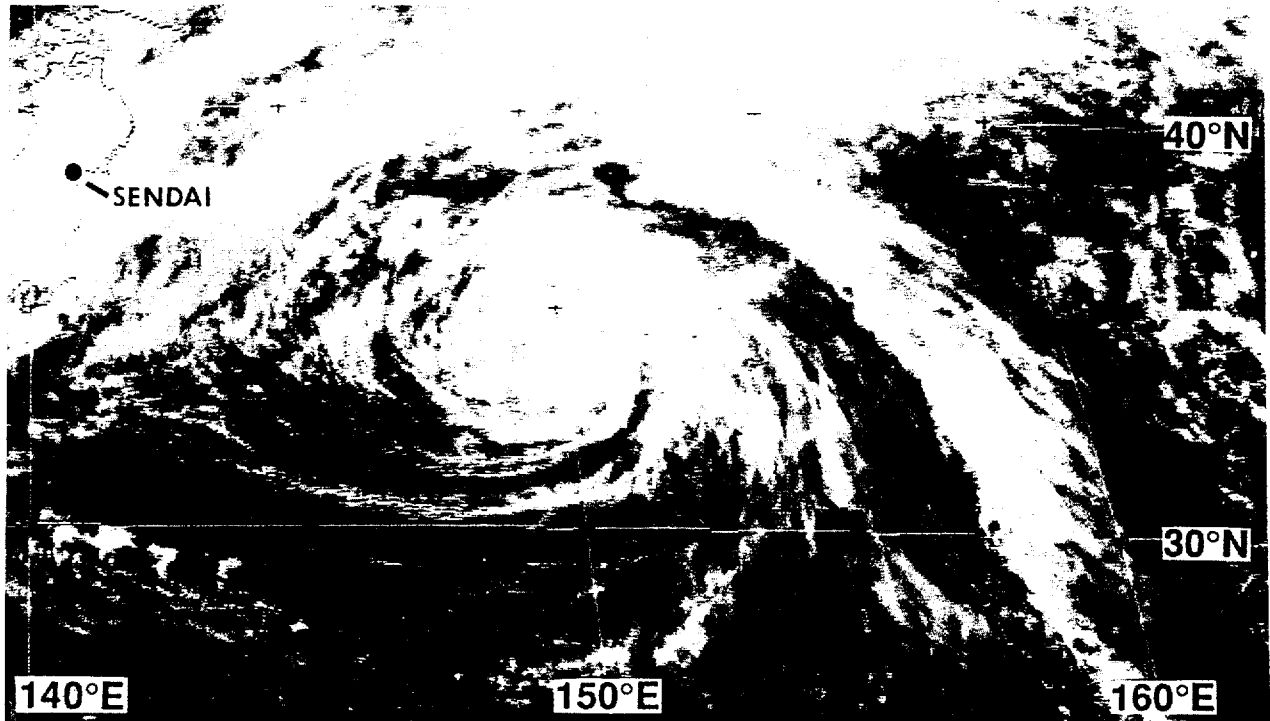


Figure 3-29-6 The single vortex that is the merged Pat and Ruth (30W). Deep central convection is absent, but ship reports and tightly wound low-level cloud lines support surface winds of tropical storm intensity (270031Z September visible GMS imagery).

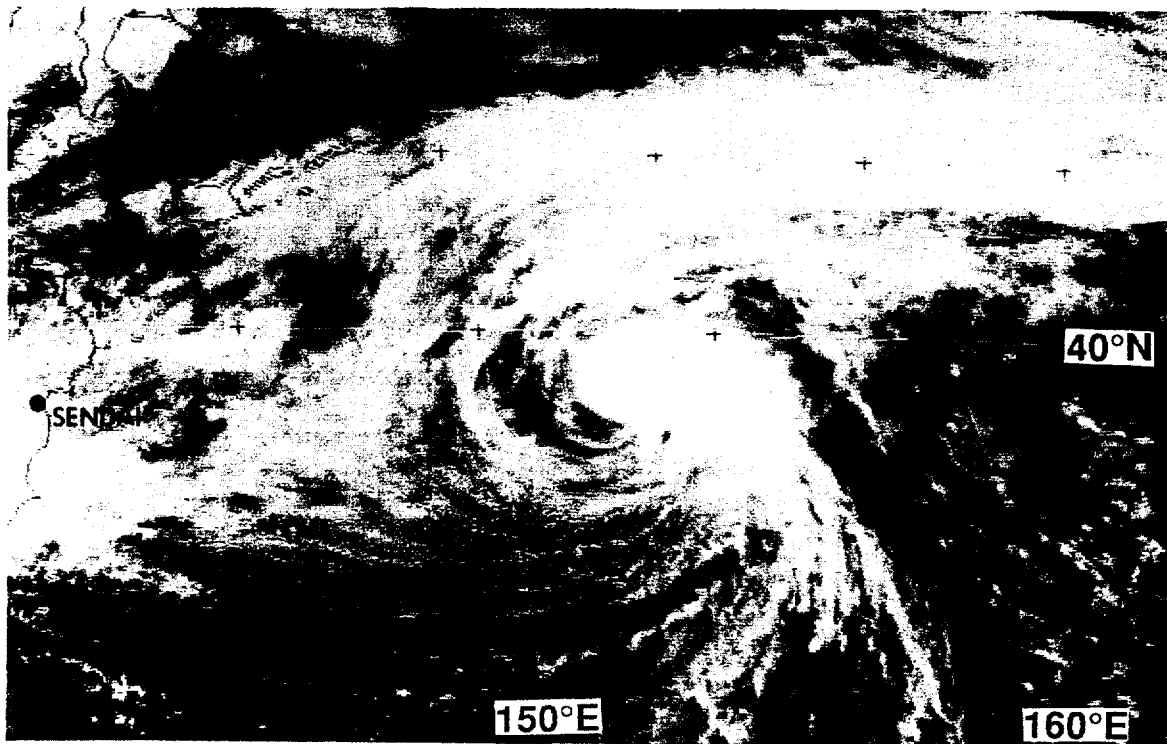
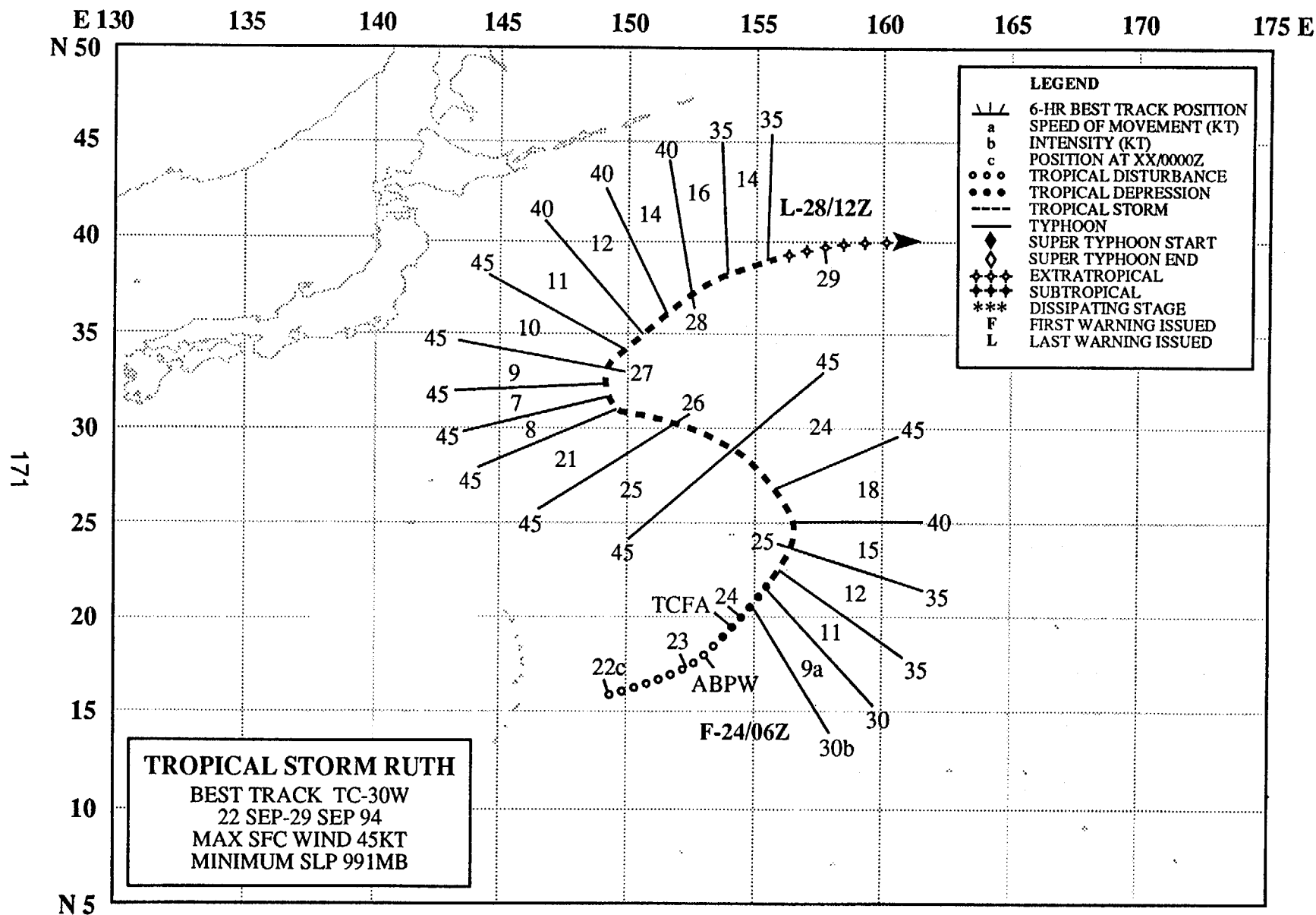


Figure 3-29-7 Central deep convection has been re-established as the merged Pat and Ruth begins its recurvature into midlatitudes (280031Z September visible GMS imagery).



TROPICAL STORM RUTH (30W)

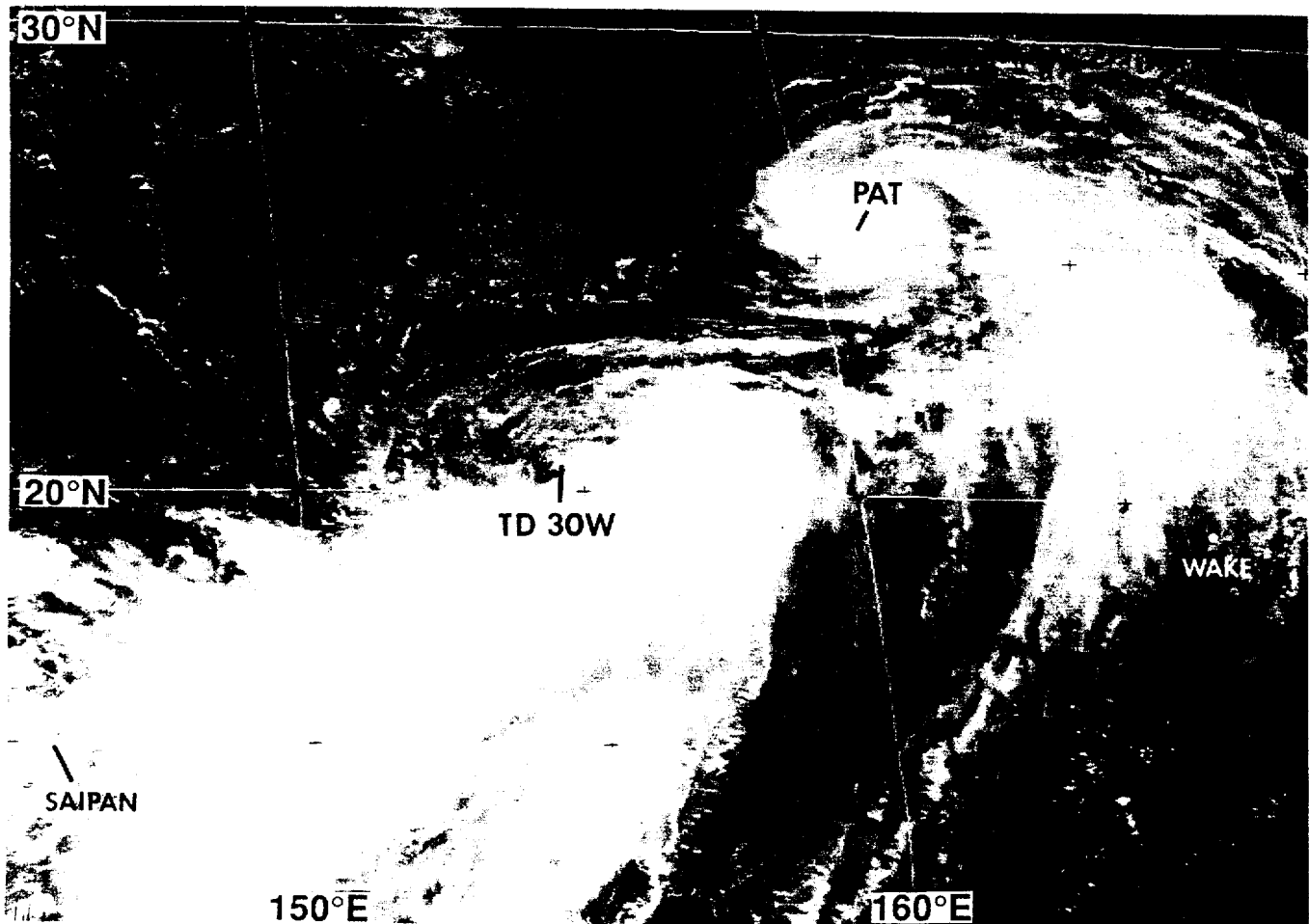


Figure 3-30-1 Cyclonically curved lines of deep convection and low-level cloud lines indicate that the tropical disturbance, which later became Tropical Storm Ruth, was intensifying (240131Z September visible GMS imagery).

I. HIGHLIGHTS

The symmetrical collapse of deep convection during the merger of Ruth with Pat (29W) is the first documented case of such an event (Lander 1995b). Ruth exhibited unusual motion: a north-oriented “S”-shaped track.

II. TRACK AND INTENSITY

Based on 24 hours of persistence, an area of deep convection (located along the axis of a reverse-oriented monsoon trough) was first identified as a tropical disturbance on the 230600Z September Significant Tropical Weather Advisory. Increased cyclonic curvature of the convective cloud bands in this tropical disturbance prompted the JTWC to issue a Tropical Cyclone Formation Alert at

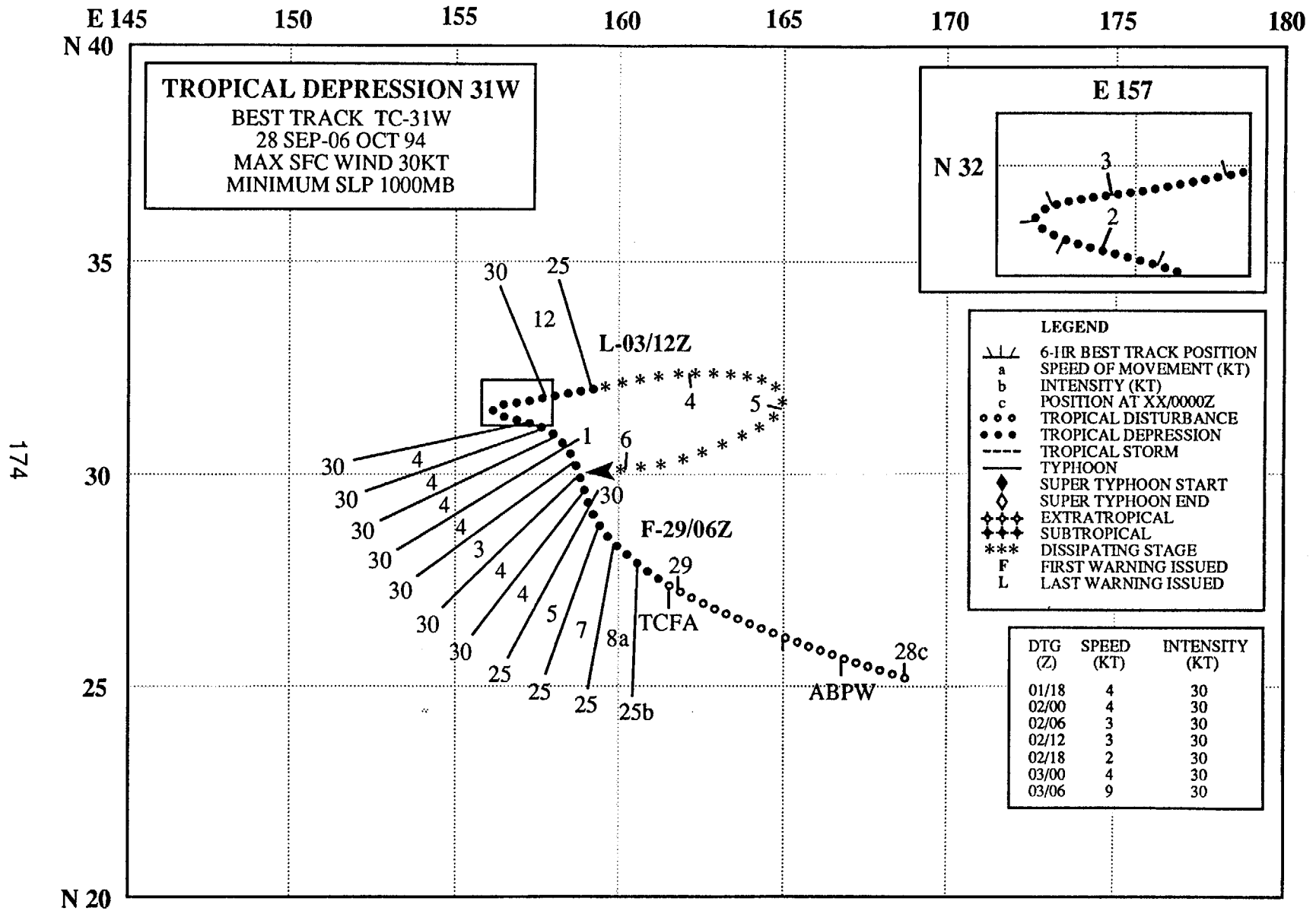
231800Z. Continued improvement in the organization of the deep convection and the presence of well-defined, cyclonically curved, low-level cloud lines during the daylight hours of 24 September (Figure 3-30-1) led to the first warning on Tropical Depression 30W at 240600Z. The system was upgraded to Tropical Storm Ruth at 250600Z. Ruth initially moved northeastward under the steering influence of deep southwesterly monsoonal flow. As it moved northeastward, the separation distance between Ruth and Pat (29W) steadily decreased and a binary interaction ensued. The binary interaction culminated in merger, and at 261200Z, Ruth and Pat (29W) became one vortex. The merged Ruth and Pat (29W) then recurved and the final warning was issued at 281200Z.

III. DISCUSSION

For a complete discussion of the first documented case of the symmetrical collapse of the deep convection of both tropical cyclones during merger, see the discussion section in the summary of Typhoon Pat (29W).

IV. IMPACT

No reports of significant damage or fatalities were received.



TROPICAL DEPRESSION 31W

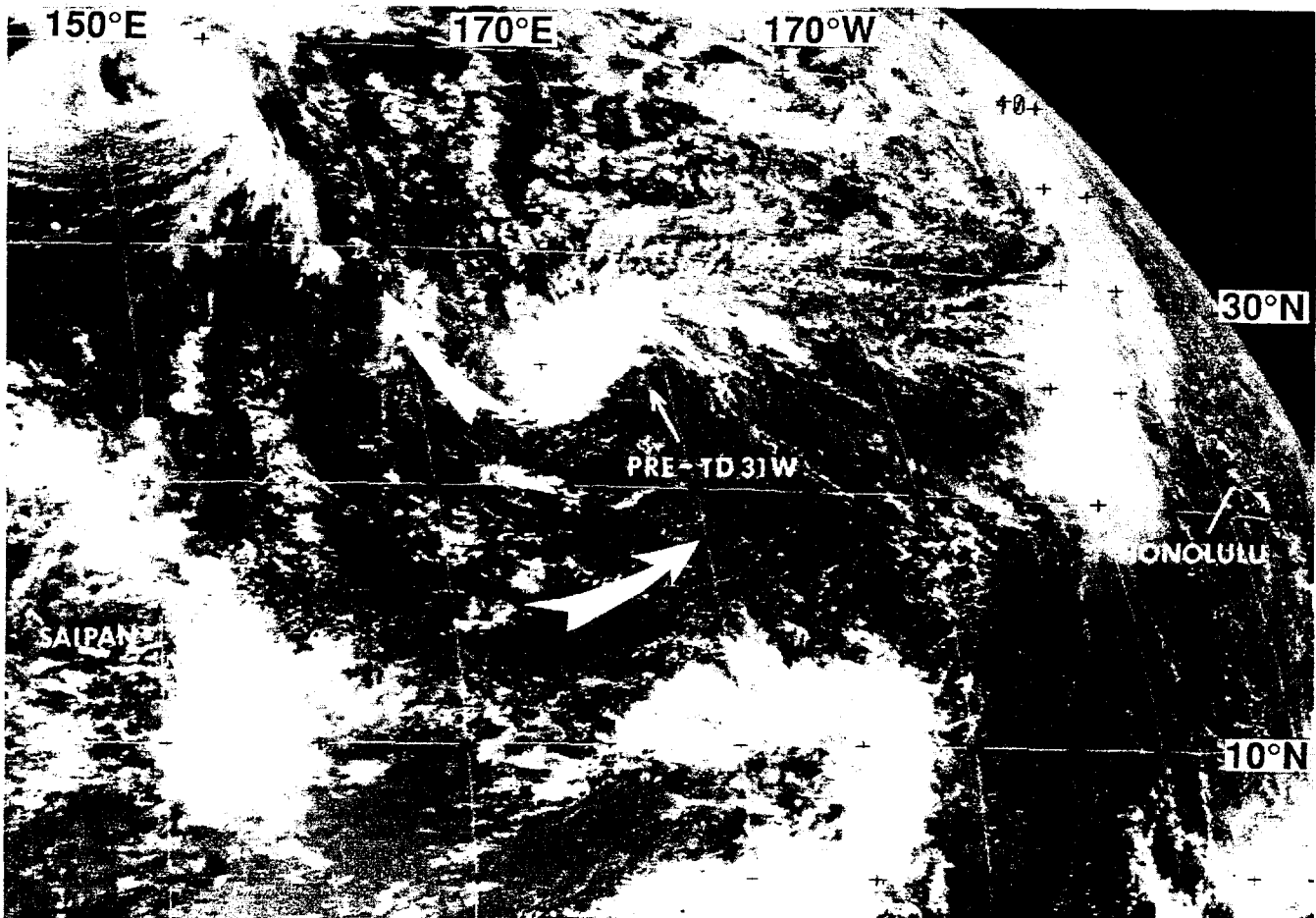


Figure 3-31-1 An area of deep convection located on the north side of an upper-level cold-core cyclonic vortex (i.e., a TUTT cell) precedes the formation of Tropical Depression 31W. Arrows indicate upper-tropospheric wind flow. (280031Z September GMS visible imagery.)

I. HIGHLIGHTS

Tropical Depression 31W was one of two tropical cyclones during 1994 — the other was Tropical Storm Yuri (36W) — that developed in direct association with a cyclonic vortex in the tropical upper tropospheric trough (TUTT) (i.e., a TUTT cell). TD 31W was a small tropical cyclone that developed at high latitude (25°N).

II. TRACK AND INTENSITY

During the last week of September, an area of persistent cloudiness associated with an upper-level trough was quasi-stationary northwest of the Hawaiian Islands. On 26 September, an upper-tropospheric cyclonic vortex detached from this trough and began to drift westward toward the international date line (i.e., it became a westward moving TUTT cell). Accompanying this TUTT cell was a small area of deep convection which was associated with some low-level cloud lines indicating the possibility of a low-level circulation. The TUTT cell moved rapidly westward, and crossed the international date line on 27 September. The small area of deep convection persisted on its north side (Figure 3-31-1), and it

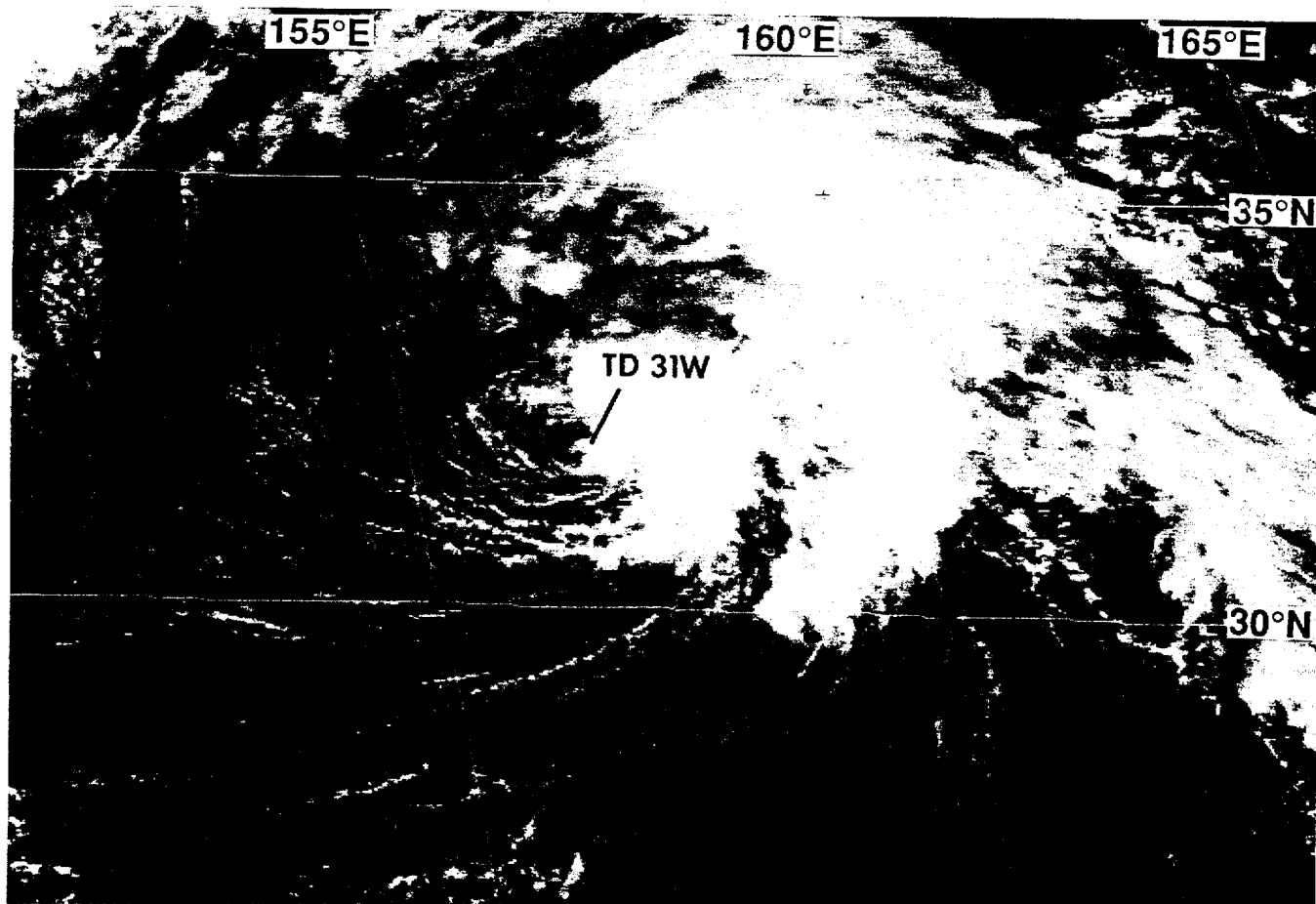


Figure 3-31-2 Well-organized low-level cloud lines accompany an area of deep convection as Tropical Depression 31W moves eastward and begins to dissipate (030031Z October visible GMS imagery).

was included on the 280600Z September Significant Tropical Weather Advisory. At 290600Z, the first warning was issued on Tropical Depression 31W. Remarks on this first warning included:

“ . . . The tropical disturbance east of Marcus island [WMO 47991] has intensified into Tropical Depression 31W. This system is well organized but lacks any significant deep convection. Some moderate convection has developed around the system center and numerous low-level cloud lines were noted spiraling into the tight circulation. . . .”

Tropical Depression 31W failed to become a tropical storm. For most of its life it lacked significant deep convection. Often, it was merely composed of tightly wound low-level cloud lines. After the system recurved at 021200Z October, it acquired significant deep convection and exhibited its most impressive satellite signature (Figure 3-31-2). The final warning was issued at 031200Z, as the system moved eastward and weakened.

III. DISCUSSION

The formation of Tropical Depression 31W in direct association with a cold low in the tropical upper tropospheric trough (i.e., a TUTT cell) is hypothesized to be a distinct mechanism of tropical cyclogenesis that has not been previously addressed (see also the discussion section in Yuri's (36W) summary). The closest description of this process is Sadler (1976). However, in Sadler's model, the

tropical cyclone forms about 1000 km to the southeast of a TUTT cell where diffluent upper-level southwesterly wind enhances deep convection (Figure 3-31-3a). The TUTT cell also acts to enhance upper-level outflow from the incipient tropical cyclone. In Sadler's model, the tropical cyclone may originate in the low-level monsoon trough, and as such, it is indirectly affected by the TUTT cell. Tropical cyclones like Tropical Depression 31W and Yuri (36W), form near the core of the TUTT cell, embedded in low-level tradewind flow at sub-tropical latitudes (i.e., north of 20°N) (Figure 3-31-3b). The cloud systems of such tropical cyclones tend to be isolated in the cloud-free zone between the cloudiness associated with the monsoon trough and the extensive cloudiness associated with the polar front.

IV. IMPACT

No reports of damage or injuries were received.

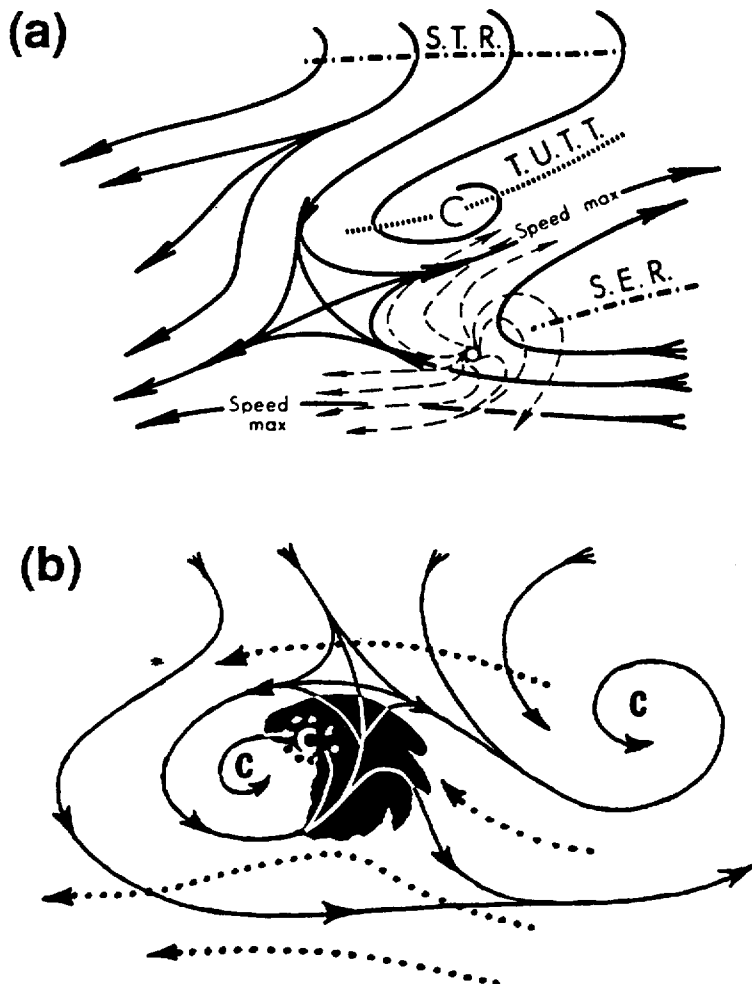


Figure 3-31-3 (a) Sadler's (1976) model of the indirect role of a TUTT cell in tropical cyclogenesis. S.T.R. = subtropical ridge, T.U.T.T. = tropical upper tropospheric trough, and S.E.R. = sub-equatorial ridge. (b) Schematic illustration of the direct role of a TUTT cell in the genesis of Tropical Depression 31W and of Tropical Storm Yuri (36W). Solid lines are 200 mb streamlines, dotted lines are low-level flow. Black-shaded area shows deep convection.

E 110 115 120 125 130 135 140 145 150 155 160 165 170 175 180

N 50

45

40

35

30

25

20

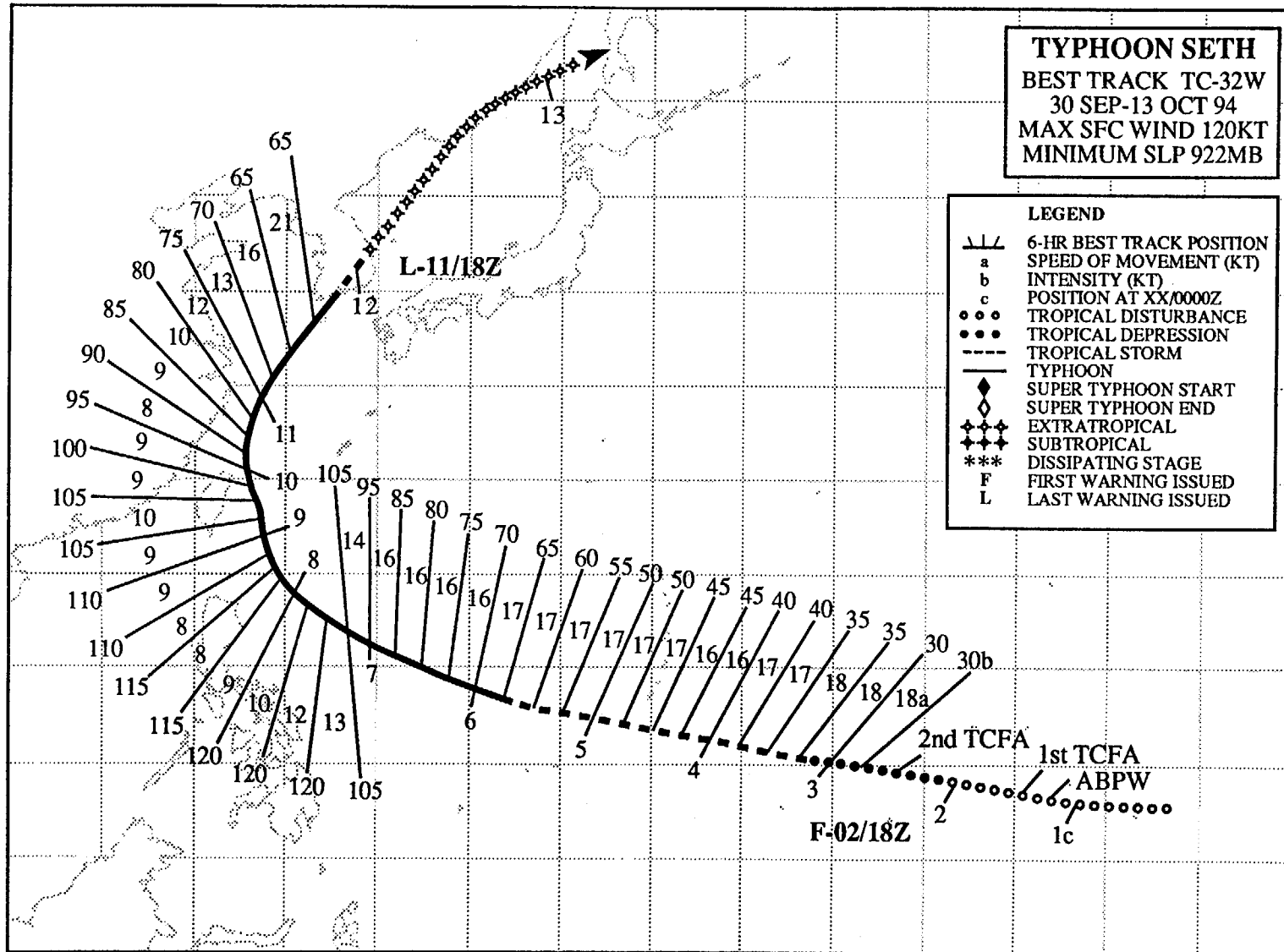
15

10

5

EQ

178



TYPHOON SETH (32W)

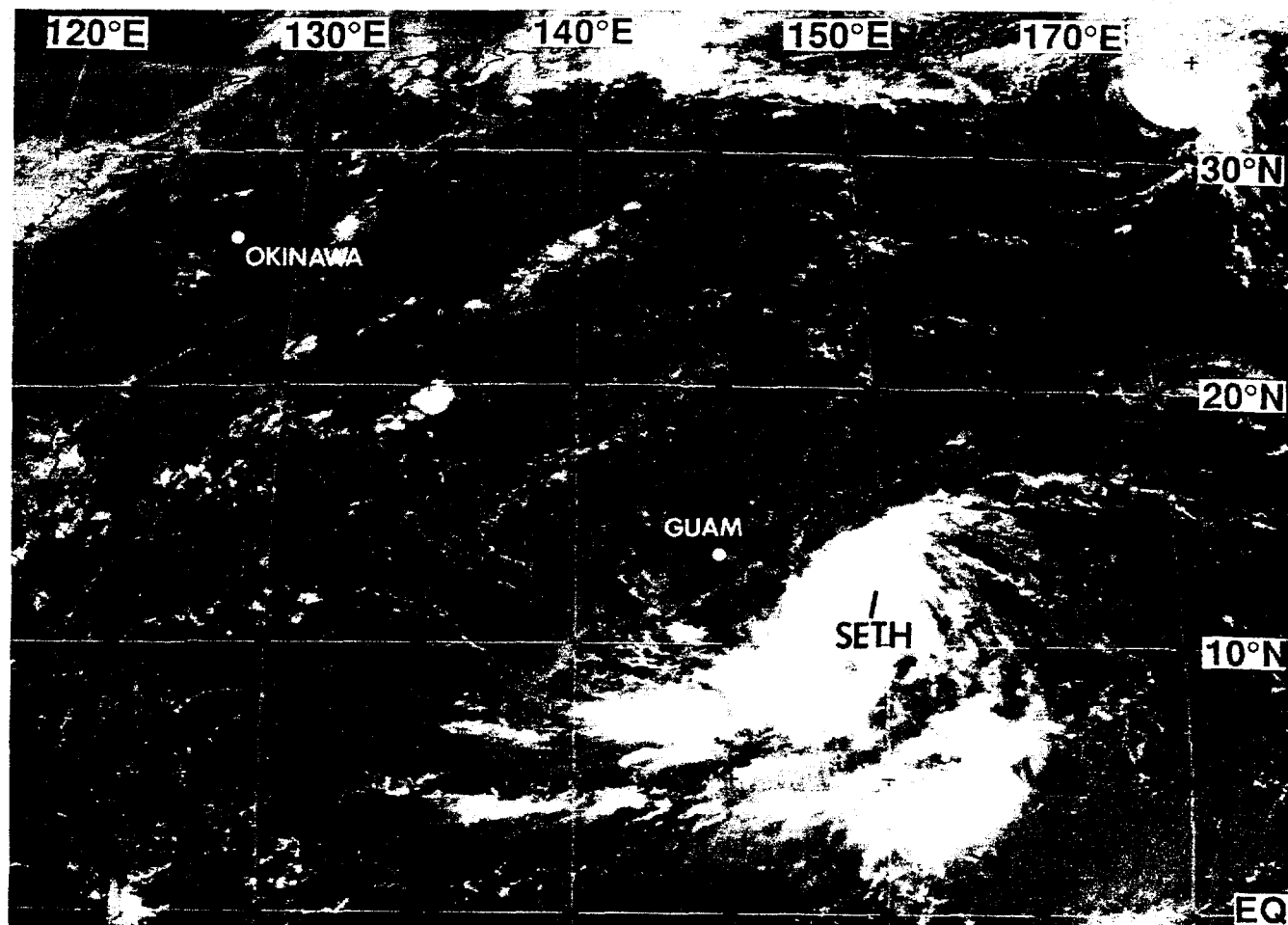


Figure 3-32-1 Seth and accompanying rain bands are seen isolated in an unusually cloud-free tropics (032331Z October visible GMS imagery).

I. HIGHLIGHTS

Seth originated from a tropical disturbance at low latitude in the Marshall Islands and moved on a typical recurving track. After recurving east of Taiwan, Seth moved northeastward and impacted the Korean peninsula. During the period of Seth's extra-tropical transition, as it moved through the Yellow Sea toward Korea, intensity estimates made from satellite imagery were low and illustrate the need for the development of new diagnostic techniques to address extra-tropical transition.

II. TRACK AND INTENSITY

Seth developed from an isolated area of deep convection in the Marshall Islands and tracked across the western North Pacific during a period when the basin was relatively cloud-free, and the monsoon circulation (which had earlier been extremely active) had become very weak (Figure 3-32-1). Synoptic data at 010000Z October indicated that a low-level cyclonic circulation center developed in the Marshall Islands in association with this area of deep convection. This tropical disturbance was first mentioned on the 010600Z October Significant Tropical Weather Advisory. At 011100Z, a Tropical Cyclone Formation Alert (TCFA) was issued by JTWC. Remarks in this TCFA included:

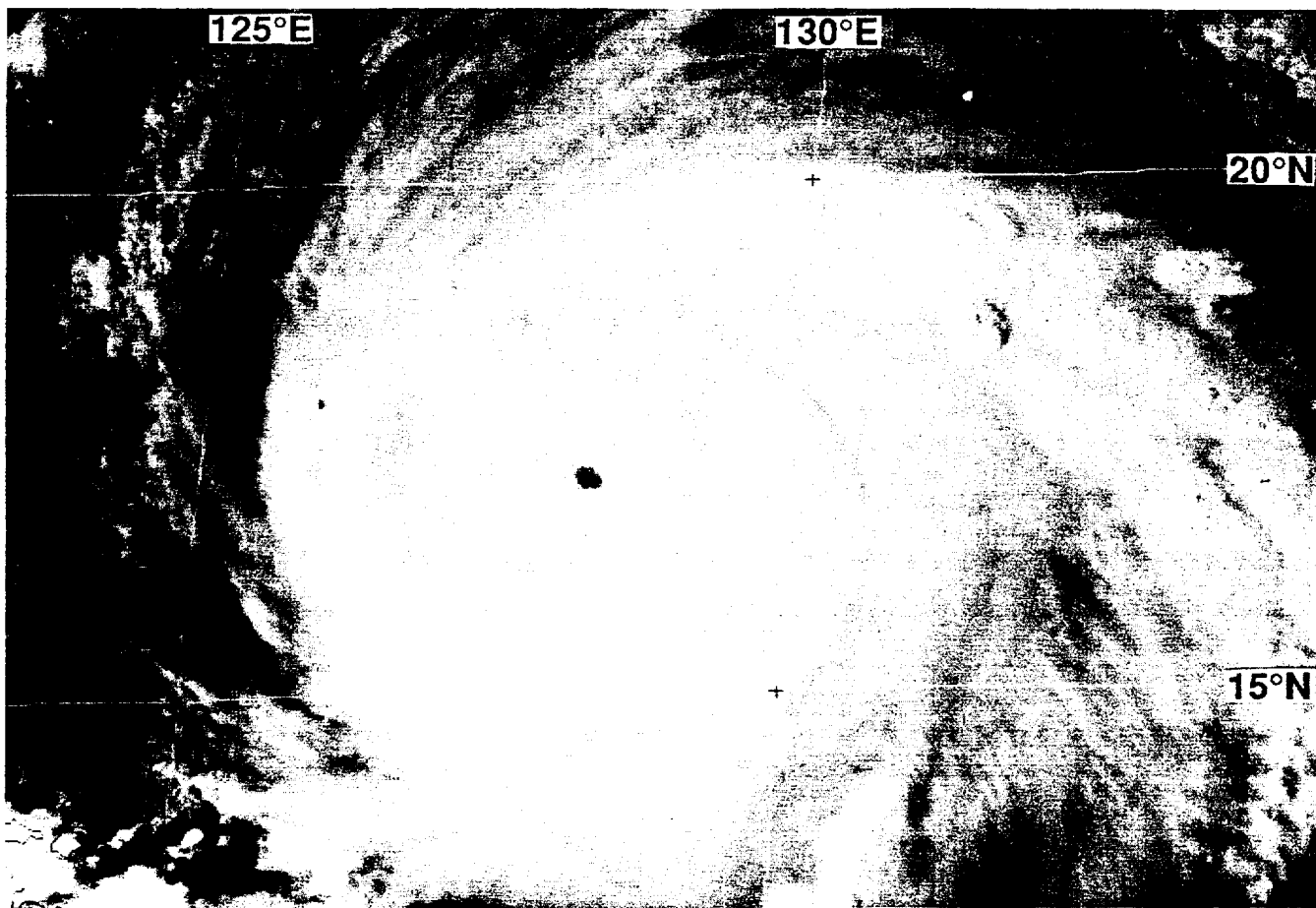


Figure 3-32-2 Nearing its peak intensity, Seth's eye becomes well-defined (070631Z October visible GMS imagery).

“... [The] tropical disturbance passing through the Marshall Islands has exhibited signs of development over the past 12 hours. Satellite imagery and synoptic data indicate a persistent low-level circulation center ... 24 hour pressure falls at Kwajalein were close to three millibars as the system passed by. ... If the system continues moving at its present rapid forward speed, the potential for further development will be reduced. ...”

Failing to intensify, a second TCFA was issued 24 hours later (at 021100Z). The first warning on Tropical Depression 32W was issued at 021800Z when satellite imagery indicated that deep convection associated with the system had increased and become more centralized. A normal rate of intensification of one “T” number per day ensued as Seth moved on a west-northwestward track. Typhoon intensity was attained at 051800Z. Turning gradually to the northwest, Seth steadily intensified (Figure 3-32-2) and reached peak intensity of 120 kt (62 m/sec) at 071200Z. Seth then moved on a broad recurving track, passing to the east of Taiwan and later over the Korean Peninsula. The point of recurvature occurred at 100600Z when Seth was 90 nm (170 km) north-northeast of Taipei. By this time Seth's intensity dropped to 90 kt (46 m/sec). Seth accelerated as it approached the Korean Peninsula. At 111800Z, it passed directly over the island of Cheju Do (located in the Yellow Sea about 100 km south of the Korean Peninsula). Moving at a forward speed in excess of 30 kt (55 km/hr), the system crossed the Korean Peninsula, entering the Sea of Japan shortly after 120000Z. Based upon the acquisition of extratropical characteristics, the final JTWC warning was issued at 111800Z. After entering the Sea of



Figure 3-32-3 An eye within an eye. Concentric wall clouds appear as Seth begins to weaken (080331Z October visible GMS imagery).

Japan, the system continued to move rapidly northeastward toward the Kamchatka Peninsula with winds in excess of 50 kt (26 m/sec) until 130000Z.

III. DISCUSSION

a. Concentric eye walls

Approximately 30 hours after attaining peak intensity, Seth acquired well-defined concentric eye walls (Figure 3-32-3). After another 24 hours, and with continued weakening, vestiges of the inner eye wall — seen clearly in Figure 3-32-3 — were still present in satellite imagery. At this time (approximately 090000Z), Seth came within range of the Hualien radar. At first, poorly defined concentric eye walls appeared on the radar image (not shown). Then, while moving northward through the southwestern end of the Ryukyu Islands, Seth's eye became quite ragged.

Well-defined concentric eye-walls (Figure 3-32-3) are rarely seen in conventional satellite imagery. The JTWC suspects that they are more common than indicated by their rate of appearance in satellite imagery. For example, even though they were obscured by cirrus in satellite imagery, well-defined concentric eye walls appeared on radar as Gladys (20W) approached Hualien (see the discussion of concentric eye walls in the Gladys summary).

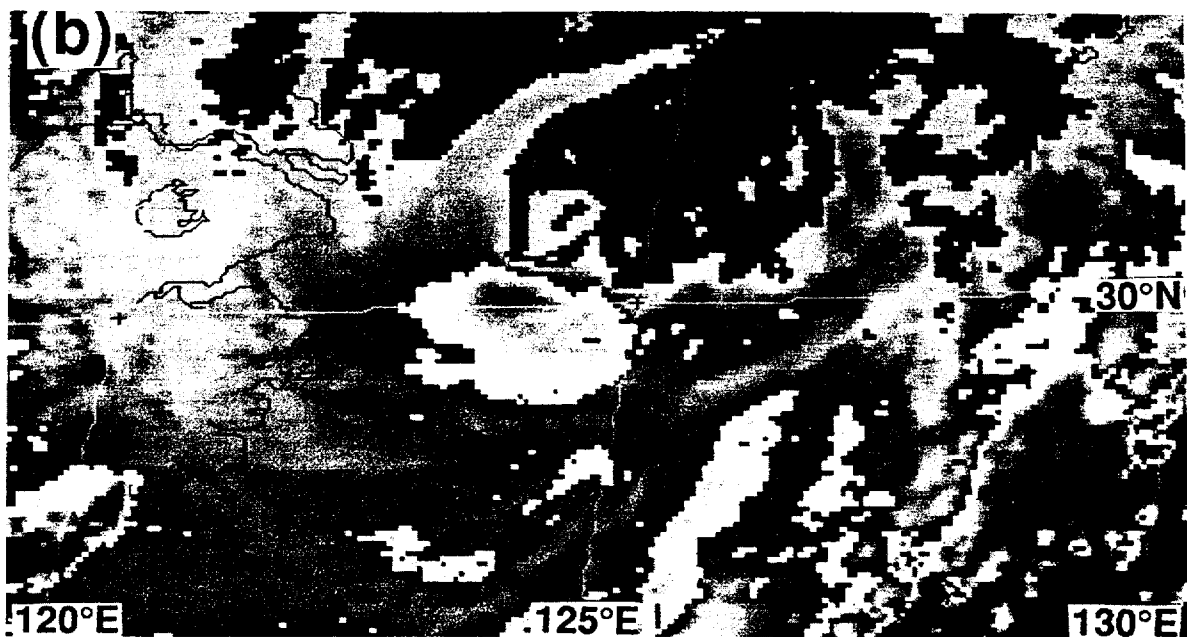
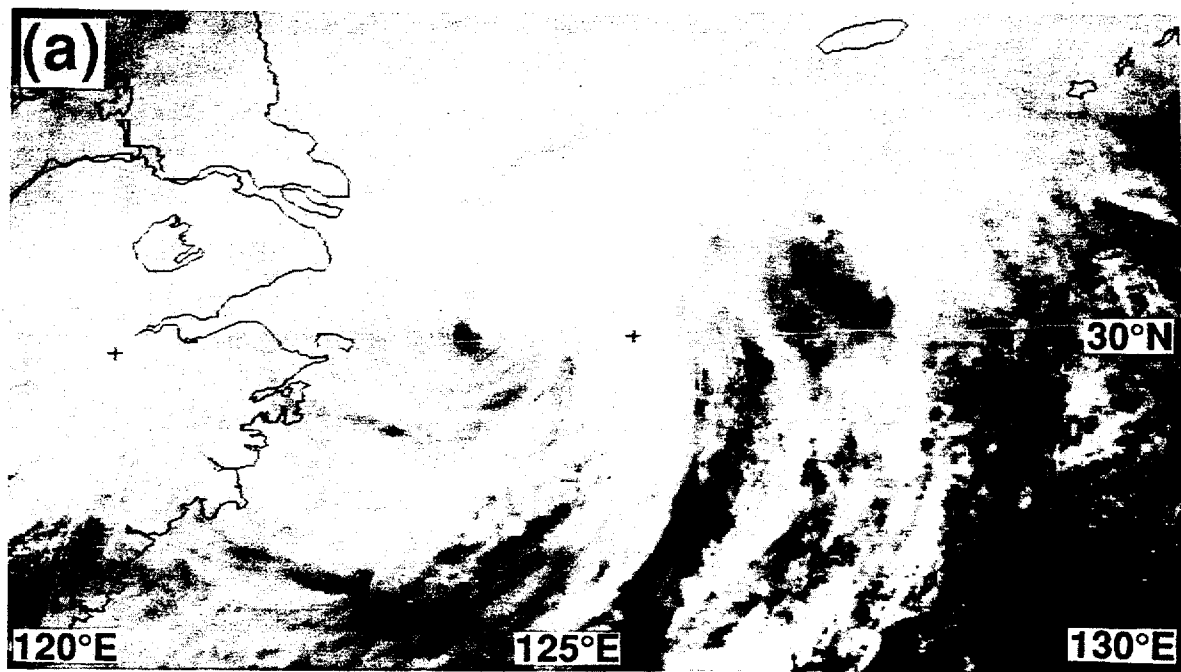


Figure 3-32-4 Satellite intensity estimates begin to decrease as Seth's central dense overcast is sheared away to the north side of the low-level circulation center by southwesterly winds aloft as the process of extra-tropical transition begins: (a) 110131Z October visible GMS imagery, and (b) 110131Z October enhanced infrared GMS imagery. The enhancement is the Basic Dvorak (BD) curve.

b. Extratropical transition

One of the more difficult forecast and warning challenges faced by the JTWC for Seth occurred as the typhoon approached the Korean peninsula. Eighteen hours prior to landfall on the peninsula, Seth began to lose its central deep convection while in the process of transitioning into an extratropical low (Figure 3-32-4a,b). Applying Dvorak's satellite intensity analysis to the transitioning system, the diag-

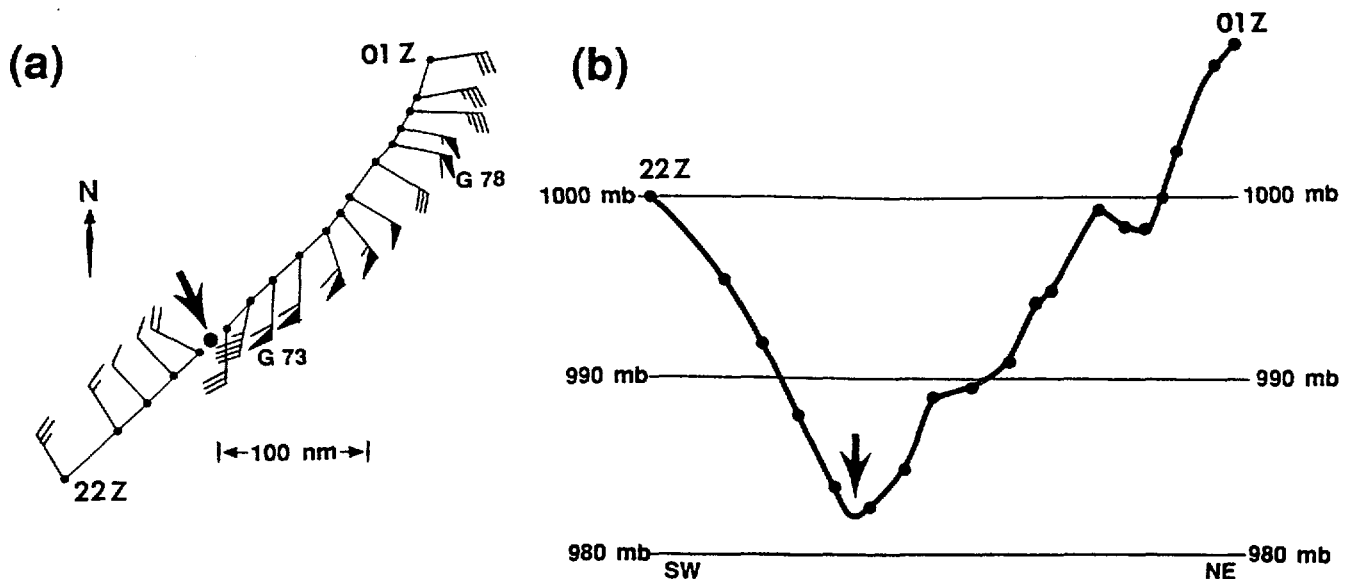


Figure 3-32-5 Schematic depictions of (a) winds and (b) sea-level pressure recorded at Cheju Do (WMO 47187) during Seth's passage. The data are plotted with respect to Seth's center (indicated by an arrow).

nosed intensity began to fall to unrealistically low values (Table 3-32-1). Wind and pressure reports from Cheju Do (WMO 47187) (Figure 3-32-5a,b), and from other stations, indicated that Seth retained typhoon intensity up to its landfall on the southern coast of South Korea.

Application of Dvorak's satellite intensity estimates to Seth as it began to acquire extratropical characteristics yielded values which were as much as three "T" numbers below the real-time intensity (Table 3-32-1). In an attempt to produce more accurate intensity estimates (from satellite imagery) on recurving tropical cyclones that are undergoing extra-tropical transition, the subtropical classification scheme of Hebert and Poteat (1975) has been used. For Seth, this scheme yielded "ST" numbers which corresponded to intensities far lower than those observed. This is not surprising since the scheme developed by Hebert and Poteat was intended to be applied to intensifying midlatitude lows that have acquired organized deep convection. The attempt to use Hebert and Poteat's system in reverse (i.e. on tropical cyclones that are becoming extratropical following recurvature) is most probably a misapplication. Analysts at the JTWC also tried to apply to the recurving Seth, a technique for estimating the intensity of mid-latitude cyclones from satellite imagery (Smigielski and Mogil 1992). Again, it was difficult to derive intensities high enough.

IV. IMPACT

At 041800Z, Seth, with a best-track at an intensity of 50 kt (26 m/sec), passed 102 nm (190 km) south of Guam, where a peak wind gust of 41 kt (21 m/sec) was recorded. No reports of damage or injuries were received. The next region affected by Seth was Taiwan and the southern Ryukyu Islands. A peak gust of 110 kt (57 m/sec) and a minimum pressure of 952 mb was recorded at Yonaguni Jima (WMO 47912) as the western inner edge of Seth's eye-wall cloud passed over. No reports of damage or injuries were received from this region. At Cheju Do (WMO 47187), a peak wind gust of 78 kt (40 m/sec) was recorded as Seth approached from the southwest. Wind gusts to near 70 kt (36 m/sec) and rainfall in excess of 300 mm (11.8 inches) affected portions of South Korea. Torrential rains near the

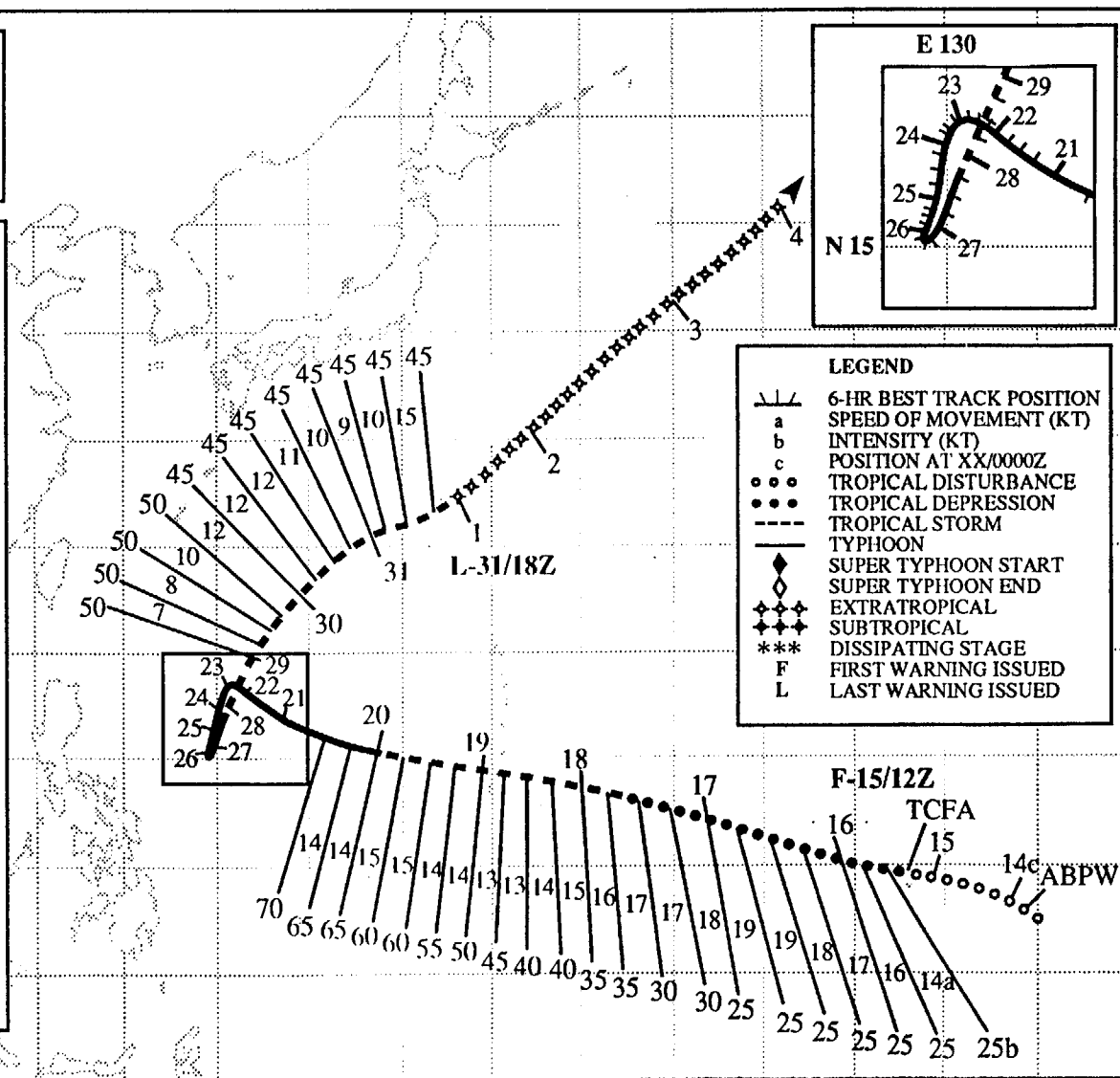
eastern port city of Samchok resulted in flooding that killed one person, forced the evacuation of 550 people, inundated 178 houses and interrupted rail traffic. However, the rain from Seth brought relief to many drought-parched areas of South Korea.

Table 3-32-1 Intensity estimates derived from satellite imagery during Seth's extratropical transition. In the code, T = Dvorak tropical numbers, ST = Hebert and Poteat subtropical numbers, and the number that follows the "/" is the current intensity, which is always held higher in cases when the cyclone is weakening.

Time (Z)	Code	Best Track <i>Current Intensity</i>	Best Track <i>Best Track</i>
		Intensity (kt)	Intensity (kt)
102330Z	T 3.0/4.0	65	75
110144Z	T 3.0/4.0	65	70
110232Z	T 3.5/4.0	65	70
110530Z	T 2.5/3.5	55	70
111115Z	T 1.5/2.5	35	65
111130Z	ST 1.5/2.5	35	65
111151Z	T 1.5/2.5	35	65
111300Z	ST 1.0/2.0	30	65
111730Z	ST 1.0/2.0	30	65
112330Z	ST 1.0/2.0	30	60
120125Z	ST 1.0/1.0	25	60
120530Z	ST 1.0/2.0	30	60

MINIMUM SLP 927MB

	DTG (Z)	SPEED (KT)	INTENSITY (KT)
40	20/12	13	70
	20/18	10	70
35	21/00	8	75
	21/06	6	75
	21/12	5	75
	21/18	4	80
30	22/00	3	80
	22/06	3	80
	22/12	3	85
	22/18	3	90
	23/00	1	90
25	23/06	2	95
	23/12	1	105
	23/18	3	115
	24/00	3	115
	24/06	4	115
	24/12	4	110
20	24/18	4	105
	25/00	3	105
	25/06	2	105
	25/12	2	100
	25/18	2	100
15	26/00	2	95
	26/06	1	95
	26/12	2	90
	26/18	4	85
	27/00	4	80
10	27/06	5	75
	27/12	6	70
	27/18	7	65
	28/00	6	60
	28/06	7	55
5	28/12	7	55
	28/18	7	50



TYPHOON VERNE (33W)

I. HIGHLIGHTS

Typhoon Verne was a relatively long-lived tropical cyclone that passed within range of Guam's NEXRAD. Several special cross-sections of reflectivity and radial velocity were obtained through Verne's center and peripheral cloud bands. Verne underwent unusual motion in the Philippine Sea: for over seven days it meandered within 150 nm (280 km) of 17°N ; 130°E.

II. TRACK AND INTENSITY

During the first week of October, the deep tropics of the western North Pacific became inactive (Figure 3-33-1a). Higher-than-normal pressure accompanied a reduction in deep convection. By mid-October, deep convection began to increase in low latitudes, especially east of 140°E, and an active monsoon trough formed along about 10°N (Figure 3-33-1b). By the third week of October, this monsoon trough evolved into a chain of four tropical cyclones: Teresa (34W), Verne, Wilda (35W), and Yuri (36W) (Figure 3-33-1c).

The tropical disturbance that became Verne was first mentioned on the 131800Z October Significant Tropical Weather Advisory when an area of deep convection associated with a broad low-level cyclonic circulation formed in the Marshall Islands. At 150800Z, a Tropical Cyclone Formation Alert was issued when this disturbance showed signs of increased organization. Continued improvement in the convective banding features prompted the first warning at 151200Z. Tropical Depression 33W moved west-northwestward along the axis of the monsoon trough, and its intensification rate remained slow. At 171800Z Tropical Depression 33W was upgraded to Tropical Storm Verne. Continuing on a steady west-northwestward track, Verne passed 50 nm north of Guam during the early morning hours of October 19. Verne acquired a CDO and its estimated intensity was 50 kt (26 m/sec). At 200000Z Verne was upgraded to a typhoon based upon intensity estimates from satellite imagery. Verne continued on a steady west-northwestward track until 210600Z when it abruptly slowed. It then meandered within 150 nm of 17°N ; 130°E for seven days. Verne reached a peak intensity of 115 kt (59 m/sec) at 231800Z while moving slowly southward in the Philippine Sea (Figure 3-33-2). After Verne turned northward at 260600Z, it steadily weakened, and by 280600Z it had dropped below typhoon intensity. The final warning was issued at 010000Z November as Verne recurved east of Japan and became extratropical.

III. DISCUSSION

a. NEXRAD's view of Verne

Verne's closest point of approach to Guam was 50 nm (90 km) to the north at 180000Z. In addition to Verne's CDO, peripheral cloud bands tracked well-within the 124 nm (230 km) range of the NEXRAD's Doppler velocity sensor. Many radar products were examined, including: the base reflectivity, the base velocity, animation of the base reflectivity, convective cell tracking, and the one- and three-hour integrated precipitation products.

1. STORM-TOTAL PRECIPITATION

For almost two days (180420Z to 200030Z), Guam's NEXRAD provided a continuous integration of the precipitation associated with Verne (Figure 3-33-3). NEXRAD-estimated rainfall of over one inch fell in a 120 nm (220 km)-wide swath along Verne's track. Maximum estimated storm-total rainfall values of four to six inches occurred in a narrower swath. The NEXRAD underestimated storm-total pre-

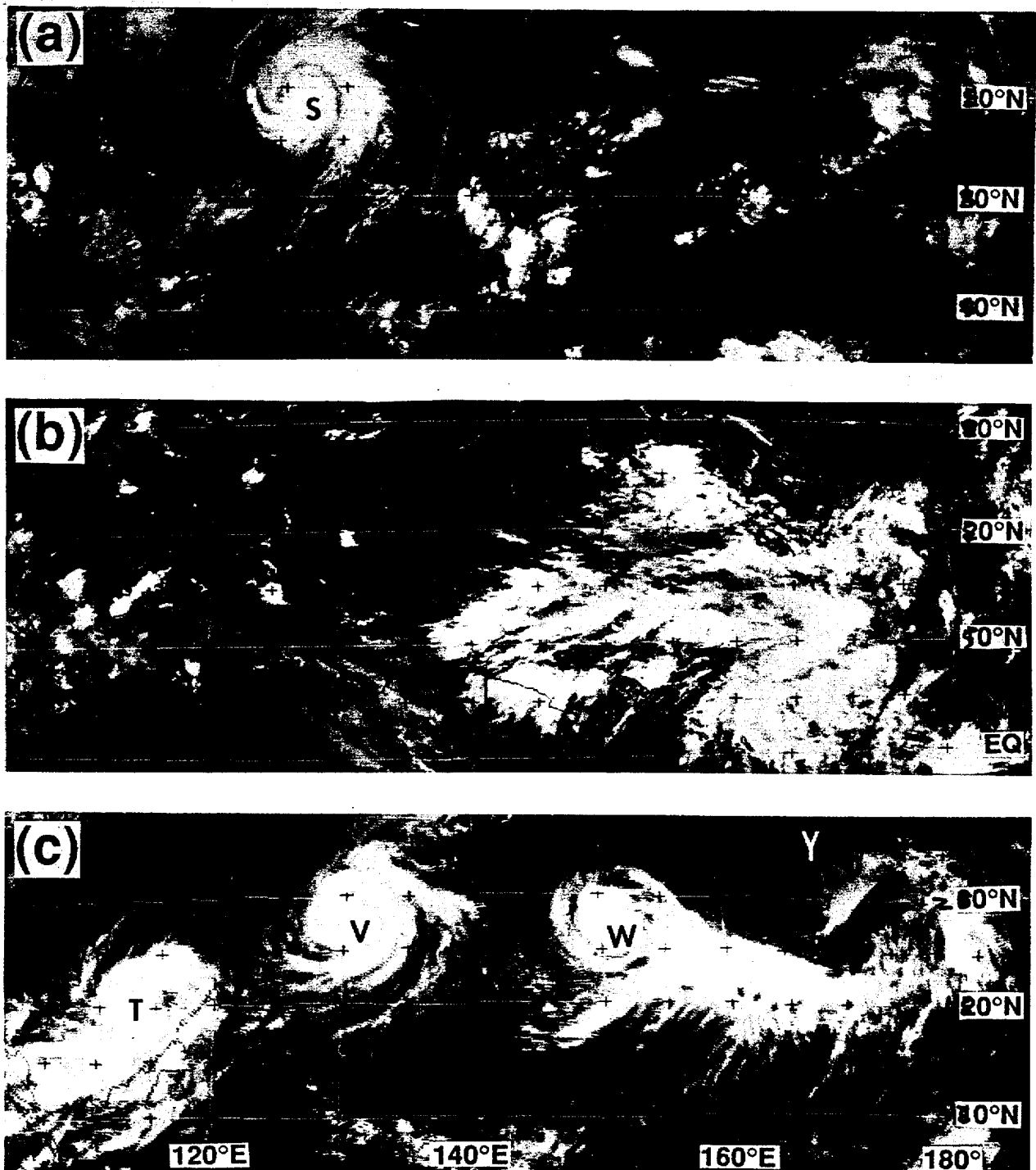


Figure 3-33-1 Evolution of the large-scale distribution of deep convection in the western North Pacific during October. (a) Things are very quiet in the tropics as Seth (S) moves out of the region (080031Z October infrared GMS imagery). (b) An increase in the amount of deep convection accompanies near-equatorial westerlies east of 140°E (140031Z October infrared GMS imagery). (c) Four named tropical cyclones — T = Teresa (34W), V = Verne, W = Wilda (35W) and Y = Yuri (36W) — are lined up WSW-ENE across the western North Pacific basin (230531Z October infrared GMS imagery).

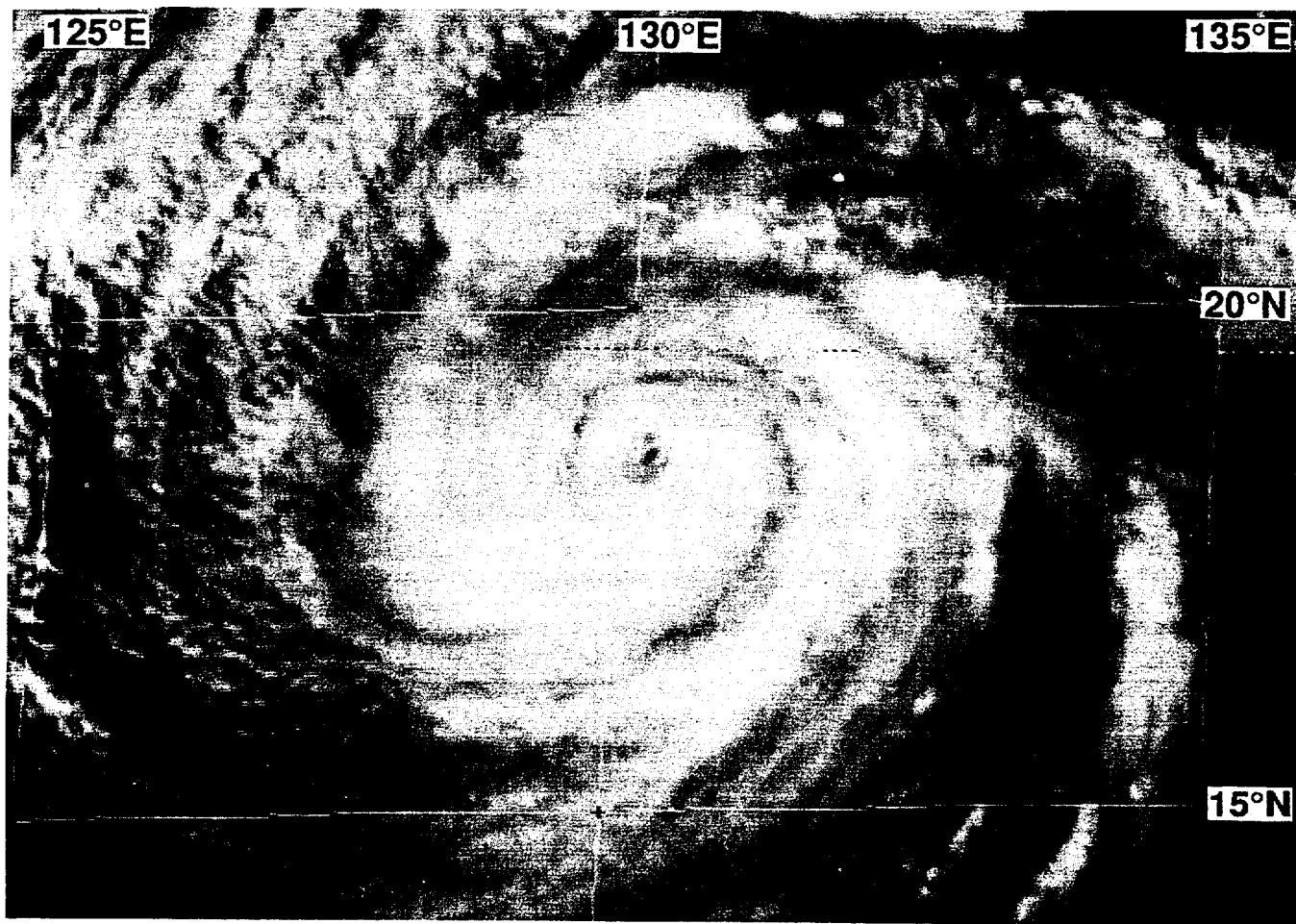


Figure 3-33-2 Verne's eye is becoming better defined as it nears its peak intensity (230424Z October visible GMS imagery).

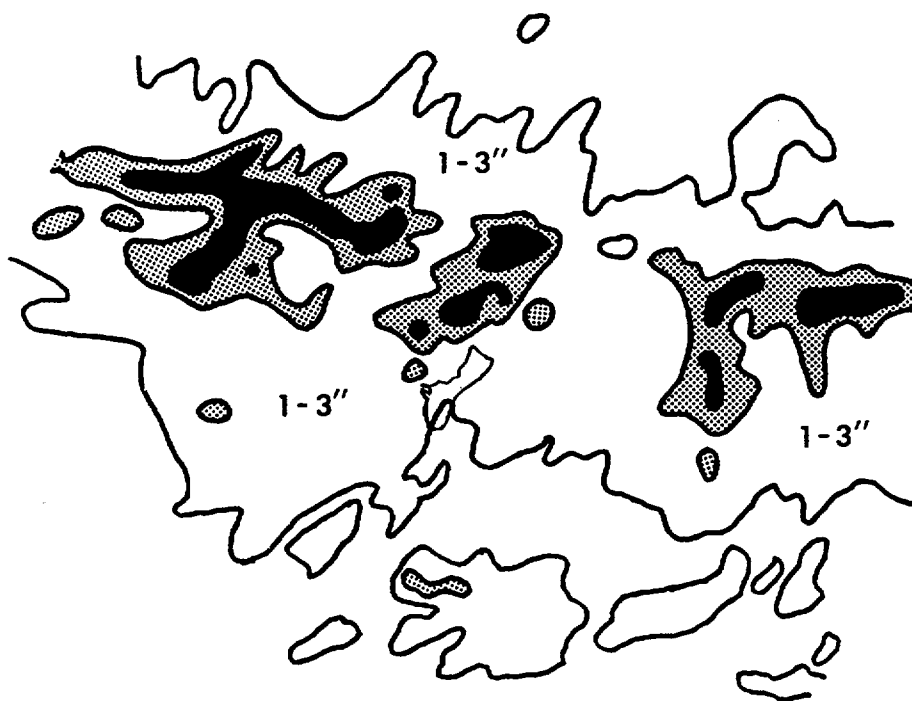


Figure 3-33-3 Estimated precipitation deposited by Verne as it tracked north of Guam (NEXRAD storm-total precipitation algorithm for the period 180420Z to 200030Z October). Outer contour = 1", shaded region received between 3" and 4", black regions received 4" or more.

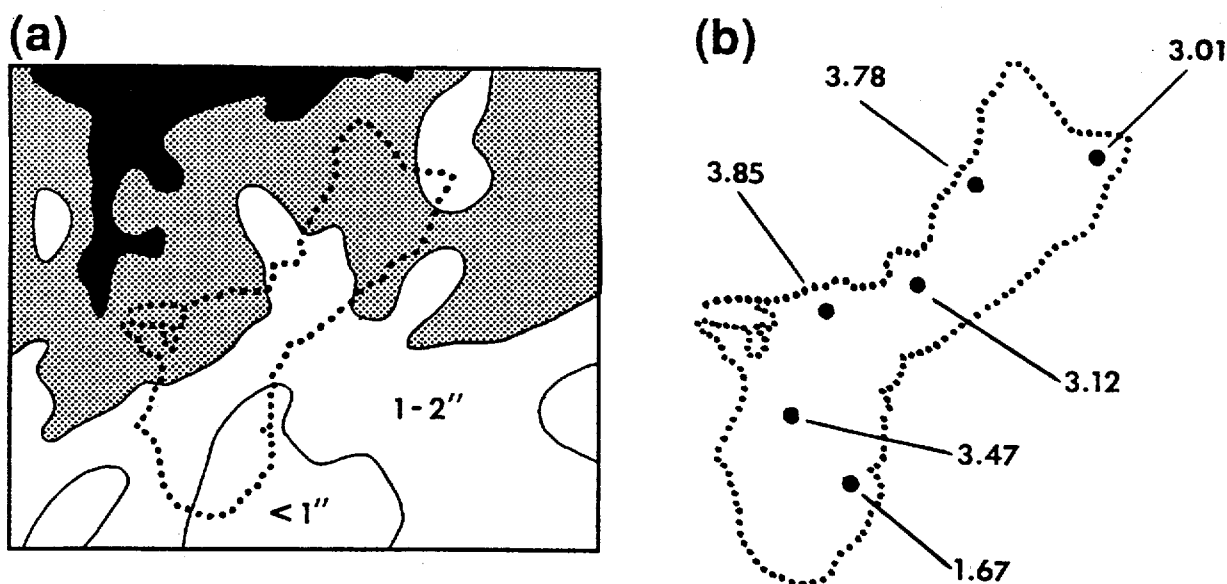


Figure 3-33-4 (a) Enlargement of the Guam region showing NEXRAD storm-total precipitation during Verne. Outer contour = 1", shaded region received between 2" and 3", black region received 3" or more. (b) Storm-total precipitation during Verne measured on Guam.

precipitation by 33% to 50% when compared to rainfall measured on Guam (Figure 3-33-4a,b). In almost all heavy rain events on Guam for which NEXRAD storm-total precipitation estimates were available for comparison to actual observations from around the island, the NEXRAD estimates are short by 25%-50% of the measured values. Despite these under-estimations, the rainfall distribution shown by NEXRAD has agreed quite well with the observed distribution.

2. PATTERN AND EVOLUTION OF THE WIND AND DEEP CONVECTION

When Verne passed to the north of Guam, it was a tropical storm with a satellite intensity estimate of 50 kt (26 m/sec). Its satellite-observed structure was a CDO pattern with a banding feature (Figure 3-33-5). The thick cirrus canopy of Verne's CDO in early morning, low-sun-angle, visible satellite imagery (not shown) was seen to have an overshooting convective tower embedded in rather featureless dense cirrus. The dense cirrus obscured highly organized lower-level cloud structures as observed by the NEXRAD. The base reflectivity, vertical cross-sections through Verne's core, and the echo-top product obtained from Guam's NEXRAD showed that Verne was composed of a central arc of deep convection wrapping roughly half-way around the southeastern semi-circle of Verne's cloud-free center. This deep convection rose to at least 60,000 ft (18 km) in one convective cell (i.e., hot tower) on the eastern side of Verne's inner core (Figure 3-33-6). This convective hot tower was not steady-state, but was observed to go through three episodes of intense build-up followed by a period of weakening. With each pulse of the central hot tower, the inner-core convection became more organized and nearly formed an eye wall. As the hot tower weakened, the curvature of the inner-core convection lessened. In synchrony with the pulses of the inner-core hot tower, the reflectivity in the nearest rainband to the south of the inner core intensified, then subsided.

Even the wind structure of Verne's inner core was affected by the pulsing of Verne's central hot tower. Prior to a major pulse of the hot tower when Verne was near its closest point of approach to

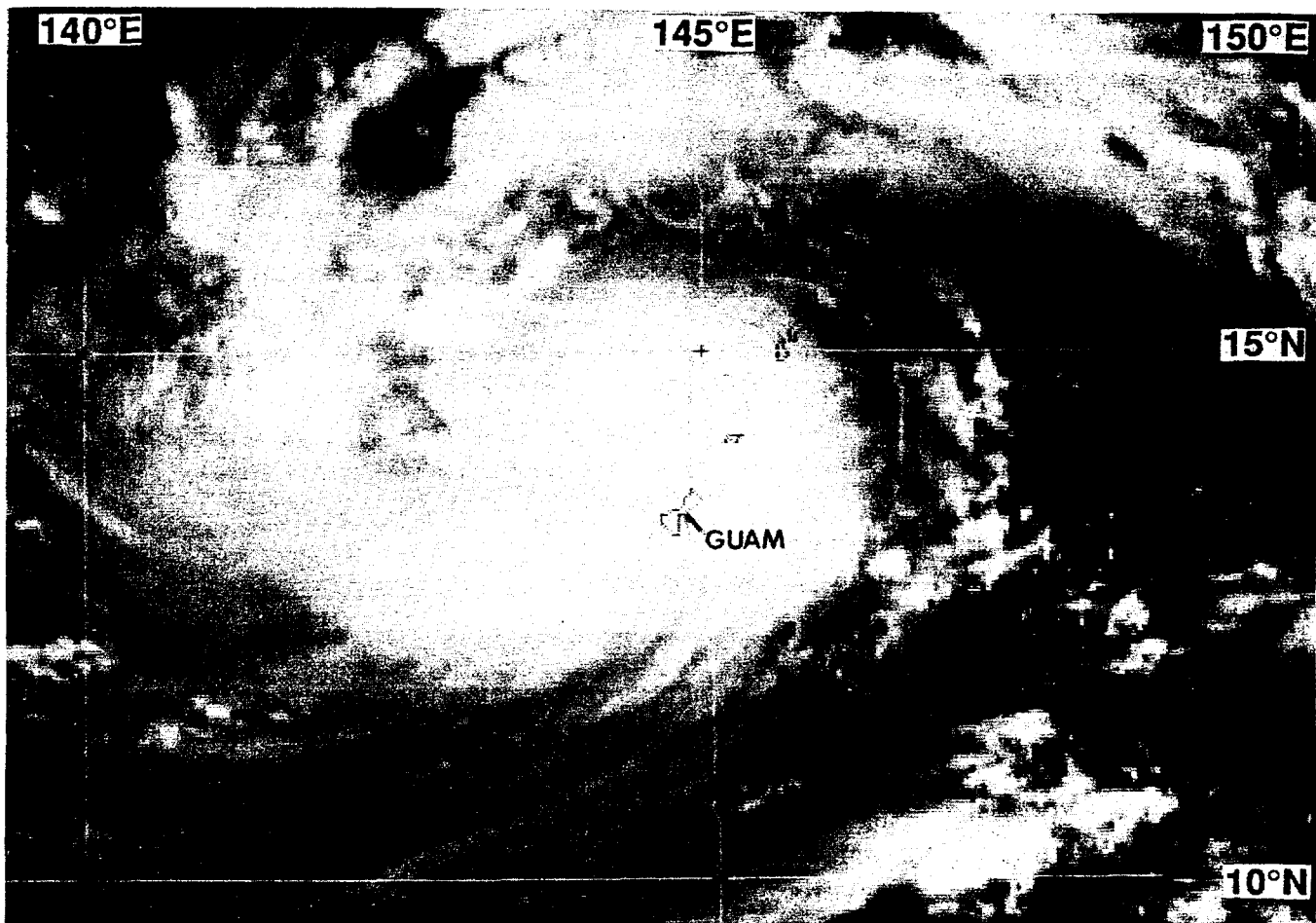


Figure 3-33-5 Verne near its closest point of approach to Guam. Verne's CDO obscures its low-level center (182331Z October visible GMS imagery).

Guam, the NEXRAD-observed wind speed on a vertical slice cut east-west through Verne's center showed the text-book signature of a low-level cyclone overlain by an upper-level anticyclone. When the hot tower became very active, the wind on the same slice cut through Verne's core showed that in the hot tower, the outbound southerlies were carried upward throughout the column (Figure 3-33-7). Another feature of the vertical structure of the wind in Figure 3-33-7, is that the maximum low-level winds (both inbound and outbound) were at 4,000 ft (1.2 km), which was the lowest elevation observable by the radar at this range.

b. Unusual motion

Verne continued on a steady west-northwestward track until 210600Z when it abruptly slowed and then meandered within 150 nm (275 km) of 17°N ; 130°E for seven days. In finer detail, Verne's motion during this period consisted of a slow westward drift between 210600Z to 230000Z, a slow southward drift between 230000Z to 260600Z, and a turn to the north-northeast after 260600Z. Later, shortly before 281200Z, Verne began a modest acceleration toward the north-northeast. Verne's period of unusual motion began when the monsoon trough axis acquired a reverse orientation (see Figure 3-33-1c). At this time, 500 mb heights became higher in the ridge axis southeast of the trough than in the ridge axis to the north of the trough. Additionally, strong low-level northeasterly winds persisted over

* SAIPAN
* TINIAN



Figure 3-33-6 Echo tops as seen by Guam's NEXRAD at 182318Z showing Verne's lone "hot tower" on the southeastern side of its inner core. Outer contour = 35,000 ft, black shaded region shows tops over 40,000 ft. Maximum top at this time was 56,000 ft. Small "x" denotes estimated location of Veme's low-level circulation center.

the western half of the Philippine Sea and the South China Sea. It is likely that these two environmental factors combined to cause Verne to stall.

c. Air-sea interactions

It has long been known that tropical cyclones leave a trail of reduced sea surface temperature (SST) across the ocean surface. This cooling, which can reach 6°C and may persist for several weeks, is predominantly caused by turbulent mixing which deepens the oceanic mixed layer (Kepert 1993). Modeling and observational studies show the bulk of the cooling occurs to the right of the track in the northern hemisphere (Price 1981, Holland 1987). One might expect that the cooling of the SST by a tropical cyclone might alter the horizontal and vertical structure of the atmospheric boundary layer in such a way so as to affect the intensity, structure and behavior of the tropical cyclone itself. In coupled air-sea models (e.g., Kurihara 1992), the maximum surface wind

in a tropical cyclone is reduced by upwards of 5-10% by the induced cooling of the SST.

Given that a tropical cyclone causes cooling of the sea surface, it might be of particular interest to observe the intensity changes of tropical cyclones which stall over water for extended periods of time. A testable hypothesis is that tropical cyclones which remain quasi-stationary over water for extended periods of time weaken (or at best, do not increase in intensity) as the underlying SST falls. Such reasoning has been used operationally in the past by the JTWC to forecast rapid weakening of a tropical cyclone (e.g., Jack 1989). While Verne remained quasi-stationary for seven days within 150 nm (280 km) of 17°N ; 130°E, it intensified from 75 kt to 115 kt (its peak intensity) during the first two days of its stall, it weakened from 115 kt to 105 kt during the next two-day period of its seven-day stall, and then began to lose intensity more rapidly (a 60 kt decrease from 105 kt to 55 kt) during the latter three days. Although Verne weakened significantly during the latter portion of its stall, it is inappropriate to claim that the storm-induced cooling of the SST was the major factor contributing to this weakening. More research is necessary to confirm the role of tropical cyclone induced SST changes upon the tropical cyclone itself.

IV. IMPACT

Verne brought gusty winds and heavy rain to Guam, Rota, Tinian and Saipan. Some minor damage to vegetation was reported on Guam. Reports from Saipan indicated more extensive fallen or uprooted trees. No reports of storm-related injuries or damage to houses or buildings were received. The maximum wind gust measured on Guam was 60 kt (31 m/sec).

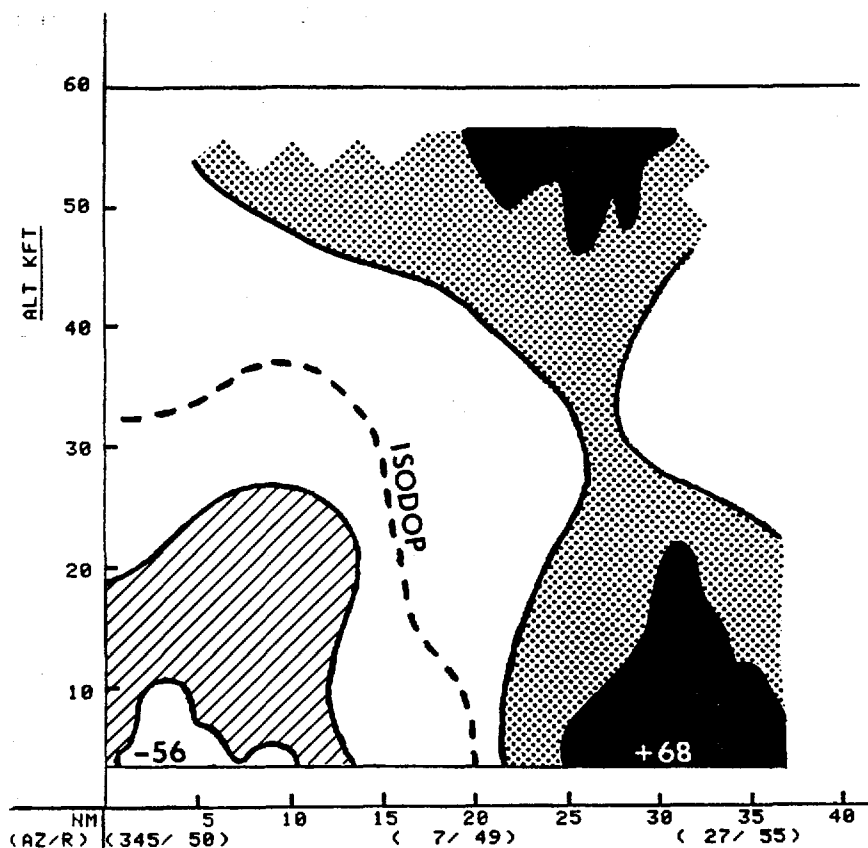


Figure 3-33-7 East-west cross-section (looking north) cut through the center of Verne shows inbound or outbound velocity with respect to Guam's NEXRAD. The hot tower on the eastern side of Verne's low-level center appears to have carried southerly (outbound) winds aloft resulting in a deepening of Verne's cyclonic circulation (182324Z October NEXRAD velocity cross section).

E 100 105 110 115 120 125 130 135 140 145 150 155 160 165 170 E
N 35

TYPHOON TERESA
BEST TRACK TC-34W
14 OCT-27 OCT 94
MAX SFC WIND 80KT
MINIMUM SLP 963MB

LEGEND

- 6-HR BEST TRACK POSITION
- a SPEED OF MOVEMENT (KT)
- b INTENSITY (KT)
- c POSITION AT XX/0000Z
- TROPICAL DISTURBANCE
- TROPICAL DEPRESSION
- TROPICAL STORM
- TYPHOON
- ◆ SUPER TYPHOON START
- ◇ SUPER TYPHOON END
- ◆◆◆ EXTRATROPICAL
- ◆◆◆ SUBTROPICAL
- *** DISSIPATING STAGE
- F FIRST WARNING ISSUED
- L LAST WARNING ISSUED

193

30

25

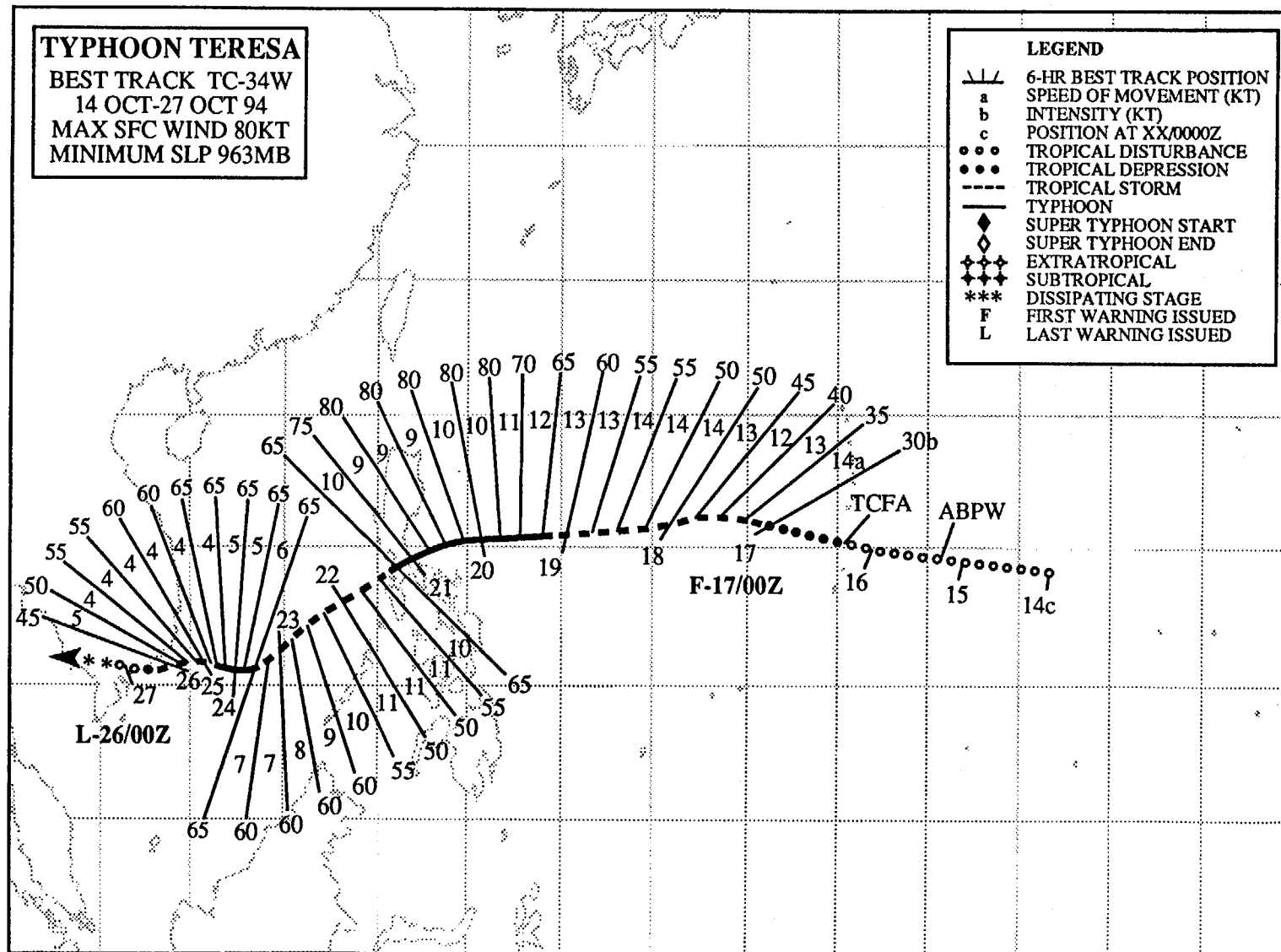
20

15

10

5

EQ



TYPHOON TERESA (34W)

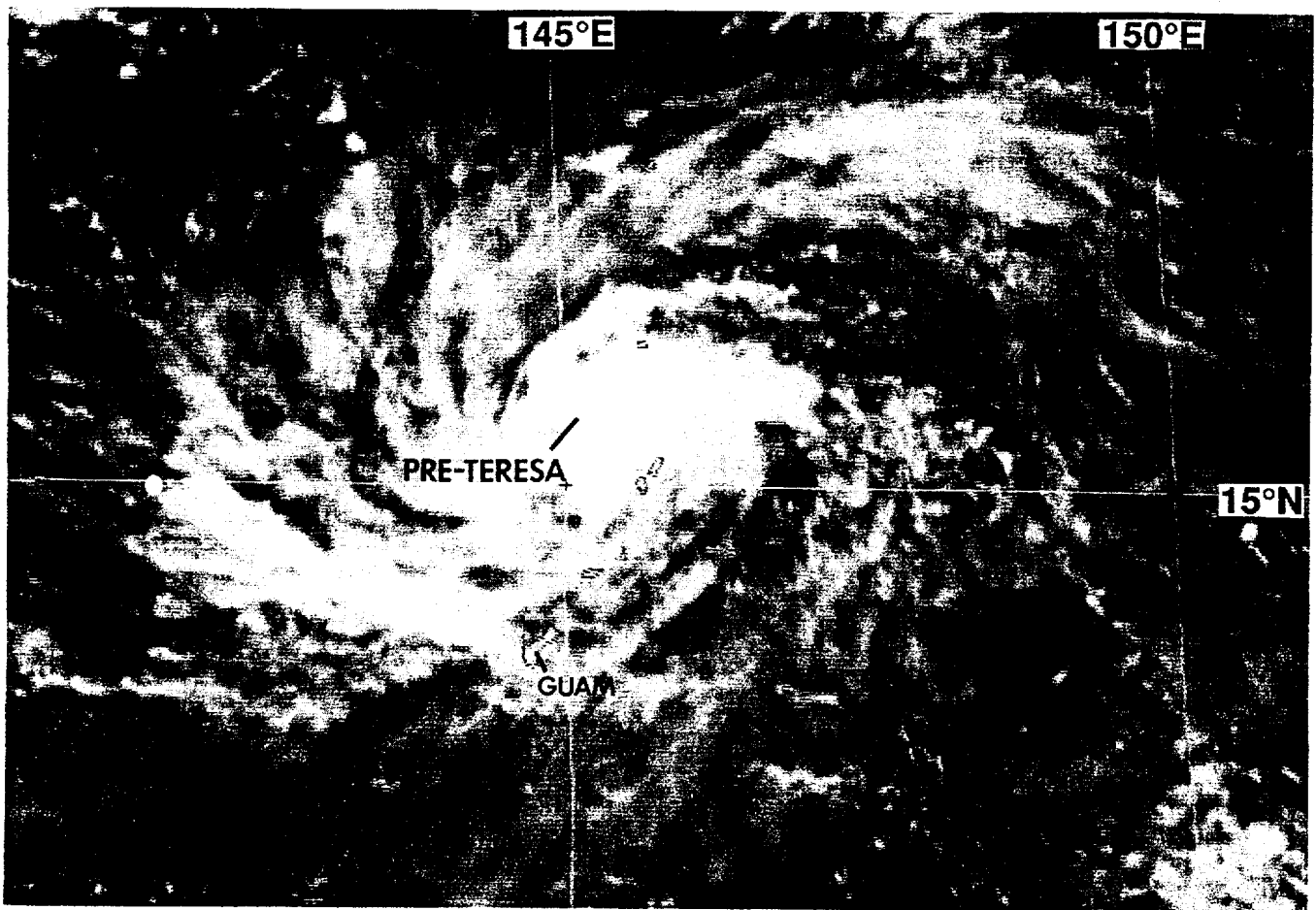


Figure 3-34-1 Well-organized low-level cloud lines and a symmetrical pattern of cirrus outflow prompted the JTWC to issue a Tropical Cyclone Formation Alert shortly after the time of this picture (160531Z October visible GMS imagery).

I. HIGHLIGHTS

Unusual southwestward motion brought Typhoon Teresa on a path across the central Philippine islands where it caused loss of life and much damage. The forecast performance of the objective guidance was especially poor as Teresa impacted the Philippines. Teresa was the westernmost tropical cyclone of a multiple outbreak that, at one point, featured four tropical cyclones in the western North Pacific.

II. TRACK AND INTENSITY

By mid-October, deep convection began to increase in the low latitudes of the western North Pacific, especially east of 140°E where westerly winds south of the monsoon trough increased. The atmospheric conditions leading to the formation of Teresa are included in Verne's (33W) summary.

The tropical disturbance that became Teresa was first mentioned on the 150600Z October Significant Tropical Weather Advisory. At this time, an area of deep convection had consolidated about 300 nm (550 km) east of the southern Mariana Islands. This disturbance moved westward and passed near Saipan at approximately 160600Z (Figure 3-34-1). A Tropical Cyclone Formation Alert was issued at

160730Z, followed by the first warning on Tropical Depression 34W at 170000Z. The system was upgraded to Tropical Storm Teresa at 170600Z. Moving westward at a steady 14 kt (25 km/hr), Teresa intensified at a normal rate and became a typhoon at 190600Z. The peak intensity of 80 kt (41 m/sec) was reached at 191800Z (Figure 3-34-2). Teresa was then only 300 nm (550 km) east of the Philippine island of Luzon and heading west-southwestward. Between the hours of 200600Z and 210600Z, the system crossed southern Luzon, passing just south of Manila (Figure 3-34-3). Emerging into the South China Sea after crossing southern Luzon, Teresa had weakened to 50 kt (26 m/sec). In response to steering influences of a strong northeast monsoon over the northern half of the South China Sea, Teresa continued to move southwestward, losing about 4 degrees of latitude (14.5°N to 10.5°N) between 210600Z and 231200Z. During this time period, the system slowly reintensified and by 231200Z it became a typhoon. Upon reaching typhoon intensity for a second time, Teresa turned toward the west and its speed of forward motion slowed to 5 kt (10 km/hr). Moving westward toward the coast of southern Vietnam, Teresa began to weaken. The final warning was issued at 260000Z as the system continued to weaken over water. The remnants of Teresa made landfall on the coast of southern Vietnam shortly after 261200Z, and passed over Ho Chi Minh City at approximately 270000Z.

III. DISCUSSION

a. A NEXRAD view of Teresa

When the tropical disturbance that became Teresa passed near Saipan, it came just within the 124 nm (230 km) Doppler range of Guam's NEXRAD. A velocity cross section was obtained through its center at 160736Z (two hours after the visible satellite imagery in Figure 3-34-1). The NEXRAD velocity cross section revealed a cyclonic circulation extending from 15,000 ft (the lowest beam elevation) upward to 30,000 ft (the highest elevation of precipitation targets). The peak inbound velocity of 18 kt (9 m/sec) was located about 40 nm (75 km) to the west of the peak outbound velocity of 14 kt (7 m/sec).

b. Forecast performance

The overall official track forecasts for Teresa were exceptionally good. At two periods, the objective track guidance became unreliable: shortly before landfall in the Philippines, and later, as the system neared the coast of Viet Vietnam. While it was east of the Philippines, the objective guidance called for Teresa to stall east of the Philippines. This bias in the objective guidance was detected quickly, and the official forecast brought Teresa across the Philippines and into the South China Sea. As Teresa neared the coast of Vietnam, the NOGAPS numerical guidance exhibited a bias to the north of track. This bias was also quickly detected, and the official forecast did not err as drastically.

IV. IMPACT

Teresa swept across Manila and nearby provinces on the Philippine island of Luzon. Its typhoon intensity winds uprooted trees, toppled utility poles, and destroyed homes and crops. Six people were reported killed by falling trees and flying debris. In a separate incident, 17 people were reported to be dead or missing when a Maltese oil tanker, the *Thanassis A*, sank in the South China Sea in heavy seas associated with Teresa and the Northeast Monsoon. Nineteen other crew members were rescued.

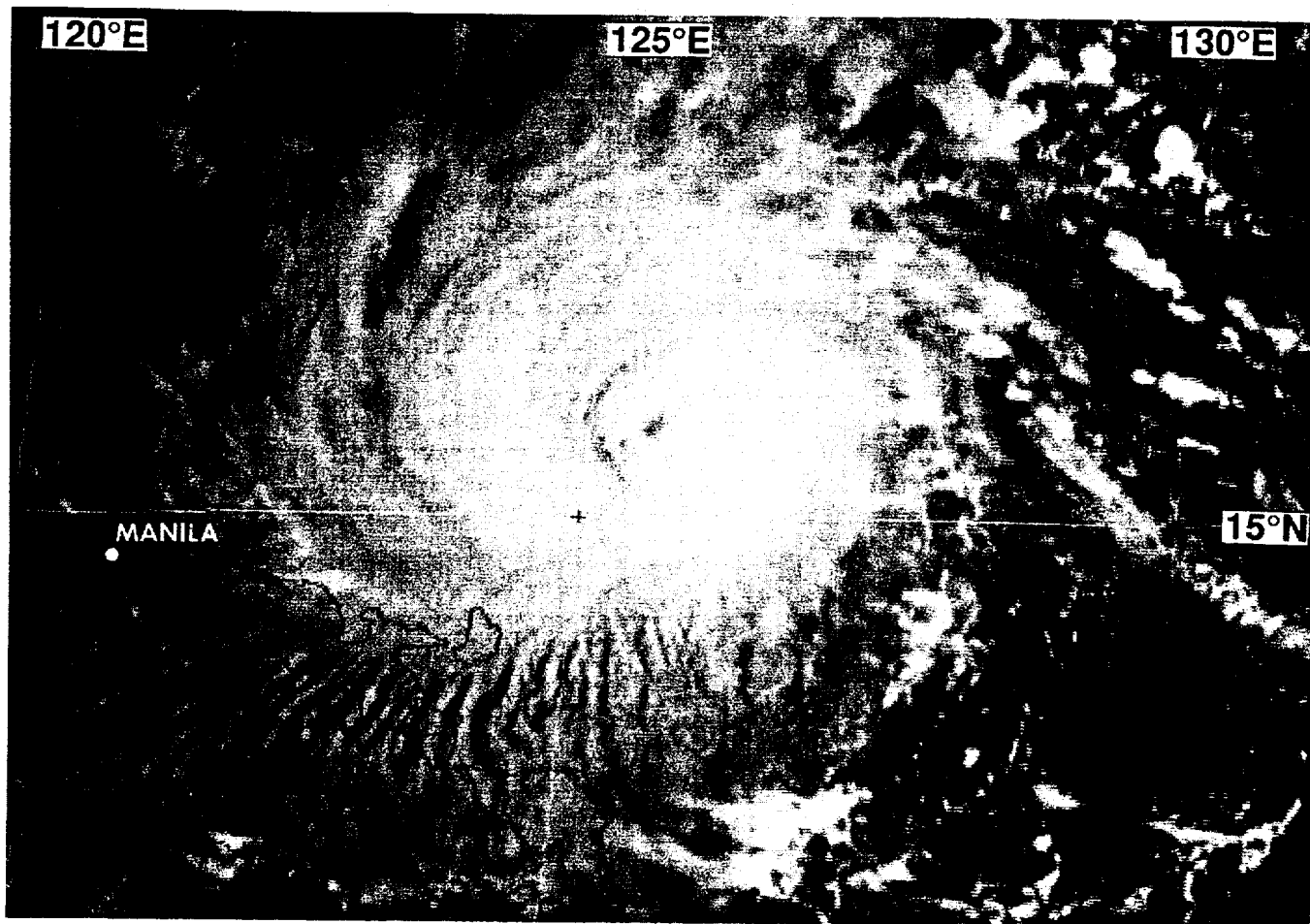


Figure 3-34-2 The low sun angle of morning helps to bring out the structure of Teresa's cloud system about eight hours prior to reaching its peak intensity (192224Z October visible GMS imagery).

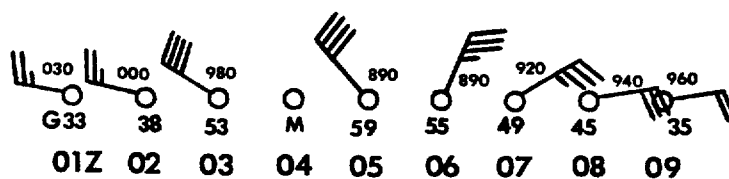


Figure 3-34-3 Hourly synoptic data recorded at Manila (WMO 98429) during Teresa's passage a short distance to the south of the city. Wind flags show sustained wind. The time of observation, gusts, and sea-level pressure are indicated.

E 120 125 130 135 140 145 150 155 160 165 170 175 180 175 170 W

N 50

TYPHOON WILDA
 BEST TRACK TC-35W
 18 OCT-01 NOV 94
 MAX SFC WIND 125KT
 MINIMUM SLP 916MB

45

40

35

30

25

20

15

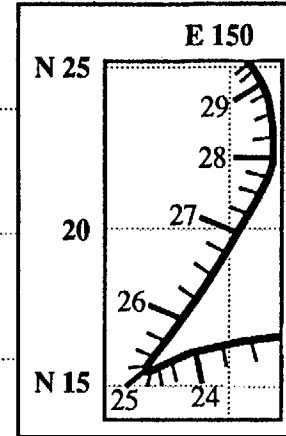
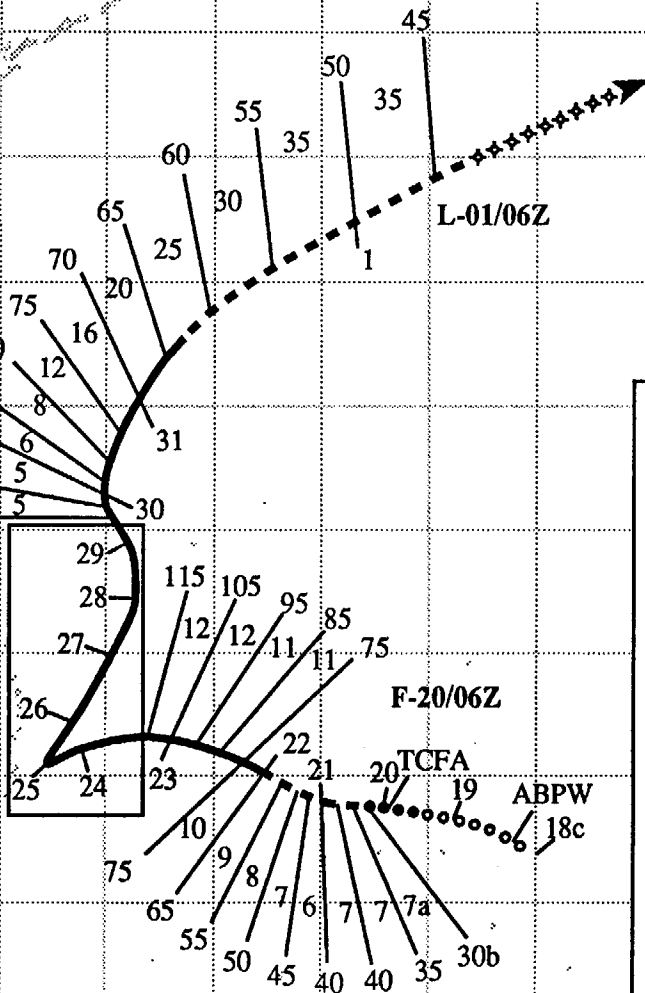
10

N 5

197

LEGEND

- 6-HR BEST TRACK POSITION
- a SPEED OF MOVEMENT (KT)
- b INTENSITY (KT)
- c POSITION AT XX/0000Z
- TROPICAL DISTURBANCE
- TROPICAL DEPRESSION
- - - TROPICAL STORM
- TYPHOON
- ◆ SUPER TYPHOON START
- ◇ SUPER TYPHOON END
- ◆ EXTRATROPICAL
- ◆ SUBTROPICAL
- *** DISSIPATING STAGE
- F FIRST WARNING ISSUED
- L LAST WARNING ISSUED



DTG (Z)	SPEED (KT)	INTENSITY (KT)
23/12	11	120
23/18	10	125
24/00	9	125
24/06	7	125
24/12	5	120
24/18	3	115
25/00	2	115
25/06	2	115
25/12	4	110
25/18	6	110
26/00	8	110
26/06	8	105
26/12	8	105
26/18	8	105
27/00	7	100
27/06	7	100
27/12	7	100
27/18	6	100
28/00	6	95
28/06	7	95
28/12	7	95
28/18	6	90
29/00	5	90
29/06	5	90
29/12	5	90

F-20/06Z
 TCFA
 ABPW
 18c
 30b
 7a
 7b
 40
 45
 50
 55
 65
 75
 85
 95
 105
 115

TYPHOON WILDA (35W)

I. HIGHLIGHTS

The third tropical cyclone of a mid-October four-storm outbreak, Wilda exhibited unusual motion. Wilda intensified to a peak of 125 kt (64 m/sec) during a quasi-stationary period near 15.6N ; 147.2E. During the stall, the monsoon trough within which Wilda was embedded acquired a reverse orientation. Coming out of the stall, Wilda moved on a slow north-oriented "S"-track.

II. TRACK AND INTENSITY

By mid-October, an active monsoon trough extended across the Philippine Sea (at 15°N), and from there, east-southeastward to a terminus in the Marshall Islands. At 180600Z, there were two named tropical cyclones — Teresa (34W) and Verne (33W) — and a tropical disturbance located along this trough axis. This tropical disturbance, which later became Wilda, was first mentioned on the 180600Z October Significant Tropical Weather Advisory when it was located near 10°N; 170°E at the eastern terminus of the monsoon trough. At 192230Z a Tropical Cyclone Formation Alert was issued based on increased central deep convection and a well-organized cirrus outflow pattern. At 200600Z the first warning was issued based upon persistence of the central deep convection and a rapid improvement in the organization of the central and peripheral deep convection. At 201800Z, Tropical Depression 35W was upgraded to Tropical Storm Wilda, and at 220000Z, Wilda was upgraded to a typhoon. Post-analysis of satellite and synoptic data indicated that Wilda most probably became a 25 kt (12 m/sec) tropical depression at 191200Z, and a tropical storm at 201200Z.

After becoming a typhoon, Wilda first moved west-northwestward, then westward along about 16.7°N, and then west-southwestward, threatening Saipan. At approximately 241200Z, Wilda abruptly slowed and remained quasi-stationary for 24 hours at a position about 90 nm (170 km) ENE of Saipan and 180 nm (330 km) NE of Guam (Figure 3-35-1). Wilda's intensity peaked at 125 kt (64 m/sec) at 231800Z, just as it began to turn west-southwestward towards Saipan. Later, during its one-day stall, it began to weaken slightly. At 251200Z, Wilda began to move toward the northeast on what would prove to be the first leg of a typical "S" track (Lander 1995a). While moving northeastward, Wilda weakened from 115 kt to 95 kt. After 280600Z, Wilda turned toward the north-northwest and weakened further. After 291800Z, Wilda turned northeastward (on the last leg of its "S" track) and accelerated. At 010600Z November, the final warning was issued as Wilda tracked northeastward at 35 kt (65 km/hr), and its cloud signature indicated that a transition to an extra-tropical cyclone had occurred.

III. DISCUSSION

a. NEXRAD's view of Wilda

When Wilda stalled northeast of Guam, it was at its closest point of approach of 180 nm (330 km). Although poorly defined, Wilda's eye was discernible on the NEXRAD reflectivity product for a short time. The poor eye definition was likely due to signal attenuation by heavy rainbands and a beam height of 20,000 ft at Wilda's 180 nm range. In contrast, Wilda's extensive peripheral cloud bands remained well-within radar range for several days.

For almost two days (240220Z to 260005Z), Guam's NEXRAD provided a continuous integration of the precipitation associated with Wilda. Estimated rainfall magnitudes and gradients were extreme (Figure 3-35-2). Over five inches fell in a narrow swath between Guam and Saipan. Within two small regions, covering an area of approximately 1400 square miles (roughly the land area of the state of

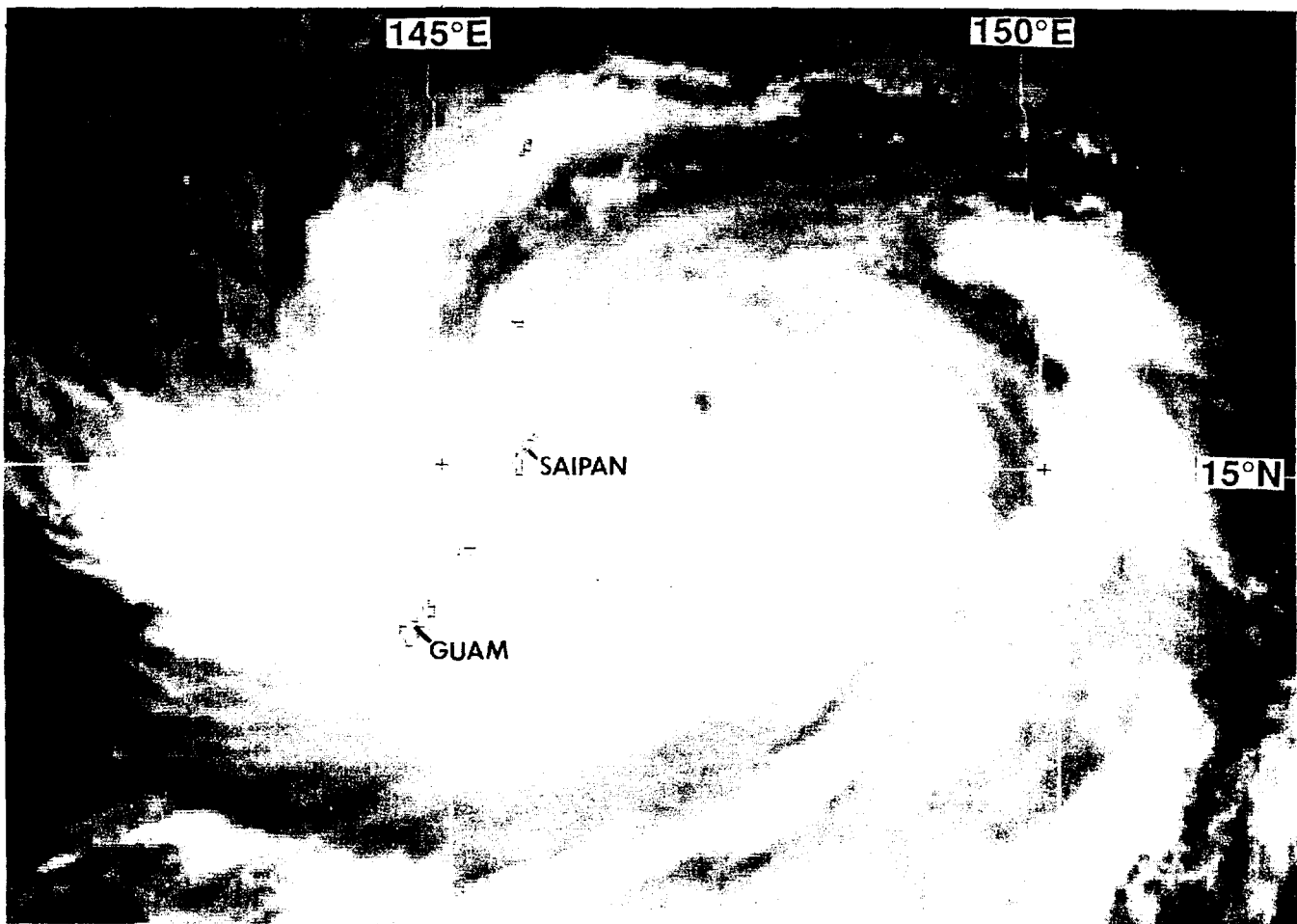


Figure 3-35-1 Wilda at an intensity of 115 kt (59 m/sec) has stalled about 90 nm (170 km) east-northeast of Saipan (242331Z October visible GMS imagery).

Rhode Island), over ten inches of rain was estimated to have fallen. On the island of Guam, the storm-total precipitation estimated by NEXRAD (Figure 3-35-3a) is about 20% short of the rainfall actually measured during Wilda's passage (Figure 3-35-3b). This was the most accurate storm-total precipitation estimated by NEXRAD on Guam to date. NEXRAD estimates are historically 25%-50% less than the measured values (for example, see Verne's (33W) summary). Its representation of the spatial distribution of rainfall (in this case, a narrow band of 3-4" inches of rain across the middle of the island with lighter amounts on the northern and southern ends of the island) was good.

b. Unusual motion

The monsoon trough which became active during mid-October was initially oriented WNW-ESE, and the tropical cyclones along its axis moved on west-northwesterly tracks consistent with climatology. Then, by virtue of the differential motions of Teresa (34W), Verne (33W), Wilda (35W), and Yuri (36W), the axis of the trough became oriented WSW-ENE (i.e., reverse oriented) at approximately 230000Z (see Figure 3-33-1c in Verne's summary). Concurrent with the monsoon trough's reverse orientation, Verne (33W) and Wilda stalled, and then moved on north-oriented tracks. After emerging from its one day stall, Wilda moved on an "S" shaped track (a track type which is almost exclusively associated with reverse orientation of the monsoon trough (Lander 1995a)).

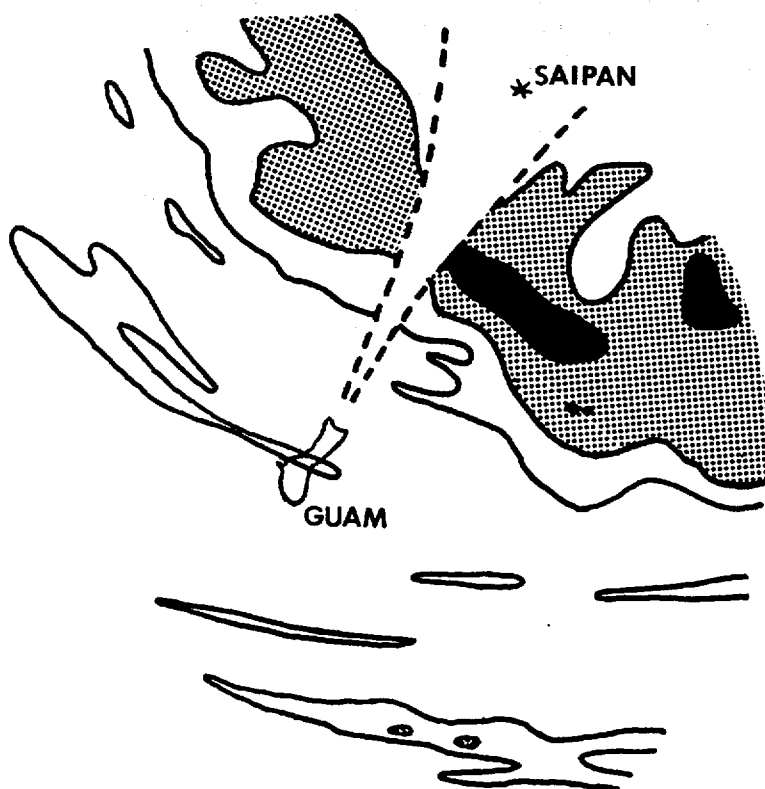


Figure 3-35-2 Estimated rainfall deposited by Wilda within 124 nm of Guam (NEXRAD storm-total precipitation for the period 240220Z to 252147Z October). Outer contour is three inches, half-tone indicates 5 to 10 inches, black-shaded area indicates 10 inches or more. The dashed lines enclose the area of radar beam blockage.

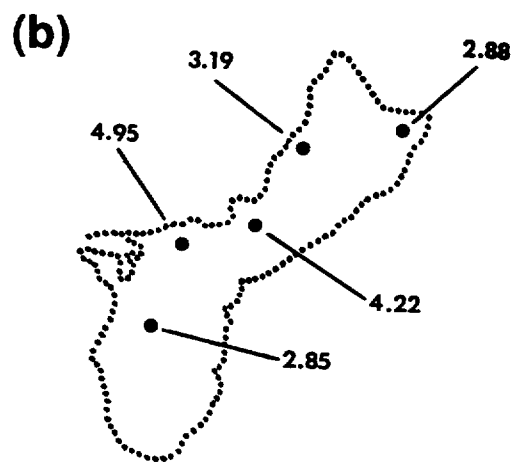
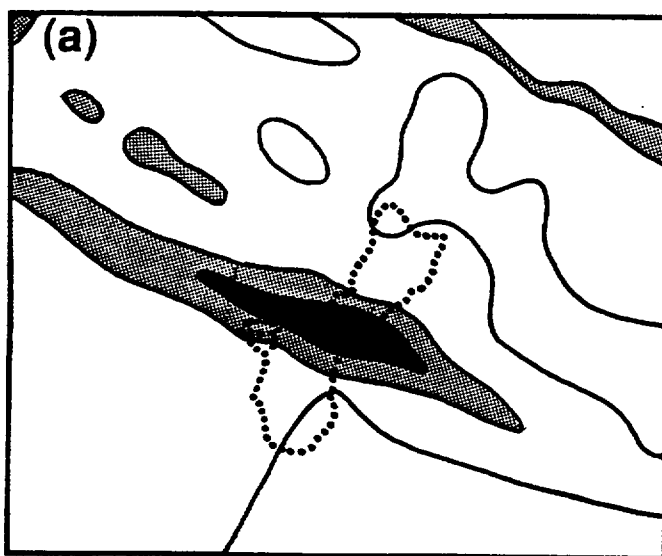


Figure 3-35-3 (a) Rainfall deposited on Guam by Wilda as estimated by NEXRAD during the period 240220Z to 252147Z October. Outer contour is 2 inches, half-tone indicates three to four inches, black-shaded area indicates four inches or more. (b) Rainfall measured on Guam during Wilda's passage.

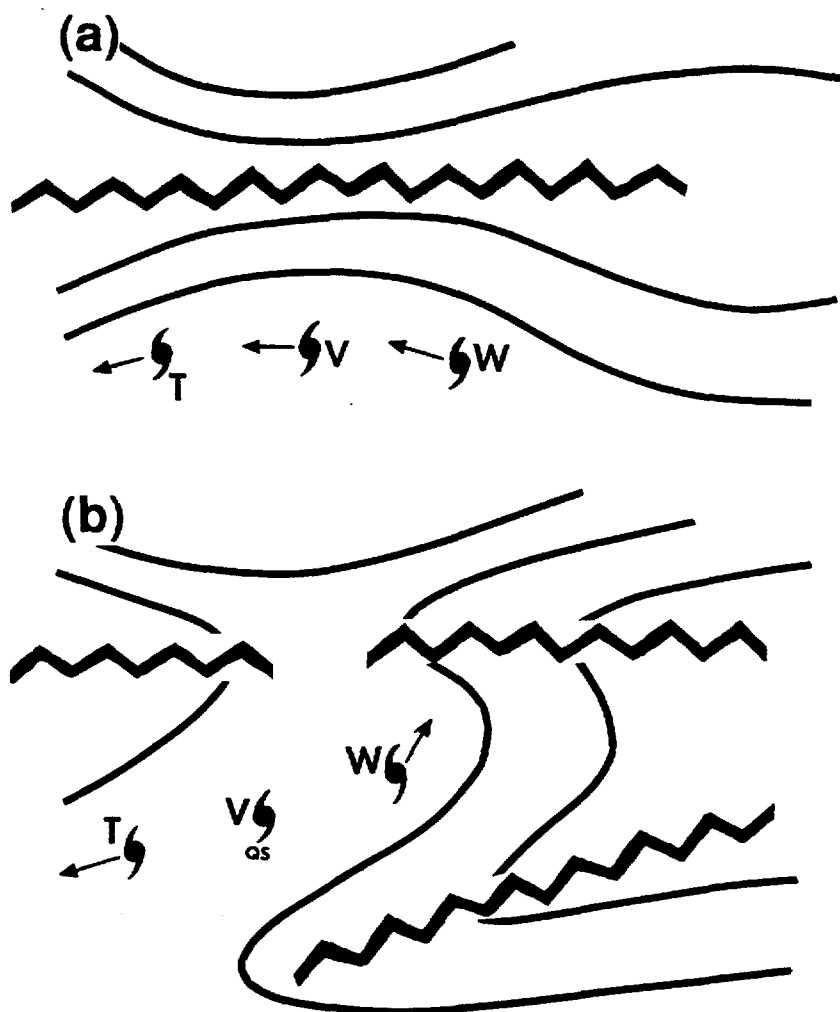


Figure 3-35-4 (a) Schematic illustration of the pattern of the 500 mb heights (adapted from NOGAPS analyses) in the western North Pacific while Teresa (T), Verne (V) and Wilda (W) moved westward. (b) Pattern of the 500 mb heights as the monsoon trough acquired a reverse orientation, and Wilda began to move northeastwards. Contours values are arbitrary. Zig-zag lines indicate ridge axes. Arrows depict motion of the tropical cyclones. QS = quasi-stationary.

The stall and the “S” track of Wilda were associated with an interesting evolution of the 500 mb pattern. At first, while Teresa (34W), Verne (33W), and Wilda were moving west-northwestward, the 500 mb height field featured a zonally oriented subtropical ridge (Figure 3-35-4a). As the monsoon trough acquired a reverse orientation, two ridge axes began to influence the motion of the tropical cyclones: one ridge axis was the preexisting subtropical ridge, and the other ridge axis developed to the southeast of the monsoon trough (Figure 3-35-4b). While Wilda was moving west-northwestward, the highest 500 mb heights were along the axis of the subtropical ridge. As Wilda stalled, pressure heights increased in the new ridge to the southeast. When pressure heights in the southeastern ridge exceeded the pressure heights along the subtropical ridge axis, Wilda began to move northeastward. The two-ridge structure at 500 mb (Figure 3-35-4b) remained in place as Wilda moved northward. The top half of Wilda’s “S” motion occurred as Wilda moved through the subtropical ridge axis and entered the mid-latitude westerlies.

c. Air-sea interactions

As discussed in Verne’s (33W) summary, tropical cyclones are known to cause cooling of the sea surface. This leads to the testable hypothesis that tropical cyclones which remain quasi-stationary over water for extended periods may weaken as the underlying sea surface temperature (SST) falls. Like

Verne (33W), Wilda provides a good test case.

While Wilda remained quasi-stationary for about 24 hours near 15.7°N ; 147.2°E, it weakened slightly from 125 kt (its peak intensity) to 115 kt. Later, coming out of its stall, it weakened slightly, but remained near 100 kt (51 m/sec) for the next three days. As was the case with Verne (33W), one can draw few conclusions from the case of Wilda about feedback of tropical cyclone induced SST changes upon the tropical cyclone itself (without rigorous study). At best, it can be shown that both Verne (33W) and Wilda induced some cooling of the SST (Figure 3-35-5).

d. Forecast performance

Despite unusual motion, the track forecasts errors for Wilda were lower than average, with mean errors at 24, 48, and 72 hours of 115, 193, and 223 nm respectively. Long-range (48 and 72-hour) track errors showed increases at three places along Wilda's track: (1) as it turned west-southwestward toward its stall position (forecasts then were for continued westward motion); (2) as it moved northeastward after the stall (forecasts then did not anticipate the magnitude of the bend back toward the north-northwest as Wilda executed the middle portion of its "S" track); and, (3) at the point of recurvature into the mid-latitude westerlies (the timing of the acceleration to the northeast was a problem).

Intensity forecasts were quite poor at two times: (1) in the early stages, the intensity was significantly under-forecast by as much as 35 kt at 24 hours, 45 kt at 48 hours and 50 kt at 72 hours ; and, (2) upon coming out of its stall and moving northeastward, the rate of weakening was over-forecast. Real-time diagnosis of intensity was 25 kt low (with respect to the final best-track intensity estimates) as Wilda reached its peak intensity; up to 20 kt too high during Wilda's stall; and then within 5 kt of the final best-track intensity as Wilda executed the "S" portion of its track.

IV. IMPACT

Wilda brought gusty winds, hazardous surf, and heavy rain to Guam, Rota, Tinian and Saipan. The highest recorded wind gust recorded on Guam was 74 kt (38 m/sec) at the JTWC. On Saipan, high winds downed trees and power lines, and pulled tin roofs from houses. Eleven people were injured in typhoon-related accidents. At the Saipan port, two tugboats sank, a flat barge was lost, and 50 welding machine units were destroyed. Offshore, the Philippine-registered ship, *M/V Ronda*, nearly sank in 30 to 40 foot high seas. On Guam, three surfers were missing and presumed drowned in rough seas off the northern end of the island. A surfboard and two boogie boards washed ashore, but the surfers were never found.

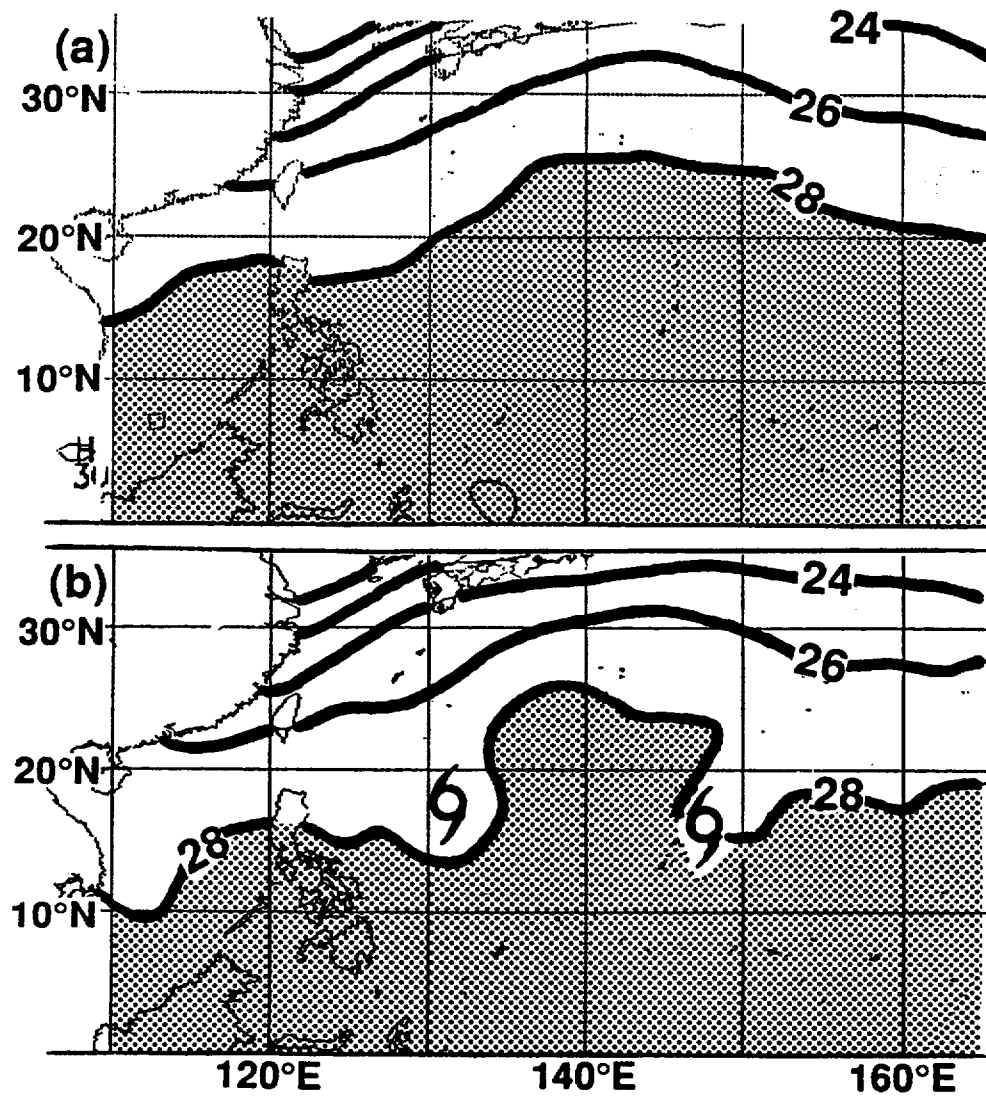
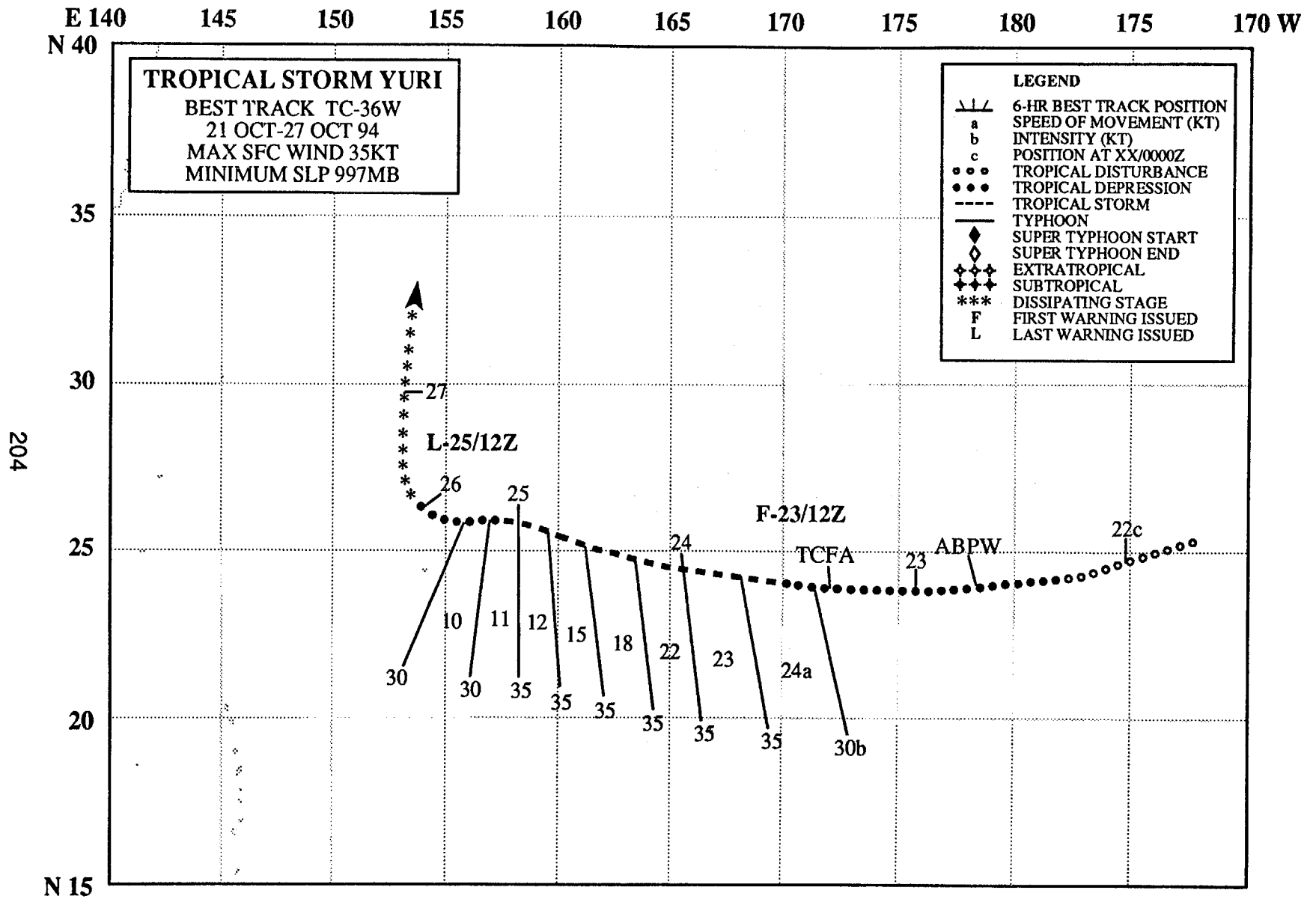


Figure 3-35-5 (a) SST analysis at 211200Z October. (b) SST analysis at 271200Z October. Notice the cooling of the SST at the stall locations of Verne (33W) and Wilda.



TROPICAL STORM YURI (36W)

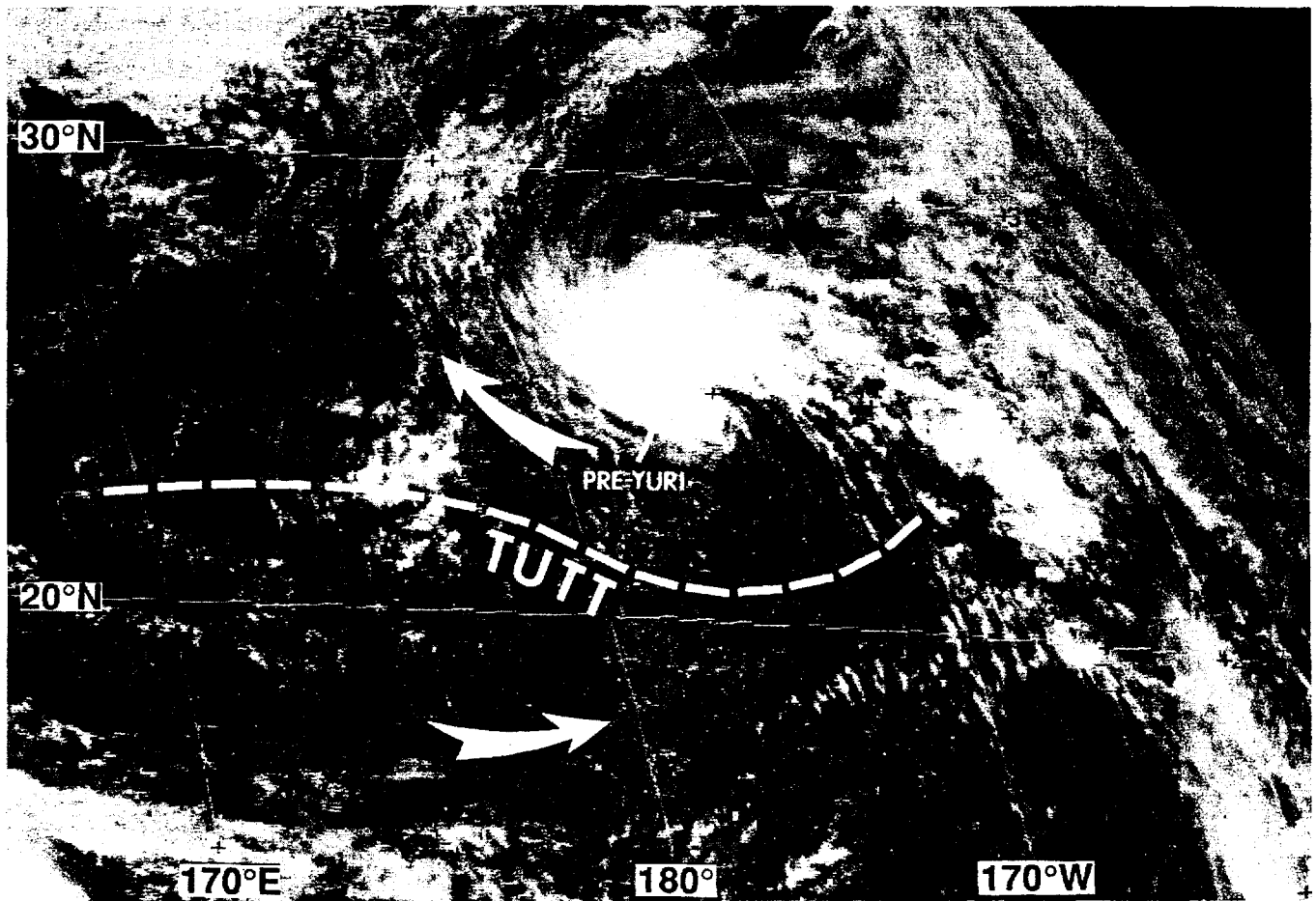


Figure 3-36-1 The tropical disturbance which later became Tropical Storm Yuri is seen northwest of Hawaii along the axis of the TUTT (212331 visible GMS imagery).

I. HIGHLIGHTS

Yuri was a small, short-lived tropical cyclone which formed at relatively high latitude (25°N) in direct association with a TUTT cell. Forming east of the international date line in a relatively cloud-free area (Figure 3-36-1), the disturbance that became Yuri, moved rapidly westward at 21 kt (40 km/hr). For a couple of days, the low-level southwest monsoon stretched from the Philippines all the way out to the south of Yuri. This temporarily placed Yuri at the eastern reaches of the reverse-oriented monsoon trough that also included Teresa (34W), Verne (33W), and Wilda (35W).

II. TRACK AND INTENSITY

The low-level circulation of the western North Pacific during late October was dominated by an active monsoon trough. In the upper troposphere, the axis of the tropical upper tropospheric trough (TUTT) stretched along 25°N from about 150°E to a position (30°N ; 160°W) northwest of Hawaii. This TUTT overlaid a relatively cloud-free region between the monsoon cloudiness to the south and the cloudiness associated with the polar front to north. A distinct area of persistent convective clouds formed in association with a TUTT cell that was northwest of Hawaii on 22 October. This area of con-



Figure 3-36-2 The remnant low-level circulation of Yuri (252331Z visible GMS imagery).

vection was clearly associated with a low-level circulation center. Moving rapidly westward at nearly 21 kt (40 km/hr), this circulation crossed the international date line shortly after 221200Z. The 221800Z October Significant Tropical Weather Advisory noted that a weak low-level circulation center which appeared to be developing beneath a TUTT cell had crossed the international date line. Based upon well-organized low-level cloud lines in satellite imagery, a Tropical Cyclone Formation Alert was issued at 230000Z. The first warning on Tropical Depression 36W was issued at 231200Z. The rationale for issuing the first warning is stated in the prognostic reasoning message (WDPN34 PGTW 231500):

“... [at 231200Z] animated infrared satellite imagery shows that Tropical Depression 36W is moving rapidly westward near Wake island. Well-defined lower level cumulus lines are evident on infrared metsat data as well as DMSP nighttime visible imagery. There is a lack of deep convection near the center, but animation shows the cloud elements spinning around the cyclone center at a velocity estimated at 30 to 40 knots. It is possible that this system is most intense at the 850-700 mb level above the surface. We have no [conventional] synoptic data to support our current intensity

estimate. The Dvorak satellite analysis model for intensity estimates does not handle these types of hybrid systems very well, so it is likely the satellite intensity estimates on Tropical Depression 36W [may] be significantly lower than the actual winds at the surface.”

During the night of 23 October, a small area of deep convection formed on the southeastern side of the well-defined low-level circulation center of Tropical Depression 36W. In addition, low-level cloud motion (obtained from the satellite-derived cloud-motion bulletin issued by the JMA) of 40 kt (20 m/sec) was observed on the north side of the circulation. These data prompted an upgrade of the system to Tropical Storm Yuri at 231800Z. Yuri remained at minimal tropical storm intensity until 250000Z. The loss of all deep convection and a degradation in the appearance of the low-level cloud lines, indicated that the system had weakened to tropical depression intensity at 250600Z. The final warning was issued at 251200Z. The remnant low-level circulation of Yuri (Figure 3-36-2) was captured nicely by the scatterometer aboard the ERS-1 satellite at 260000Z (Figure 3-36-3).

III. DISCUSSION

a. Unusual genesis

Most of the tropical cyclones of the western North Pacific form along the axis of the monsoon trough. On rare occasions, a tropical cyclone forms from a small convective cloud cluster in direct association with a TUTT cell. The cloud system of such tropical cyclones is often isolated in the relatively cloud-

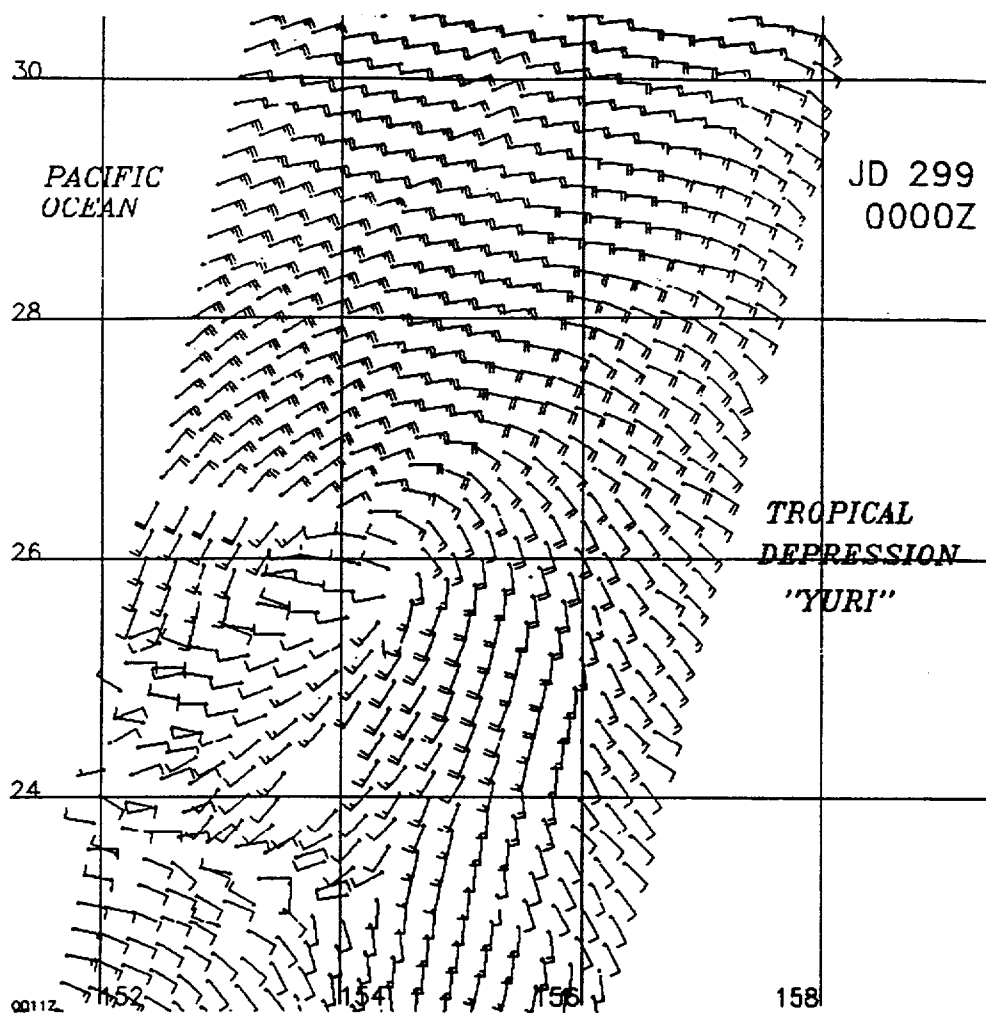


Figure 3-36-3 Low-level wind flow derived from the scatterometer aboard the ERS-1 satellite showing the remnant circulation of Yuri (260000Z October ERS-1 scatterometer-derived wind).

free region between the cloudiness associated with the monsoon trough and the cloudiness associated with the polar front. These TUTT-cell induced tropical cyclones are usually small-sized and isolated in easterly low-level winds (i.e., the low-level wind returns to easterly a few hundred kilometers equatorward of the system). (see also the summary of Tropical Depression 31W, which — like Yuri — formed in direct association with a TUTT cell.)

In recent years, we have observed that tropical cyclones which form along the TUTT axis, in association with TUTT cells, tend to form to the northeast of the center of the TUTT cell where the upper-level winds are from the south or southeast, and are highly diffluent (Figure 3-36-4a,b). This mode of formation is quite different from the influence of TUTT cells on tropical cyclone development suggested by Sadler (1976). In this paper, Sadler hypothesizes that TUTT cells aid tropical cyclone development by providing a diffluent upper-level outflow region in the southeast quadrant of a TUTT cell which is located to the northwest of a developing tropical cyclone (Figure 3-36-4c). In an earlier paper by Sadler (1967), he hypothesizes that TUTT cells may penetrate to the surface and create an inverted trough or a vortex in the tradewind flow. In fact, he claims that TUTT-cell penetration to the surface is the primary source for disturbances in the trade winds during summer. This process, though providing a better description of the formation of Yuri and TD 31W (and of other recent tropical cyclones (e.g., Gordon, 1989) observed to have formed in direct association with TUTT cells), lacks a description of the role of

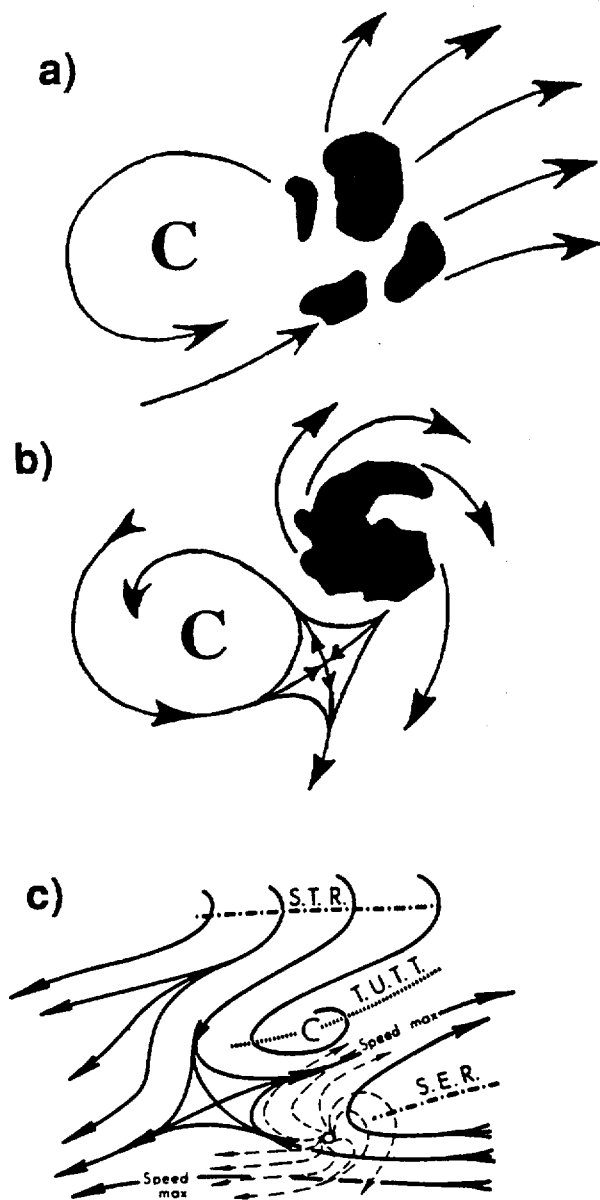


Figure 3-36-4 (a) Cloud clusters to the east of a TUTT cell prior to development of a low-level circulation center. (b) A tropical cyclone which has evolved from a cloud cluster near a TUTT cell. Black silhouettes represent deep convection, arrows depict 200 mb flow, large "C" represents the center of the TUTT cell. (c) A TUTT cell provides an upper-level outflow channel to a developing tropical cyclone (After Sadler, 1976). STR is the subtropical ridge; SER the sub-equatorial ridge; TUTT, the tropical upper tropospheric trough.

deep convection in the formation of the surface low, and is vague about whether the tropical cyclones that form in such cases are initiated by the reflection of the TUTT cell at the surface or whether they are independently produced by convective processes associated with the TUTT cell.

IV. IMPACT

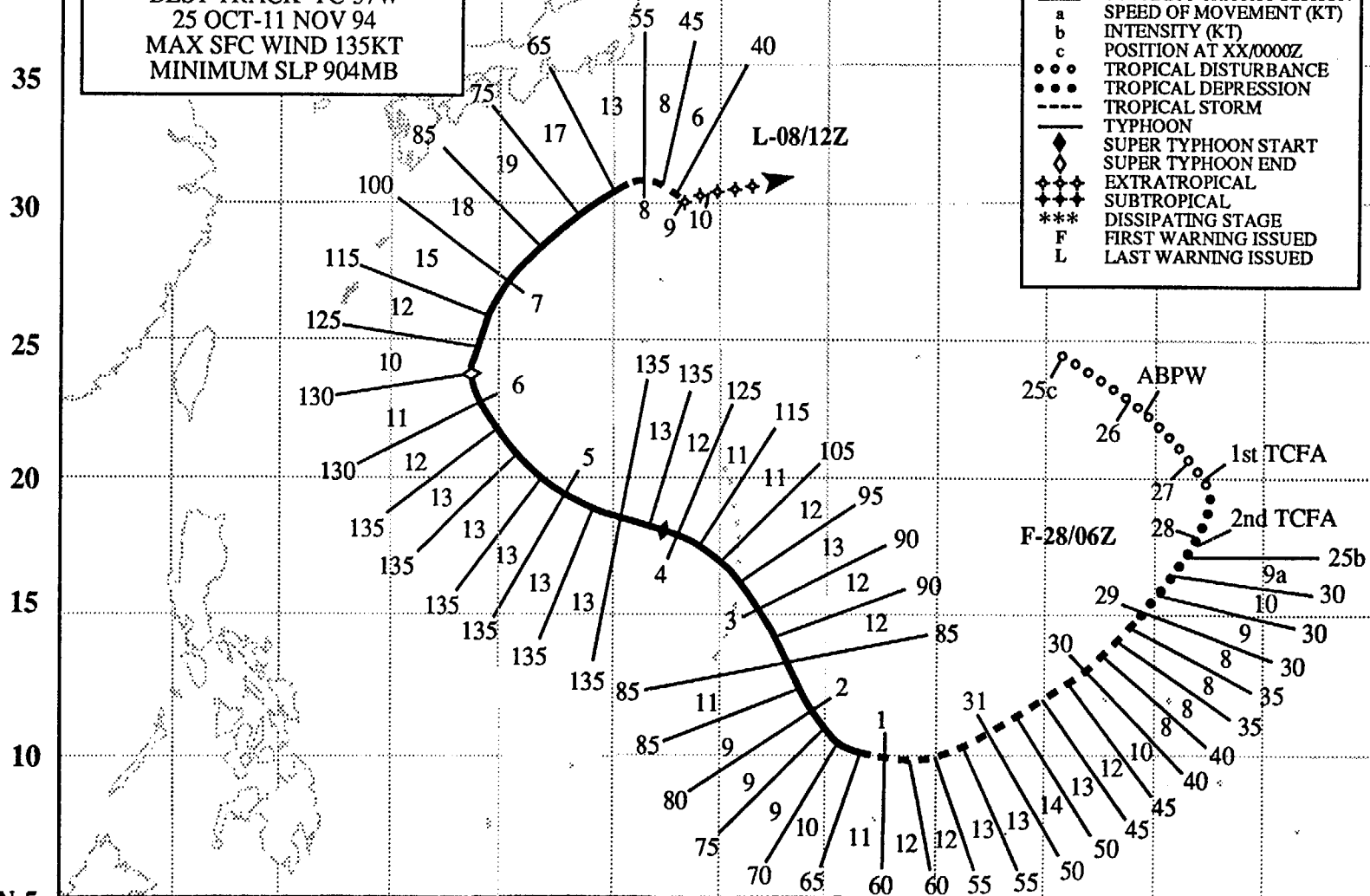
No reports of serious damage or injuries were received.

E 115 120 125 130 135 140 145 150 155 160 165 170 175 E
N 40

SUPER TYPHOON ZELDA
BEST TRACK TC-37W
25 OCT-11 NOV 94
MAX SFC WIND 135KT
MINIMUM SLP 904MB

LEGEND
 \ / \ 6-HR BEST TRACK POSITION
 a SPEED OF MOVEMENT (KT)
 b INTENSITY (KT)
 c POSITION AT XX/0000Z
 ○ ○ ○ TROPICAL DISTURBANCE
 ● ● ● TROPICAL DEPRESSION
 --- TROPICAL STORM
 --- TYPHOON
 ◆ SUPER TYPHOON START
 ◇ SUPER TYPHOON END
 ◆ ◆ ◆ EXTRATROPICAL
 ◆ ◆ ◆ SUBTROPICAL
 *** DISSIPATING STAGE
 F FIRST WARNING ISSUED
 L LAST WARNING ISSUED

209



N 5

SUPER TYPHOON ZELDA (37W)

I. HIGHLIGHTS

Zelda was the sixth, and final, super typhoon of 1994. During the first half of Zelda's life, it exhibited unusual motion: it moved from a subtropical latitude (25°N) southward into the deep tropics (10°N). Zelda passed to the north of Guam, and within range of Guam's NEXRAD.

II. TRACK AND INTENSITY

The tropical disturbance that became Zelda developed at the eastern reaches of a reverse-oriented monsoon trough that was defined by a line drawn SW-NE through the centers of Teresa's (34W) remnants, Typhoon Verne (34W), and Typhoon Wilda (35W) (Figure 3-37-1a). The first mention of this disturbance on the 260600Z October Significant Tropical Weather Advisory stated, in part:

"... the low level circulation that is part of the reverse oriented monsoon trough ... has had persistent convection for over 12 hours. ... the potential for significant tropical cyclone development is fair. ..."

Based on satellite imagery that showed tightly wound low-level cloud lines to the northwest of an area of deep convection, and on synoptic reports that verified the presence of a low-level cyclonic circulation, a Tropical Cyclone Formation Alert (TCFA) was issued at 270500Z. Over the next 18 hours, the system did not show any signs of intensifying. Based on satellite imagery (e.g., see Figure 3-37-2) and on synoptic reports from Wake Island (WMO 91245), a second TCFA was issued at 280230Z. Quoting from this second TCFA:

"The tropical disturbance [pre-Zelda] is now located south-southeast of Wake Island. Wake reported sea-level pressures as low as 1006.1 mb as the system [which was moving southward] passed to the east. Satellite imagery shows an exposed low level circulation center with weak convection sheared 50 nm to the south-southwest. Minimum sea level pressure is estimated at 1004 mb."

At 280600Z, the first warning on Tropical Depression 37W was issued as the satellite signature of the system improved. At this time, it was thought that Tropical Depression 37W was unlikely to become a tropical storm. Its history of slow development and evidence on satellite imagery of northeasterly shear on the system led JTWC forecasters to expect little further intensification. However, at 290600Z, Tropical Depression 37W was upgraded to tropical storm intensity based upon an improved satellite signature. Thereafter, Zelda continued to intensify at a slow pace, and, at 011200Z November, it was upgraded to typhoon intensity.

From the disturbance stage to the attainment of typhoon intensity, Zelda dropped equatorward from 25°N to 10°N along a very unusual "backwards C" -shaped track. This unusual motion is discussed in the next section. After becoming a typhoon (at 010600Z November), Zelda turned toward the north-northwest and continued to slowly intensify. At 030000Z November, Zelda turned toward a more westward heading, and six hours later, at 030600Z, its eye passed over the island of Anatahan (Figure 3-37-3). After passing over Anatahan with an intensity of 95 kt (50 m/sec), Zelda's rate of intensification increased. During the 120-hour period 290000Z October to 030000Z November, the intensity increased at a fairly steady rate of 10 kt per day. Then, over the 24-hour period 030600Z to 040600Z November, there was a 40 kt increase of intensity from 95 kt (49 m/sec) to 135 kt (69 m/sec). For 36 hours (040600Z to 051800Z), Zelda's intensity held steady at its peak value of 135 kt (69 m/sec) (Figure 3-37-4). Zelda reached the point of recurvature at 060600Z November, 48 hours after reaching peak intensity. (Reaching peak intensity prior to recurvature is typical for most very intense tropical cyclones that

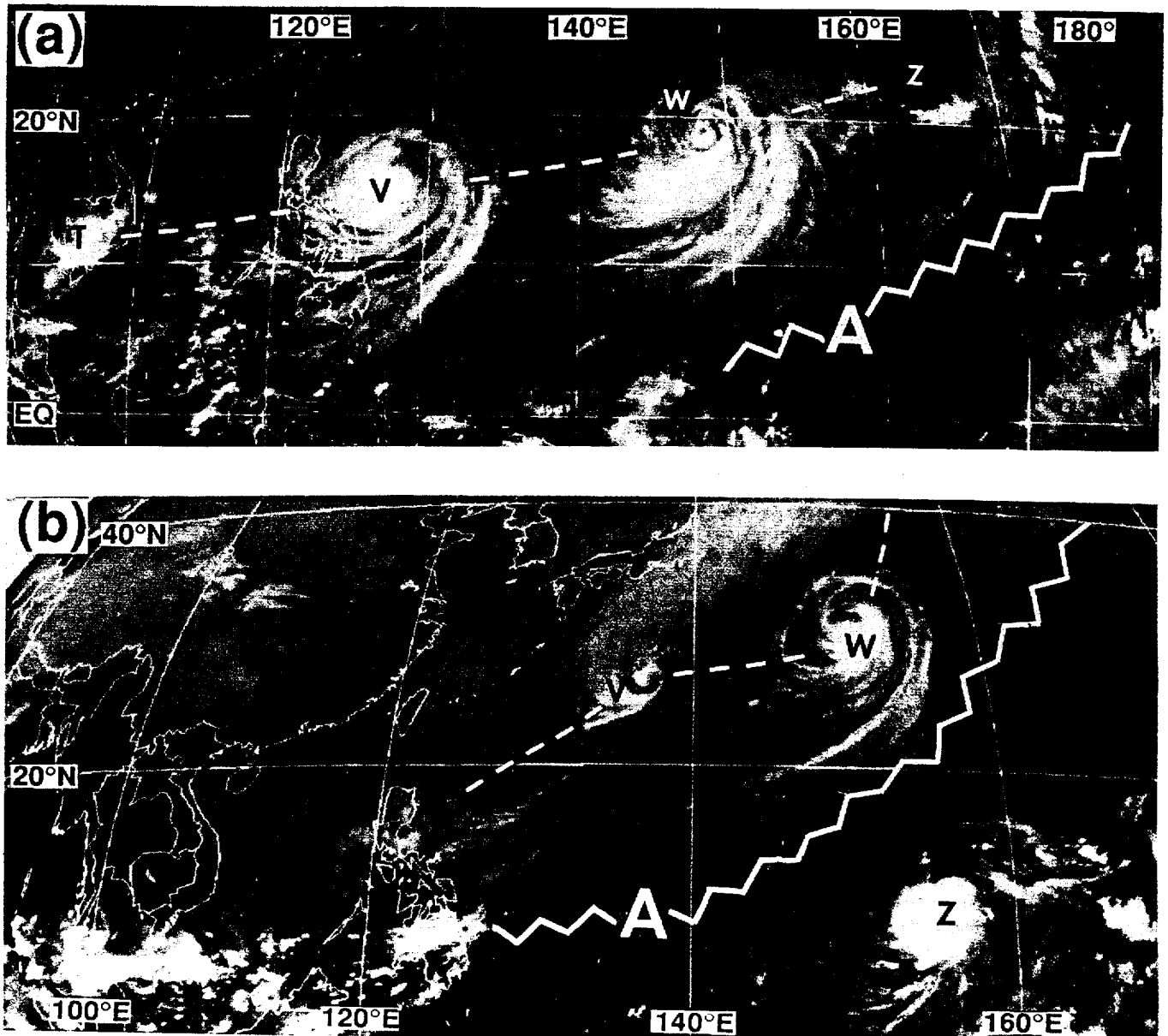


Figure 3-37-1 (a) The disturbance that would become Zelda (labeled, Z) lies at the eastern reaches of a reverse-oriented monsoon trough (dashed white line) that stretches from the remnants of Typhoon Teresa (34W) (T) — located over south-east Asia — northeastward through Verne (33W) (V) and Wilda (35W) (W). Zig-zag line indicates induced ridging south-east of the monsoon trough (260633Z October infrared GMS imagery). (b) Typhoons Verne (33W) (labeled, V) and Wilda (35W) (W) have gained latitude while Zelda (Z) has dropped southward (302332 October GMS IR imagery).

recurve — see the discussion of peak intensity versus timing of recurvature in the Typhoon Page (03W) summary.) After passing through the point of recurvature, Zelda began to weaken rapidly. In the 48-hour period 060600Z to 080600Z there was an 85 kt decrease in intensity from 130 kt (69 m/sec) to 45 kt (23 m/sec). The final warning was issued at 081200Z as Zelda acquired extratropical characteristics. The extratropical remnant of Zelda drifted eastward and dissipated over water near 30°N 145°E, almost back to where Zelda had begun.

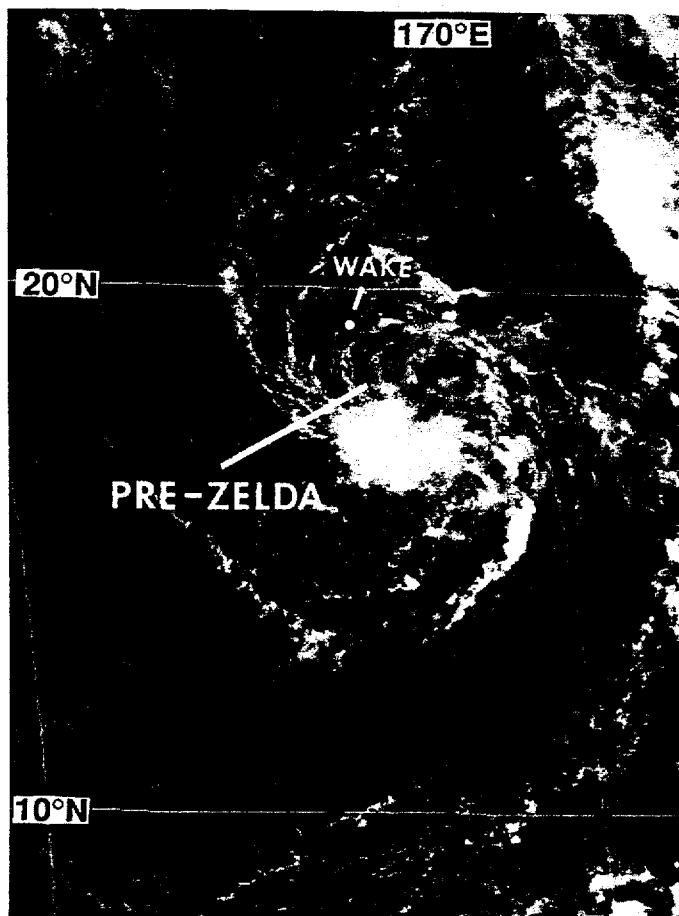


Figure 3-37-2 The exposed low-level circulation center of the tropical disturbance that would become Zelda can be seen to the north of a small area of deep convection, and is about 90 nm (165 km) south-southeast of Wake island (272331Z October visible GMS imagery).

turn to the northwest and pass near or over Guam. As the northwestward turn ensued after 010000Z, the motion became even more northward than forecast. By the 020000Z forecast, a new scenario was anticipated: numerical guidance and the official forecast now indicated that Zelda would move northwestward for 24 hours and then turn toward the west-northwest and pass near or over Saipan. However, from 021334Z to 021734Z the radar fixes indicated a north-northwestward movement. Incorporating this information, the warning at 021800Z indicated that Zelda would pass about 50 nm northeast of Saipan and then over Anatahan (a small island about 70 nm north of Saipan). At a critical time period — shortly after 021800Z — when JTWC forecasters were closely watching for evidence of Zelda's anticipated west-northwestward turn, the NEXRAD fixes (at 021832Z, 021936Z, and 022035Z) jogged to the west (see Figure 3-37-6). If interpreted as indicative of the onset of a major track change, these fixes could have been extrapolated to indicate that Zelda would pass very near or over Saipan. However, the next five radar fixes beginning at 022133Z showed northwestward motion that when extrapolated, indicated once again that Zelda would pass to the north of Saipan. Zelda passed 30 nm (55 km) to the northeast of Saipan and then directly over Anatahan.

The six-hour time step of the best track (Figure 3-37-6) and its subjective smoothing can not accommodate the short-term track changes indicated by the radar.

III. DISCUSSION

a. Unusual motion

The full trace of Zelda's motion — from its early stages as a tropical disturbance near 25°N 160°E, to its dissipation near 30°N 145°E — forms one of the oddest shaped tracks of 1994. Particularly unusual was the early portion of Zelda's track wherein the system moved southward on a "backwards C" - shaped track. One hypothesis for this unusual motion is that Zelda was carried southward in the flow around an anticyclone which had formed to the southeast of typhoons Wilda (35W) and Verne (33W) (Figure 3-37-1a,b and Figure 3-37-5).

b. NEXRAD's view of Zelda

Beginning at 020740Z November and continuing through 031432Z, forecasters at Andersen Air Force Base, Guam, were able to provide to the JTWC hourly fixes on the center of Zelda's large eye (Figures 3-37-6 and 3-37-7). The high frequency (approximately hourly) of accurate fixes obtained from the NEXRAD for Zelda were very useful overall, but illustrated that the short-term track changes that are resolvable with the NEXRAD must be interpreted with caution. For several forecasts prior to 020000Z, numerical guidance and the official forecast indicated that Zelda, which was then moving westward, would

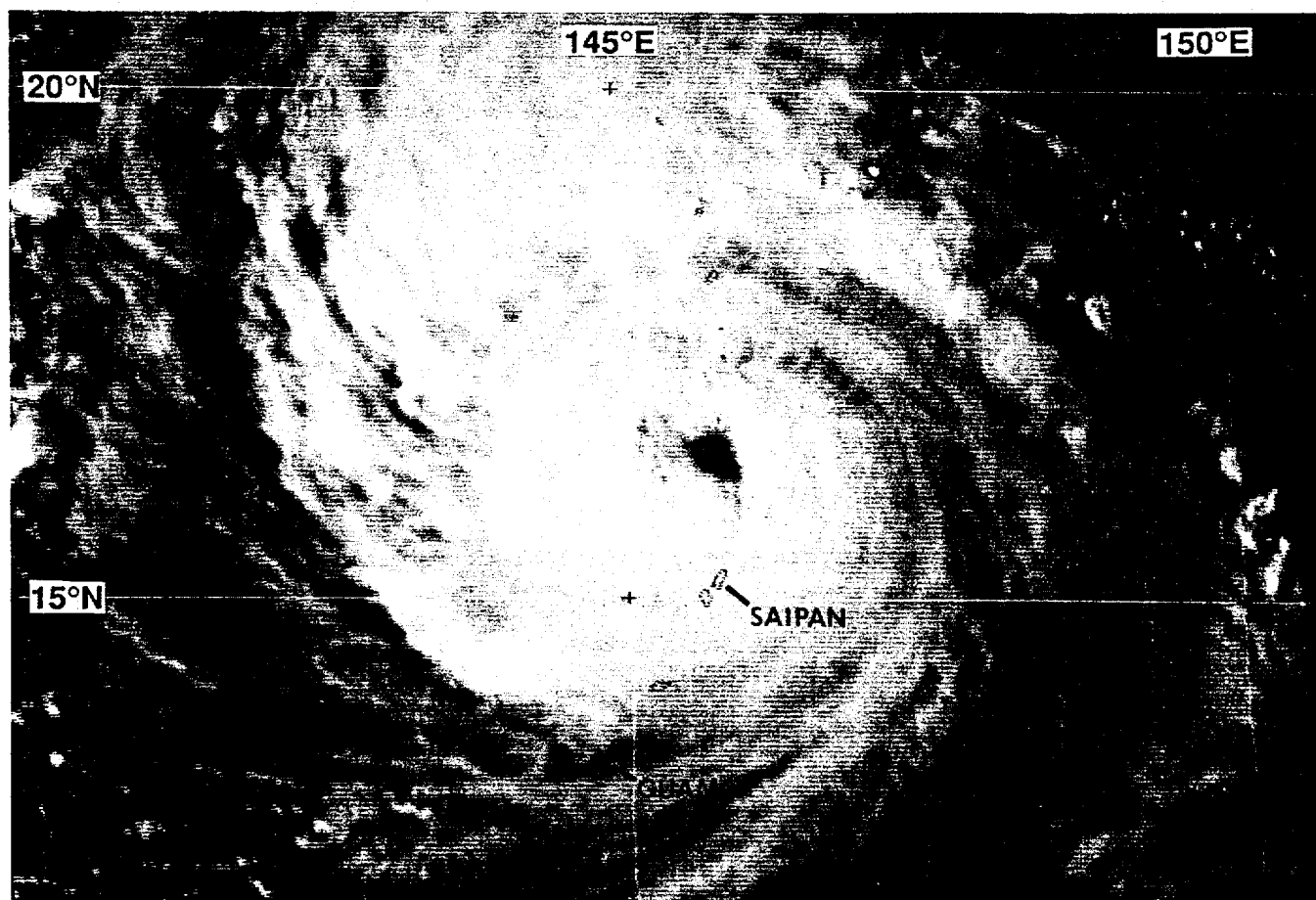


Figure 3-37-3 The island of Anatahan lies within Zelda's eye at the time of this satellite image (030631Z November visible GMS imagery).

IV. IMPACT

Of all the tropical cyclones that affected the Mariana island chain during 1994, Zelda had the most impact. High wind damaged homes in Saipan and Tinian. Hardest hit was the island of Anatahan — the northernmost inhabited island of the Commonwealth of the Northern Mariana Islands. The large eye of Zelda passed over Anatahan where the homes and crops of the 39 residents were devastated. All 39 residents were evacuated by the U.S. Navy and transferred to Saipan. Fortunately, no reports of serious injuries or deaths were received.

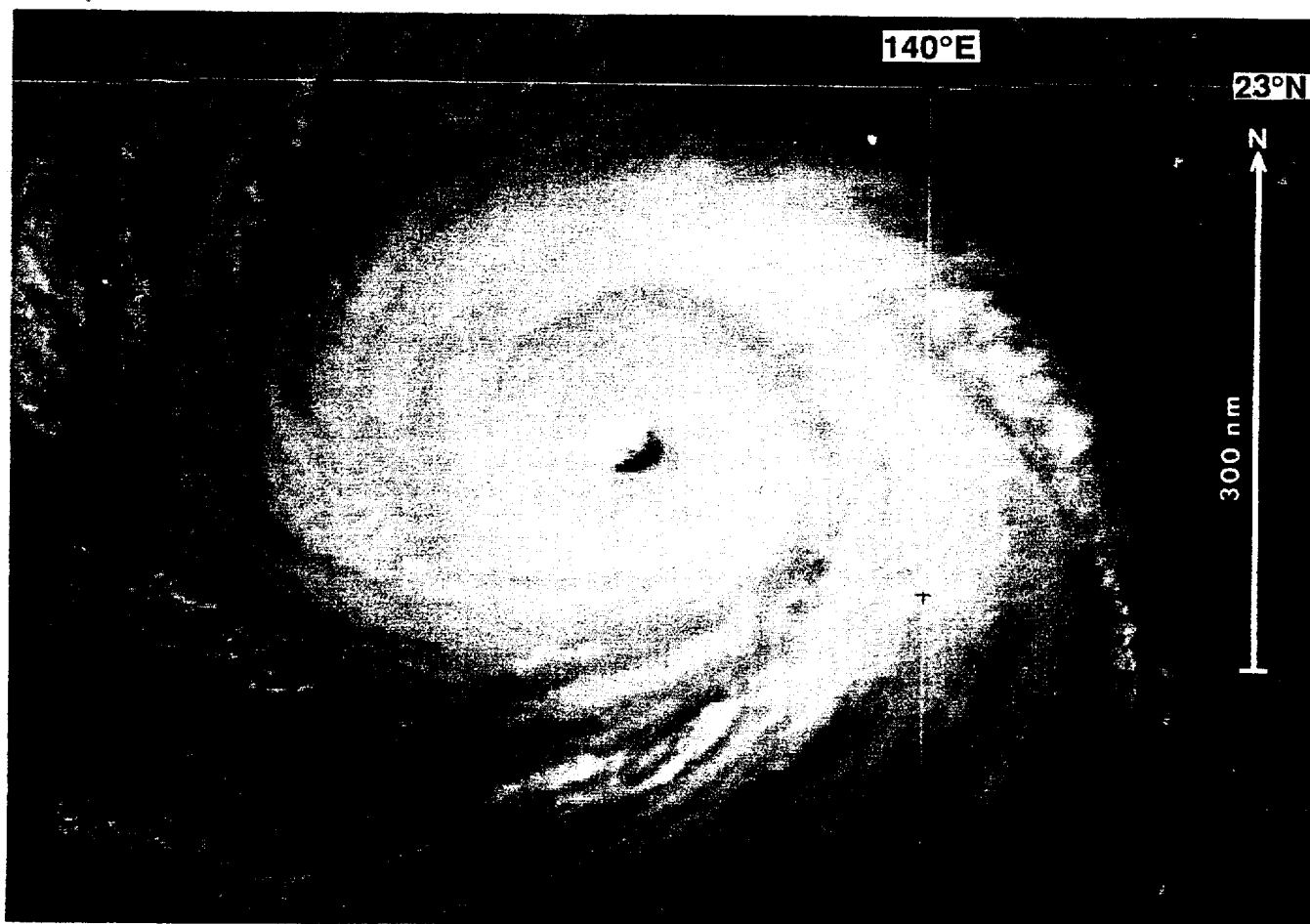


Figure 3-37-4 Super Typhoon Zelda at its peak intensity of 135 kt (69 m/sec) (042331Z November visible GMS imagery).



Figure 3-37-5 Schematic illustration of environmental factors possibly contributing to Zelda's unusual southward motion. Typhoons Verne (33W) (labeled, V) and Wilda (35W) (W) lie along the axis of a reverse oriented monsoon trough, whose axis is moving northward along with these two typhoons. A ridge (zig-zag line) has been induced in the lower and middle troposphere to the southeast of the monsoon trough, and Zelda (Z) has been steered southward around the anticyclonic circulation (labeled, A) along this ridge. The tracks of the tropical cyclones are indicated. Open circle = tropical storm intensity, filled circle = typhoon intensity. Black shaded regions are silhouettes of the deep convection.

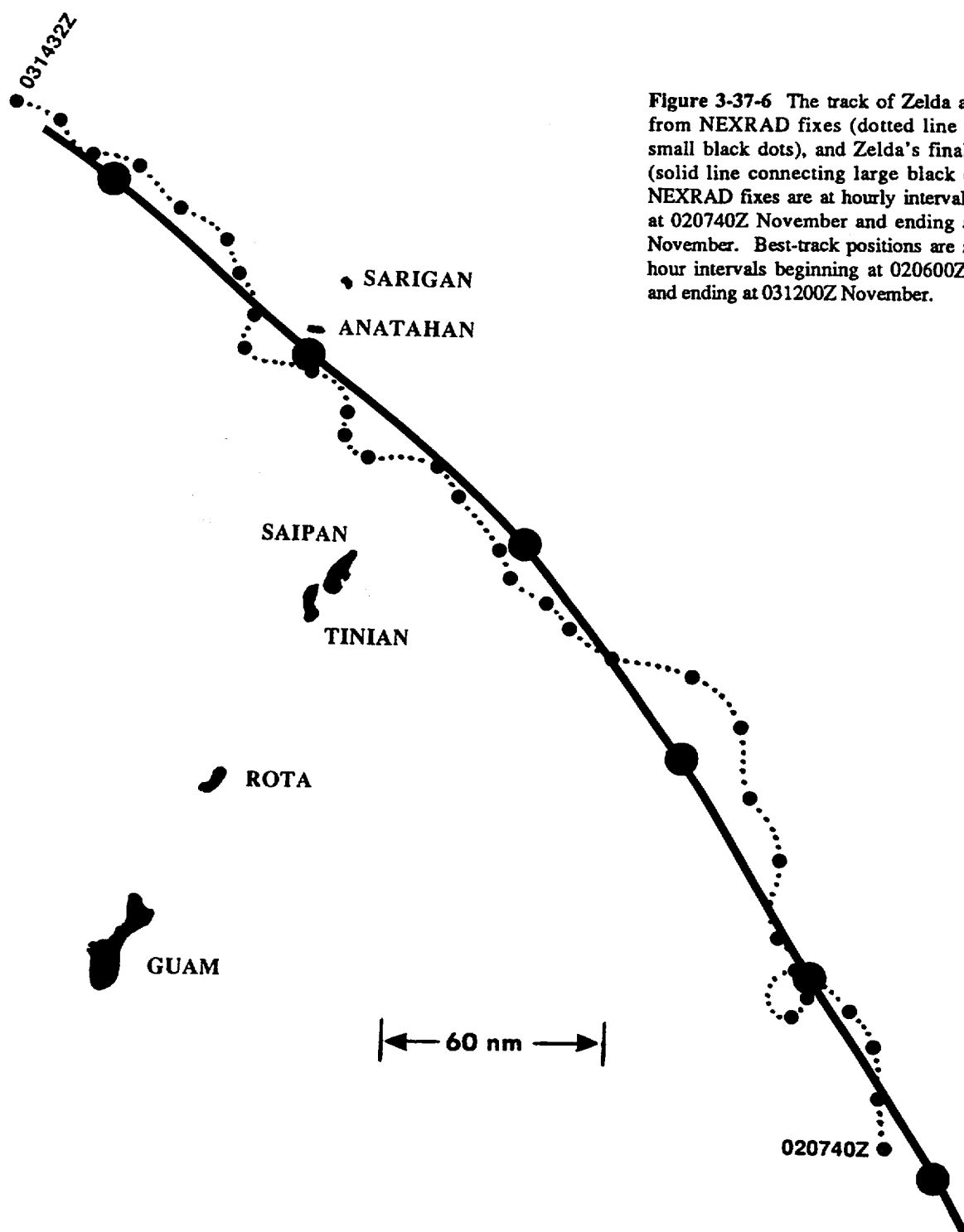


Figure 3-37-6 The track of Zelda as estimated from NEXRAD fixes (dotted line connecting small black dots), and Zelda's final best track (solid line connecting large black dots). The NEXRAD fixes are at hourly intervals beginning at 020740Z November and ending at 031432Z November. Best-track positions are shown at 6-hour intervals beginning at 020600Z November and ending at 031200Z November.

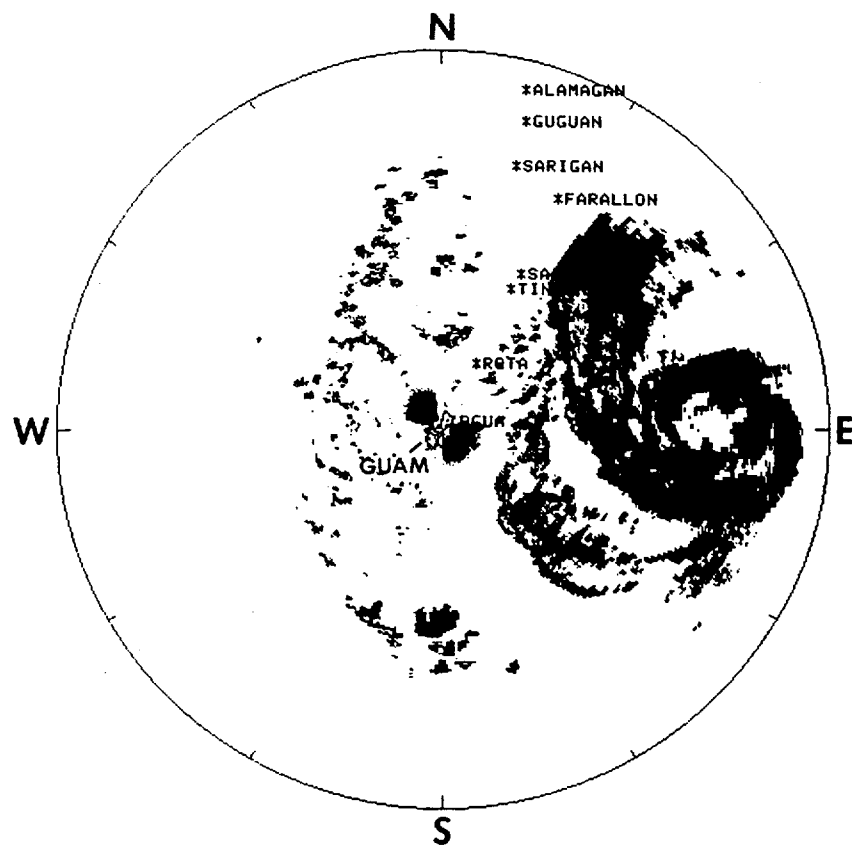
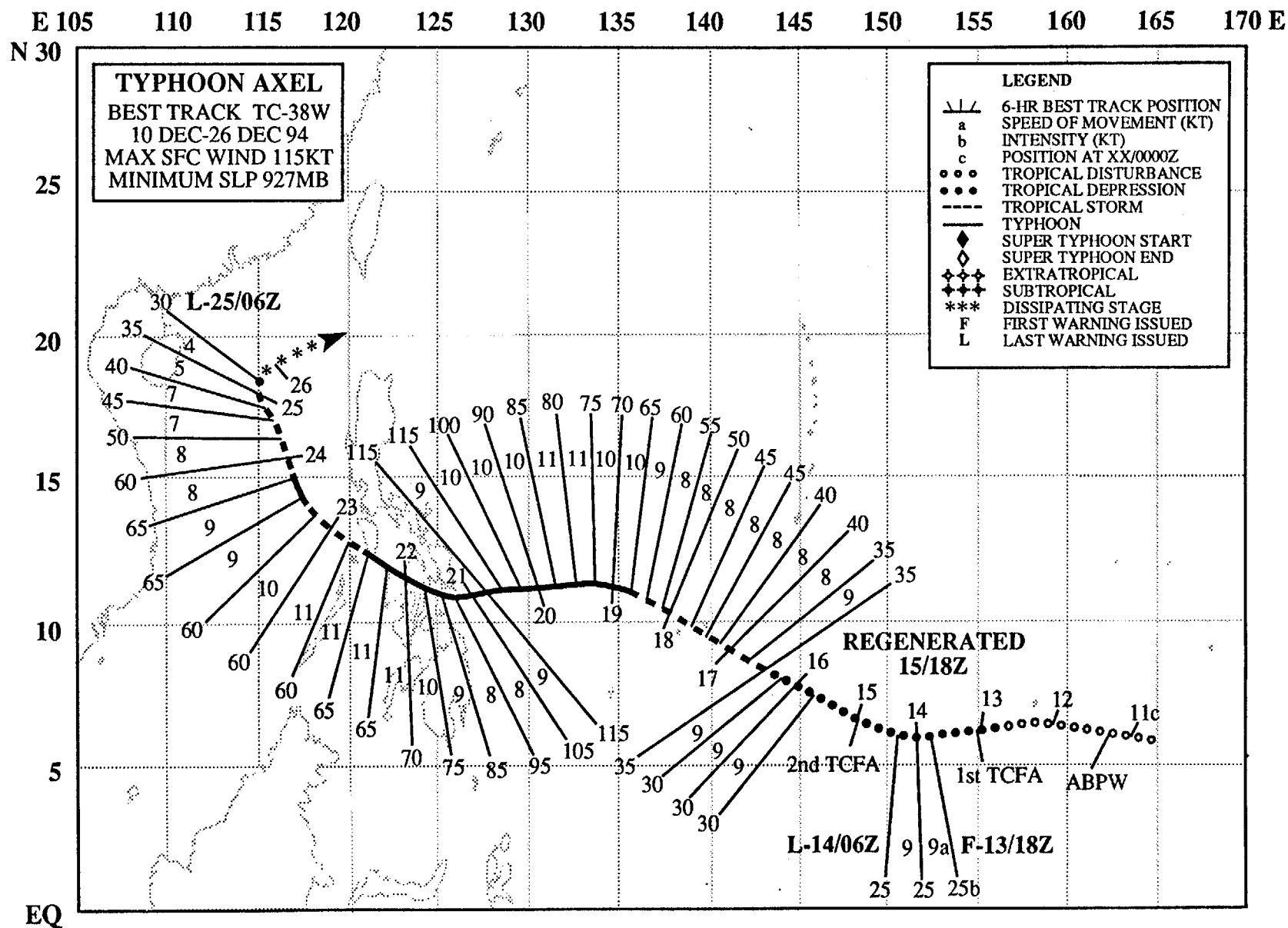


Figure 3-37-7 Zelda's relatively large eye is centered about 170 nm (315 km) to the east of Guam (021415Z November NEXRAD base reflectivity product).



TYPHOON AXEL (38W)

I. HIGHLIGHTS

Axel formed in an active near-equatorial trough during the second week of December after a month of no tropical cyclone activity in the western North Pacific basin. At first, the tropical depression that became Axel failed to mature. The JTWC issued its first warning on the system when it was near Chuuk, then issued a final warning 12 hours later. Thirty-six hours after this final warning, regeneration occurred, and the JTWC resumed warning on the system. Axel crossed the central Philippines and caused extensive damage and loss of life. Approximately 24 hours prior to impacting the Philippines, satellite imagery indicated a very rapid, but brief intensification followed by rapid weakening.

II. TRACK AND INTENSITY

After Zelda (37W) dissipated east of Japan in early November, the tropics of the western North Pacific became very quiet (i.e., the amount of deep convection was greatly reduced), and for more than a month thereafter, no significant tropical cyclones occurred. Axel ended this long period of inactivity as it formed in an active near-equatorial trough (Figure 3-38-1) during the second week of December. For several days prior to Axel's formation, the equatorial region near the international date line was the site of a large cluster of mesoscale convective complexes loosely organized in the twin-trough pattern of Figure 3-38-1a. By 13 December, a distinct low-level circulation center broke away from the cloud cluster and move toward the west. This circulation (pre-Axel) was accompanied by a twin circulation in the Southern Hemisphere (pre-TC 04P) (Figure 3-38-1b).

The tropical disturbance that became Axel was first mentioned on the 110600Z December Significant Tropical Weather Advisory based upon indications from surface reports in the eastern Caroline Islands that a broad surface circulation with an estimated minimum sea-level ppressure of 1006 mb lay beneath an upper-level anticyclone. A Tropical Cyclone Formation Alert was issued at 130100Z based upon 20-30 kt winds measured at an automated weather station on Oroluk Atoll, and also upon improvements in the satellite-observed organization of deep convection in the system. When synoptic observations at Chuuk (WMO 91334) included a gradient-level wind of 35 kt (18 m/sec) and a sea-level pressure below 1004 mb, the first warning was issued on Tropical Depression 38W at 131800Z. Twelve hours later, at 140600Z, a final warning (warning number 3) was issued on Tropical Depression 38W. Quoting from the remarks on this final warning:

“... Tropical Depression 38W has lost its organization, and has weakened over the past 12 hours. The system is ill defined, and has multiple, weak circulations associated with it. ... [it] will be closely monitored for signs of regeneration. ...”

At 142330Z, a second formation alert was issued as the remnants of Tropical Depression 38W began to show signs of regeneration (i.e., an increase in the amount and organization of deep convection near the center of the broad low-level circulation). At 151200Z, warning number 4 was issued on the regenerated Tropical Depression 38W. At 161200Z, the system was upgraded to Tropical Storm Axel. Then, based on satellite imagery that revealed an 11 nm banding eye, Axel was upgraded to typhoon intensity at 190000Z.

Upon reaching 11°N at 181800Z, Axel turned from a west-northwestward heading to a westward heading. The prognostic reasoning for the track forecast at 190000Z included the following comments:

“... our track forecast is still for Axel to lift slightly [i.e., gain latitude] over the next 24-36 hours

then track westward under the subtropical ridge. In the latter part of the forecast period, Axel should begin to dip back [i.e., move west-southwestward] over the southern Philippine islands. . . .”

After moving straight westward until 201200Z, Axel dipped slightly in latitude and passed south of the Philippine island of Samar between 210600Z and 211200Z, and then made landfall on the island of Leyte shortly after 211200Z. The estimated peak intensity of 115 kt (59 m/sec) occurred at 201200Z while Axel was east of the Philippines. As Axel neared the Philippine archipelago, the intensity fell to 85 kt (44 m/sec). The intensity dropped below the typhoon threshold after Axel crossed the Philippines and entered the South China Sea. Later, while in the South China Sea west of Luzon, Axel re-intensified to a minimal typhoon for two warning periods (231200Z and 231800Z). Thereafter, Axel weakened, and the final warning was issued at 250600Z when the deep convection and upper-level cloud cover was sheared away to the east of the exposed low-level circulation center. The system dissipated over water about 200 nm (370 km) southeast of Hong Kong.

III. DISCUSSION

a. Genesis in a near equatorial trough

According to climatology (e.g., Sadler et al. 1987), during November and December, the low-level monsoon westerly winds of the western Pacific collapse into a narrow band straddling the equator between 5°N and 5°S. At these latitudes, near-equatorial troughs are found which separate the monsoonal westerlies from the tradewinds to their north and south. Tropical cyclones may develop in the trough of either hemisphere, and sometimes they do so symmetrically, resulting in tropical cyclone twins.

The eastward penetration of monsoonal westerlies can be correlated to the values of the indices of the El Niño/Southern Oscillation (ENSO) (Lander 1994b); it is greatest when the Southern Oscillation Index (SOI) is strongly negative. During some years when the SOI is very low, the equatorial westerlies extend beyond the international date line. During the summer and autumn of 1994, the SOI was very low. By November 1994, equatorial westerlies pushed eastward into the Marshall Islands. Associated with these equatorial monsoonal westerlies was a region of large-scale deep convection resembling the depiction in Figure 3-38-1a.

The disturbance which became Typhoon Axel developed in the near-equatorial trough of the northern hemisphere (Figure 3-38-1b) in a large-scale monsoonal cloud system such as the one shown in Figure 3-38-1a. Typical of many tropical cyclones that form in the latter part of the year at low latitude in the eastern reaches of a near-equatorial trough, Axel intensified very slowly. After Axel moved a significant distance to the west along the trough axis, gained latitude, and broke from the extensive cloudiness associated with the equatorial westerlies it intensified more rapidly (Figure 3-38-1c). Axel was associated with a twin — TC 04P. Twin tropical cyclones develop simultaneously in each hemisphere and are symmetrical with respect to the equator (Lander 1990) (e.g., see Figure 3-38-1b).

b. Very short-lived high-intensity cloud signature

During the 24-hour period spanning 200000Z through 210000Z, Axel's satellite-observed cloud pattern underwent a remarkable evolution from a pattern indicative of a moderately intense typhoon, to a cloud pattern indicative of an extremely intense typhoon, and then back to a cloud pattern indicative of a moderately intense typhoon. The intensity of a tropical cyclone may be estimated from certain characteristics of its satellite cloud signature using techniques developed by Dvorak (1975, 1984). Most of the time, these characteristics evolve gradually, and the estimated intensity of a deepening tropical cyclone

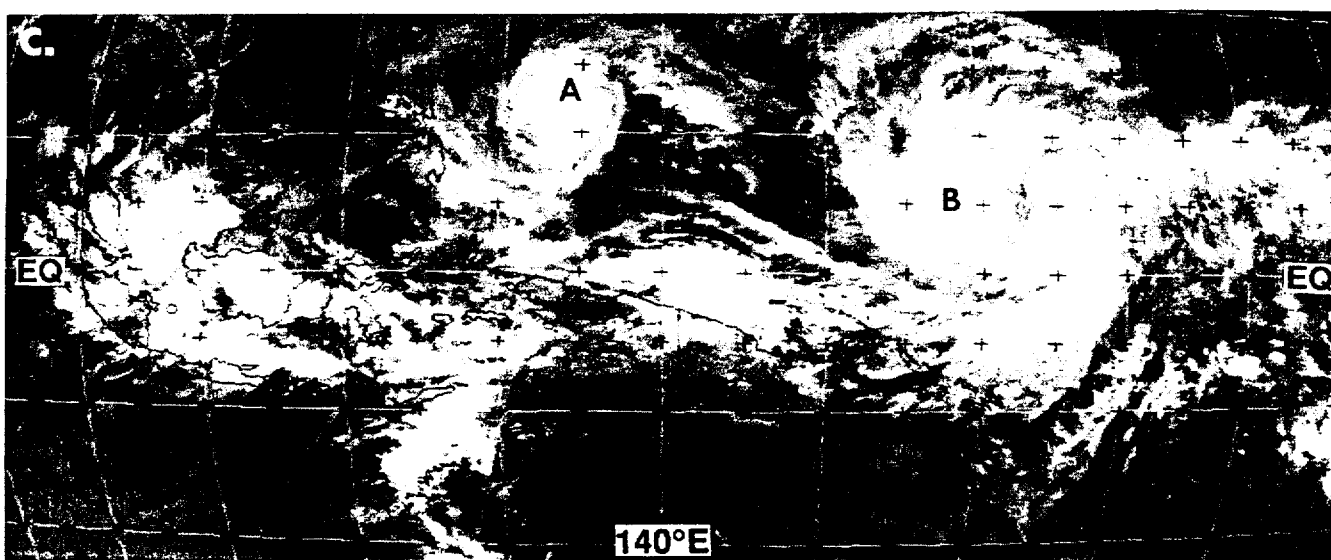
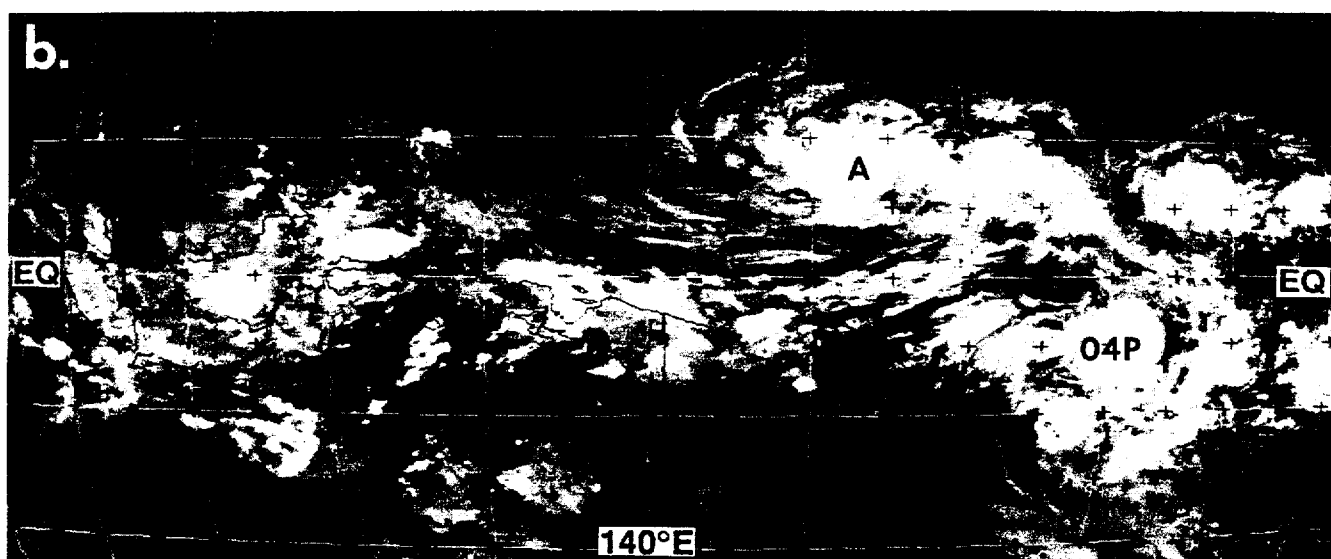
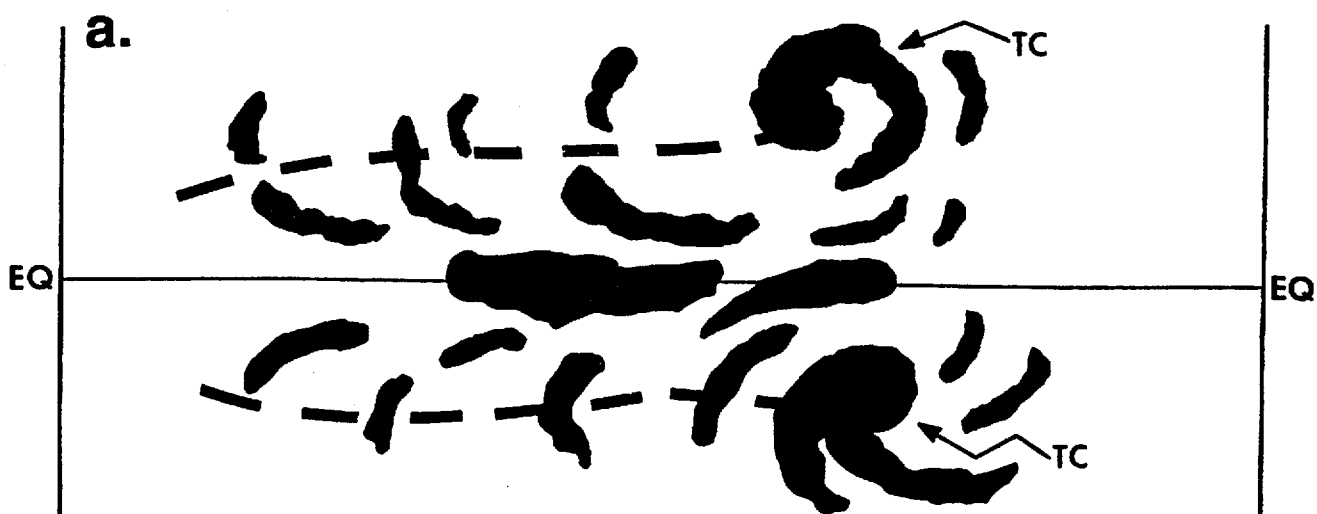


Figure 3-38-1 (Preceding page)(a) Schematic illustration of the twin-trough pattern that is common in the western Pacific during November and December. Black silhouettes indicated deep convection. Dashed line shows axes of the near-equatorial troughs. Tropical cyclones (labeled TC) are forming in each hemisphere. (b) Axel (labeled A) and Tropical Cyclone 04P are seen developing in near symmetry within a cloud pattern associated with twin near-equatorial troughs (122131Z December infrared GMS imagery). (c) Axel (labeled A) has moved west-northwestward along the axis of the monsoon trough and has become separated from the monsoonal cloudiness along the equator. A large monsoon depression (labeled B) that became Bobbie (39W) is seen forming at the eastern reaches of the monsoon trough in approximately the same area that Axel had formed a week earlier (190031Z December infrared GMS imagery).

typically rises by one “T” number per day until the peak intensity is reached. Few tropical cyclones reach a peak intensity above a T 6.0 (i.e., greater than 115 kt).

At 200532Z, the estimated intensity of Axel, based upon satellite imagery, was 77 kt (40 m/sec) (i.e., a “T” number of 4.5). A dramatic sharpening of Axel’s eye, accompanied by thickening and cooling of the tops of the eye wall cloud, took place over the next six hours. An intensity estimate of T 7.0 may be derived from the 201231Z cloud signature (Figure 3-38-2). Zehr (personal communication), who developed an automated Dvorak routine, registered a T 7.3 for Axel at this time. However, soon after this peak, the eye (and the eye wall cloud) became poorly defined: the eye wall cloud tops warmed, and breaks appeared. At 202331, the estimated T number had dropped to 5.0 (see Table 3-38-1). For deepening tropical cyclones, the intensity of the tropical cyclone parallels the T number (i.e., there is no lead or lag between the satellite-observed T number and the corresponding intensity of the tropical cyclone). Axel is a rare case where the satellite intensity estimates exhibited extraordinarily large and extremely rapid changes. Without ground truth or in situ measurements, it is not possible to determine if the

changes in the satellite-observed cloud signature of Axel corresponded to similar extraordinarily large and extremely rapid changes in the maximum sustained wind.

IV. IMPACT

Axel’s greatest impact was to the central Philippines. At 180000Z, with an intensity of 50 kt (26 m/sec), Axel passed 30 nm (55 km) to the north of Yap where only minor damage to vegetation was reported. In the Philippines, however, Axel’s impact was far more serious. At least 12 people died in the central Philippines. Flood waters breached a dam, drowning five people and injuring 25 in Bacolod City, 260 nm (480 km) southeast of Manila. In Talcoban City, capital of Leyte province, seven people died and 17 were reported missing. On the southern

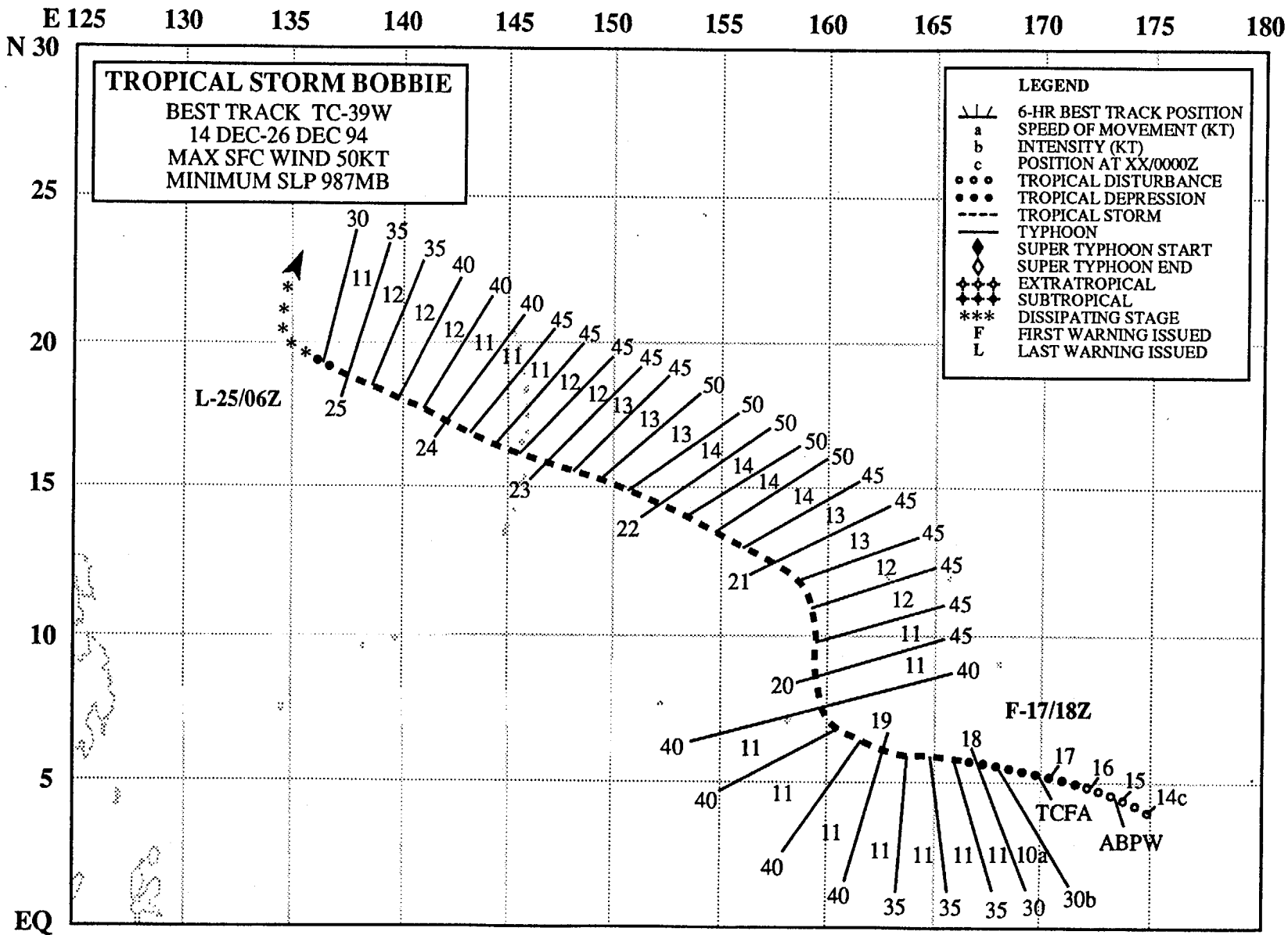


Figure 3-38-2 Axel shown at a time when its satellite cloud signature acquired characteristics of an extremely intense typhoon. The enhancement curve known as MB highlights the well-defined eye and the azimuthally symmetric wide and cold-topped eye wall. (201231Z December infrared GMS imagery).

island of Mindanao, huge waves whipped up by the approaching typhoon destroyed 163 houses, leaving 897 people homeless. In total 1,443 houses were destroyed, leaving at least 7,930 people homeless. A 12-hour power blackout affected Manila when strong winds knocked down a major transmission line on Luzon.

TABLE 3-38-1 Estimated intensity of Axel from Enhanced Infrared Imagery (EIR) during the period 200031Z December to 202331Z December.

Time	T number	Corresponding wind speed
200031Z	4.5	77 kt (40 m/sec)
200532Z	4.5	77 kt (40 m/sec)
200831Z	5.5	102 kt (53 m/sec)
200931Z	5.5	102 kt (53 m/sec)
201024Z	6.0	115 kt (59 m/sec)
201131Z	7.0	140 kt (72 m/sec)
201231Z	7.0	140 kt (72 m/sec)
201331Z	7.0	140 kt (72 m/sec)
201531Z	6.5	127 kt (65 m/sec)
201624Z	6.5	127 kt (65 m/sec)
201831Z	5.5	102 kt (53 m/sec)
202031Z	5.5	102 kt (53 m/sec)
202331Z	5.0	90 kt (46 m/sec)



TROPICAL STORM BOBBIE (39W)

I. HIGHLIGHTS

Bobbie was the last significant tropical cyclone of 1994 in the western North Pacific. For its entire life, it was a sheared system with the low-level circulation center displaced from the deep convection. Its low-level circulation center was often obscured beneath cirrus debris. The cirrus shield over its deep convection lacked the typical characteristics produced by shear. SSM/I imagery from the DMSP satellites, and scatterometer-derived winds from the ERS-1 satellite (in conjunction with conventional IR and visible imagery) were instrumental in determining the location and structure of Bobbie.

II. TRACK AND INTENSITY

During mid-December 1994, the large-scale low-level wind pattern of the deep tropics of the western North Pacific featured equatorial westerlies bounded by near-equatorial troughs at roughly 5°N and 5°S. The equatorial westerlies and associated large-scale deep convection extended eastward beyond the international date line. This flow pattern occurs frequently during the Spring and late Fall, and has been defined as the "twin trough" pattern (see Figure 3-39-1). Most episodes of twin tropical cyclones occur in association with this large-scale low-level wind pattern. On 15 December, an area of persistent convection associated with a broad, weak surface circulation in the Marshall Islands was mentioned in the 150600Z December Significant Tropical Weather Advisory. At 170430, a Tropical Cyclone Formation Alert was issued. It stated, in part:

"... a pre-existing [low-level] circulation with persistent convection [is intensifying]. ... surface pressures [have dropped] in the vicinity of Majuro. Their synoptic observation from 170300Z showed [the] surface pressure at 1002.7 mb ... this system is elongated east-west and may have several circulation centers."

Based on further synoptic data from the Marshall Islands, a tropical depression warning was issued at 171800Z. Remarks contained on this warning included:

"... this system is poorly organized at the present time, but is showing signs of steady development. The minimum central pressure in the broad low pressure region is estimated to be 1002 mb. If the

[JTWC] anticipates that this tropical depression will reach tropical storm intensity, then a standard 72-hour tropical cyclone warning will be issued ..."

At 181800, JTWC forecasters predicted that the the tropical depression would become a tropical storm in 24 hours, so a standard 72-hour tropical cyclone warning was issued. Remarks on this warning stated:

"... synoptic data from Micronesia

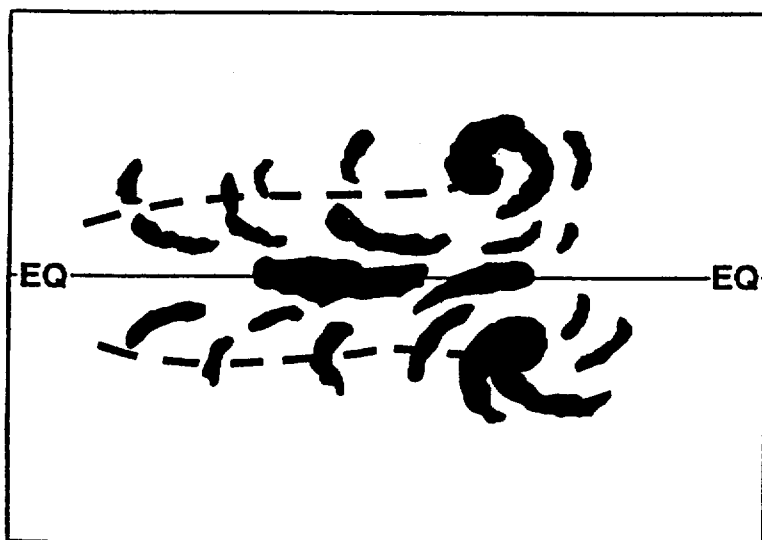


Figure 3-39-1 Schematic illustration of the distribution of deep convection associated with the "twin-trough" pattern. The axes of the near-equatorial troughs are represented by dashed lines.

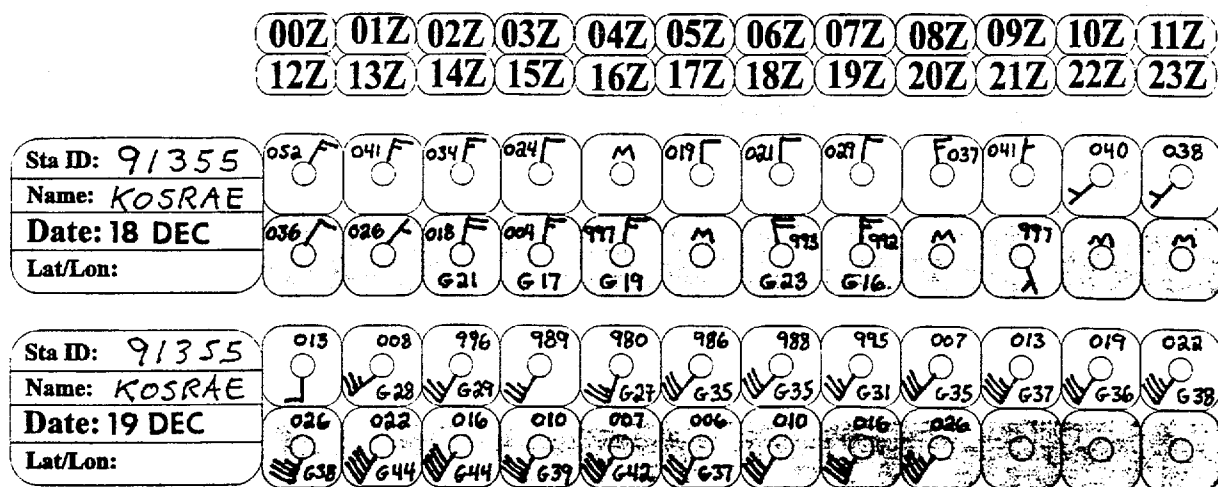


Figure 3-39-2 Time series of hourly synoptic observations at Kosrae (WMO 91355) as Bobbie passed near the island from east to west.

indicate that Tropical Depression 39W is steadily deepening over a large area. Near-gale force winds are present north of the broad low pressure center. . . . [the] warning position is based on the estimated position of the low pressure center from synoptic data; satellite imagery does not reveal a single, well-defined cyclone center and is considered to be unreliable at the present time. . . .”

This disturbance had the characteristics of a monsoon depression (JTWC 1993): a large (1500 km diameter) region of cyclonic wind flow, a relatively large (200 km diameter) light wind core, and a lack of persistent central convection. At 190000Z, the system was upgraded to Tropical Storm Bobbie based upon visible satellite imagery and synoptic reports from Kosrae (WMO 91355) and Pingelap (91352). Synoptic data from Kosrae (Figure 3-39-2) indicated that a band of 40 kt (21 m/sec) southwesterly wind existed in the southeastern quadrant of Bobbie.

At 191200Z, Bobbie turned toward the north for 24 hours and then, at 201200Z, resumed a west-northwestward track. Bobbie intensified very slowly and reached its peak intensity of 50 kt (26 m/sec) at 220000Z. Between 230000Z and 230600Z, the broad low-level center of Bobbie passed 60 nm (110 km) to the north of Saipan. Bobbie continued on a west-northwestward track until 251800Z when its remnant low-level circulation turned north and recurved.

III. DISCUSSION

In its simplest form, the deep convection associated with a “shear”-type tropical cyclone is displaced down-shear of the low-level circulation center (LLCC). The cirrus emanating from the top of this deep convection is carried farther down-shear leaving the LLCC exposed (i.e., not obscured by deep convection or by cirrus debris) (Figure 3-39-3). In such cases, the diagnosis of the position and intensity is relatively easy, especially during the daylight hours when the LLCC is easily detected in visible satellite imagery. The intensity is estimated based upon the tightness of curvature of the low-level cloud lines (Dvorak 1975) and by the separation distance of the LLCC from the edge of the cirrus canopy over the deep convection. On IR imagery, the intensity is estimated from the separation distance of the LLCC

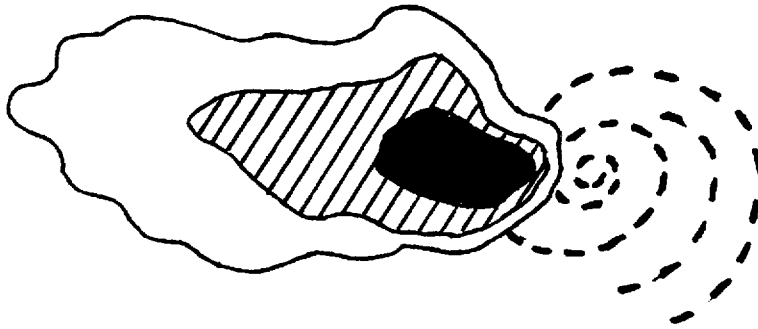


Figure 3-39-3 Schematic illustration of the structure of a typical sheared tropical cyclone. Black-shaded region shows coldest cloud top temperature. Dashed lines show low-level cloud lines. Vertical shear from the east has sharpened the temperature gradient on the eastern side of the deep convection, and has caused the low-level circulation center to become exposed on the eastern side of the deep convection.

from the edge of dense cirrus with a threshold equivalent black-body temperature of -42°C (Dvorak 1984). The highest intensity that can be diagnosed for a developing TC with a “shear” type cloud pattern is 55 kt (28 m/sec).

At intensities greater than 55 kt (28 m/sec), the LLCC tends to be under the dense cirrus canopy, or surrounded by spiral bands of deep convection. As soon as the LLCC is deemed to have moved under the cirrus canopy, the pattern type changes to “central dense overcast” (CDO). On visible satellite imagery, the intensity of a tropical cyclone with a CDO cloud pattern is determined primarily by the diameter of the CDO. On IR imagery, it is determined by the estimated embedded distance of the LLCC under the cold cirrus cloud canopy.

On some occasions, the LLCC of a tropical cyclone that possesses a “shear” type cloud pattern is often difficult to locate with conventional visible and IR imagery. Cirrus debris may obscure the low-level cloud lines. This is especially true at night when only IR imagery is available, and thin cirrus, which may not obstruct the view of the low-level cloud lines in visible imagery, is completely obstructive to the view of low-level features. The nighttime difficulty of tracking an exposed LLCC has led to the common diagnostic error that has come to be known as the “sunrise surprise”. This occurs when the analyst estimates the position of the LLCC too close to the deep convection at night, only to find it displaced a larger distance from it on the first visible image of morning.

Even in the absence of distinct low-level cloud lines marking the LLCC of a “shear” type tropical cyclone, the position of the LLCC may be estimated (with less confidence) by other manifestations of shear in the deep convection. Under shearing conditions, the up-shear side of the cold-cloud canopy usually has a sharp edge (Figure 3-39-3), and the down-shear side the cirrus thins more gradually. On enhanced IR (EIR) imagery, sharp temperature gradients are found on the up-shear side of the cirrus cloud shield and much less steep gradients of temperature are found down-shear (Figure 3-39-3). For diagnostic purposes, it is best to position the LLCC on the up-shear edge of the cloud at a separation distance consistent with earlier visible imagery, and consistent with the past motion and expected changes of intensity.

For much of its life, Bobbie’s cirrus outflow exhibited no apparent manifestation of shear. Its cirrus canopy and cirrus outflow were symmetrical with respect to the cloud system center (CSC). The persistent convection on the western side of the LLCC — at first showing conventional manifestations of shear (i.e., an easily detected LLCC east of the deep convection and cirrus outflow streaming westward from this deep convection) — became symmetrical in appearance (Figure 3-39-4). In addition to the

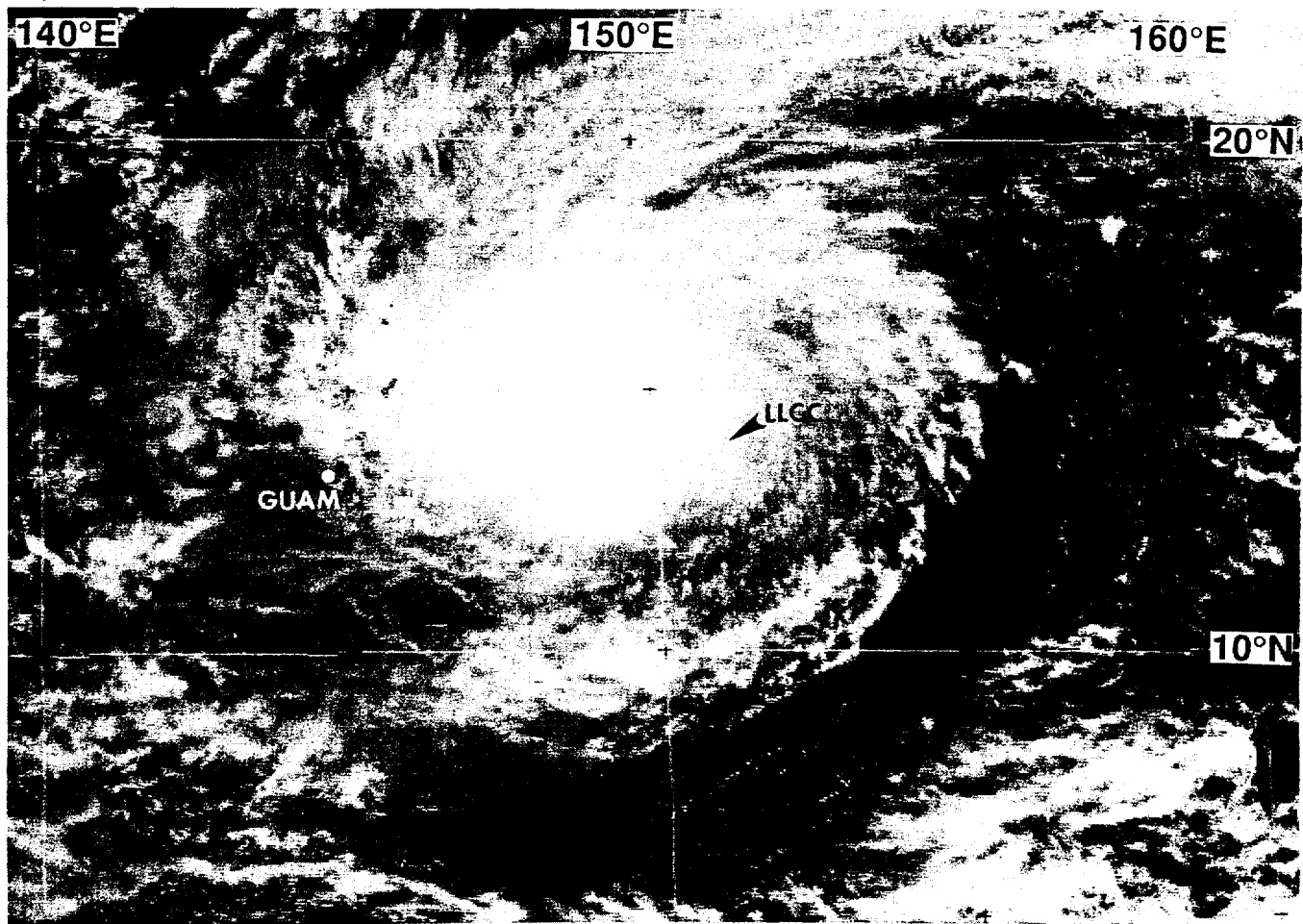


Figure 3-39-4 Bobbie at its peak intensity of 50 kt (26 m/sec). The low-level circulation center (labeled "LLCC") is displaced about 120 nm to the southeast of the center of the deep convection (220031Z December visible GMS imagery).

symmetry of the cloud shield, the LLCC was obscured by cirrus debris. At the time of the imagery in Figure 3-39-4, the LLCC was difficult to locate. Satellite analysts at the JTWC considered the option of locating the LLCC closer to the CSC, thereby increasing the intensity estimate of Bobbie to the typhoon threshold. However, the rapid motion resulting from such a placement, and the constraint of prior knowledge of the sheared structure of the system were factored into the decision to position the LLCC east of the CSC and thereby hold the intensity estimate below the typhoon threshold. Wind vectors obtained from the scatterometer aboard the ERS-1 satellite (Figure 3-31-5) later confirmed the large displacement of the LLCC from the CSC at the time of the satellite image in Figure 3-39-4.

A day later, the large displacement of the LLCC of Bobbie to the east-southeast of the CSC was confirmed by visible satellite imagery (Figure 3-39-6a) and by microwave imagery (Figure 3-39-b) obtained from a DMSP satellite. Conventional unenhanced IR imagery (Figure 3-39-6d) and enhanced IR imagery (Figure 3-39-6e) gave little indication of the large displacement of the LLCC from the CSC. Microwave images of Bobbie (Figures 3-39-6b,c) clearly depict the structure of the system: the roots of the deep convection responsible for the large oval-shaped cirrus cloud canopy seen in the visible and IR imagery (Figure 3-39-6a,d,e) are to the west of the LLCC along a major spiral band leading into a well-defined LLCC. Additional confirmation of the large (120 nm ; 220 km) displacement of the LLCC of

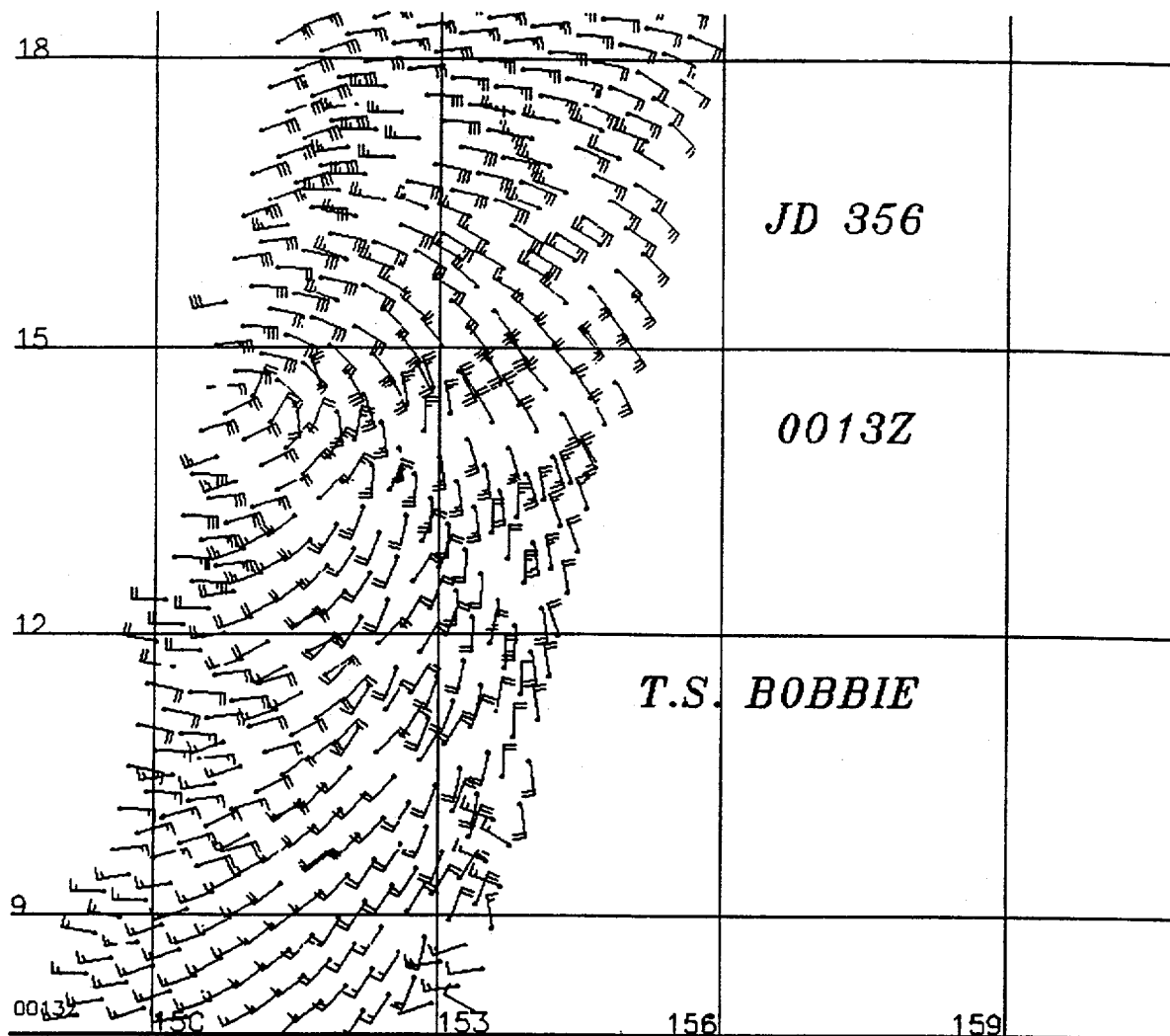


Figure 3-39-5 Wind vectors derived from the scatterometer aboard the ERS-1 satellite clearly indicate the location of Bobbie's low-level circulation center. Maximum wind vector is 35 kt (17 m/sec) on the north side of the circulation center. The timing of this pass (220013Z December) is nearly coincident with the visible image in Figure 3-39-4.

Bobbie from its CSC was obtained from synoptic reports in the Mariana Islands during Bobbie's passage through that region.

To summarize, the structure of Bobbie was difficult to diagnose for a large portion of its track, especially as it neared and passed through the Mariana island chain. Despite the presence of a persistent, large, oval-shaped dense cirrus canopy (which could have been diagnosed as the CDO of the system), a very careful study of visible satellite imagery, coupled with valuable additional information from microwave imagery and scatterometer winds indicated that the LLCC of Bobbie was well-displaced from the CSC (Figures 3-39-7). The total suite of multi-spectral information (visible, IR, active and passive microwave, and radar reflectivity) from numerous remote sensing platforms (i.e., the GMS, NOAA, DMSP, and ERS-1 satellites; and, Guam's NEXRAD), was absolutely essential to accurately locating the LLCC of Bobbie, and reasonably diagnosing its intensity.

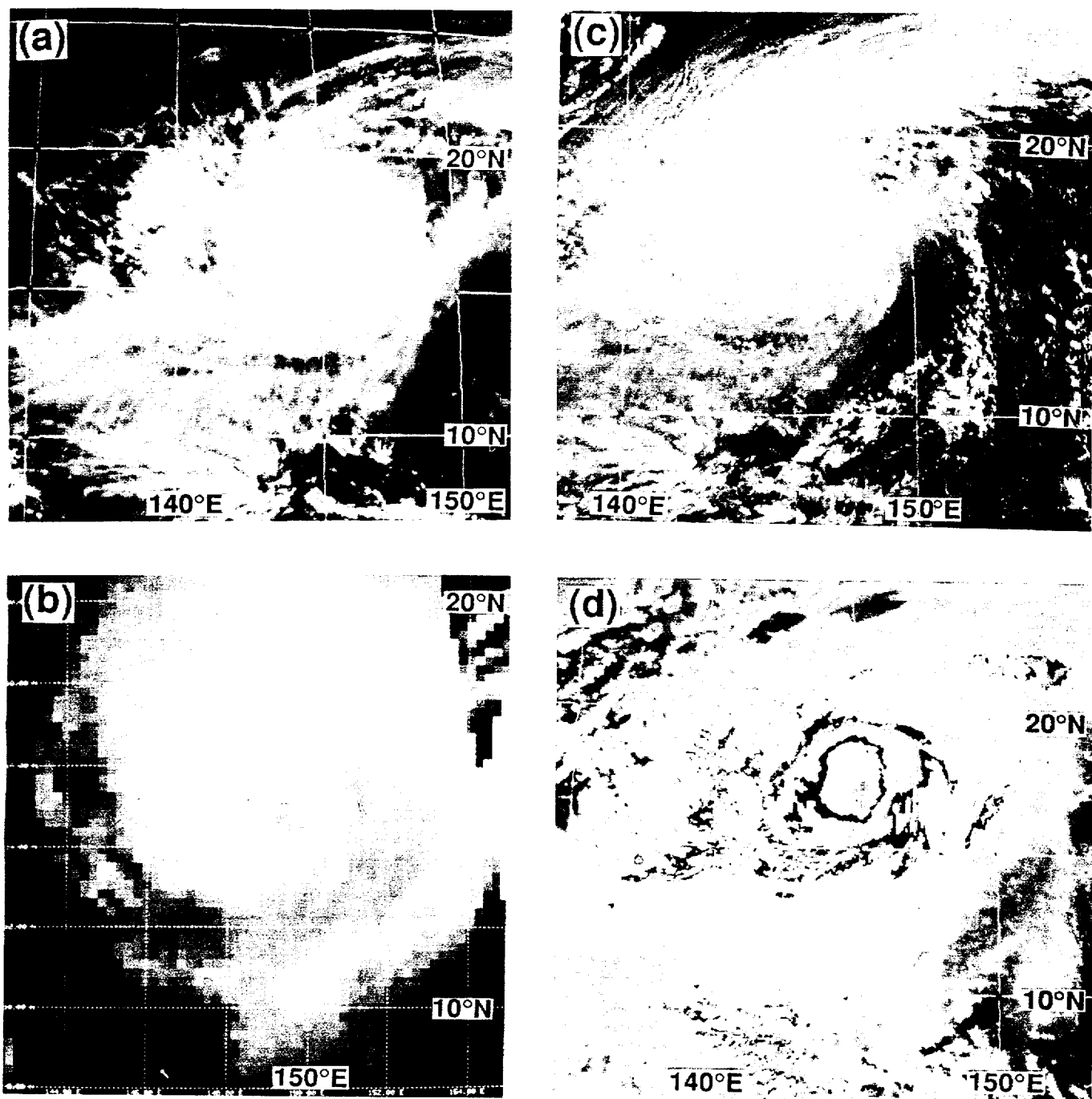


Figure 3-39-6 (a) Cirrus outflow from Bobbie's deep convection appears to be nearly symmetrical (230031Z December infrared GMS imagery). (b) Bobbie's deep convection is seen to be located on a major spiral band which wraps into a well-defined low-level circulation center (230014Z December DMSP 85H microwave imagery). (c) The low-level circulation center of Bobbie is relatively easy to locate beneath thin cirrus to the east-southeast of the deep convection (230031Z December GMS visible imagery). (d) Enhancing the IR imagery in (a) fails to reveal any of the traditional manifestations of vertical shear (230031Z December enhanced infrared GMS imagery).

IV. IMPACT

Bobbie brought heavy rain and gales to some islands and atolls in Micronesia. No reports of injuries or significant damage were received.

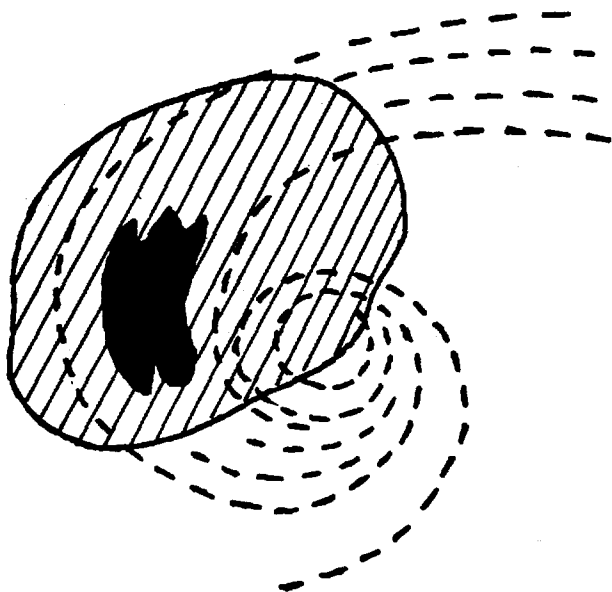


Figure 3-39-7 Schematic illustration of the structure of Bobbie as it passed through the Mariana island chain. Deep convection (black-shaded region) is located well to the west-northwest of the low-level circulation center, and is producing a large nearly symmetrical cirrus canopy (hatched region). The symmetry of the cirrus canopy, and its blocking of the view of the low-level circulation center, made diagnosis of the position and intensity of Bobbie relatively difficult. Microwave imagery and scatterometer-derived winds were valuable in defining the structure of Bobbie.

3.2 NORTH INDIAN OCEAN TROPICAL CYCLONES

1994 was an average year for North Indian Ocean tropical cyclone activity. Spring and fall in the North Indian Ocean are periods of transition between major climatic controls, and are the most favorable seasons for tropical cyclone activity. Of the five significant tropical cyclones that occurred this year; three were in the spring (TC 01B, TC02B, and TC 03A), and two were in the fall (TC 04B and TC05A) (Table 3-5). The climatological average for tropical cyclone occurrence in this basin is five, with peaks in the spring and fall (Table 3-6).

The best track composites for the 1994 North Indian Ocean tropical cyclones are shown in Figure 3-14. The most notable of these storms is Tropical Cyclone 02B. Its track and intensity characteristics are nearly identical to Tropical Cyclone 02B of 1991, which was responsible for 138,000 deaths in Bangladesh. Fortunately, the death toll from this year's TC 02B was far lower. The two tropical cyclones which occurred in the North Arabian Sea (TC 03A in June and TC 05A in November) are interesting in that they both moved along non-climatological westward tracks.

Table 3-5 NORTH INDIAN OCEAN SIGNIFICANT TROPICAL CYCLONES FOR 1994

TROPICAL CYCLONE	PERIOD OF WARNING	NUMBER OF WARNINGS ISSUED	MAXIMUM SURFACE WINDS-KT (M/SEC)	ESTIMATED MSLP (MB)
TC 01B	22 MAR - 25 MAR	11	40 (21)	994
TC 02B	29 APR - 03 MAY	18	125 (64)	916
TC 03A	07 JUN - 09 JUN	8	45 (23)	991
TC 04B	30 OCT - 31 OCT	4	45 (23)	991
TC 05A	15 NOV - 20 NOV	19	55 (28)	984
TOTAL		60		

The criteria used in Table 3-6 are as follows:

1. If a tropical cyclone was first warned on during the last two days of a particular month and continued into the next month for longer than two days, then that system was attributed to the second month.
2. If a tropical cyclone was warned on prior to the last two days of a month, it was attributed to the first month, regardless of how long the system lasted.
3. If a tropical cyclone began on the last day of the month and ended on the first day of the next month, that system was attributed to the first month. However, if a tropical cyclone began on the last day of the month and continued into the next month for only two days, then it was attributed to the second month.

TABLE 3-6 LEGEND

Total for the month/year	→	2
Typhoons	→	2 0 0
Tropical Storms	→	
Tropical Depressions	→	

Table 3-6 DISTRIBUTION OF NORTH INDIAN OCEAN TROPICAL CYCLONES FOR 1975-1994

YEAR	JAN	FEB	MAR	APR	MAY	JUN	JUL	AUG	SEP	OCT	NOV	DEC	TOTALS
1975	1	0	0	0	2	0	0	0	0	1	2	0	6
	010	000	000	000	200	000	000	000	000	100	020	000	3 3 0
1976	0	0	0	1	0	1	0	0	1	1	0	1	5
	000	000	000	010	000	010	000	000	010	010	000	010	0 5 0
1977	0	0	0	0	1	1	0	0	0	1	0	2	5
	000	000	000	000	010	010	000	000	000	010	000	110	1 4 0
1978	0	0	0	0	1	0	0	0	0	1	2	0	4
	000	000	000	000	000	000	000	000	000	010	200	000	2 2 0
1979	0	0	0	0	1	1	0	0	2	1	2	0	7
	000	000	000	000	100	010	000	000	011	010	011	000	1 4 2
1980	0	0	0	0	0	0	0	0	0	0	1	1	2
	000	000	000	000	000	000	000	000	000	000	010	010	0 2 0
1981	0	0	0	0	0	0	0	0	1	0	1	1	3
	000	000	000	000	000	000	000	000	010	000	100	100	2 1 0
1982	0	0	0	0	1	1	0	0	0	2	1	0	5
	000	000	000	000	100	010	000	000	000	020	100	000	2 3 0
1983	0	0	0	0	0	0	0	1	0	1	1	0	3
	000	000	000	000	000	000	000	010	000	010	010	000	0 3 0
1984	0	0	0	0	1	0	0	0	0	1	2	0	4
	000	000	000	000	010	000	000	000	000	010	200	000	2 2 0
1985	0	0	0	0	2	0	0	0	0	2	1	1	6
	000	000	000	000	020	000	000	000	000	020	010	010	0 6 0
1986	1	0	0	0	0	0	0	0	0	0	2	0	3
	010	000	000	000	000	000	000	000	000	000	020	000	0 3 0
1987	0	1	0	0	0	2	0	0	0	2	1	2	8
	000	010	000	000	000	020	000	000	000	020	010	020	0 8 0
1988	0	0	0	0	0	1	0	0	0	1	2	1	5
	000	000	000	000	000	010	000	000	000	010	110	010	1 4 0
1989	0	0	0	0	1	1	0	0	0	0	1	0	3
	000	000	000	000	010	010	000	000	000	000	100	000	1 2 0
1990	0	0	0	1	1	0	0	0	0	0	1	1	4
	000	000	000	001	100	000	000	000	000	000	001	010	1 1 2
1991	1	0	0	1	0	1	0	0	0	0	1	0	4
	010	000	000	100	000	010	000	000	000	000	010	000	1 3 0
1992	0	0	0	0	1	2	1	0	1	3	3	2	13
	000	000	000	000	100	020	010	000	001	021	210	020	3 8 2
1993	0	0	0	0	0	0	0	0	0	0	2	0	2
	000	000	000	000	000	000	000	000	000	000	200	000	2 0 0
1994	0	0	1	1	0	1	0	0	0	1	1	0	5
	000	000	010	100	000	010	000	000	000	010	010	000	1 4 0
(1975-1994)													
AVERAGE	0.2	0.1	0.1	0.2	0.6	0.6	0.1	0.1	0.3	0.9	1.5	0.5	4.9
CASES	3	1	1	4	12	12	1	1	5	18	29	10	97

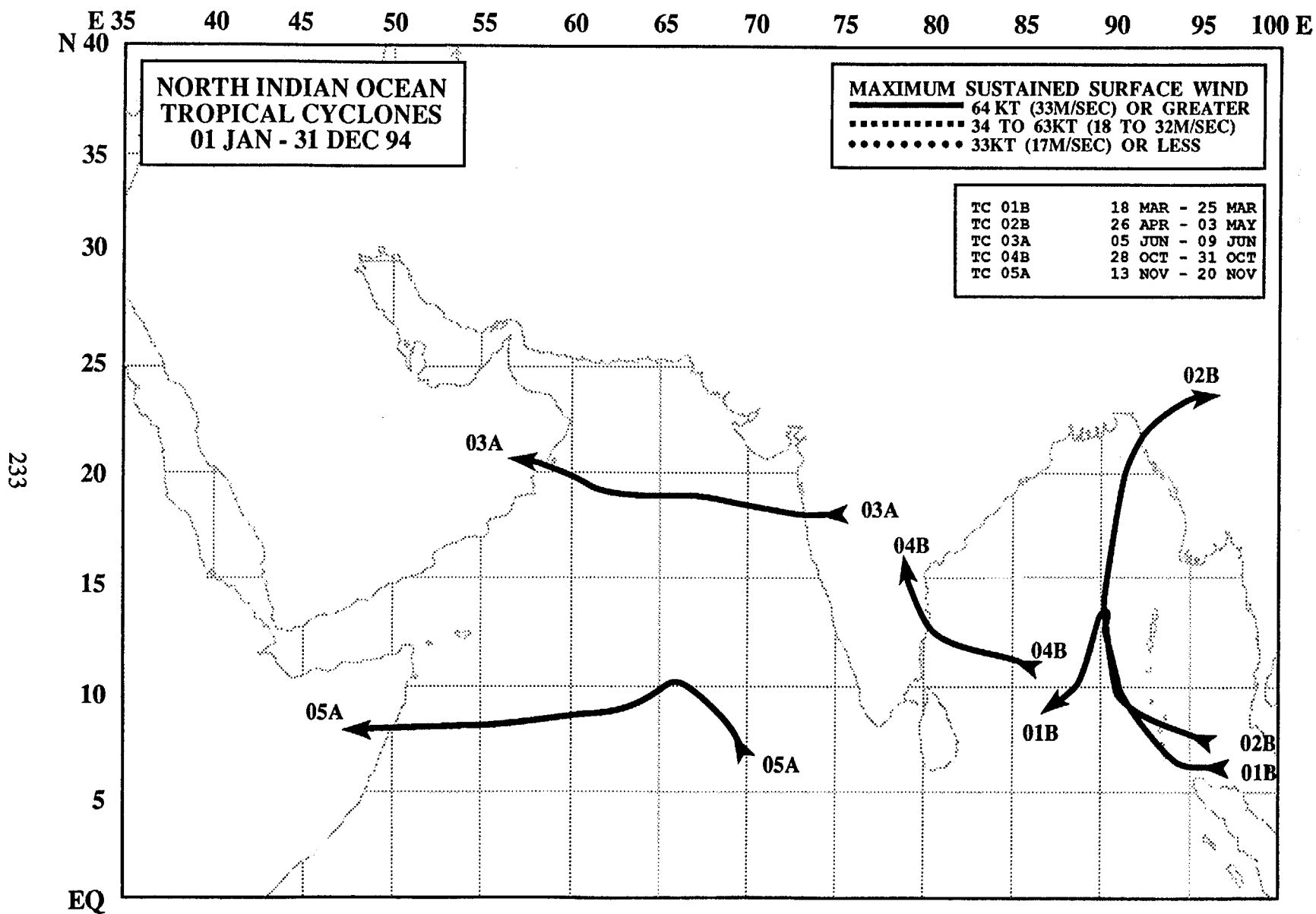
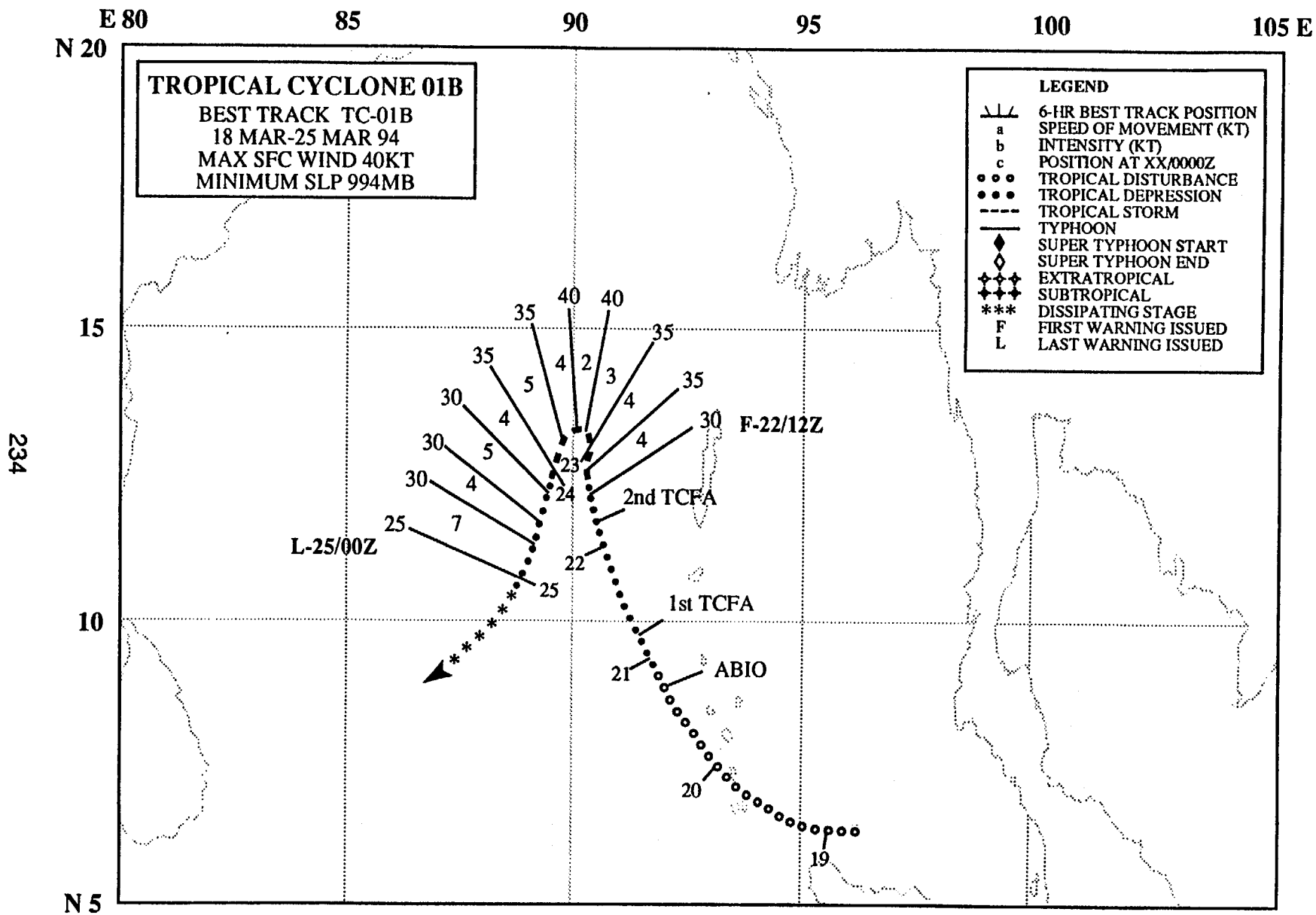


Figure 3-14 Composite best track for the North Indian Ocean tropical cyclones for 1994.



TROPICAL CYCLONE 01B

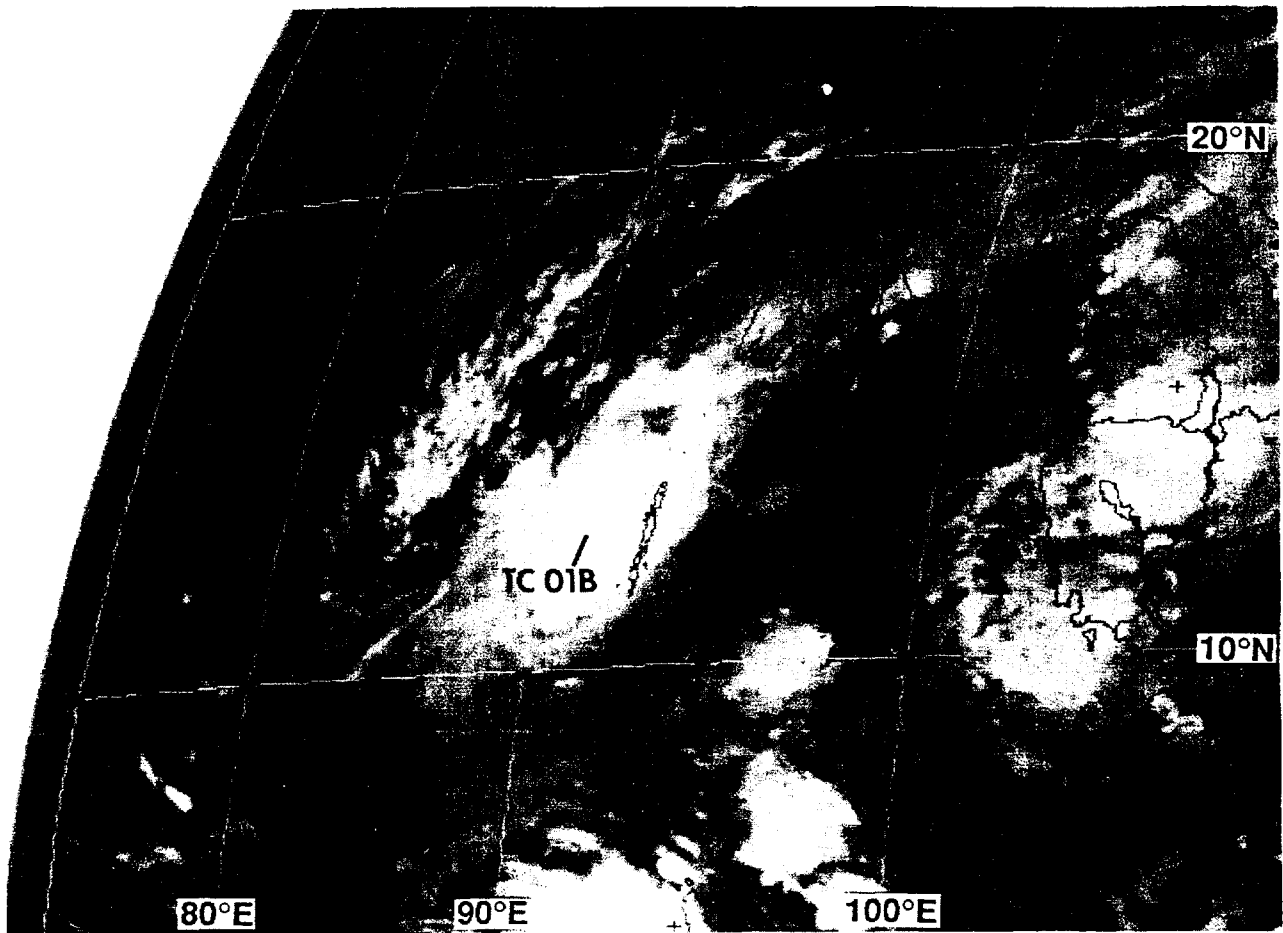
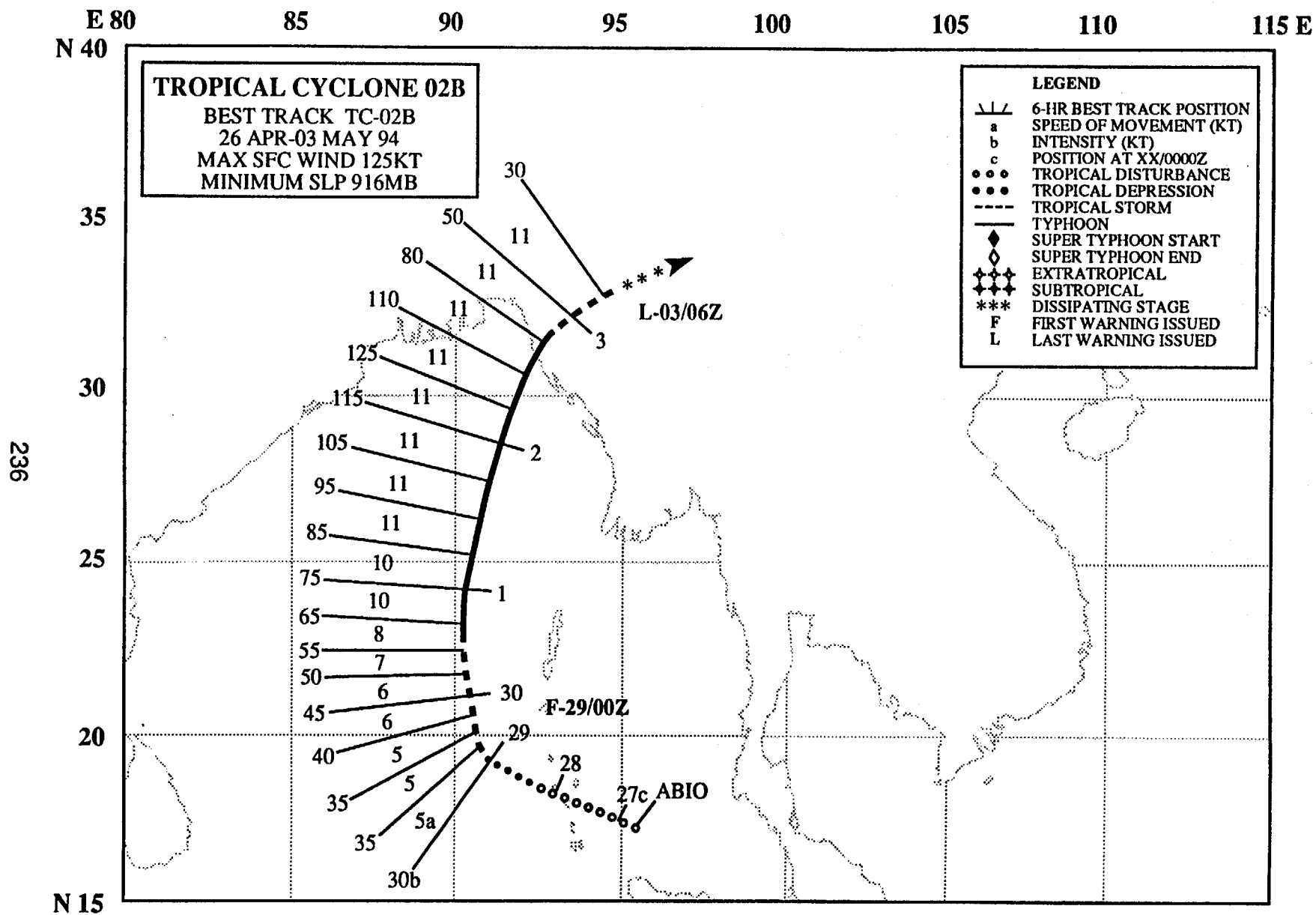


Figure 3-01B-1 Tropical Cyclone 01B near peak intensity in the central Bay of Bengal (222331Z March infrared GMS imagery).

Tropical Cyclone 01B was the first significant tropical cyclone to occur in the Northern Indian Ocean during 1994. It was first mentioned on the 201800Z March Significant Tropical Weather Advisory as area of persistent deep convection in the Bay of Bengal southwest of the Andaman Islands. Continued development led to a Tropical Cyclone Formation Alert, issued by JTWC at 210400Z. A second Tropical Cyclone Formation Alert at 220400Z was followed by the first warning at 221200Z. The tropical cyclone moved slowly and north-northwestward, reaching a peak intensity of 40 kt (21 m/sec) at 230600Z. The final warning was issued at 250000Z, as the weakening low-level vortex drifted south-southwestward.



TROPICAL CYCLONE 02B

I. HIGHLIGHTS

Tropical Cyclone 02B was by far the most intense tropical cyclone in the North Indian Ocean during 1994. Its track and intensity evolution was very similar to that of the devastating TC 02B of 1991, which was responsible for extremely heavy loss of life in the densely populated Chittagong region of Bangladesh. The combination of a lower than expected storm tide, and a massive evacuation effort by disaster preparedness officials in Bangladesh helped to keep this year's casualties to a relative minimum.

II. TRACK AND INTENSITY

The tropical disturbance which became Tropical Cyclone 02B was first mentioned on the 261800Z April Significant Tropical Weather Advisory as an area of persistent convection in the southeastern Bay of Bengal. At 290000Z the first warning was issued based on consolidation of deep convection near the system center. TC 02B tracked generally north-northeastward and intensified at a normal rate (i.e. one "T" number per day). It reached a peak intensity of 125 kt (64 m/sec) — nearly supertyphoon intensity — on 02 May (Figure 3-02B-1). The system weakened slightly prior to making landfall in the vicinity of Cox's Bazar near the Bangladesh-Burma border. The system weakened rapidly over land and the final warning was issued at 030600Z May.

III. IMPACT

In virtually every respect (i.e. track, intensity, location and time of year) TC 02B of 1994 and TC 02B of 1991 were similar. However, the impact of the 1991 storm was far more devastating (138,000 dead in 1991 as opposed to less than 300 dead in 1994). A key difference associated with the impact of the two storms was the astronomical tides: TC 02B (1991) struck close to high tide (12.5 ft (3.8 m) above mean lower low water (MLLW)) and TC 02B (1994) made landfall almost exactly at low tide (3.5 ft (1.0 m) above MLLW). This large astronomical tidal range may have made a substantial difference in the amount of storm surge related flooding. A massive evacuation in which officials moved approximately 350,000 people to safety prior to the landfall of 1994's TC 02B, also played a role in the relatively low number of fatalities. Even so, wire reports indicated relatively heavy losses from TC 02B (1994). In addition to the official death toll of 285, over one half million people were left homeless, with total losses estimated at \$125 million.

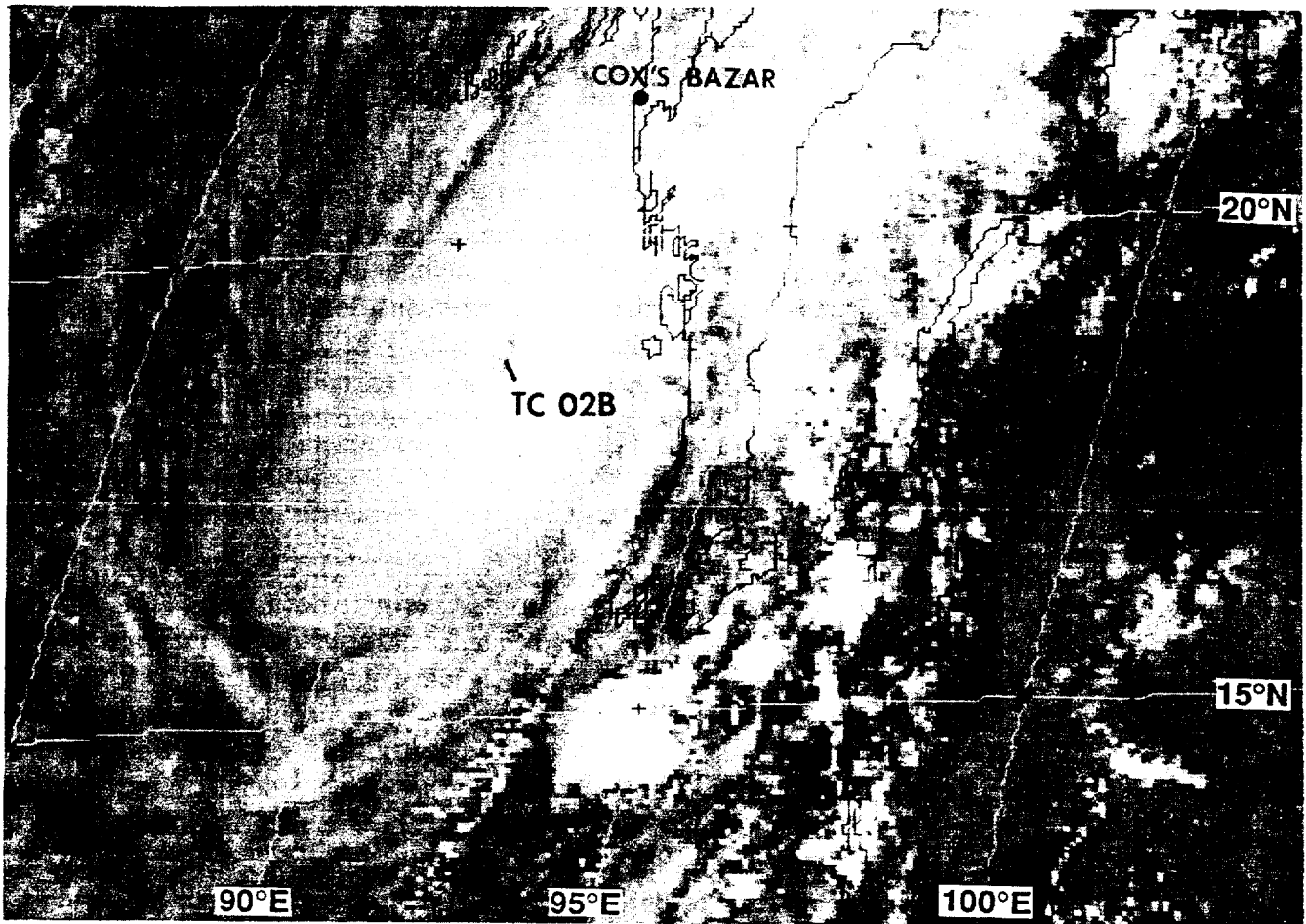


Figure 3-02B-1 Tropical Cyclone 02B moving north-northeastward in the Bay of Bengal. Maximum sustained winds at this time were estimated at 115 kt. (020031Z May visible GMS imagery).

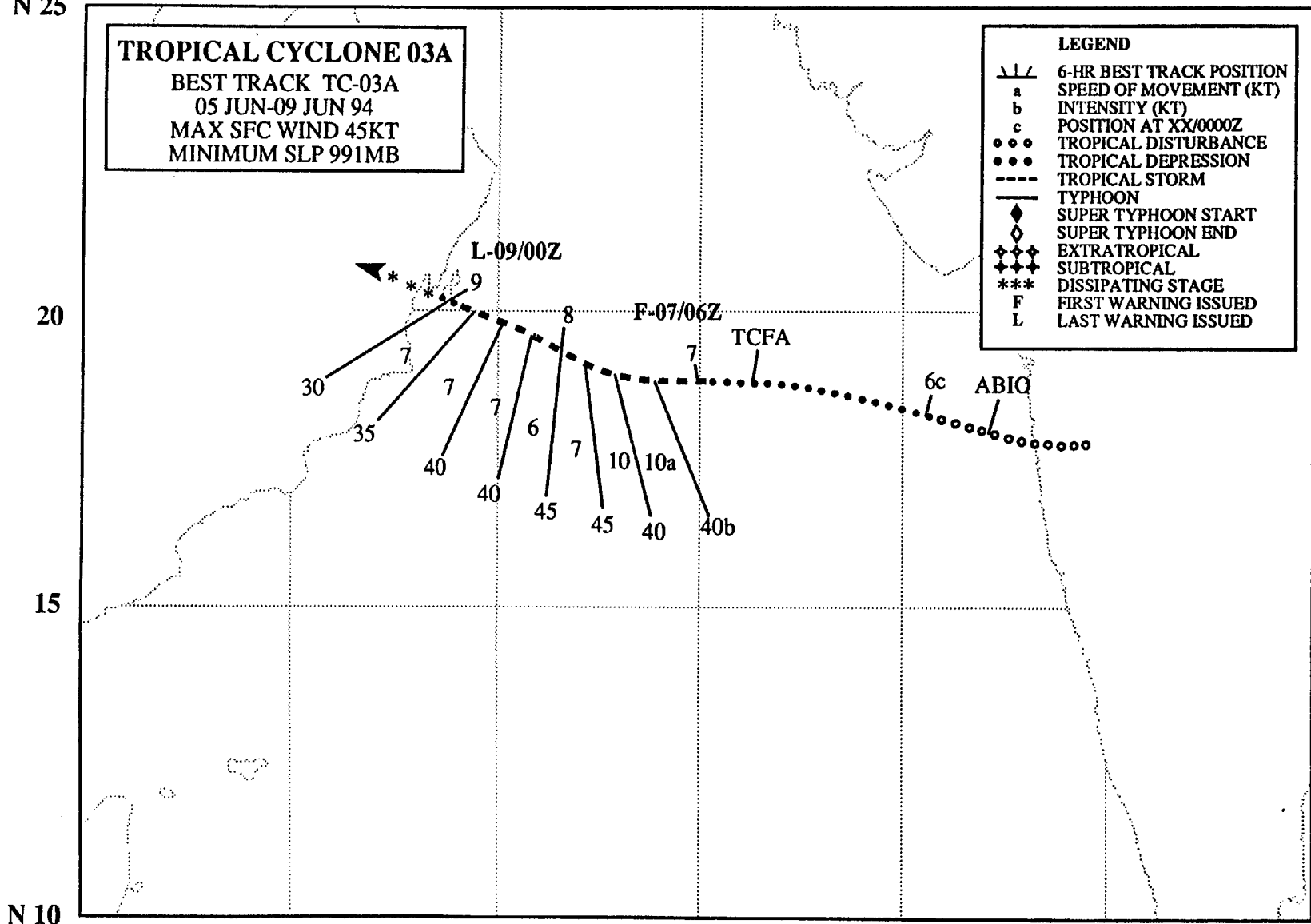
E 50 55 60 65 70 75 80 E

N 25

TROPICAL CYCLONE 03A
 BEST TRACK TC-03A
 05 JUN-09 JUN 94
 MAX SFC WIND 45KT
 MINIMUM SLP 991MB

LEGEND

- 6-HR BEST TRACK POSITION
- a SPEED OF MOVEMENT (KT)
- b INTENSITY (KT)
- c POSITION AT XX/0000Z
- TROPICAL DISTURBANCE
- TROPICAL DEPRESSION
- TROPICAL STORM
- TYPHOON
- ◆ SUPER TYPHOON START
- ◇ SUPER TYPHOON END
- ◆◆◆ EXTRATROPICAL
- ◆◆◆ SUBTROPICAL
- *** DISSIPATING STAGE
- F FIRST WARNING ISSUED
- L LAST WARNING ISSUED



239

N 10

TROPICAL CYCLONE 03A

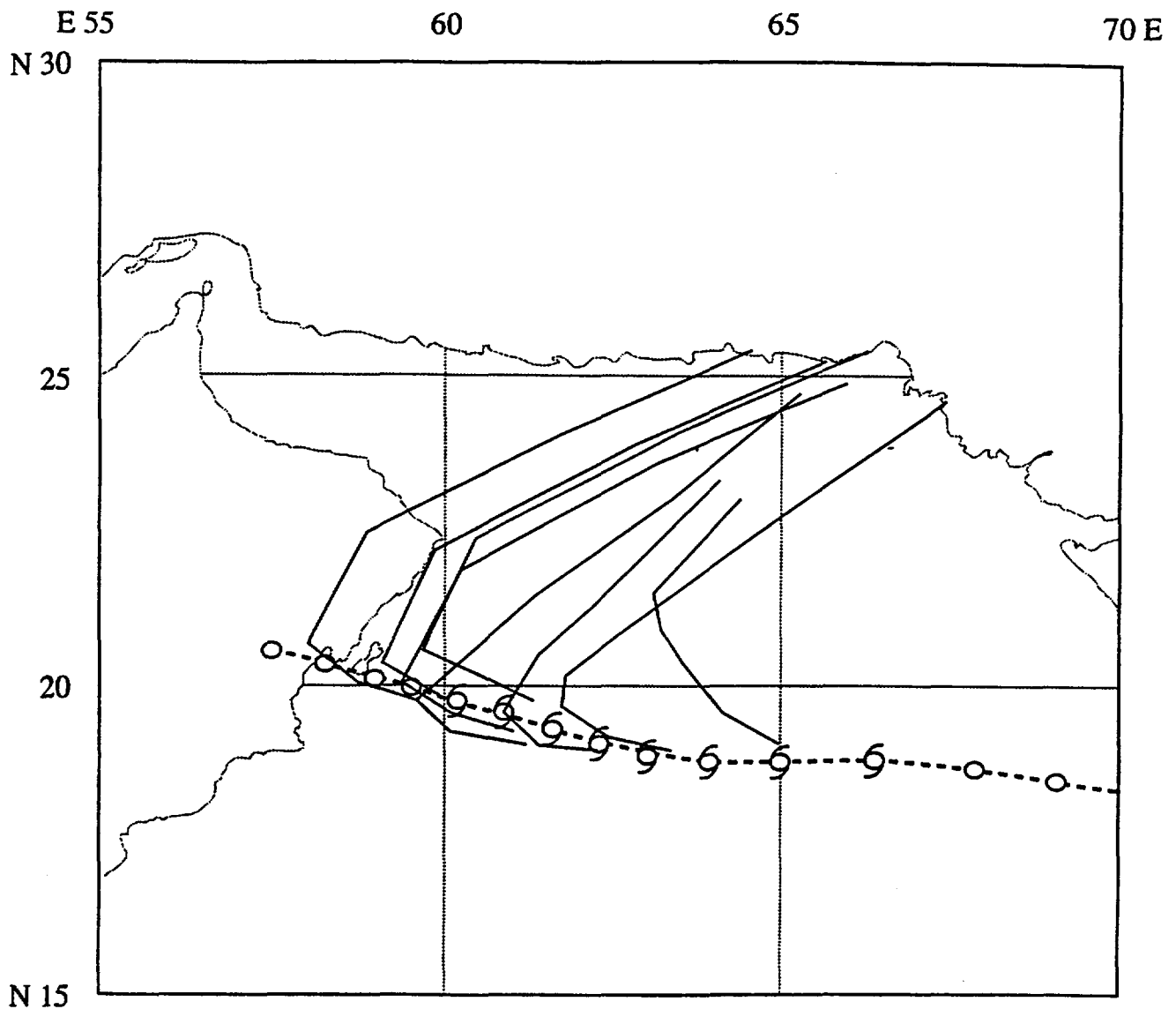
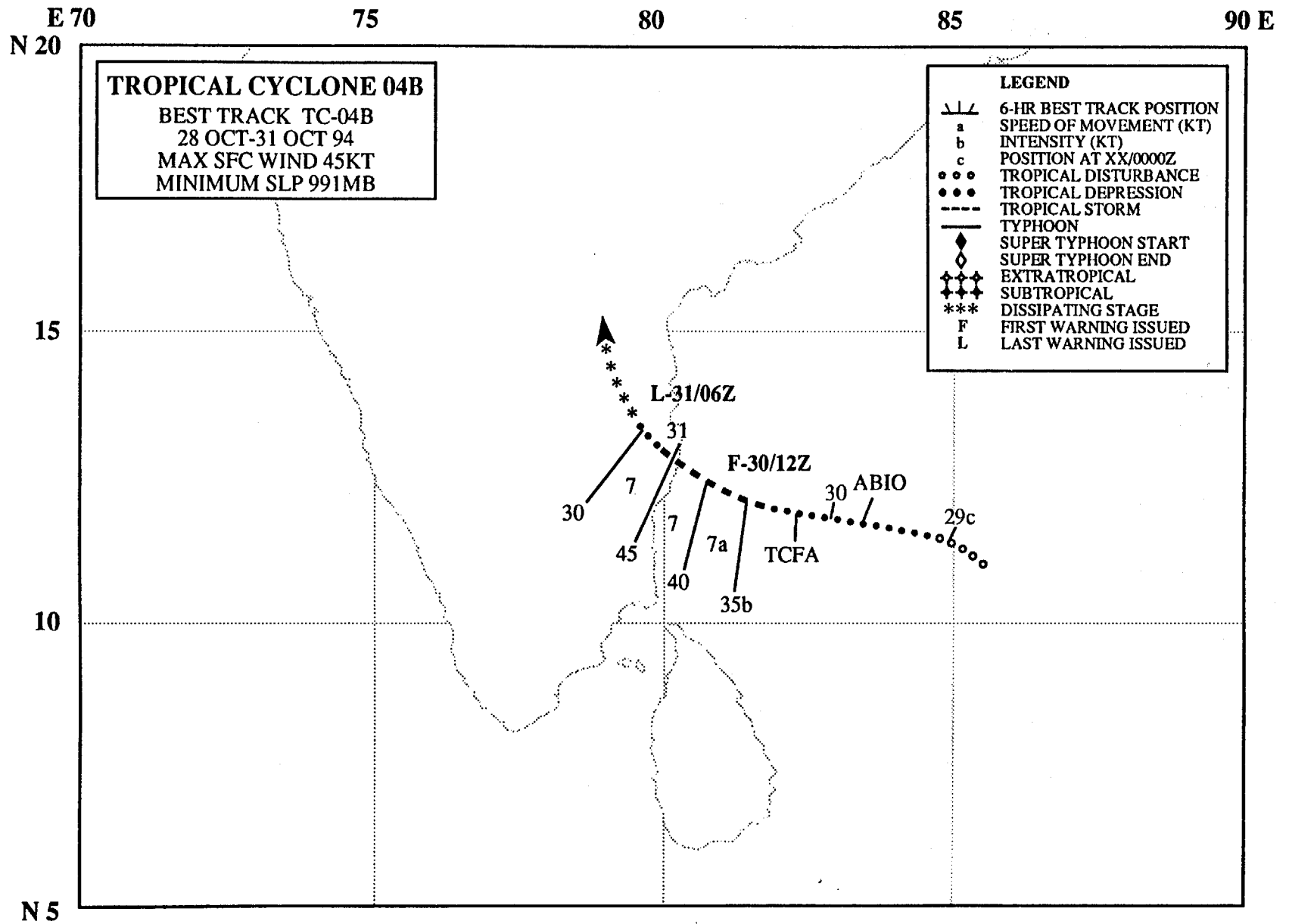


Figure 3-03A-1 The nonclimatological nature of TC 03A's track is shown by the forecast aid "CLIM", which is derived from the climatological data base for the area.

Tropical Cyclone 03A originated as a surface heat low over central India. It was first mentioned on the 051800Z June Significant Tropical Weather Advisory when the heat low moved westward into the North Arabian Sea, merged with the southwesterly monsoonal flow, and convection increased. Convective organization improved, and a Tropical Cyclone Formation alert was issued at 061800Z. The first warning followed at 070600Z. The system moved on a nonclimatological west-northwestward track (Figure 3-03A-1) and reached a maximum intensity of 45 kt (23 m/sec) at 071800Z. TC 03A began to weaken as it approached the coast of Oman, and the final warning was issued at 090000Z.



TROPICAL CYCLONE 04B

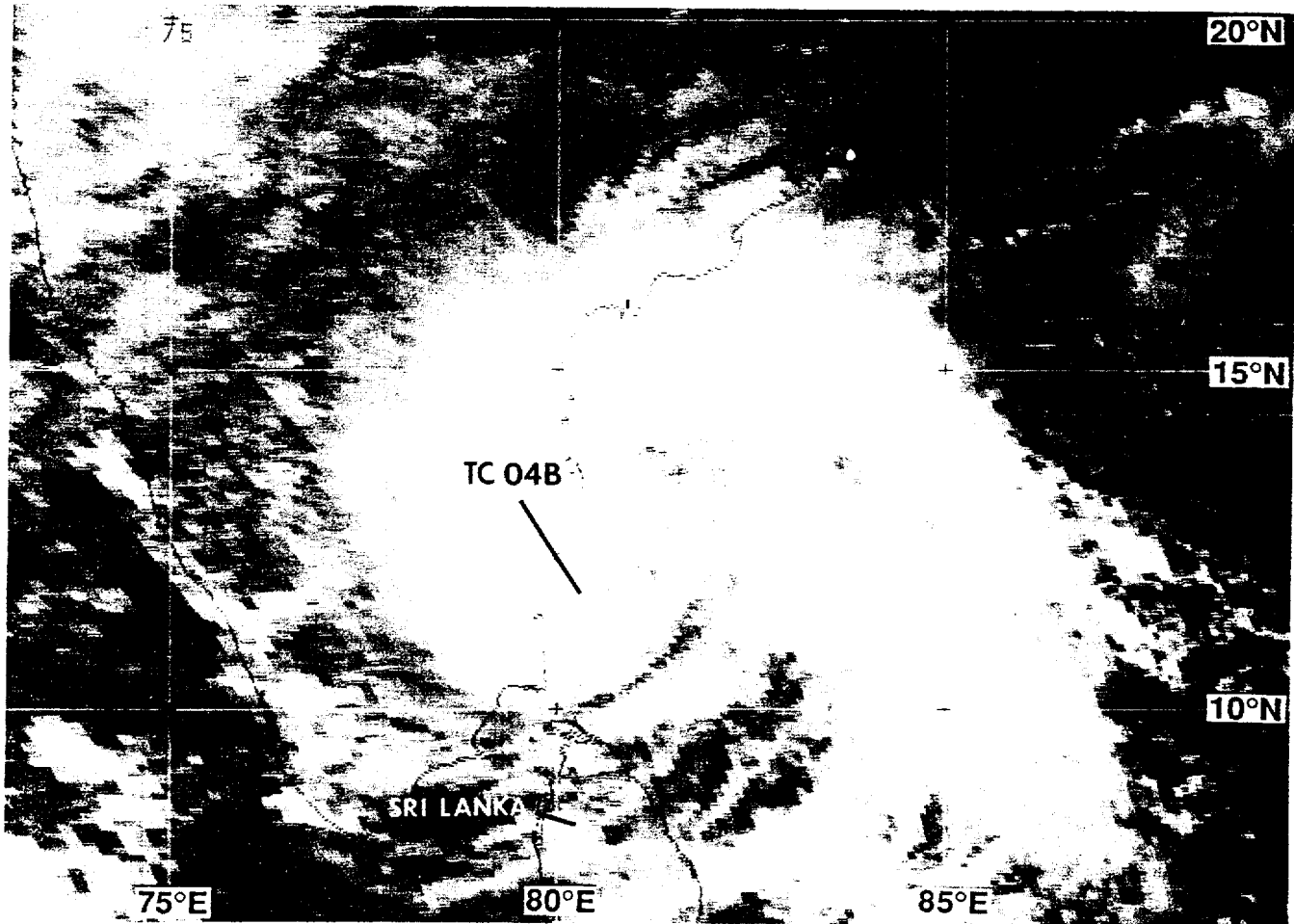
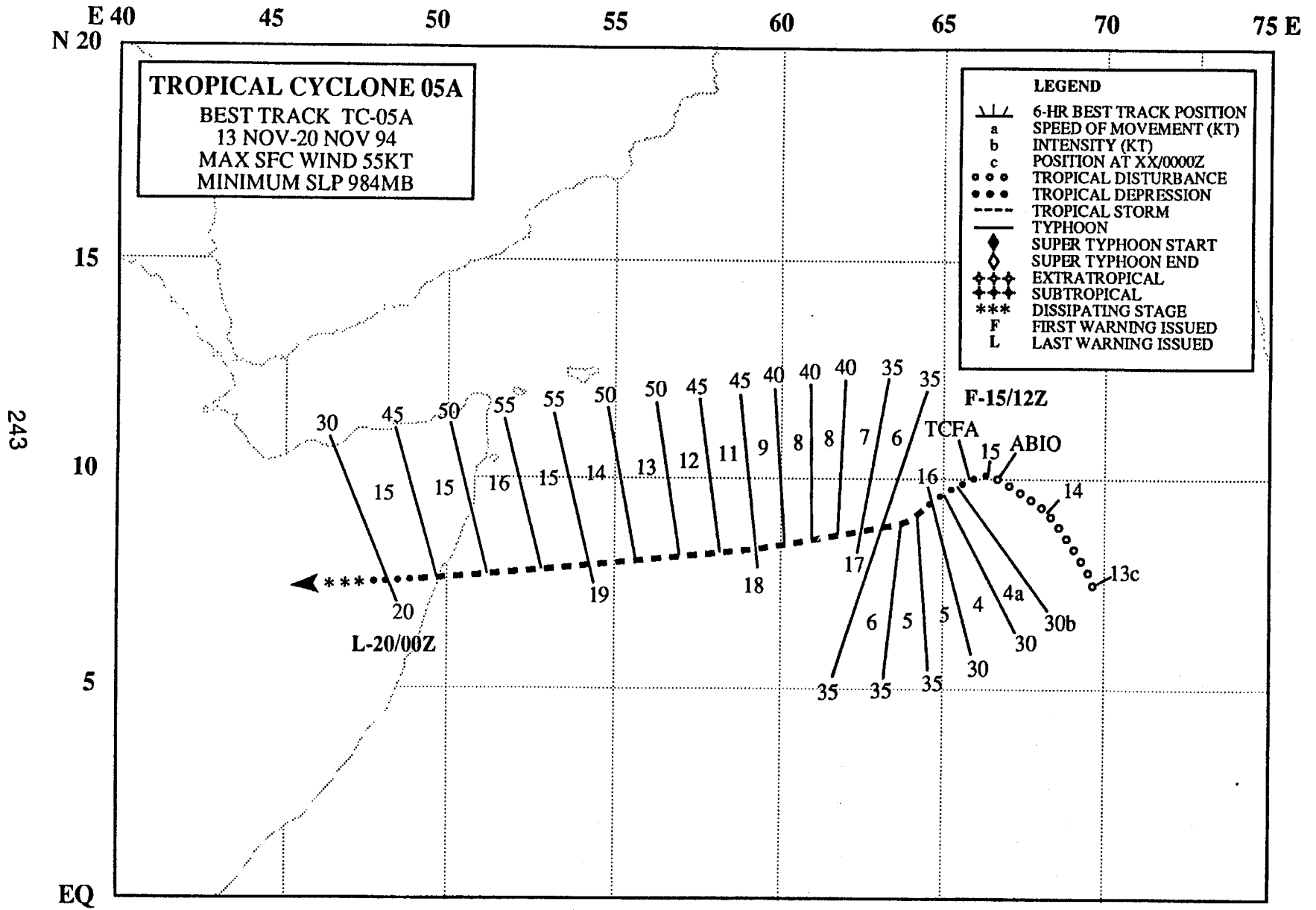


Figure 3-04B-1 Tropical Cyclone 04B approaches the southeast coast of India. The system reached peak intensity as it made landfall (300831Z October visible GMS imagery).

The disturbance that became Tropical Cyclone 04B was first mentioned on the 291800Z October Significant Tropical Weather Advisory, as an area of persistent convection began to consolidate northeast of Sri Lanka. Based on continued convective development, a Tropical Cyclone Formation Alert was issued at 300430Z, followed at 301200Z by the first warning. The tropical cyclone tracked westward towards India, and reached its peak intensity of 45 kt (23 m/sec) immediately prior to landfall, at 310000Z. A land synoptic station near TC 04B at landfall reported 40 kt (21 m/sec) winds and a 994.3 mb SLP. The final warning was issued at 310600Z as TC 04B weakened inland.



TROPICAL CYCLONE 05A

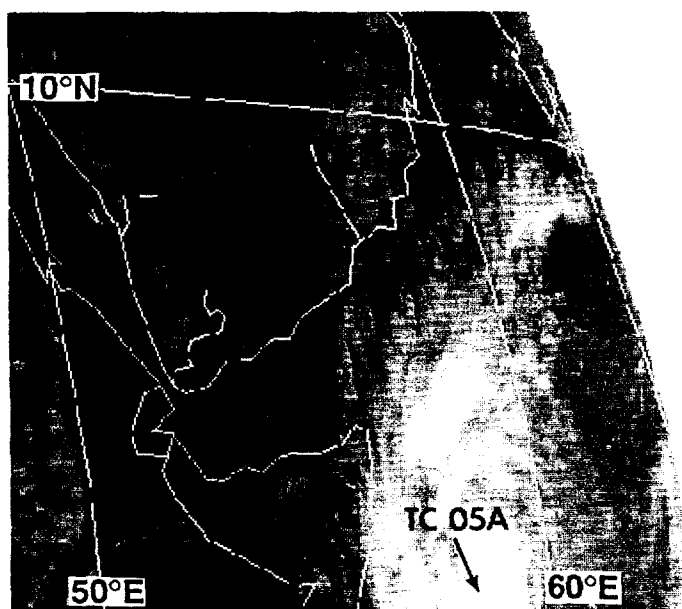


Figure 3-05A-1 Tropical Cyclone 05A approaching peak intensity (181714Z November infrared Meteosat imagery).

Tropical Cyclone 05A was first mentioned on the 041800Z November Significant Tropical Weather Advisory, as an area of convection in the eastern North Arabian Sea began to organize. Convection associated with this system increased and a Tropical Cyclone Formation Alert was issued at 150700Z, followed by the first warning at 151200Z. The system tracked toward the west-southwest and steadily intensified, reaching a peak intensity of 55 kt (28 m/sec) at 190000Z. The system made landfall over Somalia at 191800Z, and the final warning was issued at 200000Z, as the system dissipated rapidly over northeastern Africa.